



# **Next Generation Flight Management Systems for Manned and Unmanned Aircraft Operations**

*Automated Separation Assurance and  
Collision Avoidance Functionalities*

*A thesis submitted in fulfilment of the requirements for the degree of*

**Doctor of Philosophy (Aerospace Engineering)**

**Subramanian Ramasamy, MEng**

**Supervisors:**

**Professor Roberto Sabatini**

**Dr Reece Clothier**

**School of Engineering**

**College of Science, Engineering and Health**

**RMIT University**

**February 2017**

This page is intentionally left blank to support presswork tasks

## Declaration

I certify that except where due acknowledgement has been made, this work is that of the author alone; this work has not been submitted previously, in whole or in part, to qualify for any other academic award; the content of this thesis is the result of work, which has been carried out since the official commencement date of the approved research program; any editorial work, paid or unpaid, carried out by a third party is acknowledged; and, ethics procedures and guidelines have been followed.

I acknowledge the support I have received for my research through the provision of an Australian Government Research Training Program Scholarship.

Subramanian Ramasamy

20 February 2017



*"The desire to fly is an idea handed down to us by our ancestors who, in their gruelling travels across trackless lands in prehistoric times, looked enviously on the birds soaring freely through space, at full speed, above all obstacles, on the infinite highway of the air". - Wilbur Wright*

## Acknowledgements

First and foremost, I want to express my sincere gratitude and admiration to my primary supervisor Professor Roberto (Rob) Sabatini for nurturing me in line with one of Albert Einstein's quotes that reads "*It is the supreme art of the teacher to awaken joy in creative expression and knowledge*". Following the anecdote "to perceive innovation as an extension of an ardent imagination leading to profound excellence and deep satisfaction towards the benefit of mankind", I wholeheartedly thank Prof Rob Sabatini for his infinite insights and encouragement throughout my doctoral work.

The support I received from my secondary advisor, Dr Reece Clothier has been extremely important throughout my research work at RMIT University. Many thanks to the Higher Degrees by research (HDR) milestone review panel committee members for their constructive feedback. The scientific quest and support that I always received from my fellow research colleagues and compadres: Dr Alessandro G.M. Gardi, Dr Matthew Marino, Mr Francesco Cappello, Ms Jing Liu, Mr Yixiang Lim, Mr Suraj Bijjahalli, Mr Rohan Kapoor, Mrs Eranga Batuwangala and Mr Lanka Bogoda (RMIT University), and others at Cranfield University (UK), has been highly instrumental during my doctoral work. I would like to thank wholeheartedly the THALES Australia CASiA collaborators including Mr Trevor Kistan, Mr Mark O'Flynn and Mr Philippe Bernard-Flattot as well as RMIT Intelligent and Cyber-Physical Transport Systems (ICTS) research group's members. I take this opportunity to acknowledge the financial support offered by the School of Engineering, RMIT University and the Government of Australia through the Endeavour International Postgraduate Research Scholarship and Australian Postgraduate Award. I extend my impeccable gratitude to the technical and administrative staff including Mrs Lina Bubic, Mrs Jeneffer Thompson and Mrs Emilija Simic. Above all, I dedicate this work to my parents, Prof A.M.S. Ramasamy and Mrs Girija Ramasamy for opening innumerable doors in me into the world of science and technology from my childhood.

## Summary

The demand for improved safety, efficiency and dynamic demand-capacity balancing due to the rapid growth of the aviation sector and the increasing proliferation of Unmanned Aircraft Systems (UAS) in different classes of airspace pose significant challenges to avionics system developers.

The design of Next Generation Flight Management Systems (NG-FMS) for manned and unmanned aircraft operations is performed by addressing the challenges identified by various Air Traffic Management (ATM) modernisation programmes and UAS Traffic Management (UTM) system initiatives. In particular, this research focusses on introducing automated Separation Assurance and Collision Avoidance (SA&CA) functionalities (mathematical models) in the NG-FMS. The innovative NG-FMS is also capable of supporting automated negotiation and validation of 4-Dimensional Trajectory (4DT) intents in coordination with novel ground-based Next Generation Air Traffic Management (NG-ATM) systems.

One of the key research contributions is the development of a unified method for cooperative and non-cooperative SA&CA, addressing the technical and regulatory challenges of manned and unmanned aircraft coexistence in all classes of airspace. Analytical models are presented and validated to compute the overall avoidance volume in the airspace surrounding a tracked object, supporting automated SA&CA functionalities. The scientific basis of this approach is to assess real-time measurements and associated uncertainties affecting navigation states (of the host aircraft platform), tracking observables (of the static or moving object) and platform dynamics, and translate them to unified range and bearing uncertainty descriptors. The SA&CA unified approach provides an innovative analytical framework to generate high-fidelity dynamic geo-fences suitable for integration in the NG-FMS and in the ATM/UTM/defence decision support tools.

# Table of Contents

Declaration .....	iii
Acknowledgements .....	v
Summary.....	vi
List of Figures .....	xiv
List of Tables .....	xx
List of Abbreviations.....	xxii

## 1. Introduction

1.1	Research Context and Motivation .....	1
1.2	Research Gap Identification .....	8
1.3	Research Questions.....	8
1.4	Research Aim .....	9
1.5	Research Objectives.....	9
1.6	Research Methodology.....	9
1.7	Thesis Outline .....	11
1.8	References.....	12

## 2. Literature Review

2.1	Introduction .....	15
2.2	Avionics and ATM System Modernisation .....	15
2.3	Flight Management Systems.....	18
2.4	Maintenance of Separation .....	29
2.4.1	Airspace Categories and Classes.....	29
2.4.2	Rules of Air .....	30

2.4.3	General Operation Principles and Flight Rules .....	31
2.4.4	Separation Standards .....	33
2.5	Collision Detection and Avoidance .....	34
2.5.1.	Conflict Detection and Resolution Approaches .....	40
2.5.2.	Theoretical Techniques for CD&R .....	41
2.5.3.	Applied/Implemented Air Traffic Solutions for CD&R .....	43
2.6	SA&CA Technologies .....	45
2.6.1	State-of-the-art SA Technologies .....	43
2.6.2	State-of-the-art SA supported by an ATM System .....	60
2.6.3	CA Sensors/Systems .....	62
2.6.4	Attributes/Capabilities of UAS SA&CA Technologies .....	63
2.7	Tracking, Decision-Making and Avoidance Loop .....	65
2.7.1	TDA Functions .....	66
2.8	Multi-Sensor Data Fusion Algorithms for SA&CA .....	68
2.9	UTM System .....	78
2.10	Dependency on LoS and BLoS Communications .....	86
2.11	Towards Higher Levels of Autonomy .....	87
2.12	SA&CA Requirements .....	89
2.13	Research on SA&CA Avoidance Volumes .....	91
2.14	Case for a Unified Approach to SA&CA .....	94
2.15	Conclusions .....	97
2.16	References .....	97

### **3. Next Generation Flight Management Systems**

3.1	Introduction .....	109
3.2	NG-FMS and NG-ATM Systems .....	109



3.3	System Requirements and New Functions .....	117
3.4	NG-FMS Architecture .....	122
3.5	NG-FMS Algorithms.....	129
3.6	System State Error Analysis .....	135
3.7	CNS Performance.....	138
3.8	NG-FMS Case Studies.....	139
3.8.1	Platforms .....	139
3.8.2	Long-haul Flight.....	142
3.8.3	Medium-haul Flight.....	146
3.8.4	UAS.....	148
3.9	Negotiation and Validation Features.....	150
3.9.1	Evaluation Process.....	150
3.10	Conclusions .....	152
3.11	References.....	153

## **4. Separation Assurance and Collision Avoidance Functionalities**

4.1	Introduction .....	157
4.2	Unified Approach to SA&CA .....	157
4.3	Distinctiveness of an Unified Approach to SA&CA .....	169
4.4	Implementation in NG-FMS .....	171
4.5	Conclusions .....	174
4.6	References.....	175

## **5. Performance Analysis of SA&CA Functionalities**

5.1	Introduction .....	177
5.2	Avoidance Volumes .....	177

5.3	SA&CA Test Bed Architecture .....	178
5.4	Sensor/System Error Modelling.....	183
5.4.1	Test for Correlation .....	188
5.4.2	Covariant and Contravariant Components.....	190
5.4.3	Possible Cases .....	190
5.4.4	Effects of Data Size and Methodology .....	191
5.4.5	Example: ADS-B Error Modelling .....	192
5.5	Sensor/System Error Modelling.....	197
5.5.1	Errors in Range.....	197
5.5.2	Errors in Bearing Measurements at a Given Range .....	199
5.5.3	Uncertainty in Velocity Measurements .....	203
5.5.1	Wind and Wake Turbulence .....	204
5.6	Relative Dynamics between Platforms .....	206
5.7	CNS Performance and Error Models.....	211
5.8	Avoidance Trajectory Optimisation .....	214
5.9	SA&CA Certification Framework.....	216
5.9.1	SA&CA Hardware and Software.....	217
5.9.2	Approach to Certification .....	219
5.10	Conclusions .....	221
5.11	References.....	221

## **6. Ground Obstacles SA&CA Case Study**

6.1	Introduction .....	225
6.2	Ground Obstacle Detection and Warning Systems .....	225
6.3	UAS Obstacle Warning and Avoidance System .....	228

6.4	Operational Requirements .....	229
6.5	System Description .....	230
6.6	Obstacle Detection and Classification Software .....	232
6.7	Mathematical Algorithms.....	234
6.8	Formats and Functions.....	236
6.9	Simulation Case Study .....	237
6.10	Conclusions .....	240
6.11	References.....	240

## **7. Aerial Obstacles SA&CA Case Study**

7.1	Introduction .....	243
7.2	Non-Cooperative SA&CA – FLS .....	243
7.3	Cooperative SA&CA – ADS-B .....	246
7.4	Simulation Case Studies.....	249
7.4.1	Tracking and Detection Performance .....	249
7.5	Conclusions .....	258
7.6	References.....	258

## **8. Potential UAS Traffic Management Applications**

8.1	Introduction .....	261
8.2	UTM System in the CNS+A Framework.....	261
8.3	Multi-UTM System .....	263
8.4	Pathways to Implementation .....	265
8.4.1	Multi-Platform Scenario .....	265
8.4.2	TMA Environment.....	268
8.5	Simulation Case Studies.....	271

8.5.1	Geofences.....	275
8.5.1	Multi-Platform Coordination Scenario.....	277
8.6	Conclusions .....	280
8.7	References.....	280

## **9. Conclusions and Future Directions**

9.1	Conclusions .....	283
9.1.1	Summary of Original Contributions.....	283
9.1.2	Achieved Research Objectives .....	285
9.2	Future Directions .....	289

## **Appendix A: UAS Integrated Navigation Systems**

A.1	Introduction .....	295
A.2	Multi-sensor Data Fusion Techniques.....	295
A.3	Integrated Multi-sensor Data Fusion Architectures .....	300
A.4	Conclusions .....	302
A.5	References.....	303

## **Appendix B: Certification Standards and Recommended Practices**

B.1	Requirements .....	305
-----	--------------------	-----

## **Appendix C: Elements of Human Machine Interface & Interactions**

C.1	Introduction .....	309
C.2	Human Machine Interface and Interactions .....	309
C.3	Formats and Functions for Automatic SA&CA.....	313
C.4	Information Display.....	317

C.5	Adaptive HMI <sup>2</sup> .....	321
C.6	Conclusions .....	324
C.7	References.....	324

## Appendix D: List of Relevant Publications

D.1	Scientific Dissemination .....	327
-----	--------------------------------	-----

## List of Figures

Figure 1.1.	Combined objectives. ....	2
Figure 1.2.	Automated SA&CA tasks.....	7
Figure 2.1.	State-of-the-art FMS architecture.....	19
Figure 2.2.	Waypoint types (a) fly-by and (b) fly-over.....	24
Figure 2.3.	FMS guidance loop. ....	25
Figure 2.4.	FMS and AFCS interactions.....	27
Figure 2.5.	SA&CA system processes. ....	38
Figure 2.6.	CATH, SSV and SST boundaries. ....	40
Figure 2.7.	Trajectory prediction/estimation approaches.....	42
Figure 2.8.	Collision detection and resolution taxonomy. ....	42
Figure 2.9.	Onboard collision avoidance system - early radar systems. ....	46
Figure 2.10.	Onboard collision avoidance system – BCAS. ....	46
Figure 2.11.	Onboard collision avoidance system – TCAS.....	46
Figure 2.12.	Example of an encounter geometry. ....	50
Figure 2.13.	Limited robustness of TCAS.....	51
Figure 2.14.	Uncertainty propagation in ACAS. ....	54
Figure 2.15.	ACAS top-level architecture.....	56
Figure 2.16.	Functional component of ADS-B.....	57
Figure 2.17.	Detection range of CA technologies for UAS.....	65
Figure 2.18.	Collision scenario at different time epochs. ....	67
Figure 2.19.	GNC and TDA loops. ....	68
Figure 2.20.	SA&CA tasks.....	68
Figure 2.21.	Intelligent techniques for SA&CA MSDF. ....	78
Figure 2.22.	UTM system architecture.....	79
Figure 2.23.	UTM functions and stakeholders.....	80
Figure 2.24.	Role of SA&CA in UTM. ....	83
Figure 2.25.	UTM system concept - operational geographies.....	85
Figure 2.26.	Operational geographies of multiple UAS.....	86
Figure 2.27.	Well-clear threshold.....	93
Figure 2.28.	Well-clear based confliction detection method. ....	93

Figure 2.29.	Number of SA&CA research gaps identified. ....	95
Figure 3.1.	4DT intent negotiation and validation.....	112
Figure 3.2.	4-PNV system initiated intent negotiation/validation loop. ....	115
Figure 3.3.	NG-FMS initiated intent negotiation/validation loop.....	115
Figure 3.4.	SESAR trajectory management concept. ....	116
Figure 3.5.	Multi-criteria departure procedure.....	118
Figure 3.6.	Multi-criteria departure procedure.....	119
Figure 3.7.	Continuous descent approach procedure.....	120
Figure 3.8.	NG-FMS and NG-ATM system interactions.....	122
Figure 3.9.	NG-FMS integrity monitor.....	124
Figure 3.10.	NG-FMS overall architecture.....	125
Figure 3.11.	NG-FMS 4DT planner and optimiser. ....	126
Figure 3.12.	NG-FMS integrity flag generation.....	126
Figure 3.13.	NG-FMS performance management. ....	127
Figure 3.14.	CNS+A systems. ....	128
Figure 3.15.	RTSP elements and time frames. ....	138
Figure 3.16.	Airbus A380. ....	139
Figure 3.17.	Airbus A320. ....	140
Figure 3.18.	AEROSONDE™ UAS.....	141
Figure 3.19.	4D trajectories.....	144
Figure 3.20.	Climb Phase 4D Trajectory Intents.....	145
Figure 3.21.	Cruise Phase 4D Trajectory Intents. ....	145
Figure 3.22.	Simulated set of 4DT intents.....	146
Figure 3.23.	4D trajectory deviations.....	147
Figure 3.24.	Results of the 4DT optimisation for climb phase.....	149
Figure 3.25.	Results of the 4DT optimisation for descent phase. ....	149
Figure 3.26.	NG-FMS air-to-ground and air-to-air negotiation loops.....	150
Figure 3.27.	NG-FMS and NG-ATM system negotiation and validation.....	152
Figure 4.1.	Navigation and tracking error ellipsoids. ....	158
Figure 4.2.	Uncertainty volume (uncorrelated errors). ....	160
Figure 4.3.	Uncertainty volumes obtained from range only errors. ....	161

Figure 4.4.	Combination of navigation and tracking errors. ....	161
Figure 4.5.	Uncertainty volume due to error in bearing measurements. ...	163
Figure 4.6.	Avoidance volumes at different time epochs. ....	163
Figure 4.7.	Avoidance volumes at time of collision. ....	164
Figure 4.8.	Considered avoidance volume. ....	168
Figure 4.9.	Real function after parameterisation. ....	168
Figure 4.10.	Complex function after parameterisation. ....	169
Figure 4.11.	NG-FMS architecture including SA&CA functions. ....	172
Figure 4.12.	SA&CA software functional architecture. ....	172
Figure 4.13.	Surveillance data processing. ....	173
Figure 4.14.	Interactions within the NG-FMS. ....	174
Figure 5.1.	Reconfigurable UAS SA&CA test bed architecture. ....	180
Figure 5.2.	FTA for autonomous decision-making tasks. ....	181
Figure 5.3.	Error and radar ranges. ....	190
Figure 5.4.	Error and reference ranges. ....	194
Figure 5.5.	$\{\sigma_{x\_N}, \sigma_{y\_N}, \sigma_{z\_N}\} = 3, 2, 4$ and $\{\sigma_{x\_T}, \sigma_{y\_T}, \sigma_{z\_T}\} = 8, 12, 3$ ....	197
Figure 5.6.	$\{\sigma_{x\_N}, \sigma_{y\_N}, \sigma_{z\_N}\} = 6, 2, 4$ and $\{\sigma_{x\_T}, \sigma_{y\_T}, \sigma_{z\_T}\} = 8, 12, 3$ ....	197
Figure 5.7.	$\{\sigma_{x\_N}, \sigma_{y\_N}, \sigma_{z\_N}\} = 3, 8, 4$ and $\{\sigma_{x\_T}, \sigma_{y\_T}, \sigma_{z\_T}\} = 8, 12, 3$ ....	198
Figure 5.8.	$\{\sigma_{x\_N}, \sigma_{y\_N}, \sigma_{z\_N}\} = 3, 2, 6$ and $\{\sigma_{x\_T}, \sigma_{y\_T}, \sigma_{z\_T}\} = 8, 12, 3$ ....	198
Figure 5.9.	$\{\sigma_{x\_N}, \sigma_{y\_N}, \sigma_{z\_N}\} = 3, 2, 4$ and $\{\sigma_{x\_T}, \sigma_{y\_T}, \sigma_{z\_T}\} = 3, 12, 3$ ....	198
Figure 5.10.	$\{\sigma_{x\_N}, \sigma_{y\_N}, \sigma_{z\_N}\} = 3, 2, 4$ and $\{\sigma_{x\_T}, \sigma_{y\_T}, \sigma_{z\_T}\} = 8, 5, 3$ .....	199
Figure 5.11.	$\{\sigma_{x\_N}, \sigma_{y\_N}, \sigma_{z\_N}\} = 3, 2, 4$ and $\{\sigma_{x\_T}, \sigma_{y\_T}, \sigma_{z\_T}\} = 8, 12, 1$ ....	199
Figure 5.12.	Covariant case. ....	200
Figure 5.13.	Contravariant case. ....	201
Figure 5.14.	Effect of correlation coefficient. ....	201
Figure 5.15.	Errors in azimuth/elevation measurements = 35 degrees. ....	202
Figure 5.16.	Errors in azimuth/elevation measurements = 35 degrees. ....	202
Figure 5.17.	Errors in azimuth/elevation measurements = 10 degrees. ....	203
Figure 5.18.	Uncertainty in velocity = 7 m/sec. ....	204
Figure 5.19.	Uncertainty in velocity = 3 m/sec. ....	205
Figure 5.20.	Illustration of a conflict event. ....	206



Figure 5.21.	Obtained resolution.....	208
Figure 5.22.	Two objects in a collision course. ....	208
Figure 5.23.	Collision scenario. ....	209
Figure 5.24.	Navigation and surveillance sensors/systems. ....	212
Figure 5.25.	Illustration of a collision detection & resolution mechanism. ....	213
Figure 5.26.	Role of CNS performance and error models.....	213
Figure 5.27.	FAA FoR (a) and a possible sensors' installation (b).....	218
Figure 5.28.	NG-FMS hardware and software interface. ....	219
Figure 5.29.	Two-way approach to certification.....	220
Figure 6.1.	LOWAS FOV. ....	230
Figure 6.2.	LOWAS scan pattern for a slowly advancing platform. ....	231
Figure 6.3.	LOWAS avionics integration architecture for UAS. ....	232
Figure 6.4.	LOWAS signal processing software architecture. ....	233
Figure 6.5.	Target sections. ....	236
Figure 6.6.	Obstacle avoidance scenario. ....	238
Figure 6.7.	Case study scenario. ....	238
Figure 6.8.	Results of the avoidance trajectory generation algorithm.....	239
Figure 7.1.	Acquired and stabilised visual image. ....	244
Figure 7.2.	Tracked object. ....	244
Figure 7.3.	Acquired thermal image and tracked object.....	245
Figure 7.4.	Measured and estimated X position.....	250
Figure 7.5.	Measured and estimated Y position.....	250
Figure 7.6.	Measured and estimated Z position. ....	251
Figure 7.7.	Acquired thermal image and tracked object.....	251
Figure 7.8.	MSE in X, Y and Z. ....	252
Figure 7.9.	MSE in X, Y and Z. ....	252
Figure 7.10.	Conflict probability. ....	253
Figure 7.11.	Real and required separation.....	253
Figure 7.12.	Avoidance volume at time of conflict. ....	254
Figure 7.13.	Conflict scenario. ....	255
Figure 7.14.	Range and bearing data.....	255

Figure 7.15.	Real and required separation.....	256
Figure 7.16.	Range and bearing data.....	256
Figure 7.17.	Avoidance of other traffic by host aircraft platform.....	257
Figure 8.1.	UTM system concept. ....	262
Figure 8.2.	UTM and surveillance nodes. ....	264
Figure 8.3.	Multi-platform scenario. ....	267
Figure 8.4.	Deconfliction scenario in the TMA. ....	269
Figure 8.5.	Fully autonomous deconfliction scenario in the TMA. ....	270
Figure 8.6.	Simulated urban environment. ....	271
Figure 8.7.	Simulated urban environment in MATLABTM.....	272
Figure 8.8.	Vertices of imported objects. ....	272
Figure 8.9.	Simulated urban environment in MATLABTM (3D). ....	273
Figure 8.10.	Simulated urban environment in MATLABTM (2D). ....	273
Figure 8.11.	UAV and the current FoV. ....	274
Figure 8.12.	Optimised trajectory of the unmanned aircraft. ....	275
Figure 8.13.	Avoidance of a ground obstacle geofence. ....	276
Figure 8.14.	Avoidance of an aerial obstacle geofence.....	277
Figure 8.15.	Multi-platform coordination sceanario. ....	277
Figure 8.16.	Horizontal and vertical resolution – intruder 1. ....	278
Figure 8.17.	Horizontal and vertical resolution – intruder 2. ....	278
Figure 8.18.	Horizontal and vertical resolution – intruder 3. ....	279
Figure 8.19.	Re-optimised host platform trajectory.....	279
Figure A.1.	Multi-sensor data fusion process.....	296
Figure C.1.	CDTI display showing other traffic.....	315
Figure C.2.	PFD display showing resolution information.....	316
Figure C.3.	CDTI display showing resolution information. ....	316
Figure C.4.	Case 1 - Detection of wires and an extended structure.....	318
Figure C.5.	CDTI - Case 1. ....	318
Figure C.6.	Case 1 - Detection of wires and an extended structure.....	319
Figure C.7.	TID - Case 2. ....	319
Figure C.8.	Case 3 - Detection of wires and an extended structure.....	320

Figure C.9. TID - Case 3. ....	320
Figure C.10. Adaptive HMI <sup>2</sup> architecture. ....	321
Figure C.11. Adaptive HMI <sup>2</sup> integration in the NG-FMS. ....	322

## List of Tables

Table 2.1.	State-of-the-art FMS functions.....	22
Table 2.2.	Waypoint categories.....	23
Table 2.3.	Lateral guidance modes.....	25
Table 2.4.	Vertical guidance modes. ....	26
Table 2.5.	ICAO separation standards. ....	34
Table 2.6.	SA&CA core capabilities. ....	36
Table 2.7.	SA&CA crosscutting capabilities.....	37
Table 2.8.	ACAS X variants.....	55
Table 2.9.	Airborne surveillance systems. ....	60
Table 2.10.	Classification of autonomy levels.....	88
Table 2.11.	Research gaps for SA&CA.....	96
Table 3.1.	Performance weighting layout.....	119
Table 3.2.	Airbus A380 specifications.....	140
Table 3.3.	Airbus A320 specifications.....	141
Table 3.4.	AEROSNDETM UAS specifications. ....	142
Table 3.5.	AEROSNDETM UAS ADM parameters and derivatives. ....	143
Table 3.6.	Navigation system performance.....	147
Table 4.1.	Summary of equipage.....	173
Table 5.1.	SA&CA technologies.....	179
Table 5.2.	Correlation analysis. ....	191
Table 5.3.	Traffic application specific requirements summary. ....	195
Table 5.4.	Traffic ID specific requirements summary. ....	196
Table 6.1.	EGPWS modes, causes and warnings. ....	227
Table 6.2.	Obstacle detection technologies.....	229
Table 6.3.	LOWAS alerts.....	237
Table 7.1.	Navigation uncertainty categories.....	248
Table 7.2.	Navigation uncertainty categories - velocity. ....	248
Table A.1.	Integrated NGS systems.....	300
Table B.1.	Operational requirements. ....	305
Table B.2.	Technical and safety requirements. ....	306

Table B.3.	Human factors and T&E requirements.....	307
Table C.1.	Symbology of CDTI display.....	314
Table C.2.	Aural annunciations. ....	317

## List of Abbreviations

3D	Three Dimensional
4D	Four Dimensional
3-DoF	Three Degrees-of-Freedom
6-DoF	Six Degrees-of-Freedom
A/THR	Auto-Throttle
ABAS	Aircraft-Based Augmentation System
ACARE	Advisory Council for Aviation Research and innovation in Europe
ACARS	Aircraft Communications Addressing and Reporting System
ACAS	Airborne Collision Avoidance System
ACC	Area Control Centre
ACL	Aeronautical Clearance Services
ACM	ATC Communication Management
ACP	ATM Collision Prevention
ADAC	Automated Dynamic Airspace Controller
ADC	Air Data Computer
ADM	Aircraft Dynamics Model
ADS	Automatic Dependent Surveillance
ADS-A	Automatic Dependent Surveillance – Address
ADS-B	Automatic Dependent Surveillance – Broadcast
ADS-C	Automatic Dependent Surveillance – Contract
ADS-R	Automatic Dependent Surveillance – Rebroadcast
AFCS	Automatic Flight Control System
AGC	Automatic Gain Control

AGL	Above-Ground Level
AIRAC	Aeronautical Information Regulation and Control
AMC	Acceptable Means of Compliance
ANSP	Air Navigation Service Provider
AOC	Airline Operation Centre
APD	Avalanche Photodiode
AP/FD	Auto-Pilot and Flight Director
API	Application Programming Interface
APPR	Approach
APV	Approach with Vertical Guidance
ARINC	Aeronautical Radio Incorporated
ASAS	Airborne Separation Assistance System
ASBU	Aviation System Block Upgrades
ASTM	American Society for Testing and Materials
ASTRAEA	Autonomous System Technology Related Airborne Evaluation and Assessment
A/THR	Auto-Throttle
ATA	Air Transport Association
ATC	Air Traffic Control
ATCo	Air Traffic Controller
ATCRBS	Air Traffic Control Radar Beacon System
ATFM	Air Traffic Flow Management
ATM	Air Traffic Management
ATN	Aeronautical Telecommunications Network
ATO	Along-Track Offset
ATS	Air Traffic Services
ATSA	Air Traffic Situation Awareness

ATZ	Aerodrome Control Zone
AVR	Automatic Voice Recognition
BADA	Base of Aircraft Data
BDL	Boolean Decision Logic
BITE	Built-In-Test Equipment
BLoS	Beyond Line-of-Sight
BRLoS	Broad RLoS
CAA	Civil Airworthiness Authority
CARATS	Collaborative Action for Renovation of Air Traffic Systems
CAS	Calibrated Air Speed
CASA	Civil Aviation Safety Authority
CASiA	Centre for Advanced Studies in Air Traffic Management
CAT	Category (Instrument Landing)
CATH	Collision Avoidance Threshold
CC	Capability Class
CCD	Continuous Climb Departure
CD	Collision Detection
CD&R	Collision Detection and Resolution
CDA	Continuous Descent Approach
CDM	Collaborative Decision Making
CDO	Continuous Descent Operations
CDTI	Cockpit Display of Traffic Information
CFIT	Controlled Flight Into Terrain
CIF	Caution Integrity Flag
CKF	Cubature Kalman Filter
CM	Conflict Management



CNS	Communications, Navigation, Surveillance
CNS+A	Communication, Navigation and Surveillance/ Air Traffic Management and Avionics
CONOPS	Concept of Operations
CPDLC	Controller Pilot Data Link Communications
CRM	Crew Resource Management
CTA	Control Area
DAM	Dynamic Airspace Management
DCB	Demand-Capacity Balancing
DF	Direct to a Fix
DM	Domain Mode
DOD	Department of Defence
DSS	Decision Support System
DTD	Distance-To-Destination
DTED	Digital Terrain Elevation Database
DU	Display Unit
EASA	European Aviation Safety Authority
ECEF	Earth-Centred Earth-Fixed
EFI	Electronic Fuel Injection
EFIS	Electronic Flight Instrument System
ELOS	Equivalent Level of Safety
EKF	Extended Kalman Filter
EPU	Estimated Position Uncertainty
ERA	Environmentally Responsible Aviation
ERAM	En-Route Automation Modernization
ESM	Electronic Surveillance Module
ETA	Estimated Time of Arrival

EUROCAE	European Organisation for Civil Aviation Equipment
EVIGA	Enhanced VBN-IMU-GNSS-ADM
FAA	Federal Aviation Administration
FAF	Final approach Fixed
FAR	Federal Aviation Regulations
FANS	Future Air Navigation System
FANS-1	Future Air Navigation System implemented by Boeing
FANS-A	Future Air Navigation System implemented by Airbus
FCP	Flight Control Panel
FCU	Flight Control Unit
FHA	Functional Hazard Assessment
FIC	Flight Information Centre
FIANS	Future Indian Air Navigation System
FIR	Flight Information Region
FIS	Flight Information Service
FL	Flight Level
FLIR	Forward Looking Infrared
FLS	Forward-Looking Sensors
FIS-B	Flight Information Service – Broadcast
FMECA	Failure Modes Effects and Criticality Analysis
FMGU	Flight Management Guidance Unit
FMS	Flight Management System
FOR	Field-of-Regard
FOV	Field-of-View
FPA	Flight Path Angle
FPGA	Field Programmable Gate Array

FPLN	Flight Plan
FTA	Fault Tree Analysis
FTE	Flight Technical Error
GA	Go Around
GAL	Generic Array Logic
GBAS	Ground-Based Augmentation System
GCS	Ground Control Station
GLONASS	GLObalnaya NAvigatsionnaya Sputnikovaya Sistema
GM	Guidance Materials
GNC	Guidance Navigation and Control
GNSS	Global Navigation Satellite System
GPWS	Ground Proximity Warning System
GPS	Global Positioning System
GM	Gauss-Markov
GS	Ground Speed
GVA	Geometric Vertical Accuracy
GW	Gross Weight
HF	Human Factors
HFE	Human Factors Engineering
HFOM	Horizontal Figure of Merit
HITL	Human-In-The-Loop
HLP	High Level Processing
HM S/D	Helmet-Mounted Sight/Display
HMI <sup>2</sup>	Human–Machine Interface and Interactions
HUD	Head-Up Display
IAF	Initial Approach Fix

IBO	Intent-Based Operations
ICAO	International Civil Aviation Organisation
ICT	Information, Communication and Technology
ICTS	Intelligent and Cyber-Physical Transport Systems
IDA	Institute for Defense Analyses
IF	Initial Fix
IFF	Identify Friend or Foe
IFG	Integrity Flag Generator
IFR	Instrument Flight Rule
ILF	Integrated LOWAS/FLS
ILS	Instrument Landing System
IMU	Inertial Measurement Unit
INS	Inertial Navigation System
IRNSS	Indian Regional Navigational Satellite System
IVHM	Integrated Vehicle Health Management
JAA	Joint Aviation Authorities
JAUS	Joint Architecture for Unmanned Systems
JTI	Joint Technological Initiative
LIDAR	Light Detection and Ranging
LNAV	Lateral Navigation
LoS	Line-of-Sight
LOWAS	Laser Obstacle Warning and Avoidance System
LLP	Low Level Processing
M	Mach number
MAC	Mid-Air Collision
MAG DEV	Magnetic Deviation

MASPS	Minimum Aviation System Performance Standard
MATS	Mobile Aircraft Tracking System
MCDP	Multi-Criteria Departure Procedure
MCDU	Multi-Function Control and Display Unit
MFD	Multi-Function Display
MIDCAS	Mid Air Collision Avoidance System
Mode A	ATC Transponder Mode signifying aircraft call sign
Mode C	ATC Transponder Mode signifying aircraft call sign and altitude
Mode S	ATC Transponder Mode signifying call sign, altitude and additional aircraft data
MOA	Military Operations Area
MOPS	Minimum Operational Performance Standards
MOUT	Military Operations in Urban Terrain
MS	Mode-Status
MSDF	Multi-Sensor Data Fusion
MSE	Mean Square Error
MSSR	Mono-pulse Secondary Surveillance Radar
MSR	Message Success Rate
MTOM	Maximum Take-Off Mass
NACp	Navigation Accuracy Category for Position
NACv	Navigation Accuracy Category for Velocity
NADP	Noise Abatement Departure Procedures
NAS	National Airspace System
NASA	National Aeronautics and Space Administration
NAVDB	Navigation Database
NCDC	National Climatic Data Center
ND	Navigation Display

NextGen	Next Generation Air Transport Management System (USA)
NFZ	No-Fly Zone
NG-FMS	Next Generation Flight Management System
NG-ATM	Next Generation Air Traffic Management
NG-ACS	Next Generation Aeronautical Communication System
NGS	Navigation and Guidance System
NIC	Navigation Integrity Category
NM	nautical mile
NMAC	Near Mid-Air Collisions
NLP	Non-Linear Programming
NOAA	National Oceanic and Atmospheric Administration
NSA	Noise Sensitive Area
NTD	Navigation and Tactical Display
OMD	Object Modifiable Databases
OP	Operational
OUSD	Office of the Under Secretary of Defense
OWS	Obstacle Warning System
PACT	Pilot Authority and Control
PAL	Programmable Array Logic
PLA	Programmable Logic Array
PBC	Performance-Based Communication
PBN	Performance-Based Navigation
PBO	Performance-Based Operations
PBS	Performance-Based Surveillance
PCFR	Persistent Contrail Formation Region
PERBDB	Performance Database

PF	Pilot Flying
PNF	Pilot Non-Flying
PFD	Primary Flight Display
PID	Proportional-Integral-Derivative
PMF	Point Mass Filter
PPI	Plan Position Indicator
PRNAV	Precision Area Navigation
PSR	Primary Surveillance Radar
PU	Processing Unit
PVA	Position, Velocity and Attitude
QZSS	Quasi-Zenith Satellite System
R&D	Research and Development
RA	Resolution Advisory
RADAR	Radio Detection And Ranging
RAM	Random Access Memory
RALT	Radio Altitude
RCP	Required Communication Performance
RDDT&E	Research, Development, Demonstration, Testing and Evaluation
RLoS	Radio Line-of-Sight
RNAV	area navigation
RNP	Required Navigation Performance
RNP APCH	RNP Approach
ROA	Range-of-Applicability
RoC	Risk-of-Collision
ROM	Read-Only Memory
RSP	Required Surveillance Performance

RVSM	Reduced Vertical Separation Minima
RTA	Required Time of Arrival
RTCA	Radio Technical Commission for Aeronautics
RWY TRK	Runway Track
RTSP	Required Total System Performance
SAF	Safety
SA&CA	Separation Assurance and Collision Avoidance
S&A	See-and-Avoid
SAA	Sense-And-Avoid
SAE	Society of Automotive Engineers
SARP	SAA Science and Research Panel
SAS	Stability Augmentation System
SESAR	Single European Sky ATM Research
SESAR JTI	SESAR Joint Technology Initiative
SBAS	Space-Based Augmentation System
SCM	Strategic Conflict Management
SDA	System Design Assurance
SHU	Sensor Head Unit
SID	Standard Instrument Departure
SIL	Source Integrity Level
SIS	Signal-in-Space
SL	Safety Line
SLR	Sideways-Looking Radar
SMC	Sequential Monte Carlo
SP	Separation Provision
SPKF	Sigma-Point Kalman Filter



SPO	Single Pilot Operations
SR-UKF	Square Root-UKF
SS	Self Separation
SSR	Secondary Surveillance Radar
SST	Self-Separation Threshold
SSV	Self-Separation Volume
SSVR	Surveillance State Vector
STANAG	NATO Standardization Agreement
STAR	Standard Terminal Arrival Route
SUA	Special User Area
SVR	Synthetic Voice Reply
SWaP	Size, Weight and Power
SWIM	System-Wide Information Management
TA	Traffic Advisory
TACAN	Tactical Air Navigation
TAWS	Terrain Avoidance Warning System
TBO	Trajectory-Based Operations
TC	Technical
TCA	Terminal Control Areas
TCAS	Traffic Collision Avoidance System
TDA	Tracking, Decision-Making and Avoidance
TDMA	Time Division Multiple Access
TE	Test and Evaluation
TIO	Tailored Input/Output
TIS-B	Traffic Information Service – Broadcast
TMA	Terminal Manoeuvring Area

TOGA	Take Off/Go Around
UAV	Unmanned Aerial Vehicles
UAS	Unmanned Aerial Systems
UKF	Unscented Kalman Filter
URSV	Unmanned Reusable Space Vehicle
UTM	UAS Traffic Management
UTMS	UTM System
V2V	Vehicle-to-Vehicle
V2I	Vehicle-to-Infrastructure
VBN	Vision-Based Navigation
VHF	Very High Frequency
VIGA	VBN-IMU-GNSS-ADM
VOR	VHF Omni-directional Ranging radio
VNAV	Vertical Navigation
VS	Vertical Speed
VTOL	Vertical Take-Off and Landing
WAM	Wide-Area Multilateration
WCET	Worst Case Execution Time
WGN	White Gaussian Noise
WGS	World Geodetic System
WIF	Warning Integrity Flag
WN	White Noise
WP	Waypoint
W&P	Wires & Poles

This page is intentionally left blank to support presswork tasks

This page is intentionally left blank to support presswork tasks

# CHAPTER 1

## INTRODUCTION

*"Innovation is hard. It really is. Because most people do not get it. Remember, the automobile, the airplane, the telephone, these were all considered toys at their introduction because they had no constituency. They were too new". -*  
Nolan Bushnell

### 1.1 Research Context and Motivation

Scientific advances in microelectronics, sensing technologies, data fusion techniques and automation are driving the design and development of high-performance and reliable avionics systems for manned and unmanned aircraft operations. The proliferation of avionics systems has been significant in both civil and military aviation. It is to be noted that civil avionics systems account for 35-40 % of the total aircraft cost while more than 50 % of the total cost in Research & Development (R&D) of military aircraft is spent on avionics systems [1]. Global and regional air traffic is growing at a rapid pace and it is predicted that current air passenger traffic will double in the next 15 years [2]. Therefore, R&D efforts in aviation are now focussing on the introduction of novel systems that enhance safety, cost-effectiveness and operational efficiency as well as address the environmental sustainability aspects of the air transportation system. Accordingly, a number of large-scale and regional research initiatives are addressing the avionics and Air Traffic Management (ATM) modernisation challenges [3, 4]. The prominent programmes in Europe include Single European Sky Air Traffic Management Research (SESAR) and the Clean Sky Joint Technological Initiative (JTI) for Aeronautics and Air Transport. These two programmes are defining future air transportation in Europe by addressing the challenges and benefits of increased air traffic growth [5 - 8]. The Advisory Council for Aviation Research and Innovation in Europe (ACARE) has set an ambitious target aiming to address the environmental sustainability of aviation in its Strategic Research Agenda [9, 10]. Across the Atlantic Ocean, the Next Generation Air Transportation System (NextGen) and National Aeronautics and Space Administration

(NASA) Environmentally Responsible Aviation (ERA) programmes are the major research initiatives leading the transformation efforts in the USA [11, 12]. Under the Airspace Operations and Safety Program (AOSP), NextGen technologies are developed to further improve the safety of current and future aircraft in collaboration with the Federal Aviation Administration (FAA), industry and academic partners. Specific projects include Airspace Technology Demonstrations (ATD), Shadow Mode Assessment Using Realistic Technologies for the National Airspace System (SMART-NAS) for Safe Trajectory Based Ops (TBO) and Safe Autonomous Systems Operations (SASO). Other programmes worldwide include OneSKY in Australia, Collaborative Action for Renovation of Air Traffic Systems (CARATS) in Japan, SIRIUS in Brazil and the Future Indian Air Navigation System (FIANS) [13]. The International Civil Aviation Organization (ICAO) in its Global Air Navigation Capacity and Efficiency Plan (Doc 9750) has identified the following four key overarching performance improvement areas [14]:

- Efficient flight path;
- Optimum capacity and flexible flights;
- Airport operations;
- Globally interoperable systems and data.

The requirements set by the modernisation programmes largely provide the design drivers for avionics and ATM system developers, who are faced with the following key challenges:

- Improving safety;
- Improving efficiency;
- Providing cost-effective solutions;
- Increasing demand-capacity balancing;
- Improving environmental sustainability of aviation.

The combined objectives are illustrated in Figure 1.1.

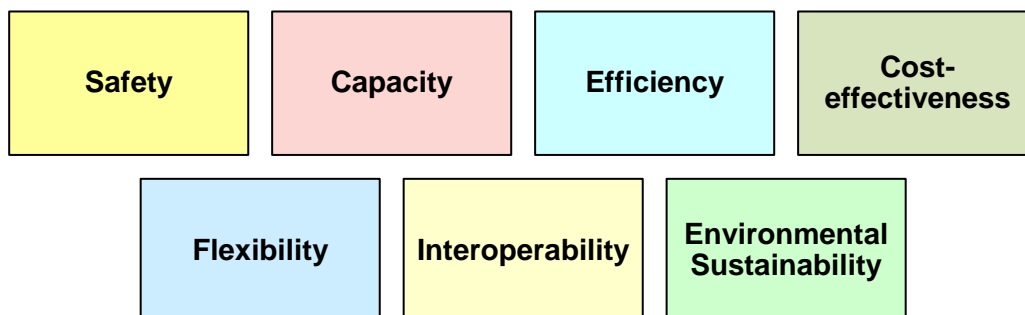


Figure 1.1. Combined objectives.

Scientific advances in Communication, Navigation, Surveillance/Air Traffic Management (CNS/ATM) and Avionics (CNS+A) systems are required to achieve the ambitious goals set by national and international aviation organisations. The CNS+A concept was first introduced by the ICAO Future Air Navigation Systems (FANS) committee and was later implemented by Boeing, Airbus and other original equipment manufacturers as FANS-1 and FANS-A products. The key CNS+A concepts are [13]:

- Four Dimensional (4D) Trajectory/Intent-Based Operations (TBO/IBO);
- Performance-Based Communication, Navigation, Surveillance (PBC/PBN/PBS), supporting Performance-Based Operations (PBO);
- TBO/IBO facilitated by System Wide Information Management (SWIM);
- Enhanced ground-based and satellite-based surveillance, including Automatic Dependent Surveillance (ADS) and automated self-separation;
- Improved Human Machine Interface and Interactions (HMI<sup>2</sup>), interoperability for airborne and ground interfaces and increased levels of automation;
- Enhanced Line-of-Sight (LoS) and Beyond Line-of-Sight (BLoS) aeronautical communications, involving a substantial exploitation of data-links;
- Collaborative Decision Making (CDM) to allow all stakeholders involved in flight planning and management to participate in the enhancement of system performance by utilising more accurate information from airborne systems;
- Air Traffic Flow Management (ATFM) and Dynamic Airspace Management (DAM).

These CNS+A concepts enable more accurate estimation of CNS performance and involve higher levels of automation. It is to be emphasised that in recent years, Unmanned Aircraft Systems (UAS) are being extensively employed in a variety of civil and military applications as these vehicles provide cost-effective and safe alternatives to manned aircraft in a wide range of operational scenarios. UAS offer a safer and cost-effective alternative to manned aircraft in dangerous, sensitive and/or dull tasks because of the absence of a pilot on board the aircraft. These distinctive abilities of UAS are a result of adopting a number of enabling CNS+A concepts and technologies in a phased manner and the widespread availability of a number of diverse airborne sensors and systems. Accurate and fail-safe algorithms for navigation, guidance and effective control of the platform are required to accomplish such missions. Currently, UAS can only operate in segregated airspace, where collision risks are largely eliminated by preventing or strictly controlling entry into this class of airspace by other aircraft. In order to address the challenges of integrating UAS in all classes of airspace, and in existing

ATM and future UAS Traffic Management (UTM) systems, the required levels of safety and operational regulations need to be determined. Recent research shows that small UAS could pose less risk to life and inanimate objects on the ground when compared with manned aircraft [15]. The long term vision of the aviation community is to achieve coordinated manned and unmanned aircraft operations in all classes of airspace. Initial steps have been taken in this regard by the launch of programmes such as NASA's Unmanned Traffic Management (UTM) initiative [16]. Some recommendations for research in the area of manned and unmanned aircraft coexistence in all classes of airspace and aerodromes have been identified as part of the Aviation System Block Upgrades (ASBU) by the ICAO [17]. Due to the fact that there are no definitive standards available now, there are a number of groups and special committees working on UAS including ASTM F38, EUROCAE WG-73, ICAO UASSG and RTCA SC-228 [18 - 20]. Specifically, in the CNS+A context, the first recommendation addressing the operational and certification issues for civil UAS was issued by the Joint Aviation Authorities (JAA) CNS/ATM Steering Group [19]. Some key recommendations include the development of innovative methods and algorithms for dynamic allocation of airspace resources as well as the introduction of CNS+A technologies enabling unrestricted access of UAS to all classes of airspace. Subsequently, the EUROCAE Working Group (WG-73) endeavours to address:

- UAS operations and collision avoidance functions;
- Command, control, communication, spectrum and security issues;
- Airworthiness and continued airworthiness.

The architectures, interfaces, communication protocols, data elements and message formats for operation of UAS are defined in the NATO Standardisation Agreement (STANAG) 4586 [21]. In terms of general applicability, the Joint Architecture for Unmanned Systems (JAUS) provides a better perspective than STAGNAG 4586. The JAUS standard Domain Model (DM) and a reference architecture provide mechanisms for UAS interoperability including integration into the airspace, architecture framework, message formats and a set of standard messages [22]. UAS support is one of the key performance improvement areas identified by the ICAO for ASBU [17]. In the TBO context, the following are included:

- Initial integration of UAS into non-segregated airspace: implementation of basic procedures and functions including Sense-and-Avoid (SAA) for operating UAS;
- UAS integration in traffic: implementation of defined procedures addressing lost link as well as enhanced SAA functions;



- UAS transport management: implementation of UAS operations on the airport surface and in non-segregated airspace similar to manned aircraft.

The integration of UAS into the non-segregated airspace requires recommendations from committees for standardisation (RTCA SC-203, ASTM F 38, EUROCAE WG 73, and others), which aim to develop the Minimum Aviation System Performance Standards (MASPS). In this perspective, the key CNS+A systems/elements are:

- LoS and BLoS communication systems;
- High-integrity airborne and ground-based UAS navigation systems and integrated fail-safe avionics architectures;
- The adoption of fused cooperative/non-cooperative surveillance systems incorporating collision avoidance and collaborative conflict resolution capabilities in a network centric operational scenario;
- Provision and integration of Separation Assurance and Collision Avoidance (SA&CA) capabilities in the Next Generation Flight Management System (NG-FMS);
- Interactions between Guidance, Navigation and Control (GNC) and Track, Decision-Making and Avoidance (TDA) loops.

Other issues that are addressed for a safe integration of the UAS in the airspace include the definition of automation functions and standards for Human-In-The-Loop (HITL) interactions, operational contingency procedures and certification processes. Additionally, the air safety nets that can be used as a last resort necessity have to be clearly defined for all UAS types to address the emergency scenarios rising in a CNS+A context. Cooperative and non-cooperative SA&CA performance-based requirements are currently developed in a research context and need to be accepted into a regulatory framework in order to support the UAS operational improvements [23, 24]. The initial integration of UAS requires capabilities including ground-based SAA systems and the adoption of a combination of policies, procedures, and technologies intended to facilitate safe airspace access. The SAA technology will be integrated in the flight management system of the UAS to meet collision and hazard avoidance responsibility and to provide situational awareness. UAS integration in traffic requires the development of on board SA&CA algorithms, which must be able to fulfil the requirements for detecting and successfully resolving any mid-air collisions in non-segregated airspace for both cooperative and non-cooperative targets [23, 24]. In particular, this technology enabler will cope with both air and ground obstacles of various characteristics (natural and man-made) including long and thin structures such as electrical cables, poles and

aerial obstacles such as other UAS and manned aircraft. Significant impacts are also expected in the areas of SAA airworthiness and design standard evolutions. The UAS research community is working on a number of SA&CA algorithms to replicate and even to provide a higher level of performance of the see-and-avoid (S&A) capability of humans. Despite a huge number of efforts that have been devoted to the integration of UAS in non-segregated airspace, the standards as well as a certification framework for SA&CA has yet to be established. Furthermore, the maturity of SA&CA techniques and enabling technologies is considered very limited when viewed in the perspective of civil airworthiness regulations for manned aircraft, raising concerns to certification authorities and airspace users [25, 26]. Furthermore, large amounts of established reliability data are not available as in the case of civil aviation. The separation assurance function is not addressed in conjunction with the collision avoidance problem. A unified approach to SA&CA for manned and unmanned aircraft is required to meet the challenges of UAS integration and to provide a pathway to certification. One of the key technology enablers to achieve this goal is the implementation of suitable hardware components and data fusion techniques for cooperative and non-cooperative SA&CA tasks. Such functions will provide manned and unmanned aircraft the capability to consistently and reliably perform equally or even to exceed the see-and-avoid performance while allowing a seamless integration of unmanned aircraft in the ATM and UTM network. In a typical operational scenario, the host aircraft (manned/unmanned) would have to ensure the required separation (horizontal and vertical) is maintained with other traffic and also have to see/sense in advance any potential conflicts and avoid them. The host aircraft and other traffic are conventionally equipped with a different set of non-cooperative sensors and cooperative systems as shown in Figure 1.2.

Automated SA&CA tasks have to be carried out to ensure safety and in order to allow the exploitation of the enhanced CNS+A concepts and capabilities, new ground-based and airborne CNS+A systems have to be designed and developed. The key technology enablers are novel CNS technologies onboard the aircraft (manned and unmanned) and CDM based ground systems. These CNS+A systems include:

- Modern avionics and ground-based systems for planning and real-time execution of 4-Dimensional Trajectory (4DT) functionalities, including multi-objective 4D trajectory optimisation, negotiation and validation in the TBO/IBO context. These include the airborne component - NG-FMS and the ground component - Next Generation ATM (NG-ATM) system;
- Network-centric systems for strategic, tactical and emergency scenarios;

- Enhanced ground-to-ground, air-to-ground and ground-to-air communication systems;
- Avionics, Ground and Satellite Based Augmentation Systems (ABAS/ GBAS/SBAS) enabling multi-constellation Global Navigation Satellite System (GNSS) as primary means of navigation;
- Enhanced ground-based and satellite-based surveillance including the exploitation of non-cooperative sensors and cooperative systems supporting automated SA&CA functions;
- High-integrity, high-throughput, secure and reliable Next Generation Aeronautical Communication System (NG-ACS) networking all the CDM stakeholders;
- CNS+A systems for UAS, targeting coordinated operation of manned and unmanned aircraft;
- Systems that satisfy the Required Navigation Performance (RNP), the Required Communication Performance (RCP), the Required Surveillance Performance (RSP) and ultimately the Required Total System Performance (RTSP).

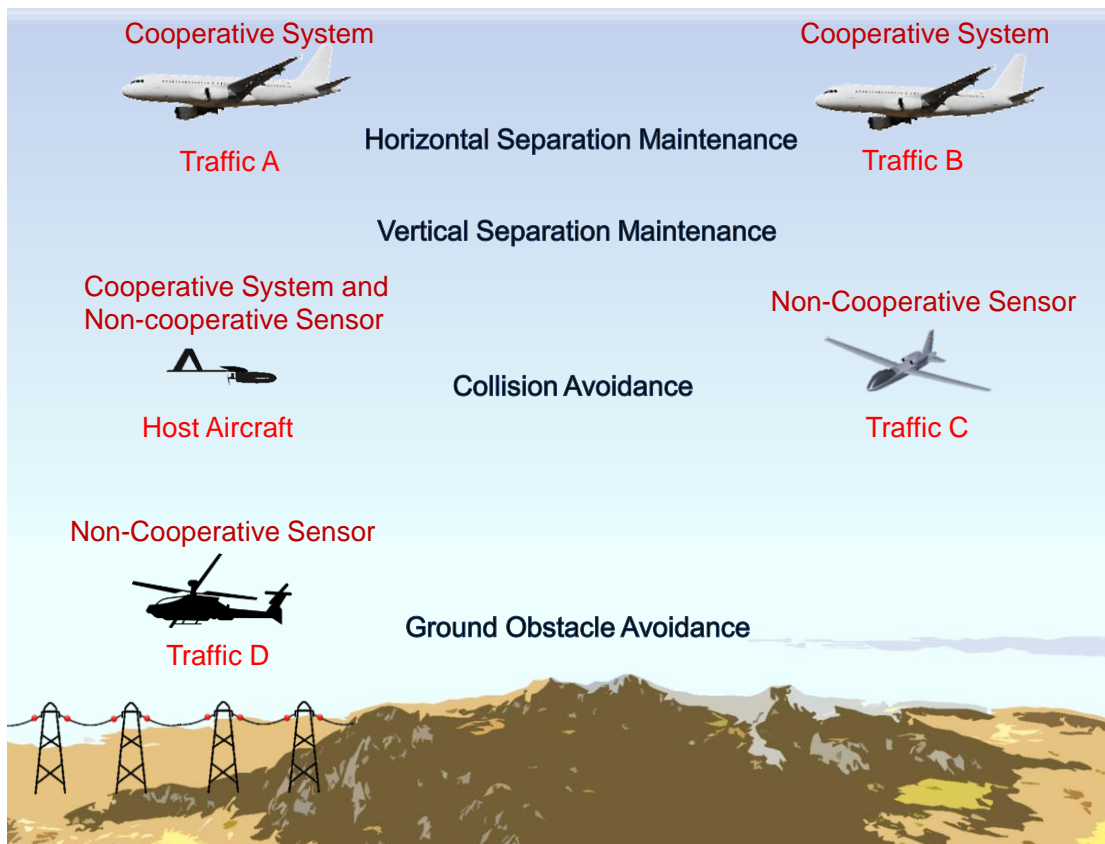


Figure 1.2. Automated SA&CA tasks.

The CNS systems provide better and more precise airborne navigation services, optimal collision avoidance and separation assurance, as well as secure and reliable communication links.

## 1.2 Research Gap Identification

State-of-the-art aircraft are equipped with FMS, which provide automated navigation and guidance services that are largely restricted to the use of 3D trajectories. Time is not used as a control variable, although setting Required Time of Arrival (RTA) and Estimated Time of Arrival (ETA) at en-route waypoints and at the destination respectively provide some initial implementations of time based operations. Hence a NG-FMS is required for the full implementation of TBO/IBO.

On the other hand, one of the key challenges for the aviation community is to introduce the SA&CA capability for manned and unmanned aircraft. It is also timely that a solid mathematical framework be used for certifying the SA&CA. The maturity of the available SA&CA techniques and enabling technologies is considered very limited when viewed in the perspective of civil airworthiness regulations for manned aircraft, raising concerns to certification authorities and airspace users. With the growing adoption of UAS for a number of civil, commercial and scientific applications there is a need to certify SA&CA systems according to established national and international standards.

## 1.3 Research Questions

This thesis addresses the challenges of introducing novel software algorithms in flight management system (specifically separation maintenance and collision avoidance automation functionalities for manned and unmanned aircraft) and answers the following key research questions:

- How are innovative analytical models adapted within the trajectory-based operations context?
- How is a unified approach to cooperative and non-cooperative separation assurance and collision avoidance realised for manned and unmanned aircraft?
- How is the safety and efficiency of aircraft operations improved by the introduction of automated separation assurance and collision avoidance algorithms?
- How are the automated separation assurance and collision avoidance tasks affected by the performance of onboard navigation and tracking sensors?

## 1.4 Research Aim

This research endeavours to develop and implement novel mathematical algorithms for automated SA&CA tasks. Within this framework, the key aim is to develop a unified methodology for cooperative and non-cooperative SA&CA.

The aim of this research work is:

*To develop novel mathematical models (software functionalities) for manned and unmanned aircraft NG-FMS primarily focussed on improving safety and efficiency by providing automated SA&CA functions.*

## 1.5 Research Objectives

The following objectives were identified:

- Perform a detailed review of the existing literature on modern FMS focussing on GNC and TDA functions;
- Define the system level functional architecture of a NG-FMS suitable for manned and unmanned aircraft operations;
- Adapt suitable NG-FMS models and algorithms for on board planning and optimisation of four dimensional trajectories to support TBO/IBO in the CNS+A context;
- Perform simulation case studies to test the validity of the NG-FMS models and algorithms for safe and efficient operations;
- Develop the mathematical models required to introduce a novel unified approach to cooperative and non-cooperative SA&CA for manned and unmanned aircraft;
- Evaluate the mathematical models introduced for SA&CA in representative simulation case studies (multiple manned and unmanned aircraft operations);
- Define possible pathways for certification of SA&CA functions, allowing safe and unrestricted operations of manned and unmanned aircraft in the future UTM context.

## 1.6 Research Methodology

The methodology followed in this work is presented below:

In the first phase, a comprehensive review of all existing work in the flight management system functionalities, challenges of UAS integration into all classes of airspace and SA&CA algorithms was undertaken.

In the second phase, novel mathematical models were developed to determine the overall uncertainty volume in the airspace. These models were then evaluated to test for fitness of use. The design and development of NG-FMS (including identification of optimal system architecture and algorithms required for TBO/IBO) was carried out. Furthermore, a performance analysis was carried out to investigate and explore the potential of the unified approach to cooperative and non-cooperative SA&CA for manned and unmanned aircraft.

In the third phase, modelling and simulation activities were performed to validate the NG-FMS algorithms for 4D trajectory optimisation and SA&CA tasks.

The research methodology adopted is summarised as follows:

- NG-FMS requirements definition;
- Conceptual design and development of the NG-FMS implementing dedicated functions for manned and unmanned aircraft operations:
  - NG-FMS conceptual design;
  - Development of tailored algorithms for 4D trajectory optimisation supporting TBO/IBO;
  - Implementation of near real-time 4DT estimation, negotiation and validation functions, in synergy with ATM Decision Support Systems (DSS) for TBO/IBO;
  - Mathematical modelling and implementation of a unified approach for cooperative and non-cooperative SA&CA functions;
  - Tailoring of tracking and avoidance algorithms for implementing the unified approach to separation maintenance and collision avoidance for non-cooperative and cooperative scenarios;
- Verification of the NG-FMS functions by performing modelling and simulation activities. The application case studies are in a MATLAB/Simulink simulation environment. Case studies that are representative of typical manned/unmanned aircraft operational flight envelope were also considered. Additionally, the facilities available at the THALES Australia Centre for Advanced Studies in ATM (CASiA) including TopSky - ATM solutions and at the RMIT University avionics and ATM system laboratory were utilised to verify some of the software functionalities.

## 1.7 Thesis Outline

This section provides a general outline of the successive chapters of this thesis. In chapter 2, the theoretical background and algorithms of the GNC and TDA loops are presented. The chapter starts with an introduction to state-of-the-art FMS and its functions. The chapter then goes on to describe the SA&CA algorithms currently employed. Some theoretical description of various multi-sensor data fusion techniques used for tracking in the context of SA&CA are also described. The chapter also presents some general considerations on SA&CA requirements in terms of available information, functions, implementation and regulatory issues.

Chapter 3 provides the general design principles of NG-FMS. More specifically, it provides an overview of system requirements, functions and implementation of NG-FMS for manned and unmanned aircraft. Furthermore, the navigation, guidance and performance management algorithms employed in NG-FMS are also described. The general architecture of the simulation environment integrating the developed NG-FMS system and the NG-ATM system is then summarised.

The unified approach to cooperative and non-cooperative SA&CA is described in Chapter 4. The mathematical models required for the unified approach are then documented in this chapter. Furthermore, the automated separation maintenance and collision avoidance functions of NG-FMS are discussed in this context.

Performance analysis of navigation and surveillance sensor/system errors is presented in Chapter 5. Covariance analysis and other statistical methods employed for determination of navigation and tracking errors are described in detail. Some description of assumptions and of the solutions used for conflict detection, resolution evaluation and autonomous avoidance trajectory generation are also presented. Pathways to certifying avionics systems that provide SA&CA functionalities in manned and unmanned systems are also described. Appendix A provides a summary of multi-sensor data fusion techniques implemented for UAS integrated navigation systems. Appendix B provides a compilation of the certification standards, Acceptable Means of Compliance (AMC), Guidance Materials (GM) and recommended practices.

Chapters 6 and 7 include the various case studies performed for evaluating the unified approach in both cooperative and non-cooperative scenarios. The sensor modelling techniques and assumptions used to choose various scenarios are spelled out. Key aspects of the Human Machine Interface and Interaction (HMI<sup>2</sup>) design based on the presented case studies are summarised in Appendix C.

Chapter 8 provides an overview of the methodology to apply the unified approach to SA&CA in an UTM context. Preliminary simulation case studies are also presented for validation of the presented SA&CA algorithms in the UTM framework.

Finally chapter 9 ends with conclusions drawn from this work. Recommendations for future research work are also presented. A list of relevant publications developed based on the work carried out during this PhD research is provided in Appendix D.

## 1.8 References

1. P. Bieber, F. Boniol, M. Boyer, E. Noulard and C. Pagetti, "New Challenges for Future Avionic Architectures", Aerospace Lab Journal, Issue 4, May 2012.
2. Airbus, "Future Journeys, 2013-2032", Global Market Forecast, 2013. Downloadable from:  
[http://www.airbus.com/company/market/forecast/?eID=dam\\_frontend\\_push&docID=33752](http://www.airbus.com/company/market/forecast/?eID=dam_frontend_push&docID=33752)
3. C. Haissig, "Air Traffic Management Modernization: Promise and Challenges", Encyclopedia of Systems and Control, pp. 28-33, 2015.
4. M.T. DeGarmo, "Issues Concerning Integration of Unmanned Aerial Vehicles in Civil Airspace", MITRE, 2004.
5. SESAR JU, "European ATM Master Plan", Edition 2, Brussels, Belgium, 2012.
6. SESAR JU, "SESAR Consortium - Modernising the European Sky", Brussels, Belgium, 2011.
7. SESAR JU, "SESAR Content Integration Team", SESAR ATM Target Concept, Brussels, Belgium, 2007.
8. Clean Sky JTI, Accessible at: [www.cleansky.eu](http://www.cleansky.eu)
9. Advisory Council for Aviation Research and Innovation in Europe (ACARE), "Strategic Research Agenda, Volume 2", 2004. Downloadable from:  
<http://www.acare4europe.org/sites/academy4europe.org/files/document/ASD-Annex-final-211004-out-asd.pdf>
10. Advisory Council for Aviation Research and Innovation in Europe (ACARE), "Strategic Research & Innovation Agenda (SRIA)", Volume 1, 2012. Downloadable from:  
<http://www.acare4europe.org/sites/academy4europe.org/files/attachment/SRIA%20Volume%201.pdf>
11. FAA, "Avionics Roadmap, Version 2.0", Federal Aviation Authority, Washington, September 2011.
12. Federal Aviation Administration (FAA), "NextGen Implementation Plan", Washington DC, USA, 2011.



13. R. Sabatini, A. Gardi, S. Ramasamy, T. Kistan and M. Marino, "Modern Avionics and ATM Systems for Green Operations", Encyclopedia of Aerospace Engineering, eds. R. Blockley and W. Shyy, John Wiley: Chichester, 2015. DOI: [10.1002/9780470686652.eae1064](https://doi.org/10.1002/9780470686652.eae1064)
14. ICAO, "Global Navigation Plan, 2013-2028", Doc 9750-AN/963, Capacity and Efficiency, Fourth Edition, 2013.
15. R. Melnyk, D. Schrage, V. Volovoi and H. Jimenez, "A Third-Party Casualty Risk Model for Unmanned Aircraft System Operations", Reliability Engineering & System Safety, Vol. 124, pp. 105-116, 2014.
16. P.H. Kopardekar, "Unmanned Aerial System (UAS) Traffic Management (UTM): Enabling Low-Altitude Airspace and UAS Operations", NASA Technical Report, 2014.
17. The International Civil Aviation Organization (ICAO), Working Document for the Aviation System Block Upgrades - The Framework for Global Harmonization, Montreal, Canada, 2013.
18. JAA, UAV TASK-FORCE, Final Report - A Concept for European Regulations for Civil Unmanned Aerial Vehicles (UAVs), 2004.
19. G. Amato, EUROCAE WG-73 on Unmanned Aircraft Systems, ed: EUROCAE.
20. L. Cary, "International Regulatory Framework for Remotely Piloted Aircraft Systems", ICAO Representative, Remotely Piloted Aircraft Systems (RPAS) Conference, Paris, France, 2012.
21. J.T. Platts, M.L. Cummings and R.J. Kerr, "Applicability of STANAG 4586 to Future Unmanned Aerial Vehicles", AIAA Infotech@ Aerospace Conference, Rohnert Park, California, USA, 2007.
22. A. Oztekinmet and R. Wever, "Development of a Regulatory Safety Baseline for UAS Sense and Avoid", Handbook of Unmanned Aerial Vehicles, pp. 1817-1839, Springer Verlag, Netherlands, 2015.
23. S. Ramasamy, R. Sabatini and A. Gardi, "A Unified Approach to Separation Assurance and Collision Avoidance for Flight Management Systems", Proceedings of the 35<sup>th</sup> AIAA/IEEE Digital Avionics Systems Conference (DASC2016), Sacramento, CA, USA, September 2016.
24. S. Ramasamy, R. Sabatini and A. Gardi, "Avionics Sensor Fusion for Small Size Unmanned Aircraft Sense-and-Avoid", IEEE Workshop on Metrology for Aerospace, pp. 271-276, Benevento, Italy, May 2014. DOI: [10.1109/MetroAeroSpace.2014.6865933](https://doi.org/10.1109/MetroAeroSpace.2014.6865933)
25. K. Dalamagkidis, K.P. Valavanis and L.A. Pieggl, "On Unmanned Aircraft Systems Issues, Challenges and Operational Restrictions Preventing Integration into the National

Airspace System", Progress in Aerospace Sciences, Elsevier, vol. 44, issue 7, pp. 503-519, 2008. DOI: [10.1016/j.paerosci.2008.08.001](https://doi.org/10.1016/j.paerosci.2008.08.001)

26. K.D. Davis and S.P. Cook, "Achieving Sense and Avoid for Unmanned Aircraft Systems: Assessing the Gaps for Science and Research", Handbook of Unmanned Aerial Vehicles, pp. 1841-1855, Springer Netherlands, 2015.

# CHAPTER 2

## LITERATURE REVIEW

*"The first rule of any technology used in a business is that automation applied to an efficient operation will magnify the efficiency. The second is that automation applied to an inefficient operation will magnify the inefficiency". - Bill Gates*

### 2.1 Introduction

This chapter presents the system architecture and algorithms employed in FMS. The two key avionics system loops required to provide automated guidance, as well as SA&CA functionalities are described in this chapter. A background on the currently available SA&CA algorithms is presented. The chapter also provides a background of the role of SA&CA in the modern ATM and UTM systems, describes the development process of SA&CA functions, provides a review of the Conflict Detection and Resolution (CD&R) algorithms and presents the case for introducing a unified approach to SA&CA within modern avionics systems for manned and unmanned aircraft. A theoretical summary of various multi-sensor data fusion techniques tailored for accomplishing an effective SA&CA is also presented.

### 2.2 Avionics and ATM System Modernisation

The present day ATM system originated as a result of a mid-air collision over the Grand Canyon (US) in 1956. It is essential to modernise the existing infrastructure (air and ground) to attain substantial benefits in safety, efficiency and environmental sustainability of aviation, and to ensure optimal demand-capacity balancing [1]. The limited capacity of the ground infrastructure has to be increased by introducing dynamic capacity-demand balancing to cope with growing air traffic [2]. The European and U.S. airspace are good examples for this development. There are generally two categories of airspace namely regulatory and non-regulatory. Within these two categories, there may be controlled, uncontrolled, special use, and other airspace. With a share of 65% in worldwide air traffic, the world's busiest airspace areas and capacity

problems have been experienced in the past in both of these areas [3]. The lessons learned from the traffic situations in these areas are becoming driving factors supporting the redesign of the existing ATM system. In the Australian context, by 2021, Airservices Australia is looking at providing air traffic control services using an advanced and integrated ATM system through collaboration with the Department of Defence. The plan is to unify the Australian skies under a new, harmonised ATM system under the OneSKY program to support integrated civil and military air traffic operations [4]. This will enable a new level of operational and cost efficiency and safety, while also reducing delays for the travelling public and providing opportunities to improve environmental outcomes. The benefits of a combined civil and military air traffic management system, delivered under the OneSKY Australia program, will include safety and efficiency improvements, as well as cost savings and reliability. The key features are:

- Improved safety and efficiency;
- One flight information region;
- Modular and adaptable systems;
- Greater use of four dimensional trajectories.

The International Civil Aviation Organisation (ICAO) global ATM operational concept defines a general framework for the ATM system operational concept. The concept foresees that the key conceptual change for traffic synchronisation will be the implementation of 4-Dimensional (4D) trajectory optimisation algorithms [5]. The trajectories are expected to be negotiated between the airborne and ground systems, and are targeted to be conflict-free. Regarding airspace user operations, the concept anticipates that individual aircraft performance, flight conditions and capacity-demand balancing will allow dynamically-optimised 4D trajectory planning, negotiation and validation. In the context of conflict management, the concept identifies a three-layered approach namely: Strategic Conflict Management (SCM), Separation Provision (SP) and CA.

SCM is considered to be achieved through airspace organisation and management and covers the earliest planning stage up to shortly pre-departure. ICAO uses the term strategic in this context, as opposed to tactical; because pre-flight phases do not possess the same real deadlines as flight short term CD&R. Though, especially for long-haul flights, strategic conflict management may also be applied after departure, depending on the best means to resolve a conflict. Strategic conflict management is comprised of:

- Airspace organisation and management;
- Demand and capacity balancing;
- Traffic synchronisation.

SP is the second layer of conflict management, which guarantees that aircraft are separated according to the applicable standards. According to ICAO, separation provision may be seen as an iterative process in which a conflict is detected, and then a resolution is identified and communicated to the conflicting entities. The execution of the resolution is monitored and, in case applicable minimum separation is not achieved, resolution manoeuvres are identified. ICAO defines the operator for separation management (separator) as the agent responsible for separation provision which can, depending on the separation mode, also be delegated to an aircraft. Several notions are defined in this context of conflict management including:

- Self-separation: the airspace user is responsible for separation in respect to one or more hazards;
- Distributed: different predetermined separators are defined for different hazards;
- Cooperative: role of separation is delegated temporarily until a termination condition sets in.

Hazards to which aircraft need to be separated from are classified as:

- Airborne:
  - Other aircraft;
  - Terrain;
  - Atmospheric constraints (weather, wake turbulence, etc.);
  - Restricted airspaces.
- Ground:
  - Vehicles operating in the airport (including other aircraft on the taxiway or runway);
  - Other obstructions while on the apron and manoeuvring area.

Common to both hazard situations is that for each hazard a separator needs to be responsible for separation provision. The authority is vested on air traffic service providers, governed by regulations and standards set out by international/national aviation authorities providing guidelines for enforcement rules, discrepancies, etc. Collision avoidance is essential in both layers, when strategic conflict management and separation provision have failed.

In addition to the need for implementing automated SA&CA functionalities for increasing safety, efficiency and demand-capacity balancing, there is also the requirement for supporting safe and widespread UAS operations. A system similar to an ATM system is envisaged to be implemented and it is foreseen that low-altitude UAS operations will occur in the same airspace where today's gliders, general aviation and helicopter operations occur [6]. Hence automated SA&CA functionalities are required to be implemented for safe and efficient manned/unmanned aircraft as well as multiplatform coordinated operations. These automated guidance and SA&CA functionalities can be implemented as software modules (mathematical models) in novel FMS onboard manned and unmanned aircraft, which is the focus of next section.

## 2.3 Flight Management Systems

Automated navigation and flight guidance functions on board modern aircraft are designed to guide the aircraft along a safe and efficient trajectory. The first modern FMS was introduced onboard the Boeing 767 in 1982 [7]. The original systems had 16-bit processors using bit-slice technology and removable memory cards with 128 KB of Random Access Memory (RAM), 128 KB of Read-Only Memory (ROM), clock rates of only 24 MHz. A dedicated hard drive provided 100 KB of non-volatile storage. State-of-the-art FMS are primarily responsible for providing automated navigation and guidance services from take-off to landing. The hardware components of modern FMS include the Multi Control Display Unit (MCDU) and FM dedicated processor. FMS of modern aircraft typically have a 64-bit Power PC micro-processor, 120 MB of RAM, 50 Mbytes of flash memory and a clock rate of 800 MHz. The FMS operates in close relation with the Automatic Flight Control System (AFCS). Flight plans are generated by the state-of-the-art FMS in coordination with the Airline Operation Centre (AOC) and Air Navigation Service Provider (ANSP). The modern FMS is hence an integrated set of avionics systems that provides the flight crew with the ability to operate an aircraft in compliance with the ANSP requirements in a manner that meets the expectations of the AOC. The flight path of an aircraft is represented in the FMS as lateral and vertical profiles over time. Typically, an FMS Flight Plan (FPLN) consists of lateral FPLN and vertical FPLN, which is in turn divided into a number of segments, sections and integral steps. Each segment is constructed based on a given set of local objectives with respect to the variables provided by the guidance component. The core of an FMS consists of one or more flight management computers/embedded processors and one or more Multifunction Control Display Units (MCDU). The software component embedded in the FMS processor performs the following functions [8, 9]:

- Positioning and navigation algorithms involving a number of multi-sensor data fusion techniques;
- Guidance computations in terms of lateral and vertical guidance algorithms;
- Trajectory generation and optimisation algorithms;
- Short-term and long-term performance computation algorithms;
- Dual and single FM mode (single and dual) protocols;
- Processing, sorting and selection of databases;
- Built-In-Test Equipment (BITE) and monitoring;
- Interface management.

A conceptual representation of a state-of-the-art FMS architecture is shown in Figure 2.1.

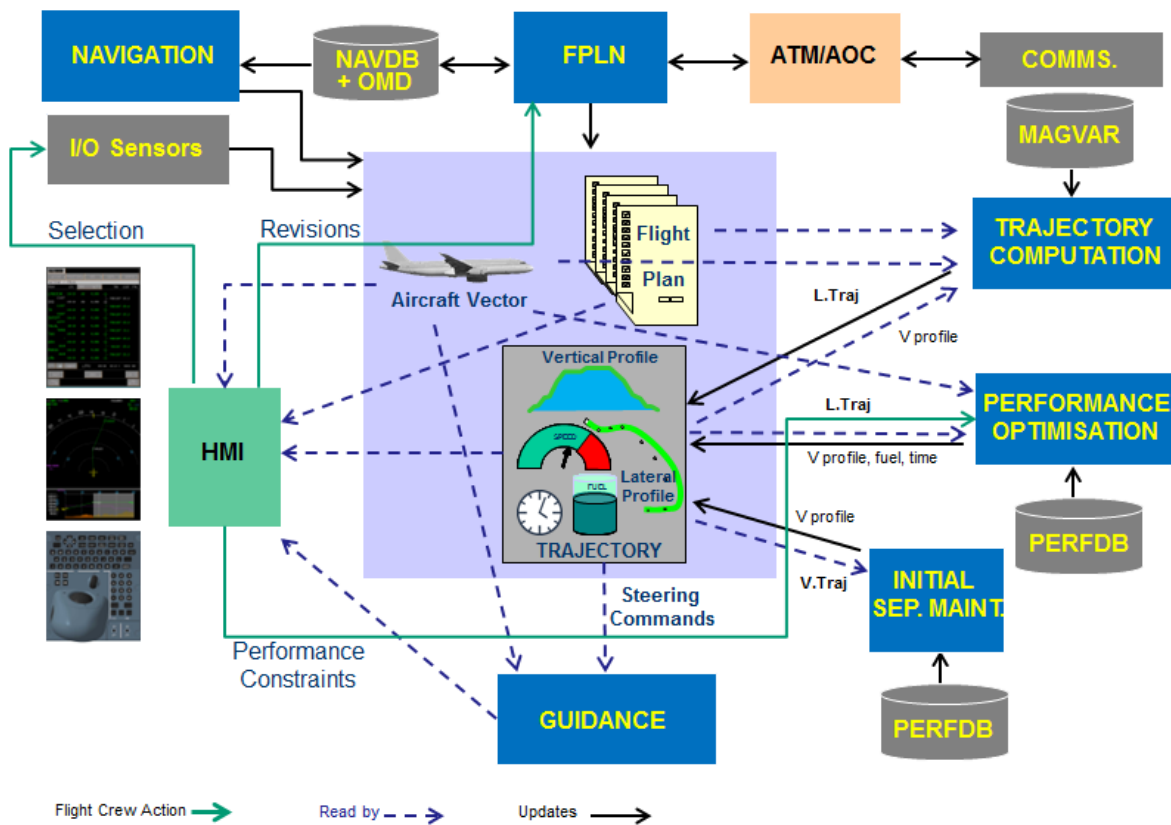


Figure 2.1. State-of-the-art FMS architecture.

The Primary Flight Display (PFD) and the Navigation Display (ND) are the most commonly used HMI<sup>2</sup> that provide display information to the crew. The lateral flight planning activity includes an initialisation FPLN and lateral revisions. The same concept applies to the vertical FPLN as well. The main navigation functions include [8]:

- Selection of navigation modes;
- Radio navigation functions including manual and auto selection;
- Inertial Reference System (IRS) initialisation and alignment;

- GNSS initialisation. These might include Global Positioning System (GPS), Galileo, GLObalnaya NAVigatsionnaya Sputnikovaya Sistema (GLONASS), BeiDou (or Compass), Indian Regional Navigational Satellite System (IRNSS), Quasi-Zenith Satellite System (QZSS) or a combination of the available constellations.

The traditional databases associated with FMS are Magnetic Deviation (MAG DEV), Performance Database (PERBDB) and Navigation Database (NAVDB). In addition to these databanks, weather, demographic distribution, digital terrain elevation, environmental and Object Modifiable Databases (OMD) can be introduced for TBO/IBO. The FMS navigation function is interfaced with the NAVDB, which is updated every 28 days as a pre-flight process, based on the ICAO's Aeronautical Information Regulation and Control (AIRAC) cycle. The NAVDB is structured to provide information on standard navigational aids, waypoints, holding patterns, and airport information. Airport data include information on terminal gates, runways, Standard Instrument Departure (SID), Standard Terminal Arrival Route (STAR) approaches and missed approach procedures. Uncertainty in the navigation performance requires large separation distances between aircraft to ensure safety. This is often considered as a technical constraint limiting the dynamic airspace allocation in the next generation ATM (SESAR/NExtGen) environment. Hence, performance-based navigation enabled by the introduction of satellite navigation systems (GNSS) are employed to improve the RNP in order to meet the requirements specified in RTCA DO-236B.

State-of-the-art FMS provides automated navigation functionalities for estimation of the aircraft's position using the World Geodetic System (WGS-84) system coordinates. The position of the aircraft is determined by using information from multiple navigation sensors including the Inertial Reference System (IRS), VHF Omnidirectional Range (VOR), Distance Measuring Equipment (DME), Instrument Landing System (ILS) and Microwave Landing System (MLS). With the development of satellite-based navigation systems, GNSS data are becoming the main source of navigation information in all flight phases. In addition, FMS sends radio tuning commands for VOR, DME and ILS sensors based on the radio frequencies retrieved from the navigation database [8, 9]. Turning of radio parameters (frequency, etc.), is performed either manually by the pilot, or automatically by the FMS by performing database management queries on the NAVDB. Engine parameters and aircraft configuration from the Mode Control Panel (MCP), throttle management and other pilot controls are provided to the thrust management module of the FMS. This module supports the generation of vertical flight guidance steering commands and provides engine-trim commands to the Full Authority Digital Engine



Control (FADEC) or other engine control units. The FMS thrust management function also offers the ability to control the throttle with minimum fuel consumption.

The vertical FPLN defines the speed, altitude and time constraints at each waypoint based on the lateral FPLN plan, temperature, atmospheric pressure, aircraft weight, wind conditions, aircraft performance (given by PERFDB), cost index and flight predictions (short and long term). The state-of-the-art FMS have advanced design features primarily employing an intuitive use of the system and thereby reducing significantly the crew workload. These functions are summarised in Table 2.1 [10].

The cost index varies among various airlines, routes and the selected FPLN. The cost index is used to compute the best trip cost, which evidently affects the speed (economical CAS/Mach speed) and altitude used in the vertical FPLN. Climbs are computed with a transition from constant Calibrated Air Speed (CAS) to constant Mach number assuming maximum climb thrust. Cruise segments are calculated at constant Mach number and descents are programmed with a transition (dictated by a transition altitude) from constant Mach number to constant CAS using idle thrust. The cost index is given by:

$$\text{Cost Index} = \frac{\text{Time Cost}}{\text{Fuel Cost}} \quad (2.1)$$

The cost index is dictated by the cost of fuel/kg, time cost per minute of flight (given by hourly maintenance cost, flight crew/cabin crew cost, depreciation/leasing cost) and time of flight. A lower cost index this value put more emphasis on reducing fuel flow. With a higher value the emphasis changes to high speed. The total cost is given by:

$$\text{Cost} = \text{Fuel Used} + \text{Cost Index} * \text{Time} \quad (2.2)$$

Each FMS manufacturer provides a different range of CI and predominately, this index varied from 0 to 99 or from 0 to 999.

Taking the Airbus A380 as a reference, the CI varies from 0 to 999 denoting maximum range and maximum time respectively. Furthermore additional CIs can be introduced such as long range cruise, maximum endurance and maximum range cruise. The conventionally used CI is often revised when deviations occur between the nominal flight plan and what is being actually flown, based on the aircraft dynamics and environmental/external conditions. Typical deviations are delayed departures at airports or errors in the predetermined en-route winds/weather conditions.

Table 2.1. State-of-the-art FMS functions.

CREW FUNCTIONS	<ul style="list-style-type: none"> <li>-Overfly a designated terrain point/waypoint/navigational aid</li> <li>-Add/Delete a WPT of the initial Flight Plan</li> <li>-Avoid a new reported Threat Zone</li> <li>-Change initial Assault Landing to an alternate destination</li> </ul>
CHARACTERISTICS	<ul style="list-style-type: none"> <li>Worldwide standard and users navigation databases</li> <li>-Standard navigation database (ARINC 424)</li> <li>-Standard databases for aircraft performance and magnetic deviation</li> <li>-Multi-sensor localization</li> <li>-Manual position updating</li> <li>-Position monitoring</li> </ul>
Predictions based upon modelled aircraft performances	<ul style="list-style-type: none"> <li>-Aircraft weight management</li> <li>-Flight phase parameters computation</li> <li>-Time and fuel prediction</li> <li>-Range/ Endurance computation</li> </ul>
Tactical features	<ul style="list-style-type: none"> <li>-Low Level Flight</li> <li>-Air dropping</li> <li>-Assault landing</li> </ul>
Lateral navigation	<ul style="list-style-type: none"> <li>-Active flight plan (all ARINC 424 leg types)</li> <li>-Temporary flight plan with multiple revisions</li> <li>-Secondary flight plan with chaining capability</li> <li>-SID, STAR, approach management</li> <li>-Holding patterns</li> <li>-Lateral offset</li> <li>-Overfly/fly by selection</li> <li>-Reverse route, Direct to -RTA management</li> <li>-Time/Altitude constraints management</li> </ul>
Vertical navigation	<ul style="list-style-type: none"> <li>-Multiple steps</li> </ul>
Digital Map	<p>Source Data Format:</p> <ul style="list-style-type: none"> <li>-Vector, raster and various picture formats</li> <li>-Matrix: Digital terrain elevation database</li> </ul> <p>Map Display Format:</p> <ul style="list-style-type: none"> <li>-2D/3D high resolution digital map generation</li> <li>-Combined elevation, raster and vector databases</li> <li>-Hypsometric and anti-collision display modes</li> <li>-Vertical profile</li> </ul>
Map Management through keyboard and cursor unit	<ul style="list-style-type: none"> <li>-Altitude point or zone</li> <li>-Zoom</li> <li>-Map reference point change</li> <li>-Decluttering</li> </ul>
Radio Management	<ul style="list-style-type: none"> <li>-VOR-DME-civil nav aids -VHF-ATC mode S</li> </ul>
Training and Mission Planning System (TMPS)	<ul style="list-style-type: none"> <li>-FMS training on PC-based environment</li> </ul> <p>Preparation and download of:</p> <ul style="list-style-type: none"> <li>-Navigation data base</li> <li>-Aircraft performance and magnetic deviation data base</li> <li>-Routes preparation and download</li> <li>-Communication plan</li> </ul>

Similarly to the way a strategic CI is adopted for a given flight, a dynamic tactical CI is often defined in a state-of-the-art FMS. For any given CI, flight legs are constructed according to DO-206. Accordingly, non-deterministic legs-such as course legs or legs ending at an unspecified position-are often avoided, since they could involve problems for air traffic separation and bring added complexity to the FMS path construction by being dependent on the aircraft performance [11 - 13]. DO-206 recommends the use of track legs with a specified terminator. In particular, the use of track legs is advantageous with respect to course legs, since they do not depend on wind conditions and avoid problems related to magnetic variation. Among the deterministic terminators, the most relevant are the Waypoints (WPs). In particular, the users can define the WP position on a horizontal plane in a variety of ways as summarised in Table 2.2 [13].

Typically, a WP constructed in FMS can be of two different types, according to the way by which the conjunction between the relative legs is flown (Figure 2.2):

- Fly-By (also named short turn): the WP is not overflown and the aircraft links the two legs with a turn;
- Fly-over (also named fly-through): the WP is overflown and then the aircraft returns on the leg.

Table 2.2. Waypoint categories.

WP category	Description
PBD	Polar coordinates (bearing and range) from another fix.
PB/PB	Intersection of bearings from two defined WPs.
ATO	Specified by an Along-Track Offset (ATO) from an existing flight path fix.
LAT/LON	WP is defined at the point an aircraft is entering a specified latitude or longitude.
LAT/LON crossing WP	WP is placed at the intersection of a specified point (LAT/LON) with the active FPLN.
Airways intersection	First point at which two given airways intersect. An airway is a defined route consisting of a number of waypoints.
Runway extension WP	WP is placed at a given distance from the runway threshold along the runway heading.
Abeam WP	Activation of DIRECT TO function. Abeam WPs are created at their abeam position on the DIRECT TO path.
FIR/SUA intersection WP	WP is placed at the cross between the active flight plan and the Flight Information Region (FIR) or Special User Areas (SUA) boundary.

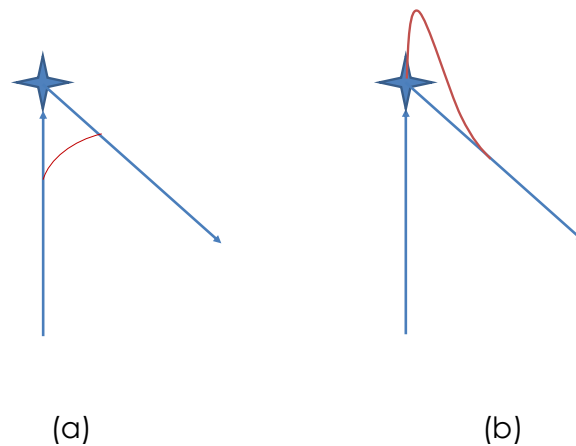


Figure 2.2. Waypoint types (a) fly-by and (b) fly-over.

RTCA DO-206 recommends the use of fly-by type WPs, since in most cases the next waypoint in the planned trajectory is not accurately predictable if there are any deviations [14]. The requirement to be levied on unmanned aircraft FMS is to prove the required levels of safety in the presence of anomalies such as unexpected traffic, on board failures, and conflicting data. This is essential because existing lateral and longitudinal autopilots in commercial aircraft (and business jets) can support flight in all flight phases but do not provide the capability for fully autonomous flight.

Automation is mostly considered rigid in the current implementation because the avionics system designers have largely preferred simplicity over adaptability in their strategies [15]. To operate efficiently in controlled airspaces and to realise coordinated operations of manned and unmanned aircraft, all aircraft are required to be equipped with a FMS that replicates current functionality, including precise following of the approved flight plan, a Communication, Navigation and Surveillance (CNS) system monitoring capability and Human Machine Interface and Interactions (HMI<sup>2</sup>) capability [16, 17]. The steering commands generated by the FMS are used to automatically follow the FPLN. Manoeuvres (given by ARINC 424 flight legs) are performed with respect to the change of one guidance mode to another [18]. In this case, the guidance of the aircraft is managed entirely by the FMS. In a selected mode, the pilot takes over the control of the flight guidance systems, imposing a different set of modes and guidance parameters. The selected mode is often used during take-off and landing phases. Other instances of employing a selected mode occur when alerts are raised from a path monitoring block, or when collision threats are provided. A conceptual representation of the FMS guidance loop is shown in Figure 2.3.

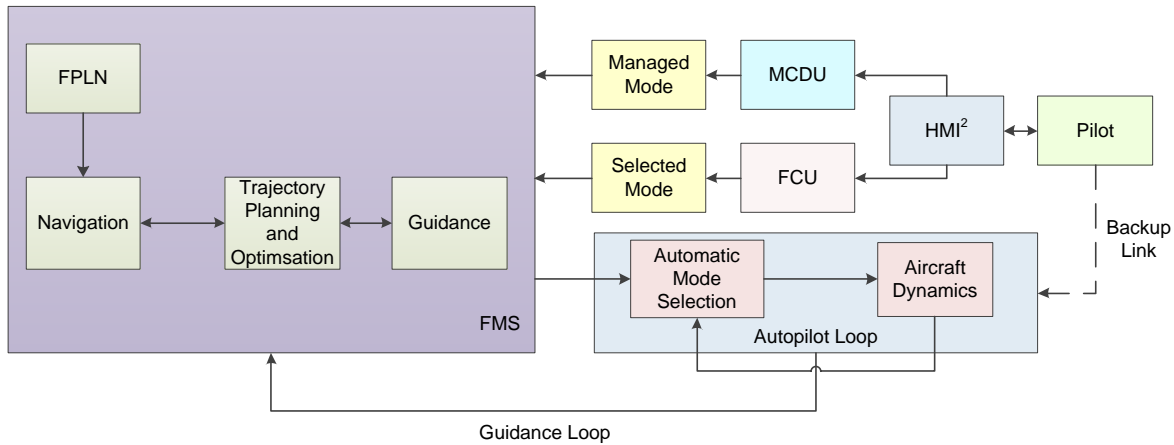


Figure 2.3. FMS guidance loop.

The guidance modes can be categorised into lateral and vertical guidance modes. The lateral mode is used to control the altitude of the aircraft by implementing algorithms for modifying and fine-tuning the roll angle. Similarly the vertical mode is used to control the perpendicular motion of the aircraft by implementing algorithms for modifying and fine-tuning the pitch angle. The typical lateral modes of operation are summarised in Tables 2.3.

Table 2.3. Lateral guidance modes [19].

Mode	Description
Runway (RWY) [MANAGED]	Activated after pilot sets thrust levers to FLX or Take Off/Go Around (TOGA). This mode is categorised into: RWY mode - Activated to maintain the runway middle. Runway Track (RWY TRK) mode - activated after take-off and passes 30 ft Radio Altitude (RALT).
Navigation (NAV) [MANAGED]	This mode is used for en-route navigation and non-precision approaches. It will capture and track the lateral guidance.
Approach (APPR) [MANAGED]	In the lateral guidance, this mode captures and tracks the lateral guidance for ILS localizer and VOR non-precision approaches. This mode is selected manually by pressing the Approach (APPR) button on the Flight Control Panel (FCP). First it will arm APP NAV mode. It is similar to NAV mode and guide the aircraft to a target flight path. If there is no Final approach Fixed (FAF) point defined in the flight plan before next airport, LOC mode is activated.
Go-Around (GA) [MANAGED]	GA TRK - This mode generates a command to track a heading reference. Only activated during a GA.
Heading Track (HDG-TRK) [SELECTED]	This mode generates a command to capture and maintain a selected heading reference. The heading reference can be adjusted by the pilot.
Roll Out [MANAGED]	This mode guides the aircraft along the runway following an automatic landing.

The speed (CAS/Mach) and thrust are controlled by the auto-throttle subsystem. In general, generic modes such as navigation, climb, etc. are typically managed modes while other modes including heading, altitude hold and speed hold can be either managed or selected modes. Vertical guidance modes (Table 2.4) are controlled by the Auto-Pilot and Flight Director (AP/FD). Then the Auto-Throttle (A/THR) controls the target Speed/Mach (SPD/MACH) and fixes thrust to react to the AP/FD mode selected.

Table 2.4. Vertical guidance modes [19].

Mode	Description
Speed Reference (SRS) [MANAGED]	It commands the aircraft pitch in order to maintain a speed target and guides the aircraft during take-off, initial climb and after a GA.
Climb (CLB) to Descent (DES)	<p>To change altitude, the auto-throttle commands constant thrust and aircraft pitch to maintain the aircraft speed. This mode is also known as the Pitch Mode. There are many types of these modes:</p> <p>OP CLB and OP DES [SELECTED]: Open climb or open descent such that aircraft reach an altitude without considering the altitude constraints.</p> <p>CLB and DES [MANAGED]: The aircraft will level off at an altitude constraint.</p> <p>EXP CLB and EXP DES [SELECTED]: Similar to OP CLB and OP DES but differs in the speed target the aircraft assumes.</p>
Altitude (ALT)	<p>The aircraft will maintain the pressure altitude. This mode has multiple modes depending on the circumstances.</p> <p>ALT [SELECTED] and ALT* [CAPTURE]. These modes are activated once the altitude target is reached and one of climb or descent mode is active or VS mode is active. ALT* mode is activated first, and once the aircraft reaches level-off the ALT mode engages.</p> <p>ALT CRZ [MANAGED]: Similar to the previous ALT mode except that the selected altitude must be at or above Cruise altitude define in MCDU.</p> <p>ALT CST [MANAGED] and ALT CST* [CAPTURE]: This mode considers the altitude constraint.</p>
Approach (APPR) [MANAGED]	Final Mode: Aircraft is guided along the vertical flight path as defined in the flight plan. If the flight plan contains no Non-precision part for the airport and ILS tuned-in, the glide slope mode is engages to capture the glide slope of the ILS.
Vertical Speed (VS) / Flight Path Angle (FPA) [SELECTED]	The aircraft will maintain the specified vertical speed (climb or descent) reference, defined by the vertical speed dial on the FCP or a Flight Path Angle. Once the altitude is read this mode will change to ALT.
FLARE [MANAGED]	The aircraft is aligned with runway centerline on yaw axis and flare on the pitch axis, such that the AP/FD commands a suitable pitch angle for the flare.

The interaction between the A/THR and AP/FD are based on the pitch mode controls. If the AP/FD pitch modes controls the vertical trajectory or the pitch mode is not engaged then the A/THR modes controls the target SPD/MCH. However if the pitch mode controls a target speed or Mach then the A/THR controls the thrust. Typical thrust control by the A/THR is during the climb and descent modes. All the vertical guidance modes can be initiated, and controlled by, managed or selected mode.

When designing flight guidance systems, it is also necessary to consider flight guidance protection to ensure safety. Flight guidance protection is a means to alert the flight crew when a hazardous situation is detected in the planned aircraft trajectory. Guidance protection laws programmed in the FMS depend on input data from Ground Proximity Warning System (GPWS), weather radar/wind shear alert systems and/or a Traffic Collision Avoidance System (TCAS) [20, 21]. The design of control laws and guidance laws are based on the adoption of a state representation approach of flight dynamics including trim conditions, pilot models and stabilisation augmentation given by:

$$\vec{u}(t) = -G \vec{x}(t) + H \vec{y}(t) \quad (2.3)$$

where  $\vec{u}$  is the control vector,  $\vec{x}$  is the state vector,  $\vec{y}$  is the output reference vector,  $G$  is the feedback gain matrix and  $H$  is the feed-forward gain matrix. The flight control laws depend on the flight guidance mode employed (selected or managed mode). The development of flight control laws is very intricate and it is a multi-disciplinary development process. The control laws need to be carefully designed in order to cope with the complexity of the control task itself. The interactions between FMS and Auto Flight Control System (AFCS) are illustrated in Figure 2.4.

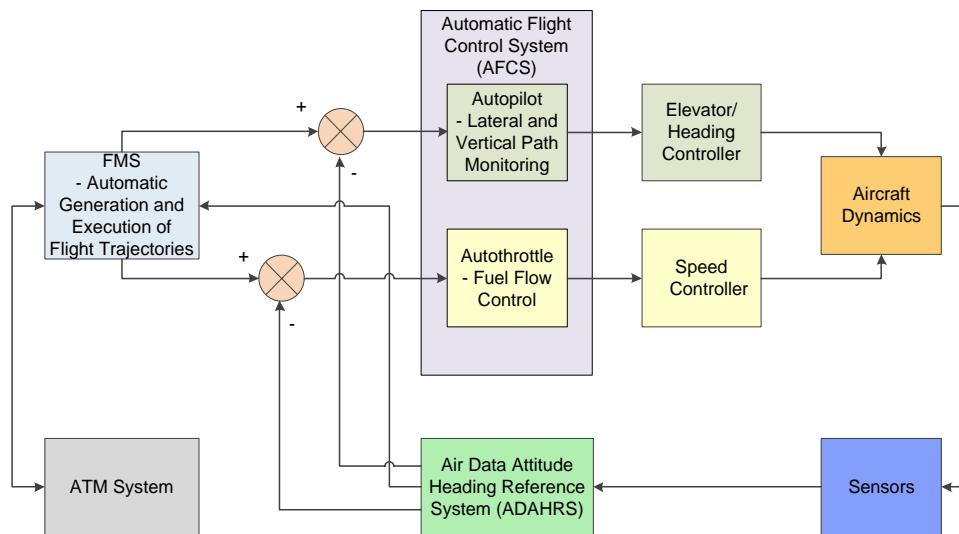


Figure 2.4. FMS and AFCS interactions.

A typical FCS consists of control surface actuators, motion sensors and controllers. Either the pilot or flight guidance system provides the reference inputs i.e., command signals. The actuators translate the command signals into control surface deflections, while motion sensors detect the changes in aircraft motion variables (linear / angular accelerations and velocities). If there is a difference between the commanded state and measured state, the controller generates command signals in accordance with the implemented control law such that the actual state is driven towards the desired state. The guidance system continuously monitors the path of the aircraft. In the case of any deviation from the desired path, the guidance system issues path correction commands to the flight control system. The flight control system then translates these commands into control surface deflections to cause the required change in the motion of the aircraft.

Usually, an AFCS contains two loops: an inner loop known as a Stability Augmentation System (SAS) and an outer flight path control loop known as an autopilot [22]. The purpose of SAS is to augment the values of certain stability derivatives of the aircraft through feedback control. The SAS improves the flying qualities of an aircraft and helps in rejecting atmospheric disturbances. Usually, a SAS is engaged for the entire duration of the flight to ensure that the airframe exhibits a stable behaviour. A dedicated SAS is designed for each mode of aircraft motion. The most commonly used SAS functions are: yaw damper, pitch rate stability augmentation and roll rate damper. The autopilot enables an aircraft to follow a desired lateral / vertical profile, without any input from the pilot. Essentially, the autopilot facilitates an aircraft at a desired altitude / heading / airspeed. The autopilot comprises two sub-systems: the attitude control system and the flight path control system [23]. Attitude control systems are used to place an aircraft in the desired orientation in space and keep that orientation for the required duration of time. Flight path control systems allow an aircraft to follow a predefined path with high accuracy. The basic modes of an autopilot are listed below:

Longitudinal Channel:

- Auto-throttle (speed control);
- Altitude hold/select mode;
- Vertical speed hold/select mode;
- Attitude hold mode (pitch attitude).

Lateral Channel:

- Attitude hold mode (roll attitude);
- Heading hold/select mode.



## 2.4 Maintenance of Separation

In this section, a short summary of the top-level components of airborne and ground surveillance systems are defined and a brief description of the lower-level services, functions, equipment, roles and procedures under each component are presented. The top-level components of the ATM system as given by ICAO are CM, traffic synchronisation, demand and capacity balancing, aerodrome/airspace operations, and airspace and service delivery management.

### 2.4.1 Airspace Categories and Classes

The airspace is defined as the portion of the atmosphere controlled by a country above its territory, including its territorial waters or, more generally, any specific 3D area of the atmosphere [25]. According to CFR, Title 14, part 71-73 and the Aeronautical Information Manual, the US national airspace is divided into two categories and four types based on the complexity or density of aircraft movements, proximity to airports, altitude, the nature of the operations conducted within the airspace, the level of safety required, and the national and public interest. These categories and types are regulated as follows:

- Explicit regulations for airspace class A, B, C, D, E, restricted and prohibited areas;
- A non-regulatory framework that includes airspace class G, Military Operations Area (MOA), warning areas, alert areas, and controlled firing areas.

While classes are mutually exclusive, categories can be defined within any class as needed. Categories are typically used to provide additional information to pilots about hazards activities common to the airspace. There are four types within these two categories:

- Controlled airspace;
- Uncontrolled airspace;
- Special use airspace;
- Other airspace.

Airspace classes A through E, ordered from most restrictive to least, corresponds to controlled airspace. However, when overlapping airspace designations apply to the same airspace, the operating rules associated with the more restrictive airspace designation apply [CFR §71.9].

## 2.4.2 Rules of the Air

By definition, control areas are volumes of airspace that are sufficient to contain the flight paths of Instrument Flight Rules (IFR) or portions thereof for which it is desired to provide certain Air Traffic Services (ATS). Control areas also include ATS routes (airways) and Terminal Control Areas (TCA), frequently known as Terminal Manoeuvring Areas (TMA). Control zones complement control areas in their purpose and are specifically conceived to contain arrival and departure IFR flight paths in close proximity to the ground. For minor and isolated airports with limited IFR traffic, an appropriate combination of control zones and ATS routes is usually sufficient to contain IFR traffic safely. This is due to the fact that tactical deconfliction by ATM operators is almost never required and occasional peaks of traffic can be successfully managed by exploiting multiple approach and departure procedures and en-route holdings. Larger airports or combinations of multiple minor airports in close proximity to each other require more frequent tactical ATM interventions in terms of path stretching and separation measures. Whenever additional allowance for these tactical measures is necessary, TCA/TMA is established. In order to maximise safety of IFR traffic TCA/TMA are most commonly granted the highest levels of ATS, corresponding to airspace classes "A", "B" or, less frequently, "C".

Due to their distinctive nature, TCA/TMA have become the paradigm of dense air traffic scenarios, where arriving, departing and overflying aircraft intersect leading to frequent conflict situations. The highest levels of ATS assigned to TCA/TMA, implies that most of the responsibilities for conflict detection, separation maintenance, sequencing and spacing lies on the ATM side. This is effectively the opposite of recreational airspace assigned classes "G" and "F", and has important consequences for manned and unmanned aircraft SA&CA.

CA algorithms have to take into account the same collision avoidance requirements of the rules of the air for manned aviation, delineated in the ICAO Annex 2 [24], in order to guarantee the Equivalent Level of Safety (ELOS).

Aviation regulations in the United States, collectively known as Federal Aviation Regulation (FAR), are codified in the Code of Federal Regulations (CFR), Title 14, Chapter I [26]. The CFR, along with supplementary material like handbooks, orders, advisory circulars and technical standards orders issued by the FAA, define appropriate standards, procedures, and practices to ensure that manufacturers and operators are able to establish a minimum level of safety and reliability required for civil operations

[27]. Aviation authorities in other countries (UK, Australia, etc.) have an equivalent code of regulations applicable regionally.

### 2.4.3 General Operation Principles and Flight Rules

Code of Federal Aviation, Title 14, part 91 has established right-of-way rules, aircraft speed, minimum safe altitudes, equipment, instrument, and certificate requirements, maintenance, preventive maintenance, special flight operations i.e. aerobatic flight, flight test areas, etc. for the US. Federal regulations do not permit pilots to fly below 10,000 ft or in proximity of airspace Class B, C, and D at speed exceeding 250 knots. It is not allowed for aircraft to operate close to another aircraft in a way that creates a collision hazard. The pilot is required to contribute to collision avoidance by being alert in order to "see and avoid" other aircraft [CFR §91.111]. The flight rules that need to be considered for implementing effective SA&CA algorithms for manned and unmanned aircraft are summarised as follows:

- Right-of-way rules – Except water operations: When an aircraft has the right-of-way, other traffic shall give way to that aircraft and may not pass over, under, or ahead of it unless well clear [CFR §91.113]. The main right-of-way rules are:
  - The aircraft that is in distress has right of way over all other traffic;
  - Landing aircraft or aircraft on final approach to land have right of way over other aircraft in flight or operating on the surface. If two or more aircraft are landing then the aircraft at the lower altitude has the right of way;
  - Aircraft being overtaken have the right of way. Overtaking aircraft shall alter course to the right to pass well clear;
  - In an head-on scenario, each aircraft shall alter course to the right to pass well clear;
  - In case of a converging scenario:
    - ✓ when the aircraft are of the same category, then the aircraft to the other's right has the right of way;
    - ✓ if the aircraft are of different categories, then both aircraft have to follow the rules provided in CFR; §91 for converging encounters.
- Aircraft speed: The minimum safe airspeed defined by the [CFR; §91.117] is 250 knots (288 mph) for any particular aircraft operating below 10,000 ft MSL. However, the minimum safe airspeed is 200 knots (230 mph) for any aircraft operating at or below 2,500 ft above the surface within 4 NM of the primary airport of a Class C or Class D airspace area. In regards to Class B, [CFR §91.117] indicates that no person may operate an aircraft in the airspace underlying a

Class B airspace designated for an airport or in a VFR corridor designated through Class B airspace at an indicated airspeed of more than 200 knots (230 mph);

- Minimum safe altitude: According to [CFR §91.199], the minimum safe altitudes are categorized as follows:
  - Over congested areas: an aircraft shall maintain an altitude of 1,000 ft above the highest obstacle within a horizontal radius of 2,000 ft of the aircraft;
  - Non-congested areas: minimum of 500 ft Above Ground Level (AGL) shall be maintained (except over open water or sparsely populated areas);
  - Anywhere else: an aircraft should maintain an altitude such that if the engine fails, an emergency landing may be executed without undue hazard to persons or property on the surface.
- Failure of power unit(s): in case of power unit failure, the aircraft shall not fly below the altitude necessary to make an emergency landing;
- Land clear rule: when in densely populated areas, the aircraft shall not fly below the altitude necessary to make a landing outside of the congested area, in the event of a power unit failure;
- Flying over open air assemblies: when flying over an organised open-air assembly of more than 1000 persons, the aircraft shall fly above 1000 ft. Such an altitude permits landing in the event of a power unit failure.

The CFR Title 14, Part 91 defines two types of flight rules, namely visual flight rules and instrument flight rules, which apply to all aircraft except moored balloons, kites, unmanned rockets, and unmanned free balloons.

The CFR Title 14, Part 27 (Airworthiness Standards: Normal Category Rotorcraft) and CFR Title 14, Part 29 (Airworthiness Standards: Transport Category Rotorcraft) provide the airworthiness standard for normal and transport category rotorcraft respectively. In most countries, at airports/helipads, established standard departure and arrival procedures ensure that (wherever possible), twin engine Vertical Take-Off and Landing (VTOL) aircraft do not fly over residential areas below 1500ft. Normal flight is permitted down to 1000ft over residential areas and lower levels are permitted during landing and take-off. The following conditions shall be applied in the authorisation of VTOL aircraft when flying according to VFR:

- such flights may be conducted during day only, unless otherwise permitted by the competent authority;
- by the pilot: (i) clear of cloud and with the ground surface in sight, (ii) the flight visibility is not less than 800 m; (iii) fly at a speed of 140 kts (instrument

air speed) or less to give adequate chance to observe other traffic and any obstacles to avoid a collision and take and timely actions if necessary.

In some circumstances, VTOL aircraft need to fly at lower altitudes (law enforcement, search and rescue, emergency, medical and surveying purposes, etc.), which might require authorisation from the regulatory authority. If a VTOL aircraft pilot requires to cross a controlled zone around an airport, it may be necessary for the ATCo to hold the VTOL aircraft in one place until it is safe to continue operations.

#### 2.4.4 Separation Standards

Separation standards refer to the minimum distance that aircraft operating in controlled airspace and at airports with an operational control tower must keep between them [28]. Different separation standards apply to aircraft operating under IFR and VFR. In Australia, aircraft flying under IFR in controlled airspace up to 29,000 ft altitude are separated by 1000 ft vertically, unless they are separated horizontally. When above 29,000 ft, the vertical separation increases to 2000 ft, except in airspace where Reduced Vertical Separation Minima (RVSM) is applied. It is generally guaranteed that when aircraft are separated vertically, horizontal separation can be reduced without compromising safety. In controlled en route airspace, the horizontal separation standard between aircraft flying at the same altitude is 5 Nautical Miles (NM) while in terminal area airspace, the minimum separation is 3 NM. For general aviation aircraft (non-commercial aircraft) outside of controlled airspace, separation can be as close as 500 ft vertically and 500 ft horizontally. ICAO rules divide aircraft into three main categories including light, medium and heavy, in order to establish separation between aircraft based on wake vortices. The classification is based on the maximum take-off weight of the aircraft and the separation distances are based on experimental flight data (flight tests). The ICAO classification is provided in Table 2.7 (adapted from [29]). The only exception is for Airbus A380 aircraft, which has a different set of separation distance standards.

An analytical model has been proposed for calculating the safe separation distance between aircraft and is especially valuable in non-cooperative sensor based aircraft separation. The safe separation distance is given by:

$$s = \frac{A/B}{f \eta} \quad (2.3)$$

where  $s$  is the safe separation distance,  $f$  is the fraction of the available control moment that is used,  $\eta$  is the turbulent kinematic shear viscosity and :

$$A = \frac{I_f r^2}{2} \quad (2.4)$$

where  $I_f$  is the incident flow velocity and  $r$  is the vortex core radius.  $B$  is given by:

$$B = \frac{12}{h} \frac{v_2}{v_1} \frac{S_a}{S} \frac{b_a}{b_2} \frac{a_1}{b_1} \frac{a_1}{c_1} \quad (2.5)$$

where  $h$  is a dimensionless factor specified by the wing planform,  $v_2$  and  $v_1$  are the volume loading (wing loading divided by span) of the preceding and following aircraft,  $S_a$  is the aileron area,  $S$  is the wing area,  $b_a$  is the moment arm of ailerons,  $b$  is the wing span,  $a$  is the core radius of the wing-tip vortices and  $c$  is the wing chord. It is to be noted that equation (2.3) is not symmetric (i.e., heavy-light is not equal to light-heavy).

Table 2.5. ICAO separation standards.

Designation	Maximum Take-off Weight	Aircraft Example	* Separation Distances for a Pair of Aircraft
Heavy	$W > 136 \text{ t}$	Boeing B 747-400 ( $W = 396,893 \text{ kg}$ )	Heavy-Heavy 4 NM Heavy-Medium 5 NM Heavy-Light 6 NM
Medium	$7 \text{ t} < W < 136 \text{ t}$	Boeing B 737-300 ( $W = 70,080 \text{ kg}$ )	Medium-Heavy 3 NM Medium-Medium 3 NM Medium-Light 5 NM
Light	$W < 7 \text{ t}$	Cessna Citation 500 ( $W = 5,375 \text{ kg}$ )	Light-Heavy 3 NM Light-Medium 3 NM Light-Light 3 NM

\*where the first aircraft is the leading aircraft and the second aircraft is the following aircraft.

## 2.5 Collision Detection and Avoidance

A key objective of the ATM modernisation concept is the delegation of the task of separation assurance from air traffic controller to the flight crew, where the whole task is supported by higher levels of automation. In order to be able to satisfy this goal, aircraft are required to implement automated means for airborne conflict management, which is categorised as:

- Conflict detection,
- Conflict prevention;
- Conflict resolution.

Onboard systems will need to be able to identify violation of separation minima in strategic (long-term), tactical and emergency timeframes. Resolutions for these conflicts need to be computed in order to offer the flight deck crew alternative routing. In case coordination with other traffic participants is required, those updated trajectories need to be communicated, shared (involves negotiation and agreement of trajectories between two aircraft) and validated. This has to be achieved independent of ground infrastructure.

One of the key goals of this thesis is to describe the system design aspects that will support airborne separation assurance and conflict management in line with the ATM modernisation as well as UTM concepts of operations.

Over the years, many efforts have been made in order to develop SA&CA requirements and, in 2004, the Radio Technical Commission for Aeronautics (RTCA) Special Committee 203 (SC-203) was formed [30]. SC-203 was given the task of defining Minimum Aviation System Performance Standards (MASPS) for SA&CA.

Between December 2008 and March 2009, the FAA organized several workshops in order to define the capabilities that a SA&CA system should have to be compliant with the current rules governing the notion of "see-and-avoid." The workshop published a document in October 2009 [31], where the sense-and-avoid concept was defined as "the capability of [an unmanned aircraft] to remain well clear from and avoid collisions with other airborne traffic". Moreover, the workshop defined that a SA&CA system would be characterized by two components [32]:

- A self-separation component that ensures a safe separation based on a variable time-based threshold. In this way, the aircraft remain "well-clear" of each other;
- A collision avoidance component that operates when the safe separation is lost and an extreme manoeuvre is needed to prevent a collision. In fact, for the collision avoidance manoeuvre, a distance-based threshold is considered.

The participants of the workshop identified the SA&CA core and crosscutting capabilities and they are summarised in Tables 2.6 and 2.7.

Table 2.6. SA&CA core capabilities [30, 31].

Core Capability	Description
Target Detection	Ability to determine presence and location of any airborne object that presents a collision threat to the unmanned aircraft covered by this SA&CA system
Target Tracking	Ability to refine a detected airborne object's position (2D or 3D) and velocity based on one or more target detection(s) from a single sensor
Multi-sensor Data Fusion	Ability to refine a detected airborne object's position (2D or 3D) and velocity based on one or more target detection(s) or track(s) from multiple sensors
Object Identification	Ability to discriminate type and characteristics of a detected airborne object
Threat Assessment	Ability to determine risk of collision based on relative position (2D or 3D) and velocity of the detected airborne object and the unmanned aircraft covered by the SA&CA system
Alerting	Ability to communicate that a risk threshold has been met
Manoeuvre Selection	Ability to determine the appropriate action needed to resolve identified collision risk(s) to the appropriate separation threshold
Manoeuvre Notification	Ability to communicate the selected manoeuvre in order to execute within the timing window
Manoeuvre Execution	Ability to execute the selected manoeuvre within the timing window
Return-to-Home/Mission	Ability of UAS to return to intended or amended course after an avoidance or separation manoeuvre is complete

In order to define a set of SA&CA standards, for the certification and operational approval of unmanned aircraft, the FAA workshop identified five sub functions that a SA&CA system shall perform including:

- Detection of conflicting traffic;
- Determination of the right of way;
- Analysis of the flight paths;
- Maneuvering;
- Communication.

According to the performance of the on board SA&CA technologies, it is possible to obtain different encounter sensing dimensions. This design factor is defined as the extension of space surveyed for the conflict risks monitoring. The trajectory



information of other traffic is determined after performing multi-sensor data fusion of information obtained from the SA&CA technologies (Figure 2.5).

Table 2.7. SA&CA crosscutting capabilities.

Crosscutting Capability	Description
Pilot/Operator Presentation	Ability to provide the pilot/operator with the required information required to perform/monitor the core SA&CA capabilities
System Integration	Ability to integrate the core capabilities into existing and planned manned and unmanned aircraft
Certification/Qualification	Ability to show through process and evidence that the SA&CA system meets an acceptable safety level
Concept of Operations (CONOPS)/Procedure Validation	Ability to conform to approved CONOPS and operational procedures
Data Standardization/Characterization	Ability to enable collaboration and meaningful comparisons through databases, data standards and data integrity
Airspace/ATM/UTM	Ability to assess the impact on the airspace that UAS system performance and the performance of supporting systems, such as SA&CA, may have on ATM/UTM
Traffic Separation Minima	Ability to determine the separation standards and the environmental or operational conditions which inform SA&CA design

Criticality analysis is carried out to prioritize (i.e. to determine if a collision risk threshold is exceeded for all tracked intruders) and to determine the action commands. If an evading action is required, the SA&CA system generates and optimises an avoidance trajectory according to a priority based cost function based on minimum distance, fuel, time and closure rate criteria with the aid of differential geometry algorithms to generate a smooth trajectory.

Detection of conflict risks requires the identification of potential threats in the airspace close to the own ship; along with continuous data updates, collection and recording. Therefore it is necessary to provide the system with the tools to enable the detection and identification of specific type of threats. These tools can be simple databases, e.g. for detecting ground threats, sensors set for the detection of moving threats, etc.

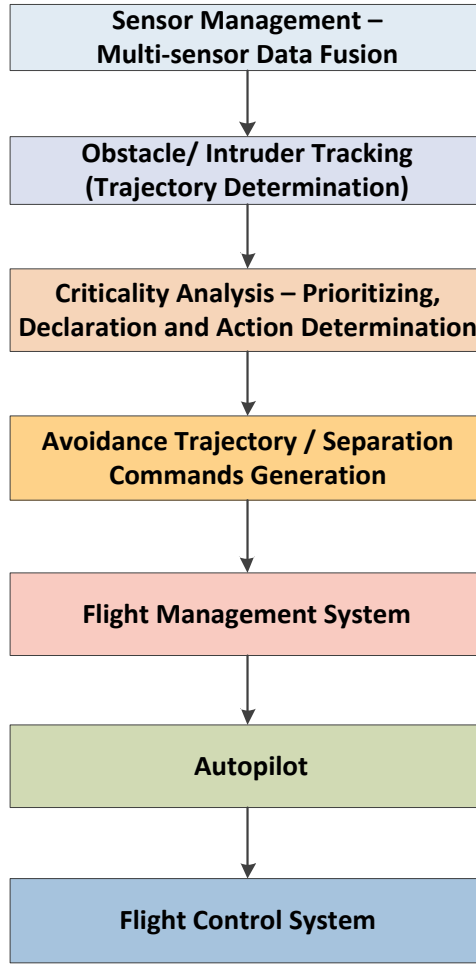


Figure 2.5. SA&CA system processes.

Consider a classical two aircraft conflict, where an aircraft on the lower segment flies at  $v_1$  m/s, and an aircraft on the upper segment flies at  $v_2$  m/s. The angle of incidence is  $\alpha$  and  $D$  is the separation standard.

Let:

$$r = \frac{v_2}{v_1} \quad (2.6)$$

If two aircraft are in conflict, the following inequality should be satisfied to avoid any conflicts.

$$(x_1 - x_2)^2 + (y_1 - y_2)^2 \leq D^2 \quad (2.7)$$

The above second degree inequality will only be satisfied if the following equation holds true:

$$(x_1 - x_2)^2 + (y_1 - y_2)^2 - D^2 = 0 \quad (2.8)$$

Equation (2.5) has at least one solution. Hence the discriminant is given by:

$$\Delta = D^2 (v_1^2 - 2v_1v_2 \cos \alpha + v_2^2) - \sin^2 \alpha (l_2v_1 - l_1v_2)^2 \quad (2.9)$$

where the aircraft on the lower segment is at a distance  $l_1$  from the intersection point and the other aircraft is at a distance  $l_2$ .  $\Delta$  must be positive and the extremal points  $r_1$  and  $r_2$  are given by:

$$r_1 = l_1 \frac{v_2}{v_1} + D \frac{\sqrt{1 + \left(\frac{v_2}{v_1}\right)^2 - 2\left(\frac{v_2}{v_1}\right) \cos \alpha}}{\sin \alpha} \quad (2.10)$$

$$r_2 = l_1 \frac{v_2}{v_1} - D \frac{\sqrt{1 + \left(\frac{v_2}{v_1}\right)^2 - 2\left(\frac{v_2}{v_1}\right) \cos \alpha}}{\sin \alpha} \quad (2.11)$$

If the length of the segment is given by  $(r_1 - r_2)$ , the function on  $r$  and  $\alpha$  does not depend on  $l_1$ . It implies that the obtain information is sufficient and there is no uncertainty of any kind. Conflicts could be exactly predicted as soon as the position of the aircraft is known, even if they are very far away from the intersection point. A number of studies have shown that only one conflict out of three to five detected and monitored would really result in separation violation. For example, on simulated traffic on a busy day of 1999 in the French airspace above FL 320, when the uncertainties on trajectory predictions increase (since it was considered as free flight), the number of necessary maneuvers also increases dramatically [33]. Without uncertainty, 972 conflicts occur and 1041 maneuvers are required to solve them. When a 2% uncertainty is considered on ground speed, and 5% uncertainty on climbing or descending rate, 2461 maneuvers are necessary to solve the detected conflicts. The number of maneuvers increases to 3881 for a 5% uncertainty on ground speed and 15% uncertainty on vertical speed and it eventually reaches 6819 maneuvers with 10% ground speed and 30% vertical speed uncertainties [33]. Figure 2.6 illustrates relevant parameters in the well-clear based conflict detection method.

Figure 2.6 shows the different SA&CA zones and the condition of CA. As can be seen, the Self-Separation Threshold (SST) and Self-Separation Volume (SSV) are boundaries where there is no threat, but an aircraft detected far away can be regarded as an obstacle. In controlled airspace, ATC ensures a safe distance is maintained from other aircraft, terrain, obstacles and certain airspace not designated for routine air travel. The ATC is in charge of giving the order to reconfigure the path and avoid crossing trajectories. The second volume is called the self-separation threshold. In this situation, ATC efforts may have failed, or another unresolved alarm may have occurred, and the aircraft detected turns out to be a threat. The SSV could be the only function provided given that the safety analysis demonstrates that the target level of safety can be met

with SSV alone. However, when all forms of SA have failed, we are now at the third volume and the CA (provided by the Collision Avoidance Threshold (CATH) boundary) takes appropriate action to prevent a threat aircraft from penetrating the Collision Volume (CV). On rare occasions the self-separation functions may conflict with ATC separation services, and as a general rule the aircraft follows the ATC separation services.

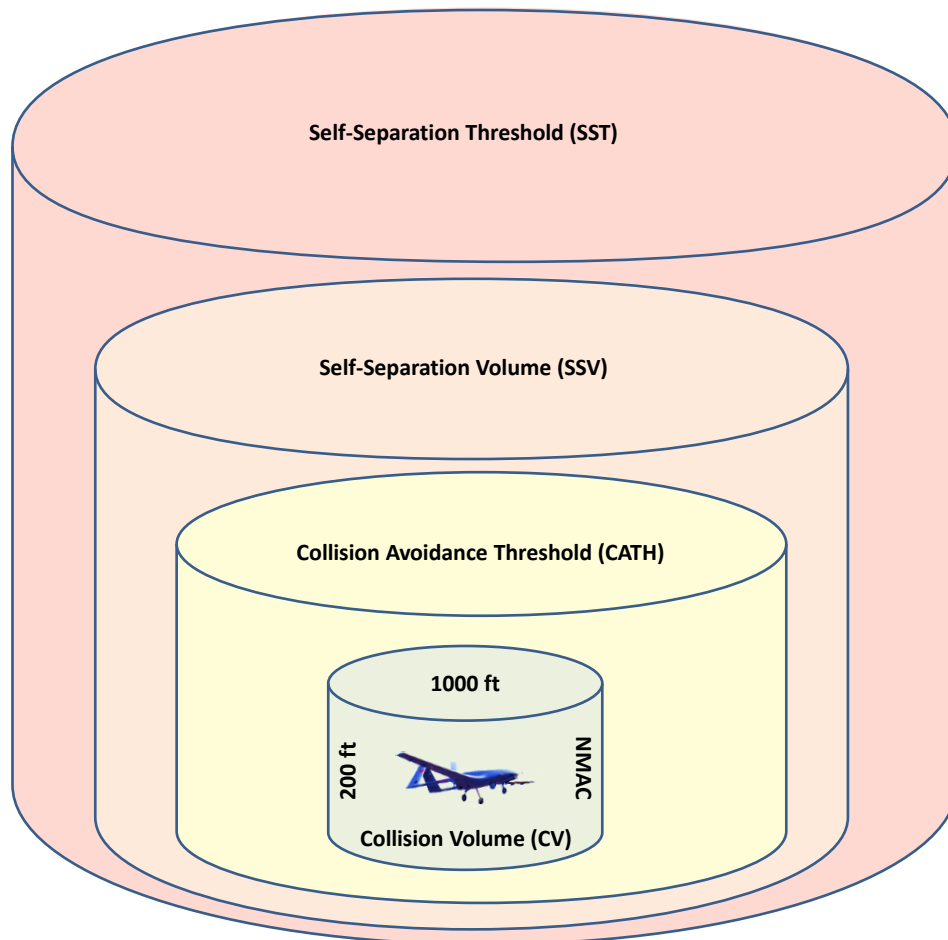


Figure 2.6. CATH, SSV and SST boundaries.

### 2.5.1. Conflict Detection and Resolution Approaches

Conflict Detection and Resolution (CD&R) algorithms are implemented to monitor the surrounding environment for both static and dynamic obstacles using onboard sensors and using information from the ground network. Cooperative systems and non-cooperative sensors are employed for object detection in the surrounding airspace.

To detect and resolve a conflict, it is important to assess and compare the trajectories of the host aircraft and the detected object. The trajectory prediction and computation module processes the raw sensor information and provides the trajectories of the host

aircraft and the tracked objects. When multiple sensors/systems are employed for tracking, then multi-sensor data fusion techniques are adopted. There are three basic models of trajectory prediction methods (Figure 2.7). In the nominal method, the trajectory is predicted directly from the sensor data without considering the possibility of any uncertainty or change. The output of the nominal trajectory predictor is a single trajectory computed from prior sensor measurements. The trajectory may be computed using different methods, i.e. linear prediction, Taylor series prediction, or prediction using the Kalman filter. The nominal method prediction is suitable for short-term predictions, where the probability of change is relatively low. The worst-case method is another modelling approach. This method covers the whole range of manoeuvres the aircraft may perform and uses a look-ahead time parameter to compute the area where the aircraft may occur. This area is then considered as the predicted trajectory. In the probabilistic prediction approach, the uncertainties are used to model the potential variations in the trajectory. To construct this model, all possible trajectories are generated (like for the worst-case prediction) and each trajectory is evaluated by the probability function. The probabilistic prediction is a trade-off between the nominal method and the worst-case prediction. The probabilistic prediction method is the most widely used technique, in which decisions are made based on the likelihood of the conflict.

### **2.5.2. Theoretical Techniques for CD&R**

The flight plan, Position, Velocity and Attitude (PVA) as well as Trajectory Change Points (TCP) exchange approaches are bound to cooperative sensors only. The aircraft exchange parts of their flight plans, TCPs or other state information and in this case, the precise trajectory is known and no prediction is needed. The conflict resolution block resolves the collision using one of the collision avoidance methods (Figure 2.8). Some of the key methods are rule-based, game theoretic, field-based, geometric, numerical optimization, combined and multi-agent methods [34, 35].

In general, the existing conflict resolution solutions can be divided into two parts: simple collision avoidance solutions, and localisation and mapping based solutions. Simple solutions are based on avoiding collisions by steering the vehicle in the opposite direction using different techniques. The biggest drawback of such solutions is the intervention into the steering which may not be desirable for the mission of the aircraft. These solutions do not allow an aircraft to control its distance from an obstacle which may be necessary [36 - 39].

Rule-based methods use a set of prescribed rules to avoid conflict. The sets of rules are fixed during the system design phase and originally were inspired by the VFR known from the civilian air traffic domain.

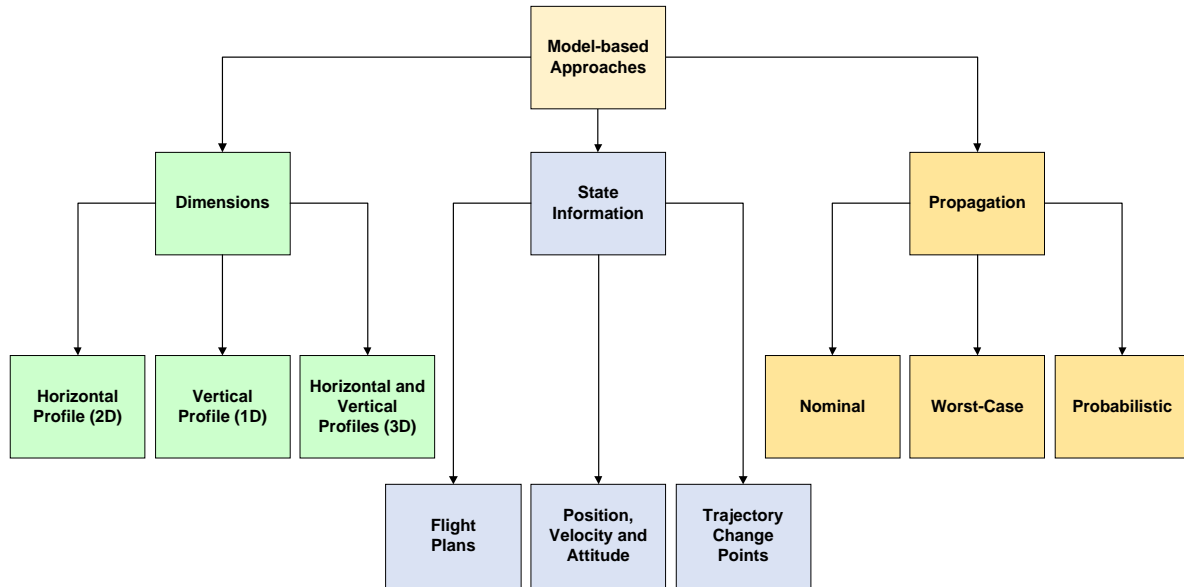


Figure 2.7. Trajectory prediction/estimation approaches.

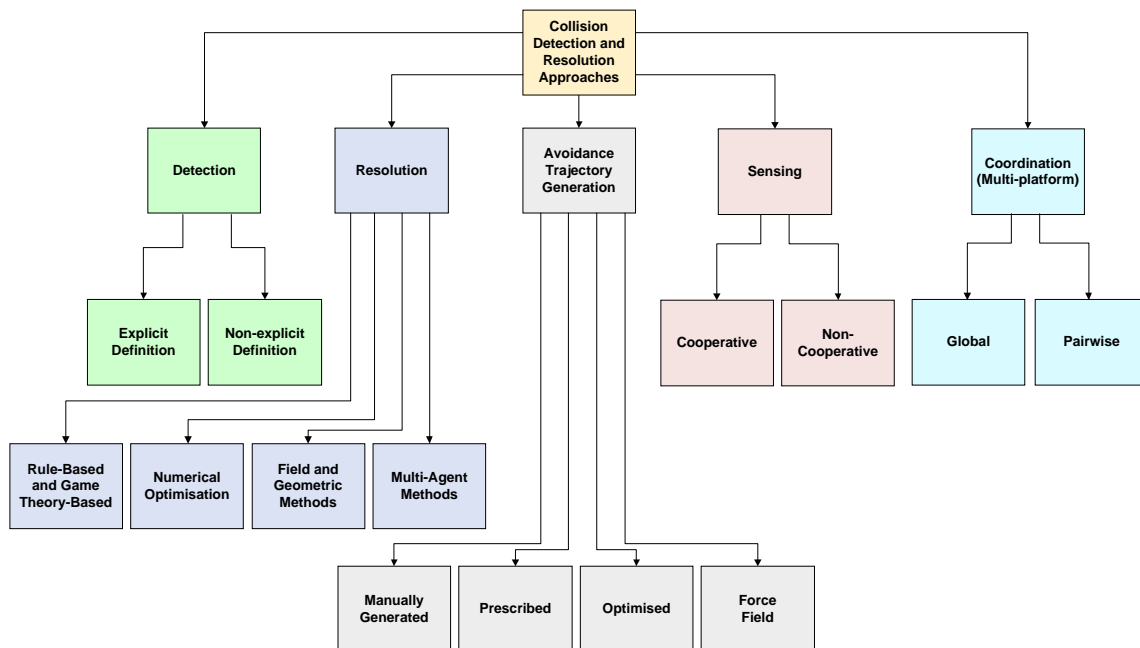


Figure 2.8. Collision detection and resolution taxonomy.

The second part can be described as localisation and mapping-based solutions. The map is loaded a priori and the fixed obstacles are provided in the associated database. Those solutions avoid collisions by mapping, positioning, and navigation within the map while the positioning and mapping is based on a complex localisation algorithm.

Compared to the first division, these solutions do not limit the mission, but the CA algorithm requires considerable memory and computational power compared to the already mentioned simple solutions, because of its complexity [40 – 42].

The rule-based methods use a set of prescribed rules to avoid conflict. The sets of rules are fixed during the system design phase and originally were inspired by the visual flight rules (VFR) known from the civilian air-traffic domain. In the game theory methods, the authors model the conflict as a two-player differential game. These algorithms are useful mainly for non-cooperative conflict resolution. The field-based methods treat each aircraft as a charged particle and are very close to a reactive control mechanism. Based on the current configuration (e.g. position of other platforms, weather condition, considered uncertainty), the field is computed. Geometrical approaches consider the whole trajectory of the airplane, not restricting to the currently observed solution. Various approaches optimize given objective functions while they are searching for the proper evasion manoeuvre. In many cases, these methods are considering only two-aircraft collision; for multi-collision situations they degrade and present sub-optimal approaches, or rely on the sequential application of two-aircraft collision avoidance, where safety is not necessarily guaranteed at all times. Geometrical optimization is a very complex problem, especially if all available actions (including change of heading, velocity, and altitude) are considered. The numerical optimization methods use a kinematic model of the vehicle together with a set of constraints, and then use cost metrics for the manoeuvre generation. The optimal evasion manoeuvre is then computed based on the most desired constraints. The major benefit of these methods is that the optimization criterion is clearly formalized and the final control is optimized with respect to the given problem definition. With increasing number of airplanes the problem becomes analytically unsolvable. The limitation of bounded receding time horizon simplifies the problem. The multi-agent methods use the multi-agent framework for solution generation. Each aircraft is controlled by one agent. The agents are able to communicate and negotiate a solution using various utility functions [34].

### **2.5.3. Applied/Implemented Air Traffic Solutions for CD&R**

Various other CD&R algorithms have been employed in specific projects on SA&CA around the globe. Within the Smart Skies project, technologies were developed to facilitate the greater utilisation of the national airspace system by both manned and unmanned aircraft [43]. These technologies include an automated separation management system capable of providing SA in complex airspace environments and CA with dynamic and static obstacles; and a Mobile Aircraft Tracking System (MATS)

that utilises cost-effective primary radar and cooperative surveillance systems. The system includes manned and unmanned aircraft, virtual aircraft, public mobile data and Iridium communication links, an Automated Dynamic Airspace Controller (ADAC) and the MATS.

The Mid Air Collision Avoidance System (MIDCAS) was a 4 year long European project funded by five European countries. Its goal was to demonstrate the baseline of acceptable solutions for the critical self-separation and mid-air collision avoidance functions to contribute to the integration of unmanned aircraft in civilian airspace [44, 45].

The Autonomous System Technology Related Airborne Evaluation and Assessment (ASTRAEA) was a UK industry-led consortium focusing on the technologies, systems, facilities, procedures and regulations that will allow autonomous vehicles to operate safely and routinely in civil airspace over the UK [46 - 48].

Sense and Avoid Flight Tests (SAAFT) were conducted by the Air Force Research Laboratory (AFRL) and Defense Research Associates, Inc. (DRA) in the US. AFRL established the SAAFT program to demonstrate autonomous collision avoidance capabilities in both cooperative and non-cooperative air traffic. The intent of the program was to equip unmanned aircraft with CA capabilities and thus allow them the same access to national and international airspace that manned aircraft have [49, 50].

## 2.6 SA&CA Technologies

To operate in civil airspace, manned and unmanned aircraft are expected to maintain safe separation from other aircraft. New self-separation and Collision avoidance systems designed for unmanned aircraft are under development to meet this requirement. To maintain airspace safety, these new systems must interoperate safely with collision avoidance system onboard manned aircraft. Therefore, the interactions of manned aircraft collision avoidance and unmanned aircraft collision avoidance and self-separation must be understood. Many of the SA&CA systems under development for unmanned aircraft provide horizontal guidance, alerting UAS to turn left or right to avoid intruders. In contrast, both TCAS (Traffic Alert and Collision Avoidance System), the internationally-mandated collision avoidance system required onboard all large transport aircraft, and its planned successor ACAS Xa1 (Airborne Collision Avoidance System X), issue only vertical resolution advisories such as climb or descend.



### 2.6.1 State-of-the-art SA Technologies

Currently most of the air traffic surveillance services around the world are achieved using Primary Surveillance Radar (PSR) and Secondary Surveillance Radar (SSR). PSR refers to a directed radio frequency source being reflected by an airborne object to a highly directional receiver that supports depiction of the source's range and azimuth information on a display. While primary radar was adequate for military early warning systems in an environment, WWII added the requirement to assign an identity to all radar returns. This resulted in the development of the Military IFF (Identify Friend or Foe) radar beacon system in which an airborne transponder issues a coded reply to interrogation by a primary radar source (located on the ground or airborne).

PSR is an independent and self-contained system, and it does not require the target (airborne aircraft) to carry any additional surveillance-related equipment. When the technology advanced, it was complemented by SSR for air traffic control. Through interrogation, all aircraft within the maximum possible range are expected to reply with their unique identification and altitude information, and thus enhancing the situation awareness for the ATCo. SSR is considered to be a dependent and cooperative surveillance system. Although SSR provides more detailed information when compared to PSR, SSR does not provide information on unequipped aircraft, or on aircraft whose SSR components have failed. Radar systems were employed for CA (Figure 2.9), until 1974, when the FAA contracted the development of the BCAS or Beacon Collision Avoidance System which is a transponder related airborne framework. BCAS uses the replies from the Air Traffic Control Radar Beacon System (ATCRBS) transponders in response to the interrogations [51] as shown in Figure 2.10. At that time, ATCRBS transponders were introduced in all military flying machine and many airplanes.

TCAS was initially developed in the United States during the 1970s and 1980s in response to a series of deadly mid-air collisions between United States civil aircraft [52]. Mandated internationally for large transport aircraft, TCAS has substantially reduced the risk of airborne collisions (Figure 2.11).

TCAS alerting logic is based on linear extrapolation of intruder trajectories and a large set of heuristic rules [53 – 55]. There are three members of the TCAS family; TCAS I, TCAS II and TCAS III. TCAS I is a pilot warning indicator which displays proximate traffic and alerts the crew to other aircraft which may become potential near mid-air collision threats.

TCAS provides an effective collision avoidance function in traffic densities as high as 0.3 aircraft per square nautical mile (24 transponder-equipped aircraft within five nautical miles of the TCAS-equipped aircraft).

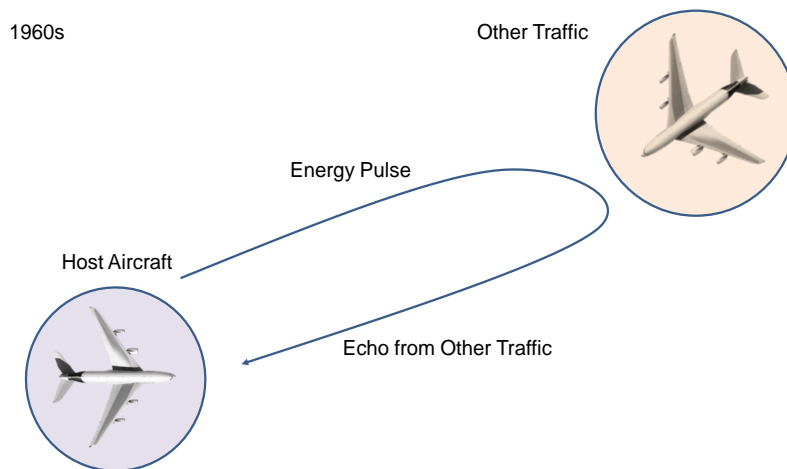


Figure 2.9. Onboard collision avoidance system - early radar systems.

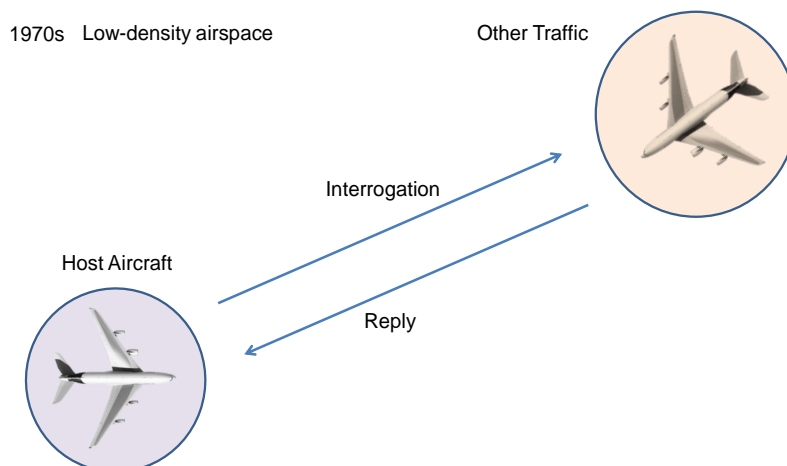


Figure 2.10. Onboard collision avoidance system – BCAS.

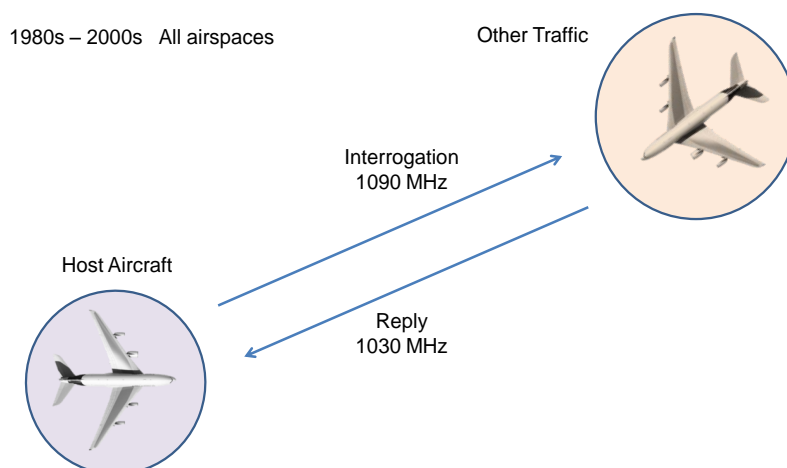


Figure 2.11. Onboard collision avoidance system – TCAS.

When TCAS operates in traffic densities of 0.3 transponder-equipped aircraft per square nautical mile or higher, it provides protection against collisions with other aircraft, so long as those aircraft are closing at speeds of less than 500 kt.

TCAS is also capable of providing protection against aircraft closing at relative speeds of up to 1200 kt in airspace characterized by densities of less than 0.06 transponder-equipped aircraft per square nautical mile, which is equivalent to eighteen transponder-equipped aircraft within ten nautical miles of the TCAS aircraft.

A TCAS I-equipped aircraft can receive limited alert and advisory information about aircraft in its vicinity. TCAS I also participates in cross-link communication with TCAS II equipped aircraft. TCAS I operates by listening for aircraft transponder transmissions (replies). The replies detected may have been:

- unsolicited transmissions from Mode S transponders (squitters);
- replies elicited by ground station or TCAS II interrogations (passive TCAS I);
- replies resulting from low-power interrogations from TCAS I (active TCAS I).

Additionally, TCAS I receives traffic advisory information from TCAS II aircraft. If an intruding aircraft is equipped with TCAS II, and if that TCAS II aircraft determines that a collision hazard exists, it will transmit advisory information to the TCAS I aircraft, which includes bearing (if available), range and relative altitude of the TCAS II aircraft with respect to the TCAS I aircraft. As an option, TCAS I can be implemented to provide an indication of the transmitting transponder's bearing.

TCAS II, in addition, provides recommended vertical escape manoeuvres to the crew to avert potential Near Mid-Air Collisions (NMAC). The term TCAS IV is reserved for future TCAS equipment that has additional capabilities beyond those of TCAS II equipment; such as the ability to generate resolution advisories in the horizontal plane (e.g., "TURN RIGHT," "TURN LEFT"). The equipment described in this thesis does not have horizontal resolution capability. In this document, TCAS I is denoted TCAS I; the use of the unqualified term TCAS refers exclusively to TCAS II; and the last version is explicitly denoted as TCAS IV. As the development of TCAS Versions 7 and 7.1 exemplified, modifying the existing rules is extremely difficult and time consuming.

TCAS II is intended to improve air safety by acting as a last-resort method of preventing mid-air collisions or near collisions between aircraft. By employing SSR technology, TCAS II equipment operates independently of ground-based aids and ATC. Aircraft equipped with TCAS II have the ability to interrogate airborne transponders to monitor range, bearing, and reported altitude of other aircraft in the vicinity and assess the risk of

collision. Non-transponding aircraft are not detected. TCAS II Version 6.0 was first introduced in the United States in 1990 with collision avoidance logic. TCAS II Version 7.0 was introduced in the US and Europe in 2000 and was subsequently mandated by ICAO for all commercial turbine-powered transport aircraft worldwide, having more than 19 passenger seats or having a maximum take-off weight above 5700 kg. TCAS II is referred to as the Airborne Collision Avoidance System II (ACAS II) in ICAO terminology. TCAS II provides traffic advisories and if warranted, resolution advisories in the vertical plane. RAs are indications given to the flight crew; they recommend manoeuvres intended to provide separation from all threats, or restrictions to maneuvers to maintain existing separation. TCAS II operating procedures in the western world give RAs priority over ATC clearances and instructions, i.e., flight crews are instructed to follow an RA even when it conflicts with ATC guidance. Controllers have no knowledge of a TCAS RA, unless they are notified by the flight crew via the radio (resolution advisory information is provided by TCAS II to Mode S SSRs, but it is not normally presented to controllers). TCAS can track up to 30 airplane in an ostensible scope of 14 nautical miles for Mode A or C targets, and 30 nautical miles for Mode S targets. This data is passed to the collision avoidance logic in the onboard electronics to decide the TAs or RAs.

The following section describes how to compute and update the CRS input variables Coarse\_Altitude, Fine\_Altitude, Own\_Corrected\_Alt, Fine\_Altitude\_Rate, Radio\_Altitude, and ZRINT. These calculations use the parameters Init\_Alt, Init\_Alt\_Rate, Alt\_Accel, Ground\_Level, and Quant specified in the encounter input file of the TCAS [56 – 60].

At  $T=1$  for own aircraft and at the time Encounter\_Start is specified for other traffic, the altitude (Alt) and altitude rate (Alt\_Rate) for each aircraft are set to Init\_Alt and Init\_Alt\_Rate, respectively. At the end of each cycle ( $T=i$ ) Alt and Alt\_Rate are updated for each aircraft for the next cycle ( $T = i+1$ ) as follows:

$$Alt_{i+1} = Alt_i + Alt\_Rate_i + 0.5 \times Alt\_Accel_i \quad (2.12)$$

$$Alt\_Rate_{i+1} = Alt\_Rate_i + Alt\_Accel_i \quad (2.13)$$

Calculations for Alt and Alt\_Rate always use the exact value of Alt, rather than rounding to the nearest 100 ft. The CRS input variables:

- Coarse\_Altitude;
- Fine\_Altitude;
- Own\_Corrected\_Alt;
- Fine\_Altitude\_Rate;
- Radio\_Altitude;

- ZRINT.

These input variables are calculated at the beginning of each cycle from these values as follows [56]:

$$Coarse\_Altitude_i = Alt\_Own_i \quad (2.14)$$

$$Fine\_Altitude_i = Alt\_Own_i \quad (2.15)$$

$$Own\_Corrected\_Alt_i = Alt\_Own_i \quad (2.16)$$

$$Fine\_Altitude\_Rate_i = Alt\_Rate\_Own_i \quad (2.17)$$

$$Radio\_Altitude_i = Alt\_Own_i - Ground\_Level_i \quad (2.18)$$

$$ZRINT_i = Round(Alt_{Other_i}, 100) \text{ if } QUANT = 100 \quad (2.19)$$

$$ZRINT_i = Round(Alt_{Other_i}, 25) \text{ if } QUANT = 25 \quad (2.20)$$

These values are used to compute and update the CRS input variables RR (relative range), BEAR (bearing), and Bear\_Meas (raw bearing). These calculations use the parameters Air\_Speed, Init\_Range, Range\_Space, and Angle specified in the encounter Input File.

Figure 2.12 illustrates an example of the encounter geometry. For all encounters, the own aircraft is assumed to be travelling at a constant speed in the positive x-direction. Forward\_Range is the x-component of the distance of the other aircraft from own aircraft. Side\_Range is the y-component of the distance of the other aircraft from own aircraft, with positive distance being measured to the right of own aircraft. Angle is the heading angle of the other aircraft measured clockwise from the x-axis. Initially, at the time Encounter\_Start is specified, Forward\_Range is set to Init\_Range and Side\_Range is set to Range\_Space.

At the end of each cycle Forward\_Range and Side\_Range are updated for the next cycle as follows:

$$Forward\_Range_i = Forward\_Range_i - Air\_Speed\_Own - Air\_Speed\_Other_i \times \cos(Angle_{i+1}) \quad (2.21)$$

$$Side\_Range_i = Side\_Range_i - Air\_Speed\_Own - Air\_Speed\_Other_i \times \sin(Angle_{i+1}) \quad (2.22)$$

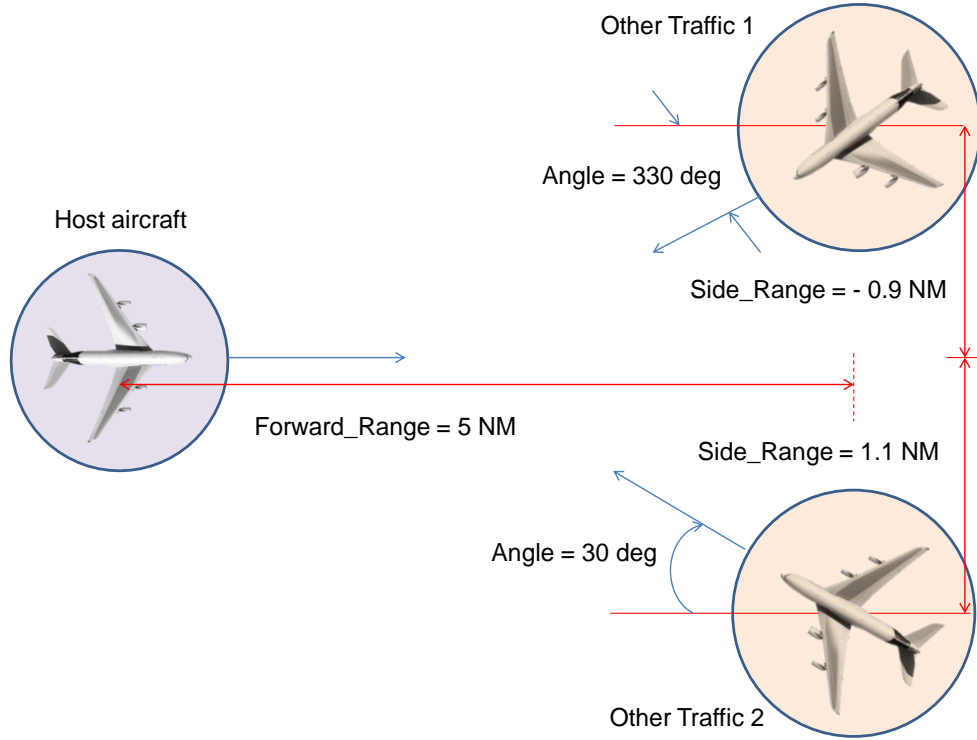


Figure 2.12. Example of an encounter geometry.

*Air\_Speed\_Own* and *Air\_Speed\_Other* are constant throughout each test and, if the value of Angle changes, it is updated before the new *Forward\_Range* and *Side\_Range* are computed. The CRS input variable *RR* is computed at the beginning of each cycle from these values as follows:

$$RR_i = \sqrt{Forward\_Range_i^2 + Side\_Range_i^2 + Relative\_Alt_i^2} \quad (2.23)$$

where *Relative\_Alt* is the real altitude difference between own and other aircraft. *Relative\_Alt* is computed using the altitudes computed in the previous paragraph:

$$Relative\_Alt_i = Alt\_Own_i - Alt\_Other_i \quad (2.24)$$

Finally, the CRS input variables *BEAR* and *BEAR\_MEAS* are calculated at the beginning of each cycle as follows:

$$Bear_i = \arctan \left( \frac{Side\_Range_i}{Forward\_Range_i} \right) \quad (2.25)$$

$$Bear\_Meas_i = \arctan \left( \frac{Side\_Range_i}{Forward\_Range_i} \right) \quad (2.26)$$

and then adjusted for the quadrant in which the other aircraft is located.

TCAS has been very successful in preventing mid-air collisions over the years, but the way in which the logic was designed limits its robustness [56 - 60]. Fundamental to TCAS

design is the use of a deterministic model. However, recorded radar data show that pilots do not always behave as assumed by the logic. Not anticipating the spectrum of responses limits TCAS's robustness, as demonstrated by the collision of two aircraft in 2002 over Überlingen, Germany. TCAS instructed one aircraft to climb, but one pilot descended in accordance with the air traffic controller's instructions (illustrated in Figure 2.13), leading to a collision with another aircraft whose pilot was following TCAS. If TCAS recognized the noncompliance of one of the aircraft and reversed the advisory of the compliant aircraft from descend to climb, the collision would have been prevented. To overcome the above issues and to ensure safe and effective collision avoidance in the future airspace environment, in 2009, the FAA TCAS program office began formal research on a next generation airborne collision avoidance system: ACAS X. Whereas TCAS logic is based on linear extrapolation and heuristic rules, ACAS X logic is based on a dynamic model of aircraft movement and a computer optimized lookup table of collision avoidance actions.

In ACAS X, traffic alerts are issued to advise pilots that another aircraft is a potential threat and to prepare for a resolution advisory if necessary. A resolution advisory commands specific vertical-only manoeuvres that will satisfy safety goals with minimal manoeuvring. Resolution advisories include the following:

- Climb or descend;
- Level off;
- Maintain climb or descend;
- Don't or limit climb or descent rate.

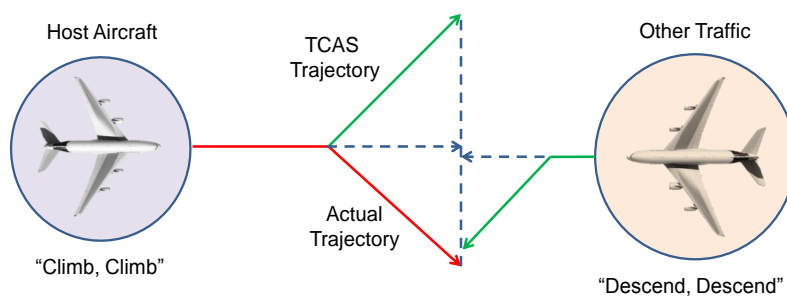


Figure 2.13. Limited robustness of TCAS.

Like TCAS, ACAS X avoids collisions by giving vertical guidance to an aircraft's pilot. A typical scenario involves two aircraft:

- the ownship, where ACAS X is installed;
- another aircraft called intruder that is at risk of colliding with the ownship.

The Collision Avoidance community defines a NMAC as being when two aircraft are within  $h_p = 500$  ft horizontally and  $r_p = 100$  ft vertically [61, 62]. ACAS X is designed to avoid such NMACs. ACAS X uses both discrete advisories to the pilot, and the continuous dynamics of aircraft, it is natural to formally verify it using hybrid systems.

ACAS X prevents an NMAC by giving an advisory to the pilot of the ownship. From a table of advisories and their modelling variables, every advisory, except the clear of conflict (COC), has a vertical rate range of the form  $(-\infty, \dot{h}_f]$  or  $(\dot{h}_f, +\infty]$  for some vertical rate  $\dot{h}_f$ , which we call the target vertical velocity. We therefore model any advisory by its corresponding target vertical velocity  $\dot{h}_f$ , and a binary variable  $w$ , whose value is  $-1$  if the vertical rate range of the advisory is  $(-\infty, \dot{h}_f]$  and  $+1$  if it is  $(\dot{h}_f, +\infty]$ . Note that this symbolic encoding makes it possible to represent many more advisories and is therefore robust to changes in the set of advisories that ACAS X allows. It is assumed that the ownship pilot complies with each advisory within  $d_p$  sec, and that they accelerate with at least acceleration  $a_r$ , to bring the relative vertical velocity in compliance with the advisory.

This design makes ACAS X substantially easier to adapt to specific aircraft, airspace procedures, and surveillance technologies. ACAS X is a family of adaptations, two of which are more predominantly employed: ACAS Xa and ACAS Xu. Both TCAS and ACAS Xa issue resolution advisories based in large part on the projected vertical trajectories of intruder aircraft. ACAS Xa is being designed as a direct replacement for TCAS, with the intent to provide improvements in safety and operational suitability. ACAS Xu is being designed for UAS, and as such it is optimized for the aerodynamic performance and surveillance systems characteristic of those platforms. ACAS Xu, unlike TCAS and ACAS Xa, is able to provide horizontal resolution advisory guidance. In this thesis, the interactions of a vertical collision avoidance system and a system providing UAS with horizontal guidance, ACAS Xu's horizontal logic fills the role of the system providing horizontal guidance. Note that ACAS Xu is also able to provide vertical RA guidance, but this analysis is focused solely on its horizontal logic. Even though ACAS Xu is a collision avoidance system, the results of this work are applicable to any collision avoidance or



self-separation system providing guidance that may cause vertical manoeuvres within the collision avoidance timeframe.

A UAS receiving only horizontal guidance would notionally be unconstrained in the vertical dimension, meaning it would be free to change its vertical rate at the same time it is directed to turn. Such changes to vertical rate could occur for a variety of reasons, including dynamic restrictions on the UAS (e.g., it is near its service ceiling, it may not be able to maintain its current climb rate and turn at the same time) or the actions of the UAS operator. If these changes to vertical rate occurred during the RA timeframe of an intruder equipped with TCAS or ACAS Xa, then the safety benefit provided by those systems could be degraded. For example, consider an encounter between a TCAS equipped manned aircraft and a UAS receiving horizontal guidance only. The TCAS aircraft is above the UAS and is descending towards it, while the UAS is climbing slowly near its service ceiling. As some point, TCAS issues an RA directing the manned aircraft to maintain its descent and cross altitudes with the UAS. At around the same time, the horizontal logic on the UAS directs it to turn. To comply, the UAS is forced to descend due to dynamic restrictions near its service ceiling. This creates a dangerous situation in which both aircraft are descending and the RA issued by TCAS will no longer resolve the encounter.

In ACAS X, when a collision risk is detected, an alert as well as a suggestion for a potential resolution manoeuvre is provided to the pilot. The system is capable of tracking only aircraft equipped with a mode S transponder and can detect mode A/C transponders to a certain extent. The propagation of uncertainties in the trajectory states of two aircraft are modelled in ACAS as illustrated in Figure 2.14. These consist of uncertainties in the states of host aircraft and other traffic and the resulting dynamic uncertainty at the point of conflict. Various variants of ACAS X can be employed including [61] as summarised in Table 2.8.

ACAS is different from a conventional CA system, in the sense that it does not include any autonomous resolution execution function. ACAS has characteristics and performance different from those required by a SA&CA system for UAS. One of the main reasons is that the different climb performance of various aircraft platforms (manned and unmanned) is not compatible with current TCAS requirements. More precisely, the limitations on the climb performance make it difficult for the unmanned aircraft remote pilot or the avionics systems to execute the manoeuvres suggested by TCAS advisories. General aviation aircraft and aerostatic balloons are not usually fitted with mode S transponders, requiring non-cooperative surveillance is required. Figure 2.15 shows the

top-level architecture of ACAS. The system receives sensor measurements every second. On the basis of these sensor measurements, the system infers the distribution over the aircraft's current status. This status, or state estimation, takes into account the probabilistic dynamic model and the probabilistic sensor model. This state distribution determines where to look in the numeric logic table to determine the best action to perform (e.g., whether to issue an advisory and if so, the vertical rate to adopt). This processing chain is repeated once per second with every new sensor measurement. Critical to understanding the logic optimization process inherent are two important concepts. The first is a Markov decision process, which is essentially the probabilistic dynamic model combined with the utility model. The second is dynamic programming, which is the iterative computational process used to optimize the logic.

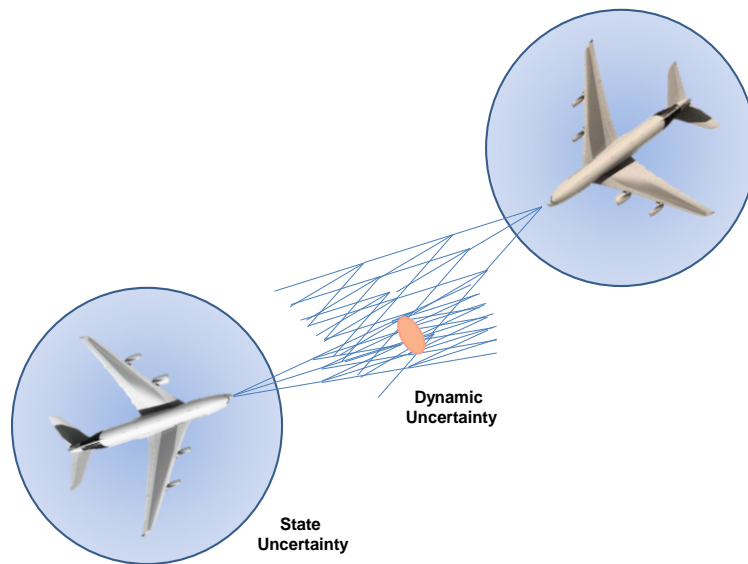


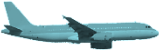



Figure 2.14. Uncertainty propagation in ACAS.

Besides being compatible with NextGen, ACAS X improves the safety of air travel and provides more operational suitability. In addition to protecting the traveling public on board every large commercial aircraft worldwide, ACAS X provides:

- Reduced pilot workload (by reducing the number of confusing and surprising advisories);
- Capacity to accommodate new surveillance inputs that provide more detailed and precise tracking data than currently used onboard transponders;
- Ability to reduced fuel costs, emissions, and flight operating times, as well as increased arrival rates at airports;
- A minimised number of interruptions to normal air traffic flow;

- A streamlined manufacturing operation process and reduced costs associated with system implementation and upgrades;
- An integration platform to facilitate the use of unmanned aircraft in defence and commercial applications.

Table 2.8. ACAS X variants.

ACAS X Type	Description	Surveillance Technology	Advisories
ACAS Xa (active) 	It is the general purpose ACAS X that will make active interrogations to establish the range of intruders. ACAS Xa is a successor to TCAS II system.	Active RADAR supplemented with passive	Same as current TCAS
ACAS Xo (operation) 	A mode of operation of ACAS X designed for particular operations for which ACAS Xa is unsuitable. It facilitates procedure-optimized alerting against a user-selected aircraft while providing global Xa protection for all other traffic.	Active RADAR supplemented with passive	Vertical and horizontal advisories
ACAS Xp (passive) 	It is specifically intended for unmanned aircraft. It accepts a variety of surveillance inputs and uses decision-logics that are optimised for a wide variety of performance capabilities.	Passive only	Reduced advisory set
ACAS Xu (unmanned) 	A version of ACAS X that relies solely on passive ADS-B inputs to track other traffic and does not make any active interrogation. It is intended for general aviation aircraft, which are not currently required to be equipped with TCAS II system.	Potentially radar, EO/IR, etc.	Vertical and horizontal advisories (for self-separation)

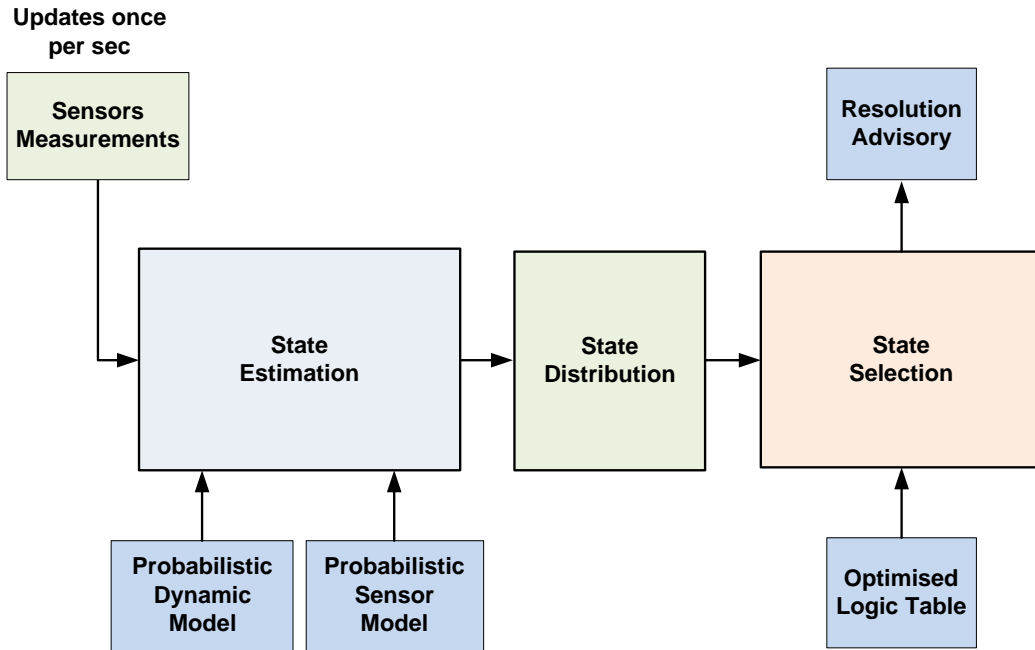


Figure 2.15. ACAS top-level architecture.

Automatic Dependent Surveillance – Broadcast (ADS-B) is operational in most countries. In Australia, ADS-B has almost complete coverage above FL250 and reasonable coverage down to 10,000ft. ADS-B messages are transmitted via the Extended Squitter Mode-S transponder data link operating at 1090 MHz. Mode S ES capable transponders and ADS-B OUT equipage mandates are detailed in [63, 64]. Automatic Dependent Surveillance – Contract A (ADS-C) separation of Instrument Flight Rules (IFR) dependent aircraft outside of radar coverage are managed procedurally, resulting in large separation standards. ADS-C relies on the automatic transmission of reports from an appropriately equipped aircraft. The content and timing of reports is described as a “contract”. Digital data link communications via satellite or VHF can be made from appropriately equipped aircraft (FANS 1/A) to enable reduced separation standards. The digital data link enables Controller Pilot Data Link Communications (CPDLC) and Automatic Dependent Surveillance – Contract (ADS-C).

Automatic Dependent Surveillance Broadcast (ADS-B) has been viewed as a low cost alternative and complement to the current primary surveillance radar. Typically, ADS-B refers to the function on a surface vehicle or airplane which broadcasts its state vector together with other relevant information periodically. ADS-B is developed to improve situation awareness, conflict detection, conflict avoidance, runway incursion avoidance as well as surveillance in remote areas without radar covering. Additionally, ADS-B

integrated with other capability is expected to enable airspace with self-separation similar to visual operation today in SESAR and NextGen programs.

All the involved vehicles including aircraft, ground vehicles and other objects periodically transmit their identification, positional information as well as intent information using a broadcast data link. ADS-B is made up of the following components:

- the transmitting subsystem which includes a message generation as well as transmission function at the source aircraft;
- the propagation medium, and a receiving subsystem which is composed of message reception;
- the report assembly functions at the receiving aircraft.

Some ground-based users may have the capability to receive but not transmit. The ADS-B system consists of three functional components: receiver aircraft, transmitter aircraft as well as ground station as illustrated in Figure 2.16. The characteristics and requirements of ADS-B make it a capable sensor for CA on small UAS in the National Airspace System (NAS).

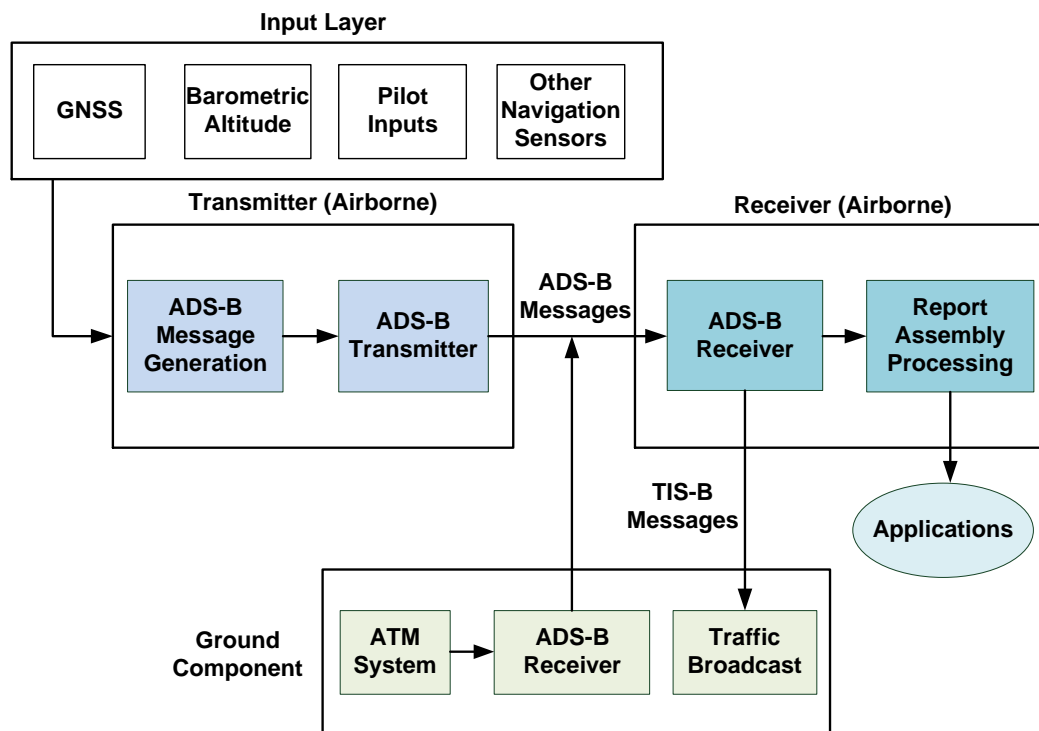


Figure 2.16. Functional component of ADS-B.

One of the key aspects of ADS-B that makes it feasible for use on small UAS is the availability of ADS-B receivers that meet the SWaP constraints of a small UAS. Another key advantage of ADS-B is the long range at which information is available. While there

is a significant amount of variation in the range of ADS-B signals, the shortest expected range is 10 NM. But, at the same time, currently, most small UAS cannot carry ADS-B transponders. Furthermore, the density of ADS-B signals if all small UAS were equipped with ADS-B would lead to communication signal collisions in the broadcast algorithm. Additionally the long range of ADS-B is advantageous in that the quality of information transmitted over ADS-B does not degrade with range. Thus the accuracy of ADS-B is not dependent on the size, power, or range of the transmitter and receiver units. This is a significant advantage over radar and optical sensors, and makes path planning for conflict detection and separation assurance at long ranges easier.

However, the limitations of ADS-B system are:

- It is heavily dependent on line-of-sight availability of GPS and ADS-B transmissions. Without GPS information, ADS-B transponders are unable to transmit usable position information. Air-to-air ADS-B transmissions also require line-of-sight visibility for reliable exchange of information. Bandwidth constraints of ADS-B can also be a limitation. Due to the fact that all ADS-B Out-capable aircraft must transmit a message at least once per second on the same nominal frequency, the ADS-B protocol specifies a multiple access scheme. While the scheme is different for the 978 MHz frequency and 1090 MHz frequency, all multiple access schemes have a finite number of transmitters that they can support. This is especially applicable to small UAS, and there are limitations of employing Time Division Multiple Access (TDMA), which is typically used at 978 MHz;
- The cost of procuring ADS-B equipage is another limitation. Certified ADS-B Out hardware costs typically range from \$1,000 to \$25,000 AUD.

ADS-B uses three types of reports:

- Surveillance State Vector (SSVR) report;
- Mode-Status (MS) report;
- On-condition report.

Information provide by these reports are detailed below. The SSVR report contains information on the dynamics of the aircraft, which include geometric position, horizontal and vertical velocity, and heading. In addition, the quality of the SSVR element is contained in the MS report. The MS message includes current operational information of the transmitting aircraft including capability class codes, operational mode codes and SSV quality. The Capability Class (CC) code identifies the capability of a transmitting ADS-B participant including TCAS installation information, Cockpit Display of Traffic

Information (CDTI) capability, air referenced Velocity report capability, and trajectory change report capability. OM codes indicate the current operational mode of a transmitting element. The SSVR quality codes contain the Navigation Accuracy Category for position (NACp), Navigation Accuracy Category for Velocity (NACv) and Surveillance Integrity Level (SIL). All ADS-B participants must provide these SSVR and MS reports. Upon reception of a state vector report, the system searches for a track of the same type (ADS-B, ADS-R, TIS-B) and with the same 24-bit address as the report. If no match is found, the system generates a new track containing the following parameters:

- System time (track time of applicability);
- Position time of applicability;
- Velocity time of applicability;
- Track type (ADS-B, ADS-R, TIS-B);
- 24-bit address;
- Position (latitude, longitude, altitude);
- Velocity (East/West velocity, North/South velocity, altitude rate);
- Geometric Vertical Accuracy (GVA) = 1 (Version 2);
- System Design Assurance (SDA) = 1 (Version 2);
- State covariance matrices. (Covariance is a statistical concept, which seeks to describe how two variables are related to each other. Two variables are said to be positively related if they move in the same direction. The variables are inversely related if they move in opposite directions. Covariance is a tool to determine whether two variables are positively related or inversely related);
- ID change flag = 0;
- Index of correlated TIS-B track = null;
- Time of correlation with TIS-B track = null;
- Previous state (position and track time of applicability) matrix initialized as a row vector;
- Estimated turn rate = null.
- Navigation Integrity Category (NIC);
- NACP = 5;
- NACV = 1;
- SIL = 0;

Multilateration systems use a network of ground-based transceivers to localise aircraft based on the difference in time of arrival of aircraft transponder transmissions. Multilateration systems are currently deployed at a number of Class C CTR (for terminal

area airspace surveillance and separations services within the terminal manoeuvring area) and for en-route and terminal area surveillance. Advanced Surface Movement Guidance and Control System (A-SMGCS) provides routing, guidance and surveillance for the control of the surface movement of aircraft and vehicles. The system is based on a number of existing surveillance technologies to provide situational awareness and alerting. It is a key technology for the prevention of runway and taxiway incursions and ground collisions. A precision runway monitor is a surveillance system that supports reduced staggered separation for aircraft on the existing parallel Instrument Landing System (ILS) approaches of airports. It uses a primary radar sensor to provide accurate and high update rate surveillance of the approach and landing areas.

A summary of airborne surveillance systems currently available is provided in Table 2.9.

Table 2.9. Airborne surveillance systems.

Airspace	Conventional Systems	State-of-the-art Systems
Oceanic continental En-route airspace with low/high-density traffic	Primary radar/Secondary Surveillance Radar (SSR) Very High Frequency (VHF) voice position reports OMEGA/ Long Range Navigation Customized Navigation Database (LORAN-CNDB)	Automatic Dependent Surveillance (ADS)
Continental airspace with high-density traffic	Primary radar  SSR Mode A (ATC Transponder Mode signifying aircraft call sign)  SSR Mode C (ATC Transponder Mode signifying aircraft call sign and altitude)	SSR Mode A SSR Mode C SSR Mode S (ATC Transponder Mode signifying call sign, altitude and additional aircraft data) ADS
Terminal areas with high-density	Primary radar SSR Mode A/C	SSR [Mode A/C/S] ADS

### 2.6.2 State-of-the-art SA supported by an ATM System

CM function of ATM System provides SA features for ensuring safety and avoidance of terrain, weather, wake turbulence, and airspace. CM can be further divided into:



- SCM, which is achieved through airspace organisation and management, demand and capacity balancing, and traffic synchronisation;
- SP, which is the second layer and describes a range of primarily tactical sub-functions intended to ensure separation minima are maintained. SP function includes the issuing of instructions, clearances and information advisories to airspace users. SP is supported by route adherence monitoring, cleared level adherence monitoring and approach path monitoring. In the future, ASAS will be available to complement the ATM SP functions (e.g., ADS-B In and Cockpit Display of Traffic Information);
- ATM Collision Prevention (ACP) services are provided to aid pilots in maintaining well clear of other aircraft and hazards in the event that safe separation minima have been lost. From an ATM system perspective, this involves the issuing of safety alerts, which are defined as the provision of advice to an aircraft when an ATS Officer becomes aware that an aircraft is in a position that is considered to place it in unsafe proximity to terrain, obstructions or another aircraft. For example:
  - Aircraft conflict alerts – alerts initiated by an ATM system when an ATCo becomes aware of aircraft that are considered to be in unsafe proximity;
  - Terrain/obstruction alerts – the provision of advice to an aircraft when an ATS officer becomes aware that an aircraft is in a position which is considered to place it in unsafe proximity to terrain or obstructions.
- PSR is operational at Class C aerodromes and some military aerodromes. ATCRBS SSR is used for approach and en-route surveillance in most nations. Coverage is primarily limited to areas surrounding the Control Area (CTA). The returned coded reply is processed by a SSR system. In the case of the modern Mode 3/A ATCRBS, the system provides coded aircraft identification (4 digits octal) and a Mode C pressure altitude. ATCRBS sends a directional interrogation signal during the radar volume scan on a 1030 MHz carrier frequency and expects a Mode 3/A (and Mode C) reply in the 1090 MHz band. The advent of denser air traffic has resulted in the need for a greater volume of data from the target transmitter (primarily for more detailed identification) and considerably faster and more reliable digital processing has given birth to a solution in the form of the Mode-S transponder standard.

CM is a component of the ATM system that will be impacted by the integration of UAS into the current ATM system.

### 2.6.3 CA Sensors/Systems

A number of non-cooperative sensors have been adopted as part of research projects dealing with developing CA functions. The technologies that have been used can be divided into two macro areas [65]:

- Cooperative technologies that typically require a transponder on board the aircraft: they require other aircraft to equip with the same devices when sharing the same airspace.
- Non-cooperative technologies that identify all the aircraft not equipped with a transponder or, for example, gliders, hot air balloons, and so on. They do not require other aircraft to equip the same devices when sharing the same airspace.

Multi-sensor platforms for obstacle detection by using millimetre-wave radar, electro-optic/infrared, Light Detection and Ranging (LIDAR) and acoustic sensors are currently employed. Ground-based CA systems using electronic sensors are also currently developed and they provide information for manoeuvre decision tasks especially in TMA operations. The adoption of a multi-sensory approach to CA (employing passive and active MMW radar, Forward Looking Infra-Red (FLIR), LIDAR and an Electronic Surveillance Module (ESM) for obstacle detection) has resulted in adequate performance in low- to medium-dynamics platform applications. A non-cooperative collision avoidance system for UAS utilising pulsed Ka-band radar and optical sensors has been developed [66]. Acoustic-based CA systems for small UAS may adopt a multi sensor platform with acoustic sensors that allows detection of obstacles and intruders in a 360 ° FoV, and performs quick-reaction manoeuvres for avoidance [67]. This system allows all weather operations and offers advantages in terms of power consumption and cost. Encounter models and their applications to CA strategies address both cooperative and non-cooperative scenarios.

Ground-based CA systems using electronic sensors, which are also currently being developed [68]. These ground based systems provide information for manoeuvre decisions for terminal manoeuvring area operations. The states of the tracked obstacles are obtained by adopting Extended/Unscented Kalman Filter (EKF/UKF) or other multi-sensor data fusion techniques, which are used in order to predict the trajectory in a given time horizon. On-board trajectory re-planning with dynamically updated constraints based on the intruder and the host dynamics is at present used to generate obstacle trajectories. Coarse-resolution radar based CA solutions are implemented for small size UAS and the information is often fused with data from an ADS-B system. In the

case of cooperative scenarios, ADS-B and TCAS are adopted for implementing CA functions [69]. The avoidance trajectory is generated with the use of an on-board trajectory re-planning module, which has dynamically updated constraints based on the intruder and the host dynamics. The avoidance trajectories are also generated with the use of a nonlinear differential geometric guidance law based on a collision cone approach and dynamic inversion, which, combined with a first order autopilot, allows for satisfactory guidance of the vehicle. The possible synergies attainable with the adoption of different detection, tracking and trajectory avoidance algorithms are addressed in the later chapters of the thesis.

In an operational perspective, guidelines and regulations are required to support the CA system requirements development. The requirements for designing and developing an effective CA system are derived from the current regulations applicable to the see-and-avoid capability of manned aircraft. The proposed detection range and Field-of-Regard (FoR) must be adequate to ensure separation from the intruder, in order to prevent a probable near mid-air collision. This criterion is also naturally applicable in the case of small UAS, since the vast majority of mid-air collision events occur below 3000 ft. In the case of see-and-avoid, the main roles and responsibilities of pilot and crew are stated in FAA AC 90-48C and FAR §91.113 regulations as follows: vigilance shall be maintained at all times, regardless of whether the operation is conducted under IFR/VFR. Initial requirements recognized by SC-203 and other aviation/UAS working groups state that any UAS shall have a system capable of monitoring the surroundings at all times. This system has to maintain a minimum separation distance with any cooperative or non-cooperative obstacle/intruder.

#### **2.6.4 Attributes/Capabilities of UAS SA&CA Technologies**

The attributes/capabilities of SA&CA technologies can be summarized as follows [65]:

- Optical sensors (pixel/visual):
  - low cost, size, and weight;
  - suffer from various atmospheric disturbances;
  - have to be arranged in various positions on the aircraft;
  - a visual radar can be used that is highly comparable to a human's ability;
  - dictated by the required Field-of-View (FoV);
  - payload size and mounting issues.

- Infrared sensors:
  - higher cost than optical sensors;
  - low size and weight;
  - useful in conducting night time operations;
  - operate under severe weather conditions;
  - to achieve the required FOV, sensors have to be arrayed in various positions on the aircraft, taking up valuable external area;
  - some sensors do not pick up objects lacking some type of heat signature (cables or gliders);
  - development and integration efforts are generally expensive.
- Microwave RADAR:
  - very mature technology;
  - useful in detecting the intruder aircraft at great distances;
  - generally bulky.
- LIDAR:
  - the size of the detection cone is very small and it makes possible to target a specific obstacle;
  - the revisit rate is poor and it takes multitude of laser sensors to achieve the same rate as a microwave radar;
  - highly developed for large UAS but underdeveloped for small UAS;
  - high cost;
  - inadequate in adverse weather (light can be absorbed and reflected depending upon the external conditions).

The essential criteria for designing an effective CA system are as follows:

Quantitative:

- The FOV has to be equivalent or superior to that of a pilot in the cockpit. This corresponds to a primary FOV of  $-60^{\circ}$  vertically/ $70^{\circ}$  horizontally and a secondary FOV of  $-100^{\circ}$  vertically and  $120^{\circ}$  horizontally;
- Sufficient detection range. As an example, the detection range of various CA technologies available for UAS is shown in Figure 2.17.

Qualitative:

- Accurate and precise intruder detection (static and dynamic), recognition and trajectory prediction (dynamic);
- Prior obstacle detection for allowing time for executing the trajectory avoidance manoeuvres;

- Effective fusion schemes for multi-sensor data augmentation, especially by tight coupling;
- Identification of the primary means of cooperative and non-cooperative CA for integrity requirements.

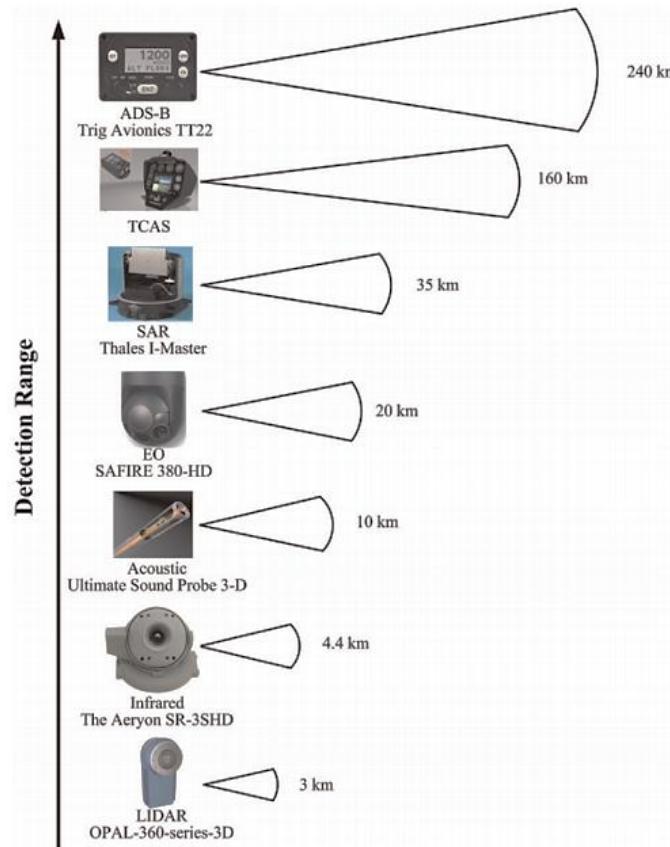


Figure 2.17. Detection range of CA technologies for UAS [65].

## 2.7 UAS Tracking, Decision-Making and Avoidance Loop

The integration of UAS into all classes of airspace presents a series of challenges in order to ensure safe operations. One of the main challenges is the SAA capability, which enables UAS to perform equally or exceed the performance of the S&A ability of the pilot in manned aircraft systems. Both cooperative and non-cooperative SAA systems are being developed to enable UAS to routinely access all classes of airspace.

The SAA capability can be defined as the automatic detection of possible conflicts by the UAS platform under consideration, resolving the collision risks and performing optimised avoidance manoeuvre tasks to prevent the identified collisions. Current advances in state-of-the-art airborne sensors and multi-sensor data fusion methods have led to a number of innovative-but at the same time dispersed-non-cooperative and

cooperative SAA solutions. Non-cooperative Collision Detection and Resolution (CD&R) for UAS is also considered to one of the major challenges that needs to be addressed carefully.

### 2.7.1 TDA Functions

The TDA loop consists of the following [70]:

- Tracking: A group of sensors collect the required data from the surrounding environment. Tracking is accomplished by the continuous acquisition of obstacle/intruder data. The sub-functions include:
  - Data Acquisition: cooperative and non-cooperative detection;
  - Low-Level Tracking: individual sensor and system tracks;
  - High-Level Tracking: data fusion (optimal estimation).
- Decision-Making: As other traffic/obstacles are tracked, suitable decision logics are employed for evaluating the risk and declaring an action to be taken (if a collision is identified). The sub-functions include:
  - Evaluate: trajectory estimation within a given time horizon, calculate risk of collision;
  - Prioritise: Risk of Collision (RoC) vs. threshold and low level tracking vs. threshold;
  - Declare: deterministic/stochastic decision making process.
- Avoidance: Once a possibility of collision is detected, then the on board FMS determines an action to avoid the collision by re-generating and optimising the flight trajectory against the set constraints and performance parameters.
  - Determine Action: avoidance trajectories generation;
  - Command: avoidance trajectory communication to pilot, Flight Control System (FCS), Flight Management System (FMS);
  - Execute: manoeuvre execution, history function, return-to-path.

Some relevant definitions are provided below.

Environment sensing: monitoring the surrounding airspace using non-cooperative sensors/cooperative systems to detect and identify every potential hazard. The primary aim is to get a synthetic description of the surrounding airspace in terms of the current state of the threats including their position and, an accurate estimation of its future states.

- Conflict detection: information collected during environment sensing is elaborated to identify which of the detected objects are real threats;
- Resolution estimation: the required resolution manoeuvre is identified if a conflict risk is detected.

Advisories communications: advisories about conflict risks and the estimated resolution manoeuvres are reported to the pilot/remote pilot. The operator task is then to accept, reject or ignore the suggested trajectory changes. In fact, even though the unmanned aircraft platform is capable of operating autonomously, a SA&CA system must normally report to and share the responsibility for its tasks (including safety) with the UAS operator, linked to the UAS via a communication data links. The collision scenario at different time epochs is illustrated in Figure 2.18.

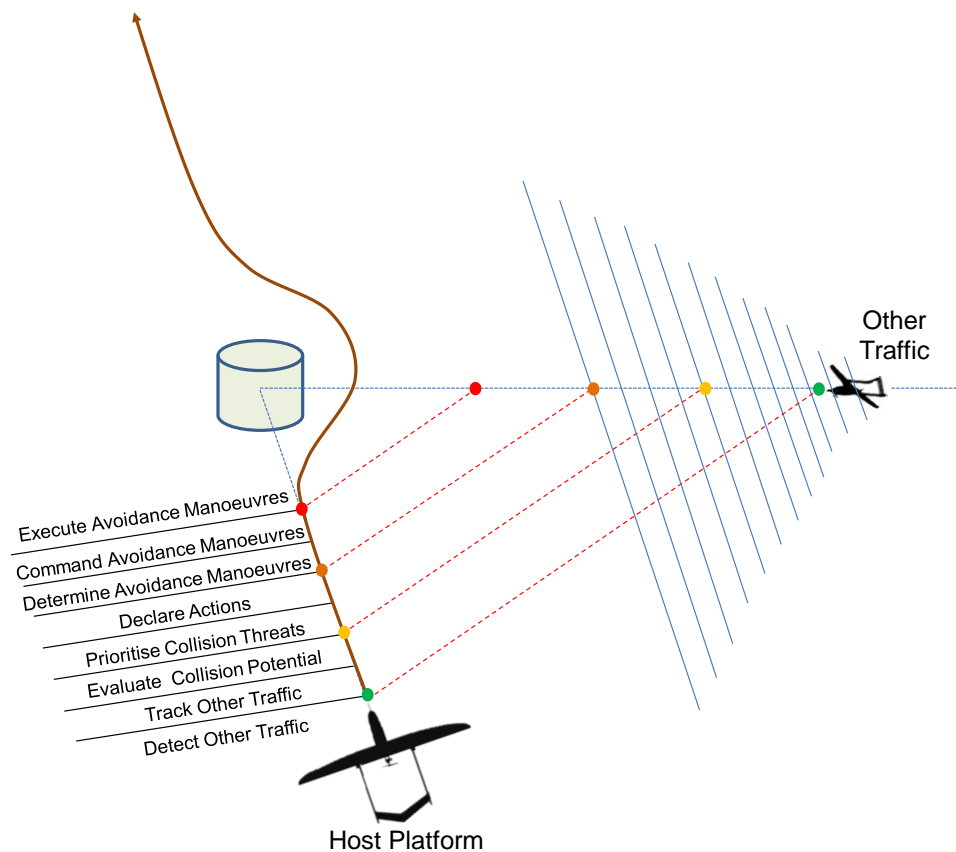


Figure 2.18. Collision scenario at different time epochs.

Autonomous resolution: execution of calculated resolution manoeuvres autonomously. It also refers to the execution of avoidance manoeuvres if the operator does not react to the advisory within the minimum safe time before impact. The GNC and TDA loops are illustrated in Figure 2.19. The SA&CA tasks are illustrated in Figure 2.20 [adapted from 71].

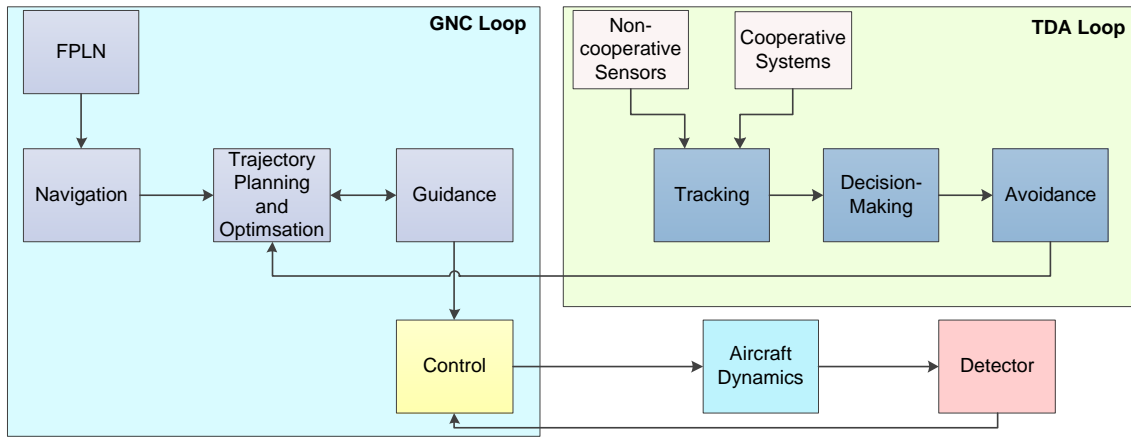


Figure 2.19. GNC and TDA loops.

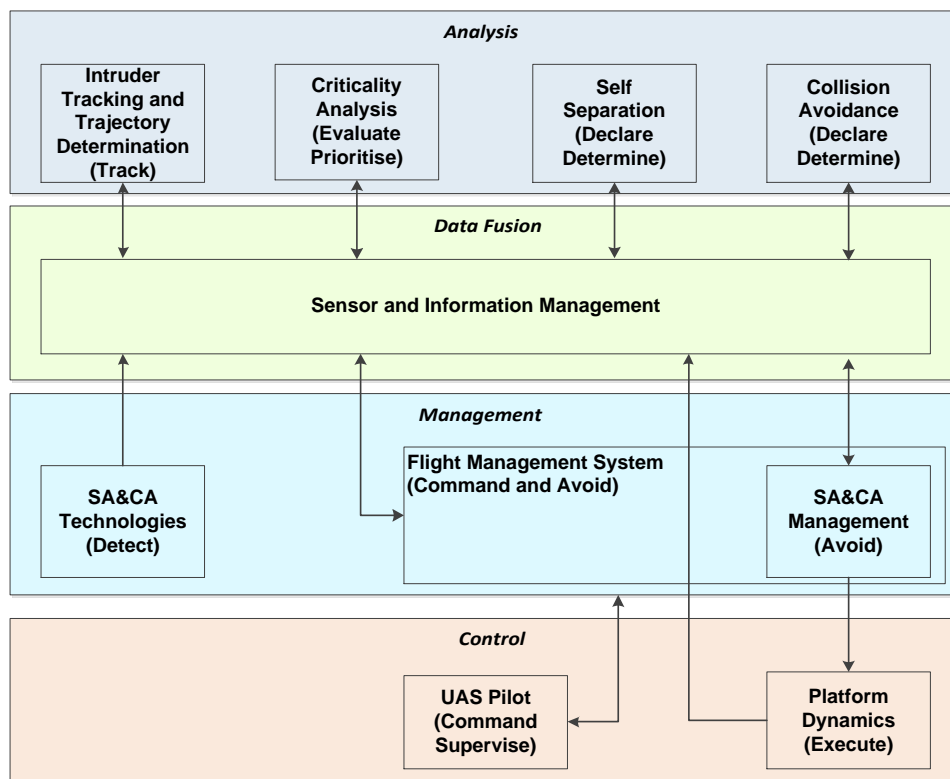


Figure 2.20. SA&CA tasks (adapted from [71]).

## 2.8 Multi-Sensor Data Fusion Algorithms for SA&CA

In Intelligent Surveillance Systems (ISS) technologies such as computer vision, pattern recognition, and artificial intelligence are developed to identify abnormal behaviors in videos. As a result, fewer human observers are needed to monitor more scenarios with high accuracy. This means that surveillance operations are constantly evolving in an increasingly autonomous fashion, where human interaction is needed less frequently. Multiple sensing is the ability to sense the environment with the concurrent use of several, possibly dissimilar, sensors [72]. The reason for multiple sensing is to be able to perform



more tasks, more efficiently, in a reliable way [72]. However, when applied to UAS, engineering focus is on an increasingly intelligent approach to design and integration for incorporating multiple sensing elements. Therefore surveillance systems on board UAS are also being developed to reduce the workload of pilots and to increase autonomy in the vehicle. Surveillance systems use a number of sensors to obtain information about the surrounding environment. Visual and thermal sensors are two of the many sensors used. To fully exploit the fact that more than one sensor is being used, the information is fused using an approach called data fusion. Data fusion is implemented in research areas such as signal processing, pattern and image recognition, artificial intelligence, and information theory. A common feature of these architectures is that they incorporate multiple levels of information processing within the data fusion process [73, 74]. More specifically, sensor fusion is the result of combining sensor data from diverse sources so the resulting information has less uncertainty than if these sources were used as an individual sensor. Current state-of-the-art airborne sensors and Multi Sensor Data Fusion (MSDF) methods for surveillance detection and tracking tasks, have employed non-cooperative and cooperative sensors/systems for SA&CA solutions. Data fusion of surveillance sensors utilizes these sensors/systems in order to detect and track obstacles and intruders.

MSDF is an effective way of optimizing large volumes of data and is implemented by combining information from multiple sensors to achieve inferences that are not feasible from a single sensor or source [75]. MSDF is an emerging technology applied to many areas in civilian and military domains, such as automated target recognition, battlefield surveillance, and guidance and control of autonomous vehicles, monitoring of complex machinery, medical diagnosis, and smart buildings [76]. Techniques for MSDF are drawn from a wide range of areas including pattern recognition, artificial intelligence and statistical estimation [75]. There are many algorithms for data fusion which optimally and sub-optimally combine information to derive a processed best estimate. Mathematically, the type of system determines if the system can be optimally estimated. In general, linear systems can be optimally estimated with the original Kalman Filter and non-linear systems are sub-optimally estimated with approximation techniques which linearize the non-linear system. Real life navigation and surveillance applications are almost always described by non-linear equations therefore approximation techniques are commonly applied, some techniques include; the Extended Kalman Filter (EKF), Unscented Kalman Filter (UKF), Square Root-UKF (SR-UKF), Cubature Kalman Filter (CKF), Point Mass Filter (PMF) and the particle filter [77-79]. In the past three decades, the EKF has become the most widely used algorithm in numerous nonlinear estimation

applications [80]. In comparison to the UKF, the EKF is difficult to manipulate (i.e. computationally intractable) due to derivation of the Jacobean matrices. Furthermore, the accuracy of the propagated mean and covariance is limited to first order Taylor series expansion, which is caused by its linearization process [81]. The UKF overcomes the limitations of the EKF by providing derivative-free higher-order approximations by approximating a Gaussian distribution rather than approximating an arbitrary nonlinear function [82]. The UKF is more accurate and robust in navigation applications by also providing much better convergence characteristics. The UKF uses sigma points and a process known as unscented transform to evaluate the statistics of a nonlinear transformed random variable. Due to the advancements in modern computing technologies, algorithms such as the UKF and the PF can now be implemented effectively for real time systems. The aim of this research is to adopt MSDF techniques to provide the best estimate of track data obtained from cooperative systems and non-cooperative sensors. The UKF is used to process the cooperative sensors and a PF is adopted to combine the non-cooperative sensor measurements. The PF or Sequential Monte Carlo (SMC) are a broad and well known category of Monte Carlo algorithms developed in the last two decades to provide approximate solutions to intractable inference problem. The methodology is used for nonlinear filtering problems seen in Bayesian statistical inference and signal processing. Using the PF for filtering or estimation problems, the observations are used to measure internal states in systems. The system dynamic process and sensors are also filled with random noise utilised in the filtering process. The objective is to compute the posterior distributions of states or hidden variable, from the noisy and partial observations. The main objective of a PF is estimating the posterior density of the hidden state variables using the observation variables if applicable. The PF is designed for a hidden Markov model, where the system consists of hidden and observable variables. The dynamical system describing the evolution of the state variables is also known probabilistically obtained from the prediction and updating process of the PF. A set of particles is initialised in the PF to generate a sample distribution, where each particle is assigned a weight, which represents the probability of that particle to be sampled from the probability density function. Weight disparity leading to weight collapse is a common issue encountered in these filtering algorithms; however it can be mitigated by including a resampling step before the weights become too uneven.

ADS-B and TCAS are exploited in the MSDF architecture, which provide position and velocity estimates for the detection and tracking solution. The MSDF technique used to fuse the cooperative sensors is the UKF (which is MSDF technique N), the MSDF technique

used to fuse the non-cooperative sensors is the PF (which is MSDF technique NC) and the MSDF technique used to fuse the MSDF N and MSDF NC sensors is based on a memory based learning. In order to estimate the non-linear functions, approximation methods are used. On-board trajectory replanning, with dynamically updated constraints based on the intruder and the host dynamics, is at present used to generate obstacle avoidance trajectories. The states of the tracked obstacles are obtained by adopting UKF/PF or other MSDF techniques, which are then used in order to predict the trajectory in a given time horizon.

The real world may be described by nonlinear differential equations, and measurements may not be a function of those states. In many problems, in this case, the measurements are a linear function of the states, but the model of the real world is nonlinear. In order to predict the track of the target object/aircraft MSDF techniques are used to obtain the best estimate and then a probabilistic model is used. The UKF is used to obtain a better estimate; therefore a better prediction will be obtained because the errors are essentially reduced. The detection information provided by several awareness sensors should be evaluated and prioritized taking into account the rest of the UAS information such as telemetry, flight plan and mission information [83]. A multi-sensor surveillance system includes function such as detection and tracking which utilize cooperative and non-cooperative information sources in a multi-sensor architecture. The output of an effective multi-sensor tracker provides a unified surveillance picture with a relatively small number of confirmed tracks and improved target localization. Global multi-sensor fusion and tracking should be capable of processing (potentially anomalous) AIS tracks and contact-level or track-level data from other sensors to produce a single, consolidated surveillance picture. The following filters have been used for implementing TDA loops [84]:

*Tracking for single object non maneuvering target*

1. Optimal Bayesian filter
2. Kalman Filter
3. Extended Kalman Filter
4. Unscented Kalman Filter
5. Point Mass Filter
6. Particle Filter

*Manoeuvring object tracking*

1. Optimal Bayesian filter
2. Generalized pseudo-Bayes Filters (of order 1 and order 2)

3. Interactive Multiple Models
4. Bootstrap Filter (Auxiliary)
5. Extended Kalman Auxiliary Particle Filter

*Single Object Tracking in Clutter*

1. Optimal Bayesian filter
2. Nearest neighbour filter
3. Particle filter
4. Extended Kalman auxiliary particle filter

*Single- and Multiple-Object Tracking in Clutter: Object-Existence-Based Approach*

1. Optimal Bayes' recursion
2. Joint Probabilistic Data association (JPD)
3. Interacting Multiple Models – Joint Integrated Probabilistic Data Association (IMM-JIPDA)

*Multiple-object tracking in clutter: random-set-based approach*

*Random Finite Set Formalism (RFS)*

1. Optimal Bayesian multi-object tracking filter
2. Probabilistic hypothesis density approximation

*Approximate filters*

1. Gaussian mixture probability hypothesis density filter
2. Particle probability hypothesis density filter
3. Gaussian mixture cumulative probability hypothesis density algorithm

*Object-existence-based tracking filter*

1. Integrated probabilistic data association filter

Several well-known Bayesian filtering algorithms are employed for the single, multiple, manoeuvring and non-maneuvring object tracking problem. Manoeuvring objects are those objects whose dynamical behaviour changes overtime. An object that suddenly turns or accelerates displays a manoeuvring behaviour with regard to its tracked position [84]. While the definition of a manoeuvring object extends beyond the tracking of position and speed, historically it is in this context that manoeuvring object tracking theory developed. This service has to incorporate 4D navigation in order to know at what moment the aircraft is going to arrive at the different flight plan waypoints.

The Unscented Kalman Filter (UKF):

The UKF is an alternative to the EKF, and shares its computational simplicity while avoiding the need to derive and compute Jacobians and achieving greater accuracy

[84]. The UKF is based upon the unscented transformation process: this method approximates the moments of a non-linearly transformed random variable. The unscented transformation can be used as the basis of a non-linear filtering approximation which has the same form as the EKF but is derived in a quite different manner. The posterior PDF of  $x_k$  using Bayes' rule is given by:

$$p(X_k|y^k) = p(X_k, y_k|y^{k-1})/p(y_k|y^{k-1}) \quad (2.27)$$

The UKF approximates the joint density of the state  $x_k$  and measurement  $y_k$  conditional on the measurement history  $y^{k-1}$  that is approximated by a Gaussian density expressed as:

$$p(x_k, y_k|y^{k-1}) = N\left(\begin{bmatrix} X_k \\ y_k \end{bmatrix}; \begin{bmatrix} \hat{x}_{k|k-1} \\ \hat{y}_{k|k-1} \end{bmatrix}, \begin{bmatrix} P_{k|k-1} & \Psi_k \\ \Psi_k^T & S_k \end{bmatrix}\right) \quad (2.28)$$

This implies that:

$$p(y_k|y^{k-1}) = N(y_k; \hat{y}_{k|k-1}, S_k) \quad (2.29)$$

In general, the moments appearing in these equations cannot be computed exactly and so must be approximated. The UT is used for this purpose. The state prediction is performed by predicting the mean and covariance matrix of  $x_k$ , which represent the moments of transformation given by:

$$x_k = f(x_{k-1}) + v_k \quad (2.30)$$

where the statistics are taken for  $x_{k-1}$  given  $y^{k-1}$ . The predicted mean and covariance matrix are given by:

$$E(x_k|y^{k-1}) = E(f(x_{k-1}) + v_k|y^{k-1}) = E(f(x_{k-1})|y^{k-1}) \quad (2.31)$$

$$\begin{aligned} cov(x_k|y^{k-1}) &= cov(f(x_{k-1}) + v_k|y^{k-1}) = \\ &= cov(f(x_{k-1})|y^{k-1}) + cov(v_k) \end{aligned} \quad (2.32)$$

Approximations to the predicted mean and covariance matrix are to be obtained using the unscented transformation. Sigma points  $\chi_{k-1}^1, \dots, \chi_{k-1}^s$  and weights  $w^1, \dots, w^s$  are selected to match the mean and the covariance matrix of  $p(x_{k-1}|y^{k-1})$ . With  $\chi_k^i = f(\chi_{k-1}^i)$  where  $i = 1, \dots, s$ , the approximations for the predicted mean and covariance matrix are given by:

$$\hat{x}_{k|k-1} = \sum_{i=1}^s w^i \chi_k^i \quad (2.33)$$

$$P_{k|k-1} = Q_k + \sum_{i=1}^s w^i (\chi_k^i - \hat{x}_{k|k-1})(\chi_k^i - \hat{x}_{k|k-1})^T \quad (2.34)$$

The measurement prediction: The predicted statistics for the measurement  $y_k$  are moments of the transformation given by:

$$y_k = h(x_k) + w_k \quad (2.35)$$

where the statistics of  $x_k$  given  $y^{k-1}$  are available from the prediction step. Hence we have:

$$E(y_k | y^{k-1}) = E(h(x_k) | y^{k-1}) \quad (2.36)$$

$$\text{cov}(y_k | y^{k-1}) = \text{cov}(h(x_k) | y^{k-1}) + \text{cov}(w_k) \quad (2.37)$$

$$\text{cov}(x_k, y_k | y^{k-1}) = \text{cov}(x_k, h(x_k) | y^{k-1}) \quad (2.38)$$

Let  $\chi_k^1, \dots, \chi_k^s$  and  $w^1, \dots, w^s$  denote the sigma points and weights, respectively, selected to match the predicted mean and covariance matrix. The transformed sigma points are  $y_k^i = h(\chi_k^i)$ ,  $i = 1, \dots, s$ . The UT approximations to the moments are [83]:

$$\hat{y}_{k|k-1} = \sum_{i=1}^s w^i y_k^i \quad (2.39)$$

$$S_k = R_k + \sum_{i=1}^s w^i (y_k^i - \hat{y}_{k|k-1})(y_k^i - \hat{y}_{k|k-1})^T \quad (2.40)$$

$$\Psi_k = \sum_{i=1}^s w^i (\chi_k^i - \hat{x}_{k|k-1})(y_k^i - \hat{y}_{k|k-1})^T \quad (2.41)$$

The resulting expression for the posterior probability distribution function is given by:

$$p(x_k | y^k) = N(x_k; \hat{x}_{k|k}, P_{k|k}) \quad (2.42)$$

where:

$$\hat{x}_{k|k} = \hat{x}_{k|k-1} + \Psi_k S_k^{-1} (y_k - \hat{y}_{k|k-1}) \quad (2.43)$$

$$P_{k|k} = P_{k|k-1} + \Psi_k S_k^{-1} \Psi_k^T \quad (2.44)$$

As with the EKF, the UKF is strongly reminiscent of the KF, with the main difference being the dependence of the posterior covariance matrix on the observed measurements. In

UKF this occurs because the calculated sigma points generated in the UT process are moment approximations and are determined based on state estimates which are measurement dependent. Before concluding, we note that the assumption of additive noise in the dynamic and measurement equations has been made only for the sake of convenience [84]. The UT is equally applicable for non-additive noise. For instance, if the dynamic equation is  $x_k = g(x_{k-1}, v_k)$ , then the quality undergoing a non-linear transformation is the augmented variable  $z_k = [x_{k-1}^T, v_k^T]^T$ , which has the statistics  $E(z_k|y^{k-1}) = [\hat{x}_{k-1|k-1}^T, 0_{n,1}^T]^T$  and  $cov(z_k|y^{k-1}) = diag(P_{k-1|k-1}, Q_k)$ . The UT can be applied to the random variable  $z_k$  transformed through the function  $g$  to approximate the predicted state statistics. Since  $z_k$  is of dimension  $n_x + n_v$ , a larger number of sigma points will be required than for the case where the dynamic noise is additive. Similar comments hold for a measurement equation which is non-linear in the measurement noise. A summary of the UKF is given by below.

Algorithm:

1. Determine sigma points  $\chi_{k-1}^1, \dots, \chi_{k-1}^s$  and weights  $w^1, \dots, w^s$  to match a mean  $\hat{x}_{k-1|k-1}$  and covariances matrix  $P_{k-1|k-1}$ .
2. Compute the transformed sigma points  $\chi_k^i = f(\chi_{k-1}^i)$ ,  $i = 1, \dots, s$ .
3. Compute the predicted state statistics:

$$\hat{x}_{k|k-1} = \sum_{i=1}^s w^i \chi_k^i \quad (2.45)$$

$$P_{k|k-1} = Q_k + \sum_{i=1}^s w^i (\chi_k^i - \hat{x}_{k|k-1})(\chi_k^i - \hat{x}_{k|k-1})^T \quad (2.46)$$

4. Determine the sigma points  $\chi_k^1, \dots, \chi_k^s$  and weights  $w^1, \dots, w^s$  to match mean  $\hat{x}_{k|k-1}$  and covariance matrix  $P_{k|k-1}$ .
5. Compute the transformed sigma points  $y_k^i = h(\chi_k^i)$ ,  $i = 1, \dots, s$ .
6. Compute the predicted measurement statistics

$$\hat{y}_{k|k-1} = \sum_{i=1}^s w^i y_k^i \quad (2.47)$$

$$S_k = R_k + \sum_{i=1}^s w^i (y_k^i - \hat{y}_{k|k-1})(y_k^i - \hat{y}_{k|k-1})^T \quad (2.48)$$

$$\Psi_k = \sum_{i=1}^s w^i (\chi_k^i - \hat{x}_{k|k-1})(y_k^i - \hat{y}_{k|k-1})^T \quad (2.49)$$

7. Compute the posterior mean and covariance matrix

$$\hat{x}_{k|k} = \hat{x}_{k|k-1} + \Psi_k S_k^{-1} (y_k - \hat{y}_{k|k-1}) \quad (2.50)$$

$$P_{k|k} = P_{k|k-1} - \Psi_k S_k^{-1} \Psi_k^T \quad (2.51)$$

The Particle Filter:

There are different methods for target tracking, but particle filtering is one of the most important and widely used methods. The particle filter is an implementation of Bayesian recursive filtering using a sequential Monte Carlo sampling method. It is used in statistics and signal processing, where it is known as a bootstrap filter and a Monte Carlo filter respectively [85]. The target state is represented by  $x_t$  where  $t$  is time.  $z_t$  is the set of all observations. The posterior density function  $p(x_t|z_t)$  is represented by a set of weighted samples. Observations  $p(z_t|x_t)$  can be non-gaussian. The main aim is the estimation of the probability distribution function of the target object by a set of weighted samples  $S = \{(s^{(n)}, w^{(n)}) | n = 1, \dots, N\}$  such that  $\sum_{n=1}^N w^{(n)} = 1$  [86]. Based on the observations, the likelihood of each particle is applied in weight assignment by the equation below in each step:

$$\omega^{(n)} = p(z_t|x_t = s_t^{(n)}) \quad (2.52)$$

The particle filter consists of two stages, prediction and update. In the prediction state, next step particles are calculated by using current step particles and target state transition equations. In the update stage, the weights are assigned to new particles by the following equation [86]:

$$\omega_t^i \propto \omega_{t-1}^i \frac{p(z_t x_t^i) p(x_t^i | x_{t-1}^i)}{q(x_t^i | x_{t-1}^i, z_t)} \quad (2.53)$$

where  $q$  is the importance density function which is used in the sampling function. The posteriori density function is estimated by using the following equation:

$$p(x_t|z_t) = \sum_{i=1}^N \omega_t^i \delta(x_t - x_{t-1}^i) \quad (2.54)$$

The next step state vector is estimated by using the weighted average on current step particles with the following equation [86]:

$$\hat{x}_t = \sum_{i=1}^N w_t^i x_t^i \quad (2.55)$$

Sequential Importance Resampling Particle Filter:



One of the basic challenges in implementation of a PF is the appropriate choice of the proposal density function. One of the common suboptimal choices of the proposal density function is the transitional prior distribution [86].

$$q(x_t|x_{t=1}^i, z_t) = p(x_t|x_{t=1}^i) = N_{x_t}(x_t, \Sigma_t) \quad (2.56)$$

By substituting  $q(\cdot)$  into each particle's weight, a new weighting can be calculated based on:

$$\omega_t^i \propto \omega_{t=1}^i p(z_t|x_t^i) \quad (2.57)$$

In each step of the SIR algorithm, re-sampling is done after state estimation. After re-sampling, weights of all particles are equal to  $\frac{1}{N}$  where  $N$  is the number of particles. Hence the above equation is modified as:

$$\omega_t^i = p(z_t|x_t^i) \quad (2.58)$$

The implemented algorithm involves the initialisation of the particles using prior distribution of the tracked object.

Then, for all the particles, the following steps are implemented:

- a. Prediction: Generate particles using dynamic model

$$\hat{x}_{t+1}^i \sim p(x_{t+1}|x_t^i) \quad (2.59)$$

- b. Weighting: Calculate weight for particle

$$\omega_{t+1}^i \sim p(z_{t+1}|x_t^i) \quad (2.60)$$

The normalization of the particle weights is given by:

$$\hat{\omega}_{t+1}^i = \frac{\omega_{t+1}^i}{\sum_{i=1}^N \omega_{t+1}^i} \quad (2.61)$$

- c. Resampling:

The particles are resampled and new particles are obtained with same weight and repeat from stage 2.

$$\left\{ \left( x_{t+1}^i, \frac{1}{N} \right) \right\}_{i=1}^N = \text{Re-sampling} \left\{ (x_{t+1}^i, w_{t+1}^i) \right\}_{i=1}^N \quad (2.62)$$

Statistical Learning Techniques:

Statistical learning theory is a framework for machine learning drawing from the fields of statistics and functional analysis. Statistical learning concerns itself with finding a predictive function for a task/problem. The goal of learning is prediction. Learning falls into many categories, including supervised learning, unsupervised learning, online learning, and reinforcement learning. From the perspective of statistical learning theory, supervised learning is best understood. Supervised learning involves learning from a training set of data. Every point in the training set is an input-output pair, where the input maps to an output. The learning problem consists of inferring the function that maps between the input and the output in a predictive fashion, such that the learned function can be used to predict output from future input. In machine learning problems, a major problem that arises is that of over fitting. Because learning is a prediction problem, the goal is not to find a function that most closely fits the (previously observed) data, but to find one that will most accurately predict output from future input [86, 87]. Some examples of statistical learning techniques include, but are not limited to: artificial neural networks, instance based learning, learning with hidden variables and kernel machines, which are succinctly depicted in Figure 2.21 [88].

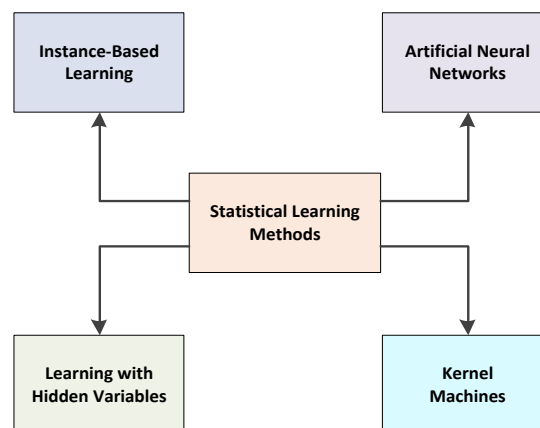


Figure 2.21. Intelligent techniques for SA&CA MSDF (Adapted from [89]).

## 2.9 UTM System

UAS Traffic Management (UTM) supports civilian low-altitude airspace and UAS operations [90]. The UTM system comprises of all of the elements required to support and execute UAS operations in the low-altitude airspace. Specifically, the integration of small size UAS (typically 55 lbs and below), is targeted in the NASA's initiative under AOSP to ensure safety and operation efficiency.

Some lessons learnt from low-altitude uncontrolled airspace operations of helicopters, gliders and general aviation aircraft can also be helpful. UTM system development

accommodates manned aircraft along with Line-of-Sight (LoS) and Beyond LoS (BVLoS) UAS operations in the low-altitude airspace. The supporting components include, but are not limited to, the NAS information, Communication and Technology (ICT) systems, UAS systems, regulations, policies, and procedures. The operation of multiple conventional and autonomous transport vehicles is an important emerging issue to be considered in the development of future traffic management systems.

- Near-term Goal: Safely enable initial low-altitude UAS as early as possible;
- Long-term Goal: Accommodate increased demand with highest safety, efficiency, and capacity.

Figure 2.22 depicts the functional description of the UTM, and its functions are shown in Figure 2.23.

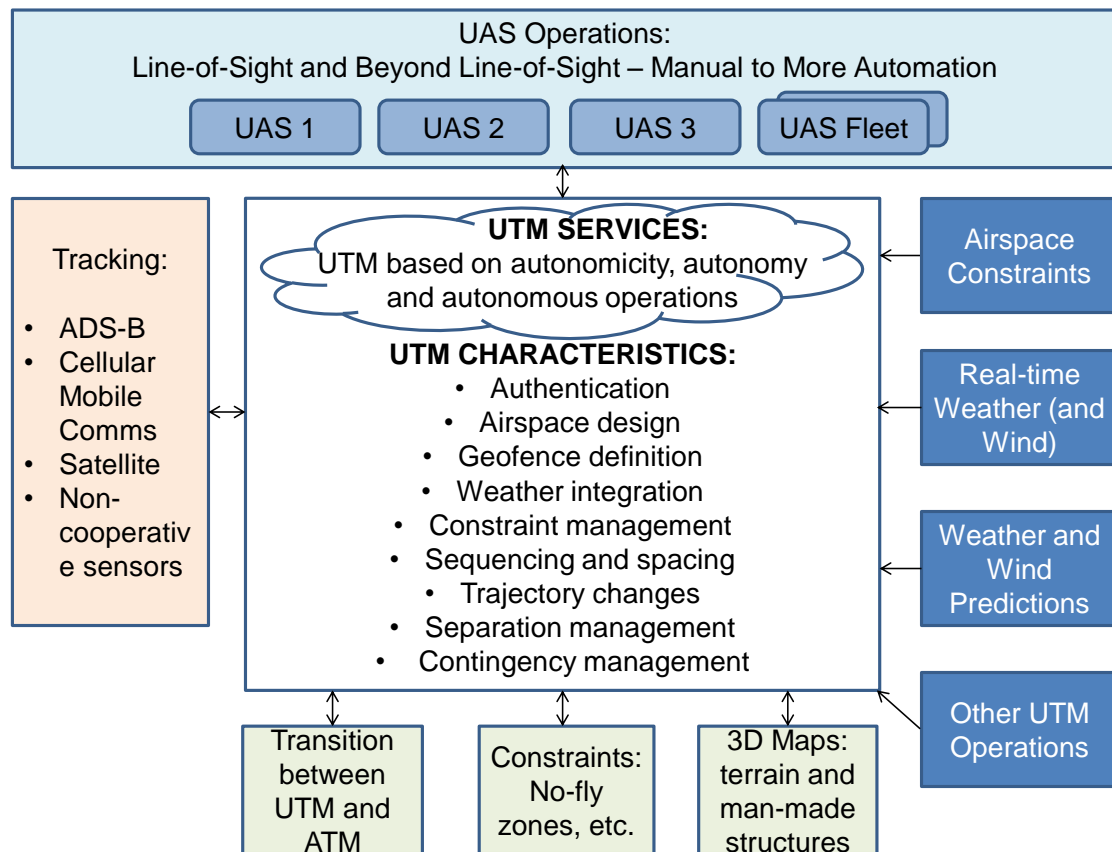


Figure 2.22. UTM system architecture.

The UTM will support a wide variety of UAS, from those equipped with minimalistic avionics to autonomous UAS [91-95]. The inputs to UTM will include: UAV mission/business flight plan or trajectory, real-time weather and wind, predicted wind and weather, airspace constraints (dynamically adjusted), community needs about sensitive areas (dynamically adjusted), and three-dimensional maps that include man-made structures

as well as natural terrain. The UTM will need persistent Communication, Navigation and Surveillance (CNS) coverage to ensure and monitoring conformance to the constraints. This could be provided by a combination of low-altitude radar, cellular tower, satellite, and other means. The important aspect is that coverage is continuous robust, reliable, and redundant in order to ensure the monitoring and support needed for safe operations. Although the role of human operators needs to be carefully defined, it is anticipated that the humans will provide overall direction and goal-setting for the UTM system. The self-configuration aspect of UTM will determine whether the operations should continue given the current and/or predicted wind/weather conditions.

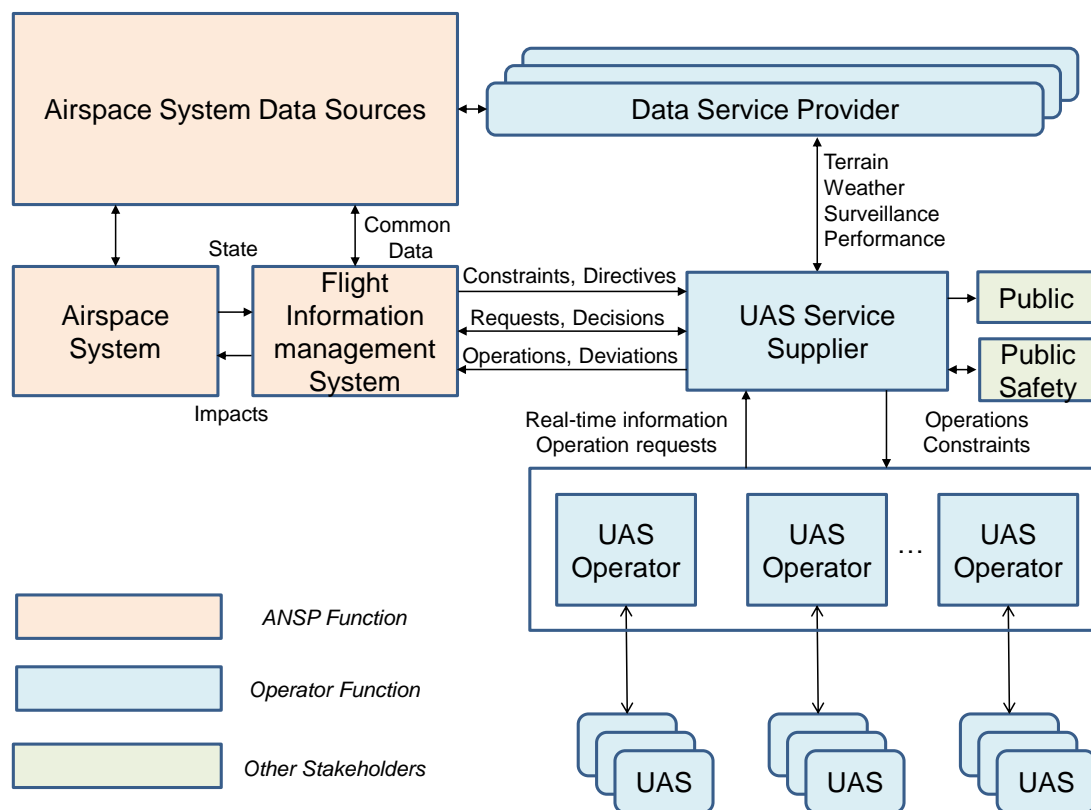


Figure 2.23. UTM functions and stakeholders.

The self-optimization aspect of UTM refers to given the traffic demand, and how the airspace must be configured to make the operations most efficient in light of traffic demand. The self-protection aspect will ensure that all sensor data related to CNS and vehicles is accurate and operating at the desired integrity. Should the data integrity, sensor inputs, and precision reduce, the self-configuration aspect will identify the appropriate strategy such as increased separation buffer or gradually halting the operations. The self-healing aspect refers to safely returning to normalcy. The human

may be the ultimate decision-maker regarding the continuation and return to normalcy of the operations.

A list of UTM functions is provided below:

#### 1. Airspace Operations and Management

- Current: ~500 ft. and below;
- Geographical needs and applications;
- Rules of the airspace: performance-based;
- Geofences: dynamic and static.

#### 2. Wind and Weather Integration

- Actual and predicted winds/weather;
- Operator responsibility.

#### 3. Congestion Management

- Demand/capacity imbalance;
- Only if needed –corridors, altitude for direction, etc.

#### 4. Separation Management

- Airspace reservation;
- Vehicle-to-vehicle and vehicle-to-UTM;
- Tracking: ADS-B, cellular, & satellite based;
- Traffic avoidance;
- SA&CA to manned aircraft predicated on right of way;
- Status and intent exchange in accordance with standards;
- Collaborative decision making;
- Contingency planning and response (system outages, unreported weather, etc.).

#### 5. Route Structure

- Only where needed for safety or efficiency of flight;
- Procedural rules-of-road (corridors, altitudes, etc.).

#### 6. Air Traffic Control

- Integrated with manned air traffic control, where positive UAS control is required for safety or efficiency of flight;
- Static or dynamic application (e.g., ability to respond in crisis situation where sustained mixed operations are required).

#### 7. Flow Management

- Only where needed for safety or efficiency of flight;
- Manage access into areas of operation, not particular operation;

#### 8. Contingency Management

- Large-scale GPS or cell outage;
- Cyber-physical attacks.

9. Track and Locate (cellular communication systems, ADS-B, satellite, etc.)

- Conflict (V2V, sense and avoid) and hazard avoidance.

10. Last and First 50 Feet Operations

In terms of granting the required levels of operational safety when considering the integration of autonomous traffic in the existing ATM and planned UTM networks characterised by dense/mixed traffic and high levels of service, the emphasis is on network-centric equipment that can meet strict performance requirements while also supporting enhanced traffic management and optimisation functionalities. In particular, in order to grant the required surveillance performance and autonomous Separation Assurance and Collision Avoidance (SA&CA) capabilities for unrestricted access to controlled airspace, UAS surveillance equipment involve a combination of non-cooperative sensors and cooperative systems. Ground-based and satellite based data-link communication systems act as the backbone of LoS and BLoS Vehicle-to-Vehicle (V2V) and Vehicle-to-UTM (V2U) information exchanges [96].

The UTM system development is aimed at introducing safe separation functionalities by exploiting the concept of dynamic geo-fences and providing a solution driven by the unified approach to SA&CA. In the long term and to support faster-moving hybrid unmanned vehicles, UTM research will have to develop efficient network-centric functionalities for trajectory prediction and negotiation both within individual controlled airspace/network sectors and across multiple sectors belonging to the same region, also considering the inbound/outbound flows from adjacent regions. Three different operating environments within the airspace systems that will be in the UTM system concept of operations are [90]:

- UAS operations inside uncontrolled Airspace (class G): In this environment, no interaction with controlled air traffic will occur as the UAS operations occur outside of controlled airspace operations. However, UAS share the airspace with other airspace users, such as general aviation aircraft, helicopters, gliders, balloons, and parachutists;
- UAS operations inside controlled airspace, but segregated from controlled air traffic: As many use cases of small UAS operations would benefit from operating near airports and inside controlled airspace, there could be segregated areas within the controlled airspace that can be made available for UAS operations. These could be transition tunnels or blocks of airspace that are made available

depending on current airport and airspace configurations and other criteria related to controlled airspace operations and

- UAS operations integrated into the controlled air traffic flows: When UAS are integrated into the controlled air traffic flows they are expected to behave exactly like traditional aviation and meet all the requirements set forth currently for operations in the controlled airspace classes.

SA&CA is the underlining core element of any UTM system implementation as shown in Figure 2.24. The approach will support both avionics/ATM system mediated scenarios as well as support a fully autonomous implementations.

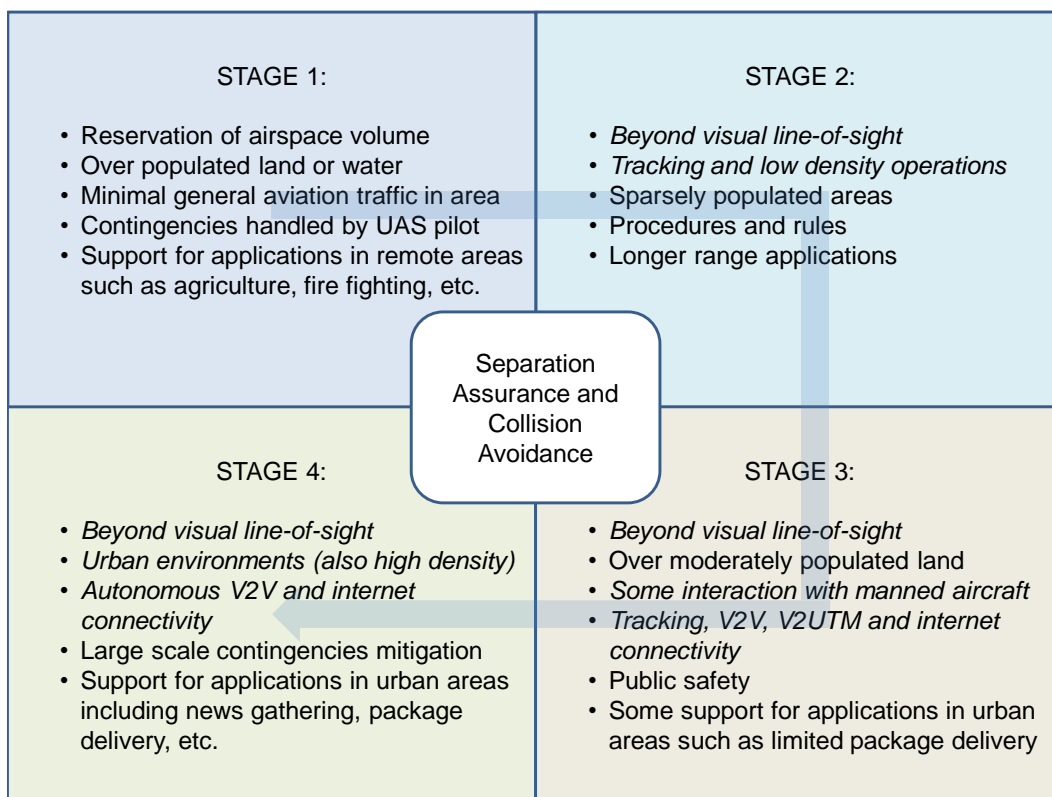


Figure 2.24. Role of SA&CA in UTM.

In order to address the identified challenges, a number of strategies can be implemented. One such challenge is the definition of a number of UTM system operational geographies described for ensuring safety of UAS operations. There are multiple geographical regions specific to an operational plan including flight geographies, conformance geographies and protected geographies. The specifications of each of these defined geographical regions have been described within the UTM system. In a general case, the flight geography is dictated by the plan provided by the

UAS operator. Then the UTM system adds a conformance buffer and computes the conformance geography.

Operation of the UAS is expected to stay within the conformance geography at any point of time, and all violations will be notified as appropriate. The UTM system then adds a second buffer and computes a protected geography that the system uses for deconflicting purposes. The final plan is prepared by also including constraints at the time of submission and then activation is performed. It is ensured that protected geographies from separate operations never overlap in 4D (space and time) with each other or with any no-fly constraint. Some envisioned rules for operation plan validation are:

- at least one operational volume has to be included;
- there cannot be more than 10 operational volumes;
- the minimum time for validating each operational volume should be 2 minutes;
- a minimum time for each operational volume (dictated by mission endurance requirements and operational complexity);
- a fixed area for a flight geography (given by a polygon). E.g., 55756800ft<sup>2</sup> (2 square miles);
- a fixed length for a flight geography (given by a line string). E.g., 5280ft (1 mile).

The UTM system verifies the identification (by assigning a unique number) and other information (e.g. maximum speed in given weather considerations). This information is used to determine the conformance geometry. The conformance buffer can also be determined using other variables such as vehicle type (fixed wing or rotor), Size, Weight, and Power (SWaP) requirements. UTM system also verifies the validity of altitude information of a given plan by using the available digital terrain elevation data. The system also checks the plan and vehicle capability with respect to weather (wind) conditions and favourable conditions [97, 98].

Flight geography is the topography submitted by the operator via the UTM system and it describes the physical location of the planned operation. A single flight geography contains the geographic information together with time data to effectively form a reservation for a 4D volume of airspace. Multiple flight geographies may be submitted with a single operation submission to form a chain of volumes that will be used by that operation. This allows for more efficient use of the airspace by reserving smaller pieces for longer running operations. The collection of flight geographies is called the operation volumes. Operational volumes are used for determining the dynamic geo-fences using the unified approach to SA&CA. In a near-term implementation, the collection of



operation volumes would contain exactly one flight geography and the entire flight geography would necessarily be required to be within line of sight of the UAS Controller. In the long term, there could be either multiple flight geographies or at least one that may be beyond visual LoS of the UAS controller, or both.

Conformance geographies are defined by the UTM System and are derived from the UAS operation centre submitted flight geography/geographies. There is exactly one conformance geography per flight geography. The approach is, if the operator submits a polygon area for the flight geography, the conformance geography would be represented by the same polygon. But efficient use of flight geography can be performed by using a structured polygon based approach, by constructing a group of hexagons and also by incorporating cellular infrastructure concepts. In that case, the operator submits a line string for the flight geography and the conformance geography would be a polygon containing that line string. If an active operation violates its conformance geography, there will be a trigger in the UTM system to mark that operation as nonconforming. The UTM system notifies the UAS operational centre that the operation is nonconforming and must take immediate corrective action to bring the operation back into conformance with its submitted plan.

The UTM system defines an additional region around the conformance geography called the protected geography. This volume will be used by the UTM system to strategically deconflict operations from each other, along with other constraints in the system. If the UTM system defined protected geography for a proposed operation intersects any known constraints in the system, the proposed plan will be rejected. Thus, it is the protected geography that drives acceptance or rejection of an operational plan. The operational geographies are shown in Figure 2.25.

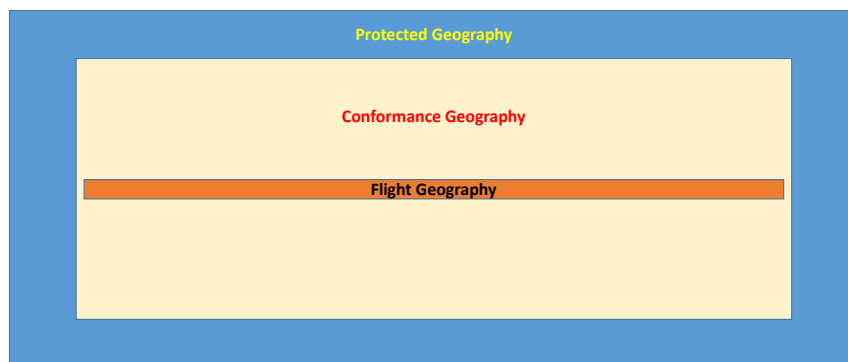


Figure 2.25. UTM system concept - operational geographies.

When there are multiple UAS operating in the same topography, then operational geographies are defined distinctively for each UAS occupying the topography. The operational geographies of multiple UAS accessing the same topography are shown in Figure 2.26.

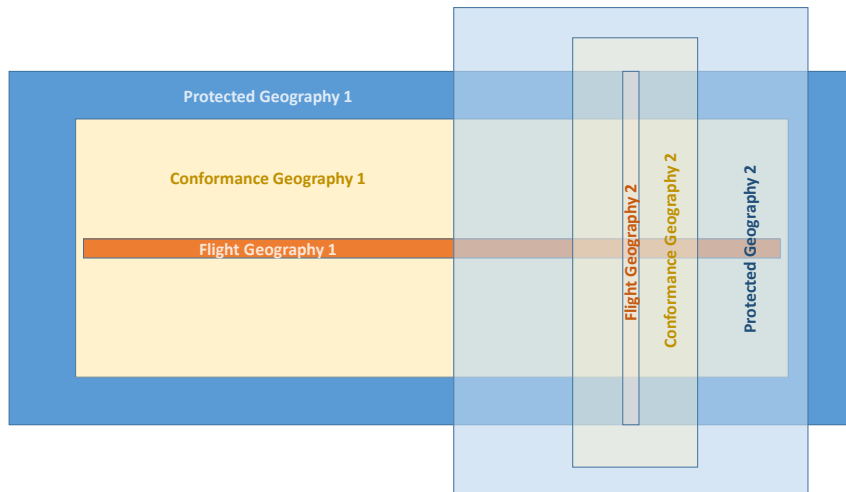


Figure 2.26. UTM system concept - operational geographies of multiple UAS.

By evaluating these operational geographies, the NG-FMS generates 4D trajectories that are then evaluated for SA&CA, given the surveillance information from the UTM system.

## 2.10 Dependency on LoS and BLoS Communications

The airworthiness requirements regarding CA&CA capabilities are highly dependent on the operating modes. These modes are defined below.

Visual line-of-sight is defined by ICAO as being “a mode of UAS operation in which the flight crew monitors the flight path in relation to other aircraft, persons, vehicles or structures through direct and unaided visual contact with the aircraft, in order to maintain separation and collision avoidance.”

Beyond VLoS (BVLoS): In this mode the aircraft is controlled from a GCS that is equipped with necessary instrumentation and displays. When a communication relay is employed, say using satellites, it is generally referred to as Broad RLoS (BRLoS). An UAV can be operated in BRLoS but it can be still within the visual line-of-sight. There might be propagation effects including interference and others, but the UAV can still be observed in a clear sky.

In VLoS flight conditions, unmanned aircraft are constrained to very low altitudes in order to be visible and also to enable control by the remote pilot/operator. ICAO rules state that, except for take-off and landing flight phases, the minimum flight altitude has to be

above 500 ft. In BVLoS/BRLoS operations, SA&CA algorithms are required to support the remote pilot in the accomplishment of the following tasks:

- maintaining appropriate separation distance from other airspace users;
- avoidance of collision with terrain and obstacles;
- avoidance of severe/adverse weather;
- maintaining appropriate flight visibilities and distance from clouds;
- visual observation of lighting and markings;
- visual observation of any in flight interception signals;
- visual observation of the landing/departure runway;
- visual observation of next aircraft where reduced separation is approved.

## 2.11 Towards Higher Levels of Autonomy

Autonomy can be defined as the capability of making decisions without assistance by human operators. Autonomy in UAS is essential to both increase the utility of the UAS and the safety of its operation, as it allows the unmanned aircraft to avoid hazardous situations if failures occur in the C2 loop [99]. Levels of autonomy were initially defined by Sheridan [100]. Sheridan's 10-level scale of autonomy is based on the decision-maker (human or system) and on how the decisions are executed. Different implementations of Sheridan's scale were considered. UAS can be configured for autonomous, overridable, aided and deliberate operations and are listed in Table 2.10.

These levels are based on information acquisition, information analysis, decision and action selection, as well as action implementation functions. According to the classification identified in the autonomous modes, UAS usually operates at Pilot Authority and Control (PACT) level 3 [100].

The system communicates to the UAS GCS remote pilot any potential hazards that are detected and the suggested resolution to enable him/her to make a decision for executing an avoidance manoeuvre.

However, in the case of imminent collision situations, if the remote pilot does not react in time, the SAA systems operates at PACT level 5 (autonomous mode of operations) and executes the avoidance actions. The expert processing required is grant UAS the appropriate levels of autonomy can be attained either by knowledge-based algorithms or by more advanced forms of machine intelligence. Notwithstanding, it shall be noted that autonomous decision-making in UAS is not limited to safety-critical purposes, and usually accounts for other features, such as performance optimisation. Therefore, the

costs of certification could be managed by reducing the number of sub-systems/lines of code subject to certification requirements. Licensing already-certified software modules could also help manage these costs. However, unlike software safety, in terms of system safety requirements, new systems deploying certified algorithms still need to be certified themselves in very specific contexts, as the software may be running on different hardware, be configured differently, be employed in different operational contexts, etc.

Table 2.10. Classification of autonomy levels (Adapted from [100]).

Automation mode	Operator Control	Sheridan Scale	Outline of the Human-Systems Interaction
Autonomous	Executive	9-10	The system performs all aspects of decision-making and informs the operator after execution, if required, per pre-planned criteria or on operator's request.
Overridable	Supervisory	6-8	The system generates decision alternatives and a preferred option for execution and informs the operator in time for override intervention.
Aided	Consent-Based	3-5	The system generates decision alternatives and recommends one to be carried out – but only after operator's approval. The operator may select alternative options.
Deliberate	Manual	1-2	The system executes commands initiated by the operator (the system may provide and/or recommend decision alternatives to the operator).

The technologies for airborne and ground systems are largely evolving independent from UAS autonomy technologies except for the emerging air taxi (on-demand aviation) entrepreneurs who assume fully-autonomous, human-occupied platforms analogous to self-driving cars. Emerging technologies in the autonomous car domain are supporting the tasks to carry out by a human occupant, who has no particular driving expertise. Some recently evolving research is available about this emerging application that links UAS-centric autonomy technologies with manned aviation [101-103]. It is also required to consider the implications of the proposed UTM system techniques on existing policies and practices. These include addressing the new requirements for risk management (UAS collision with another UAS when flying over unpopulated areas), specifications, system architecture, required CNS performance, etc. [104-106].

## 2.12 SA&CA Requirements

It will be necessary that automated SA&CA systems provide a level of safety equalling or exceeding that of manned aircraft (Title 14 Code of Federal Regulations). In July 2004, an endeavour to set the standards for this equivalent level of safety was attempted when the ASTM subcommittee released Document F2411-04 (since amended to F2411-04e1) "Standard Specification for Design and Performance of an Airborne Sense-and-Avoid System" [107]. Since its release, this document has served as a guideline for developers and researchers working on UAS. In 2005, the United States Department of Defense (DoD) adopted these performance standards for its UAS program.

In order to safely integrate UAS into all classes of airspace, UAS must adhere to the same separation standards as manned aircraft and thus must be able to complete an ATC clearance in a timely manner. However, UAS are inherently different from manned aircraft in several aspects that affect end-to-end response time [108, 109].

For manned aircraft, the pilot is on board the aircraft and the control input is wired to the control surfaces and other systems of the aircraft. For UAS, the pilot is in a control station that is removed from the aircraft and the control input must travel wirelessly through the air or through a satellite relay, depending on the data link architecture, adding a delay not present with manned aircraft. The variable control delays can make the control of the UAS more difficult [110]. A summary of the SA&CA requirements for manned and unmanned aircraft are provided below:

General requirements include:

- The SA&CA algorithms shall detect both cooperative and non-cooperative collision threats during day and night and consider adverse weather conditions;
- The SA&CA algorithms shall notify the operator for any imminent collision risk and provide a collision resolution or execute an autonomous avoidance manoeuvre;
- The SA&CA algorithms shall consider any direction or warning from other avoidance systems;
- The SA&CA algorithms shall provide a recommended course to resume action after any avoidance manoeuvre.

Requirements of SA and CA include:

- The SA&CA algorithms shall warn the operator of obstacles within an estimated distance of 3000 m. In case of cooperative vehicles, the minimum separation

shall follow the standards stated by the FAA or other aviation regulatory authorities;

- The generated avoidance manoeuvre shall be based in the standards established in FAR §91.113 Appendix 3;
- The generated avoidance manoeuvre shall prevent mid-air collision and has to consider other avoidance manoeuvres generated by other systems such as TCAS;
- If the pilot avoidance manoeuvre increases the risk of collision with any other obstacle the system shall override the pilot command;
- If the pilot does not execute a return to course manoeuvre after an avoidance action, either from the FCS or from the operator, then the aircraft shall autonomously return to its original course.

Requirements for implementing autonomous actions include:

- The SA&CA algorithms shall execute an autonomous avoidance manoeuvre if the pilot does not perform the suggested resolution from the SA&CA system;
- The SA&CA algorithms shall provide the operator the necessary information on the progress of the autonomous manoeuvre (time and weather permitting);
- The SA&CA algorithms shall execute a return-to-course action after an autonomous manoeuvre is executed.

UTM requirements include:

- Communication, Navigation, and Surveillance, Prediction and Separation Management including SA&CA;
- Persistent communication, navigation, and surveillance coverage under day and night conditions;
- Communication, navigation, and surveillance coverage under all visibility conditions;
- Ability to sense, detect and track all moving objects at an altitude up to 10,000 ft. Most of the UAS for package delivery, wildlife monitoring, fire fighting, crop dusting, and other applications will operate at much lower altitudes. A starting point is Class G airspace under 2000 ft;
- Ability to predict potential collisions between UAS as well as between UAS and other moving objects including but not limited to birds, gliders, helicopters, model aircraft, general aviation aircraft, personal air vehicles, special purpose balloons, jet wind turbines, etc.;

- Ability to predict the trajectory for next mile and/or within the 5 minutes, whichever is higher.
- Ability to monitor separation among UAS and predict conditions where the crossing or separation minima will be violated. The horizontal separation minima be set to 1 mile at the beginning of UTM activity and will be reduced over time;
- Ability to provide persistent, redundant, coverage by sensors to areas where operations will be conducted.

The SA&CA requirements presented above assume a pilot-centric, manned-vehicle perspective. But there is a requirement to look at existing policies and best practices to modify them based on the new UAS requirements. For example, there is a possibility that a UAS can hit another UAS without risk when an overflying unpopulated region, which requires suitable policy changes but they are still at an embryonic stage when writing this thesis.

## 2.13 Research on SA&CA Avoidance Volumes

Some work that has been previously performed on calculating the avoidance/uncertainty volume in the context of SA&CA (manual as well as automated) are highlighted below:

- Collision Avoidance System and Method utilizing Variable Surveillance Envelope (Patent): In this work, the size and shape of the safety volume is monitored by the sensors and the volume is modified according to the speed and motion vectors of the aircraft or other traffic, so as to maximize efficient use of sensor capabilities and minimize the size, cost and power requirements of the system [111].
- UAS Collision Encounter Modelling and Avoidance Algorithm Development for Simulating Collision Avoidance: Detection of other traffic is performed by defining a geometric sensor model and a collision cone approach. Avoidance algorithms consist of proportional navigation guidance that uses information from the collision potential between the unmanned aircraft and other traffic [112].
- Dynamic Separation Thresholds for a Small Airborne Sense and Avoid System: In this method, the distance-based thresholds are replaced with time-based thresholds that account for intruder performance using turning flight geometry to implement a computationally inexpensive solution [113].
- UAS Collision Avoidance Algorithm Minimizing Impact on Route Surveillance: An aggregated collision cone approach is implemented to detect and avoid

collision with two or more aircraft simultaneously (geometric collision avoidance system) [114].

- UAS Insertion into Commercial Airspace - Europe and US Standards Perspective: The SC-203 and WG-73 definitions are considered, which define SAA to encompass two high level functions: Self Separation (SS) and Collision Avoidance (CA). Self-Separation is intended to resolve any conflict early, so that a UAS remains "well clear" of other aircraft and avoids the need for last-minute collision avoidance manoeuvres [115].
- 3D Obstacle Avoidance Strategies for UASs (Uninhabited Aerial Systems) Mission Planning and Re-Planning: The research presented in this work focuses upon mission planning tasks. A planning algorithm is described, which allows the vehicle to autonomously and rapidly calculate 3D routes [6]. The calculation of routes is based on obstacle avoidance strategies and on specific vehicle performance constraints [116].
- Development of a Mobile Information Display System for UAS Operations in North Dakota: This research focusses on estimating the current aircraft position uncertainty volume. The volume of any overlap of any aircraft's uncertainty volume with a UAV's uncertainty volume determines the current risk [117].
- Sensor Resource Management to Support UAS Integration into the National Airspace System: The research aims at proving resource allocation strategies and ensures aircraft adhere to the minimum separation requirement. An evolutionary algorithm is implemented and the Kalman filter's covariance matrices are used to determine positional uncertainty to predict separation requirement violations [118].
- Coordination of Multiple UAS for Tracking under Uncertainty: The research shows how Partially Observable Markov Decision Processes (POMDPs) can be used for controlling fleets of UAS under uncertainty [119].
- Self-Separation Support for UAS: Criteria are identified for defining requirements for a future SA and CA system Concept of conflict probing and the associated stability for the available data, interfaces and display are identified [120].
- Analysis of Well-Clear Boundary Models for the Integration of UAS in the NAS: A definition of well clear is provided to the SA concept for the integration of UAS into civil airspace. This research by NASA presents a family of well-clear boundary models based on the TCAS II resolution advisory logic. Analytical techniques are used to study the properties and relationships satisfied by the models. Some of these properties are numerically quantified using statistical methods [121]. Figure



2.27 shows the well-clear threshold. Based on the current ATM operations, a conflict is defined when an aircraft encounter happens within 3.5 NM of one another horizontally and within 2000 ft above an altitude level of 29,000 ft and 1000 feet below the 29,000 ft level. A self-separation volume is defined much larger than the collision volume but it may vary in size with operational area and airspace class [121]. In this case, a conflict is defined to occur when other traffic enters the self-separation volume. The self-separation threshold is then defined as the threshold boundary at which the host aircraft performs a maneuver to prevent other traffic from penetrating the self-separation volume. Hence, it can be the addition of the self-separation volume provides a performance goal that is analogous to the collision volume. The encounter geometry is then evaluated in the relative coordinate frame where the relative motion of the aircraft is analysed by investigating the dynamics of the intruder aircraft with respect to the host aircraft (Figure 2.28).

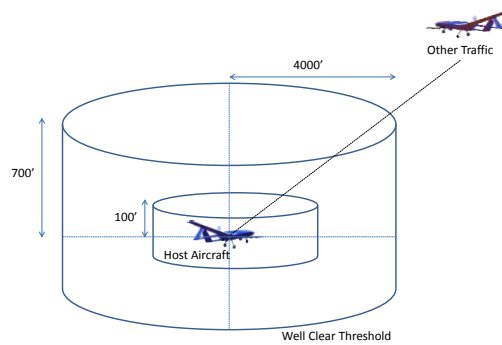


Figure 2.27. Well-clear threshold.

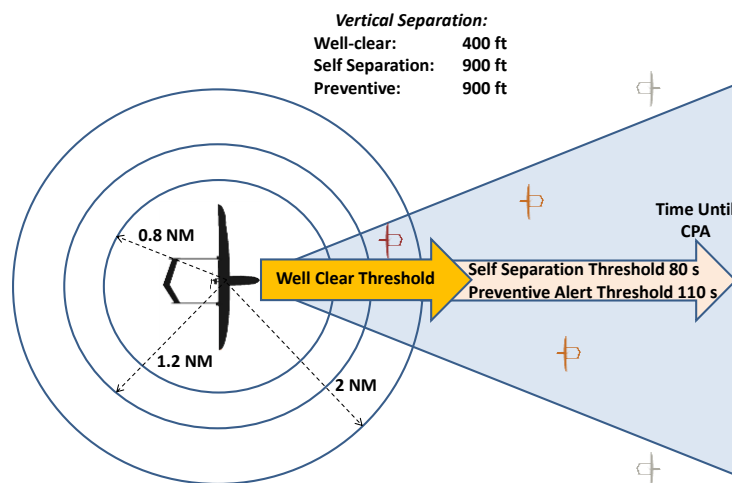


Figure 2.28. Well-clear based conflict detection method.

## 2.14 Case for a Unified Approach to SA&CA

In addition to the unique airworthiness, spectrum, and security considerations that come with having the cockpit outside the aircraft, UAS have challenges in complying with several of the 14 Code of Federal Regulations, Part 91 (general operating rules). Specifically, compliance with the following critical rules is [122]:

- Sec. 91.111 Operating near other aircraft:  
No person may operate an aircraft so close to another aircraft as to create a collision hazard.
- Sec. 91.113 Right-of-way rules - except water operations:  
When weather conditions permit, regardless of whether an operation is conducted under instrument flight rules or visual flight rules, vigilance shall be maintained by each person operating an aircraft so as to see and avoid other aircraft. When a rule of this section gives another aircraft the right-of-way, the pilot shall give way to that aircraft and may not pass over, under, or ahead of it unless well clear.

In response to the need for identifying the gaps in SA&CA functionalities, the U.S. Office of the Under Secretary of Defense (OUSD) established the SAA Science and Research Panel (SARP) in February 2011. The SARP consists of a panel of experts in technologies necessary to provide UAS with the ability to sense and avoid other aircraft. It advises the UAS Airspace Integration IPT chaired within OUSD and is currently co-chaired by individuals outside of the DoD to provide a more independent perspective of the state of the research and science efforts. The outcome of the workshops conducted by SARP was threefold [122]:

- A relationship between the, MIL-STD-882D safety methodology and the target level of safety methodology was proposed;
- A method to identify the contribution of qualitative hazards/mitigations to a quantitative level of safety was proposed;
- A list of disciplines that should undergo qualitative hazard analysis or comparable (instead of direct quantification) analysis was established.

Figure 2.29 indicates the highest number of research gaps belongs to SA&CA certification and qualification. The SARP certification workshop was held with the objective of determining the research and science efforts needed to answer key questions related to civil use UAS SA&CA certification.

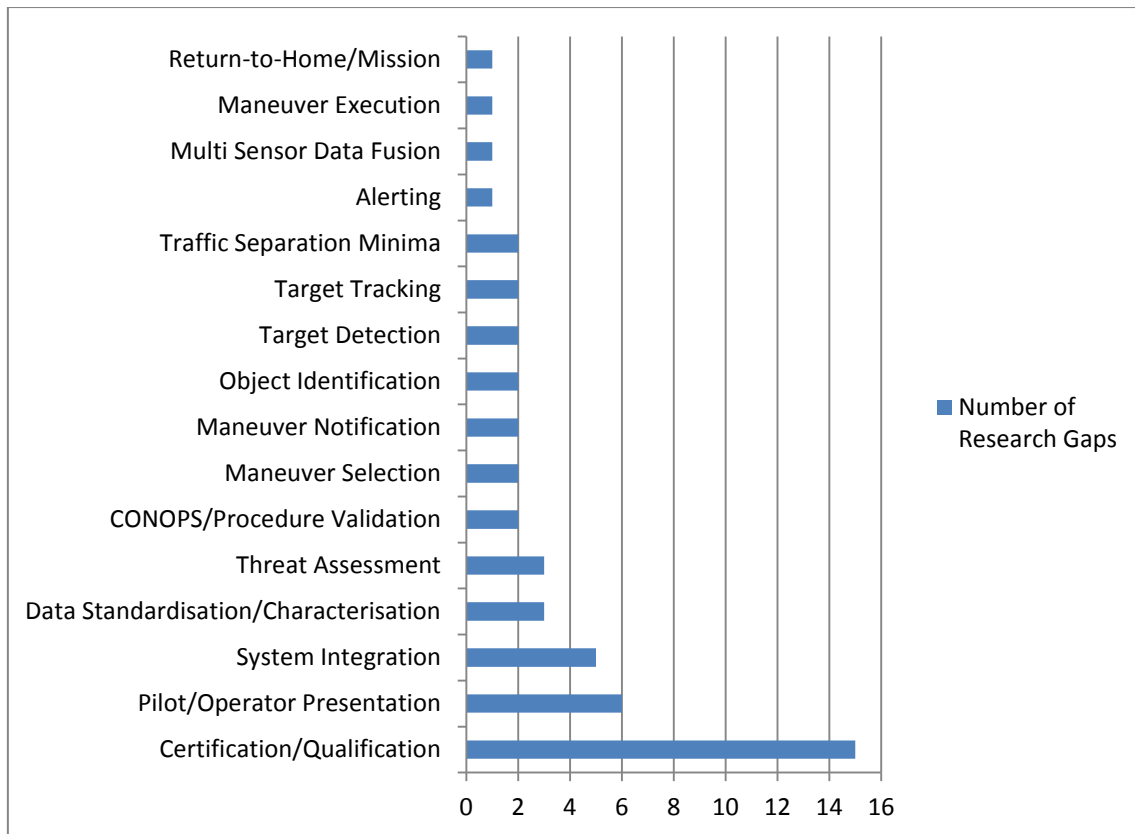


Figure 2.29. Number of SA&CA research gaps identified.

The workshop participants examined 12 research gaps identified by the SARP specific to SA&CA certification/qualification as shown in Table 2.11. The highest number of research gaps belongs to SA&CA certification and qualification. The SA&CA certification workshop was held with the objective of determining the research and science efforts needed to answer key questions related to civil UAS SA&CA certification.

Additionally, the following research questions arise in the context of UTM system implementation:

- What is the minimum separation between UAS and other operations in the considered airspace?
- How do we maintain safe separation among UAS, gliders, helicopters, model aircraft, general aviation, and in future, personal air vehicles?
- What is the separation minimum among different types of manned aircraft, UAS and general aviation and other vehicles that operate in the same airspace?
- What is the (minimum) requirement on UAS for SA&CA?
- What are different architectures (ground-based and air based) for SA&CA and how they would work together?
- What are the different SA&CA architectures to provide persistent coverage?

- What are the different sensor options, redundancies and sensor data integrity needs?
- What is the minimum equipment requirement on the UAS?
- Where do we need geo-fencing?
- What is the minimum functionality of the UTM in terms of airspace design, geofencing definition, self-configuration, weather/wind integration, congestion management, trajectory management, and separation assurance?
- What are the inputs, outputs, and processing functions of UTM?

Table 2.11. Research gaps for SA&CA (Adapted from [105]).

Research Gap	Description
Airspace Characterisation	How should airspace characterisation be included as part of SA&CA certification?
Non-cooperative Data Collection and Assurance	What types and amount of data must be collected from non-cooperative sensors to assure the certifying authority that all non-cooperative traffic is sensed?
Safety Case	What safety strategies and artefacts must be included in a SA&CA safety case?
Human Factors	What human factor considerations must be applied to GCS for certification?
Commercial-off-the-Shelf (COTS) Technologies	How can COTS equipment be used for SA&CA system-of-systems that minimizes recertification and redesign?
SA&CA Architectures	How should SA&CA concept of operations and concepts of employment be matched to safe, cost-effective and optimal system architectures?
Modelling and Simulation (M&S)	How should the M&S tools used in the SA&CA certification process be evaluated and validated as accurate and representative of the SA&CA system?
Airworthiness	How do the service 3-tier airworthiness certification levels input into a target level of safety calculation for the SA&CA system?
Segregated Certification	What are the criteria to determine which parts of the overall SA&CA system can be certified independently (e.g., non-cooperative sensor, cooperative system) in a system of systems approach?
Multi-UAS Integration & Coordinated Operations	What are the certification challenges associated with multiple UAS operating in close proximity to each other (e.g., determining how to change SA&CA thresholds for formation flight)?
FAR Compliance	What challenges exist for all aircraft (manned and unmanned) in complying with the FARs in their present form (e.g., right-of-way rules in 14 CFR 91.113)?
Software and Hardware Assurance	How do civil assurance considerations in RTCA DO-178C software assurance and DO-254 hardware assurance apply to public UAS airspace integration?

All the existing SA&CA technologies do not provide a cohesive mathematical framework or and a system implementation approach that includes both cooperative and non-cooperative means of implementing TDA loops and supports the case for certification. One of the key technology enablers to achieve the goal of safe integration of UAS in non-segregated airspace is the implementation of suitable data fusion techniques supported by a unified approach to non-cooperative and cooperative SA&CA. A unified approach would meet the requirements for manned and unmanned aircraft coordinated operations. Such SA&CA functionalities can provide UAS the capability to consistently and reliably perform equally the see-and-avoid performance of a human pilot in manned aircraft, while allowing a seamless integration of UAS in the current and planned dual-use civil/military ATM system and in the future UTM context.

## 2.15 Conclusions

This chapter provided an introduction to the system architecture and algorithms of Flight Management Systems (FMS). The Guidance, Navigation and Control (GNC) and Tracking, Decision-Making and Avoidance (TDA) avionics loops were described in detail. The existing Separation Assurance and Collision Avoidance (SA&CA) procedures and algorithms currently employed were also presented. The key multi-sensor data fusion techniques tailored for accomplishing an effective TDA loop was also presented. Furthermore, the UTM system requirements and the implications on SA&CA technologies, standards and practices were also discussed.

## 2.16 References

1. R. Sabatini, A. Gardi, S. Ramasamy, T. Kistan and M. Marino, "Modern Avionics and ATM Systems for Green Operations", Encyclopedia of Aerospace Engineering, eds R. Blockley and W. Shyy, John Wiley: Chichester, 2015. DOI: 10.1002/9780470686652.eae1064
2. M. Samà, A. D'Ariano, P. D'Ariano and D. Pacciarelli, "Air Traffic Optimization Models for Aircraft Delay and Travel Time Minimization in Terminal Control Areas", Public Transport, Vol. 7, Issue 3, pp.321-337, 2015.
3. European Commision, "Flightpath 2050 Europe's Vision for Aviation Report of the High Level Group on Aviation Research", EUR 098 EN, Belgium, 2011.
4. P. Hartley, "Joint Command and Control of Australian Airspace", Australian Defence Force Journal, Vol. 197, 2015.

5. ICAO, "Global Air Traffic Management Operational Concept", Doc 9854 AN/458, The International Civil Aviation Organization, Montreal, Canada, 2005.
6. P. Kopardekar, "Unmanned Aerial System (UAS) Traffic Management (UTM): Enabling Low-altitude Airspace and UAS Operations", ARC-E-DAA-TN32373, NASA Ames Research Center, NASA, Moffett Field, CA, USA, 2016.
7. Boeing, "Contribution of Flight Systems to Performance-Based Navigation", Boeing Aero Magazine, 2009.
8. M.R. Cramer, A. Herndon, D. Steinbach and R.H. Mayer, "Modern Aircraft Flight Management Systems", Encyclopedia of Aerospace Engineering, eds R. Blockley and W. Shyy, John Wiley: Chichester, 2015.
9. R. Walter, "Flight Management Systems", Digital Avionics Handbook, eds. C. Spitzer, U. Ferrell, T. Ferrell, Third Edition, 2014.
10. Thales, "Interactive Flight Management System", THALES GROUP, 2016. Accessed December 2016. Available at: <https://www.thalesgroup.com/en/worldwide/defence/what-we-do-air-forces-defence-onboard-electronics/military-interactive-flight>
11. K. Elikar, H. Bouadi and M. Haddad, "Flight planning and guidance features for an UAV Flight Management Computer", Proceedings of IEEE 21<sup>st</sup> International Conference on Emerging Technologies and Factory Automation (ETFA), pp. 1-6, Berlin, Germany, 2016.
12. J. Villarroel and L. Rodrigues, "Optimal Control Framework for Cruise Economy Mode of Flight Management Systems", Journal of Guidance, Control, and Dynamics, pp.1022-1033, 2016.
13. RTCA, "Minimum Aviation System Performance Standards for Radiodetermination Satellite Service (RDSS)", DO-206, Radio Technical Commission for Aeronautics, Washington DC, USA, 1990.
14. E.M. Atkins, "Certifiable Autonomous Flight Management for Unmanned Aircraft Systems", Winter Issue of The Bridge on Frontiers of Engineering, Vol. 40, No. 4, 2010.
15. C. Pasaoglu, N. Akcam, E. Koyuncu, A.F. Tarhan and G. Inalhan, "Collaborative Intent Exchange Based Flight Management System with Airborne Collision Avoidance for UAS", Journal of Intelligent & Robotic Systems, pp.1-26, 2016.
16. P.F. Di Donato, S. Balachandran, K. McDonough, E. Atkins and I. Kolmanovsky, "Envelope-aware Flight Management For Loss Of Control Prevention given Rudder Jam", Journal of Guidance, Control, and Dynamics, pp.1-15, 2016.
17. ARINC, "Navigational Data", ARINC 424, Aeronautical Radio, Incorporated, Annapolis, Maryland, US.

18. A. Miele, "Optimal Trajectories and Guidance Trajectories for Aircraft Flight through Windshears", Proceedings of the 29<sup>th</sup> IEEE Conference on Decision and Control, pp. 737–746, 1990.
19. C.S. Ha, S.E. Kang, J.H. Mok, S. Ko and Y.W. Lee, "3-Dimensional Path Planning and Guidance using the Dubins Curve for an 3-DOF Point-mass Aircraft Model", Journal of the Korean Society for Aviation and Aeronautics, Vol. 24, no. 1, pp.1-9, 2016.
20. M.A. Wahid, "Flight Guidance along 3D+T Trajectories and Space Indexed Traffic Management, Doctoral dissertation, Université de Toulouse, Université Toulouse III-Paul Sabatier, 2015.
21. L. Song, H. Yang, J. Xie, C. Ma and J. Huang, "Method for Improving the Natural Lateral-Directional Stability of Flying Wings", Journal of Aerospace Engineering, p.06016003, 2016.
22. D. McLean, Automatic Flight Control Systems, Prentice Hall, Michigan, US, 1990.
23. ICAO, "International Standards Annex 2 - Amendment 44", The International Civil Aviation Organization, Montreal, Canada, 2005.
24. FAA, "Code of Federal Regulations", CFR, Federal Aviation Administration, Washington DC, USA.
25. Airservices, "Separation Standards", Airservices Australia, Australian Capital Territory, Australia, 2016.
26. Eurocontrol, "European Airspace Concept Handbook for PBN Implementation", Third Edition, Brussels, Belgium, 2013.
27. N. Durand, D. Gianazza, J.B. Gotteland and J.M. Alliot, "Airspace Management", Metaheuristics for Air Traffic Management, pp.69-83, 2016.
28. Air Services Australia, "Separation Standards", Australia's Air Navigation Service Provider, Canberra, Australia, 2016.
29. L.M.B.C. Campos and J.M.G. Marques, "On an Analytical Model of Wake Vortex Separation of Aircraft", The Aeronautical Journal, Vol. 120, No. 1232, pp. 1534-1565, 2016.
30. A. Oztekin and R. Wever, "Development of a Regulatory Safety Baseline for UAS Sense and Avoid", Handbook of Unmanned Aerial Vehicles, Springer, Netherlands, pp. 1817-1839, 2015.
31. FAA, 'Sense and avoid (SAA) for unmanned aircraft systems (UAS)', Sense and Avoid Workshop, Federal Aviation Administration, October 2009.
32. M.C. Consiglio, J.R. Comstock Jr, R.W. Ghatas and M.J. Vincent, "Unmanned Aircraft Systems (UAS) Controller Acceptability Study 3 (CAS3): Collision Avoidance, Self Separation, and Alerting Times (CASSAT): Combined PER/FER", UAS in the NAS Project

Briefing to FAA and Industry, NASA Langley Research Center, Hampton, VA, United States, 2015.

33. G. Granger, "Détection et résolution de conflits aériens: modélisations et analyse", Doctoral Thesis, Informatique de l'Ecole Polytechnique, 2002.
34. S. Kopřiva, D. Šišlák and M. Pěchouček, "Sense and Avoid Concepts: Vehicle-Based SAA Systems (Vehicle-to-Vehicle)", Sense and Avoid in UAS: Research and Applications ed P. Angelov, John Wiley & Sons, Ltd, Chichester, UK, 2012. DOI: 10.1002/9781119964049.ch6
35. M. Melega, "Autonomous Collision Avoidance for Unmanned Aerial Systems", Doctoral Dissertation, Cranfield University, 2014.
36. R. Pablo, E. Santamaria, J.M. Lema, E. Pastor and C. Barrado, "Integration of SAA Capabilities into a UAS Distributed Architecture for Civil Applications", Sense and Avoid in UAS: Research and Applications 61, 2012.
37. S. Bouabdallah, M. Becker, V. de Perrot and R. Siegwart, "Toward obstacle avoidance on Quadrotors", Proceedings of the 12<sup>th</sup> International Symposium on Dynamic Problems of Mechancis, Ilhabela, Brazil, pp. 1-10, 2007.
38. J.F. Roberts, T.S. Stirling, J.C. Zufferey and D. Floreano, "Quadrotor using Minimal Sensing for Autonomous Indoor Flight", Proceedings of MAV Conference (EMAV 2007), Toulouse, France, pp. 1-8, 2007.
39. S. Scherer, S. Singh, L. Chamberlain and M. Elgersma, "Flying Fast and Low among Obstacles: Methodology and Experiments", International Journal of Robotics Research, Vol. 27, Issue 5, pp. 549-574, 2008.
40. S. Shen, N. Michael and V. Kumar, "Autonomous Multi-Floor Indoor Navigation with a Computationally Constrained MAV", Proceedings of the IEEE International Conference on Robotics and Automation, Shanghai, China, pp. 20-25, 2011.
41. M. Achtelik, A. Bachrach, R. He, S. Prentice and N. Roy, "Autonomous Navigation And Exploration of a Quadrotor Helicopter in GPS Denied Indoor Environments", Proceedings of the 1<sup>st</sup> Symposium on Indoor Flight, 2008. Available online at: <http://robot-chopper.googlecode.com/svnhistory/r479/trunk/References/2009MIT.pdf>
42. G. Chowdhary, E.N. Johnson, D. Magree, A. Wu and A. Shein, "GPS Denied Indoor and Outdoor Monocular Vision Aided Navigation and Control of Unmanned Aircraft", Journal of Field Robotics, Vol. 30, Issue 3, pp.415-438, 2013.
43. R. Clothier, R. Walker, R. Baumeister, M. Brünig, J. Roberts, A. Duggan and M. Wilson, "The Smart Skies Project", IEEE Aerospace and Electronic Systems Magazine, Vol. 26, Issue 6, pp.14-23, 2011.



44. M. Orefice, V. Di Vito and G. Torrano, "Sense and Avoid: Systems and Methods", Encyclopedia of Aerospace Engineering, eds R. Blockley and W. Shyy, John Wiley: Chichester, 2015.
45. J. Pellebergs, The MIDCAS Project, Proceedings of the 27th International Congress of the Aeronautical Sciences (ICAS), Nice, France, 2010.
46. P. Angelov, "Sense and Avoid in UAS: Research and Applications, John Wiley & Sons, 2012.
47. P. Woods, "FLAVIIR—An Integrated Programme of Research for UAVs", Proceedings of the 3<sup>rd</sup> AIAA Flow Control Conference, San Francisco, USA, pp. 5-7, 2008.
48. A.E. Heaton, "A Method to Support the Requirements Trade-Off of Integrated Vehicle Health Management for Unmanned Aerial Systems", PhD Thesis, Cranfield Univeristy, 2014.
49. O. Shakernia, W.Z. Chen, S. Graham, J. Zvanya, A. White, N. Weingarten and V.M. Raska, "Sense and Avoid (SAA) Flight Test and Lessons Learned", Proceedings of 2<sup>nd</sup> AIAA Infotech@ Aerospace Conference and Exhibit, pp. 1-12, 2007.
50. B.C. Karhoff, J.I. Limb, S.W. Oravsky and A.D. Shephard, "Eyes in the Domestic Sky: an Assessment of Sense and Avoid Technology for the Army's Warrior Unmanned Aerial Vehicle", IEEE Systems and Information Engineering Design Symposium, pp. 36-42, 2006.
51. T. Williamson and N.A. Spencer, "Development and Operation of the Traffic Alert and Collision Avoidance System (TCAS)", Proceedings of the IEEE, Vol. 77, Issue 11, pp.1735-1744, 1989.
52. W. Harman, "TCAS-A System for Preventing Midair Collisions", The Lincoln Laboratory Journal, Vol. 2, Issue 3, pp.437-457, 1989.
53. H. Lenz and J. Gottstein, "TCAS Compatibility of Advanced Airborne Separation Assurance System Operations", Proceedings of the AIAA Infotech at Aerospace Conference, ISSN: 0731-5090, 2015.
54. J.E. Kuchar and A.C. Drumm, "The Traffic Alert and Collision Avoidance System", Lincoln Laboratory Journal, vol. 16, issue 2, 2007.
55. C. Livadas, J. Lygeros and N.A. Lynch, "High-level Modeling and Analysis of the Traffic Alert and Collision Avoidance System (TCAS)", Proceedings of the IEEE, vol. 88, no. 7, pp.926-948, 2000.
56. RTCA, "Minimum Operational Performance Standards for Traffic Alert and Collision Avoidance Systems II (TCAS II)", DO-185B, Radio Technical Commission for Aeronautics, Washington DC, USA, 2008.
57. FAA, "Introduction to TCAS II", Version 7.1, Federal Aviation Administration, Washington DC, USA, February 2011.

58. W.H. Harman, "TCAS: A System for Preventing Midair Collisions," Lincoln Laboratory Journal, vol. 2, no. 3, pp. 437–458, 1989.
59. J.K. Kuchar and A.C. Drumm, "The Traffic Alert and Collision Avoidance System," Lincoln Laboratory Journal, vol. 16, no. 2, pp. 277–296, 2007.
60. T.B. Billingsley, M.J. Kochenderfer, and J.P. Chryssanthacopoulos, "Collision Avoidance for General Aviation," in IEEE/ AIAA Digital Avionics Systems Conference, Seattle, Washington, 2011
61. M.J. Kochenderfer, M.W.M. Edwards, L.P. Espindle, J.K. Kuchar, and J.D. Griffith, "Airspace Encounter Models for Estimating Collision Risk," Journal of Guidance, Control, and Dynamics, vol. 33, no. 2, pp. 487–499, 2010.
62. M.J. Kochenderfer, J.E. Holland and P. James, "Chryssanthacopoulos: Next Generation Airborne Collision Avoidance System", Lincoln Laboratory Journal, Vol. 19, issue 1, pp. 17– 33, 2012.
63. CASA, "ADS-B mandates 2014-2017", Civil Aviation Safety Authority, Woden, Australian Capital Territory, Australia, 2016.
64. E. Valovage, "Enhanced ADS-B Research", IEEE Aerospace and Electronics Systems Magazine, Vol. 22, Issue 5, pp. 35–38, 2007.
65. X. Yu and Y. Zhang, "Sense and Avoid Technologies with Applications to Unmanned Aircraft Systems: Review and Prospects, Progress in Aerospace Sciences, vol. 74, pp.152-166, 2015.
66. G. Fasano, D. Accardo, A. Moccia, C. Carbone, U. Ciniglio, F. Corrado, and S. Luongo. "Multi-Sensor-Based Fully Autonomous Non-Cooperative Collision Avoidance System for Unmanned Air Vehicles," Journal of Aerospace Computing, Information, and Communication, vol. 5, no. 10, pp. 338-360, 2008.
67. A. Finn and S. Franklin, "Acoustic sense & avoid for UAV's", Seventh IEEE International Conference on Intelligent Sensors, Sensor Networks and Information Processing (ISSNIP), 2011.
68. P. Cornic, P. Garrec, S. Kemkemian, L. Ratton, "Sense and Avoid Radar using Data Fusion with Other Sensors," in Proceedings of the IEEE Aerospace Conference, Big Sky, USA, March 2010.
69. C.P. Lai, Y.J. Ren and C. Lin, "ADS-B based Collision Avoidance Radar for Unmanned Aerial Vehicles", Proceedings of IEEE Microwave Symposium Digest 2009 (MTT'09), IEEE MTT-S International, pp. 85-88, 2009.
70. S. Ramasamy, R. Sabatini and A. Gardi, "A Unified Approach to Separation Assurance and Collision Avoidance for Flight Management Systems." Proceedings of the 35<sup>th</sup>

AIAA/IEEE Digital Avionics Systems Conference (DASC2016). Sacramento, CA (USA), September 2016.

71. C.K. Lai, "A Novel Collision Avoidance Logic for Unmanned Aerial Vehicles using Real-Time Trajectory Planning", PhD Thesis, Cranfield University, UK, 2014.
72. J.K. Aggarwal, "Multisensor Fusion for Computer Vision," vol. 99. Springer Science & Business Media, 2013.
73. D.L. Hall and J. Llinas, "An Introduction to Multisensor Data Fusion", Proceedings of the IEEE, Vol. 85, Issue 1, pp.6-23, 1997.
74. D.J. Dailey, P. Harn and P.J. Lin, "ITS Data Fusion," Final Research Report, Research Project T9903, Task 9, ATIS/ATMS Regional IVHS Demonstration, 1996.
75. A. Gad and M. Farooq, "Data Fusion Architecture for Maritime Surveillance," Proceedings of the Fifth IEEE International Conference on Information Fusion, Vol. 1, 2002.
76. T. Tagarev and P. Ivanov, "Computational Intelligence in Multi-Source Data and Information Fusion," Issue: Information and Security, vol. 2, 1999.
77. D.L. Hall, "An Introduction to Multisensor Data Fusion," Proceedings of the IEEE, vol. 85, issue 1, 1997.
78. F. Cappello, S. Ramasamy and R. Sabatini, "A Low-Cost and High Performance Navigation System for Small RPAS Applications", Aerospace Science and Technology, Elsevier, 2016. DOI: [10.1016/j.ast.2016.09.002](https://doi.org/10.1016/j.ast.2016.09.002)
79. R. Sabatini, F. Cappello, S. Ramasamy, A. Gardi and R. Clothier, "An Innovative Navigation and Guidance System for Small Unmanned Aircraft using Low-Cost Sensors", Journal of Aircraft Engineering and Aerospace Technology, vol. 87, issue 6, 2015. DOI: [10.1108/AEAT-06-2014-0081](https://doi.org/10.1108/AEAT-06-2014-0081)
80. F. Cappello, R. Sabatini, S. Ramasamy and M. Marino, "Particle Filter based Multi-sensor Data Fusion Techniques for RPAS Navigation and Guidance," Proceedings of the Second International Workshop on Metrology for Aerospace (MetroAeroSpace 2015), Benevento, Italy, 2015.
81. A.W. Eric and R.V.D. Merwe, "The Unscented Kalman Filter for Nonlinear Estimation", The IEEE Adaptive Systems for Signal Processing, Communications, and Control Symposium, AS-SPCC, 2000.
82. R.V.D. Merwe, "Sigma-point Kalman Filters for Probabilistic Inference in Dynamic State-space Models", Dissertation, Oregon Health & Science University, 2004.
83. S.M. Oh, "Nonlinear Estimation for Vision-Based Air-to-Air Tracking", Dissertation, Georgia Institute of Technology, 2007.

84. P. Angelov, "Sense and Avoid in UAS: Research and Applications," John Wiley & Sons, 2012.
85. S. Challa, "Fundamentals of Object Tracking", Cambridge University Press, 2011.
86. Y. Bengio, A. Courville and P. Vincent, "Representation Learning: A Review and New Perspectives", IEEE Transactions on Pattern Analysis and Machine Intelligence. 2013 Aug; vol. 35, issue 8, pp. 1798-828, DOI: [10.1109/TPAMI.2013.50](https://doi.org/10.1109/TPAMI.2013.50)
87. M.H.G. Anthony and N. Biggs, "Computational Learning Theory", Cambridge University Press, 1997.
88. M.A. Welling, "First Encounter with Machine Learning", University of California, Irvine, CA, USA, pp. 1-93, 2011.
89. F. Cappello, R. Sabatini and S. Ramasamy, "Multi-Sensor Data Fusion Techniques for RPAS Detect, Track and Avoid", SAE Technical Paper 2015-01-2475, SAE 2015 AeroTech Congress & Exhibition, Seattle, Washington, USA, 2015. DOI: [10.4271/2015-01-2475](https://doi.org/10.4271/2015-01-2475)
90. P. Kopardekar, "Safely Enabling Low-Altitude Airspace Operations: Unmanned Aerial System Traffic Management (UTM)", ARC-E-DAA-TN22234, NASA Ames Research Center, NASA, Moffett Field, CA, USA, 2015.
91. J. Robinson, M. Johnson, J. Jung, P. Kopardekar, T. Prevot and J. Rios, "Unmanned Aerial System Traffic Management Concept of Operations (v0.5) (UTM CONOPS)", NASA TM draft, Moffett Field, CA, USA, 2015.
92. C.W. Johnson, "The Safety Research Challenges for the Air Traffic Management of Unmanned Aerial Systems (UAS)", Proceedings of the 6<sup>th</sup> EUROCONTROL Experimental Centre Safety Research and Development Workshop, Munich, Germany, October, Vol. 21, 2009.
93. Y. Kim, J. Jo and M. Shaw, "A Lightweight Communication Architecture for Small UAS Traffic Management (SUTM)", IEEE Integrated Communication, Navigation and Surveillance Conference (ICNS), pp. T4-1, 2015.
94. T. Prevot, J. Homola and J. Mercer, "From Rural to Urban Environments: Human/Systems Simulation Research for Low Altitude UAS Traffic Management (UTM)", 16<sup>th</sup> AIAA Aviation Technology, Integration, and Operations Conference, Washington DC, USA, pp. 3291, 2016.
95. V. Milanés, J. Godoy, J. Pérez, B. Vinagre, C. González, E. Onieva and J. Alonso, "V2I-Based Architecture for Information Exchange among Vehicles", IFAC Proceedings, Vol. 43, Issue 16,, pp. 85-90, 2010.
96. P. Kopardekar, P. Lee, T. Prevot, J. Mercer, J. Homola, M. Mainini, N. Smith, A. Aweiss and K. Lee, "Feasibility of Mixed Equipage Operations in the Same Airspace", Eighth

USA/Europe Air Traffic Management Research and Development Seminar (ATM2009), Napa, CA, USA, 2009.

97. K. Legrand, S. Puechmorel, D. Delahaye and Y. Zhu, "Aircraft Trajectory Planning under Wind Uncertainties", 35th AIAA/IEEE Digital Avionics Systems Conference, Enabling Avionics For UAS/UTM (DASC 2016), Sacramento, CA, USA, 2016.
98. C. White, E.W. Lim, S. Watkins, A. Mohamed and M. Thompson, "A Feasibility Study of Micro Air Vehicles Soaring Tall Buildings", Journal of Wind Engineering and Industrial Aerodynamics, Vol. 103, pp.41-49, 2012.
99. T.B. Sheridan, "Adaptive automation, level of automation, allocation authority, supervisory control, and adaptive control: Distinctions and modes of adaptation," IEEE Transactions on Systems, Man and Cybernetics, Part A: Systems and Humans, Vol. 41, pp. 662-667, Jul 2011.
100. R.M. Taylor, "Capability, Cognition and Autonomy", DTIC Document, 2003.
101. R.V. Hemm, D. Duncan and V.L. Stouffer. "On-Demand Aviation Regulatory Obstacles and Resulting Research Roadmaps", 16<sup>th</sup> AIAA Aviation Technology, Integration, and Operations Conference, AIAA Aviation Forum, Washington DC, USA, 2016.
102. D.S. Jang, C. Ippolito, S. Sankararaman and V. Stepanyan, "Concepts of Airspace Structures and System Analysis for UAS Traffic flows for Urban Areas", AIAA Information Systems-AIAA Infotech@ Aerospace (p. 0449), Grapevine, Texas, USA, 2017.
103. V.C. Nneji, A. Stimpson, M.M Cummings and K.H. Goodrich, "Exploring Concepts of Operations for On-Demand Passenger Air Transportation", 17<sup>th</sup> AIAA Aviation Technology, Integration, and Operations Conference, pp. 3085, Denver, Colorado, USA, 2017.
104. L. Ren, M. Castillo-Effen, H. Yu, E. Johnson, T. Nakamura, Y. Yoon and C.A. Ippolito, "Small Unmanned Aircraft System (sUAS) Trajectory Modeling in Support of UAS Traffic Management (UTM)", 17<sup>th</sup> AIAA Aviation Technology, Integration, and Operations Conference, pp. 4268, Denver, Colorado, USA, 2017.
105. R. Fontanella, A.R. Vetrella, G. Fasano, D. Accardo and R.S. Lo, "Requirements, Platform Specifications, and System Architectures for Future Unmanned Traffic Management Systems", AIAA Information Systems-AIAA Infotech @ Aerospace, AIAA SciTech Forum, (AIAA 2017-0225, Grapevine, Texas, USA, 2017.
106. V. Kumar, B.M. Horio and S. Hasan, "Modeling Approach for Evaluation of Traffic Management Requirements and Policies for Unmanned Aircraft Systems", 17<sup>th</sup> AIAA Aviation Technology, Integration, and Operations Conference Denver, Colorado, USA, 2017.

107. ASTM, "Standard Specification for Design and Performance of an Airborne Sense-and-Avoid System", ASTM F2411-04, American Society for Testing and Materials, 2004.
108. V.J. Gawron, "Human Factors Issues in the Development, Evaluation and Operations of Uninhabited Air Vehicles", Proceedings of the Association for Unmanned Vehicle Systems International, Huntsville, AL, USA, pp. 431-438, 1998.
109. P.W. Merlin, "Ikhana Unmanned Aircraft System Western States Fire Missions", National Aeronautics and Space Administration, Washington DC, USA, 2009.
110. M. Mouloua, R. Gilson, J. Kring and P. Hancock, "Workload, Situational Awareness, and Teaming Issues for UAV/UCAV Operations", Proceedings of the Human Factors and Ergonomics Society 45<sup>th</sup> Annual Meeting of the Human Factors and Ergonomics Society, Santa Monica, USA, pp. 162-165, 2001.
111. D. Wood, "Collision Avoidance System and method Utilizing Variable Surveillance Envelope", U.S. Patent 6,804,607, 2004.
112. A. Smith, D.M. Coulter and C.S. Jones, "UAS Collision Encounter Modeling and Avoidance Algorithm Development for Simulating Collision Avoidance", AIAA Modeling and Simulation Technologies Conference, 2008.
113. M. Mullins, M. Holman, K. Foerster, N. Kaabouch and W. Semke, "Dynamic Separation Thresholds for a Small Airborne Sense And Avoid System", AIAA Infotech@ Aerospace Conference, Boston, MA, USA, pp. 19-22, 2013.
114. A.L. Smith and F.G. Harmon, "UAS Collision Avoidance Algorithm Minimizing Impact on Route Surveillance", AIAA Guidance, Navigation, and Control Conferenc, pp. 1-20, 2009.
115. E.A. Euteneuer and G. Papageorgiou, "UAS Insertion into Commercial Airspace: Europe and US Standards Perspective", 30<sup>th</sup> AIAA/IEEE Digital Avionics Systems Conference (DASC), pp. 5C5-1, 2011.
116. F. De Crescenzo, G. Miranda, F. Persiani and T. Bombardi, "3D Obstacle Avoidance Strategies for UAS (Uninhabited Aerial System) Mission Planning and Replanning", Proceedings of the 26<sup>th</sup> Congress of the International Council of the Aeronautical Sciences, 2008.
117. R. Marsh, K. Ogaard, M. Kary, J. Nordlie and C. Theisen, "Development of a mobile information display system for UAS operations in North Dakota", International Journal of Computer Information Systems and Industrial Management Applications, vol. 3, pp.435-443, 2011.
118. N. Hanlon, K. Cohen and E. Kivelevitch, "Sensor Resource Management to Support UAS Integration into the National Airspace System", AIAA SciTech 2015 Conference, 2015.

119. J. Capitán, L. Merino and A. Ollero, "Coordination of Multiple UAS for Tracking under Uncertainty", Proceedings of the 1<sup>st</sup> Workshop on Research, Education and Development on Unmanned Aerial Systems, RED-UAS, 2011.
120. J. Tadema, E. Theunissen and K.M Kirk, "Self Separation Support for UAS", American Institute of Aeronautics and Astronautics (AIAA), 2010.
121. J. Upchurch, C. Munoz, A. Narkawicz and J. Chamberlain, "Analysis of Well-Clear Boundary Models for the Integration of UAS in the NAS", Langley Research Center, Hampton, Virginia, TM-2014-218280, NASA, 2014.
122. K.D. Davis and S.P. Cook, "Achieving Sense and Avoid for Unmanned Aircraft Systems: Assessing the Gaps for Science and Research," Handbook of Unmanned Aerial Vehicles, pp. 1841-1855, Springer Netherlands, 2015.

This page is intentionally left blank to support presswork tasks



# CHAPTER 3

## NEXT GENERATION FLIGHT MANAGEMENT SYSTEMS

*"The philosopher is nature's pilot. And there you have our difference:  
to be in hell is to drift: to be in heaven is to steer". - George Bernard Shaw*

### 3.1 Introduction

This chapter presents the system architecture and key design features of NG-FMS. The next generation airborne and ground (NG-FMS and NG-ATM) systems are first introduced. Then a system requirement analysis and a description of the novel functionalities required in an advanced NG-FMS are described. Subsequently, the main modules of the NG-FMS architecture that allow the generation of 4DT planning and optimisation algorithms are presented. The features required for achieving full interoperability with the NG-ATM system, enabling automated TBO/IBO are described. Validation of the adopted trajectory optimisation algorithms is performed through dedicated simulation test cases.

### 3.2 NG-FMS and NG-ATM Systems

In recent years, research interest has gathered in improving safety, capacity and efficiency of air operations as well as attaining environmentally sustainable solutions. In line with European Union's SESAR, US's NextGen, Australia's OneSKY and other ATM modernisation programmes, research on NG-FMS is aimed to provide 4D TBO/IBO with NG-ATM and Next Generation Airborne Data Link (NG-ADL) systems.

The efficiency and effectiveness of NG-ATM system are increased by introducing more information sharing and improving the operational and technological frameworks. According to the SESAR ATM master plan [1], the foreseen future deployments evolve from radar-based operations to TBO/IBO to achieve performance-driven ATM. As

covered in Chapter 2 (Section 2.6), the current surveillance infrastructure is largely composed of PSR, SSR, Mono-pulse Secondary Surveillance Radar (MSSR) and MSSR Mode-S. Recent technological advances including the emergence of ADS-B and Wide-Area Multilateration (WAM) have reached maturity and are being deployed in many parts of the world supporting the evolution to performance-driven ATM. In addition to ground-based surveillance, satellite based ADS-B is also becoming available as a source for surveillance information, especially in oceanic and remote areas. ADS-B is also supporting the development of new airborne surveillance operational services, including Air Traffic Situational Awareness (ATSA) and the Airborne Separation Assistance System (ASAS), which provide services such as sequencing and merging and self-separation in SESAR and NextGen. Future airborne applications will require changes in the avionics to process surveillance information in an automated manner and to display the airspace situation to the pilot.

NextGEN is composed of programs including ADS-B, data communications, en-route automation modernization, terminal automation modernization and replacement, the national airspace system voice system and system wide information management. To reduce the costs inherent in ground based radar systems and improve aircraft tracking accuracy, an air traffic system based entirely on self-reporting traffic is proposed. The cornerstone of this program is ADS-B for SA&CA. When all users are capable of determining their three dimensional position and velocity vector, and then transmitting that information to the appropriate ATC facility, the requirement for ground based radar acquisition becomes obsolete. Because the system must remain safe and robust during transition, and because the cost of the mandated new equipment is an issue, there are many additional elements to the program to smooth transition. This incentive came in the form of Broadcast Weather information, termed Flight Information Service – Broadcast (FIS-B). To provide effective situational awareness, each ADSB-in receiver must see all the traffic in the vicinity. With some users transmitting ADS-B on UAT and others on 1090ES, it was necessary to provide a translating repeater and hence ADS-R (Rebroadcast) was introduced. Hence, the ATC received UAT transmissions, which are rebroadcast on 1090ES and vice versa.

Because mandatory compliance is still a few years away, there are targets that will be identified by ATCRBS that are not reporting position on either 1090ES or UAT. In an endeavour to provide a comprehensive traffic picture, ATC provides a Traffic Information Service – Broadcast (TIS-B) with these additional targets to all ADS-B (out) equipped traffic.

In the CNS+A context, the NG-FMS acts as the airborne counterpart that implements the operational 4D trajectory concept. One of the key drawbacks in the current FMS is the inability to handle traffic uncertainties in a predictive real-time manner. This results in system inefficiencies that affect the system performance (both airborne and ground systems). Hence, it is of paramount importance to implement the TBO/IBO concept through the design and development of a NG-FMS and NG-ATM system providing [2]:

- enhanced capability to exploit the CDM concept among all stakeholders utilising accurate real-time information acquired from the airborne counterpart. In this respect, the NG-FMS generates, synchronises and negotiates the predicted aircraft intents with the ground NG-ATM based on real-time CNS system performance, observed airspace and atmospheric conditions. CDM involves all stakeholders in the ground communication network including 4-PNV systems, Air Traffic Controllers (ATCo), Air Navigation Service Providers (ANSP) and Airline Operation Centres (AOC);
- introduction of higher levels of automation supporting role shifting of the ground NG-ATM system from traditional command and control oriented units to highly automated decision-making nodes in an interoperable environment. The transition is supported by the introduction of user-preferred trajectories downlinked from the aircraft. The changes to flight plans may be the result of weather and traffic hazards, emergency situations, and system degradation/failures resulting in a breach of agreed trajectory contract;
- introduction of environment-related objectives based on cost functions to reduce emissions in all flight phases and noise at the vicinity of airports whilst minimising the total cost of a flight;
- controlled time of arrival and strict adherence to required time of arrival enforced by both ground and airborne systems;
- continuous synchronisation of trajectory and state information to support the introduction of time as a control variable in the trajectory optimisation process;
- enhancing transition from voice communication to data-driven operations.

An innovative ground based 4D Trajectory Planning, Negotiation and Validation (4-PNV) system for NG-ATM is assumed to be the 4DT planning, data exchange, negotiation and validation counterpart of NG-FMS. The 4-PNV system incorporates CDM and global optimisation criteria adhering to airspace constraints, and dedicated trajectory de-confliction algorithms to enable IBO/TBO. The 4-PNV system receives multiple options of 4DT intents from each aircraft equipped with NG-FMS (both manned aircraft and UAS).

Then the 4-PNV system validates, through near real-time negotiation with the aircraft, the trajectory intents and resolves any traffic conflicts (implementing adequate separation and avoidance methods), and thus establishing an optimal and safe solution for each aircraft in the strategic and tactical timeframes. Three time horizons are defined, given the time before a predicted conflict or hazard. These include the Online Strategic (OS – more than 20 minutes before the predicted conflict or hazard) and Online Tactical (OT – between 20 and 10 minutes look ahead) and emergency situations (less than 10 minutes ahead). The introduction of Separation Assurance and Collision Avoidance (SA&CA) functions within NG-FMS becomes especially significant in the emergency time horizon.

Airspace constraints, flight path restrictions, and global optimisation criteria are shared by the 4-PNV system with the NG-FMS, which generate intents consisting of a number of flyable optimal trajectories. Figure 3.1 depicts the conceptual negotiation between the NG-FMS and the 4-PNV of a family of trajectory intents.

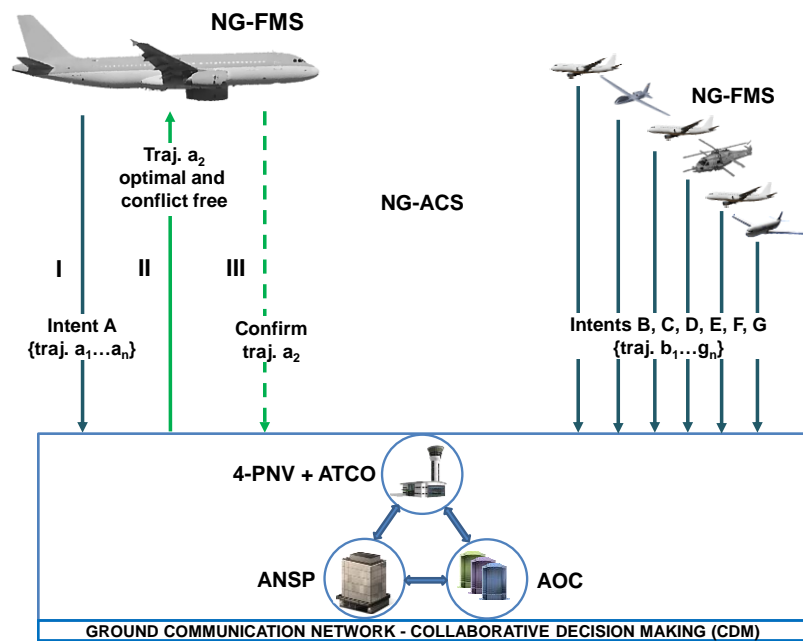


Figure 3.1. 4DT intent negotiation and validation.

The key objectives of the NG-FMS/4-PNV trajectory negotiation and validation concepts are:

- enhancing the performance of 4D trajectory optimisation process;
- improving the human situational awareness without imposing excessive workload;
- reducing air/ground 4D trajectory negotiation loops;
- avoiding endless negotiation loops;

- avoiding unnecessary information exchange.

The air-to-ground negotiation involves the process of receiving and validating the new set of 4DT intent from the 4-PNV system or sending the updated 4DT intent information to the 4-PNV system for validation. The air-to-air negotiation involves updating the aircraft state information and is specifically essential for updating information on any collision threats, if the aircraft have on board cooperative surveillance sensors. Introduction of new constraints or any updates triggers the NG-FMS/4-PNV system to initiate a strategic negotiation by up-linking new constraints. In case a negotiation is initiated by the 4-PNV system after onboard processing, the NG-FMS discovers performance or constraint violations (e.g., exceeding the aircraft performance characteristics), the NG-FMS downlinks a rejection message notifying that the aircraft is unable to satisfy the new constraints, together with a new intent for validation by the 4-PNV system. Specifically, in the tactical online context, either the NG-FMS or the 4-PNV system may initiate the intent negotiations, through the ATM system acts as a key decision maker. In general, the NG-FMS would initiate the trajectory negotiations due to newly detected local weather changes, performance degradations, equipment failures or on-board emergency situations. Other manoeuvre-related factors such as inefficient heading changes, unachievable climb/descent rates and altitudes may also trigger negotiation loops. In the tactical online scenario, a single-loop negotiation is always sought, due to the reduced time and stringent traffic management requirements. Similarly, if a solution cannot be obtained through trajectory negotiation, then ATCo and pilots' direct intervention will be considered.

For example, consider a TMA case: when the aircraft is approaching its destination airport, the 4-PNV system might initiate a 4D trajectory intent negotiation process at specific predefined 4D waypoints. This 4D trajectory intent is then negotiated via data-link between the 4-PNV system and the aircraft. The negotiation and validation process can be implemented by the following approaches:

- A 3D flight plan can be agreed upon between the NG-FMS and 4-PNV system, considering all relevant constraints and approach procedures including Standard Terminal Arrival Route (STAR), GNSS curved approaches, ILS approaches, etc. at the destination airport. After the negotiation and validation process is complete for the 3D route, time can be introduced as a control variable in the NG-FMS 4D trajectory optimisation software, defining the ETA at the destination point and RTA at all the intermediate waypoints. Arrival management algorithms can then compute a controlled time of arrival within a specified window and ensure that

the aircraft is able to follow the validated 4D trajectory intent, thereby optimising the arrival sequence. The 4-PNV system, after coordination between the involved sectors, then sends the optimised intent to the onboard NG-FMS system;

- Instead of negotiating and validating a 3D flight plan and then negotiating a 4DT intent, these processes can involve a direct 4D trajectory intent negotiation and validation process during the trigger point.

In the OS time horizon, the 4-PNV system acts as the main partner, since it captures an ever-updated global situational awareness, thanks to the ground network and the associated trajectory prediction algorithms. Uncertainties, such as long-term forecast weather phenomena, airport closures or sectors saturations trigger the 4-PNV system to initiate a strategic negotiation by uplinking new constraints to the NG-FMS. These constraints are used by the NG-FMS for on-board trajectory optimisation and negotiation/validation. If, after onboard evaluation, performances/constraint violations exist, the aircraft will downlink a rejection message together with a new intent to the 4-PNV for validation. In the OT time horizon, either the NG-FMS or the 4-PNV may initiate trajectory negotiations. The NG-FMS may initiate the trajectory negotiation due to freshly detected weather changes, performances degradation, equipment failures or on-board emergency situations. The fundamental objective of this is to compute an optimal trajectory addressing minimum fuel consumption, flight time, operative cost, noise impact and persistent contrail formation. Multiple negotiation loops will be allowed in the OS scenarios, as shown in Figure 3.2 but eventually prevented due to data-link bandwidth concerns. In the OT time horizon, either the NG-FMS or the 4-PNV may initiate trajectory negotiations. The 4-PNV will act mainly as a key decision maker. The NG-FMS may initiate the trajectory negotiation due to newly detected weather changes, performances degradation, equipment failures or any on-board emergency situations. Other manoeuvre-related factors such as inefficient heading changes, and unachievable climb/descent rates and altitudes due to the actual aircraft weight may also be the cause of negotiation. In the OT scenario, a single-loop negotiation is always preferred and aimed for, due to the stringent time constraints. Similarly, if a solution cannot be obtained through trajectory negotiation, a direct intervention by the ATCo/pilot or both will be considered. Examples of the trajectory negotiation process are shown in Figures 3.2 and 3.3 (NG-FMS and 4-PNV system initiated respectively).

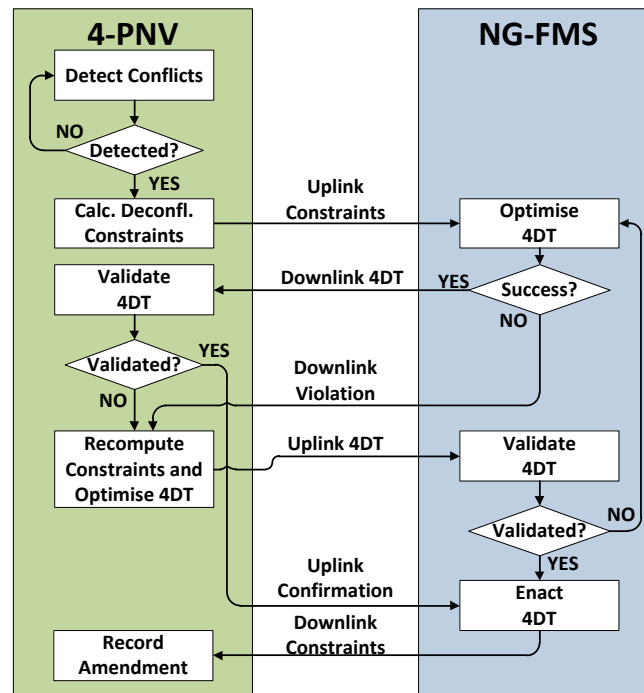


Figure 3.2. 4-PNV system initiated intent negotiation/validation loop.

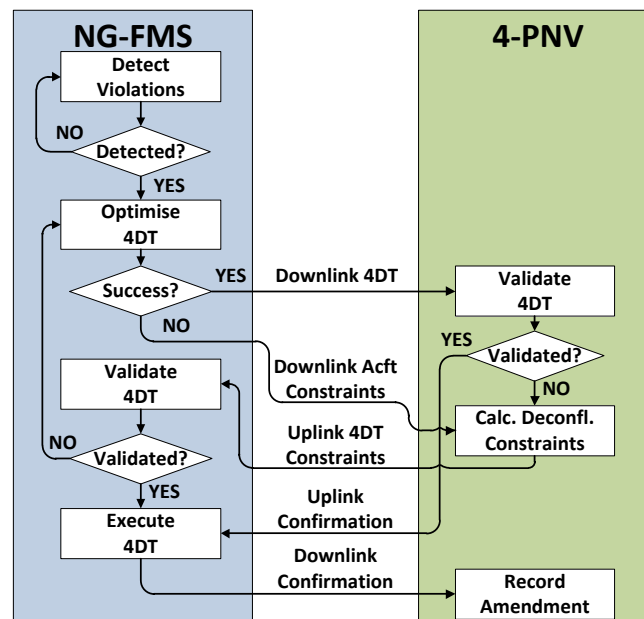


Figure 3.3. NG-FMS initiated intent negotiation/validation loop.

The key long-term goals of ATM modernisation programmes include the integration of trajectory management processes in planning and execution [1, 3]. According to the SESAR concept of operations, these refer to the management, negotiation and sharing of the Shared Business Trajectory (SBT) as well as the management, updating, revision

and sharing of the Reference Business Trajectory (RBT), and finally the transition from the SBT to RBT (Figure 3.4).

During the planning process the trajectory may undergo certain refinements which then lead to the RBT. For the flight execution the RBT is the reference. Upon deviation – intended or unintended – from the RBT, the Predicted Trajectory (PT) is calculated with the aim to return the aircraft to its RBT.

This concept introduces the 4D Trajectory, which in SESAR is defined as 'a set of consecutive segments linking waypoints and/or points computed by the airborne or by the ground systems to build a vertical profile and the lateral transitions; each point defined by a longitude, a latitude, a level and a time'.

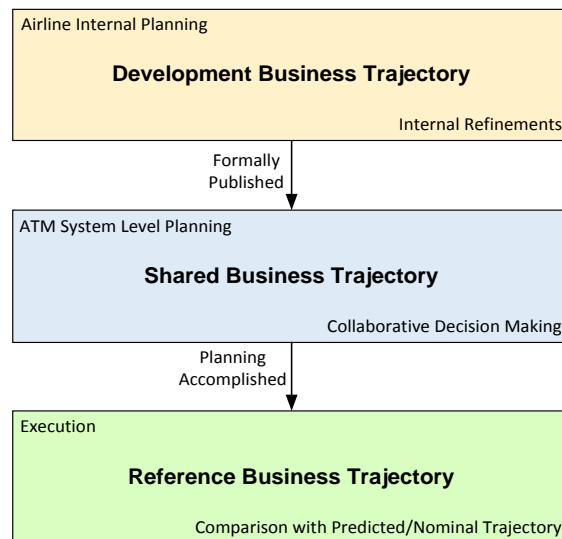


Figure 3.4. SESAR trajectory management concept.

It is envisaged that the enhanced mission trajectory will be integrated into the TBO/IBO environment throughout all phases of trajectory planning and execution. The enhanced mission trajectory is subject to trajectory management processes and contains 4D targets and ATM constraints. The introduction of System Wide Information Management (SWIM) for air-to-ground, air-to-air and ground-to-ground information sharing supports ATM operational improvements and provides better situational awareness (including CDM) while airborne SA&CA systems supporting integration of UAS replicate the human ability to See-and-Avoid (S&A). It has been identified that UAS should have this capability, as it is one of the cornerstones of aviation, entitled 'rules-of-the-air', in which the pilot is ultimately responsible for the safety of the flight. Other aspects to be considered include avionics integration, CNS ground segment integration as well as test and evaluation algorithms [1].



## 3.2 System Requirements and New Functions

In addition to the navigation and guidance automated services, a NG-FMS offers a significant benefit by supporting 4-Dimensional trajectory planning, optimisation and re-optimisation [4]. Furthermore, the introduction of SA&CA functions and CNS performance monitoring services are supported by the NG-FMS. In summary, the following novel functionalities are implemented in the NG-FMS:

- navigation algorithms involving a number of multi-sensor data fusion techniques;
- guidance computation (lateral and vertical guidance algorithms);
- 4D trajectory planning, generation and optimisation algorithms;
- short-term and long-term performance computation algorithms;
- advanced SA&CA algorithms;
- CNS performance monitoring;
- dual and single mode protocols in case of conventional two pilot aircraft;
- single mode protocols for single pilot operations;
- processing algorithms for navigation, performance, magnetic deviation, demographic and digital elevation terrain databases;
- novel Human-Machine Interface and Interaction (HMI<sup>2</sup>) system protocols including adaptive forms.

In addition to the traditional databases mentioned earlier in Chapter 2, weather, demographic distribution, digital terrain elevation, environmental and pilot modifiable databases are also introduced in the NG-FMS. The environmental performance of the NG-FMS requires additional data to be included in the existing databases or including a separate database exclusively for environmental functions. Noise abatement operational procedures in use today are: Noise abatement flight procedures including Continuous Descent Arrival (CDA), Noise Abatement Departure Procedures (NADP), modified approach angles, staggered, or displaced landing thresholds, low power/low drag approach profiles and minimum use of reverse thrust after landing. Other procedures include spatial management, including noise preferred arrival and departure routes and runways, flight track dispersion or concentration, as well as noise preferred runways for achieving benefits operationally and environmentally, and ground management.

Multi-Criteria Departure Procedure (MCDP) enables trajectories to be optimised operationally and environmentally during the take-off and climb flight phases (Figure

3.5). The concept is based on NADP adopted from Procedures for Air Navigation Services/Operations ICAO document 8168 and is extended to emissions reduction [5].

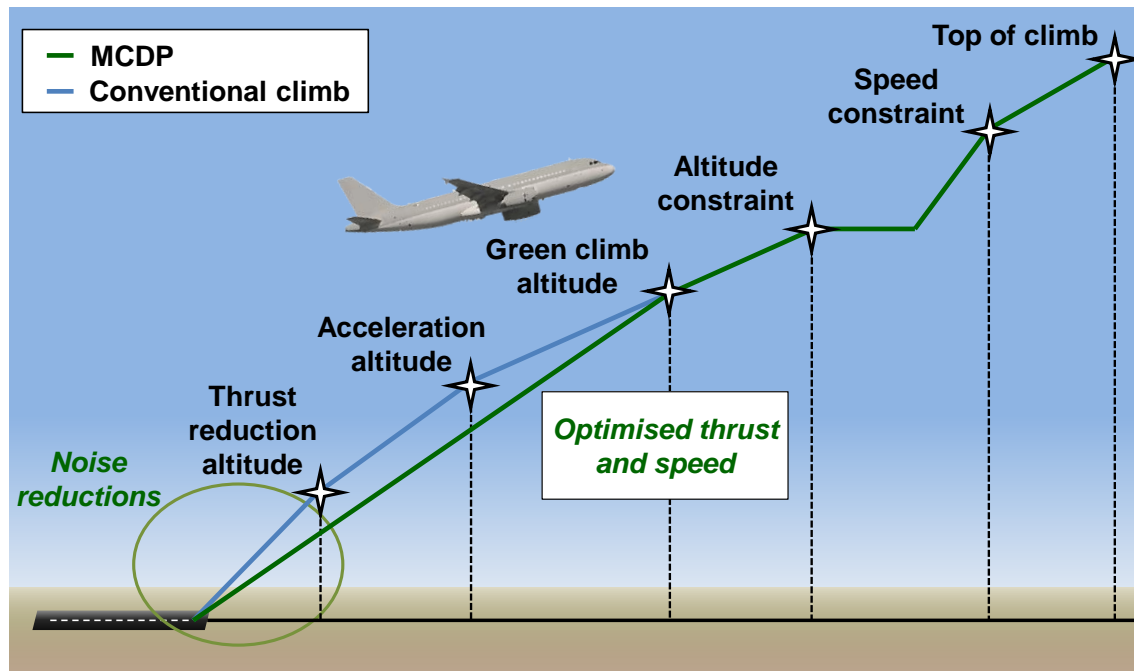


Figure 3.5. Multi-criteria departure procedure.

In addition to the conventional databases, the demographic distribution and digital terrain elevation databases are included for noise assessments. These allow the aircraft to reduce the take-off noise while taking into account actual aircraft parameters and ambient conditions. The 4DT optimisation algorithms for take-off and climb flight profiles ensure a combined optimization of noise and emissions while at the same time meeting the constraints of the planned mission including following the best Standard Instrument Departure (SID) from the available choices. For obtaining costs benefits in terms of fuel consumption and emission factors, the design is to achieve an optimum cruise level, but with a time varying cost function. These cost functions can be based on the priority levels agreed on a-priori basis by the CDM participants. An example of the performance weighting parameters used is listed in Table 3.1. Recently, multi-step algorithms are implemented in cruise phase that: i) "step to" a different cruise flight level at a fixed waypoint, ii) "step from" a fixed waypoint to another flight level and iii) "step level" at different cruise altitude. The current aircraft state vector, temperature and wind profile are considered for implementing the multi-step function.

During cruise, the NG-FMS optimizes the set of vertical and lateral trajectories based on the aircraft performance and weather constraints (Figure 3.6). Path constraints are introduced in the optimisation loop as functions of either the system state or control

variables, and are defined to comply with the operational or safety procedures. These constraints include the No-Fly Zones (NFZ), weather cells and Persistent Contrail Formation Regions (PCFR). These constraints take into account traffic separation aspects, terrain obstacles, and weather hazards, as well as a primitive representation of noise-sensitive areas.

Table 3.1. Performance weighting layout.

Precedence	Weightings						
	$K_{fuel}$	$K_{time}$	$K_{WC}$	$K_{contrail}$	$K_{CO_2}$	$K_{HC}$	$K_{SO_x}$
I	$K_{fuel} 1$	$K_{time} 1$	$K_{WC} 1$	$K_{contrail} 1$	$K_{CO_2} 1$	$K_{HC} 1$	$K_{SO_x} 1$
II	$K_{fuel} 2$	$K_{time} 2$	$K_{WC} 2$	$K_{contrail} 2$	$K_{CO_2} 2$	$K_{HC} 2$	$K_{SO_x} 2$
III	$K_{fuel} 3$	$K_{time} 3$	$K_{WC} 3$	$K_{contrail} 3$	$K_{CO_2} 3$	$K_{HC} 3$	$K_{SO_x} 3$
IV	$K_{fuel} 4$	$K_{time} 4$	$K_{WC} 4$	$K_{contrail} 4$	$K_{CO_2} 4$	$K_{HC} 4$	$K_{SO_x} 4$

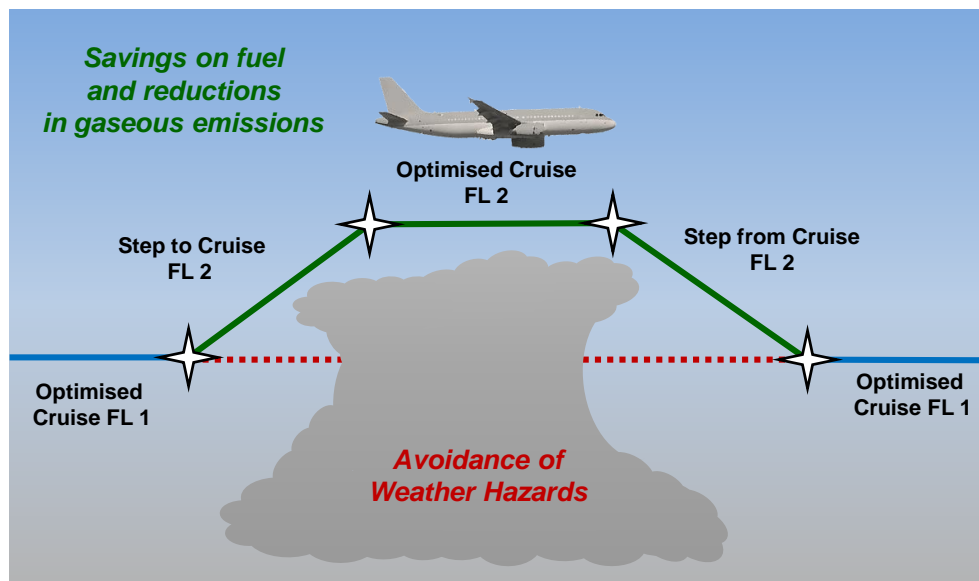


Figure 3.6. Multi-criteria departure procedure.

Fuel planning is indispensable to ensure safety and compliance to aeronautical rules. Fuel surveillance has always been part of pilot workload as performing a mission consists in making accommodations between safety, fuel savings and timing depending on the airline strategy. The strategies including cost index variation or speed changes to obtain a cruise speed that will permit the aircraft to perform arrival right on time, planning

around the optimum flight level, clearance at flight levels differing at a minimum value from the optimum flight level and “Direct TO” functionality use. The advantage of using “Direct TO” is the reduction of fuel consumption, along with a reduced flight time. In the descent and approach phase, enhancements such as the Continuous Descent Approach (CDA) concept are adopted even in dense traffic environments (Figure 3.7). The 4DT optimal descent profile is generated by the NG-FMS by considering speed, altitude and time constraints in the nominal path in addition to weather updates from the NG-ATM system. Since the optimum descents are based on idle thrust, they can differ from one aircraft to another; hence synchronization at the airport is essential to obtain the required fuel savings and environmental benefits.

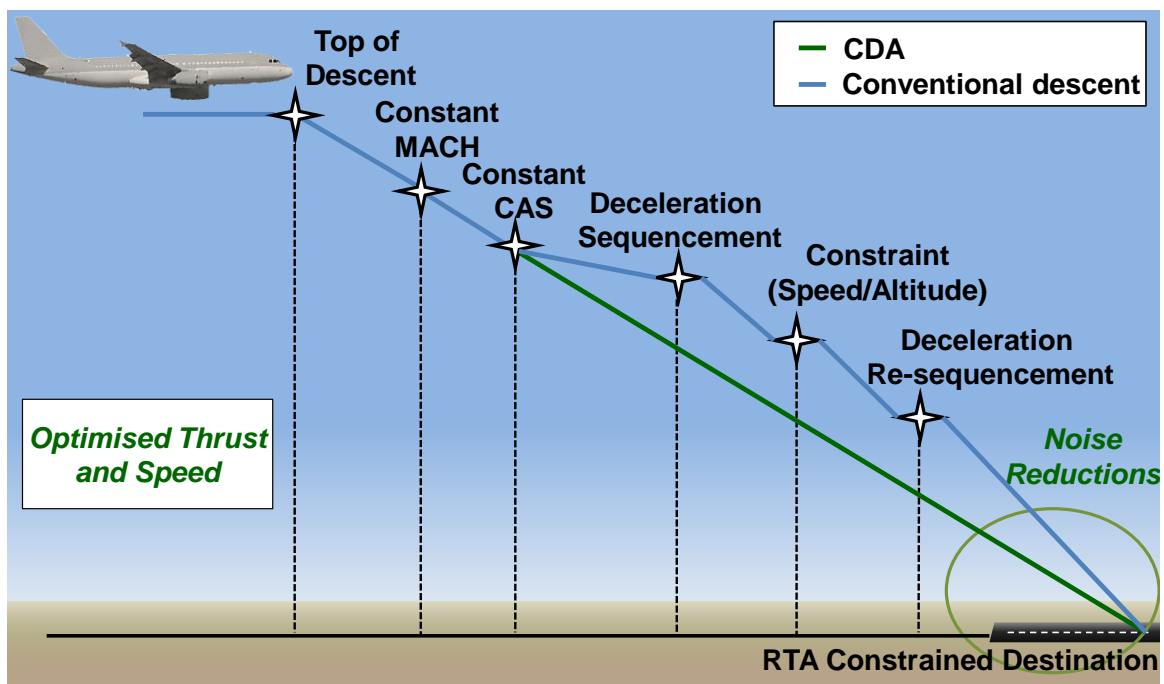


Figure 3.7. Continuous descent approach procedure.

The NG-ATM system receives multiple options of 4DT intents from each aircraft equipped with NG-FMS. These 4DT intents will be based on performance weighting that are collaboratively agreed upon and are targeting the global optimisation criteria. The system validates, through real-time negotiation with the aircraft, the trajectory intents and resolve traffic conflicts (implementing adequate separation and avoidance methods), thus establishing an optimal and safe solution for each aircraft. NG-FMS generates intents consisting of a number of flyable optimal trajectories (in order of priority). The 4DT intents are updated on a timely basis, as well as when there are changes. The intents contain information about the complete trajectory of the aircraft,

until it reaches its destination. The intent data includes all the waypoints (lateral and vertical), leg and turn information [6].

In 4D TBO, time is introduced as one of the variables that can be controlled during all flight phases. In initial TBO implementation, the RTA concept is introduced, which mostly involves variation of speed in the lateral profile. The cruise altitude is fixed for an idle-thrust performance path in most cases to achieve an efficient variation of the ETA at the WPTs along the trajectory. Awareness of winds and meteorological data can be used for all relevant timeframes (strategic, tactical and emergency). The weather and temperature data for the entire flight plan is obtained from the AOC and is updated at regular intervals with the information obtained from the ground systems or other aircraft via the data link. The 4DT optimisation problem includes a number of environmental objectives and operational constraints, also accounting for economic and operational performances, as well as weather forecast information from various external sources. Reduction of fuel consumption begins early in the process with route planning and the filing of the flight plan. Companies have tools to optimise flight plan depending on the predicted meteorological conditions, aircraft performances and available routes. The flight plans provided by operations centres can include steps meant to remain close to the computed optimum flight level. But these steps become geographical steps when they are uploaded into the FMS before departure, and pilots generally clear them at the beginning of cruise to update them as optimum steps using updated aircraft state. These various methods are very efficient to saving time and fuel, but they have to face operational limitations, which need to be taken into account:

- flight envelope boundaries;
- ATC clearance;
- flight level availability;
- traffic capacity of geographical zone.

It is highly desirable to set up optimum flight levels or use DIRECT TO for achieving the RTA at the end of each flight phase and the ETA at the planned destination. Efficient trajectories, based on more precise, reliable and predictable three dimensional flight path will be optimized for minimum noise impact and low emissions and include agile trajectory management, in response to meteorological hazard.

The sensing of atmospheric perturbations and atmospheric humidity is based on the characterization and surveillance of the environment. It is achieved by the employment of improved weather radar algorithms. These methods improve on board detection accuracy for potentially hazardous weather conditions.

### 3.3 NG-FMS Architecture

The NG-FMS software is based on multi-objective and multi-model 4DT optimisation algorithms for strategic, tactical and emergency scenarios. The NG-FMS not also considers large fixed-wing UAS (likely be able to use a substantial part of the NG-FMS design given that they will operate in the NAS with other commercial transport aircraft), but also non-traditional designs (VTOL, hybrid configurations such as tilt rotor, etc.) and small UAS that are expected to be increasingly autonomous for safety as well as efficiency reasons. The NG-FMS have broad applicability to UAS and emerging on-demand aviation operations and applications. The implications of older general aviation aircraft are also considered. The transition time from equipping all aircraft with NG-FMS is also crucial, during which the general aviation will still be in service without undergoing a retrofit of existing avionics or upgrading of new avionics systems (NG-FMS). Information exchange is supported by NG-ACS as shown in Figure 3.8. Emergency scenarios involve avoidance of other traffic and obstacles with data obtained from multi-sensor data fusion algorithms. Prevention of collisions takes into account weather and airspace sector information in addition to tactical intervention and emergency avoidance tasks.

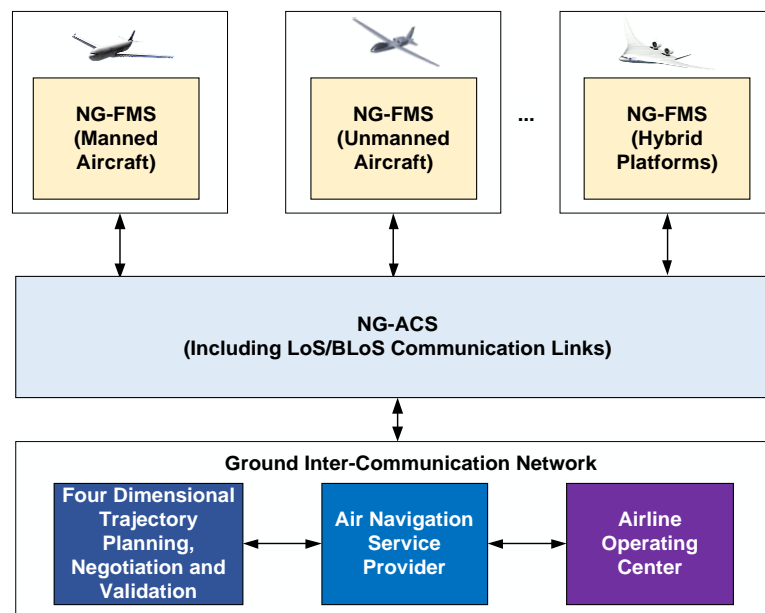


Figure 3.8. NG-FMS and NG-ATM system interactions.

The key NG-FMS software modules are:

- 4D trajectory planning and optimisation: to perform 4D trajectory planning and optimisation functions for strategic (offline and online), tactical (offline and online) and emergency tasks. The 4DT optimiser includes a model and constraint

suite. A number of performance criteria and cost functions are used for optimisation, including minimisation of fuel consumption, flight time, operative cost, noise impact, emissions and contrails. The databases include navigation, performance, magnetic deviation and environmental databases;

- 4D trajectory monitoring: to perform state estimation, calculating the deviations between the 4D trajectory intents and the estimated/predicted aircraft states;
- Path correction: to correct for any deviations in terms of lateral, vertical and time profiles (required and estimated time of arrival). The generated steering commands are provided to the automatic flight control system;
- Trajectory negotiation and validation: to carry out the process of negotiation that can be initiated by the pilot via the NG-FMS, making use of the information available on board, or by the air traffic controller via the 4-PNV system. The negotiation and validation of 4DT intents by the NG-FMS/4-PNV system is dependent on [10, 11]:
  - ✓ on-board validation based on synchronization, sufficient fuel, compliance with dynamics (time performances, turn performances, speed, altitude), obstacle separation, locally sensed weather, and compliance with health monitoring status;
  - ✓ ground-based validation based on air traffic separation (lateral, vertical, longitudinal), sector occupancy, airspace restrictions (special use areas) and time based restrictions (night time noise abatement procedures).
- NG-FMS performance manager: to monitor the active 4D trajectory intents for errors and addresses the full set of CNS performance requirements throughout the different phases of 4DT intent negotiation and validation;
- NG-FMS integrity manager: to generate integrity C/N/S caution (predictive) and warning (reactive) flags based on inputs from different sensors/systems and predefined decision logics (Figure 3.9). For instance, the main causes of GNSS signal degradations in flight, namely antenna obscuration, multipath, fading due to adverse geometry and Doppler shift are identified and modelled to implement integrity thresholds and guidance algorithms in the Avionics-Based Integrity Augmentation (ABIA) system [7, 8].

The RNP, RCP and RSP integrity performance management modules provide information to the integrity management software modules that are used, in turn, to generate usable, timely and valid caution and warning alerts. Figure 3.10 shows a schematic of

the NG-FMS architecture. Airline, airspace, aircraft performance (derived from the performance database) and ATM operational constraints are taken into account in the trajectory prediction and performance optimisation tasks. Each aircraft equipped with NG-FMS generates 4DT intents. 4DT intents are defined according to the Flight Management Computer (FMC) ARINC 702A-3 characteristic as a string of 4D points that define the predicted trajectory of the aircraft along with the point type and turn radius associated with the flight path transition [9, 10]. Intent data are updated in situations such as a change in the nominal flight path, or the addition of new sequencing points and weather data. The trajectory computation and optimisation component of the NG-FMS is reconfigurable with that of the ground-based counterpart to enable negotiation and validation updates in real-time (Figure 3.11).

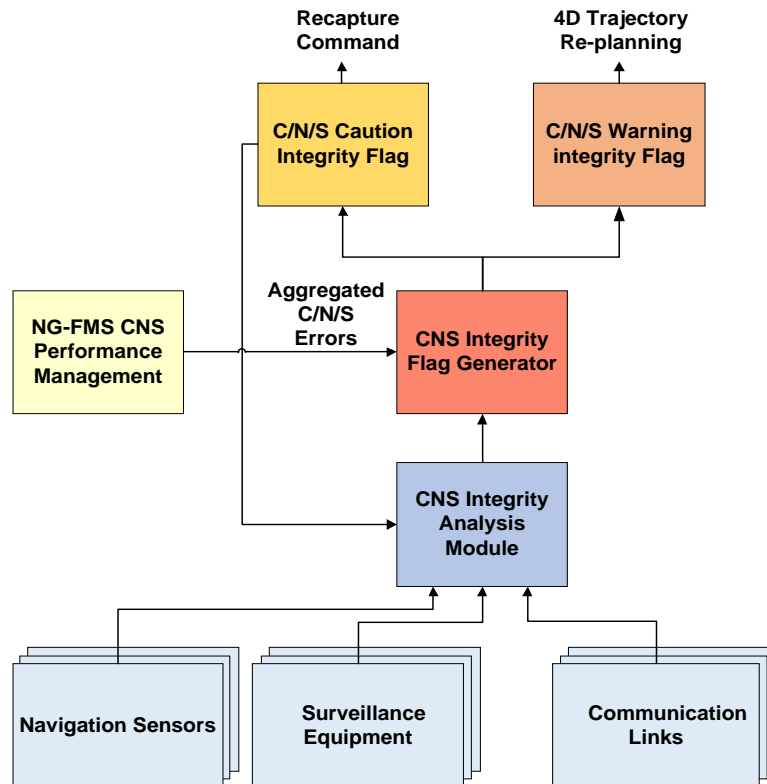


Figure 3.9. NG-FMS integrity monitor.

Additionally, the intents are recomputed according to flight plan revisions, weather updates, guidance mode modification, cost index modification and corrections for position uncertainties in real-time based on the 4D trajectory optimisation algorithms described earlier. The efficiency and effectiveness of 4DT planning, negotiation and validation functionalities of the NG-FMS are directly driven by the nature of information sharing. Subject to various in-flight changes, trajectory calculations are refreshed to maintain consistency and downlinked to the 4-PNV system via the NG-ACS.



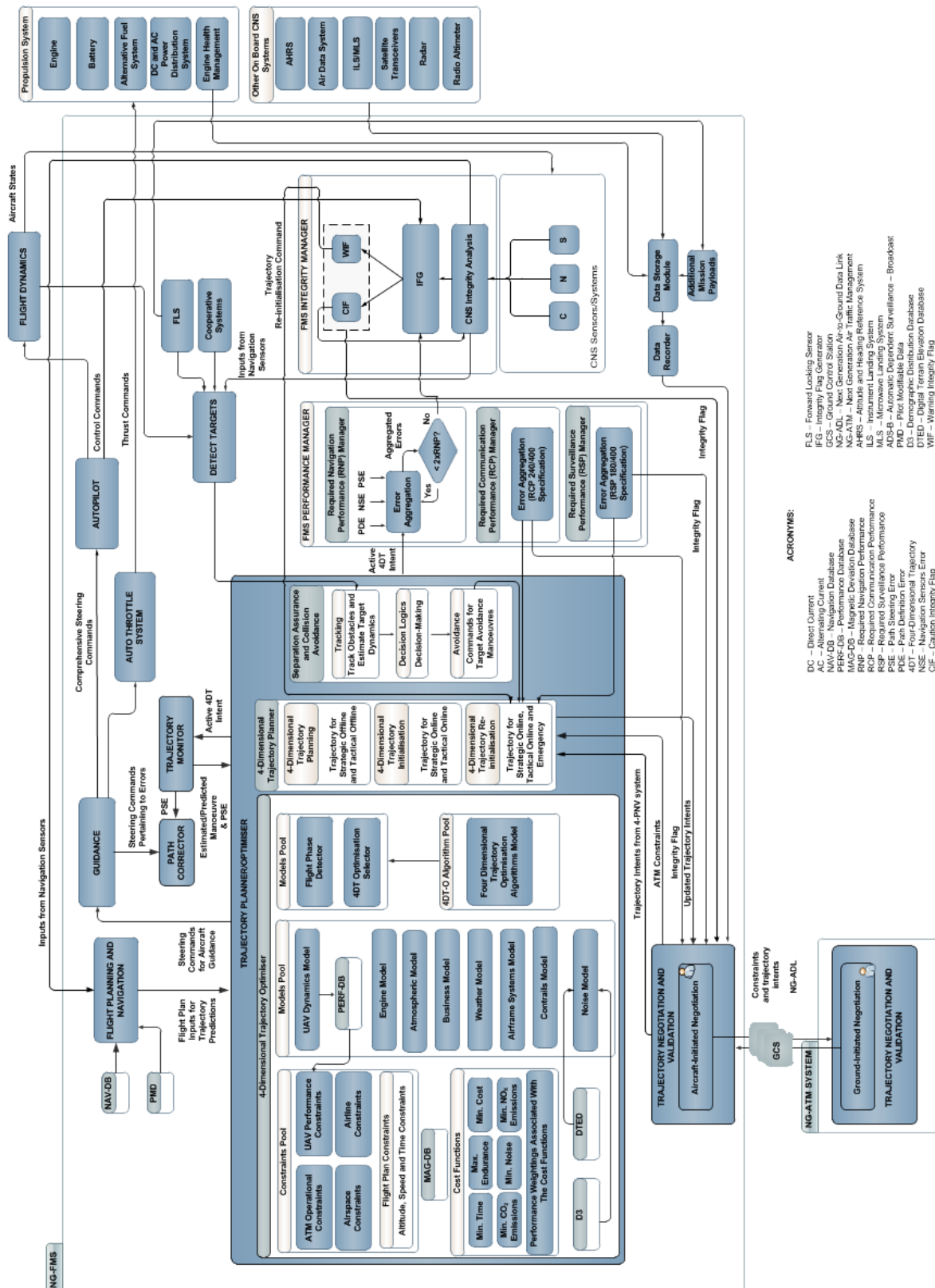


Figure 3.10. NG-FMS overall architecture.

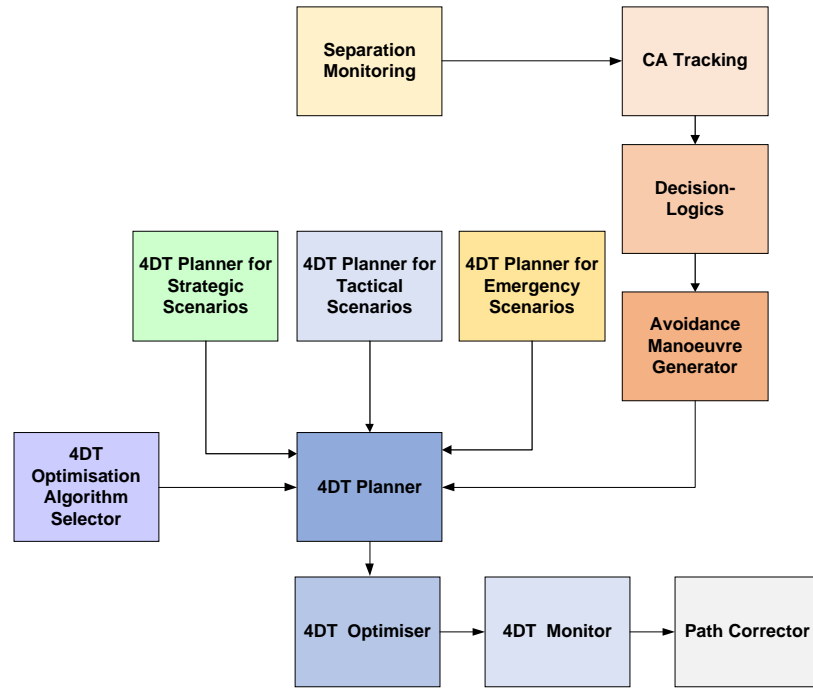


Figure 3.11. NG-FMS 4DT planner and optimiser.

With the increasing levels of on-board automation, integrity monitoring and augmentation systems have occupied a fundamental role. Errors affecting the CNS+A systems (e.g., pseudo-range GNSS observables) are taken into account in evaluating the CNS performance. As illustrated in Figure 3.12, the performance manager module provides inputs to the Integrity Flag Generator (IFG) based on the errors affecting the CNS systems.

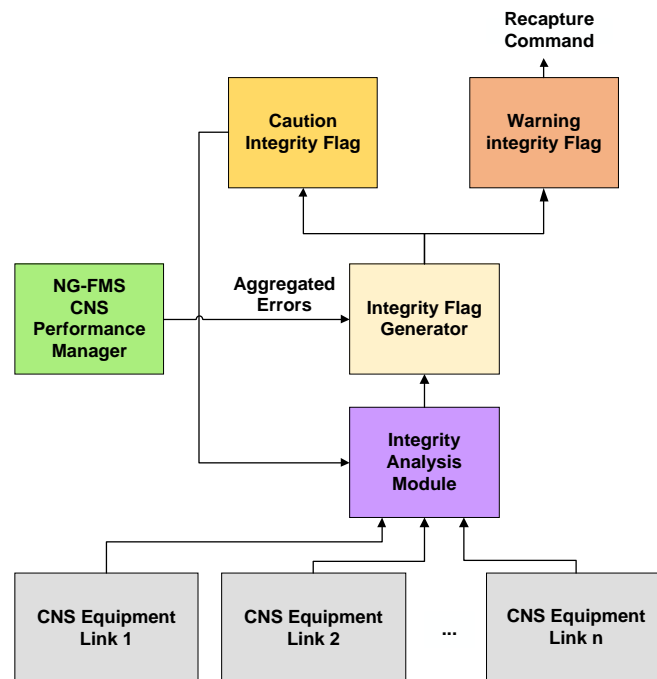


Figure 3.12. NG-FMS integrity flag generation.

The IFG uses a set of predefined Caution and Warning Integrity Flag (CIF/WIF) threshold parameters to trigger the generation of both caution and warning flags associated with CNS performance degradations. In case a warning flag is generated, a recapture command is used to trigger the 4DT regeneration and optimisation process.

Figure 3.13 is a schematic block diagram of the NG-FMS performance management modules. The performance management tasks are defined for all CNS+A parameters. These modules receive data from the 4DT planner/optimiser module.

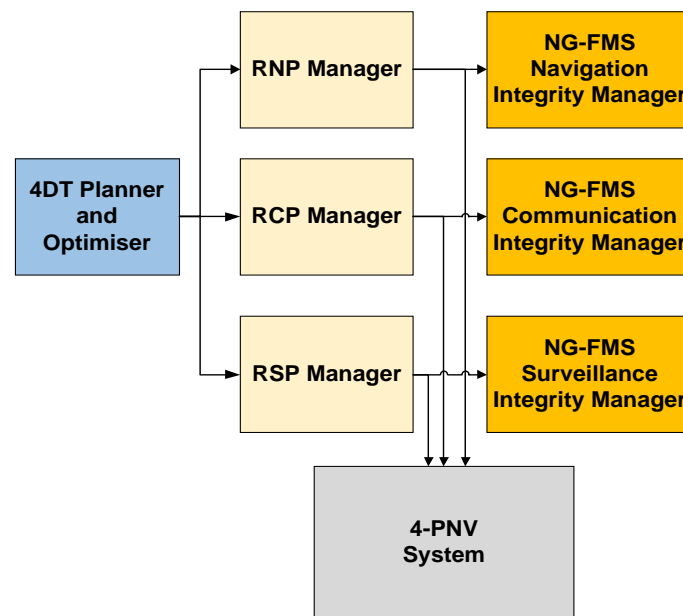


Figure 3.13. NG-FMS performance management.

The RNP, RSP and RCP integrity performance management modules provide data to the integrity management blocks that in turn generate CIF/WIF. The CNS+A performance management blocks are interfaced with the NG-ATM system.

The optimisation of 4DT trajectories is performed on-board by the NG-FMS. A number of manned and unmanned aircraft equipped with NG-FMS can be controlled by the ground command, control and intelligence system aided by LOS and BLoS communication links. HMI<sup>2</sup> for the pilot and UAS remote pilot are equipped with navigation, tactical, health management and engine management displays. The ground inter-communication system consists of a ground-to-ground communication network. Figure 3.13 is a schematic block diagram of the CNS+A systems including NG-FMS, NG-ATM and NG-ACS. In Figure 3.14, airborne systems (coloured) and subsystems (white) are represented by rectangular blocks, while ground-based systems are represented by hexagonal blocks.

Since the early UAS adoption stages, military operators have overcome most issues successfully by opportune implementations of airspace segregation. In particular, the combined operations of military UAS and manned aerial and terrestrial vehicles have been typically designed to minimise the reciprocal threats and introduce adequate safety margins. A similar approach has been pursued in the civil jurisdiction whenever commercial and recreational UAS operators have been granted access to limited portions of the airspace, where conventional manned aircraft operations are denied, such as in proximity to the ground. In these cases, the risk of Mid Air Collisions (MAC) between manned aircraft and UAS is effectively removed thanks to the reciprocal segregation in place. The introduction of a new regulatory framework and CNS+A decision support systems for TBO involve several important research activities including the development of 4DT algorithms for conflict-detection, planning, negotiation and validation that enable unrestricted access of UAS to all classes of airspace. The increasing adoption of UAS poses technological and regulatory challenges, which have hindered a quickly growing number of UAS operators, national regulators, and international aviation organisations.

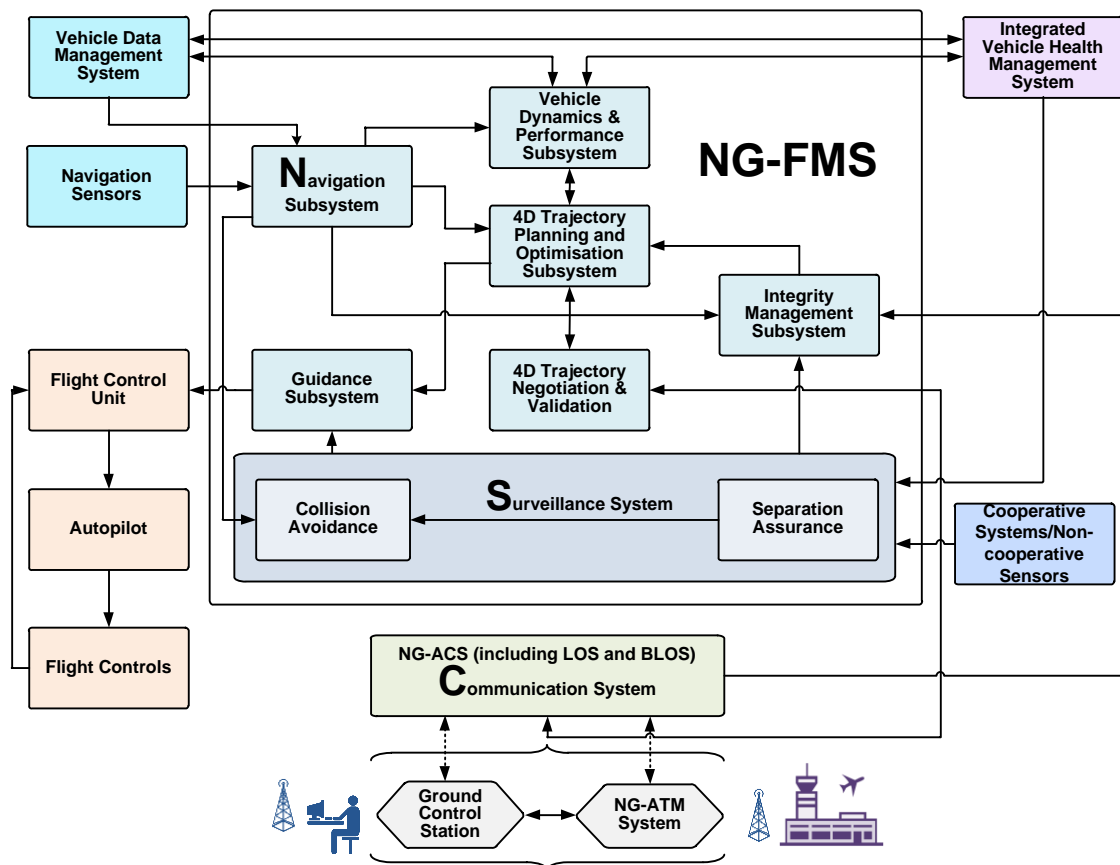


Figure 3.14. CNS+A systems.

A progressive integration of UAS by means of a gradual exploitation of the conventional civil airspace structure and regulations has been considered. In particular, the safety of manned aircraft would be substantially unaffected if UAS were to be granted access to regions where conventional aircraft operations are very sparse. From this perspective, an integration of UAS starting from less restrictive classes of airspace is traditionally favoured. This would decrease requirements in terms of CNS and Avionics (CNS+A) equipment, and require limited compliance to ATM clearances. The less demanding requirements, especially in classes "F" and "G", are certainly valued from the UAS perspective, as UAS reliability is still far from the levels offered by manned aircraft. Nevertheless, separation in these airspace regions is the responsibility of the pilots and based on visual detection and deliberate execution of avoidance manoeuvres according to the rules of the air. These aspects involve substantially higher technological challenges for UAS developers, as separation relies uniquely upon on board SA&CA and decision-making processes, hence higher levels of on board autonomy are required to mitigate the risks arising in connection to possible failures to the Command and Control (C2) loop involving the ground pilot.

### 3.4 NG-FMS Algorithms

The motion of an aircraft can be expressed in terms of a set of equations, representing the translational and angular accelerations. Applying Newton's second law to the aircraft (which is considered to be a rigid body), the following equations are obtained:

$$\vec{F} = \frac{d}{dt} \{m \vec{V}_T\} \quad (3.1)$$

$$\vec{M} = \frac{d}{dt} \{\vec{H}\} \quad (3.2)$$

where:

$\vec{F}$  is the sum of all the applied forces;

$\vec{M}$  is the sum of applied torques;

$\vec{H}$  is the angular momentum;

$m$  is the mass of the aircraft;

$\vec{V}_T$  is the total velocity vector.

The sum of external forces can be subdivided into: aerodynamic forces, gravitational force and propulsive force. The forces and moments about the six degrees of freedom, are expressed as:

$$\Sigma \vec{F}_x = \frac{d}{dt} \{m\vec{u}\} \quad (3.3)$$

$$\Sigma \vec{F}_y = \frac{d}{dt} \{m\vec{v}\} \quad (3.4)$$

$$\Sigma \vec{F}_z = \frac{d}{dt} \{m\vec{w}\} \quad (3.5)$$

$$\Sigma \vec{L} = \frac{d\vec{h}_x}{dt} \quad (3.6)$$

$$\Sigma \vec{M} = \frac{d\vec{h}_y}{dt} \quad (3.7)$$

$$\Sigma \vec{N} = \frac{d\vec{h}_z}{dt} \quad (3.8)$$

where  $\vec{u}$ ,  $\vec{v}$ ,  $\vec{w}$  are the linear velocities along the  $x$ ,  $y$  and  $z$ -axis respectively;  $\vec{F}_x$ ,  $\vec{F}_y$ ,  $\vec{F}_z$  are the forces acting on the aircraft along the three axes; and  $\vec{h}_x$ ,  $\vec{h}_y$ ,  $\vec{h}_z$  are the components of angular momentum along the three axes. The effect of angular velocities on linear velocities can be easily analysed. For example, considering the axial velocity  $\dot{x}$ , the pitch rate  $Q$  increases the velocity by a factor  $Qz$ , but the yaw rate  $R$  reduces it by a factor  $Ry$ . The equations for the linear velocities are given by [11]:

$$\dot{x} = U + Qz - Ry \quad (3.9)$$

$$\dot{y} = V - Pz + Rx \quad (3.10)$$

$$\dot{z} = W + Py - Qx \quad (3.11)$$

where  $U$ ,  $V$  and  $W$  are the rates in linear velocities and  $P$  is the roll rate. The above equations are differentiated to obtain:

$$\ddot{x} = \dot{U} + \dot{Q}z + Q\dot{z} - \dot{R}y - R\dot{y} \quad (3.12)$$

$$\ddot{y} = \dot{V} - \dot{P}z - P\dot{z} + \dot{R}x + R\dot{x} \quad (3.13)$$

$$\ddot{z} = \dot{W} + \dot{P}y + P\dot{y} - \dot{Q}x - Q\dot{x} \quad (3.14)$$

Substituting for  $\ddot{x}$ ,  $\ddot{y}$  and  $\ddot{z}$  in the above equations, the below expressions are obtained:

$$\ddot{x} = \dot{U} + QW + QPy - Q^2x - RV + RPz - R^2x + \dot{Q}z - \dot{R}y \quad (3.15)$$

$$\ddot{y} = \dot{V} - PW - P^2y - PQx + RU + RQz - R^2y - \dot{P}z + \dot{R}x \quad (3.16)$$

$$\ddot{z} = \dot{W} + PV - P^2z + PRx - QU - Q^2z + QRy + \dot{P}y - \dot{Q}x \quad (3.17)$$

The forces acting on the element of mass are given by:

$$\vec{F}_x = m\ddot{x} \quad (3.18)$$

$$\vec{F}_y = m\ddot{y} \quad (3.19)$$

$$\vec{F}_z = m\ddot{z} \quad (3.20)$$

The inertia moments acting on the mass element are given by:

$$M_x = \vec{F}_z y - \vec{F}_y z \quad (3.21)$$

$$M_y = \vec{F}_x z - \vec{F}_z x \quad (3.22)$$

$$M_z = \vec{F}_y x - \vec{F}_x y \quad (3.23)$$

The forces and moments acting on the aircraft can be calculated by summing the above equations over the complete aircraft mass. Assuming that the centre of gravity of the aircraft coincides with the origin of the chosen axis system, the terms containing  $mx$ ,  $my$  and  $mz$  in the above equations can be ignored, since their summation over the entire aircraft yields zero. Therefore, the force equations are expressed as:

$$\vec{F}_x = m\ddot{x} = m(\dot{U} + QW - RV) \quad (3.24)$$

$$\vec{F}_y = m\ddot{y} = m(\dot{V} - PW + RU) \quad (3.25)$$

$$\vec{F}_z = m\ddot{z} = m(\dot{W} + PV - QU) \quad (3.26)$$

Similarly, the moments are expressed as:

$$L = I_{xx}\dot{P} + QR(I_{zz} - I_{yy}) - I_{xz}(\dot{R} + PQ) \quad (3.27)$$

$$M = I_{yy}\dot{Q} + PR(I_{xx} - I_{zz}) + I_{xz}(P^2 - R^2) \quad (3.28)$$

$$N = I_{zz}\dot{R} + PQ(I_{yy} - I_{xx}) - I_{xz}(\dot{P} - QR) \quad (3.29)$$

where  $I_{xx}$ ,  $I_{yy}$ ,  $I_{zz}$  and  $I_{xz}$  are the moments of inertia and are given by:

$$I_{xx} = \sum \Delta m (y^2 + z^2) \quad (3.30)$$

$$I_{yy} = \sum \Delta m (x^2 + z^2) \quad (3.31)$$

$$I_{zz} = \sum \Delta m (x^2 + y^2) \quad (3.32)$$

$$I_{xz} = \sum \Delta m xz \quad (3.33)$$

The state-of-the-art FMS employ a 3-Degrees-of-Freedom (3-DoF) model for generating 3D trajectories. NG-FMS generates 4DT intents composed by groups of single trajectories  $t$  belonging to the global set  $T$ . A number of algorithms have been adopted for trajectory generation and avoidance manoeuvres [12 - 15]. The consecutive TCPs are defined with respect to the previous waypoints by conditional probability and generate

fly-by and fly-over waypoints for each flight segment up to the destination. The NG-FMS trajectory optimisation algorithms are based on a 3-Degrees-of-Freedom (3-DoF) or 6-Degrees-of-Freedom (6-DoF) Aircraft Dynamics Model (ADM) with variable mass. The 3-DoF Equations of Motion (EoM) describing the aircraft states and governing the translational movements along the longitudinal, lateral and vertical axes are:

$$\frac{d\varphi}{dt} = \frac{V \cos \gamma \sin \chi + V_{W\varphi}}{R_M + h} \quad (3.34)$$

$$\frac{d\lambda}{dt} = \frac{V \cos \gamma \cos \chi + V_{W\lambda}}{\cos \varphi (R_T + h)} \quad (3.35)$$

$$\frac{dh}{dt} = V \sin \gamma + V_{Wh} \quad (3.36)$$

$$\frac{dV}{dt} = \frac{\Delta f}{m} - g \sin \gamma \quad (3.37)$$

$$\frac{d\gamma}{dt} = \frac{g(n \cos \phi - \cos \gamma)}{V} \quad (3.38)$$

$$\frac{d\chi}{dt} = \left( \frac{N \cdot g}{V} \right) \left( \frac{\sin \phi}{\cos \gamma} \right) \quad (3.39)$$

$$\frac{dm}{dt} = -c(P, V, h) T(P, V, h) \quad (3.40)$$

$$\Delta f = T(P, V, h) - D(L, V, h) \quad (3.41)$$

The above Differential Algebraic Equations (DAEs) incorporate three control variables  $u = (P, n, \phi)$  where  $P$  is the engine power setting,  $n$  is the load factor and  $\phi$  is the bank angle. The seven state variables are  $x = (m, \varphi, \lambda, h, V, \gamma, \chi)$ , where  $m$  is the aircraft (variable) mass,  $\varphi$  is the geodetic latitude,  $\lambda$  is the geodetic longitude,  $h$  is the altitude,  $V$  is the true air speed,  $\gamma$  is the flight path angle,  $\chi$  is the heading.  $R_M$  is the meridional radius of curvature,  $R_T$  is the transverse radius of curvature,  $W$  is the wind velocity,  $T$  is the thrust,  $D$  is the drag and  $g$  is the nominal acceleration due to gravity of the Earth. This model assumes a rigid body aircraft with a vertical plane of symmetry, nil wing bending effect, a rigidly mounted aircraft engine on the vehicle body, zero thrust angle, negligible moments of inertia, varying mass only as a result of fuel consumption and uniform gravity. Wind effects are considered along the three geodetic reference axes. Earth's shape is approximated as an ellipsoid using the World Geodetic System of year 1984 (WGS 84) parameters. The lateral path is constructed in terms of segments (straight and turns) and is based on the required course change and the aircraft predicted ground speed during the turn. The specificity of the trajectory optimisation and optimal



control with respect to other mathematical optimisation branches is the application to dynamical systems. Therefore, a key component in the optimisation formulation is the set of dynamic constraints, which are meant to reproduce the feasible motion of the system within the optimisation problem [16]. A system of DAEs, consisting of the time derivatives of the state variables, is usually adopted to introduce the system dynamics, and the dynamic constraints are therefore written as:

$$\dot{x}(t) = f[x(t), u(t), t, s] \quad (3.42)$$

where  $s$  is a set of system elements. All non-differential constraints imposed on the system between the initial and final conditions are classified as path constraints, as they restrict the path, i.e. the space of states and controls of the dynamical system. In order to represent all possible non-differential restrictions on the vehicle motion, two types of algebraic path constraints are considered: inequality constraints and equality constraints. A generalised expression of an inequality constraint is [16]:

$$g_i(x(t), u(t), t; s) \leq 0 \quad (3.43)$$

whereas an equality constraint can be written as:

$$h_i(x(t), u(t), t; s) = 0 \quad (3.44)$$

Boundary conditions define the values that state and control variables of the dynamical system shall have at the initial and final times. Since in some instances the boundary conditions are not always restricted to definite values, it is useful to adopt a generalised expression including relaxed conditions. The boundary conditions are expressed as [16]:

$$\mathcal{B}_{min} \leq \mathcal{B}[x(t_0), x(t_f), u(t_0), u(t_f); s] \leq \mathcal{B}_{max} \quad (3.45)$$

where  $t_0$  is the initial time and  $t_f$  is the final time in the time domain. In order to optimise a given performance, it is necessary to introduce a scalar index: the performance index, which by means of a suitably defined cost function quantifies the achievement of that particular objective [16]. The optimal control problem can be tackled using direct and indirect methods. Global collocation methods, which are aimed at obtaining a direct solution of the optimal control problem, is attempted by enforcing the evaluation of the state and control vectors in discrete collocation points across the entire problem domain. Out of several global collocation methods, pseudospectral methods are considered as one of the most computationally effective technique available for the direct solution of large non-linear aircraft trajectory optimisation problems. They are based on a global collocation of orthogonal (spectral) interpolating functions. Uncertainties in input data, estimation models and in the trajectory propagation over

time make some key assumptions void. Hence pseudo-optimal solutions are adopted for generating 4D trajectory intents. The optimisation process is translated into the mathematical minimisation (or maximisation) of such a performance index. The optimisation problem consists of determining the controls  $u(t)$  and states  $x(t)$  that minimize a performance index,  $J$  given by the sum of Mayer ( $\Phi$ ) and Lagrange ( $L$ ) terms as follows:

$$J = \Phi[x(t_f), x(t_0), t] + \int_{t_0}^{t_f} L[x(t), u(t), t] dt \quad (3.46)$$

The optimisation is classified as single-objective when an individual performance index  $J$  is introduced and multi-objective when two or multiple performance indexes  $J_i$  are defined. The NG-FMS receives the controlled time of arrival target defined by the 4-PNV system, which becomes the RTA to be used by the NG-FMS in determining the optimal trajectory states (final time). In general, NG-FMS software for all flight phases allow incorporation of a cost index based on a manually entered CAS/Mach or a combined pair. The cost index set by the mission operators is processed by the NG-FMS to set the gain matrix weight, time, fuel, emissions, noise and other costs. The time cost,  $J_{time}$  is given by:

$$J_{time} = K_t t_f \quad (3.47)$$

Fuel consumption optimisation is achieved by minimising the difference between the aircraft initial and final mass:

$$J_{fuel} = x_f(t_f) - x_f(t_0) \quad (3.48)$$

In terms of aircraft emissions, although engine design and other factors play an influence on the total amount of emission release, engine emission is generally considered as a function of fuel burn, multiplied by a direct emission factor,  $\varrho$ . Hence, the mathematical description of the emission rate,  $J_{emission}$ , defined with respect to emissions,  $e$  and time,  $t$  is given by:

$$J_{emission} = \int_{t_0}^{t_f} \frac{de}{dt} = (m(t_f) - m(t_0)) * \varrho \quad (3.49)$$

This function is based on modelling the dependence of  $\varrho$  on the engine power setting for turbofan engines. The navigation costs,  $J_c$  is given by:

$$J_c = \sum_{c=1}^N \left( \sqrt{\frac{MTOM}{MTOM_{avg}}} \times \frac{DIS_c}{DIS_{avg}} \times URCH \right) \quad (3.50)$$

where  $MTOM$  is the Maximum Take-Off Mass,  $DIS$  is the horizontal separation between aircraft and intruder,  $DIS_{avg}$  depends on the country of implementation and  $URCH$  is the

Unitary Rate Charges for air traffic services. These charges were first established by EUROCONTROL for European countries. In order to implement the noise model, demographic distribution and digital terrain elevation data are considered. The terrain proximity cost,  $J_T$  is obtained as a trade-off between an early turn take-off, low path angle climb, low clearance margin from obstacles output and a very steep climb, long straight departure and increased obstacle clearance margin solution [19]. The numerical solution of the trajectory optimisation problem is performed by primarily combining the multiple objectives by means of weighted sum, and subsequently solving the combined optimisation problem by means of pseudospectral transcription into a constrained multi-phase Non-Linear Programming (NLP) problem [16]. Other methods such as Mixed Integer Linear Programming (MILP) can be implemented to overcome the computational complexity of the NLP problem.

### 3.5 System State Error Analysis

The lateral path is constructed in terms of segments (straight and turns) and is based on the required course change and the aircraft predicted ground speed during the turn. A turn is constructed based on the maximum ground speed during a course change and the turn radius is given by:

$$T_R = \frac{GS^2}{g \times \tan(\phi)} \quad (3.51)$$

where  $GS$  is the maximum ground speed during the turn. The turn arc length is given by:

$$T_{AL} = Course_{change} \times T_R \quad (3.52)$$

Given the  $T_R$ , the bank angle is calculated from:

$$\phi = \arctan\left(\frac{GS^2}{T_R \times g}\right) \quad (3.53)$$

The NG-FMS computes turn altitude and speed based on the selected altitude by taking into account the predicted wind at that altitude. The bank angle is determined based on aircraft dynamics and airspace configurations. In order to construct the vertical profile, a number of energy balance equations are typically adopted leading to nominal climb/descent, fixed gradients climb/descent, intermediate speed changes and level flight configurations. The integration steps are constrained by the mission profile imposed altitude, speed and time restrictions as well as performance limitations such as speed and buffet limits, maximum altitude and thrust limits. The data that drives the energy balance equations come from the airframe/engine dependent thrust, fuel

flow, drag and air speed schedule models stored in the PERFDB. The vertical profile is obtained from the energy method given by:

$$\frac{dh}{dt} = \frac{(T-D)V_T}{GW \times \left(1 + \frac{V_T}{g} \times \frac{dV_T}{dh}\right)} \quad (3.54)$$

where  $V_T$  is the true air speed and  $GW$  is the gross weight. Designing a lateral track control strategy, especially for UAS is very complex. A viable control strategy is based on the relation [17]:

$$\frac{\dot{X}_{track}}{k \times X_{track}} = \frac{\dot{Y}_{track}}{Y_{track}} \quad (3.55)$$

where  $X_{track}$  and  $Y_{track}$  are the current track position of the aircraft with respect to a TCP. The along-track and cross-track velocities are obtained from the airspeed and wind speed velocity vectors. The condition to satisfy the control strategy is given by:

$$Error = (k \times X_{track} \times \dot{Y}_{track}) - (Y_{track} \times \dot{X}_{track}) \quad (3.56)$$

A number of controllers can be implemented to complete the GNC loop including those that have been employed with reliability for a long period (Proportional-Integral-Derivative (PID) and others) as well as emerging artificial intelligence tools (neural network, fuzzy expert system, etc.). In order to study the effects of uncertainties on the generated 4DT, a detailed error analysis is performed. The errors might be due to database accuracy degradations, system modelling errors, atmospheric disturbances and subsystem errors. The system states are modified with the addition of the stochastic term,  $e(t)$  and are represented by:

$$\dot{x}(t) = f[x(t), u(t), e(t), t] \quad (3.57)$$

In order to perform a sensitivity analysis, the sensitivity of a trajectory attribute,  $J$ , including consumption of fuel, noise, emissions, etc. is considered with respect to a model parameter,  $\Delta$  and is given by:

$$\Delta = \Delta^n + d\Delta \quad (3.58)$$

The open loop sensitivity of  $J$  is given by:

$$\frac{\partial J}{\partial \Delta}_{OL} = \frac{J^{OL}(\Delta^n + d\Delta) - J^{OL}(\Delta^n)}{d\Delta} \quad (3.59)$$

The closed loop sensitivity of  $J$  is given by:

$$\frac{\partial J}{\partial \Delta}_{CL} = \frac{J^{CL}(\Delta^n + d\Delta) - J^{CL}(\Delta^n)}{d\Delta} \quad (3.60)$$

The values of  $J^{OL}$  and  $J^{CL}$  are optimised based on the 4DT optimisation algorithm adopted in the NG-FMS. Each performance index provides a quantitative measure of the attainment of a specific objective and different objectives are typically conflicting. Thus, the optimisation in terms of two or more objectives typically leads to a number of possible solutions, which are still optimal in a mathematical sense (pareto-optimality). Therefore, a trade-off analysis based on specific performance weightings is required for the operational implementation of multi-objective 4DT optimisation techniques. In the aviation domain, single and bi-objective optimisation techniques have been exploited for decades, but they accounted only for flight time-related costs and fuel-related costs. These techniques have also been implemented in a number of current generation FMS in terms of the CI, which is a scalar value to balance the relative weighting of fuel and time costs. In the NG-FMS, the weightings are varied dynamically among the different flight phases of the flight. The uncertainties associated with the position, velocity and attitudes of the aircraft depend on the uncertainty of navigation data propagated through the ADM. Since the ADM equations are non-linear functions of the navigation variables, a suitable linearization shall be introduced and this can be conveniently performed by a second-order Taylor series expansion, wherein  $S$  signifies sine and  $C$  signifies cosine of an angle:

$$\sigma_{\dot{V}} = \left( (-g \cdot C \gamma)^2 \sigma_{\gamma}^2 + \left( \frac{T_{norm}}{m} \right)^2 \sigma_{\tau}^2 \right)^{1/2} \quad (3.61)$$

$$\sigma_{\dot{h}} = \left( (S \gamma)^2 \sigma_V^2 + \sigma_{V_{Wh}}^2 + (V \cdot C \gamma)^2 \sigma_{\gamma}^2 \right)^{1/2} \quad (3.62)$$

$$\sigma_{\dot{\chi}} = \left( \left( \frac{-N \cdot g \cdot S \phi}{C \gamma \cdot V^2} \right)^2 \sigma_V^2 + \left( \frac{N \cdot g \cdot C \phi}{V \cdot C \gamma} \right)^2 \sigma_{\phi}^2 + \left( \frac{N \cdot g \cdot S \phi \cdot S \gamma}{\gamma \cdot C \gamma^2} \right)^2 \sigma_{\gamma}^2 \right)^{1/2} \quad (3.63)$$

$$\sigma_{\dot{\gamma}} = \left( \left[ \frac{g(-N \cdot C \phi + C \gamma)}{V^2} \right]^2 \sigma_V^2 + \left( -\frac{N \cdot g \cdot S \phi}{V} \right)^2 \sigma_{\phi}^2 + \left( -\frac{g \cdot S \gamma}{V^2} \right)^2 \sigma_{\gamma}^2 \right)^{1/2} \quad (3.64)$$

$$\sigma_{\dot{\phi}} = \left( \left[ \frac{1}{(R_M + h)} \right]^2 \sigma_{V_{W\phi}}^2 + \left[ \frac{-V \cdot S \gamma \cdot S \chi + V_{W\phi}}{(R_M + h)^2} \right]^2 \sigma_h^2 + \left[ \frac{-V \cdot S \gamma \cdot S \chi}{(R_M + h)} \right]^2 \sigma_{\gamma}^2 + \left[ \frac{C \gamma \cdot S \phi}{(R_M + h)} \right]^2 \sigma_V^2 + \left[ \frac{V \cdot S \gamma \cdot C \chi}{(R_M + h)} \right]^2 \sigma_{\chi}^2 \right)^{1/2} \quad (3.65)$$

$$\sigma_{\dot{\lambda}} = \left( \left[ \frac{C \gamma \cdot C \chi}{C \phi (R_T + h)} \right]^2 \sigma_V^2 + \left[ \frac{-V \cdot C \gamma \cdot S \chi}{C \phi (R_T + h)} \right]^2 \sigma_{\chi}^2 + \left[ \frac{1}{C \phi (R_T + h)} \right]^2 \sigma_{V_{W\lambda}}^2 + \left[ \frac{-V \cdot S \gamma \cdot C \chi}{C \phi (R_T + h)} \right]^2 \sigma_{\gamma}^2 + \left[ \frac{-C \phi (V \cdot S \gamma \cdot C \chi + V_{W\lambda})}{(C \phi (R_T + h))^2} \right]^2 \sigma_h^2 + \left[ \frac{S \phi \cdot C \phi (R_T + h) (V \cdot C \gamma \cdot C \chi + V_{W\lambda})}{(C \phi (R_T + h))^2} \right]^2 \sigma_{\phi}^2 \right)^{1/2} \quad (3.66)$$

where  $T_{norm}$  is the axial thrust. The resulting uncertainties in aircraft position and kinematics are conveniently described by the associated uncertainty volumes. For cooperative and non-cooperative obstacle avoidance and safe-separation maintenance, the overall uncertainty volumes are obtained by combining the navigation error with the tracking error and then translating them to unified uncertainty volumes, which are discussed in the next chapter.

### 3.6 CNS Performance

The CNS+A concepts enable more accurate estimation of CNS performance and involve higher levels of automation. Modern avionics and ground-based systems for planning and near real-time execution of Four Dimensional Trajectory (4DT) functionalities, including multi-objective 4DT optimisation, negotiation and validation in the TBO/IBO context are currently under development. CNS+A systems with integrity monitoring and augmentation functionalities fulfilling RCP, RNP and RSP, and thus meeting the RTSP levels are envisaged. The automated systems allow the aircraft equipped with novel avionic systems to fly user-preferred optimal flight paths and thus they limit the intervention of the air traffic controllers to high-level and emergency decision making. Figure 3.15 illustrates the RTSP factors and the associated timeframes.

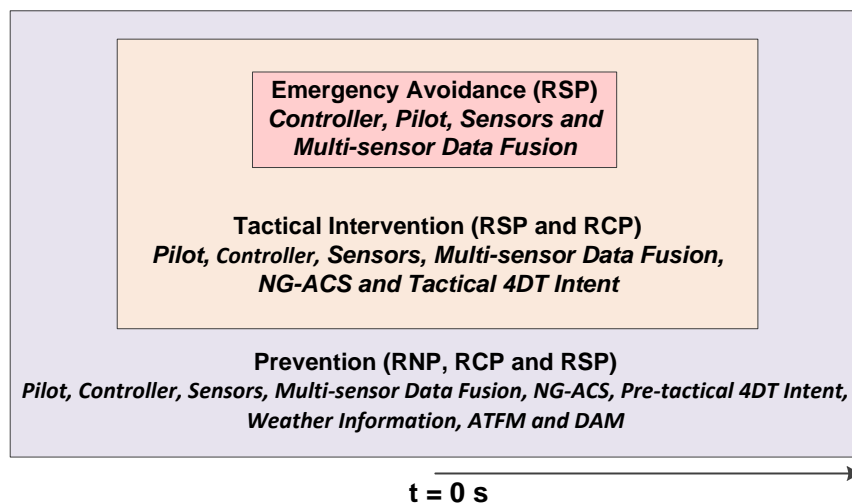


Figure 3.15. RTSP elements and time frames.

The emergency avoidance of natural and man-made obstacles involves the human pilot and controller along with data obtained from adopting multi-sensor data fusion algorithms. Tactical intervention also involves the NG-ACS and tactical 4DT intents. Prevention of collisions takes into account weather and airspace sector information in addition to tactical intervention and emergency avoidance tasks. Several architectures,

interfaces, communication protocols, data elements and message formats for operation of RPAS are defined in the NATO Standardisation Agreement (STANAG) 4586. Modelling the navigation, communication and surveillance errors as white Gaussian noise, the associated probability density functions are:

$$f_{RTSP}(x) = \frac{1}{\sqrt{2\pi}\sigma_{CNS}} e^{-\frac{x^2}{2\sigma_{CNS}^2}} \quad (3.67)$$

where  $\sigma_{CNS}$  represents the standard deviation values resulting from errors in communication, navigation and surveillance data ( $\sigma_{Comm}$ ,  $\sigma_{Nav}$ ,  $\sigma_{Sur}$ ) respectively.

## 3.7 NG-FMS Case Studies

To illustrate the capability of NG-FMS algorithms to generate and optimise 4DT intents, the typical tasks performed by the NG-FMS were simulated. Both manned and unmanned aircraft platforms were used for the case studies including Airbus A380 and AEROSONDE™ UAS.

### 3.7.1 Platforms

The Airbus A380 is a double-deck, wide-body, four-engine, long-range jet airliner manufactured by Airbus. The A380's belongs to the fly-by-wire jetliner family and has an advanced cockpit, including larger interactive displays, and an advanced flight management system with improved navigation modes. Figure 3.16 shows the dimensions of A380 while Table 3.2 provides the aircraft specifications.

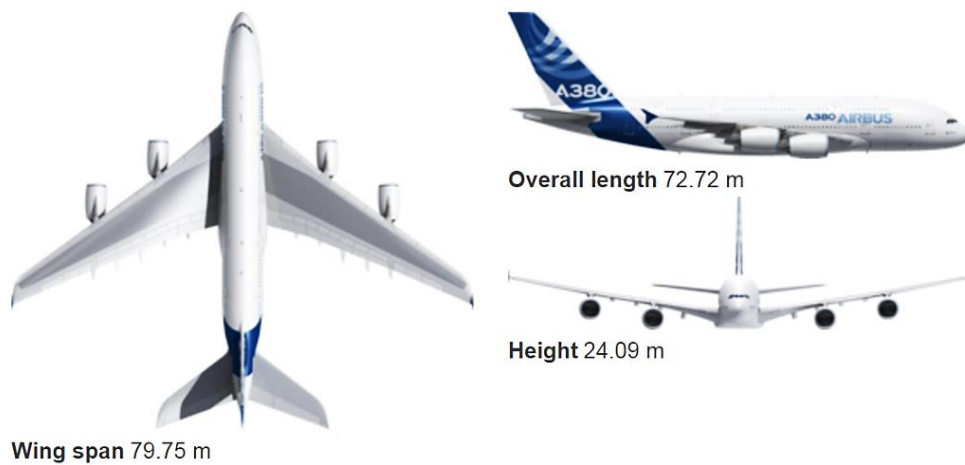


Figure 3.16. Airbus A380 [18].

The Airbus A320 belongs to the single-aisle jetliner family, which is composed of the A318, A319, A320 and A321 and variants from Boeing and other aircraft manufacturers. The introduction of sharklets (2.4-meter-tall wing tip devices) provides operators with the flexibility of either adding an additional 100 NM range or increased payload capability of up to 450 kg. Figure 3.17 shows the dimensions of A320 while Table 3.3 provides the aircraft specifications.

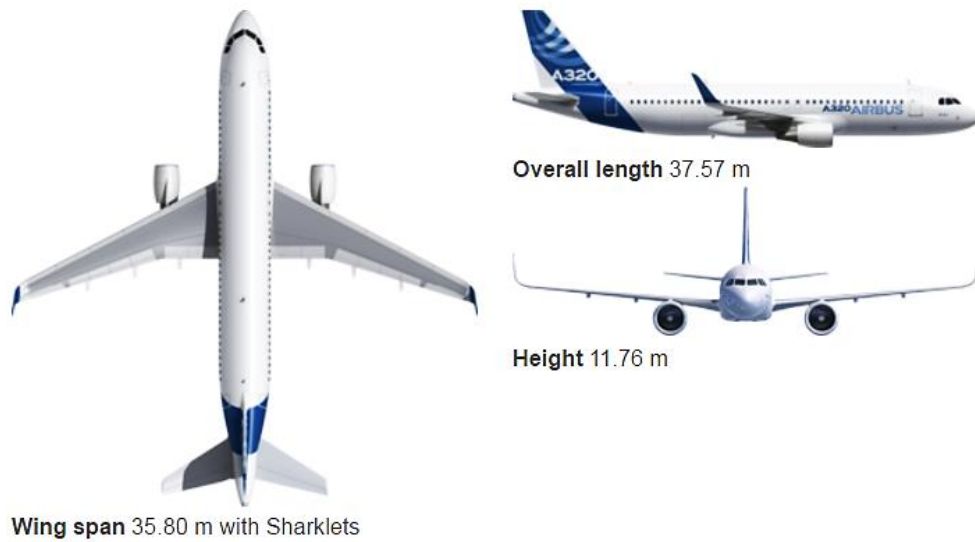


Figure 3.17. Airbus A320 [18].

Table 3.2. Airbus A380 specifications [18].

Specification	Value
Overall length	72.72 m
Fuselage width	7.14 m
Wing span (geometric)	79.75 m
Range	15,200 km
Max take-off weight	575 tonnes
Max landing weight	394 tonnes
Max fuel capacity	320,000 litres
Cruise speed	Mach 0.85

Figure 3.18 and Table 3.4 show the specifications of AEROSONDE™ UAS. Table 3.5 provides the aerodynamic parameters used in the dynamics model of AEROSONDE™ UAS. The AEROSONDE™ is a small robotic aircraft, which provides a new capability for



improving the space / time resolution of observations of the ice/ocean surface. The AEROSONDE™ has a wing span of 9 m and weighs approximately 15 kg. The small size of the AEROSONDE™ allows it to be extremely fuel efficient so that flight durations can easily exceed 20 hours. Iridium satellite communications are vital to successfully exploiting the long range/long endurance capabilities of the AEROSONDE™ aircraft (nearly 3000 km). It has an altitude range of between 100 and 7000 m.

Table 3.3. Airbus A320 specifications [18].

Specification	Value
Overall length	37.57 m
Fuselage width	3.95 m
Wing span (geometric)	35.80 m (with sharklets)
Range	6,100 km
Max take-off weight	73.5 tonnes
Max landing weight	64.5 tonnes
Max fuel capacity	24,210 litres
Cruise speed	Mach 0.84

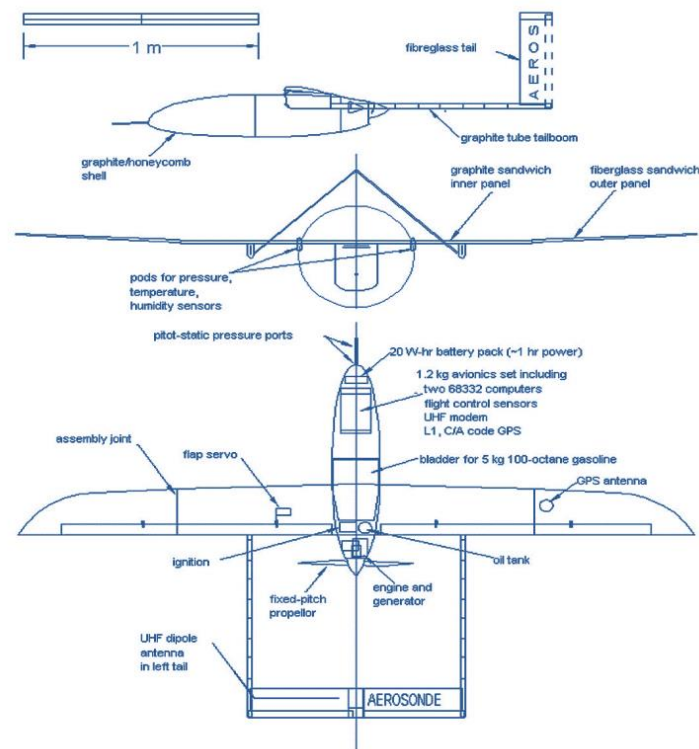


Figure 3.18. AEROSONDE™ UAS [19].

Table 3.4. AEROSNDE™ UAS specifications.

Specification	Value
Features	Auto launch and auto recover; Car Launch / Rail Launch flexibility; Multiple energy reduction landing system
Endurance	10 hours with surveillance payload
Wing span	3.6 metres
Maximum Take-Off Weight (MTOW)	17.5 kg with J-type engine and 25kg with K-type engine
Cruise Speed	50-60 Knots
Dash Speed	62-80 Knots at sea Level
Ceiling	4500m
Weight	7.5 – 10 pounds
J-Type Engine	Four-stroke 24cc. Electronic Fuel Injection (EFI)
K-Type Engine	Twin dual cylinder, four stroke, EFI
Fuel	93 Premium Octane/100 low-lead aviation gas

### 3.7.2 Long-haul Flight

A simulation case was performed with an aircraft taking off at London Heathrow airport {N 51° 28' 39", W 0° 27' 41"} and landing at Singapore Changi airport {N 01° 21' 33.16", E 103° 59' 21.57"}. The aircraft parameters and aerodynamic data were extracted from the EUROCONTROL Base of Aircraft Data (BADA). Objectives such as fuel consumption, time and path constraints are considered via an appropriate set of performance weightings obtained as a result of the CDM process. Depending on the cost functions and gains selected (i.e., minimum time, fuel and other environmental costs such as gaseous emissions of CO<sub>2</sub>, NO<sub>x</sub>, etc.), there are different trajectory possibilities for all the flight segments. Figure 3.19 illustrates the different trajectories generated, each resulting from a different cost function on time and fuel minimisation. In this case, considering the climb phase separately, the maximum CO<sub>2</sub> and NO<sub>x</sub> reductions are 281.7 kg and 1.5 kg respectively. The trajectory corresponding to minimum fuel burn provides 90 kg fuel savings when compared to the minimum time optimisation case.

Table 3.5. AEROSONDE™ UAS ADM parameters and derivatives [19].

Zero angle of attack lift derivative	$CL_0$	0.23	Sideslip roll control derivative	$CY_{da}$	-0.07
Lift angle of attack derivative	$CL_{\dot{\alpha}}$	1.97	Sideslip yaw control derivative	$CY_{dr}$	0.19
Mach number derivative	$CL_M$	0	Sideslip roll rate derivative	$CY_p$	0
Lift at minimum drag	$CL_{mind}$	0.23	Sideslip yaw rate derivative	$CY_r$	0
Pitch rate derivative	$CL_q$	7.95	Zero angle of attack derivative (pitch moment)	$Cm_0$	0.13
Lift control (flap) derivative	$CD_{df}$	0.14	Angle of attack derivative (pitch moment)	$Cm_{\dot{\alpha}}$	-2.73
Pitch control (elevator) derivative	$CD_{de}$	0.01	Lift control derivative (pitch moment)	$Cm_{df}$	0.05
Roll control (aileron) derivative	$CD_{da}$	0.03	Pitch control derivative	$Cm_{de}$	-0.992
Yaw control (rudder) derivative	$CD_{dr}$	0.03	Angle of attack derivative (pitch moment)	$Cm_{\dot{\alpha}}$	-10.38
Mach number derivative	$CD_M$	0	Pitch rate derivative	$Cm_q$	-38.2
Minimum drag derivative	$CD_{min}$	0.04	Mach number derivative	$Cm_M$	0
Sideslip derivative	$CY_{beta}$	-0.83	Sideslip derivative (roll moment)	$Cl_{beta}$	-0.13
Roll control derivative	$Cl_{da}$	-0.16	Yaw control derivative (roll moment)	$Cl_{dr}$	0.0024
Roll rate derivative	$Cl_p$	-0.50	Yaw rate derivative (roll moment)	$Cl_r$	0.25
Sideslip derivative (yaw moment)	$Cn_{beta}$	0.07	Roll control derivative (yaw moment)	$Cn_{da}$	0.01
Yaw control derivative	$Cn_{dr}$	-0.0693	Roll rate derivative (yaw moment)	$Cn_p$	-0.069
Yaw rate derivative	$Cn_r$	-0.0946	Oswald's efficiency number	$e_0$	0.75

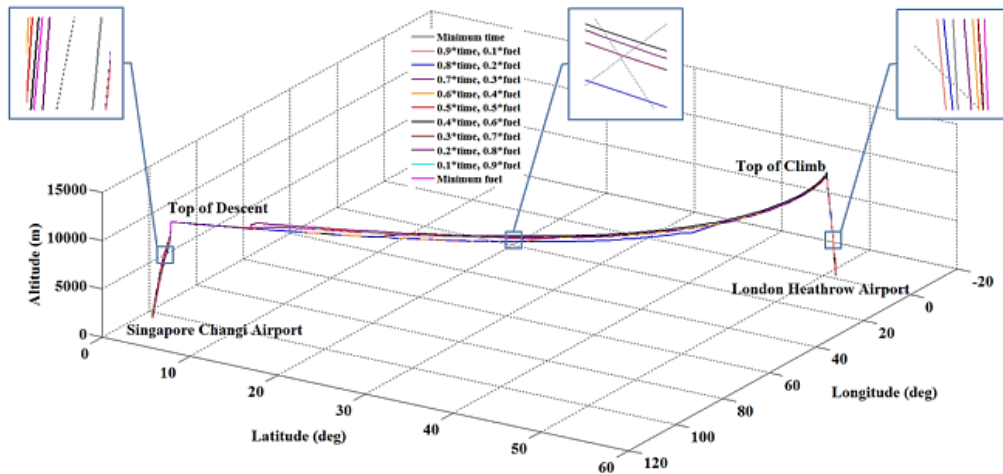


Figure 3.19. 4D trajectories.

Simulation case studies were carried out to corroborate the validity of the NG-FMS algorithms to generate and optimise 4D trajectory intents. Intents were generated by the NG-FMS and their optimisations were accomplished with respect to primarily time and fuel costs. Noise Sensitive Areas (NSA) were considered as path constraints in the climb phase (in the proximity of the airport) and weather cells were taken into account in the cruise phase. A non-rotating spherical Earth model was employed in the simulation case studies. Pseudospectral and weighted sum methods were adopted to carry out near real-time multi-objective deterministic 4DT optimisation. A typically loaded Airbus A380 aircraft with MTOW of 400,000 kg was assumed to be flying the mission. The aircraft parameters and aerodynamic data were extracted from the EUROCONTROL's BADA. The simulations were executed on a Windows 7 Professional workstation (64-bit OS) supported by an Intel Core i7-4510 CPU with clock speed 2.6 GHz and 8.0 GB RAM. The flight plan was designed for the aircraft to take-off from London Heathrow airport (ICAO code: EGLL) and flying towards AMRAL waypoint, located in the United Kingdom and then climbing up to the planned cruise flight level 330 (33,000 feet). Two avoidance regions were introduced as path constraints in the simulation case study. Figure 3.20 shows a 3D view of the 4D trajectory intents generated, each resulting from a different cost function for time and fuel minimisation. In order to account for environmental objectives, numerical data for time, fuel burn and associated emissions were analysed. The time, fuel burn and emissions ( $\text{CO}_2$  and  $\text{NO}_x$ ) change, as a result of trajectory variations (due to varying cost index). This indicates that for every kilogram of aviation fuel burned, 3.13 kg of  $\text{CO}_2$  and 0.014 kg of  $\text{NO}_x$  (as the average of  $\text{NO}_x$  emission below and above FL 330) are generated.

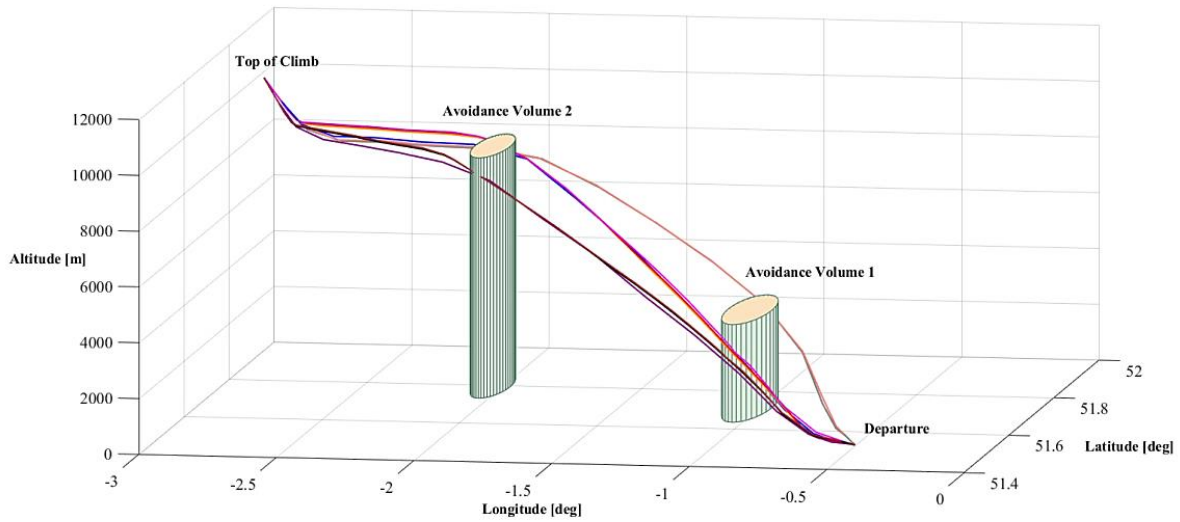


Figure 3.20. Climb Phase 4D Trajectory Intents.

In the cruise phase, two weather cells were considered and the 4D trajectory intents were able to avoid those areas as illustrated in Figure 3.21. The results demonstrate that the optimisation algorithms are able to cope with avoidance volumes as part of the cost function (numerically and analytically). The trajectory intents were optimised with contrails and weather cells as path constraints, and are generated within 10 seconds in the implemented hardware platform.

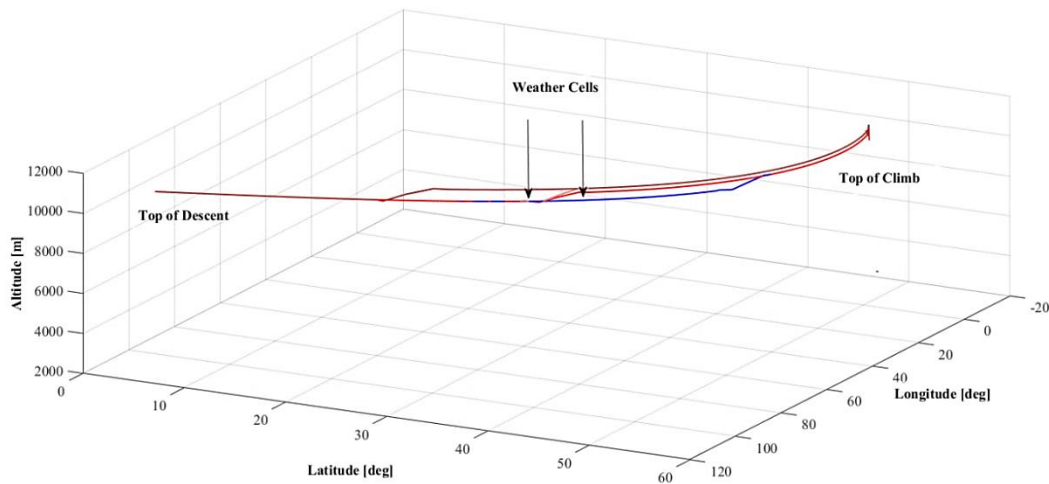


Figure 3.21. Cruise Phase 4D Trajectory Intents.

In this case, the trajectory with minimum fuel burn consumes 700 kg fuel less than that of the trajectory for minimum time. The optimisation of the active 4D trajectory took 15 seconds while the NSA avoidance trajectory required an additional 10 seconds for optimisation. Time taken in emergency scenarios such as the implementation of near real-time SA&CA functions are also well within the time frame for avoiding collisions.

During the descent and arrival phases, the aircraft proceeds from the top of descent point to Singapore Changi airport (ICAO code: WSSS). In the absence of suitable NG-FMS autopilot loops, the trajectory affected by wind / turbulence does not exceed the RNP containment boundaries. However, the NG-FMS raises a CIF after detecting the potential RNP violation due to unforeseen situations such as extreme turbulence, etc. This CIF triggers a new intent optimisation/negotiation loop with the 4-PNV system and thus prevents the production of a WIF. In the conditions described, the time required to generate the CIF was 5 seconds. To avoid a WIF event, an NG-FMS autopilot loop was performed based on the interactions with AFCS, allowing re-insertion into the original nominal trajectory immediately after a CIF event. The average difference in time (i.e. the difference between RTA and ETA) obtained for each segment was 9 seconds. The error tolerance adopted for this case was  $\pm 10$  seconds resulting in an increase of the airspeed profile by 20 m/s.

### 3.7.3 Medium-haul Flight

An Airbus A320 aircraft with take-off weight of 75,000 kg is assumed to be flying the mission. The aircraft takes off from Melbourne Tullamarine airport in Australia (ICAO code: YMML) and proceeds towards Darwin airport (ICAO code: YPDN) with a planned cruise flight level 340 (34,000 feet). Depending on the cost functions and gains selected (i.e., minimum time, minimum fuel and other environmental costs such as gaseous emissions of CO<sub>2</sub>, NO<sub>x</sub>, etc.), there are different trajectory possibilities for all flight segments. Figure 3.22 illustrates the Google Earth image of the different trajectories generated, each resulting from different weightings of time and fuel optimisation criteria. For the climb phase, the CO<sub>2</sub> and NO<sub>x</sub> reductions are approximately 251.7 kg and 1.5 kg respectively. The trajectory corresponding to minimum fuel burn provides 90 kg fuel savings when compared to the minimum time optimisation case (Figure 3.21).

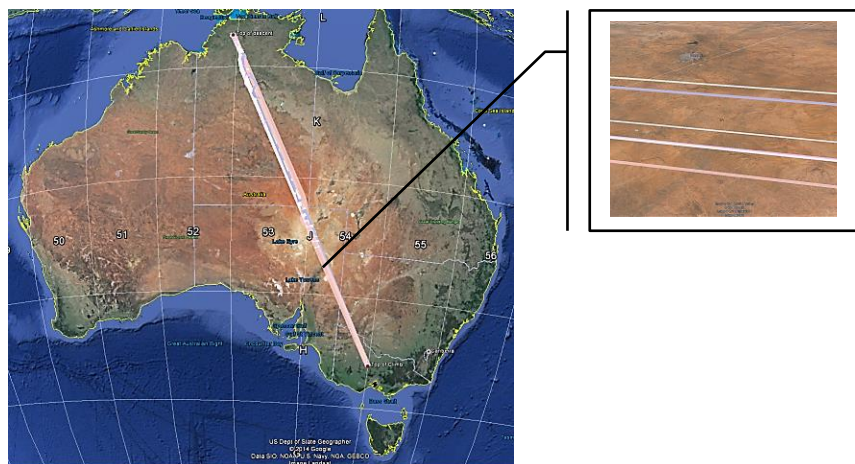


Figure 3.22. Simulated set of 4DT intents.

The introduction of position uncertainties on all the nominal parameters, allowed the transformation of the equations of motion into stochastic differential equations that were then treated with the Monte Carlo sampling technique and solved using the deterministic optimiser for 150 samples. A conservative value for the number of samples was first chosen to provide an estimate of the 4DT deviations from the RNP. Then the simulations were performed to provide a 95% confidence bound on the deviations from RNP for a given flight phase. The absolute lateral deviation of the 4D trajectories (affected by uncertainties), with respect to the reference 4D trajectory were calculated for all flight phases. Figure 3.23 shows the 4DT deviations in the climb phase. The adherence to the required CNS performances allows for assessment of any collision risks between multiple aircraft and thus supports implementation of effective separation maintenance and collision avoidance algorithms.

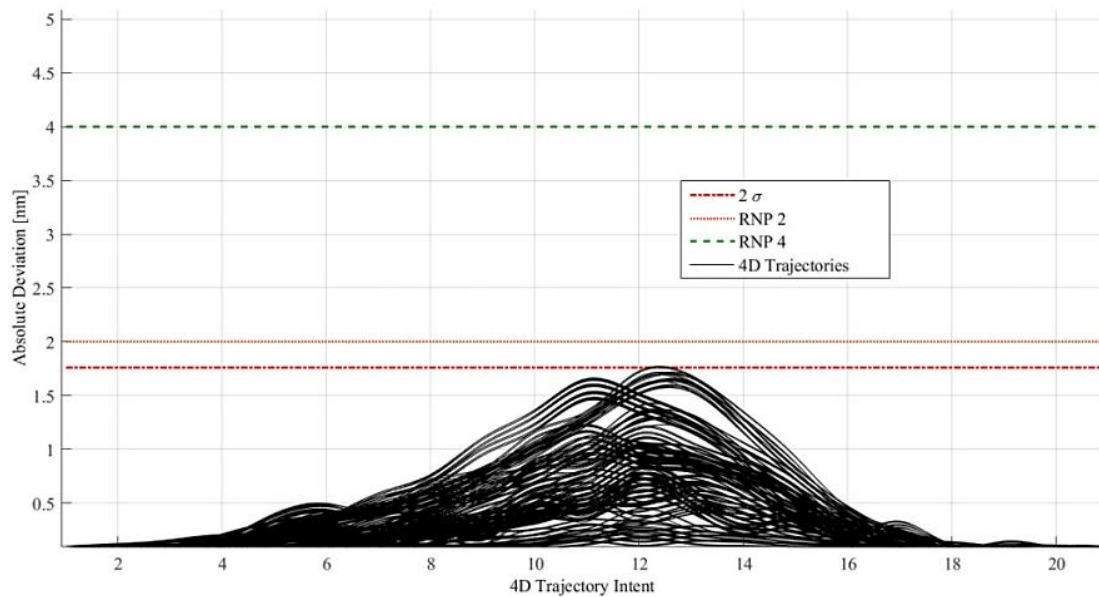


Figure 3.23. 4D trajectory Deviations (RNP).

Table 3.6 summarises the navigation performance obtained for climb, cruise and descent flight phases comparable to the RNP thresholds defined by ICAO.

Table 3.6. Navigation system performance.

Flight Phase	Performance Obtained [NM]	RNP Threshold [NM]
Climb	1.8	2
Cruise	3.2	4
Descent	1.4	2



### 3.7.4 UAS

To illustrate the capability of UAS NG-FMS to generate optimal 4D trajectories, a simulation case study is presented here [20]. The 4DT is not limited to a short sequence of 3D waypoints with time stamps. Such a definition would assume that each flight leg will be straight (with a constant heading) or a short steady-flight turn. VTOL and UAS in particular routinely execute optimised trajectories that include manoeuvres and accelerated flight segments. Furthermore, hybrid configurations (tilt rotor, etc.) will require "transition segments" to convert between vertical and horizontal flight modes. The proposed solution can handle flight plans/trajectories that can contain vertical and accelerated manoeuvres, e.g., for helicopter emergency response (medical flight) and UAS surveillance applications. The adoption of a 6-DoF aircraft dynamics model, manoeuvring recognition algorithms and operational realisation of these manoeuvres support the applicability of these algorithms to an UTM system implementation perspective to handle VTOL, manoeuvring (e.g., surveillance), and multi-UAS operations [21, 22].

An aerial recognition mission involving a loitering phase is simulated. The employed platform is an old variant of the AEROSONDE™ UAS. The departure point is St Leonards Airfield (YSLE, S38.166 E144.687), and the working area within which the recognition is performed is the AEROSONDE Testing Range, encompassed by Danger Area YMMM/D322A of the Melbourne Flight Information Region (FIR). After the recognition, the RPAS is required to land at the Point Cook Royal Australian Air Force Base (YMPC, S37.933, E144.753). The loitering was performed at the test range (S38.210 E144.860), at altitudes between 1000 and 1500 ft. Objectives such as fuel consumption, time and emissions, as well as constraints on the path and on the flight envelope are introduced in the trajectory optimization problem based on the information exchanged as a result of the 4DT negotiation process. The climb trajectory is depicted in Figure 3.24, while the descent trajectory is depicted in Figure 3.25.

The NG-FMS generated the optimal climb and descent trajectories in 47 seconds, which fully supports strategic and tactical timeframes. In order to meet the CD&R requirements for emergency timeframe less than 50 seconds, computationally inexpensive trajectory optimisation algorithms such as differential geometry techniques can be employed. The trajectory corresponding to minimum fuel burn is characterized by a fuel saving of 130 g when compared to the minimum time case.



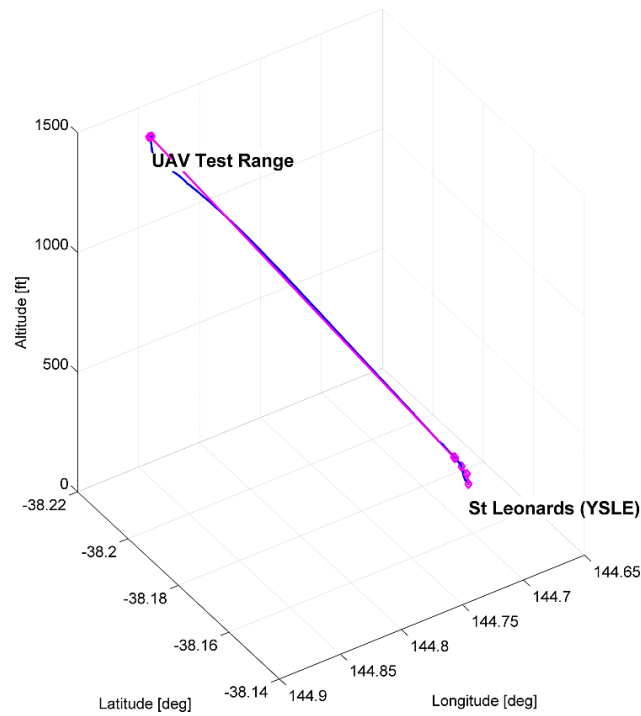


Figure 3.24. Results of the 4DT optimisation for climb phase.

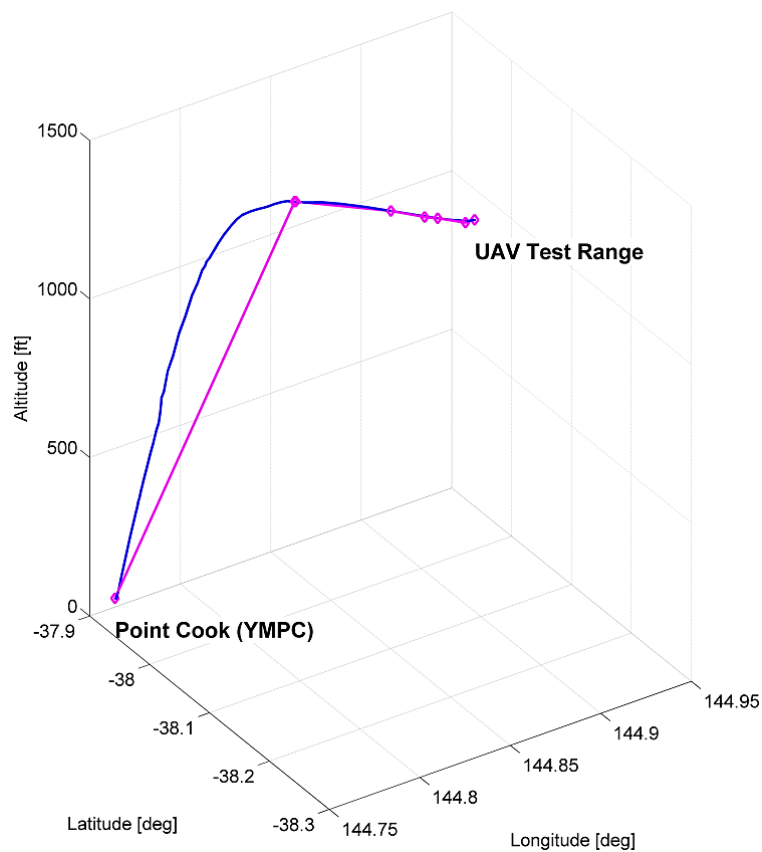


Figure 3.25. Results of the 4DT optimisation for descent phase.

A stochastic analysis case study was performed to evaluate the potential impact of system uncertainties on the trajectory generation process. The introduction of

uncertainties on all nominal parameters, with ranges equal to the standard deviations allowed for the transformation of the equation of motion into stochastic differential equations as before, which are then treated with the Monte Carlo sampling technique and solved using the deterministic optimizer for 100 samples. In these simulations, real weather data obtained with the Global Forecast System (GFS), kindly made available by the National Climatic Data Center (NCDC) of the US National Oceanic and Atmospheric Administration (NOAA), was adopted.

### 3.8 Negotiation and Validation Features

As described in Section 3.1, the negotiation and validation of 4DT intents by the NG-FMS/ATM system is dependent on a number of factors including weather updates, updated aircraft dynamics/ATM/AOC constraints, obstacle detection, Demand-Capacity Balancing (DCB), sector occupancy, and airspace and time based restrictions. A conceptual representation of the air-to-ground and air-to-air negotiation processes is illustrated in Figure 3.26.

#### 3.8.1 Evaluation Process

The negotiation and validation process between the NG-FMS and NG-ATM system was evaluated using laboratory activities by server client protocols (Figures 3.26 and 3.27).

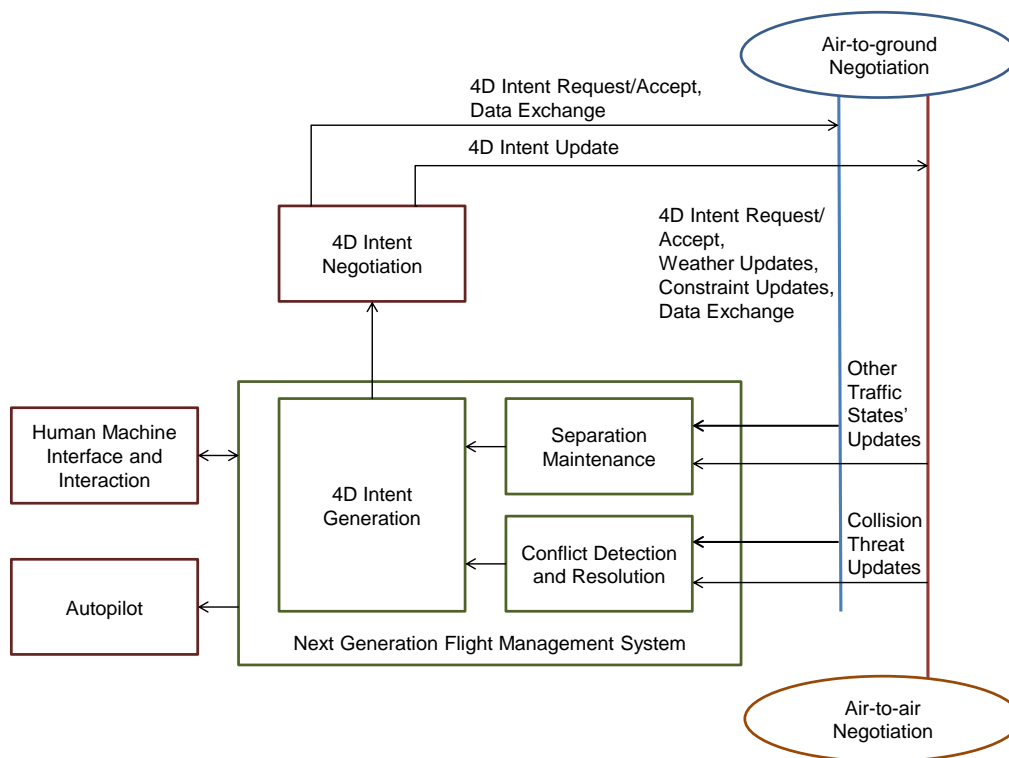


Figure 3.26. NG-FMS air-to-ground and air-to-air negotiation loops.

Since individual, per-aircraft operational and environmental benefits are marginal, to achieve significant and sustained benefits, a large proportion of the fleet will have to adopt optimised 4D TBO/IBO techniques. The rates of adoption at which these benefits will become tangible are yet to be estimated. Some Original Equipment Manufacturers (OEM) are targeting both forward fit (software update on a FANS A+C+ aircraft) and retrofit opportunities (software upgrade in a FANS B+ aircraft).

Scaling up 4DT operations in dense airspace introduces further considerations including:

- Bandwidth and data link: Increased bandwidth will be required to support the increased amounts of data link traffic between NG-FMS and NG-ATM systems. New infrastructure (such as air-ground ACS) has to play a key role, but improved protocols with compression and reduced alphabets can also be adopted;
- Maintenance of separation: As each NG-FMS negotiates a 4DT with the NG-ATM system, the NG-ATM system considers whether the requested trajectory would cause a loss of separation with other aircraft in the vicinity. As long as the look-ahead times are moderate, computational performance issues on the 4-PNV side can be addressed by distributed parallel processing. Formal methods may be employed for verifying these distributed algorithms;
- Resource loading: Several NG-FMS may request a similar 4DT, for example, to utilise favourable tailwinds or to avoid adverse weather. As successive requests are processed by the NG-ATM system, cumulative load on resources including routes and sectors increases to a point where capacity may be exceeded and DAM/DCB are required;
- Interference with CD&R function: The 4DT negotiation and validation process must be implemented to minimise interference with the CD&R functions, especially during an emergency timeframe. A minimum guaranteed safety net must be provided that is not reduced because of negotiation of 4DT intents with the 4-PNV system. Hence, it is important to have a valid solution for the 4DT intent without compromising the safety net requirements.

Other considerations include:

- Self-separation: If a wide-scale roll-out of NG-FMS equipage can be achieved in less-dense airspace, then self-separation concepts may experience a revival when coupled with surveillance technologies such as ADS-B in;
- Stability of metering and sequencing: The downstream impact of NG-FMS initiated 4DT changes may have to be considered if it impacts the sequence over scheduling points (meter fixes, terminal-area merge points, etc.). For example, an

arrival sequence may be frozen a certain time before landing or the flow of aircraft through a co-ordination point to an adjacent FIR may be subject to exit separation criteria. Until the NG-FMS system evolves to perform metering and sequencing, it may be prudent to create reduced automation zones around problematic areas of airspace.

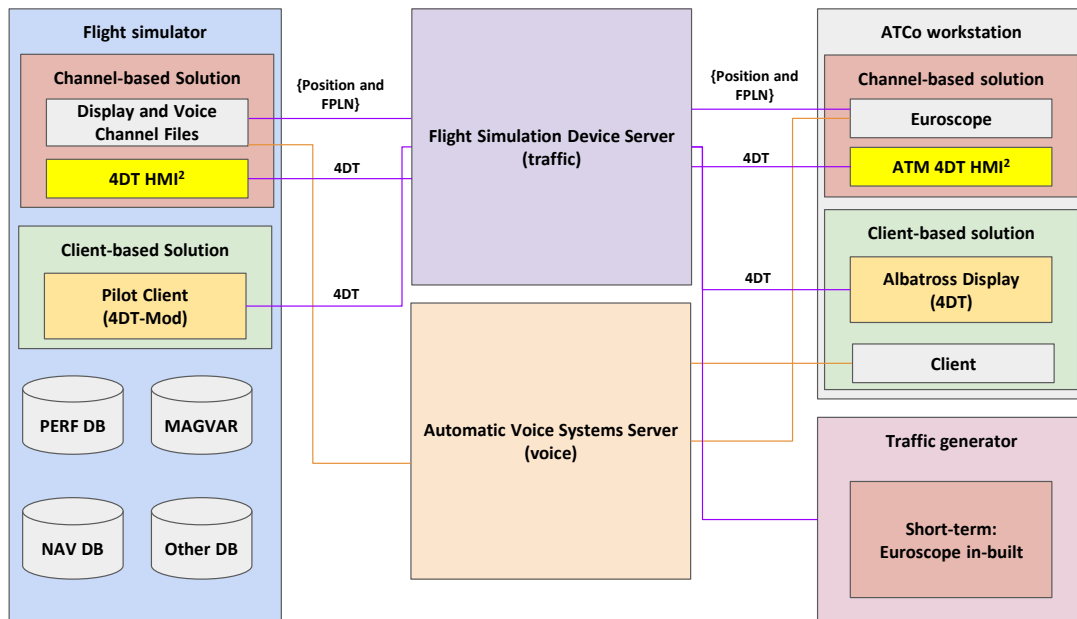


Figure 3.27. NG-FMS and NG-ATM system negotiation and validation [21].

In order to be adopted for strategic online, tactical online and in some emergency contexts requiring the use of safety nets, i.e., with a reference time horizon of say 5 minutes, it is assumed that the total duration of optimisation, negotiation and validation processes must remain under 180 seconds. Trajectories are checked for traffic conflicts and separation from hazardous phenomena. The validation algorithm assesses the lateral and vertical separation criteria and includes a simplified wake vortex modelling to assess the longitudinal separation. In line with the SESAR and NextGen concepts of operations, a near-real-time negotiation and validation process for dynamic rerouting was achieved using this framework [21].

### 3.9 Conclusions

The system architecture, design and development of a Next Generation Flight Management Systems (NG-FMS) were presented. A detailed functional architecture of the NG-FMS suitable for both manned and unmanned aircraft platforms was described.

Suitable mathematical models were developed to implement the 4DT-O capability, addressing both the deterministic and stochastic trajectory optimisation problems. Pseudospectral and weighted sum methods were adopted to carry out near real-time multi-objective deterministic 4DT optimisation. Objectives such as fuel consumption, time, noise impact and contrails were considered via an appropriate set of performance weightings. Simulation cases involving Airbus commercial transport aircraft and an AEROSONDE™ pusher prop (aviation gas fuelled) UAS were presented. These examples highlight how the NG-FMS is tailored to long-haul and short-haul transport with traditional ATM coordination, and it could be extended to an UTM system implementation to handle VTOL, manoeuvring (e.g., surveillance), and cooperative UAS operations. Investigation of the total system error boundaries was conducted to evaluate the effects of error propagation in the aircraft dynamics model. In addition, air-to-ground 4DT negotiation algorithms were developed, aiming to attempt a trajectory validation process. In line with the SESAR and NextGen concepts of operations, a near real-time negotiation and validation process for dynamic rerouting was presented.

### 3.10 References

1. SESAR, "The European ATM Master Plan", European Union and Eurocontrol, 2015.
2. R. Sabatini, A. Gardi, S. Ramasamy, T. Kistan and M. Marino, "Modern Avionics and ATM Systems for Green Operations", Encyclopedia of Aerospace Engineering, eds R. Blockley and W. Shyy, John Wiley: Chichester, 2015. DOI: [10.1002/9780470686652.eae1064](https://doi.org/10.1002/9780470686652.eae1064)
3. D. Batchelor, "Comparing European ATM Master Plan and the NextGen Implementation Plan," IEEE Conference on Integrated Communication, Navigation and Surveillance (ICNS), pp. 1-14, Washington DC, USA, 2015.
4. M. Ballin, D. Williams, "Prototype Flight Management Capabilities to Explore Temporal RNP Concepts", IEEE Digital Avionics Systems Conference, Minnesota, USA, 2008.
5. ICAO, "Procedures for Air Navigation Services - Aircraft Operations", Document 8168, Fifth Edition, The International Civil Aviation Organization, Montreal, Canada, 2006.
6. B. Honzik, "Airborne 4-Dimensional Trajectory Management", AIAA/IEEE Digital Avionics Systems Conference, Virginia, USA, 2012.
7. R. Sabatini, T. Moore and C. Hill, "A New Avionics-Based GNSS Integrity Augmentation System: Part 1 – Fundamentals", The Journal of Navigation, vol. 66, no. 3, pp. 363–384, 2013. DOI: [10.1017/S0373463313000027](https://doi.org/10.1017/S0373463313000027)
8. R. Sabatini, T. Moore, C. Hill and S. Ramasamy, Assessing Avionics-Based GNSS Integrity Augmentation Performance in UAS Mission- and Safety-Critical Tasks, Proceedings of

- International Conference on Unmanned Aircraft Systems (ICUAS 2015), Denver, CO, USA, 2015. DOI: [10.1109/ICUAS.2015.7152347](https://doi.org/10.1109/ICUAS.2015.7152347)
9. ARINC 702A-4, "Advanced Flight Management Computer System", Aeronautical Radio, Incorporated, Cedar Rapids, Iowa, US, 2014.
  10. SAE, "Flight Management System (FMS)", ARP4102/9A, Society of Automotive Engineers, Pennsylvania Troy, Michigan, USA, 2014.
  11. D. Allerton, "Principles of Flight Simulation", John Wiley and Sons Ltd, West Sussex, UK, 2009.
  12. O. von Stryk and R. Bulirsch, "Direct and Indirect Methods for Trajectory Optimization", Annals of Operations Research, vol. 37, pp. 357-373, 1992.
  13. J.T. Betts, "Survey of Numerical Methods for Trajectory Optimization", Journal of Guidance, Control and Dynamics, vol. 21, pp. 193-207, 1998.
  14. J. Z. Ben-Asher, "Optimal Control Theory with Aerospace Applications, Education Series, American Institute of Aeronautics and Astronautics (AIAA), Reston, VA, USA, 2010.
  15. A.V. Rao, "Survey of Numerical Methods for Optimal Control", Advances in the Astronautical Sciences, vol. 135, pp. 497-528, 2010.
  16. A. Gardi, R. Sabatini and S. Ramasamy, "Multi-objective Optimisation of Aircraft Flight Trajectories in the ATM and Avionics Context", Progress in Aerospace Sciences, vol. 83, pp. 1-36, 2016. DOI: [10.1016/j.paerosci.2015.11.006](https://doi.org/10.1016/j.paerosci.2015.11.006)
  17. N. Marius, "Lateral track control law for AEROSONDE UAV", 39<sup>th</sup> Aerospace Sciences Meeting and Exhibit, American Institute of Aeronautics and Astronautics, 2001.
  18. Airbus, Aircraft Specifications, Airbus S.A.S, France. Information available from: <http://www.airbus.com/aircraftfamilies/passengeraircraft>
  19. J. Maslanik, "Polar remote sensing using an unpiloted aerial vehicle", Seminar held at Colorado Center for Astrodynamics Research (CCAR), University of Colorado at Boulder. Available online at: <http://www2.hawaii.edu/~jmaurer/uav/#specifications> (overview and editing by J. Maurer), 2002. Webpage visited in 2016.
  20. A. Gardi, S. Ramasamy and R. Sabatini, "4-Dimensional Trajectory Generation Algorithms for RPAS Mission Management Systems", Proceedings of the IEEE International Conference on Unmanned Aircraft Systems (ICUAS 2015), Denver, CO, USA, 2015. DOI: [10.1109/ICUAS.2015.7152314](https://doi.org/10.1109/ICUAS.2015.7152314)
  21. A. Gardi, Y. Lim, T. Kistan, S. Ramasamy and R. Sabatini, "Air Traffic Management Simulation Environment for 4-Dimensional Trajectory Based Operations", 17<sup>th</sup> Australian International Aerospace Congress, AIAC17, Melbourne, Australia, 2017.

22. A. Gardi, "A Novel Air Traffic Management Decision Support System Multi-Objective 4-Dimensional Trajectory Optimisation for Intent-Based Operations in Dynamic Airspace", Ph.D. Thesis, School of Engineering, RMIT University, 2016.

This page is intentionally left blank to support presswork tasks



## CHAPTER 4

# SEPARATION ASSURANCE AND COLLISION AVOIDANCE FUNCTIONALITIES

*"If knowledge and foresight are too penetrating and deep, unify them with ease and sincerity". - Xun Kuang*

### 4.1 Introduction

This chapter presents the unified approach to SA&CA. In this approach, real-time safety-critical data fusion algorithms suitable for both cooperative and non-cooperative encounters are developed for a variety of safety-critical applications. The SA&CA functions are integrated in the NG-FMS and are based on mathematical algorithms that quantify in real-time the total avoidance volume in the airspace surrounding a target (static or dynamic). Building on these analytical models, data processing techniques allows the real-time transformation of navigation and tracking errors affecting the state measurements into unified range and bearing uncertainty descriptors. The investigation in later chapters focusses on representative scenarios for validating the automated separation maintenance and collision avoidance resolution functions in both non-cooperative and cooperative scenarios.

### 4.2 Unified Approach to SA&CA

The aim of the unified approach is to determine the overall avoidance volume surrounding an obstacle or an intruder track. The approach provides an innovative analytical framework to combine real-time measurements (and associated uncertainties) of navigation states, platform dynamics and tracking observables to produce high-fidelity avoidance volumes suitable for integration in future avionics, ATM and defence decision support tools.

In this approach, both the navigation error of the host platform (manned/unmanned) and the tracking error of the intruder state information are combined in order to obtain the volume of airspace that needs to be avoided, providing safe separation assurance and collision avoidance. The underlying principle is to express the Separation Assurance and Collision Avoidance (SA&CA) sensor/system error in range and bearing uncertainty descriptors [1 - 3]. In order to estimate navigation and tracking errors, sensor error modelling is adopted. Vector analysis is applied to combine the navigation and tracking ellipsoids in real-time. The variation in the state vector,  $\vec{x}$  is expressed as:

$$\delta(\vec{x}_i(t)) = \left[ \frac{\delta \vec{x}}{\delta p} \right]_t \cdot \sigma_{p_j} \quad (4.1)$$

where  $p$  is the position of the host aircraft and  $t$  is the time of measurement. Let  $R$ ,  $\alpha$  and  $\epsilon$  be the range, azimuth ( $0^\circ \leq \alpha \leq 360^\circ$ ) and elevation ( $0^\circ \leq \epsilon \leq 90^\circ$ ) obtained from any non-cooperative sensor or cooperative system. Let  $R_0$ ,  $\alpha_0$  and  $\epsilon_0$  be the nominal range, azimuth and elevation values. Consider  $\sigma_R$ ,  $\sigma_\alpha$  and  $\sigma_\epsilon$  as standard deviations of the error in range, azimuth and elevation respectively. The error ellipsoids are given as [3]:

$$\frac{(R-R_0)^2}{\sigma_R^2} + \frac{(\alpha-\alpha_0)^2}{\sigma_\alpha^2} + \frac{(\epsilon-\epsilon_0)^2}{\sigma_\epsilon^2} = 1 \quad (4.2)$$

An illustration of navigation and tracking error ellipsoids is shown in Figure 4.1.

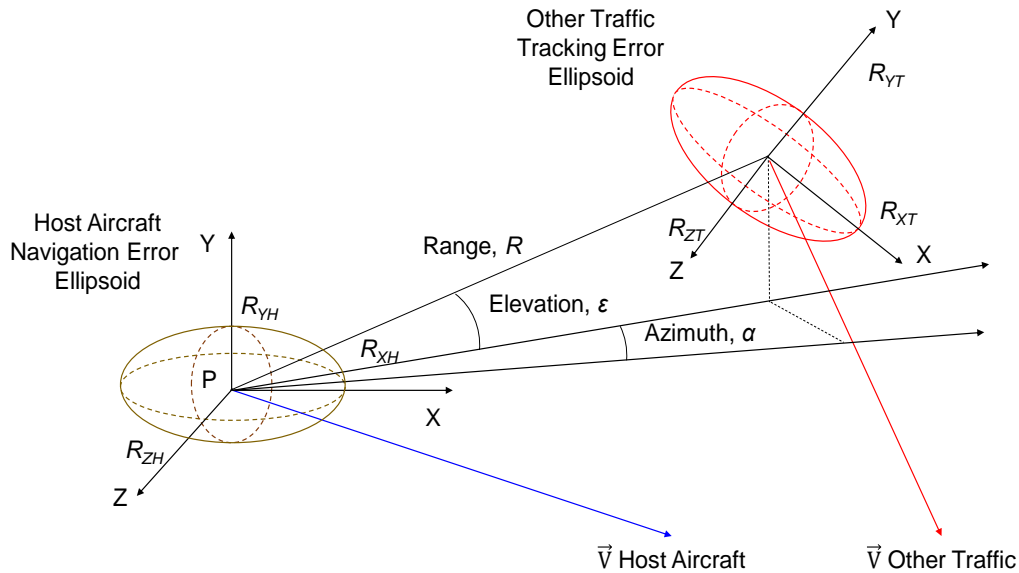


Figure 4.1. Navigation and tracking error ellipsoids.

In order to develop a unified approach to cooperative and non-cooperative SA&CA, the ellipsoids are subjected to two transforms: rotation,  $R$  and translation,  $T$  that is defined

as a projection along the Line-of-Sight (LoS) vector of the aircraft. The inverse transformation applied to one of the two ellipsoids with respect to another,  $L$ , is expressed as:

$$L^{-1} = R^{-1} T^{-1} L \quad (4.3)$$

The intruder position vector,  $p$  translated from host body frame to Earth Centred Earth Fixed (ECEF) reference frame with respect to  $R$  is given by:

$$\tilde{p} = R p \quad (4.4)$$

The intruder position vector uncertainty in ECEF frame ( $\delta\tilde{p}$ ) can be expressed as:

$$\delta\tilde{p} = \Delta_R p + R \delta p \quad (4.5)$$

where  $\delta p$  is the error of the intruder position vector in the host body frame and  $\Delta_R$  is the rotation (angular) error matrix. The rotation matrix in terms of azimuth and elevation angles is given by:

$$R = \begin{bmatrix} c\epsilon c\alpha & s\alpha & -s\epsilon c\alpha \\ -c\epsilon s\alpha & c\alpha & -s\epsilon s\alpha \\ s\epsilon & 0 & c\epsilon \end{bmatrix} \quad (4.6)$$

where  $c$  and  $s$  represent cosine and sine of azimuth and elevation angles. Therefore the position vector after rotation is expressed as:

$$\begin{bmatrix} \tilde{x} \\ \tilde{y} \\ \tilde{z} \end{bmatrix} = \begin{bmatrix} c\epsilon c\alpha & s\alpha & -s\epsilon c\alpha \\ -c\epsilon s\alpha & c\alpha & -s\epsilon s\alpha \\ s\epsilon & 0 & c\epsilon \end{bmatrix} \begin{bmatrix} x \\ y \\ z \end{bmatrix} \quad (4.7)$$

The angular error matrix is given by:

$$\Delta_R = \begin{bmatrix} -\delta\epsilon s\epsilon c\alpha - \delta\alpha c\epsilon s\alpha & \delta\alpha c\alpha & -\delta\epsilon c\epsilon c\alpha + \delta\alpha s\epsilon s\alpha \\ \delta\epsilon s\epsilon s\alpha - \delta\alpha c\epsilon c\alpha & -\delta\alpha s\alpha & -\delta\epsilon c\epsilon s\alpha - \delta\alpha s\epsilon c\alpha \\ \delta\epsilon c\epsilon & 0 & -\delta\epsilon s\epsilon \end{bmatrix} \quad (4.8)$$

and the error in position measurement is expressed as:

$$\begin{bmatrix} \delta\tilde{x} \\ \delta\tilde{y} \\ \delta\tilde{z} \end{bmatrix} = \begin{bmatrix} -\delta\epsilon s\epsilon c\alpha - \delta\alpha c\epsilon s\alpha & \delta\alpha c\alpha & -\delta\epsilon c\epsilon c\alpha + \delta\alpha s\epsilon s\alpha \\ \delta\epsilon s\epsilon s\alpha - \delta\alpha c\epsilon c\alpha & -\delta\alpha s\alpha & -\delta\epsilon c\epsilon s\alpha - \delta\alpha s\epsilon c\alpha \\ \delta\epsilon c\epsilon & 0 & -\delta\epsilon s\epsilon \end{bmatrix} \begin{bmatrix} x \\ y \\ z \end{bmatrix} + \begin{bmatrix} c\epsilon c\alpha & s\alpha & -s\epsilon c\alpha \\ -c\epsilon s\alpha & c\alpha & -s\epsilon s\alpha \\ s\epsilon & 0 & c\epsilon \end{bmatrix} \begin{bmatrix} \delta x \\ \delta y \\ \delta z \end{bmatrix} \quad (4.9)$$

In a static non-cooperative SA&CA case, the errors in range, azimuth and elevation are given by:

$$\delta R = R_0 + \sigma_R \cdot \sin \psi \quad (4.10)$$

$$\delta\alpha = \alpha_0 + \sigma_\alpha \cdot \cos \varphi \cdot \cos \psi \quad (4.11)$$

$$\delta\epsilon = \epsilon_0 + \sigma_\epsilon \cdot \sin \varphi \cdot \cos \psi \quad (4.12)$$

where  $R_0$ ,  $\alpha_0$ ,  $\epsilon_0$  are the nominal range, azimuth and elevation measurements.  $\{\varphi, \psi\}$  are the parameterisations, which support the transformation of the measurement errors to unified range and bearing descriptors. The transformation of  $\{R, \alpha, \epsilon\}$  to  $\{x, y, z\}$  is given by:

$$x = R \cdot \cos \alpha \cdot \cos \epsilon \quad (4.13)$$

$$y = R \cdot \sin \alpha \cdot \cos \epsilon \quad (4.14)$$

$$z = R \cdot \sin \epsilon \quad (4.15)$$

The correlation between the SA&CA technology employed is analysed and thus uncorrelated, covariant and contravariant cases are obtained. Considering ADS-B measurements as an example, the dependences of errors in  $\{x, y, z\}$  on the correlation between the sensor measurements are given by:

$$\sigma_x^2 = (\sigma_{x_A}^2 + \sigma_{x_O}^2 + 2 \sigma_{x_A x_O}) \quad (4.16)$$

$$\sigma_y^2 = (\sigma_{y_A}^2 + \sigma_{y_O}^2 + 2 \sigma_{y_A y_O}) \quad (4.17)$$

$$\sigma_z^2 = (\sigma_{z_A}^2 + \sigma_{z_O}^2 + 2 \sigma_{z_A z_O}) \quad (4.18)$$

where  $\{x_A, y_A, z_A\}$  is the position of the intruder obtained from ADS-B,  $\{x_O, y_O, z_O\}$  is the position of the host aircraft obtained from ADS-B and  $\{2 \sigma_{x_A x_O}, 2 \sigma_{y_A y_O}, 2 \sigma_{z_A z_O}\}$  define the correlation between the sensor measurements. An example of the two combined navigation and tracking error ellipsoids assuming error in range only, and the resulting uncertainty volume for uncorrelated (Figure 4.2) and correlated (covariant and contravariant) sensor error measurements (3 out of a total of 27 possibilities) is illustrated in Figure 4.3.

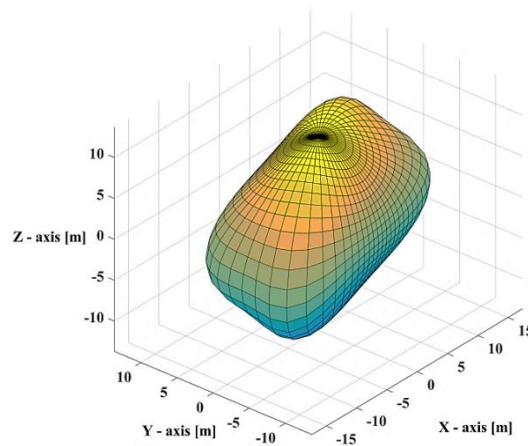


Figure 4.2. Uncertainty volume (uncorrelated errors).

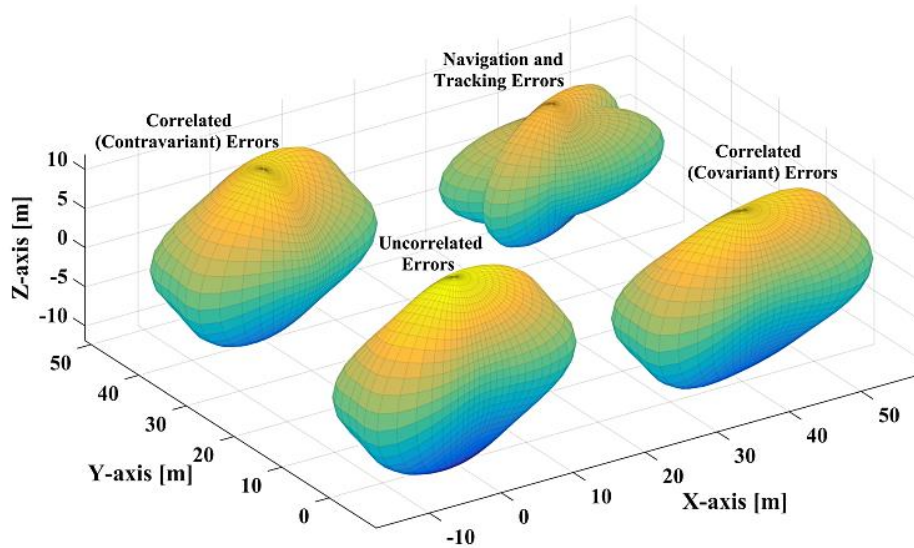


Figure 4.3. Uncertainty volumes obtained from range only errors.

The 27 possible combinations of navigation and tracking error ellipsoids are shown in Figure 4.4.

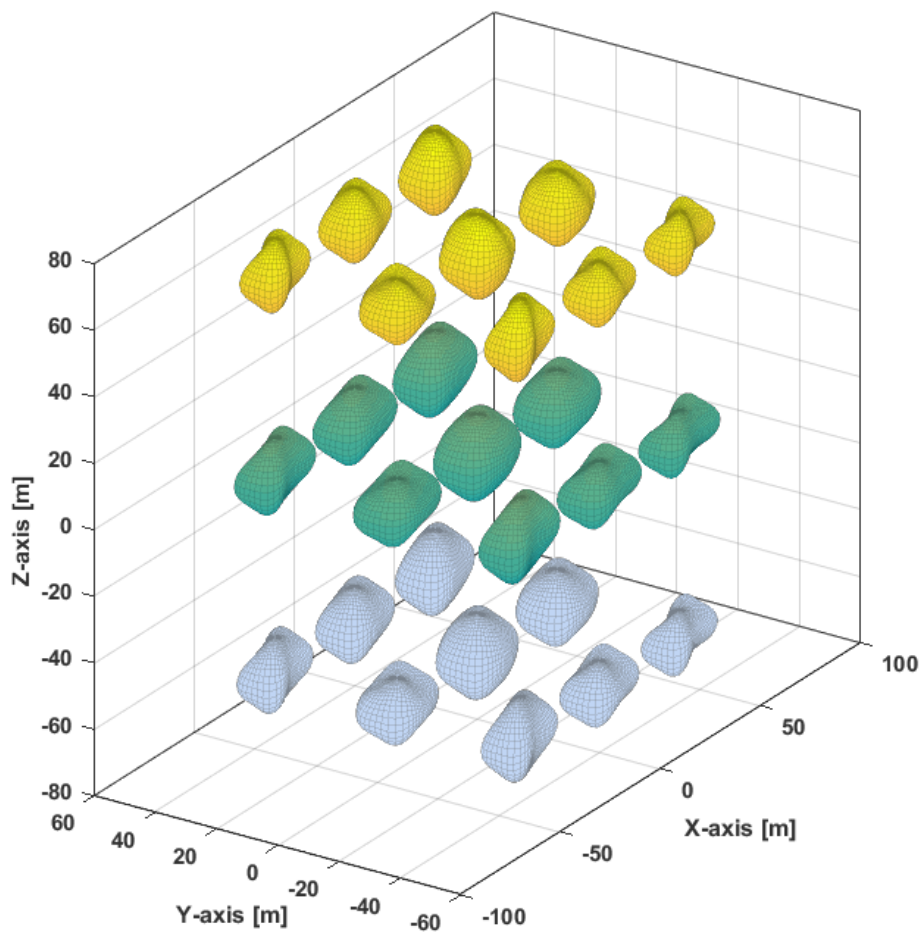


Figure 4.4. Combination of navigation and tracking errors.

In the dynamic case, the ellipsoid is obtained based on a confidence region and is given by:

$$\delta v_0 = v_0 + \sigma_{v_0} \cdot \sin \psi \quad (4.19)$$

$$\delta v_0 = v_0 + \sigma_{v_0} \cdot \cos \varphi \cdot \cos \psi \quad (4.20)$$

$$\delta v_0 = v_0 + \sigma_v \cdot \sin \varphi \cdot \cos \psi \quad (4.21)$$

The kinematic relationships are:

$$\overrightarrow{v_x} = v \cdot \cos \nu \cdot \cos v \quad (4.22)$$

$$\overrightarrow{v_y} = v \cdot \sin \nu \cdot \cos v \quad (4.23)$$

$$\overrightarrow{v_z} = v \cdot \sin v \quad (4.24)$$

and these equations are governed according to the following laws of motion:

$$\vec{x} = \vec{x_0} + \overrightarrow{v_x} \cdot t \quad (4.25)$$

$$\vec{y} = \vec{y_0} + \overrightarrow{v_y} \cdot t \quad (4.26)$$

$$\vec{z} = \vec{z_0} + \overrightarrow{v_z} \cdot t \quad (4.27)$$

where  $t$  represents the time epoch. The errors in  $\{x, y, z\}$  are given by:

$$\sigma_x^2 = (\sigma_{x0}^2 + \sigma_{v_x \cdot t}^2 + 2 \sigma_{x0} v_{x \cdot t}) \quad (4.28)$$

$$\sigma_y^2 = (\sigma_{y0}^2 + \sigma_{v_y \cdot t}^2 + 2 \sigma_{y0} v_{y \cdot t}) \quad (4.29)$$

$$\sigma_z^2 = (\sigma_{z0}^2 + \sigma_{v_z \cdot t}^2 + 2 \sigma_{z0} v_{z \cdot t}) \quad (4.30)$$

When an error exists in the measurement of elevation and azimuth angles, the resultant cone obtained at the estimated range is illustrated in Figure 4.5. In a time-varying case, the variation of avoidance volume due to errors in range and bearing measurements can be conveniently represented by this approach. An example of the uncertainty volume obtained at the estimated range due to tracking errors is shown in Figure 4.5.

The inflation of the avoidance volume due to increase in the navigation and tracking errors is shown in Figure 4.6 and the uncertainty volume considering an increasing error in the azimuth angle measurement predicted at the collision time given by  $t = t_{(coll)}$  is shown in Figure 4.7. Different uncertainty/avoidance volumes can be generated for each time epoch until the time at which a collision is predicted.

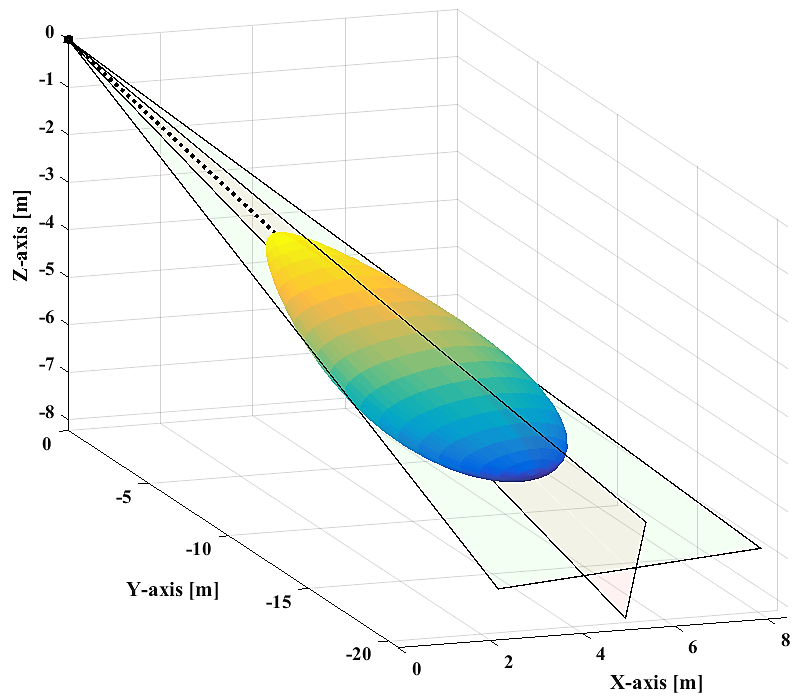


Figure 4.5. Uncertainty volume due to error in bearing measurements.

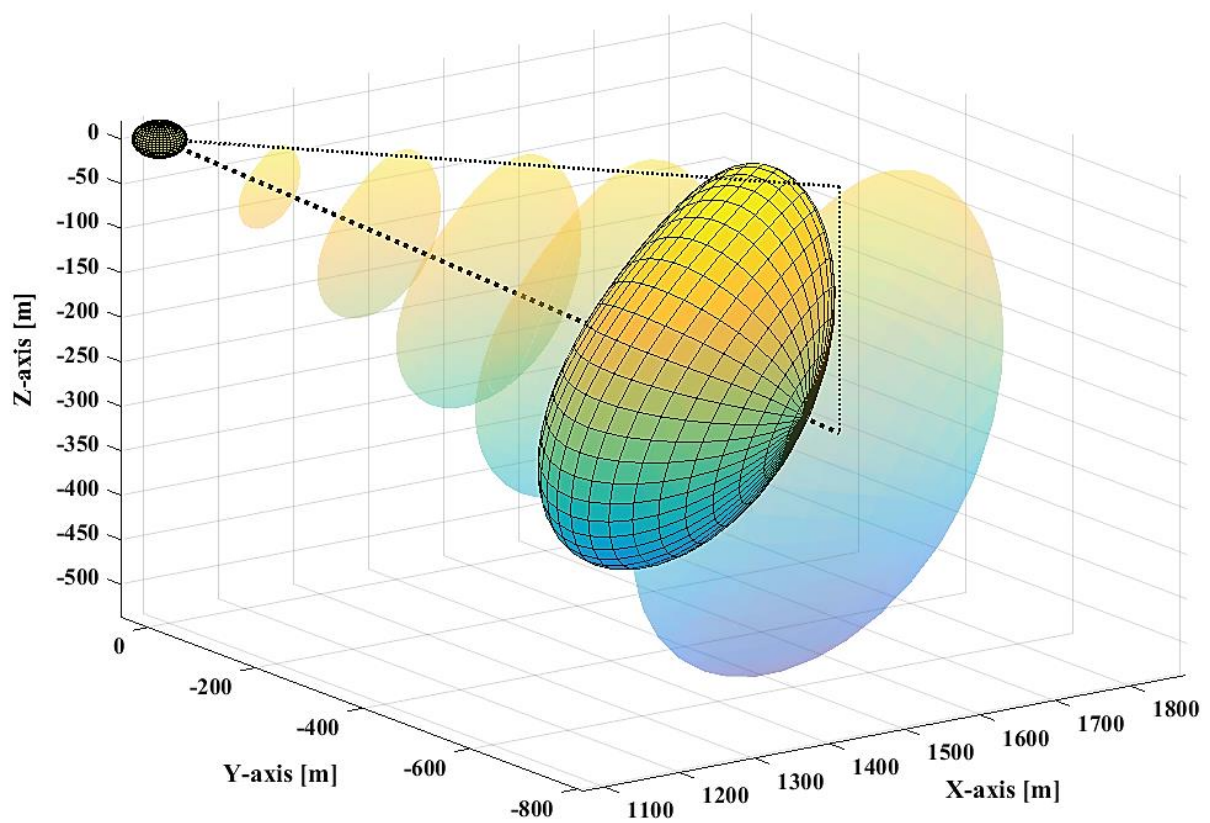


Figure 4.6. Avoidance volumes at different time epochs.

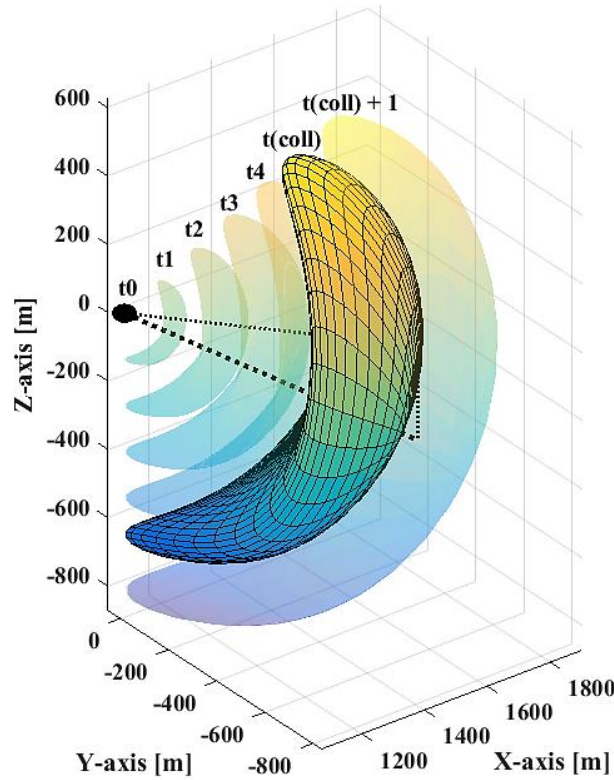


Figure 4.7. Avoidance volumes at time of collision.

In the CNS+A context, the general case is that of multiple aircraft performing either cooperative or non-cooperative surveillance [4]. In this scenario, potential conflicts are defined as close encounters in the 4D space-time domain. Close-encounters are typically evaluated as part of an intermediate step for pruning the full set of potential conflicts. Such 4D close-encounters are assumed to occur when the relative distance – i.e. the norm of the 3D relative position vector – between the nominal positions of a pair of aircraft at a certain time is below a specified threshold. For all identified close-encounters, the uncertainty volume associated with the host and intruder platforms are determined. Due to bandwidth limitations affecting current communication systems, a compact and versatile parameterisation of the uncertainty volume necessary in order to extrapolate its actual shape and size at close encounter points, with minimal data-link and computational burden. Therefore, the combined navigation and tracking uncertainty volume is conveniently described using spherical harmonics and the associated parameters are communicated to the air and ground nodes of the network. The attractive properties of adopting spherical harmonics include the ease of using rotations, spherical averaging procedures and smooth surface representations on the sphere. Spherical harmonics are single-valued and smooth (i.e. infinitely differentiable) complex functions of the parameterisation variables ( $\varphi$  and  $\psi$ ), which are indexed by



two integers, namely  $l$  and  $m$ . They consist of a complete set of orthonormal functions and hence form a vector space similar to unit basis vectors.

Let  $r(\varphi, \psi)$  be defined to represent the smooth function on the obtained uncertainty volume, so the parameterisation of this spherical harmonic representation is given by [5]:

$$r(\varphi, \psi) = \sum_{l=0}^{\infty} \sum_{m=-l}^l X_{lm} Y_{lm}(\varphi, \psi) \quad (4.31)$$

The function  $r(\varphi, \psi)$  is limited to a number of  $N$  finite coefficients, and  $l$  and  $m$  represent the direction index.  $X_{lm}$  is a factor and the function  $Y_{lm}(\varphi, \psi)$  is the spherical harmonic function. Such a parameterisation reduces the complexity and relaxes the input requirements of the algorithms required to compute and propagate the uncertainty volumes in the network. Additionally, it enables suitable corrections (e.g., inflations) to be introduced in order to account for local weather conditions. As complete weather surveillance information is generally not available to onboard aircraft, ground-based systems can uplink the parameters defining the variations of the avoidance volumes due to weather states and forecasts.

Let  $\vec{X}$  denote the points on the surface of the volume. The components of  $\vec{X}$  are  $X_1 = x$ ,  $X_2 = y$  and  $X_3 = z$ . Let the surface normal vector be denoted as  $\hat{n}$ . The normal vector is expressed as:

$$\hat{n} = \frac{\vec{X}_{\varphi} \times \vec{X}_{\psi}}{|\vec{X}_{\varphi} \times \vec{X}_{\psi}|} \quad (4.32)$$

The differential surface area element,  $d\Lambda$  which is an area of a patch of the surface at  $r(\varphi, \psi)$  is given by:

$$d\Lambda = S d\varphi d\psi \quad (4.33)$$

$$S = |\vec{X}_{\varphi} \times \vec{X}_{\psi}| \quad (4.34)$$

The decomposition is expressed in terms of parameters  $A$ ,  $B$  and  $C$ , and is given by:

$$A = \vec{X}_{\varphi} \cdot \vec{X}_{\varphi} \quad (4.35)$$

$$B = \vec{X}_{\varphi} \cdot \vec{X}_{\psi} \quad (4.36)$$

$$C = \vec{X}_{\psi} \cdot \vec{X}_{\varphi} \quad (4.37)$$

The parameters  $D$ ,  $E$  and  $F$  are given by:

$$D = -\vec{X}_{\varphi} \cdot \hat{n}_{\varphi} \quad (4.38)$$

$$E = \frac{1}{2} (\vec{X}_{\varphi} \cdot \hat{n}_{\psi} + \vec{X}_{\psi} \cdot \hat{n}_{\varphi}) \quad (4.39)$$

$$F = -\vec{X}_\psi \cdot \hat{n}_\psi \quad (4.40)$$

The derivatives of the decomposition of the above parameters can be expressed as:

$$\frac{\delta r(\varphi, \psi)}{\delta \varphi} = r_\varphi \quad (4.41)$$

$$\frac{\delta^2 r(\varphi, \psi)}{\delta \varphi^2} = r_{\varphi\varphi} \quad (4.42)$$

and so forth. The parameters D, E and F involve vector products of the derivatives of the components of  $\vec{X}$  and  $\hat{n}$ . The parameter S is expressed as:

$$S = r [r_\psi^2 + r_\varphi^2 (\sin \varphi)^2 + r^2 (\sin \varphi)^2]^{1/2} \quad (4.43)$$

The function  $Y_{lm}(\varphi, \psi)$  are given by:

$$Y_{lm}(\varphi, \psi) = \sqrt{\frac{(2l+1)(l-m)!}{4\pi(l+m)!}} P_{lm} \cos(\varphi) e^{im\psi} \quad (4.44)$$

where  $P_{lm}$  represents the Legendre functions. The Legendre polynomial function is given by:

$$P_{lm}(x) = \frac{1}{2^n n!} \frac{d^n (x^2 - 1)^n}{dx^n} \quad (4.45)$$

Expanding  $e^{im\psi}$  as  $C_{lm} \cos(m\psi) + i S_{lm} \sin(m\psi)$ , we have  $C_{lm}$  and  $S_{lm}$  defined as the spherical harmonic coefficients. The spherical harmonic coefficients are obtained as [5]:

$$L_{lm} = \{C_{m0}, S_{lm} \text{ and } C_{lm}\} \quad (4.46)$$

$$S_{lm} = 0; \quad l, m \in N \quad (4.47)$$

$$C_{lm} = 0; \quad l, m \in 2N + 1 \quad (4.48)$$

and for all other  $l$  and  $m$ :

$$C_{lm} = \frac{3}{a^l} \frac{\left(\frac{l}{2}\right)! \left(\frac{l}{m}\right)! (2 - \delta_{om})}{2^m (l+3)(l+1)!} \times \quad (4.49)$$

$$\sum_{i=0}^{(l-m)/4} \frac{(a^2 - b^2)^{(m+4i)/2} [c^2 - \left(\frac{1}{2}\right)(a^2 - b^2)]^{(l-m-4i)/2}}{16^i \left(\frac{l-m-4i}{2}\right)! \left(m + \frac{2i}{2}\right)! i!}$$

where  $\delta_{om}$  is the Kronecker delta and (a, b, c) represents the semi-major radius of the navigation or tracking error ellipsoid.  $C_{m0}$  are the zonal coefficients (functions of latitude) while  $S_{lm}$  and  $C_{lm}$  are the tesseral coefficients (functions of longitudes).  $C_{lm}$  are termed as expansion coefficients. When  $l=m$ , sectorial coefficients are obtained which are

functions of both latitudes and longitudes. The covariant and contravariant tensors are used to define the overall uncertainty volume when the errors are correlated. When the errors are correlated tensors analysis is adopted to properly account for covariant or contravariant components. Six components are associated with a rank-2 symmetrical tensor  $\phi_{ij}$ , which are three diagonal and three off-diagonal components usually occurring in pairs. The equation of an ellipsoid associated with the tensor is given by:

$$r_i \phi_{ij} r_j = 1 \quad (4.50)$$

where  $r$  is the radius vector having components  $r_i$  and  $r_j$ . Considering a three-dimensional space, the covariance tensor for the error ellipsoid is given as:

$$T = \begin{bmatrix} \phi_{ii} & \phi_{ij} & 0 \\ \phi_{ji} & \phi_{jj} & 0 \\ 0 & 0 & \phi_{kk} \end{bmatrix} \quad (4.51)$$

for components  $(i, j, k)$  along  $(X, Y, Z)$  axes. The partial derivatives of an invariant function provide the components of a covariant vector. A contravariant vector is the same as a contravariant tensor of first order.

A grid based volume can also be used with distinct faces and vertices that can easily be translated to spherical harmonic coefficients using the above analysis. The avoidance volume used for the parameterisation is shown in Figure 4.8. The real and complex functions obtained after parameterisation are shown in Figure 4.9 and 4.10 respectively.

The expansion coefficients are always unique and are used directly as a feature vector for describing an avoidance volume. In this manner, a spectral decomposition of any function can be performed, given the function is square-integrable [6]. Lower frequencies are expressed by the lower  $l$  values; they describe the overall low-resolution shape. The higher values add finer details, given by the high frequencies.

The complex-valued spherical harmonics, composed of real and imaginary parts, can be combined to give real valued functions. The resulting functions share the same orthonormal and completeness properties [6]. Real spherical harmonics are typically used for describing real surface functions. Surface harmonics are often defined as any combination of real spherical harmonics for fixed  $l$ . A surface harmonic can be described as a harmonic function whose domain is a surface and is not restricted to any specific coordinate system.

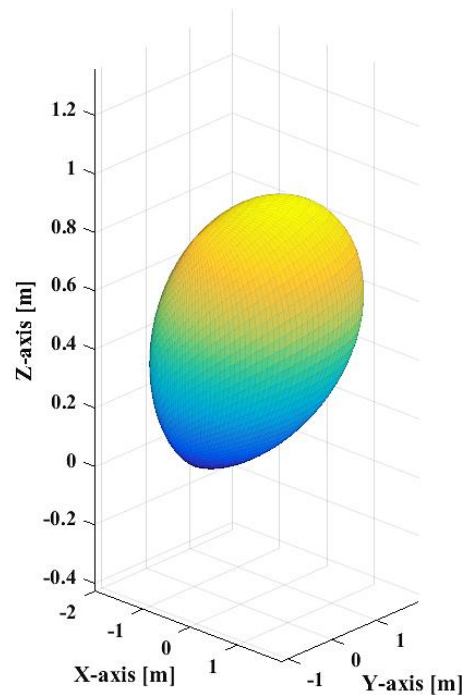


Figure 4.8. Considered avoidance volume.

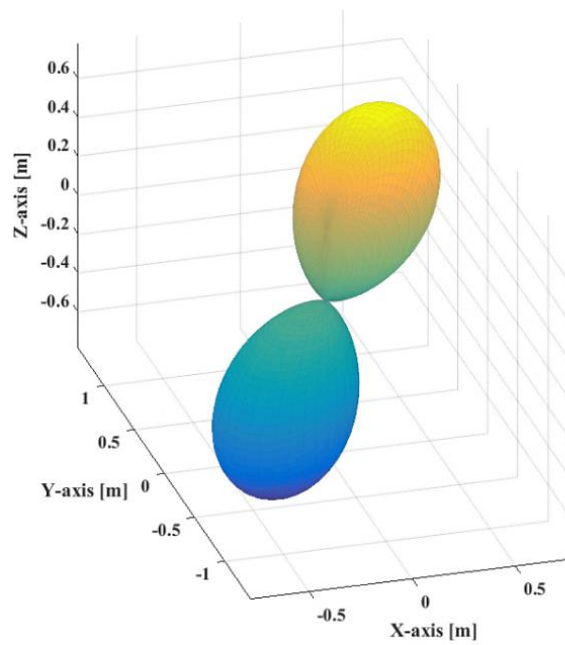


Figure 4.9. Real function after parameterisation.

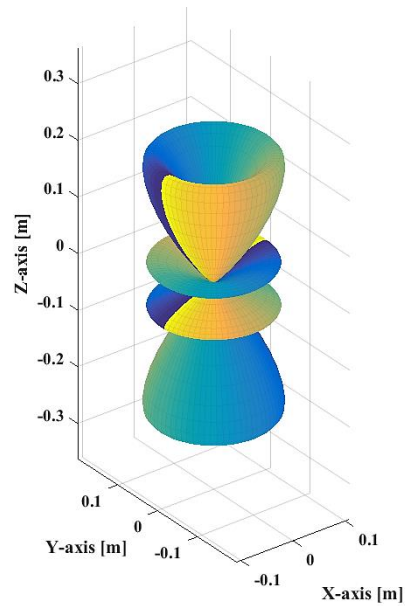


Figure 4.10. Complex function after parameterisation.

Therefore, the approach provides a compact and versatile parameterisation of the avoidance volume to extrapolate its actual shape and size at close encounter points with minimal data-link and computational burden [7].

### 4.3 Distinctiveness of an Unified Approach to SA&CA

The unified method to cooperative and non-cooperative SA&CA adds knowledge to the existing literature in the following aspects:

- Real-time quantification of the total uncertainty volume in the airspace surrounding the intruder tracks. The uncertainty volumes are estimated based on the SA&CA sensor/system measurement errors, which are expressed as uniform range and bearing uncertainty descriptors;
- Real-time transformation of host UAS navigation errors and intruder tracking errors affecting the state measurements to unified range and bearing uncertainty descriptors;
- Detection and resolution of both cooperative and non-cooperative collision threats in various weather and daylight conditions; and also in case of adverse weather conditions;
- Automated separation maintenance and collision avoidance resolution to support coordinated manned and unmanned aircraft operations;

- Real-time and close coordination of air, sea and ground operations as well as operation of multiple manned and unmanned aircraft in close proximity to each other;
- Automatic selection of sensors/systems providing the most reliable SA&CA solution, providing robustness in all flight phases (further details provided in Chapter 5);
- Generation of appropriate dynamic geo-fences, whose characteristics will be dictated by the obstacle classification and intruder dynamics, to allow computation of the optimal avoidance flight trajectories (further details provided in Chapter 8);
- Supervisory control of manned aircraft and UAS addressing various levels of autonomous vehicle-vehicle and ground-vehicle collaborations (further details provided in Appendix C);
- Robust trajectory optimisation allowing the identification of the safest and more efficient Three-Dimensional or Four-Dimensional (3D/4D) avoidance trajectory, considering relative dynamics between the host UAS and intruder platforms, airspace constraints, as well as meteorological and traffic conditions (further details are provided in Chapter 3 (Section 3.7.4) and Chapter 5 (Section 5.6));
- Optimal and dynamic sharing of airspace resources between civil and military users, as well as enabling integrated civil-military Air Traffic Management and UAS Traffic Management (ATM/UTM) operations (further details are provided in Chapter 8 (Section 8.5.2));
- Near real-time and off-line determination of the UAS safe-to-fly envelope based on the installed avionics sensors and on the own/intruder platform dynamics or, alternatively, identifying the sensors required for the UAS to safely fly a certain pre-defined envelope supporting the development of the SA&CA system certification case and can provide a pathway to certification.

As a result, it is expected that the SA&CA algorithms will allow:

- operation of multiple manned and unmanned aircraft in close proximity to each other;
- the remote pilot and/or operator to supervise and supplement the execution of various SA&CA tasks;
- seamless integration of UAS into the existing ATM system and in the UTM context.

## 4.4 Implementation in NG-FMS

In order to achieve an effective SA&CA mechanism, the tracking, decision-making and avoiding processes are classified as follows:

- detection of obstacles and traffic (air and ground) based on information derived from multi-sensor data fusion algorithms;
- tracking the detected obstacles and traffic including trajectory determination;
- prioritising and declaring flags for conflicts based on a detection threshold (that is selected so as to maximise detection rate and minimise false alarms);
- action determination, if there is a conflict;
- determining the optimised evasive manoeuvre that needs to be executed;
- execution of the optimal avoidance manoeuvre.

Using the predicted states of other traffic, criticality analysis is performed to prioritize (i.e. to determine if a collision risk threshold is exceeded for all tracked intruders) and to determine the commands required for executing an avoidance action. If possibility of a collision exists, the SA&CA algorithms generate and optimise an avoidance trajectory according to a cost function that is based on minimum distance, fuel, time and closure rate criteria with the aid of differential geometry or pseudo-spectral optimisation techniques to generate a smooth and flyable trajectory [8 - 12]. Automatic separation assurance is defined as separation assurance being implemented by airborne equipment. The autonomous SA&CA functions embedded in the NG-FMS architecture is illustrated in Figure 4.11, and the software functional architecture is shown in Figure 4.12. CDTI is adopted for displaying all information, including caution and warning flags. The equipage for ASAF is summarized in Table 4.1. The surveillance data processing is illustrated in Figure 4.13. Conflict detection and resolution is the collection of the following components [13]:

- Trajectory prediction, which estimates the flight mode of the intruder based on the information derived from cooperative/non-cooperative sensors and predicts the future trajectory of the intruder;
- Conflict detection, which calculates the time to separation violation point and conflict probability within the look-ahead time, based on relative range, velocity, and altitude difference;
- Conflict resolution, which uses all available information to resolve the conflicts;
- Monitoring the avoidance manoeuvre, which verifies that conflicts are being resolved as planned.

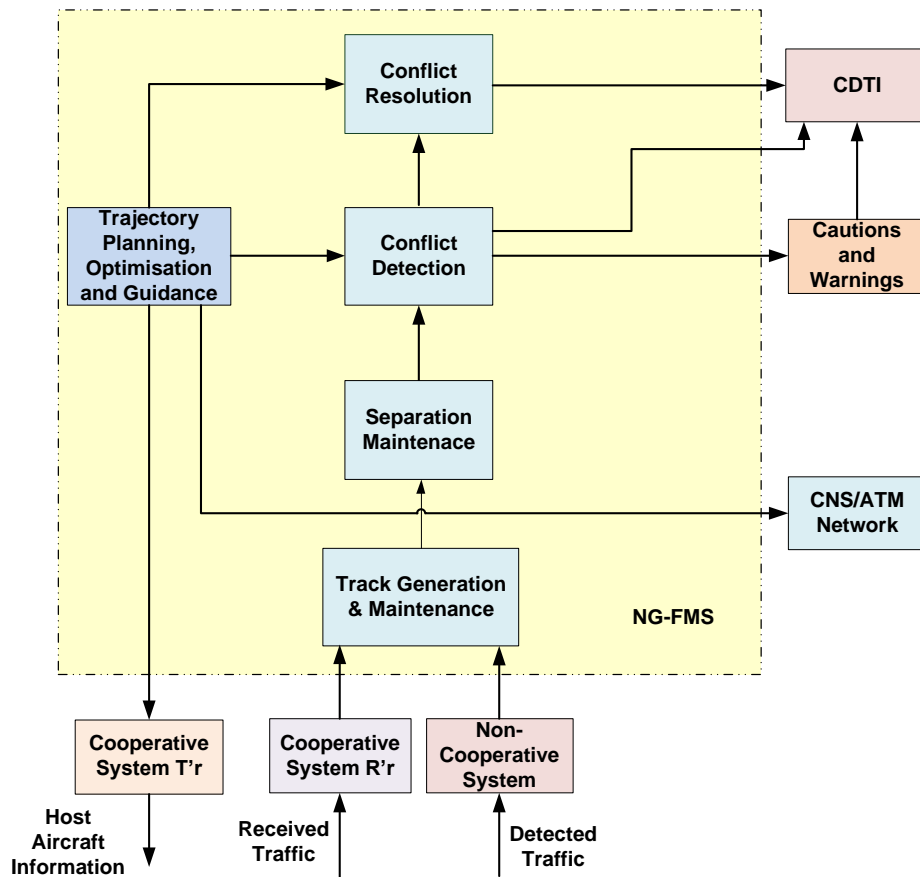


Figure 4.11. NG-FMS architecture including SA&CA functions.

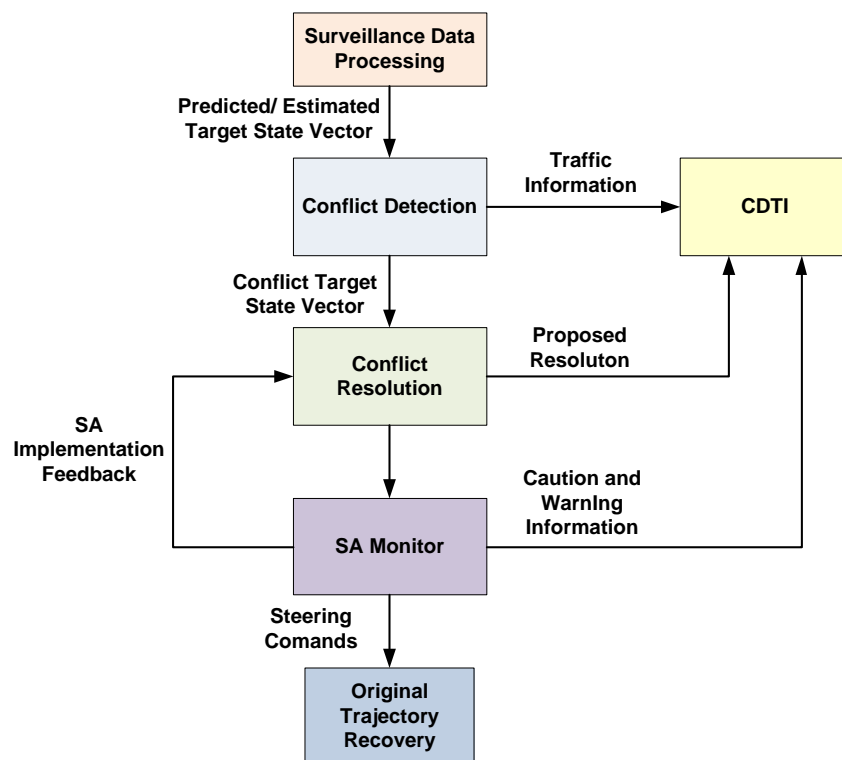


Figure 4.12. SA&CA software functional architecture.



Table 4.1. Summary of equipage.

Functions	Equipage
Communication	Voice communication, Controller Pilot Data Link Control (CPDLC), Line-of-Sight (LoS) and Beyond Los (BloS) communication data links
Navigation	Navigation sensors including Global Navigation Satellite System (GNSS), Inertial Navigation System (INS), Vision-based Navigation (VBN) sensors and Aircraft Dynamics Model (ADM) as a virtual sensor providing 3-D/4-D navigation
Surveillance	Non-cooperative Sensors including Forward Looking Sensors (FLS) Cooperative Systems including Traffic Collision Avoidance System (TCAS), Automatic Dependent Surveillance (ADS), Airborne Collision Avoidance System (ACAS)
Decision-Making	Strategic, tactical and emergency flight planning and optimisation Intelligent conflict detection, resolution and avoidance Weather/terrain/contrails/noise sensitive areas avoidance
Situational Awareness	Cockpit Display of Traffic Information (CDTI) and other displays

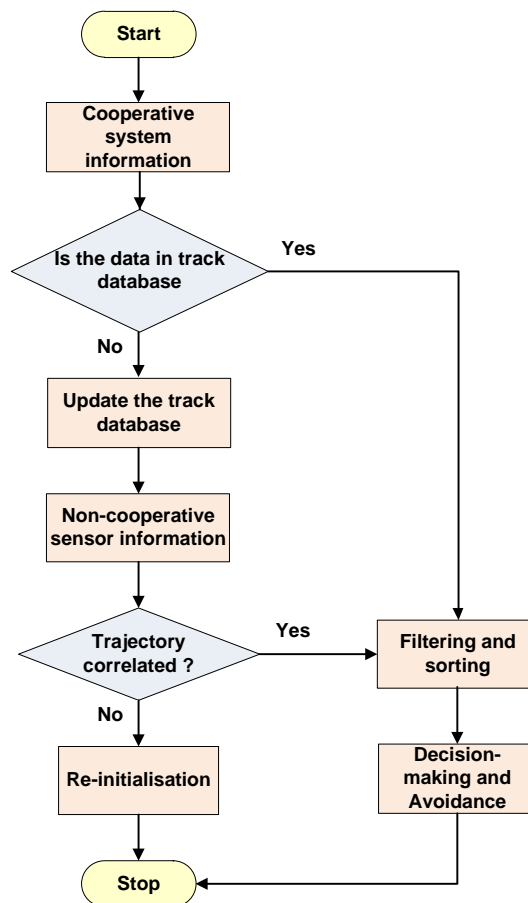


Figure 4.13. Surveillance data processing.

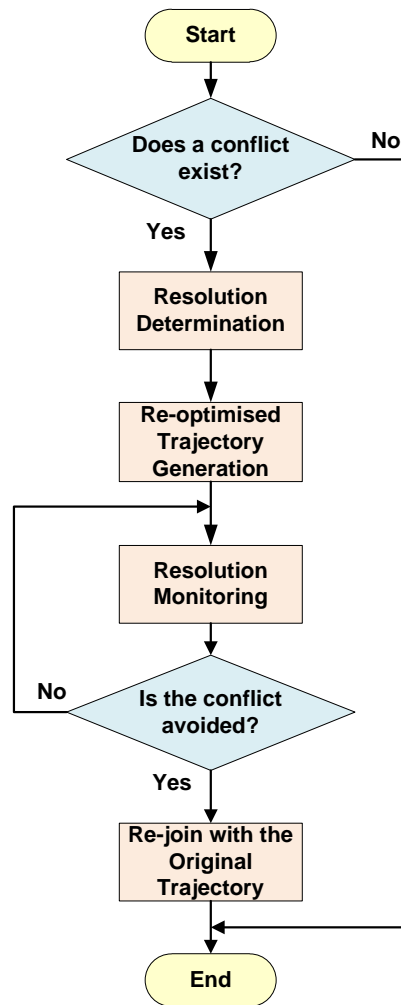


Figure 4.14. Interactions within the NG-FMS.

## 4.5 Conclusions

In this chapter, algorithms for the unified approach to SA&CA were presented. Uncertainty analysis was performed to obtain the overall avoidance volume associated with the intruder track using the presented unified approach. In this approach, both navigation error of the host platform and tracking error of intruders are combined in order to obtain the volume of airspace that needs to be considered for separation maintenance and collision avoidance. The fundamental principle in the unified approach is to express the SA&CA sensor/system measurement errors in range and bearing uncertainty descriptors. The implementation of the unified approach in the NG-FMS was also described.

## 4.6 References

1. S. Ramasamy, R. Sabatini and A. Gardi, "LIDAR Obstacle Warning and Avoidance System for Unmanned Aerial Vehicle Sense-and-Avoid", *Aerospace Science and Technology*, Elsevier, vol. 55, pp. 344–358, 2016. DOI: [10.1016/j.ast.2016.05.020](https://doi.org/10.1016/j.ast.2016.05.020)
2. A. Gardi, S. Ramasamy, R. Sabatini and T. Kistan, "Terminal Area Operations: Challenges and Opportunities", *Encyclopedia of Aerospace - UAS*, eds R. Blockley and W. Shyy, John Wiley: Chichester, 2016. DOI: [10.1002/9780470686652.eae1141](https://doi.org/10.1002/9780470686652.eae1141)
3. S. Ramasamy, R. Sabatini, A. Gardi, "Avionics Sensor Fusion for Small Size Unmanned Aircraft Sense-and-Avoid", *IEEE Workshop on Metrology for Aerospace*, pp. 271-276, Benevento, Italy, May 2014. DOI: [10.1109/MetroAeroSpace.2014.6865933](https://doi.org/10.1109/MetroAeroSpace.2014.6865933)
4. E.J. Garboczi, "Three-dimensional Mathematical Analysis of Particle Shape using X-ray Tomography and Spherical Harmonics: Application to Aggregates used in Concrete", *Cement Concrete Research*, vol. 32, no. 10, 1621–1638, 2002.
5. Z. Zhenjiang, Y. Meng, C. Hutao, C. Pingyuan, "The Method to Determine Spherical Harmonic Model of Asteroid based on Polyhedron", *Proceedings of the 3<sup>rd</sup> International Conference on Computer and Electrical Engineering, International Proceedings of Computer Science and Information Technology*, vol. 53, 2012.
6. R.J. Morris, R.J. Najmanovich, A. Kahraman and J.M. Thornton, "Real Spherical Harmonic Expansion Coefficients as 3D Shape Descriptors for Protein Binding Pocket and Ligand Comparisons", *Bioinformatics, Oxford Journals*, vol. 21, issue 10, pp. 2347-2355, 2005.
7. R. Ramamoorthi and P. Hanrahan, "An Efficient Representation for Irradiance Environment Maps", *Proceedings of the 28<sup>th</sup> ACM Annual Conference on Computer Graphics and Interactive Techniques*, Los Angeles, USA, pp. 497-500, 2001.
8. C. Carbone, U. Ciniglio, F. Corrado, and S. Luongo, "A Novel 3D Geometric Algorithm for Aircraft Autonomous Collision Avoidance", *Proceedings of the 45<sup>th</sup> IEEE Conference on Decision and Control*, San Diego, California, USA, pp. 1580-1585, 2006.
9. C.G. Prévost, A. Desbiens, E. Ganon, and D. Hodouin, "UAV Optimal Obstacle Avoidance while Respecting Target Arrival Specifications", *Preprints of the 18<sup>th</sup> IFAC World Congress*, Milano, Italy, pp. 11815-11820, 2008.
10. A. Gardi, R. Sabatini and S. Ramasamy, "Multi-objective Optimisation of Aircraft Flight Trajectories in the ATM and Avionics Context", *Progress in Aerospace Sciences*, Elsevier, vol. 83, pp.1-36, 2016. DOI: [10.1016/j.paerosci.2015.11.006](https://doi.org/10.1016/j.paerosci.2015.11.006)

11. C.K. Lai, M. Lone, P. Thomas, J. Whidboerne and A. Cooke, "On-Board Trajectory Generation for Collision Avoidance in Unmanned Aerial Vehicles", Proceedings of the IEEE Aerospace Conference, pp. 1-14, Big Sky, MT, USA, 2011.
12. D.A. Benson, G.T. Huntington, T.P. Thorvaldsen and A.V. Rao, "Direct Trajectory Optimization and Costate Estimation via an Orthogonal Collocation Method", Journal of Guidance, Control, and Dynamics, vol. 29, no. 6, pp. 1435-1440, 2006.
13. S. Ramasamy, R. Sabatini and A. Gardi, "A Unified Approach to Separation Assurance and Collision Avoidance for UAS Operations and Traffic Management", Proceedings of IEEE International Conference on Unmanned Aircraft Systems (ICUAS 2017), Miami, FL, USA, pp. 920-928, June 2017.

## CHAPTER 5

# PERFORMANCE ANALYSIS OF SA&CA FUNCTIONALITIES

*"The man of science has learned to believe in justification, not by faith, but by verification."* - Thomas Henry Huxley

### 5.1 Introduction

In this chapter, a performance analysis is carried out to investigate and explore the potential of the unified approach to cooperative and non-cooperative SA&CA for manned and unmanned aircraft. Based on the identified state-of-the-art SA&CA technologies, a Boolean-Decision Logic (BDL) driven decision tree test bed system reference architecture is presented. Implementations involving Boolean logics are generally hard wired and cannot be reconfigured; this limits the scope of a unified framework in terms of automatic decision making capability. Therefore adaptive BDL, which are based on real-time monitoring of the surveillance sensors/systems performance are implemented to provide a framework for providing autonomy in UAS operations. A scheme for selecting the onboard sensors/systems is introduced, which is based on the performance achieved at any given point of time. Covariance matrices are used for estimating sensor and system performances. After identifying a Risk-of-Collision (RoC), if the original trajectory of the host platform intersects the calculated avoidance volume, a caution integrity flag is issued. An avoidance trajectory is generated in real-time and the steering commands are provided to the flight control surfaces.

### 5.2 Avoidance Volumes

An avoidance volume is a virtual, fixed, volume-based boundary in the airspace. The overall avoidance volume obtained from the unified approach to SA&CA described in Chapter 4 is a variable boundary projected along the velocity vector of the host aircraft.

The avoidance volume is a variable depending upon the real-time navigation measurements, tracking observables, relative dynamics between platforms, collision distance, time and manoeuvrability of the platform. The inclusion of navigation error of the host aircraft and the tracking errors of all other traffic in the airspace provides a practical buffer. It also maximises the ability to predict collisions and provides the host aircraft with adequate time to generate a re-optimised trajectory and execute the required commands.

A buffer is also added taking into account the uncertainties in the aircraft states and the resulting uncertainties in the propagation of errors in the nominal trajectory. The previous research efforts on estimation of avoidance/uncertainty volume in the context of SA&CA were discussed earlier in Chapter 2 (Section 2.13).

All the highlighted approaches have attempted to define an avoidance volume, which are specific in application; meaning given a scenario or specific sensor/system, these methods can provide information for automated SA or CA. The unified approach is an innovative technique allowing the quantification of total uncertainty volume in the airspace surrounding the intruder tracks in real-time for both cooperative and non-cooperative scenarios. A thorough assessment and mitigation of the safety impact is typically required to expedite the path to certification, allowing operators (including UAS) to carry out an extended spectrum of autonomous and safety-critical tasks. The unified approach allows carrying out such assessment and supports the case for certification. Both near real-time and off-line determination of the safe-to-fly envelope is based on the installed avionics sensors as well as on the own/intruder platform dynamics. Alternatively, identifying the sensors required for the platform to safely fly a certain pre-defined envelope (in the presence of intruders with specified vehicle dynamics) can also determine the safety envelope. Further details on the certification framework are provided in the later sections of the chapter.

### **5.3 SA&CA Test Bed Architecture**

Evaluation of non-cooperative sensor/cooperative systems and the associated data fusion algorithms is a key constituent of the SA&CA system design. A number of non-cooperative sensors and cooperative systems can be employed for automated SA&CA. State-of-the-art SA&CA technologies are listed in Table 5.1 representing C for cooperative and NC for non-cooperative (both active and passive) sensors.

Table 5.1. SA&CA technologies.

Sensor/System	Type	Information	Trajectory
Visual camera	NC, Passive	Azimuth, Elevation	Extracted
Thermal camera	NC, Passive	Azimuth, Elevation	Extracted
LIDAR	NC, Active	Range	Extracted
MMW Radar	NC, Active	Range, Bearing	Extracted
SAR	NC, Active	Range, Bearing	Extracted
Acoustic	NC, Active	Azimuth, Elevation	Extracted
ADS-B	C	Position, Altitude, Velocity and Identity	State Vectors Provided
TCAS I/II/IV/ ACAS I/II/III/X	C	Range, Altitude	Extracted

The non-cooperative sensors are employed to detect intruders or other obstacles in the platform's Field-of-Regard (FoR) when cooperative systems are unavailable from the intruders. Optical, thermal, LIDAR, Millimetre Wave (MMW) radar and acoustic sensors are employed part of non-cooperative sensors. Based on the identified technologies, Boolean logics based decision tree architecture for the SA&CA system is illustrated in Figure 5.1. A typical example of prioritisation is selecting ADS-B data when both ADS-B and TCAS are present onboard the platform. A hierarchy of selecting and sorting the surveillance sensors/systems is defined based on their performance, achieved at any instant of time. Covariance matrices are used for estimating the performance of the SA&CA sensors and systems.

As discussed in Chapter 2 (Section 2.6.1), the FAA TCAS program office research led to the introduction of ACAS X technology [1, 2]. Since ACAS X logic is based on a dynamic model of aircraft movement and a computer optimised lookup table of collision avoidance actions, it is different from the conventional TCAS approach. Maintenance of separation (maintaining a safe distance from other aircraft) without triggering collision avoidance of the other aircraft is achieved by ACAS X. In an implementation perspective, ACAS X is focused on the collision avoidance aspect (after the failure of self-separation), using Markov decision processes and dynamic programming. The same approach is also extended to self-separation.

The unified approach is different from the ACAS X/well-clear method in the approach towards computation of the 3D volume in the airspace to be avoided by the host aircraft [1 – 3]. Furthermore, ACAS-X cannot handle accelerated trajectories making it less suitable for implementing UTM algorithms for small UAS and hybrid platforms. The solution proposed is indeed more general than steady flight 4D sequences taking into account complex accelerated or manoeuvring tasks. Furthermore, the proposed approach is neither limited by the onboard SA&CA technologies nor those installed on the intruders. Hence, it is a SA&CA technology independent solution.

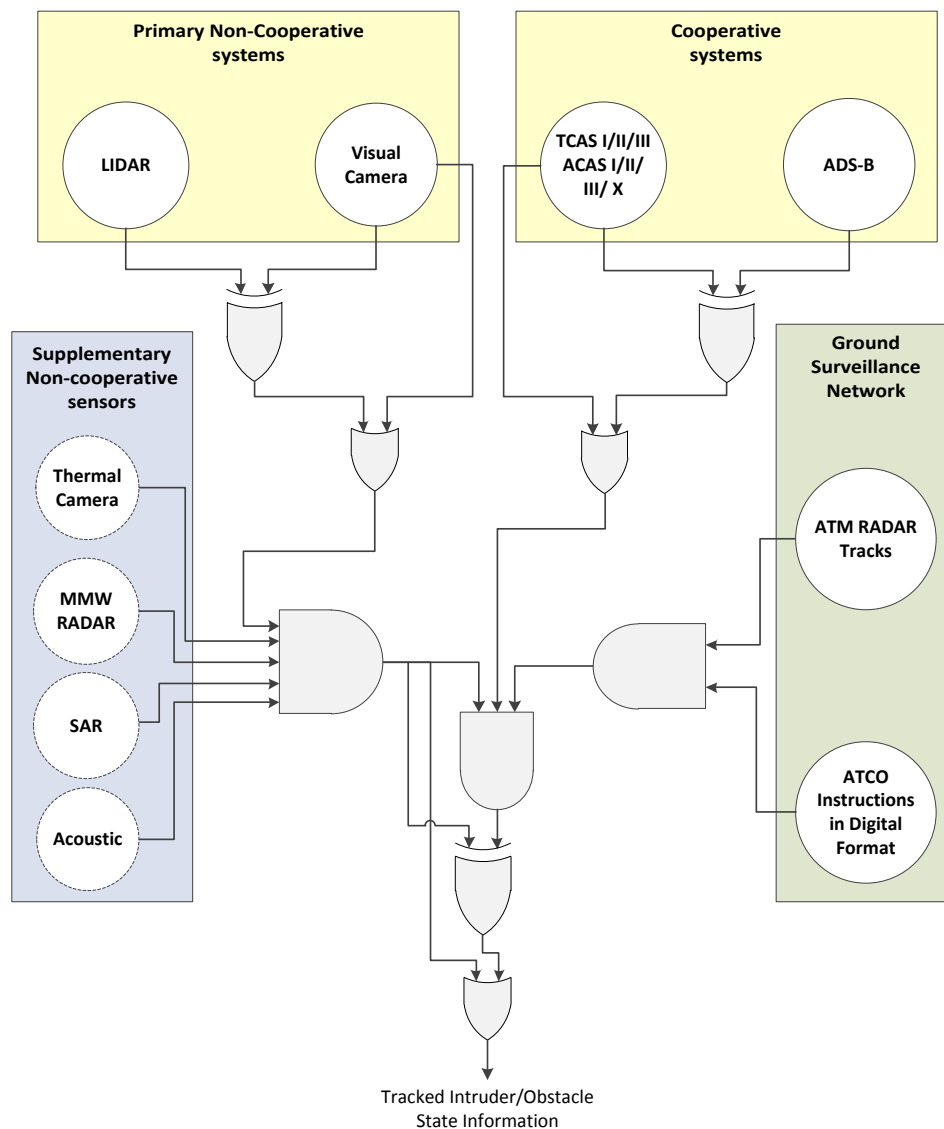


Figure 5.1. Reconfigurable UAS SA&CA test bed architecture.

Depending upon the complexity of the decision-making process, various practical implementations are possible. These include the use of microcontrollers, Programmable Array Logic (PAL), Programmable Logic Array (PLA), Generic Array Logic (GAL) and Field



Programmable Gate Array (FPGA). The programmable logic devices are especially useful in prioritising the SA&CA sensor/system according to their performance. Fault Tree Analysis (FTA) and Failure Modes Effects and Criticality Analysis (FMECA) are performed with respect to the identified state-of-the-art SA&CA technologies to determine the reliability of cooperative systems and non-cooperative sensors. A typical example of Fault Tree Analysis (FTA) performed on the reference architecture is illustrated in Figure 5.2.

Navigation and tracking performances are also improved, thanks to the robustness introduced into the system. The sensor/system, which provides the best estimate, is selected automatically. The presented approach thus provides autonomy and robustness in all flight phases, and supports all-weather and all-time operations. The method lays a foundation for the development of an airworthy SA&CA capability and a pathway for manned/unmanned aircraft coexistence in all classes of airspace. Instead of implementing hardwired decision logics (given by a pre-defined set of instructions), a dynamic reconfiguration of decision logics based on CNS systems integrity augmentation is adopted [4 - 9].

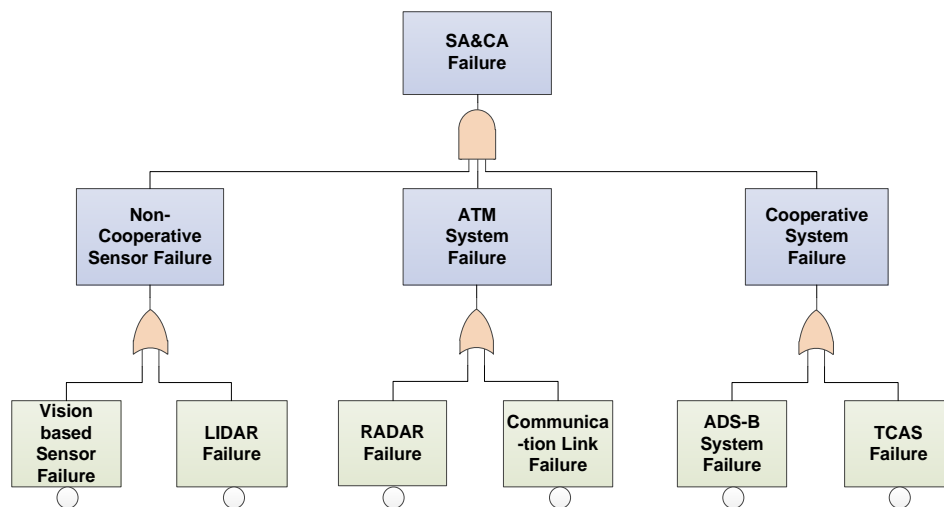


Figure 5.2. FTA for autonomous decision-making tasks.

Sensors/systems providing the most reliable SA&CA solution are automatically selected, providing robustness in all flight phases and supporting all-weather operations. This is achieved by performing a top-down and then bottom-up approaches for determining the probability of failure associated with each sensor and/or system and ATM link. The probability of failure dictates the selection of each sensor and system for strategic, tactical and emergency scenarios. It is important to remember that there are often common causes of failures across fault tree components (one of the fundamental

assumptions inherent in fault trees are that the components are independent, which is very difficult to assure in an actual system). Hence, the common causes of failures across fault tree components (here within non-cooperative sensors, cooperative systems and ATM system) need to be analysed.

Fault trees are very useful in deducing inferences about static models and situations. To introduce a temporal axis to hazard analysis, event trees are considered. Event tree analysis, which is a graphical approach, involves the assessment of the SA&CA for given sets of undesired initiating events. The initiating events are mapped against a temporal axis. For example, degradation or loss of GNSS data would impact the navigation and tracking errors (provided ADS-B is onboard the host and intruder aircraft). This impact can be modelled against time and the propagation effects can be studied. The effects also include the study of error propagation against time through the aircraft dynamics, SA&CA algorithms and NG-FMS components.

The decision logics are based on identifying the primary cooperative system and non-cooperative sensor. In the architecture defined above, the primary cooperative system is ADS-B and the key non-cooperative counterparts are vision-based sensors and LIDAR/MMW radar. Considering the ADS-B and TCAS example, representing ADS-B measurements as A, TCAS data as B and the output for cooperative scenario as O1, the expression for the Boolean logics implementation is derived as follows:

$$O1 = A + (A \oplus T) \quad (5.1)$$

$$O1 = A + (A T' + T A') \quad (5.2)$$

$$O1 = A (1 + T') + T A' \quad (5.3)$$

$$O1 = A + T A' \quad (5.4)$$

Similarly, a Boolean logics decision tree is also employed for the non-cooperative case. Denoting data from visual camera as V, thermal camera as I, LIDAR as L, MMW radar as M, acoustic as A and the output for non-cooperative CA function as O2, the expression for the Boolean logics implementation is derived as follows:

$$O2 = A \cdot M \cdot L \cdot (V + (V \oplus I)) \quad (5.5)$$

$$O2 = A \cdot M \cdot L \cdot (V + (V I' + I V')) \quad (5.6)$$

$$O2 = A \cdot M \cdot L \cdot (V + I V') \quad (5.7)$$

A combined decision tree is adopted for accommodating both non-cooperative sensors and cooperative system information. This is described by the overall output O as:

$$O = (O_1 \oplus O_2) + O_2 \quad (5.8)$$

## 5.4 Sensor/System Error Modelling

The error models of subsystems are set up respectively and the matrices of the state and measurement equations are fractional step discretisations.

The position and tracking information are given by the following formulation. A TCP is typically defined as specific 4D points in the space-time domain at which an anticipated change in the aircraft's velocity vector would cause a change in the nominal intent. The position of an aircraft is expressed as the 3-tuple,  $p = \{x(t), y(t), z(t)\}$  and  $x, y, z, t \in \mathbb{R}$  and  $t \geq 0$ .  $x$  and  $y$  are the lateral and longitudinal position of the aircraft and  $z$  provides the elevation. For any given two points, say  $p_1$  and  $p_2$ , the distances are given by:

$$H = (p_1 - p_2) | h \quad (5.9)$$

$$H = 2r \operatorname{atan} 2(\sqrt{a}, \sqrt{1-a}) \quad (5.10)$$

and

$$a = \sin\left(\frac{x_2 - x_1}{2}\right)^2 + \cos x_1 \times \cos x_2 \times \sin\left(\frac{y_2 - y_1}{2}\right)^2 \quad (5.11)$$

$$V = (p_1 - p_2) | v = (z_2 - z_1) \quad (5.12)$$

The above equations are the Haversine formulae for calculating the great circle distances between two points on an ellipsoid where  $r$  is the radius of the sphere. A TCP can be expressed as  $TCP_n = \{p_n, t_n\}$ . Given two TCPs namely,  $TCP_a$  and  $TCP_b$ , and  $t_b > t_a$ , then, the following constraints hold:

$$\psi_a \neq \psi_b \quad (5.13)$$

$$h_a \neq h_b \quad (5.14)$$

$$V_{Ta} \neq V_{Tb} \quad (5.15)$$

$$V_{Ta} \neq V_{Tb} \quad (5.16)$$

where  $\psi, h$  and  $V_T$  are the control variables.  $V$  is the velocity and  $\psi$  is the heading.

In dynamic cases, the elapsed time is important since imperfectly perceived velocity enlarges altitude uncertainty between observations, and measurements separated by known time intervals carry implicit velocity information. Weighting applied to the position measurements is influenced by three factors [10]:

- A sensitivity matrix  $H_m$  whose  $(i, j)$  element is the partial derivative of the  $i^{\text{th}}$  component of the  $m^{\text{th}}$  measured data vector to the  $j^{\text{th}}$  state variable. In this scalar measurement case  $H_m$  is a  $1 \times 2$  matrix  $[1 \ 0]$  for all values of  $m$ ;
- A covariance matrix  $P_m$  of error in state estimate at time  $tm$  (the  $i^{\text{th}}$  diagonal element is the mean squared error in estimating the  $i^{\text{th}}$  state);
- A covariance matrix  $R_m$  of measurement errors at time  $tm$  (in this scalar measurement case,  $R_m$  is a  $1 \times 1$  matrix—i.e., a scalar variance  $R_m$ ).

Some relevant definitions are:

Variance of a variable is an estimate of the squared deviations of  $n$  measures of the variable from their mean value. For a sample data with  $n$  observations for a variable  $F$ , the variance is determined by the formula:

$$\text{Var} (F) = \frac{\sum_{i=1}^n (q_i - \bar{q})^2}{n-1} \quad (5.17)$$

where  $\bar{x}$  is the sample mean of  $F$ .

For a sample data with  $n$  pairs of observations for two variables  $F$  and  $G$ , the covariance is given by:

$$\text{Cov} (F, G) = \frac{\sum_{i=1}^n (f_i - \bar{f})(g_i - \bar{g})}{n-1} \quad (5.18)$$

where  $\bar{f}$  and  $\bar{g}$  denote the sample means of  $F$  and  $G$ , respectively.  $\text{Cov} (F, G) > 0$  indicates the larger the value of  $F$ , the larger the value of  $Y$  and vice versa.  $\text{Cov} (F, G) < 0$  indicates the larger the value of  $F$ , the smaller the value of  $Y$  and vice versa. Therefore:

$$\text{Cov} (F, G) = \text{Cov} (G, F) \quad (5.19)$$

That is, covariance is symmetric in  $F$  and  $G$ .

Covariance is estimated for two variables that have different units of measurement. By measuring covariance, it can be found out whether their units are increasing or decreasing. However, covariance cannot measure the degree to which the two variables move together.

$P_m$  changes with time (e.g., the effect of velocity error on position error), as well as with any changes in the real-time measurements. In this continuous–discrete approach, uncertainty is decremented at the discrete measurement events [10]:

$$P_m^{(+)} = P_m^{(-)} - W_m H_m P_m^{(-)} \quad (5.20)$$

and, between events, dynamic behaviour follows a continuous model of the form given by:

$$\dot{P} = AP + PA^T + E \quad (5.21)$$

The system model for tracking the targets is defined as:

$$X_n = \Phi_{n-1}X_{n-1} + \xi_{n-1} \quad (5.22)$$

where  $X$  is the tracked object's state vector,  $\phi$  is the constant state transition matrix and  $\xi$  is the system noise. In a two dimensional approach the state vector  $X$  can be defined as a 4 dimensional vector  $x = (x_1, x_2, \dot{x}_1, \dot{x}_2)$ , where  $(x_1, x_2)$  correspond to the position of the tracked object in the FoV expressed on the body frame and  $(\dot{x}_1, \dot{x}_2)$  corresponds to the velocity of the object. The above equation becomes:

$$\begin{pmatrix} x_1 \\ x_2 \\ \dot{x}_1 \\ \dot{x}_2 \end{pmatrix} = \begin{pmatrix} 1 & 0 & \Delta T & 0 \\ 0 & 1 & 0 & \Delta T \\ 0 & 0 & 1 & 0 \\ 0 & 0 & 0 & 1 \end{pmatrix} \begin{pmatrix} x_{1,n-1} \\ x_{2,n-1} \\ \dot{x}_{1,n-1} \\ \dot{x}_{2,n-1} \end{pmatrix} + \begin{pmatrix} \xi_{x_1,n-1} \\ \xi_{x_2,n-1} \\ \xi_{\dot{x}_1,n-1} \\ \xi_{\dot{x}_2,n-1} \end{pmatrix} \quad (5.23)$$

The measurement model is given by:

$$z_n = H_n x_n + \mu_n \quad (5.24)$$

and expressed in matrices as:

$$\begin{pmatrix} z_{1,n} \\ z_{2,n} \end{pmatrix} = \begin{pmatrix} 1 & 0 & 0 & 0 \\ 0 & 1 & 0 & 0 \end{pmatrix} \begin{pmatrix} x_{1,n} \\ x_{2,n} \\ \dot{x}_{1,n} \\ \dot{x}_{2,n} \end{pmatrix} + \begin{pmatrix} \mu_{z_{1,n}} \\ \mu_{z_{2,n}} \end{pmatrix} \quad (5.25)$$

where  $z_n$  is the measurement vector,  $H$  is the state observation vector and  $\mu_k$  is the measurement noise. If the measurement terms and system noise are statistically uncorrelated (White Gaussian Noise (WGN)), then covariance matrices are given by:

$$Q = \begin{pmatrix} \sigma_{x_1}^2 & \sigma_{x_1 x_2} & \sigma_{x_1 \dot{x}_1} & \sigma_{x_1 \dot{x}_2} \\ \sigma_{x_2 x_1} & \sigma_{x_2}^2 & \sigma_{x_2 \dot{x}_1} & \sigma_{x_2 \dot{x}_2} \\ \sigma_{\dot{x}_1 x_1} & \sigma_{\dot{x}_1 x_2} & \sigma_{\dot{x}_1}^2 & \sigma_{\dot{x}_1 \dot{x}_2} \\ \sigma_{\dot{x}_2 x_1} & \sigma_{\dot{x}_2 x_2} & \sigma_{\dot{x}_2 \dot{x}_1} & \sigma_{\dot{x}_2}^2 \end{pmatrix} \quad (5.26)$$

$$R = \begin{pmatrix} \sigma_{z_1}^2 & \sigma_{z_1 z_2} \\ \sigma_{z_2 z_1} & \sigma_{z_2}^2 \end{pmatrix} \quad (5.27)$$

The diagonal elements of matrices  $Q$  and  $R$  correspond to the variances of the state vector and measurement vector respectively. Optimal control and estimation theory is applied for predicting and updating the system states (e.g. EKF).

The values of the Kalman gain give certain weight in the algorithm to the predictions or the measurements. For large values of Kalman gain, the measurements have a significant impact on the filter output, whereas for smaller values, predictions are obtained considering a larger weight on the filter output. The Kalman filter is initialized if the threshold of the test statistic function is exceeded. The initial conditions of the Kalman Filter can be set up to [10, 11]:

$$\hat{x}_0 = (z_{1,n}^i, z_{2,n}^j, 0, 0) \quad (5.28)$$

where  $z_{1,n}^i$  and  $z_{2,n}^j$  correspond to the target position  $(i, j)$  values obtained from the track-before-detect stage. Typically, in other SA&CA algorithms, a large value is assigned to the covariance matrix of the system states ( $1 \times 10^4$ ) due to the initial uncertainty [10, 11]. In the case of a 2D problem, such as the one analysed in this case, the uncertainty can be represented by an ellipse centred in  $\hat{x}_k$ . It is observed that the axis of the uncertainty ellipse is given by  $\pm c_k \sqrt{\lambda_k} e_k$  ( $k = 1, 2$ );  $\lambda_k$  and  $e_k$  are the eigenvalues and eigenvectors of  $P_n$  respectively;  $c_k$  is a constant.

Once the states are estimated, a future trajectory is predicted. The approach employed is based on an extension of the platform states, and on the output equation, which is given by:

$$n(k) = Sx(k) \quad (5.29)$$

where  $n = [x \ y \ z]^T$  and the matrix  $S$  locates the states in the vector  $x$  that belong to the object position:

$$\begin{bmatrix} n^{nl}(k+1|k) \\ n^{nl}(k+2|k) \\ \vdots \\ n^{nl}(k+h_p|k) \end{bmatrix} = S \begin{bmatrix} \hat{x}_T(k+1|k) \\ f[\hat{x}_T(k+1|k)] \\ \vdots \\ f[\dots f[\hat{x}_T(k+1|k)] \dots] \end{bmatrix} \quad (5.30)$$

where  $h_p$  is defined as a future horizon up to where it is desired to predict the trajectory.  $\hat{x}_T(k+1|k)$  are the estimates of the track-to-track algorithm, that contains information for all the local estimations, at the next sample time. The left hand side of equation (5.30) is expressed as:

$$\hat{n}^{nl}(1:h_p|k) \quad (5.31)$$

so the index  $(1:h_p|k)$  groups the prediction from sample time  $(k+1|k)$  to sample time  $(k+h_p|k)$ .

The quality of the predicted trajectory is also important. It can be evaluated by assessing the quality of the measurements (or by pre-estimation), which is in turn reflected in the error on the predicted value. This error is given by:

$$\sigma^2(k + \tau | k) = \text{var}\{n(k + \tau) - \hat{n}^l(k + \tau | k)\} \quad (5.32)$$

where  $n(k + \tau)$  is the modeled objected trajectory and  $\hat{n}^l(k + \tau | k)$  is the predicted optimal trajectory at sample time  $k + \tau$ . Taking this to the prediction horizon sample time  $k + h_p$ , the following error expression is obtained:

$$\sigma^2(k + \tau | k) = \begin{bmatrix} SP_{k+1|k} S^T \\ SM_{1,1} P_{k+1|k} M_{1,1}^T S^T + SW^{nl} S^T \\ SM_{1,1} P_{k+1|k} M_{1,1}^T S^T + SM_{1,2} W^{nl} M_{1,2}^T S^T + \\ SW^{nl} S^T \\ \vdots \\ SM_{h_p-1, h_p-1} P_{k+1|k} M_{h_p-1, h_p-1}^T S^T + \\ SM_{h_p-2, h_p-1} W^{nl} M_{h_p-1, h_p-1}^T S^T + \dots + SW^{nl} S^T \end{bmatrix} \quad (5.33)$$

where:

$$\begin{aligned} M_{1,T} &= A_{k+\tau} \\ M_{2,T} &= A_{k+\tau} A_{k+\tau-1} \\ M_{3,T} &= A_{k+\tau} A_{k+\tau-1} A_{k+\tau-2} \\ &\vdots \\ M_{h_p-1,} &= A_{k+\tau} A_{k+\tau-1} \dots A_{k+\tau-h_p+2} \end{aligned} \quad (5.34)$$

for all  $\tau \in \{1, 2, 3, \dots, h_p\}$  and the matrix  $P_{k+1|k}$  is the covariance matrix obtained from the track-to-track algorithm at sample  $k + 1$ .

The following characteristics are determined for the trajectory prediction process:

- The obstacle centre of mass corresponding to the position estimates;
- The geometric characteristic of a selected time invariant shape (typically an ellipsoid);
- The orientation of the vehicle, which can be estimated with the track-before-detect algorithm. It allows for heading estimation, as well as extension by the employment of the Kalman filter (when multiple sensors and/or systems measurements are supplied).

The sensor range of the platform is defined with an ellipsoidal shape. This same principle is applied to the obstacle; however, the size of the ellipsoid is dependent on the minimum separation distance,  $d_m$ , established in accordance with the mission.

### 5.4.1 Test for Correlation

The relationship between a measured and determined random variable is determined as follows. Let  $X \in \mathbb{R}^n$  be a  $n \times 1$  vector of jointly-distributed random variable with mean  $\mu_X$  and covariance matrix  $Q \in \mathbb{R}^{n \times n}$ . Let  $Y$  be a new random variable that is not measured but determined by a function, say  $Y = f(X)$ , where  $f(\cdot)$  is a function of  $X$  in the  $\mathbb{R}^n$  space. If the function is differentiable, up a certain Taylor series approximation (say first/second order), then:

$$Y \approx f(\mu_X) + \nabla f(X - f(\mu_X)) \quad (5.35)$$

where  $\nabla f(X)$  is the gradient vector evaluated at  $\mu_X$ . Then the random variable  $Y$  has mean:

$$\mu_Y \approx f(\mu_X) \quad (5.36)$$

and variance:

$$\sigma_Y^2 \approx (\nabla f)^T Q \nabla f \quad (5.37)$$

If the random variables are uncorrelated, the variance can be simplified as:

$$\sigma_Y^2 \approx (\nabla f)^T Q_d \nabla f \quad (5.38)$$

where  $Q_d$  is given by the diagonal matrix expressed as:

$$Q_d = \text{diag}([\sigma_{X1}^2, \sigma_{X2}^2, \sigma_{X3}^2 \dots \sigma_{Xn}^2]) \quad (5.39)$$

The relationship between  $\sigma_Y$  and  $\sigma_X$  is given by:

$$\sigma_Y^2 \approx \sum_{i=1}^n \left( \frac{\partial f(X)}{\partial X_i} \right)^2 \sigma_{X_i}^2 \quad (5.40)$$

assuming that  $X_i$  are independent random variables and hence the covariance  $\sigma_{X_i X_j}^2 = 0$ .

Statistical methods that can be employed for measuring correlation include Pearson, Kendall rank and Spearman correlation techniques. The most commonly used statistic is the linear correlation coefficient,  $r$ , which is often referred to as the Pearson product moment correlation coefficient and is given by:

$$r = \frac{S_{XY}}{\sqrt{S_{XX} S_{YY}}} \quad (5.41)$$

where  $S_{XY}$  is given by:

$$S_{XY} = \sum (X - \bar{X})(Y - \bar{Y}) \quad (5.42)$$

$$S_{XX} = \sum (X - \bar{X})^2 \quad (5.43)$$



$$S_{YY} = \sum (Y - \bar{Y})^2 \quad (5.44)$$

In this case,  $r$  measures the strength of the linear relationship between two variables. The magnitude of  $r$  indicates the strength, while the sign suggests the type of linear relationship. Both random variables should be normally distributed. Other assumptions include linearity and homoscedasticity. Linearity assumes a straight line relationship between each of the variables in the analysis and homoscedasticity assumes that data is normally distributed about the regression line.

Kendall rank correlation is a non-parametric test that measures the strength of dependence between two variables. If we consider two samples,  $X$  and  $Y$ , where each sample size is  $n$ , we know that the total number of pairings is  $(n - 1)/2$ . The following formula is used to calculate the value of Kendall rank correlation:

$$\tau = \frac{n_c - n_d}{\frac{1}{2}n(n-1)} \quad (5.45)$$

where  $n_c$  is the number of concordant pairs and  $n_d$  is the number of discordant pairs.

Spearman rank correlation is a non-parametric test and is used to measure the degree of association between two variables by not considering any assumptions about the distribution of the data. Is the appropriate correlation analysis when the variables are measured on a scale that is at least ordinal. The Spearman rank correlation is given by:

$$\rho = 1 - \frac{6 \sum d_i^2}{n(n^2-1)} \quad (5.46)$$

where  $\rho$  is the Spearman rank correlation,  $d_i$  is the difference between the ranks of corresponding values ( $X_i$  and  $Y_i$ ) and  $n$  is the number of value in each data set.

For example, considering ADS-B and RADAR information, typically minimum ADS-B performance requirements are based on a comparison to current RADAR performance [12, 13]. Therefore, RADAR performance must first be characterised sufficiently for each operational environment. One of the most critical parameters used for comparison is surveillance accuracy (or typically termed as position uncertainty of the tracked object). In current RADAR systems, azimuth position uncertainty is usually plotted as a function of range from the radar, given a specific radar characteristic.

In general, radar azimuth position uncertainty increases for a given target as the target moves away from the radar. Based on current operational procedures, for MSSR, two points are defined relative to supported separations. In general, 3 NM separations can be usually supported by MSSR for targets out to a maximum range of 60 NM from the

radar and beyond 60 NM, 5 NM separations must be used (to a maximum range of 200 NM) (Figure 5.3).

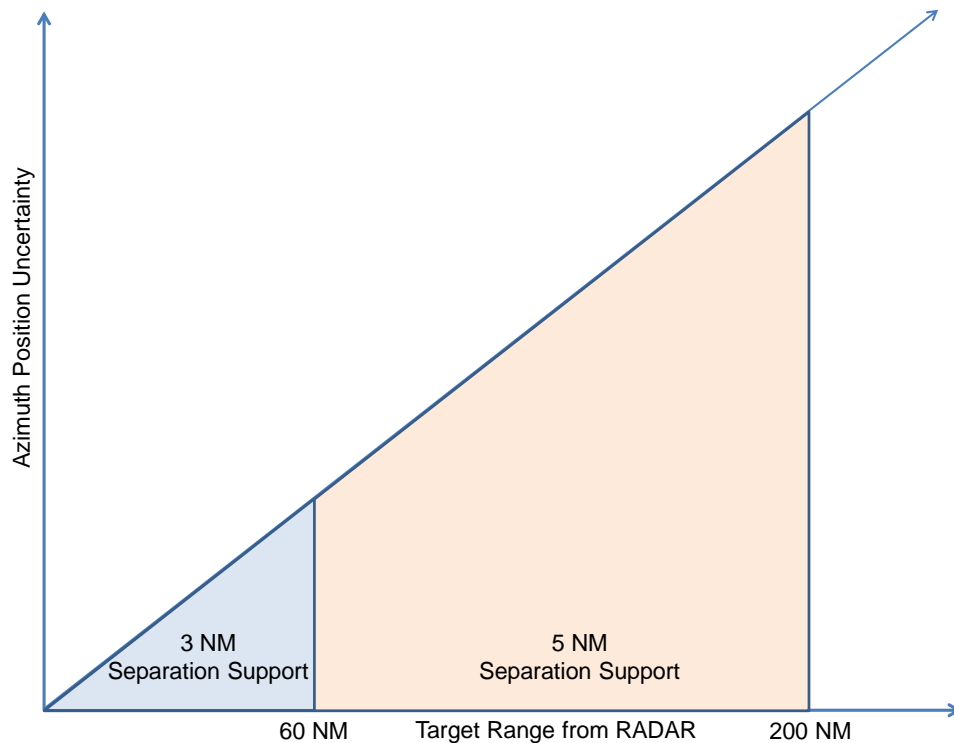


Figure 5.3. Error and radar ranges [13].

#### 5.4.2 Covariant and Contravariant Components

When the states of an aircraft do not get altered under coordinate transformations, then the relationship is invariant across time epochs. It is true that the velocity vector itself does not change when we switch coordinate systems. However, the components of the vector change. Essentially, the contravariant components of a vector are directed parallel to the coordinate axes, whereas the covariant components of a vector are directed normal (perpendicular) to constant coordinate surfaces. In the case of orthogonal Cartesian coordinates the axes are, by definition, normal to constant coordinate surfaces, so there is no distinction between contravariant and covariant components.

#### 5.4.3 Possible Cases

A number of non-cooperative sensors and cooperative systems are employed for SA&CA. An analysis for correlation between the state-of-the-art SA&CA technologies is required to determine the relationship between the navigation error of the host platform and the tracking error of the tracked traffic.

Table 5.2. Correlation analysis.

Sensor/System 1 (Host platform)	Sensor/System 2 (Tracked traffic)	Correlation
Visual camera	LIDAR	Uncorrelated/ Correlated *
Thermal camera	Radar	Uncorrelated/ Correlated *
LIDAR	ADS-B	Uncorrelated
ADS-B	ADS-B	Correlated
ADS-B	TCAS	Uncorrelated
TCAS	LIDAR	Uncorrelated
ADS-B	Acoustic Sensor	Uncorrelated

\*Depends on the environment that the sensors/systems operate in. Thus, on a foggy/rain day (water droplets, scattering, etc.), both the camera and the LIDAR will be affected and hence reduce visual activity.

When the host aircraft employs GNSS as the primary means of navigation and it employs ADS-B as the primary means of surveillance, then the errors are correlated. In all other cases, the errors are uncorrelated.

#### 5.4.4 Effects of Data Size and Methodology

The data size is a key attribute required to define the methodology to be adopted for implementing the unified approach to SA&CA. The larger the data size, the greater is the probability of determining the correlation factor and the nature of the correlation (covariant and contravariant) between the navigation error of the host aircraft and the tracking errors of the intruders.

The general methodology that is adopted is provided below:

- Determine the instantaneous position of the host aircraft;
- Obtain the error in position of the host aircraft;
- Construct the navigation error ellipsoid in 3D;
- Detect all objects and initiate the tracking process;
- Estimate/predict the trajectory of each tracked object;
- Obtain the error ellipsoid of the tracking observables in 3D;

- Compute the avoidance volume w.r.t. each tracked object assuming that the errors are uncorrelated;
- Assess the correlation between the navigation and tracking error according to the trends in the data obtained from the tracking sensors/systems;
- Recompute the avoidance volume if the errors are correlated and assume that the relationship is covariant;
- Assess the nature of the correlation between navigation and tracking errors;
- Recompute the avoidance volume if the relationship is contravariant;
- Perform an analysis for assessing the relative dynamics between the host platform and each tracked intruder;
- Compute the avoidance volumes at successive time epochs according to the correlation, the relationship associated with correlation and relative dynamics between the two platforms;
- Ensure separation assurance at all the time epochs;
- Initiate the trajectory re-optimisation module as a resolution mechanism if a collision is detected (due to non-compliance of the separation assurance function).

#### **5.4.5 Radar and ADS-B Error Modelling**

For radar, the horizontal position accuracy is normally expressed in terms of range and azimuth. The overall errors are considered to have the following component errors:

- Systematic biases;
- Stochastic errors (usually expressed as a standard deviation).

Another important term for radar is core accuracy, which is a starting point for examining radar accuracy, as compared to that of ADS-B data. Core accuracy is defined as the 95% limit of the error distribution in a certain (single direction) dimension with respect to the radar.

In the cross-range direction, the error is calculated from the azimuth error multiplied by the reference range. For ADS-B, horizontal position accuracy is defined as the radius ( $r_a$ ) of a circle cantered on the target's reported position such that the probability of the target's actual position being inside the circle is 95%. This radial error is the resultant of errors in two dimensions (x and y). Assuming that the error distributions in each dimension are independent Gaussian distributions with the same standard deviation ( $\sigma$ ), the resultant radial error distribution will be Rayleigh and the 95% point

of this distribution will be  $2.45\sigma$ . The required accuracy is derived from comparison with single dimension radar 95% accuracy.

The above discussions can be easily extended to relative position and velocity determination between ownship and intruders. For example, in addition to computing GNSS position and velocity estimates for each aircraft and exchanging these estimates through some data link, GNSS observables can be exchanged.

Expected sensor ranges might differ from one scenario to another. For example, most lightweight, low-power and low-cost UAS LIDAR systems tend to offer range of less than 1 km. But the variation of detection range for a variety of obstacles can be estimated. Flight test results obtained for detection of wire obstacles of 5 mm in diameter, in dry weather (visibilities of 800 m, 1500 m and 2000 m) and incidence angles of  $90^\circ$  and  $45^\circ$  indicated dictated the minimum LIDAR sensor performance requirements set for rotorcraft platforms [14].

In an operational scenario, these position and velocity reports are transmitted to the ground (ATM system) and other aircraft using ADS-B, and include parameters representing the accuracy and integrity performance of transmitted estimates. ADS-B does not exhibit the same uncertainty versus range characteristic as radar. ADS-B position uncertainty is primarily a function of the GNSS satellite geometry relative to the aircraft, and is not related to range from any ground-based system. The assumption takes into account the changes in satellite constellation for complex missions (military, loitering scenarios, etc.), where, with the passing of time, the satellite constellation coverage changes, even though the location does not. For this reason, ADS-B position uncertainty is assumed to be a constant for a given environment when being compared to radar performance. Hence in order to determine minimum performance requirements for ADS-B, a radar reference range must be determined for each environment to provide the appropriate comparison points between ADS-B and radar. One of the drawbacks of ADS-B on the 1090 ES base is that the interference/saturation issue. If there is a high density of air traffic, because the signals cannot be distinguished, it leads to signal layering. Therefore, it is estimated that the effective range of the ADS-B is typically 50-70 km in zones with intensive air traffic. Hence the adoption of multiple SA&CA technologies is Important. At different ranges, the employment of a suite of non-cooperative sensors or cooperative systems provides the required flexibility.

Radar position errors can be thought of in terms of a 95% error composed from range and azimuth (cross-range) components. The radar cross-range error component increases with range from the radar, however, the range error component is constant

(Figure 5.4). The radar error distributions are Gaussian in a single dimension, but in two dimensions, the 95% radar position error area is an ellipse. At the range where the radar cross-range error approximately equals the radar range error, the 95% radar position error area becomes circular. The 95% ADS-B position error area is also circular when it is based on GNSS position performance. It is relatively easy to specify a target set of Range-of-Applicability (ROA) values that span each operational domain, i.e., 60 NM to 200 NM radar ranges for En Route separation minima. However, the selection of a specific ROA value for the radar to ADS-B comparisons is much more problematic, since the most demanding environments for radar separation may not be those where radar performance is least capable, i.e., at maximum operational radar ranges.

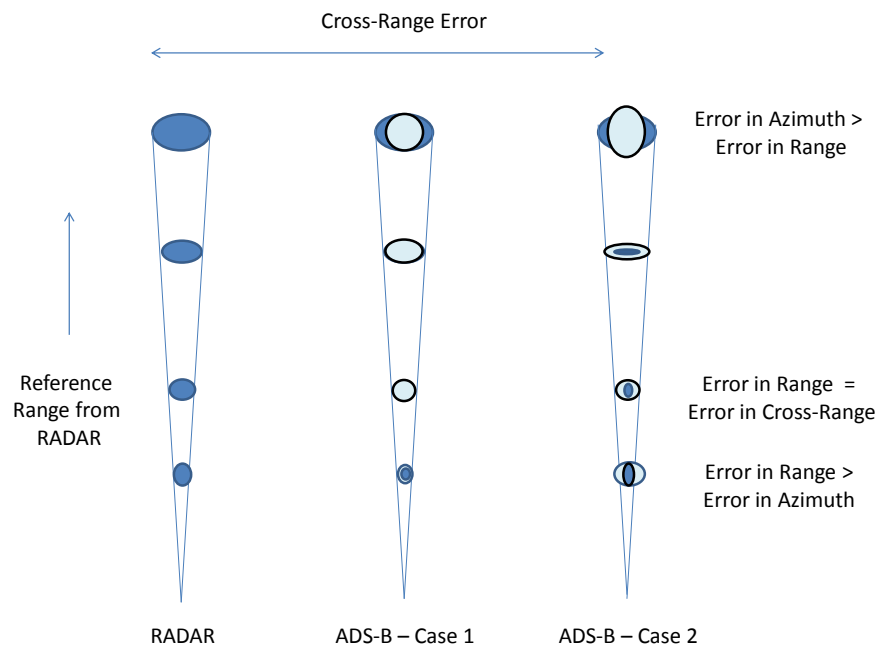


Figure 5.4. Error and reference ranges [13].

For ADS-B Case 1 in Figure 5.4, the reference range is the distance at which the radar range error equals the cross-range error. The ADS-B accuracy performance requirement is usually set such that the ADS-B position error area is approximately equal to that of radar at this point. However, the circular 95% ADS-B position error area cannot be identical to radar because the discrete ADS-B navigation accuracy categories do not exactly match the radar accuracy. The 95% ADS-B accuracy performance is constant throughout an airspace where a given navigation accuracy requirement is established. Therefore, the area bounding 95% of the radar positions is larger than that of ADS-B when the distance is greater than the ROA and smaller than that of ADS-B when the distance is less than the ROA.

A summary of the state data, state data integrity, state data status timing, as well as Traffic ID specific requirements are provide in Tables 5.3 and 5.4 respectively.

Table 5.3. Traffic application specific requirements summary [12, 13].

Requirement Category	Requirement	EVAcq/AIRB/TSAA		SURF			
		Traffic On ground When Ownship is On ground	All Other Traffic	Traffic On Ground	Traffic Airborne		
					Inside Surface Volume		Outside Surface Volume
					Ownship on Ground	Ownship Airborne	
State Data	Horizontal Position Uncertainty (95%)	< 0.1 NM (NACP ≥ 7)	< 0.5 NM (NACP ≥ 5)	< 30 m (NACP ≥ 9)	< 0.1 NM (NACP ≥ 7)	< 0.3 NM (NACP ≥ 6)	< 0.5 NM (NACP ≥ 5)
	Horizontal Velocity Uncertainty (95%) (1)	< 10 m/s (NACV ≥ 1)		< 3 m/s (NACV ≥ 2)	< 10 m/s (NACV ≥ 1)		
	Vertical Position Uncertainty (95%)	On Ground or Valid Pressure or Valid Geo (3 & 10 )		On Ground or Valid Pressure or Valid Geo (3 & 4)			
	Vertical Velocity Uncertainty (95%)	N/A		N/A			
State Data Integrity	Source Integrity Level	N/A		N/A			
	Navigation Integrity Category	N/A		N/A			
	System Design Assurance	1E-3		1E-3			
	Validation of Traffic Position with TCAS Data	N/A		N/A			
State Data And Status Timing	Maximum Total Latency	5.5 s		5.5 s			
		0.9 s		0.9 s			
		1.1 s		1.1 s			
		0.5 s		0.5 s			
		2.5 s		2.5 s			
		0.5 s		0.5 s			
	Maximum Position Data Age until Dropped	11 s (moving) 25 s (static)	25 s	11 s (moving) 25 s (static)	11 s	15 s	25 s

For ADS-B Case 2 in Figure 5.6, the reference range is chosen beyond the distance at which the range and cross-range errors are equal. At this reference range, the radar cross-range error is greater than the constant range error. The ADS-B accuracy performance requirement is set such that the ADS-B position error area is approximately equal to the radar cross-range error, the major axis of the ellipse. The 95% ADS-B position error area is slightly larger than that of radar at this distance because the radar range error is less than its cross-range error. However, as the distance from the radar increases, the radar cross-range error continues to increase and the area bounding 95% of the radar positions becomes larger than the constant circular area set for ADS-B. The required ADS-B 95% accuracy is compared against the radar 95% accuracy without systematic biases (i.e., stochastic errors only). This ensures that the normal 95% accuracy, of ADS-B is always as good as, or better than, radar accuracy at the chosen range of applicability and it also ensures that the ADS-B to ADS-B separation accuracy is always as good or better than the best-case radar to radar separation (i.e., both aircraft separated by the same RADAR). Knowing the 95% point of a Gaussian distribution as  $1.96\sigma$ , the required ADS-B 95% accuracy radius ( $r_a$ ) is given by:

$$r_a = (2.45/1.96) * 95\% = 1.25 * 0.95 \quad (5.47)$$

Table 5.4. Traffic ID specific requirements summary [12, 13].

Requirement Category	Requirement	EVAcq/AIRB/TSAA		SURF			
		Traffic On ground When Ownship is On ground	All Other Traffic	Traffic On Ground	Traffic Airborne		
					Inside Surface Volume		Outside Surface Volume
					Ownship On ground	Ownship Airborne	
Traffic ID	Maximum Latency	29 s		29 s			
		1.0 s		1.0 s			
		9.0 s		9.0 s			
		0.5 s		0.5 s			
		18 s		18 s			
		0.5 s		0.5 s			
	Maximum Data Age Until Drooped	Until track termination		Until track termination			



## 5.5 Sensor/System Error Modelling

The effect of sensor errors on the avoidance volumes is studied for all three cases of errors, including uncorrelated, covariant and contravariant errors. Different avoidance volumes are generated based on the time varying nature of the errors in navigation and tracking measurements. To illustrate the concept, considering  $\sigma_{x_N}$ ,  $\sigma_{y_N}$  and  $\sigma_{z_N}$  as the errors in navigation measurements in  $x$ ,  $y$  and  $z$  and  $\sigma_{x_T}$ ,  $\sigma_{y_T}$  and  $\sigma_{z_T}$  as the errors in tracking measurements in  $x$ ,  $y$  and  $z$ , the variation of avoidance volume is studied in the following section.

### 5.5.1 Errors in Range

The avoidance volume obtained at a given range varies according to the errors in navigation measurements and tracking observables. This variation is illustrated in Figures 5.5 to 5.11 for uncorrelated, covariant and contravariant cases respectively.

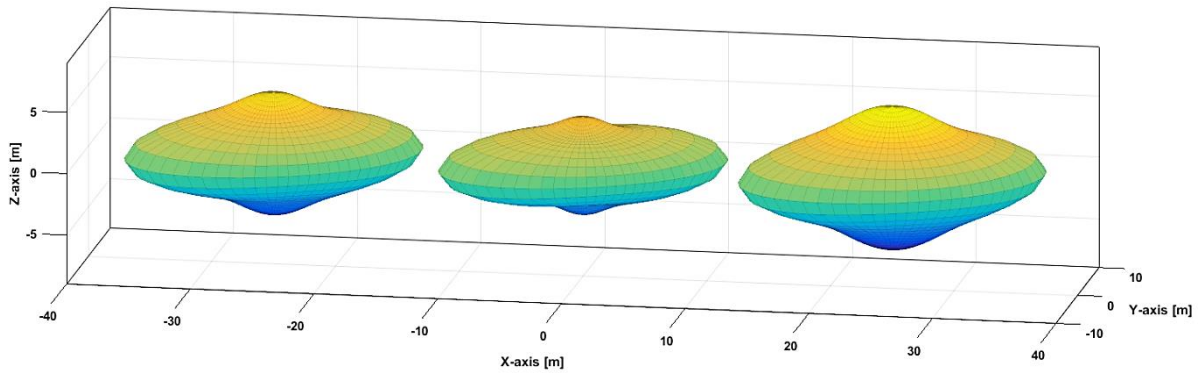


Figure 5.5.  $\{\sigma_{x_N}, \sigma_{y_N}, \sigma_{z_N}\} = 3, 2, 4$  and  $\{\sigma_{x_T}, \sigma_{y_T}, \sigma_{z_T}\} = 8, 12, 3$ .

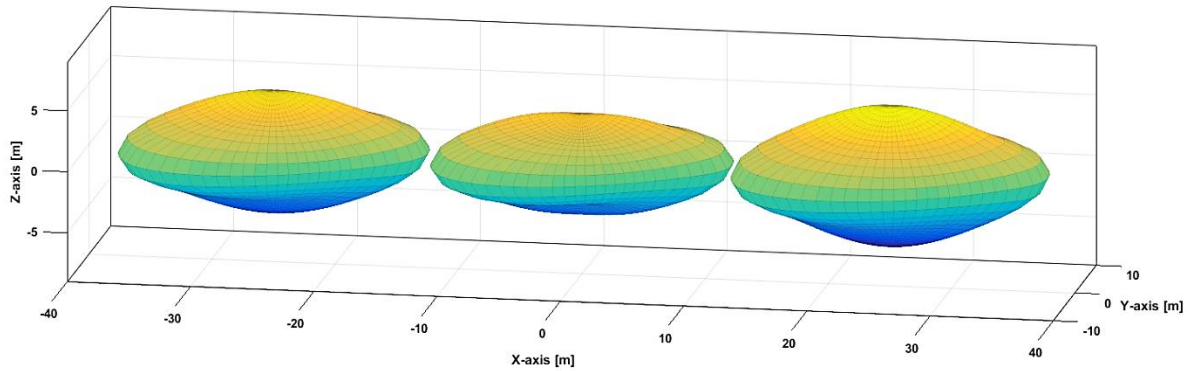


Figure 5.6.  $\{\sigma_{x_N}, \sigma_{y_N}, \sigma_{z_N}\} = 6, 2, 4$  and  $\{\sigma_{x_T}, \sigma_{y_T}, \sigma_{z_T}\} = 8, 12, 3$ .

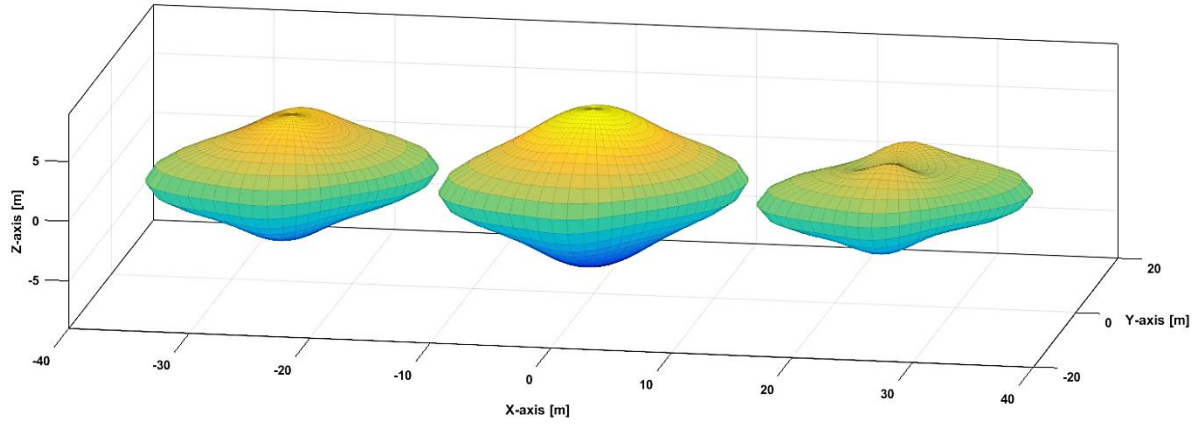


Figure 5.7.  $\{\sigma_{x_N}, \sigma_{y_N}, \sigma_{z_N}\} = 3, 8, 4$  and  $\{\sigma_{x_T}, \sigma_{y_T}, \sigma_{z_T}\} = 8, 12, 3$ .

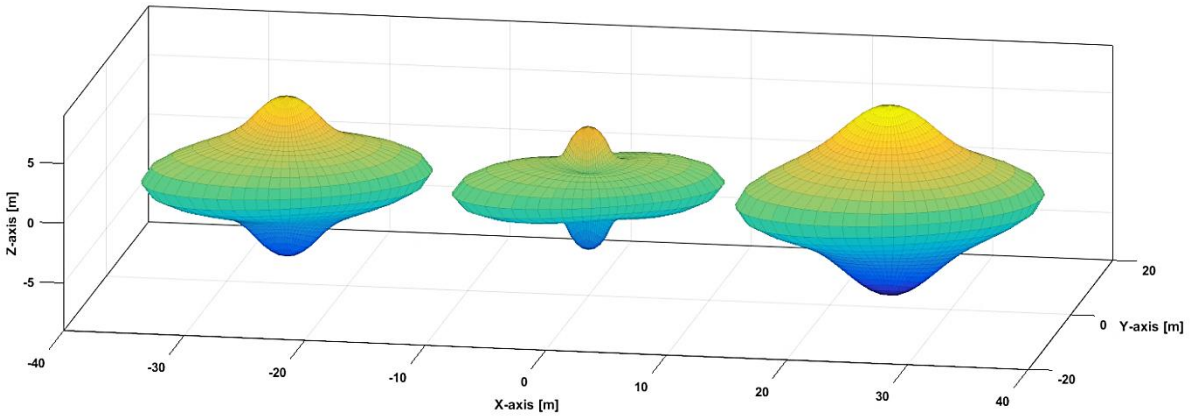


Figure 5.8.  $\{\sigma_{x_N}, \sigma_{y_N}, \sigma_{z_N}\} = 3, 2, 6$  and  $\{\sigma_{x_T}, \sigma_{y_T}, \sigma_{z_T}\} = 8, 12, 3$ .

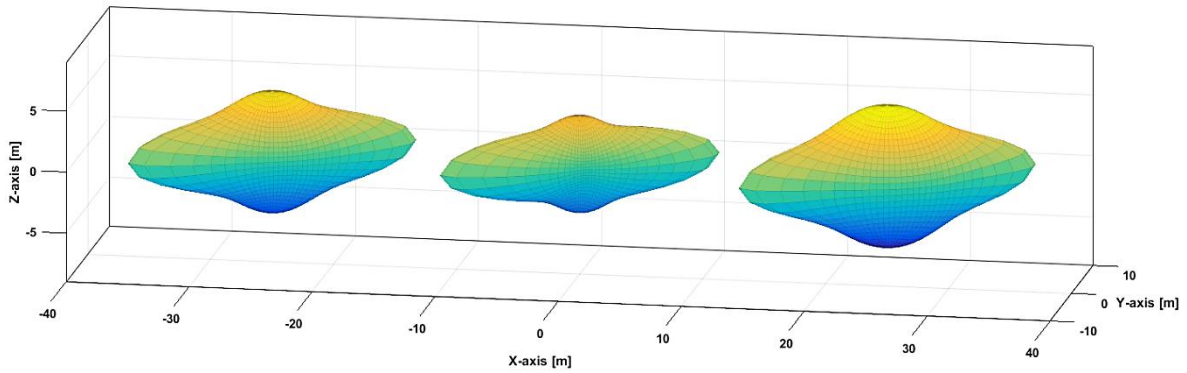


Figure 5.9.  $\{\sigma_{x_N}, \sigma_{y_N}, \sigma_{z_N}\} = 3, 2, 4$  and  $\{\sigma_{x_T}, \sigma_{y_T}, \sigma_{z_T}\} = 3, 12, 3$ .

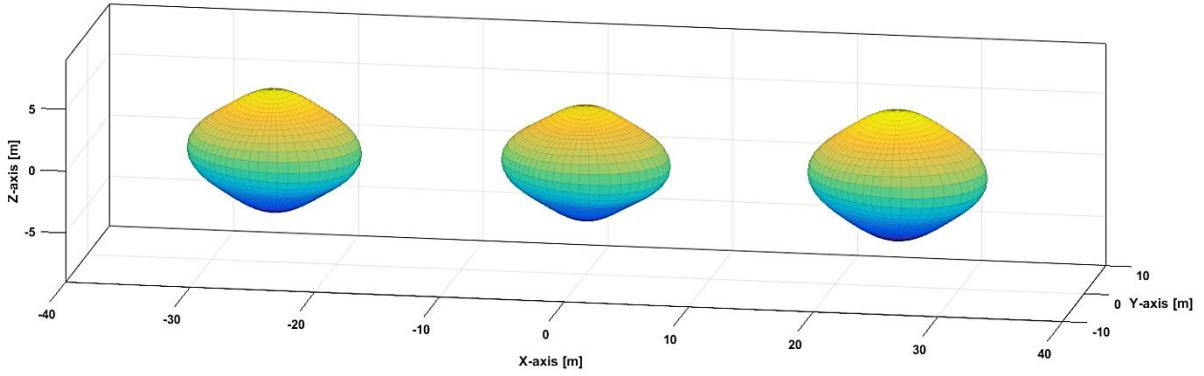


Figure 5.10.  $\{\sigma_{x_N}, \sigma_{y_N}, \sigma_{z_N}\} = 3, 2, 4$  and  $\{\sigma_{x_T}, \sigma_{y_T}, \sigma_{z_T}\} = 8, 5, 3$ .

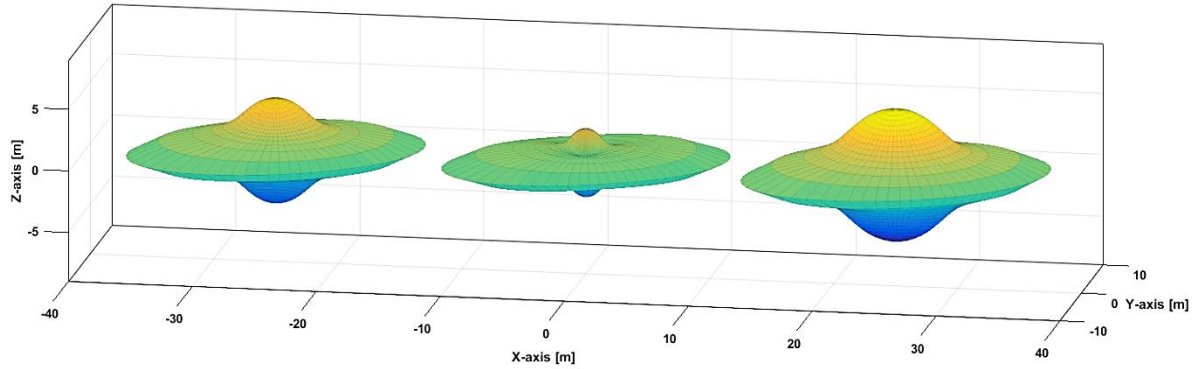


Figure 5.11.  $\{\sigma_{x_N}, \sigma_{y_N}, \sigma_{z_N}\} = 3, 2, 4$  and  $\{\sigma_{x_T}, \sigma_{y_T}, \sigma_{z_T}\} = 8, 12, 1$ .

### 5.5.2 Errors in Bearing Measurements at a Given Range

In a similar manner, the avoidance volume varies according to the errors in bearing measurements at a given range. This effect is illustrated in Figures 5.12 to 5.15.

Figure 5.14 shows the avoidance volume obtained for the following conditions (covariant case):

$$\{\sigma_{x_N}, \sigma_{y_N}, \sigma_{z_N}\} = 30, 20, 40 \text{ and } \{\sigma_{x_T}, \sigma_{y_T}, \sigma_{z_T}\} = 30, 30, 20$$

Errors in azimuth and elevation are 40 degrees and the correlation coefficient is 0.34.

Figure 5.15 shows the avoidance volume obtained for the following conditions (contravariant case):

$$\{\sigma_{x_N}, \sigma_{y_N}, \sigma_{z_N}\} = 30, 20, 40 \text{ and } \{\sigma_{x_T}, \sigma_{y_T}, \sigma_{z_T}\} = 30, 30, 20$$

Errors in azimuth and elevation are 40 degrees and the correlation coefficient is 0.34.

Figure 5.16 shows the avoidance volume obtained for the conditions as in Figure 5.14 but the correlation coefficient is 0.17.

Figure 5.17 shows the avoidance volume obtained for the following conditions (covariant case):

$$\{\sigma_{x_N}, \sigma_{y_N}, \sigma_{z_N}\} = 30, 20, 40 \text{ and } \{\sigma_{x_T}, \sigma_{y_T}, \sigma_{z_T}\} = 30, 30, 20$$

Errors in azimuth and elevation are 35 degrees and the correlation coefficient is 0.34.

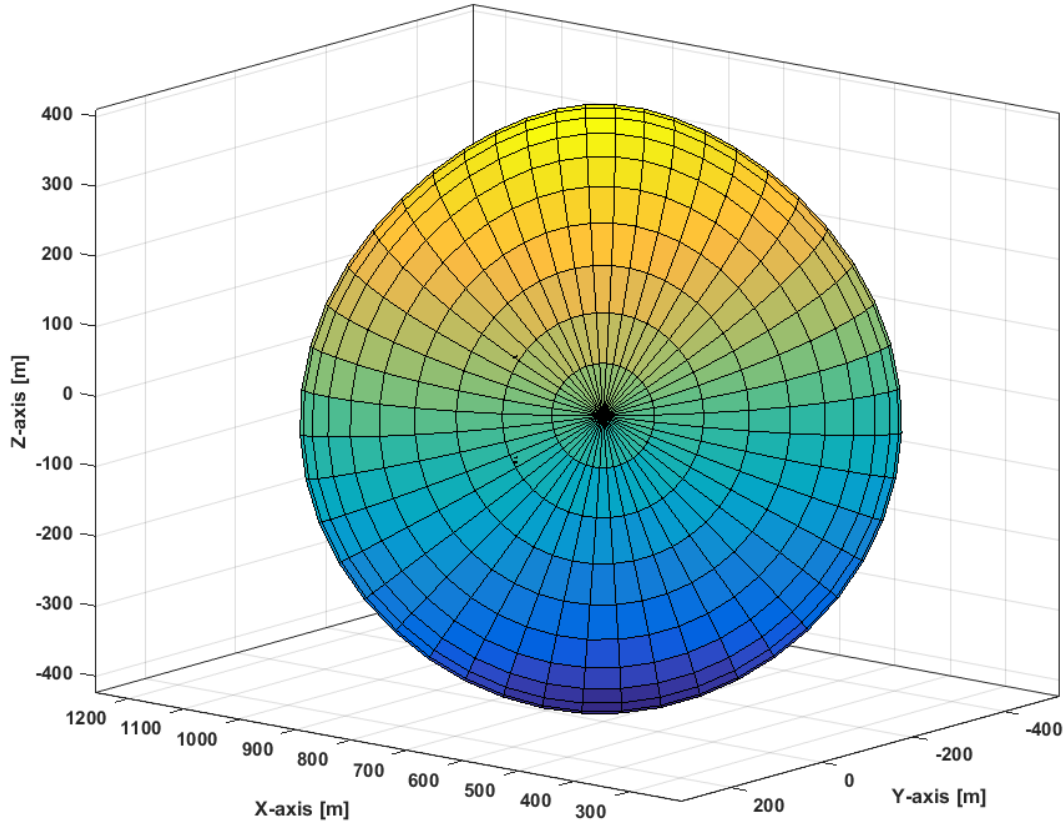


Figure 5.12. Covariant case.

Figure 5.16 shows the avoidance volume obtained for the following conditions (covariant case):

$$\{\sigma_{x_N}, \sigma_{y_N}, \sigma_{z_N}\} = 30, 20, 40 \text{ and } \{\sigma_{x_T}, \sigma_{y_T}, \sigma_{z_T}\} = 30, 30, 20$$

Errors in azimuth and elevation are 70 degrees and the correlation coefficient is 0.34.

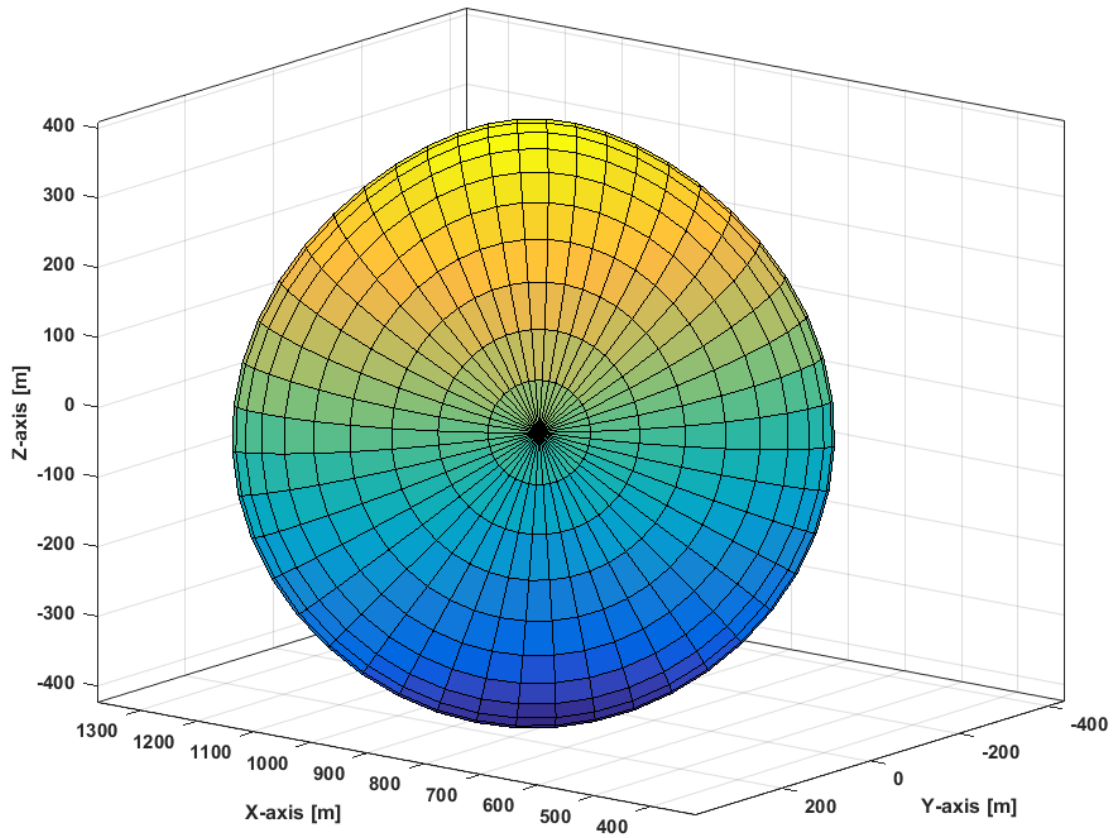


Figure 5.13. Contravariant case.

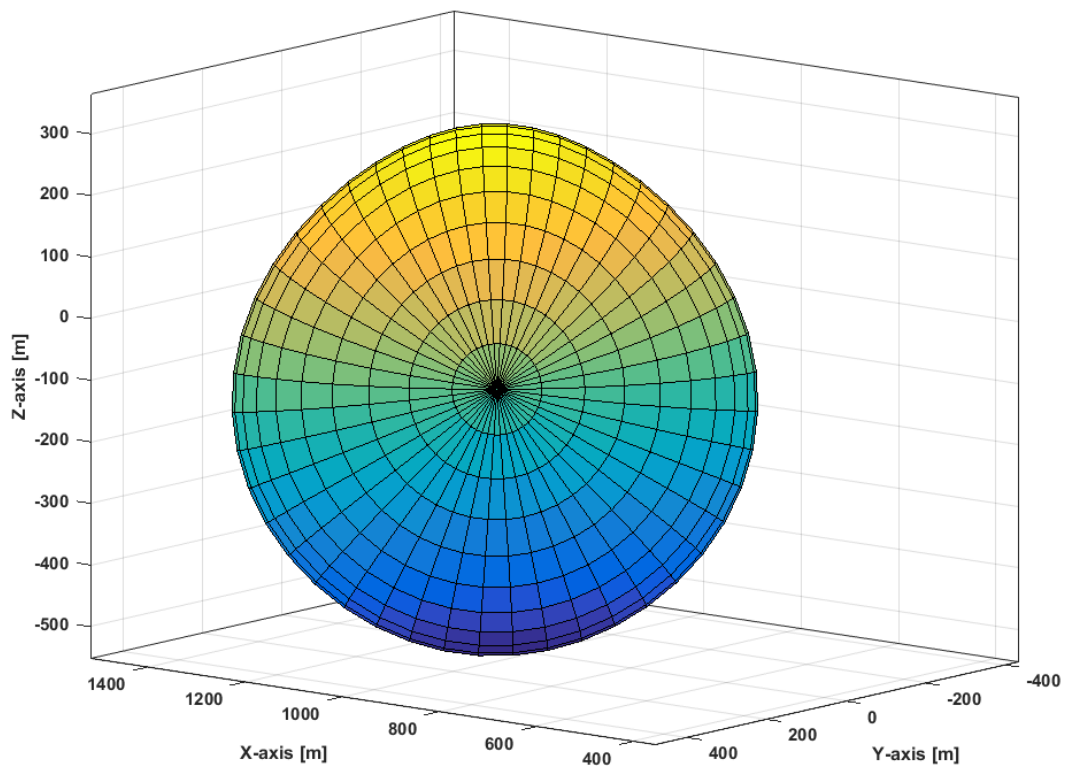


Figure 5.14. Effect of correlation coefficient.

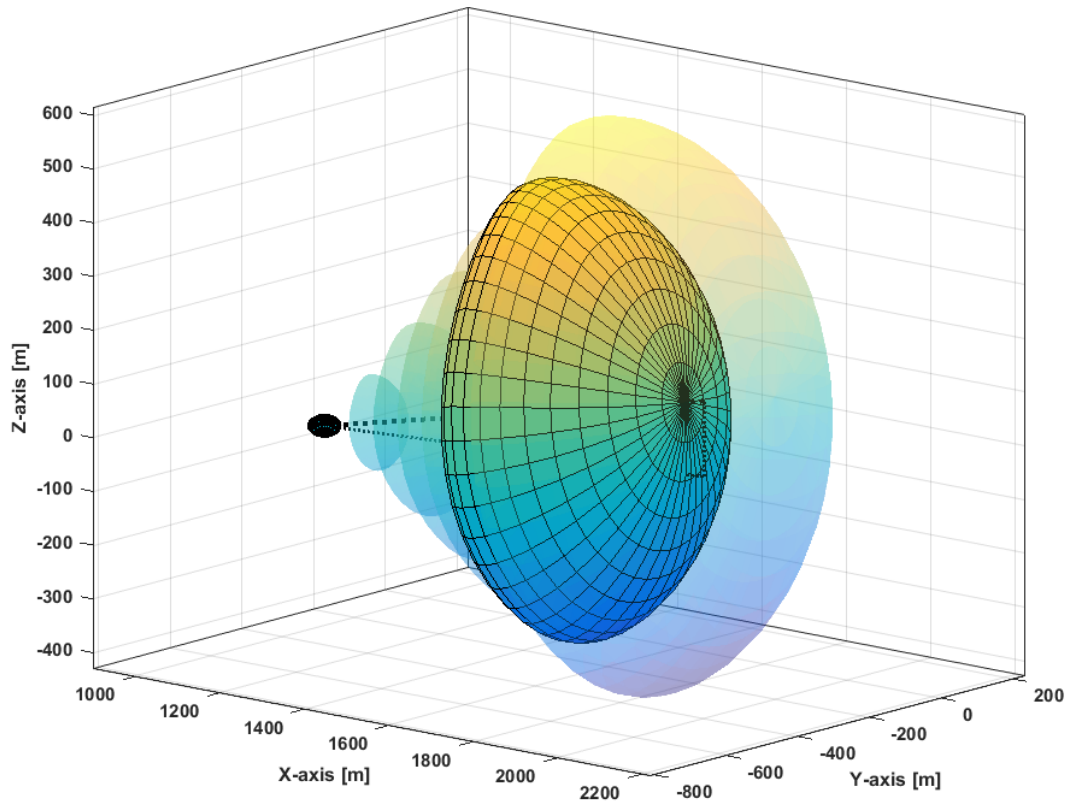


Figure 5.15. Errors in azimuth/elevation measurements = 35 degrees.

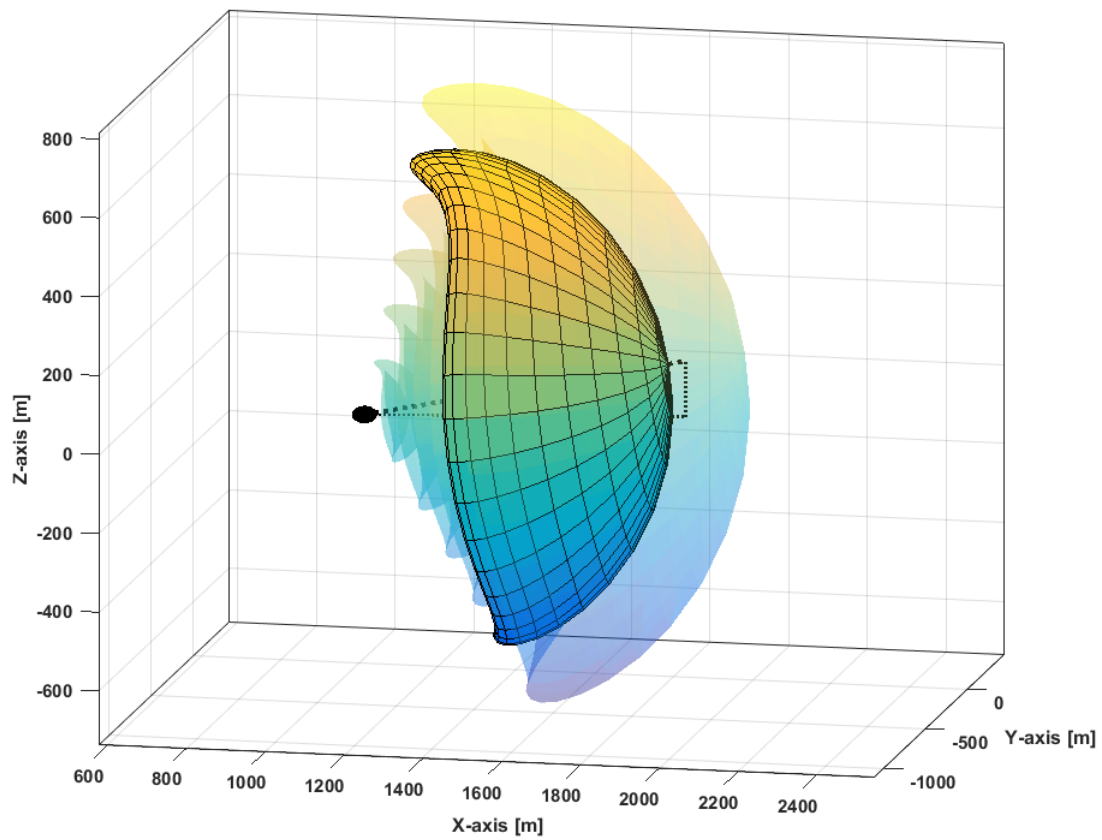


Figure 5.16. Errors in azimuth/elevation measurements = 35 degrees.



Figure 5.17 shows the avoidance volume obtained for the same conditions as for Figure 5.16 but in this case, the error in tracking observables is 10 degrees.

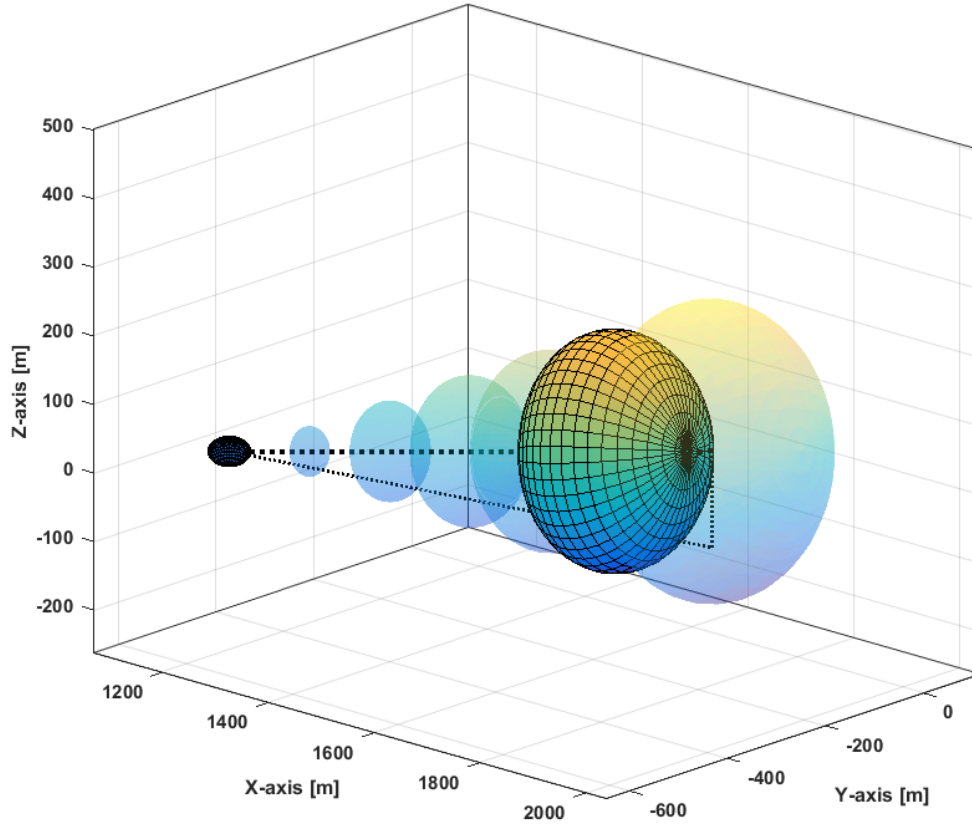


Figure 5.17. Errors in azimuth/elevation measurements = 10 degrees.

### 5.5.3 Uncertainty in Velocity Measurements

Uncertainty in the velocity measurements of the tracked object has an effect on the overall avoidance volume. The effect is intertwined with how relative dynamics between any two aerial platforms contribute to the uncertainties in measurements and to the definition of the SA&CA functionalities.

Figure 5.18 shows the avoidance volume obtained for the following conditions (covariant case):

$$\{\sigma_{x_N}, \sigma_{y_N}, \sigma_{z_N}\} = 30, 20, 40 \text{ and } \{\sigma_{x_T}, \sigma_{y_T}, \sigma_{z_T}\} = 30, 30, 20$$

Errors in azimuth and elevation are 40 degrees, the correlation coefficient is 0.34 and the uncertainty in velocity is 7 m/sec.

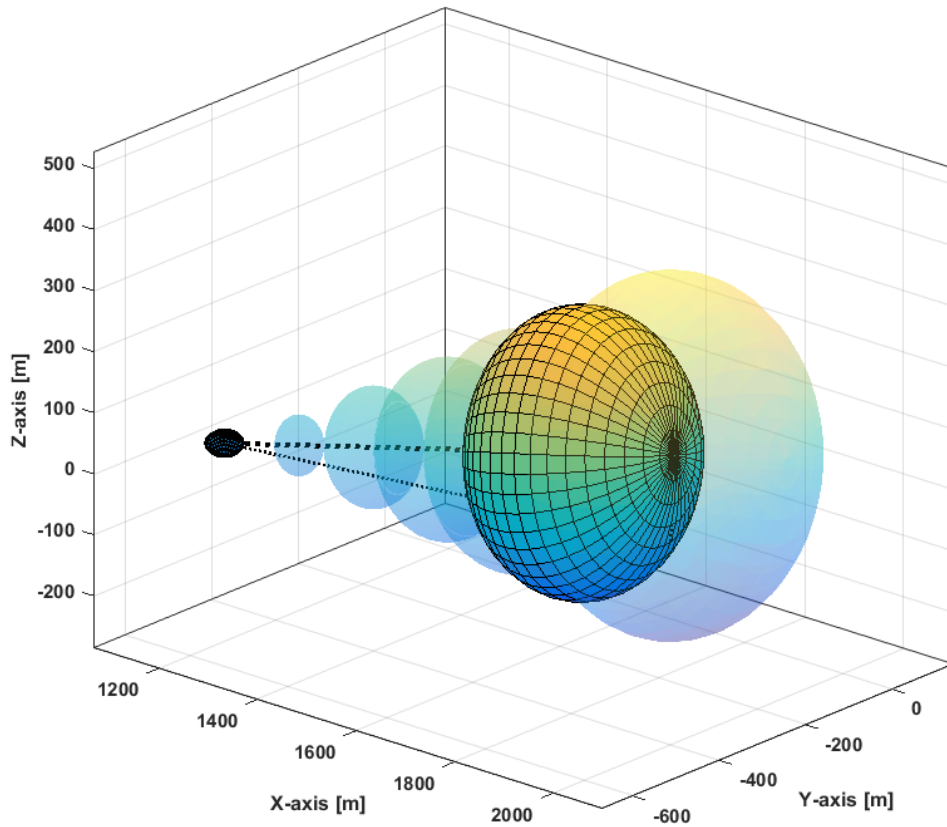


Figure 5.18. Uncertainty in velocity = 7 m/sec.

Figure 5.19 shows the avoidance volume obtained for the same condition as in the above case but the uncertainty in velocity is 3 m/sec. This directly relates to the relative dynamics between two platforms, which is studied in detail in the next section. One of the key findings of this analysis is that when SA is ensured between two platforms or when there are no conflicts between their trajectory intents, then the avoidance volumes provide the separation minima to be followed in that particular scenario. This finding holds well provided there are no coupled environmental effects (wind shear, etc.) and is applicable to both manned and unmanned aircraft, as well as coordinated operations for all classes of airspace.

### 5.5.1 Wind and Wake Turbulence

Since many unmanned aircraft are very small in size, they are quite susceptible to turbulence-induced loss-of-control and trajectory excursions, which are important factors to consider in the implementation of SA&CA functionalities. Wind effects can be conveniently included as an integral part of the aircraft dynamics model and affects the overall avoidance volume calculation. Automated means for forecasting turbulence levels in the atmosphere that effect unmanned aircraft, along with algorithms that



provide a turbulence hazard metric given the state of atmospheric turbulence are useful for this analysis.

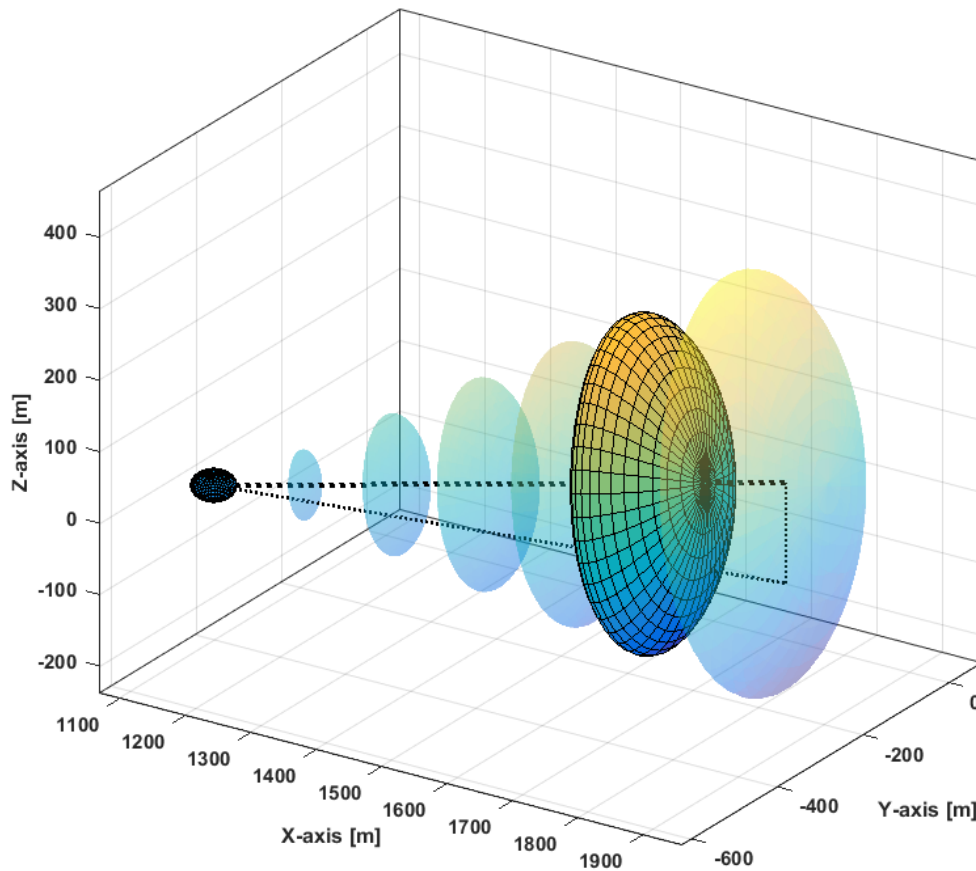


Figure 5.19. Uncertainty in velocity = 3 m/sec.

The FAA has recently implemented new rules at a number of airports for keeping airplanes far enough apart so they are not affected by each other's wake turbulence. This wake turbulence Re-Categorization (RECAT) more narrowly and accurately defines safe wake turbulence separation standards based on the performance characteristics of aircraft. Resulting from recent research in wake physics, this new system has six categories that are based on aircraft weight, approach speeds, wing characteristics and other special considerations. In a RECAT system, the required separation is modified (increased or decreased) depending on the pairings of leading and trailing aircraft. For unmanned aircraft, serious considerations must be taken to minimize the impact of wake turbulence on these light weight aircraft. It is envisioned that some of the possible impacts of hazardous wake encounters for UAS may include engine failure, temporary loss or total loss of aircraft command and control; resulting in loss of situational awareness by remote pilot and inability to respond to ATC instructions in a semi-autonomous mode of operation.

In order to provide a rigorous approach to include wake turbulence in the SA&CA functionalities, each UAS (or perhaps groups of similar type) are to be evaluated for specific reactions (attitudes and altitude excursions) when encountering various wake strengths at a range of encounter geometries. Given the onboard guidance and attitude control logic and ability to return to normal controlled flight from wake encounter induced unusual attitudes, the overall avoidance volumes are defined taking into account the existing wake models to estimate the strength of wakes generated by UAS at different speeds and configurations [15 - 18].

## 5.6 Relative Dynamics between Platforms

The geometric algorithms are defined based on definitions given in Figure 5.20.

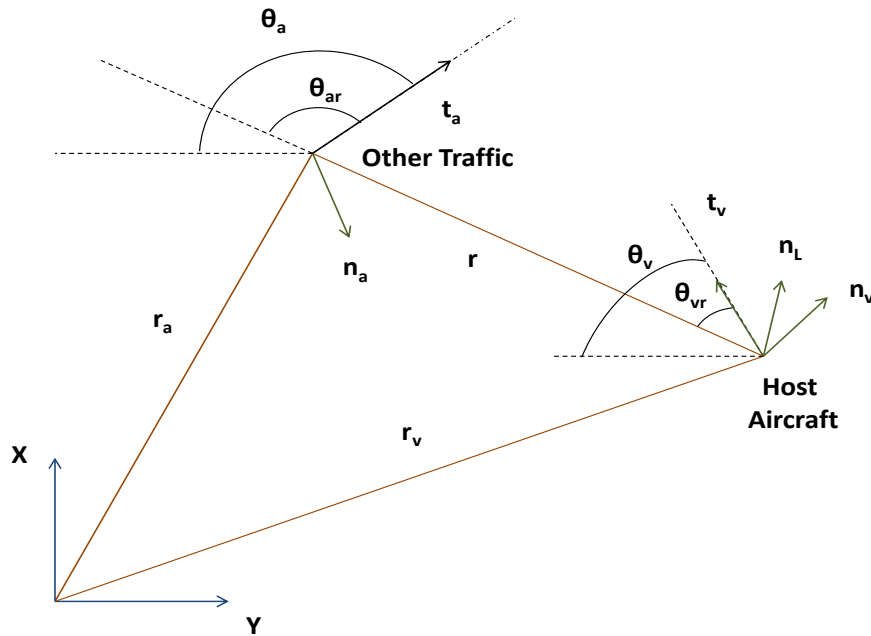


Figure 5.20. Illustration of a conflict event.

Whenever both the host aircraft and intruders are considered as points that move in a curved trajectory that can be expressed in a real space  $\mathbb{R}^3$ , then Frenet-Serret equations can be defined in order to express the relative motion [19]. Subsequently, a minimum separation distance  $d_m$  is defined. If the distance between the host aircraft and the moving intruder is or will be less than the separation distance at a specific time interval, then a conflict condition is established.

The algorithm for conflict resolution can be defined as follows, where a desired heading command  $\dot{\theta}_u$  is given by:

$$\dot{\theta}_u = \left(1 + \frac{1}{\gamma}\right) \frac{v_r}{\sqrt{r^2 - d_m}} \frac{|\theta_e|}{\theta_e} + K_p \theta_e \quad (5.48)$$

where  $\theta_e$  is the heading error between the desired heading,  $\bar{\theta}_u = \bar{\theta}_u$ , and the actual heading  $\theta_u = \theta_u$  is defined by:

$$\theta_e = \bar{\theta}_u - \theta_u = \bar{\theta}_{um} - \theta_{um} \quad (5.49)$$

It can be observed that from the matching condition in both clockwise and anticlockwise resolutions, the velocity vector can be defined as:

$$t_v = \frac{1}{\gamma} \left[ \frac{d_r}{s_a} \hat{t}_m + \hat{t}_a \right] \quad (5.50)$$

where  $\gamma$  is the heading. Also, a desired tangent vector to the circle of separation of radius  $r = d_m$  is defined as follows:

$$\bar{t}_v = \frac{1}{\gamma} \left[ \frac{d_r}{s_a} \hat{t}_s + \hat{t}_a \right] \quad (5.51)$$

where the ratio,  $\frac{d_r}{s_a}$ , is valid with the assumption of constant velocity, providing a unique solution. This ratio is obtained applying a cosine rule to the resolution geometry given by:

$$\frac{d_r}{s_a} = -\cos \theta_{am} \pm \sqrt{\gamma^2 - \sin^2 \theta_{am}} \quad (5.52)$$

The angle  $\theta_{am}$  is obtained graphically and determined for both resolution approaches (clockwise and anti-clockwise). In order to determine if a clockwise or anticlockwise solution will be performed, both desired vectors have to be considered (Figure 5.21).

Then the criterion to determine the direction is to perform the rotation to the closest desired vector. In order to extend the solution to a 3D problem, a family of trajectories is generated around the heading axis and an optimal trajectory is selected by utilizing a proper cost function. The determination of whether an obstacle/intruder poses a collision threat (collision threat detection) is resolved using a collision threat model, which is a model that describes a situation that leads to a collision.

The model and the subsequent required condition for collision occurrence are discussed in the following subsection. In order to describe a collision threat model for analysing the relative dynamics between platforms, the following scenario is considered. A host aircraft A and an intruder B are proceeding in a collision course as described in Figure 5.22.

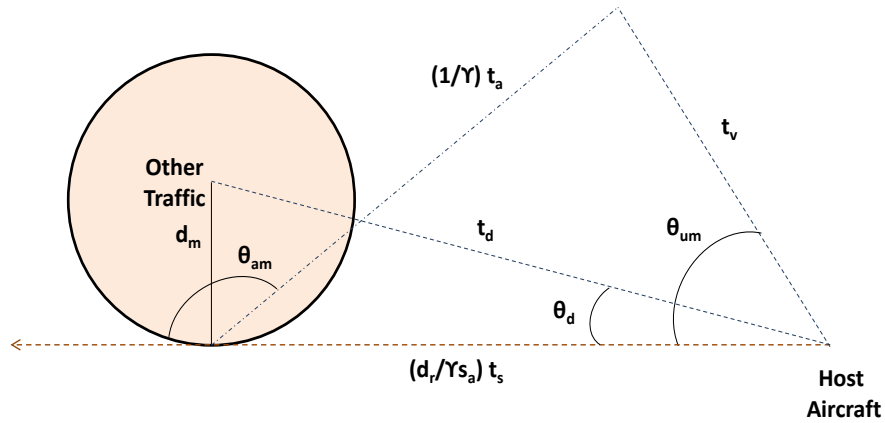


Figure 5.21. Obtained resolution.

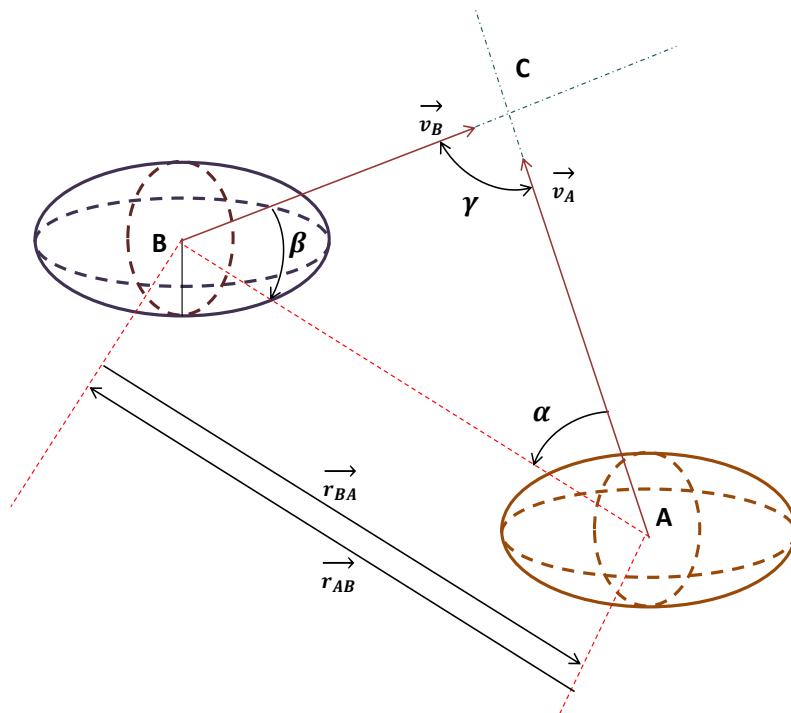


Figure 5.22. Two objects in a collision course.

Let point A be the position of host aircraft, A, and point B be that of the intruder, B. The position vectors of these aircraft are provided by  $\vec{r}_A$  and  $\vec{r}_B$  respectively. Here,  $\vec{r}_{AB}$  is the vector of the position of object B relative to object A. The collision point C, with its corresponding position vectors  $\vec{r}_{AC}$  and  $\vec{r}_{BC}$ , is the location where objects A and B would collide if the planned trajectory of the host aircraft and predicted/estimated trajectory of other aircraft do not change. But since both objects have finite size, the collision

occurs earlier. To object A, the collision occurs as it reaches point C as shown in Figure 5.23.

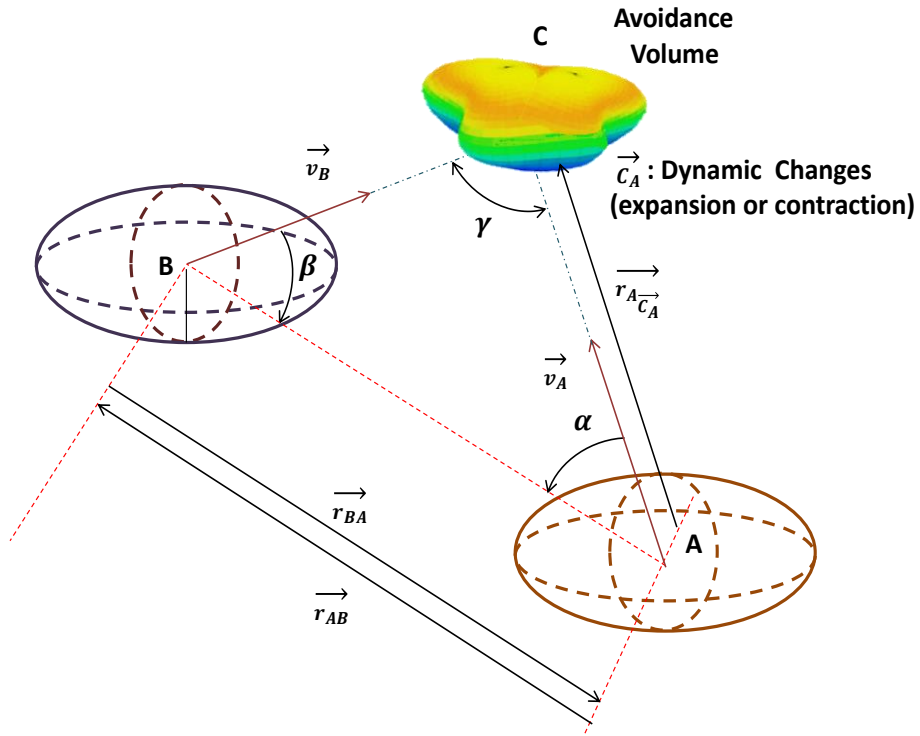


Figure 5.23. Collision scenario.

The opposite but equivalent description is applicable to object B. During the course towards collision, the radial distance between the host aircraft and intruder is decreasing. Hence, a necessary condition for a collision to occur is given by:

$$\frac{d||\vec{r}_{AB}||}{dt} < 0 \quad (5.53)$$

or

$$||\vec{r}_{AB}|| = ||\vec{r}_{BA}|| \quad (5.54)$$

Conditions can be described in relative perspective with respect to an observer in object A, or in object B. The moving object is object A and its velocity is described by its relative velocity to B. A volume given by  $r_A + r_B$  is defined around point B and this volume is a hazard to object A. The relative dynamics analysis allows for the expression of the rate of change of radial distance in terms of measured variables.

$$\frac{d||\vec{r}_{AB}||}{dt} = \vec{r}_{AB}^T \cdot \vec{v}_{AB} \quad (5.55)$$

$$\frac{d||\vec{r}_{BA}||}{dt} = \vec{r}_{BA}^T \cdot \vec{v}_{BA} \quad (5.56)$$

Relative position and relative velocity are obtainable from direct measurement by on-board range-and-direction sensors. The estimated time-to-collide ( $t_c$ ) is the time instance with respect to current condition when collision is estimated to occur and is given by:

$$t_c = \frac{|\vec{r}_{BA}| - (r_A + r_B + r_{clear})}{|\vec{v}_{ABr}|} \quad (5.57)$$

The above condition is not sufficient for a collision to occur. For example, if trajectories of the host and intruder aircraft are parallel to each other, collision may not occur if the separating distance between trajectories exceed certain value, namely the sum of both object's size radii. Therefore, another condition must be identified for describing the collision. It can be seen that the extension line of vector  $\vec{v}_A$  intrudes the avoidance volume, which means object A will collide with object B, provided the velocity vector of the host aircraft does not change in its direction.

Angle  $\psi_{AB}$  is defined as the angle of encounter, by which the host aircraft encounters the intruder aircraft. If the angle of encounter exceeds a certain predefined threshold value, a miss situation may occur instead of a collision. Such angle of encounter is called miss angle  $\psi_{ABmiss}$ , or  $\psi_{miss}$  for short. By identifying these angles, the sufficient conditions for avoiding a collision are obtained and are given by:

$$\vec{r}_{AB}^T \cdot \vec{v}_{AB} < 0 \quad (5.58)$$

or

$$\vec{r}_{BA}^T \cdot \vec{v}_{BA} < 0 \quad (5.59)$$

The other applicable conditions are given by:

$$\psi_{AB} < \psi_{miss} \quad (5.60)$$

or

$$\psi_{BA} < \psi_{miss} \quad (5.61)$$

The vectors for relative position and velocity are given by:

$$\vec{r}_{AB} = \vec{r}_A - \vec{r}_B \quad (5.62)$$

$$\vec{v}_{AB} = \vec{v}_A - \vec{v}_B \quad (5.63)$$

$$\vec{v}_{AB} = \vec{v}_{ABr} + \vec{v}_{ABt} \quad (5.64)$$

where  $\vec{v}_{ABr}$  and  $\vec{v}_{ABt}$  are the radial and tangential components of the vector. The tangent angle is the angle of encounter  $\psi_{AB}$ . The radial and tangential components are given by:

$$\overrightarrow{v_{ABr}} = ||\overrightarrow{v_{AB}}|| \cdot \cos \psi_{AB} \cdot \overrightarrow{I_{ABr}} \quad (5.65)$$

$$\overrightarrow{v_{ABt}} = ||\overrightarrow{v_{AB}}|| \cdot \sin \psi_{AB} \cdot \overrightarrow{I_{ABt}} \quad (5.66)$$

where:

$$\overrightarrow{I_{ABr}} = \frac{\overrightarrow{r_{AB}}}{||\overrightarrow{r_{AB}}||} \quad (5.67)$$

$$\overrightarrow{I_{ABt}} = \overrightarrow{I_{\psi_{AB}}} \times \overrightarrow{I_{r_{AB}}} \quad (5.68)$$

The decomposition is given by:

$$-\cos \psi_{AB} = \frac{\overrightarrow{r_{AB}}^T \cdot \overrightarrow{v_{AB}}}{||\overrightarrow{r_{AB}}|| \cdot ||\overrightarrow{v_{AB}}||} \quad (5.69)$$

$$\overrightarrow{I_{y_{AB}}} \cdot \sin \psi_{AB} = \frac{\overrightarrow{r_{AB}} \times \overrightarrow{v_{AB}}}{||\overrightarrow{r_{AB}}|| \cdot ||\overrightarrow{v_{AB}}||} \quad (5.70)$$

The miss angle is expressed as:

$$||\psi_{miss}|| = \arctan \frac{\overrightarrow{r_A} + \overrightarrow{r_B}}{||\overrightarrow{r_{BA}}||} \quad (5.71)$$

By introducing a clearance distance ( $r_{clear} > 0$ ) in  $\psi_{miss}$  expression, the miss angle is modified as:

$$||\psi_{miss}|| = \arcsin \frac{\overrightarrow{r_A} + \overrightarrow{r_B} + \overrightarrow{r_{clear}}}{||\overrightarrow{r_{AB}}||} \quad (5.72)$$

and hence:

$$\frac{||\overrightarrow{r_{AB}} \times \overrightarrow{v_{AB}}||}{||\overrightarrow{r_{AB}} \cdot \overrightarrow{v_{AB}}||} < \frac{\overrightarrow{r_A} + \overrightarrow{r_B} + \overrightarrow{r_{clear}}}{||\overrightarrow{r_{AB}}||} \quad (5.73)$$

or

$$\frac{||\overrightarrow{r_{BA}} \times \overrightarrow{v_{BA}}||}{||\overrightarrow{r_{BA}} \cdot \overrightarrow{v_{BA}}||} < \frac{\overrightarrow{r_A} + \overrightarrow{r_B} + \overrightarrow{r_{clear}}}{||\overrightarrow{r_{BA}}||} \quad (5.74)$$

## 5.7 CNS Performance and Error Models

The detection equipment for SA&CA involves a combination of non-cooperative sensors, including active/passive Forward-Looking Sensors (FLS) and acoustic sensors, as well as cooperative systems, including ADS-B and TCAS. Global Navigation Satellite Systems (GNSS), Inertial Measurement Unit (IMU) and Vision Based Navigation (VBN) sensor measurements (and possible augmentation from aircraft dynamics model) are used for navigation. Appendix A provides a summary of multi-sensor data fusion techniques implemented for UAS integrated navigation systems. The navigation and surveillance sensors/systems are shown in Figure 5.24. The intruder state measurements are obtained

from cooperative and non-cooperative equipment and are supplied through the data bus for SA&CA. The tracks of the intruders are obtained by estimating its state information in real-time. The SA&CA system functionalities are based on algorithms that quantify in real-time the total uncertainty volume in the airspace surrounding the tracked object (presented in Chapter 4). Based on these analytical models, the implemented data processing techniques allow the real-time transformation of navigation and tracking errors affecting the state measurements to unified range and bearing uncertainty descriptors. Since these errors may be statistically independent (e.g., non-cooperative sensor) or dependent (e.g., ADS-B), the overall avoidance volume is calculated in real-time for each encounter.

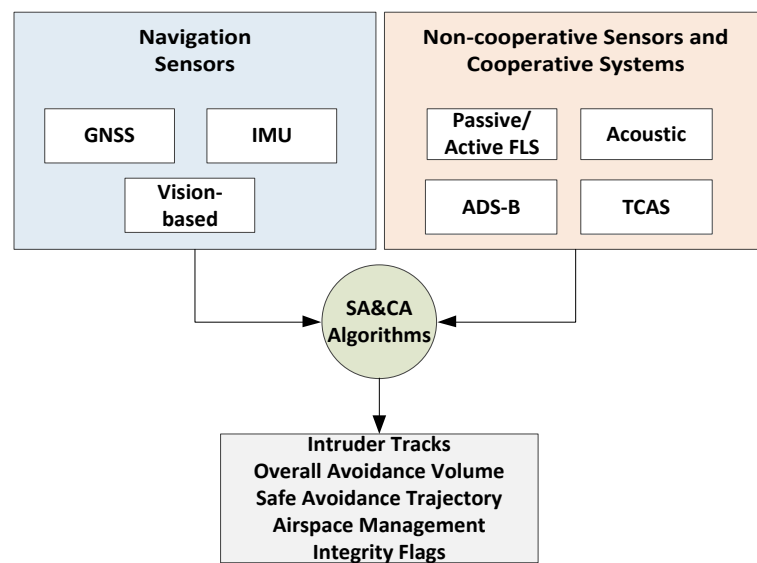


Figure 5.24. Navigation and surveillance sensors/systems.

A conceptual representation of the overall avoidance volume obtained in relation to an identified collision threat and the avoidance trajectory generated by the NG-FMS is provided in Figure 5.25. After identifying a RoC, if the original trajectory of the host platform intersects the calculated avoidance volume, a caution integrity flag is issued. An avoidance trajectory is generated in real-time and the steering commands are provided to the flight control surfaces. The SA&CA system has to sense and avoid air and ground obstacles of various characteristics (natural and man-made) including long and thin structures such as electrical cables and poles, as well as aerial obstacles such as other UAS and manned aircraft. The role of CNS performance and the error model is shown in Figure 5.26. Two different models can be defined for determining the performance of a CNS system and the errors affecting the measurements. For example, PSR can be modelled using:



- the maximum range at which the system can determine a target of a specified size;
- accuracy of target location measurement in terms of range and bearing;
- ability to recognise the type of target, etc.

Hence the performance model is different for each system.

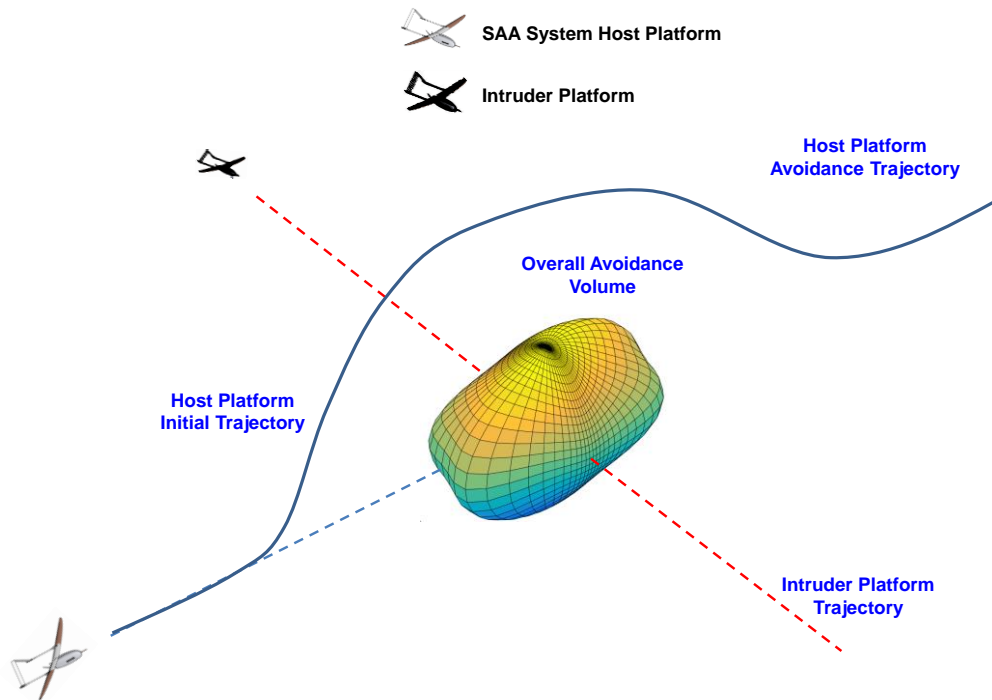


Figure 5.25. Illustration of a collision detection & resolution mechanism.

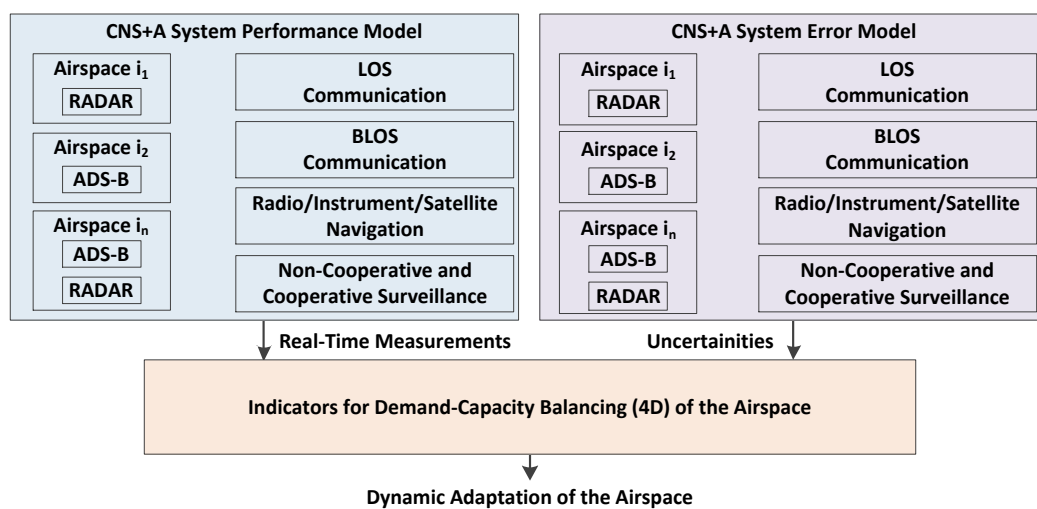


Figure 5.26. Role of CNS performance and error models.

The divergence between the performance and error models are assessed and translated into metrics in time. Integrity is translated into time (timeframe to violation) and serves as an indicator for dynamic adaptation of airspace based on CNS system performance. Capacity changes in both space and time are dependent on the performance of CNS systems. Furthermore, in order to fulfil safety requirements for SA&CA system certification, integrity monitoring and augmentation algorithms will be implemented encompassing the entire CNS sensors/systems chain and the associated navigation and tracking loops.

## 5.8 Avoidance Trajectory Optimisation

In the context of conflict identification and resolution, trajectory optimization is characterised by the identification of the most suitable 3D/4D avoidance trajectory from the time of detection to the point where the aircraft re-joins the nominal trajectory, based on dynamics/airspace constraints, user preferences, intruder trajectory, as well as meteorological and traffic conditions. Hence, the adoption of computational algorithms required for trajectory optimisation in achieving SAA represents a substantial evolution from the conventional safe-steering methodologies adopted in current systems. Advanced multi-model and multi-objective 3D/4D trajectory optimisation algorithms are used in novel ground-based and airborne CNS+A systems as described in Chapter 3. Most computationally efficient trajectory optimisation algorithms adopted in the aerospace domain belong to the family of direct methods. These solution methods involve the transcription of the infinite-dimensional problem in a finite-dimensional Non-Linear Programming (NLP) problem, hence following the approach summarised as "discretise then optimise". Safety-critical applications of trajectory optimisation algorithms are actively investigated for airborne emergency decision support systems, also known as safety-nets. These safety-critical CNS+A applications impose real time requirements on the trajectory generation algorithm. Additionally, all generated trajectories must necessarily fulfil each and every set constraint, as the obstacle avoidance and the manoeuvring envelope are formulated as constraints. These requirements limit considerably the choice of solution methods and multi-objective optimality decision logics. In particular, a number of solution methods involve the intentional violation of constraints to promote convergence to optimality, such as the conventional implementation of collocation methods. Robust parallelised direct shooting solution methods with a posteriori decision logics were implemented for the generation of safe obstacle avoidance trajectories as part of the research on laser obstacle avoidance for manned and unmanned aircraft [20 - 23]. Direct shooting

methods, involving the transcription into finite-dimensional NLP problem, can be either performed by introducing a control parameterisation based on arbitrarily chosen analytical functions, as in transcription methods, or by adopting a generalised piecewise approximation of both control and state variables based on a polynomial sequence of arbitrary degree, as in collocation methods. In both cases the transcribed dynamical system is integrated along the time interval  $[t_0; t_f]$ . The search of the optimal set of discretisation parameters is formulated as a NLP problem, which is solved computationally by exploiting efficient numerical NLP algorithms. In direct transcription methods, a basis of known linearly independent functions  $q_k(t)$  with unknown coefficients  $a_k$  is adopted as the parameterisation in the general form:

$$z(t) = \sum_{k=1}^N a_k q_k(t) \quad (5.75)$$

In direct shooting and multiple direct shooting, the parameterisation is performed on the controls  $u(t)$  only, and the dynamic constraints are integrated with traditional numerical methods such as the Runge-Kutta family, while the Lagrange term in the cost function is approximated by a quadrature approximation.

In multiple shooting, the analysed time interval is partitioned into  $n_i + 1$  subintervals. The direct shooting method is then applied to each subinterval. Parallel implementations of direct shooting involve the simultaneous integration of a family of trajectories based on different control parametrisation profiles, taking advantage of increasingly common multi-thread/multi-core hardware architectures. The optimal solution is determined a posteriori, both in the case of single objective and multi objective implementations. The following set of differential algebraic equations for the aircraft dynamics are adopted:

$$\begin{cases} \dot{v} = \frac{g}{W} (T \cos \epsilon - D - W \sin \gamma) \\ \dot{\gamma} = \frac{g}{v W} \cdot [(T \sin \epsilon + L) \cos \mu - W \cos \gamma] \\ \dot{\chi} = \frac{g}{v W} \cdot \frac{(T \sin \epsilon + L) \sin \mu}{\cos \gamma} \\ \dot{\phi} = \frac{v \cos \gamma \sin \chi + v_w \phi}{R_E + z} \\ \dot{\lambda} = \frac{v \cos \gamma \cos \chi + v_w \lambda}{(R_E + z) \cos \phi} \\ \dot{z} = v \sin \gamma + v_{wz} \\ \dot{m} = -FF \end{cases} \quad (5.76)$$

The state vector consists of the following variables:  $v$  is longitudinal velocity (scalar) [m s<sup>-1</sup>];  $\gamma$  is flight path angle (scalar) [rad];  $\chi$  is track angle (scalar) [rad];  $\phi$  is geographic latitude [rad];  $\lambda$  is geographic longitude [rad];  $z$  is flight altitude [m];  $\epsilon$  is thrust angle of

attack [rad] and  $m$  is aircraft mass [kg]; and the variables forming the control vector are:  $T$  is thrust force [N];  $N$  is load factor [dimensionless] and  $\mu$  is bank angle [rad]. Other variables and parameters include:  $D$  is aerodynamic drag [N];  $v_w$  is wind velocity, in its three scalar components [ $\text{m s}^{-1}$ ];  $g$  is the gravitational acceleration [ $\text{m s}^{-2}$ ];  $R_E$  is radius of the Earth [m] and  $FF$  is fuel flow [ $\text{kg s}^{-1}$ ]. Adopting a multi-phase trajectory optimisation formulation, the selection of the optimal trajectory along the first phase (safe steering) is typically based on minimising a cost function of the form:

$$J = w_t \cdot t_{safe} + w_f \cdot m(t_f) - w_d \cdot D(t_f) - w_{id} \cdot \int D(t)dt \quad (5.77)$$

where  $D(t)$  is the slant distance of the host platform along the avoidance trajectory from the avoidance volume associated with the obstacle,  $t_{safe} = TTT + 2 AMT$  is the time at which the safe avoidance condition is successfully attained,  $TTT$  is the time-to-threat and  $AMT$  is the avoidance manoeuvre time,  $m(t)$  is the host platform's mass and  $\{w_t, w_d, w_{id}, w_f\}$  are the positive weightings attributed to time, distance, integral distance and fuel respectively. In time-critical avoidance applications (i.e., closing obstacles with high relative velocities) appropriate higher weightings are used for the time and distance cost elements.

In terms of achieving separation maintenance, considering sector/runway capacity model, the time of separation between manned/ unmanned aircraft is given by:

$$T_{i,j} = \max \left[ \frac{r+s_{i,j}}{v_j} - \frac{r}{v_i}, o_i \right] \text{ when } v_i > v_j \quad (5.78)$$

$$T_{i,j} = \max \left[ \frac{s_{i,j}}{v_j}, o_i \right] \text{ when } v_i \leq v_j \quad (5.79)$$

where  $T_{i,j}$  is the time of separation,  $v_i$  and  $v_j$  are the velocities of adjacent aircraft,  $s_{i,j}$  is the distance of separation,  $r$  is the required separation and  $o$  represents the order.

## 5.9 SA&CA Certification Framework

One of the fundamental limitations for certification authorities for SA&CA functions is the inability to evaluate whether the system performance achieves comparable or superior levels of collision detection and resolution to manned aircraft, along with separation maintenance upon replacing the on board pilot with a Ground Control Station (GCS) remote pilot. Appendix B provides a compilation of the certification standards, AMC, GM, and recommended practices for the three categories (two-pilot aircraft, single-pilot and UAS) encompassing the Operational (OP), Technical (TC), Safety (SAF), Human Factors (HF) as well as Test and Evaluation (TE) aspects [24].

The material was sourced from national/international organizations such as the International Civil Aviation Organization (ICAO), Federal Aviation Authority (FAA), European Aviation Safety Agency (EASA), Civil Aviation Authorities (CAA) from Australia, the UK and New Zealand, the US Department of Defence (DOD) and the Institute for Defense Analyses (IDA). References are also made to standards from Aeronautical Radio Incorporated (ARINC), American Society of the International Association for Testing and Materials (ASTM), Radio Technical Commission for Aeronautics (RTCA), Society of Automotive Engineers (SAE), and NATO Standardization Agreements (STANAGs) [25 - 28].

### **5.9.1 SA&CA Hardware and Software Selection in UAS**

This section provide The avionics hardware in small UAS is typically chosen to be in the PC/104 form factor or even a smaller configuration for achieving smaller size, ruggedness and modularity. The Size, Weight and Power (SWaP) requirements are carefully analysed for the hardware implementation. The Tailored Input/Output (TIO) software needs to be able to provide information exchange from/to ARINC-429, RS-232/422/485, USB and additional interfaces as required.

The hardware design needs to ensure a straightforward path to compliance with RTCA DO-254 and other safety assessment standards for certification. The detailed hardware requirements, design information and traceability matrix is provided during the system development process. The SA&CA system is envisaged to be integrated into the existing avionics compartment (within NG-FMS) so as to minimally impact the existing payload capacity of the host aircraft.

The navigation and tracking sensors are distributed between the avionics compartment and the airframe as appropriate (avoiding mechanical/electromechanical interferences and mitigating impacts on payload capacity). A number of sensor configurations are investigated during the SAA system development phase. As an example, the FAA Field-of-Regard (FOR) recommendations are illustrated in Figure 5.27 (a). Considering two non-cooperative sensors (visual camera and radar) for Collision Detection and Resolution (CD&R) tasks, the FOR obtained is depicted in Figure 5.27 (b).

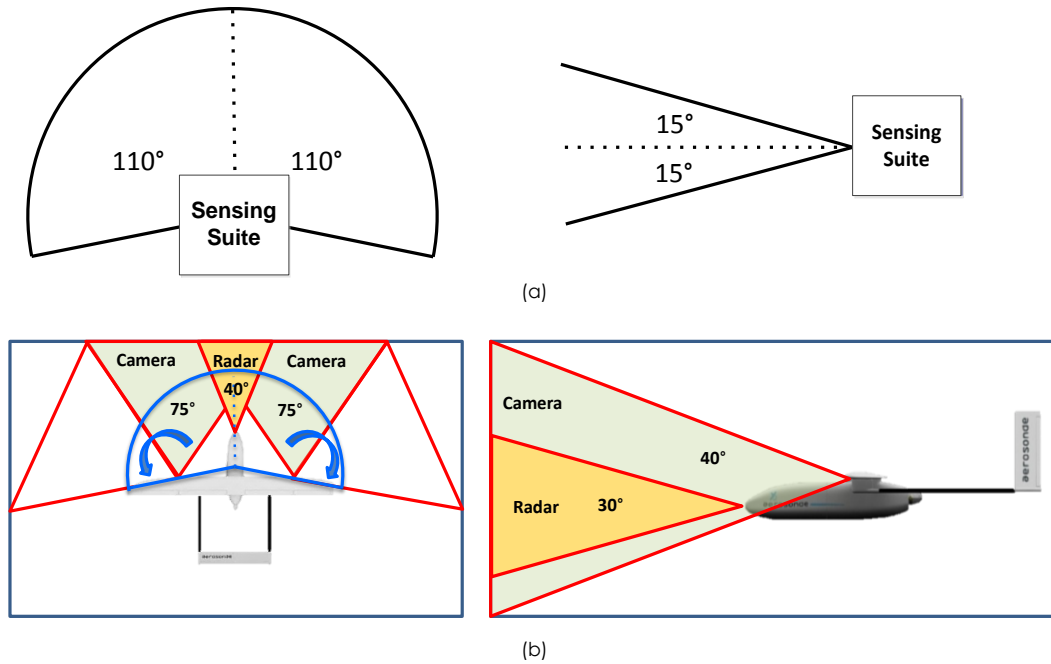


Figure 5.27. FAA FoR (a) and a possible sensors' installation (b).

This visual sensor equipped with a stabilised gimbal assembly provides an approximate FOV of 75° in azimuth and 20° in elevation. The fusion of optical sensors with other non-cooperatives sensors increases the angular accuracy. In this case, radar is employed for extracting range measurements and provides a FOV of 40° in azimuth and 15° in elevation. This sensor arrangement allows the GCS operator to select the azimuth orientation of the FOV among three possible directions: aligned with the platform heading (normal flight envelope) or 20° left or right with respect the platform heading.

The data fusion (software) techniques include a programmable core component and an Application Programming Interface (API) providing a set of commands, functions and protocols, catering to dedicated application functionalities.

The NG-FMS hardware and software interface is depicted in Figure 5.28. The applications will be partitioned according to their criticality levels. The system software needs to be programmed in the avionics mission computer (a multi-core processor) and should provide a straightforward path to compliance with RTCA DO-178C and other software certification standards.

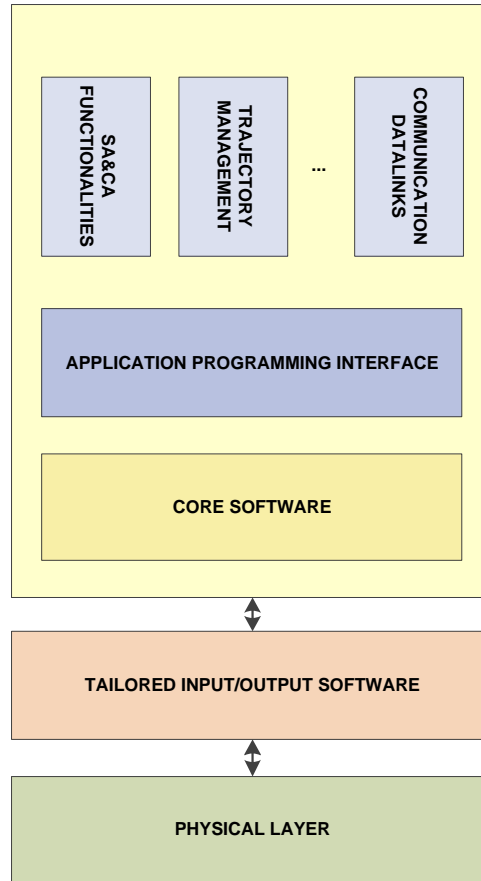


Figure 5.28. NG-FMS hardware and software interface.

### 5.9.2 Approach to Certification

The research on a certifiable SA&CA system is innovative in targeting successful certification by Civil Aviation Safety Authority (CASA), Federal Aviation Administration (FAA), Civil Aviation Authority (CAA), European Aviation Safety Agency (EASA) and other aviation safety certification organisations. The distinctive advantage that the proposed SAA system offers for achieving certification is the capability to determine the safe-to-fly UAS envelope based on the on board sensors and alternatively to identify the required sensors in order to achieve a certain predefined safety envelope. This two-way approach is represented in Figure 5.29.

In particular, considering the nominal flight envelopes of a host aircraft and the intruder as well as the on board sensors, the SA&CA software determines the attainable safety envelope. Conversely, based on a predefined (required) safety envelope and on the intruder dynamics, the SA&CA functionalities embedded in the NG-FMS support the identification of sensors that are required to be integrated onto the aircraft. As part of an

incremental approach targeting certification, extensive simulation along with ground and flight test activities need to be accomplished.

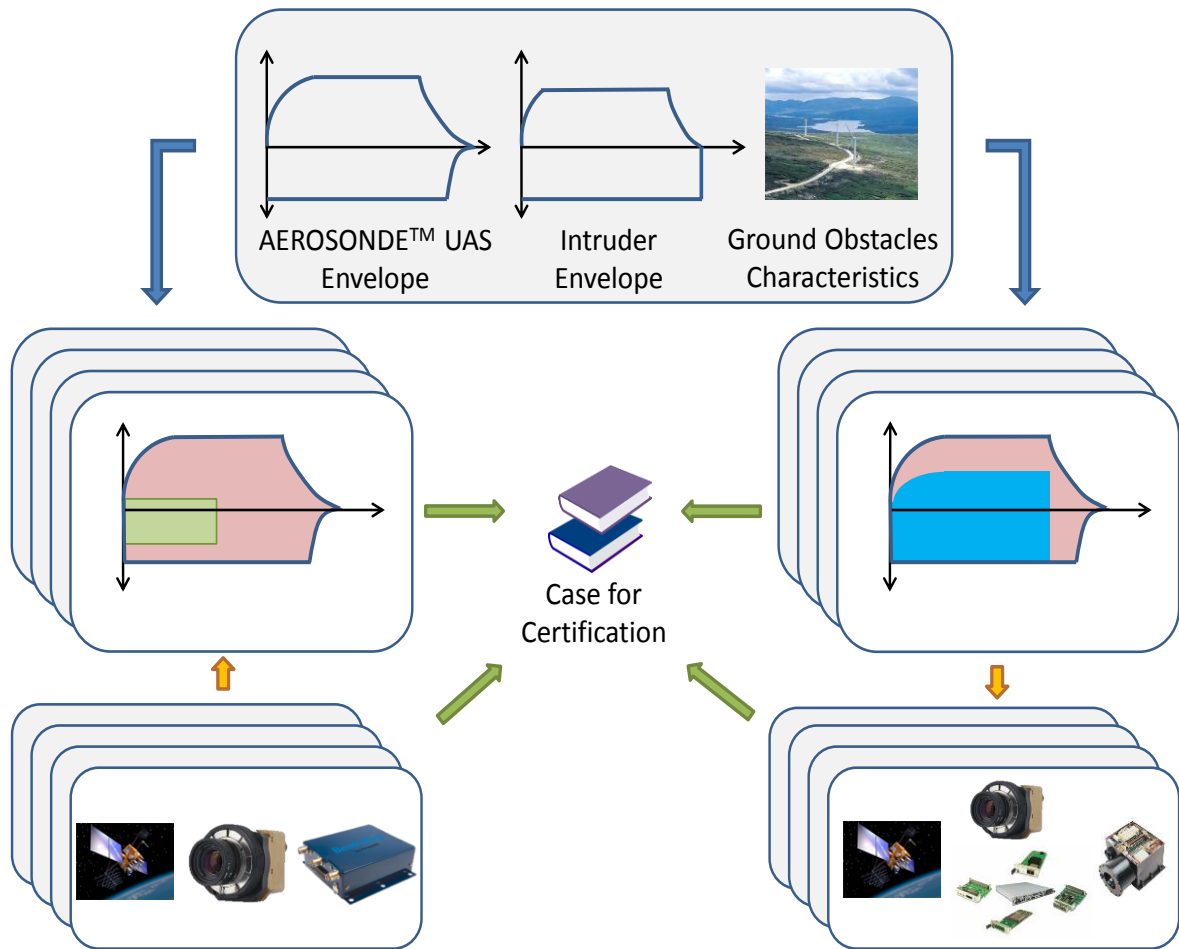


Figure 5.29. Two-way approach to certification.

The following elements are identified to be part of the SA&CA system development:

- Human factor considerations and Human Factors Engineering (HFE) elements for the design of the SA&CA specific elements in the GCS remote pilot HMI<sup>2</sup>;
- Inclusion of different non-cooperative sensor and cooperative systems equipment in the test bed system architecture;
- System hardware and software assurance;
- Test campaigns according to airspace characterisations;
- Safety cases for operations in specific airspace category;
- Low altitude flight testing in the UAS Traffic Management (UTM) context.



## 5.10 Conclusions

The algorithms employed for determining the performance of sensors/systems and determining the avoidance trajectory in the unified approach to cooperative and non-cooperative SA&CA for manned and unmanned aircraft were described. Based on the identified state-of-the-art SA&CA technologies, a BDL driven decision tree test bed system reference architecture is presented. Implementations involving Boolean logics are generally hard wired and cannot be reconfigured and this limits the scope of unified framework in terms of automatic decision making capability. An architecture for selecting the sensors/systems was defined based on their performance achieved at any instant of time. Covariance matrices were used for estimating sensor and system performances. After identifying a RoC, if the original trajectory of the host platform intersects the calculated avoidance volume, a caution integrity flag is issued. The algorithms used for avoidance trajectories (in near real-time) were also presented. The need for a certifiable SA&CA system and the implementation design drivers were also presented. The pathway to certification was described, with the unified approach emerging as an innovative method in targeting successful certification by CASA, FAA, CAA and other aviation regulatory bodies. By applying the unified approach and by considering the nominal flight envelopes of the host UAS and other traffic as well as the on board sensors, the approach determines the attainable safety envelope. Conversely, based on a predefined (required) safety envelope and dynamics of other traffic, the software is capable of identifying the sensors that are required to be integrated in the aircraft.

## 5.11 References

1. M.J. Kochenderfer, J.E. Holland and P. James, "Chryssanthacopoulos: Next Generation Airborne Collision Avoidance System", Lincoln Laboratory Journal, Vol. 19, issue 1, pp. 17– 33, 2012.
2. J.B. Jeannin, K. Ghorbal, Y. Kouskoulas, R. Gardner, A. Schmidt, E. Zawadzki and A. Platzer, "A Formally Verified Hybrid System for the Next-Generation Airborne Collision Avoidance System", International Conference on Tools and Algorithms for the Construction and Analysis of Systems, TACAS 2015: Tools and Algorithms for the Construction and Analysis of Systems, pp 21-36, Springer - Berlin Heidelberg, 2015.
3. C. Muñoz, A. Narkawicz, J. Chamberlain, M. Consiglio and J. Upchurch, "A family of Well-Clear Boundary Models for the Integration of UAS in the NAS", Proceedings of the

14<sup>th</sup> AIAA Aviation Technology, Integration, and Operations (ATIO) Conference, AIAA-2014-2412, Georgia, Atlanta, USA, 2014.

4. R. Sabatini, T. Moore, and C. Hill, "A New Avionics Based GNSS Integrity Augmentation System: Part 1 – Fundamentals," *Journal of Navigation*, vol. 66, no. 3, pp. 363-383, May 2013. DOI: [10.1017/S0373463313000027](https://doi.org/10.1017/S0373463313000027)
5. R. Sabatini, T. Moore, and C. Hill, "A New Avionics Based GNSS Integrity Augmentation System: Part 2 – Integrity Flags," *Journal of Navigation*, vol. 66, no. 4, pp. 511-522, June 2013. DOI: [10.1017/S0373463313000143](https://doi.org/10.1017/S0373463313000143)
6. R. Sabatini, T. Moore, C. Hill and S. Ramasamy, "Assessing Avionics-Based GNSS Integrity Augmentation Performance in UAS Mission- and Safety-Critical Tasks", *Proceedings of International Conference on Unmanned Aircraft Systems (ICUAS 2015)*, Denver, CO, USA, 2015. DOI: [10.1109/ICUAS.2015.7152347](https://doi.org/10.1109/ICUAS.2015.7152347)
7. P.J. Górski, A. Czaplicka and J.A. Hołyst, "Coevolution of Information Processing and Topology in Hierarchical Adaptive Random Boolean Networks", *The European Physical Journal B*, Vol. 89, no. 2, pp.1-9, 2016.
8. R.N. Kashi, M. D'Souza, S.K. Baghel and N. Kulkarni, "Formal Verification of Avionics Self Adaptive Software: A case study", *Proceedings of the 9<sup>th</sup> ACM India Software Engineering Conference*, pp. 163-169, 2016.
9. A. Thayse and M. Davio, "Boolean Differential Calculus and its Application to Switching Theory", *IEEE Transactions on Computers*, Vol. 22, Issue 4, pp.409-420, 1973.
10. J.L. Farrell, "Navigation and Tracking", Chapter 14, eds. C. Spitzer, U. Ferrell and T. Ferrell, *Digital Avionics Handbook*, Third Edition, CRC Press, 2014.
11. L.R. Sahawneh, "Airborne Collision Detection and Avoidance for Small UAS Sense and Avoid Systems", *PhD Theses*, Brigham Young University, 2016.
12. RTCA, "Minimum Operational Performance Standards (MOPS) for Aircraft Surveillance Applications (ASA) System", DO-317B, Radio Technical Commission for Aeronautics, Washington DC, USA, 2011.
13. RTCA, "Safety, Performance and Interoperability Requirements Document for Enhanced Air Traffic Services in Radar-Controlled Areas Using ADS-B Surveillance (ADS-B-RAD)", DO-318, Radio Technical Commission for Aeronautics, Washington DC, USA, 2009.
14. S. Ramasamy, R. Sabatini and A. Gardi, "LIDAR Obstacle Warning and Avoidance System for Unmanned Aerial Vehicle Sense-and-Avoid", *Aerospace Science and Technology*, Elsevier, vol. 55, pp. 344–358, 2016. DOI: [10.1016/j.ast.2016.05.020](https://doi.org/10.1016/j.ast.2016.05.020)

15. J.N. Hallock, G.C. Greene, J.A. Tittsworth, P.A. Strande and F.Y. Wang, "Use of Simple Models to Determine Wake Vortex Categories for New Aircraft", 7<sup>th</sup> AIAA Atmospheric and Space Environments Conference, AIAA AVIATION Forum, AIAA 2015-3172, 2015.
16. L. DeVries and D.A. Paley, "Wake Estimation and Optimal Control for Autonomous Aircraft in Formation Flight", Proceedinsg of the AIAA Guidance, Navigation, and Control (GNC) Conference, (AIAA 2013-4705), Boston, USA, 2015.
17. A. He, P. Tian, Z.C. Zheng, H. Chao and Y. Gu, "A Study on UAS Wake Turbulence Encounter Using Coupled Aerodynamics and Flight Dynamics Simulation", 8th AIAA Atmospheric and Space Environments Conference, AIAA AVIATION Forum, pp. 2016-3439, 2016. DOI: 10.2514/6.2016-3439
18. J.M. Alliot and N. Durand, "A Mathematical Analysis of the Influence of Wind Uncertainty on MTCD Efficiency", The controller, Meteorology and ATC (IFATCA), pp. 17-19, 2011.
19. P. Angelov, "Sense and Avoid in UAS: Research and Applications," John Wiley & Sons, 2012.
20. A. Gardi, R. Sabatini and S. Ramasamy, "Multi-objective Optimisation of Aircraft Flight Trajectories in the ATM and Avionics Context", Progress in Aerospace Sciences, vol. 83, pp. 1-36, 2016.
21. O. Von Stryk and R. Bulirsch, "Direct and Indirect Methods for Trajectory Optimization", Annals of Operations Research, vol. 37, pp. 357-373, 1992.
22. J. T. Betts, "Survey of Numerical Methods for Trajectory Optimization", Journal of Guidance, Control and Dynamics, vol. 21, pp. 193-207, 1998.
23. J. Z. Ben-Asher, "Optimal Control Theory with Aerospace Applications", Education Series, American Institute of Aeronautics and Astronautics (AIAA), Reston, VA, USA, 2010.
24. Y. Lim, B. Vincent, S. Ramasamy, J. Liu and R. Sabatini, "Commercial Airliner Single Pilot Operations: System Design Drivers and Pathways to Certification", IEEE Aerospace and Electronic Systems Magazine, 2017.
25. Federal Aviation Administration, "Integration of Civil Unmanned Aircraft Systems (UAS) in the National Airspace System (NAS) Roadmap", First edition, Washington DC, USA, 2013.
26. D.L. Edwards, "Flight Standardization Board (FSB) Report: EMBRAER S.A. EMB-500", Federal Aviation Administration (FAA), Missouri, USA, 2014.
27. Civil Aviation Authority, "CAP 722 Unmanned Aircraft System Operations in UK Airspace – Guidance", UK CAA, Norwich, UK, 2012.

28. ICAO, "Annexes 1 to 18", International Civil Aviation Organization, Montreal, Canada, 2012.
29. EASA, "Acceptable Means of Compliance (AMC) and Guidance Material (GM) to Part-CAT", European Aviation Safety Agency, Cologne, Germany, 2013.

## CHAPTER 6

# GROUND OBSTACLES SA&CA

## CASE STUDY

*"Invention consists in avoiding the constructing of useless contraptions and in constructing the useful combinations which are in infinite minority". - Henri Poincare*

### 6.1 Introduction

Based on the analytical models described in Chapter 4, data processing techniques allow the real-time transformation of navigation and tracking errors affecting the state measurements to unified range and bearing uncertainty descriptors. The investigation of this chapter focusses on validating the SA&CA algorithms for ground targets. An introduction to the available ground obstacle detection and avoidance technologies is presented, followed by a detailed case study on the LIDAR Obstacle Warning and Avoidance System (LOWAS) as one of the possible implementation technologies for the unified approach to SA&CA.

### 6.2 Ground Obstacle Detection and Warning Systems

The demand for reliable ground obstacle warning and avoidance capabilities to ensure safe low-level flight operations has led to the development of compact collision avoidance systems for a variety of fixed and rotary wing aircraft. Capabilities to prevent Controlled Flight Into Terrain (CFIT) are primarily provided by the flight crew and the ATM system ensuring safe operation of the aircraft. Safety is ensured by using primary instrumentation onboard the aircraft, carefully adhering to the ATCo instructions and being aware of the overall situation [1]. Secondary on-board guard against CFIT is provided by employing terrain proximity detection and warning devices commonly known as Terrain Awareness and Warning Systems (TAWS).

TAWS are developed to provide warnings for possible conflicts with terrain by taking into account inputs such as aircraft states, glideslope and databases (terrain, obstacles and airport). TAWS are generally classified into three types namely:

- Class-A TAWS: This class of equipment is required for turbine-powered airplanes operated under part 121 (airline) and part 135 (charter) of 10 or more passenger seats [2]. The system includes a minimum of five basic functions including forward looking terrain avoidance, premature descent alert, attention alerts, terrain awareness display and indications of imminent contact with the ground.
- TAWS Class-B: This class of equipment is required for turbine-powered airplanes operated under part 91 with six or more passenger seats and for turbine-powered airplanes operated under part 135 with six to nine passenger seats [2]. The system includes a minimum of four basic functions including forward looking terrain avoidance, premature descent alert, attention alerts and indications of imminent contact with the ground.
- TAWS Class C: This class of equipment is targeted to be used in small general aviation airplanes that are not required to install Class B equipment, which includes minimum operational performance standards intended for piston-powered and turbine-powered airplanes.

Statistics show that there is a significant drop of accidents after the introduction of radio altimeter and Ground Proximity Warning Systems (GPWS) in commercial turbo jet aircraft [1]. GPWS, also termed as Ground Collision Avoidance System (GCAS) in the military context, uses on-board sensors for estimating radio altitude, air data and attitude to assess the aircraft's current state, compares it to known hazardous situations and generates timely and usable visual and aural warnings. GPWS produces warnings in five modes/states of undesirable aircraft behaviour including [1]:

- Mode 1 - Excessive barometric sink rate with respect to terrain clearance;
- Mode 2 - Excessive rate of terrain closure with respect to terrain clearance;
- Mode 3 - Excessive altitude loss after take-off;
- Mode 4 - Unsafe terrain clearance with respect to phase of flight, airspeed, and/or aircraft configuration;
- Mode 5 - Excessive descent below the Instrument Landing System (ILS) glideslope angle.

In GPWS, a level flight towards terrain can only be implied by detecting rising terrain under the aircraft. In case of flight towards steeply rising terrain, such an implementation

may not allow enough time for corrective actions by the flight crew [3]. The Predictive GCAS (PGCAS) and Enhanced GPWS (EGPWS) were developed later to incorporate current flight path status, aircraft performance and Digital Terrain Elevation Data (DTED). GPWS and EGPWS technologies were mandated for implementation following accidents at Dulles, US in 1974 and Cali, Columbia in 1995 respectively. In particular, the EGPWS was developed to address the shortcomings of GPWS including late/no warnings and improper pilot response. A database of known runway locations, a DTED and a computer for calculating a virtual terrain clearance floor are included in the EGPWS. Seven different modes are supported by the EGPWS, with modes 1 through 4 the original GPWS modes. The recent additions are the enhanced modes supported by terrain proximity display, terrain ahead detection, and terrain clearance floor features. The modes, respective causes and warnings issued by the EGPWS are provided in Table 6.1.

Table 6.1. EGPWS modes, causes and warnings.

MODE and CAUSE		WARNING	
Mode 1: Excessive descent rate and severe descent rate	When the Rate of Descent (ROD) increases rapidly	"sink rate, sink rate"	"whoop, whoop, pull up, pull up"
Mode 2: Excessive terrain closure rate	When closure rate with the terrain increases	"terrain, terrain"	"whoop, whoop, pull up, pull up"
Mode 3: Altitude loss after take-off or go-around	Loss of altitude after take-off or go-around phase	"don't sink"	
Mode 4: Unsafe terrain clearance when not in the landing configuration	Too low condition	"too low, terrain" "too low, gear" too low, flaps"	
Mode 5: Excessive deviation below an ILS glideslope	Too low condition	"Glideslope"	
Mode 6: Bank angle / altitude callouts	Excessively steep bank angles	"Bank Angle"	
Mode 7: Wind shear callouts	Wind shear detection	"Wind Shear"	

In military aircraft, Automatic Ground Collision Avoidance System (Auto GCAS) is being used after the development of this technology for nearly three decades. Auto GCAS has been successfully integrated into a number of military platforms including the F-16.

Auto GCAS automatically assumes control of an aircraft when an imminent collision is detected (with the ground) and returns control back to the flight crew when the collision is averted. State-of-the-art Light Detection and Ranging (LIDAR) technology employing eye-safe laser sources, advanced electro-optics and mechanical beam-steering components delivers the highest angular resolution and accuracy performance in a wide range of operational conditions. LIDAR Obstacle Warning and Avoidance System (LOWAS) is thus becoming one of the most mature and successful solutions with several potential applications to manned and unmanned aircraft. The remaining sections of this chapter address specifically the employment of LOWAS as one of the possible implementation for achieving automated SA&CA of ground obstacles.

### **6.3 UAS Obstacle Warning and Avoidance System**

Small-to-medium size UAS are particularly targeted for LOWAS applications since they are very frequently operated in proximity of the ground and the possibility of a collision is further aggravated by the very limited see-and-avoid capabilities of the remote pilot.

A number of mission-and-safety critical tasks involve low-level flight activities beyond the relatively safe aerodrome perimeter. Low level and terrain-following operations are often challenged by a variety of natural and man-made obstacles. The significant number of obstacle strike accidents recorded is a major concern both for aircraft operators and for people on the ground [4, 5]. Reduced atmospheric visibility due to adverse weather conditions is frequently a contributing factor in such accidents, but the difficulty in identification of small-size obstacles such as wires has led to accidents and incidents even in clear sky conditions. Significant development activities are specifically addressing the integration of obstacle detection, warning and avoidance systems for granting separation maintenance and collision avoidance capabilities [6 - 12].

Table 6.2 compares a number of sensor technologies for Obstacle Warning System (OWS) applications in small-to-medium size UAVs. Unfortunately, state-of-the-art RADAR is not capable of detecting small natural and man-made obstacles such as trees, power line cables, and poles.



Table 6.2. Obstacle detection technologies.

REQUIREMENT	MAGNETIC	THERMAL	MILLIMETRIC WAVE RADAR	LIDAR
Wire detection	Only energized wires	Only energized wires	All wires preferably perpendicular to flight trajectory	All wires
Detection range	Short	Short	As required	As required
Coverage Area	Small	As required	As required	As required
Resolution and accuracy (obstacle type, position and distance)	Insufficient	Good for position and type, no ranging capabilities	Medium	Very high
All-weather performance in low-level flight	Good	Poor	Very good	Good*
False alarm rate	High	Low	Very low	Very low
Base technology status	Mature	Mature	State-of-the-art	State-of-the-art
* Laser energy is significantly attenuated by rain and blocked by clouds and fog.				

The outstanding angular resolution and accuracy characteristics of Light Detection and Ranging (LIDAR), as well as its good detection performance in a wide range of incidence angles and weather conditions provide an ideal solution for obstacle detection and avoidance [3]. Different types of lasers including Nd:YAG, semiconductor lasers such as GaAs and GaAlAs lasers have been employed for OWS [13]. Due to eye-safety and adverse weather (fog) propagation concerns, further development with 1.54  $\mu\text{m}$  (frequency-shifted Nd:YAG and Er:glass) solid state lasers and various semiconductor lasers has been substantially reduced, in favour of CO<sub>2</sub> lasers [14, 15].

## 6.4 Operational Requirements

The operational requirements for a reliable and effective OWS include:

- Capability to detect all types of hazardous obstacles, including topographic features, vegetation, buildings, poles/masts, towers, cables and transmission lines;
- Operability in all-time and all-weather conditions, including low-light and darkness;

- High minimum detection range, adequate for the platform airspeed performance;
- Wide Field of View (FoV), adequate for the manoeuvring envelope limits of the platform;
- High range and bearing resolutions;
- Accurate and good probability of detection, since no real obstacle threat shall remain undetected;
- Very low false alarm rate, to prevent spurious warnings that would increase the remote pilot's workload and prompt unnecessary avoidance manoeuvres, which are potentially disruptive to the safety of the mission;
- Satisfactory technological readiness levels.

## 6.5 System Description

The LOWAS is designed to detect obstacles placed in or nearby the aircraft trajectory, classify/prioritise the detected obstacles, and provide obstacle visual and aural warnings and information to the crew. The key components of the LOWAS are the Sensor Head Unit (SHU), the Processing Unit (PU), the Control Panel (CP) and the Display Unit (DU). The LIDAR beam scans periodically the area around the host platform's longitudinal axis within a FoV of  $40^\circ$  in azimuth and  $30^\circ$  in elevation (Figure 6.1).

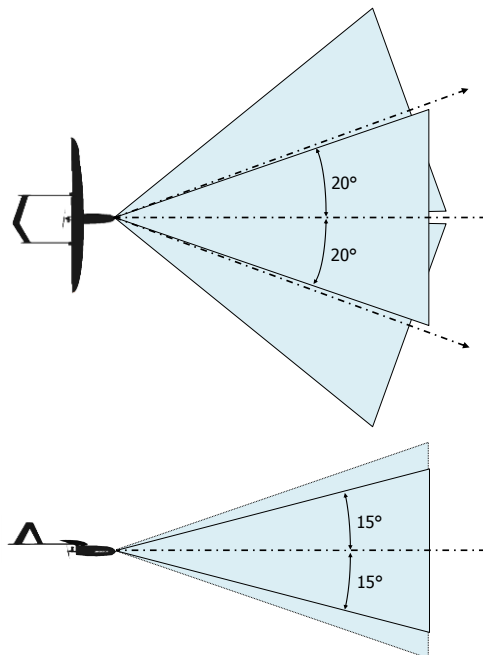


Figure 6.1. LOWAS FOV.

In order to enhance coverage during turning manoeuvres at high yawing rates, the remote pilot may vary the azimuth orientation of the LOWAS FoV by  $20^\circ$  left/right with respect to the vertical axis. As conceptually depicted in Figure 6.2, during every complete FoV scan (4 Hz refresh frequency), the LIDAR beam generates a number of elliptical scan patterns across the FoV.

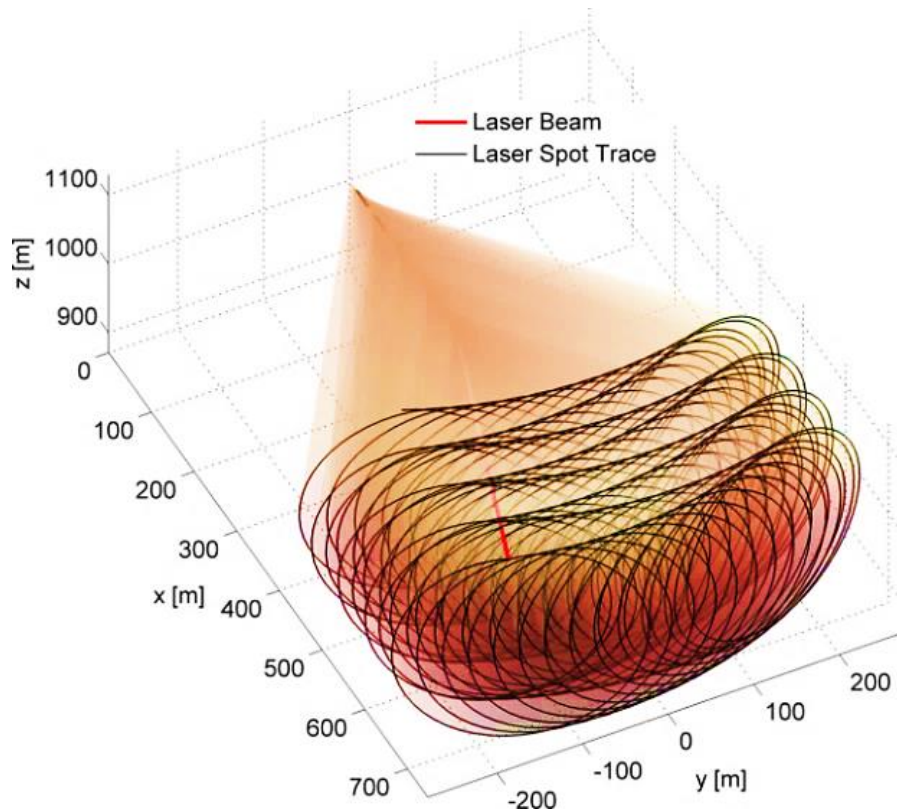


Figure 6.2. LOWAS scan pattern for a slowly advancing platform.

This scanning pattern is well suited to detect the most dangerous obstacles like wires as they produce several regularly spaced vertical lines. The electro-mechanical device that is adopted to produce the described scanning pattern is a swashing mirror. The architecture LOWAS tailored for UAS is shown in Figure 6.3 [16]. LOWAS display unit and warning generator are located in the cockpit of a manned aircraft, while in the case of an UAV, the interactions with the remote pilot involves LoS and BLoS communication links. Both LOS and BLOS communication links are necessary for providing voice and data link communications with the GCS and with the Next Generation Air Traffic Management (NG-ATM) system. Voice communications might include Automatic Voice Recognition (AVR) as well as Synthetic Voice Reply (SVR) systems [17]. Additionally, telemetry data need to be exchanged between the UAS and the GCS for aircraft control as well as for downlinking of both flight parameters and obstacle information (enabling vehicle tracking, mission control and mission profile updates).

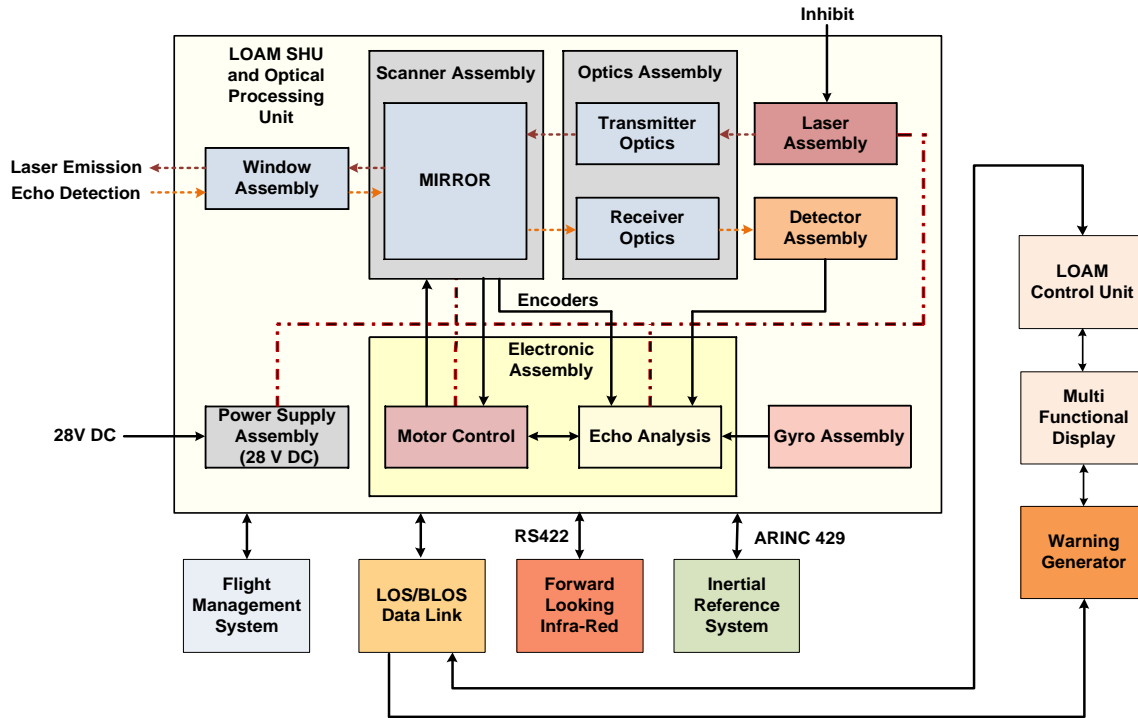


Figure 6.3. LOWAS avionics integration architecture for UAS.

## 6.6 Obstacle Detection and Classification Software

The signal pre-processing steps involve an analogue optical-electrical conversion of the echo signal by an Avalanche Photodiode (APD), a signal pre-amplification by an Automatic Gain Control (AGC) and a comparison with an adjustable threshold in order to fine-tune sensitivity on the basis of the expected return signal power in relation with the time elapsed from the LIDAR pulse emission. The threshold level may also be tuned to take into account the background conditions. These features reduce the probability of false echo detection due to atmospheric back-scattering near the laser beam output and optimise the system sensitivity in all weather conditions. Subsequently, digital signal processing is performed in order to validate positive echo detections, determine the position of the detected obstacles and their geometrical characteristics. For this purpose, the LOWAS software architecture is organised in two sequential stages: Low Level Processing (LLP) and High Level Processing (HLP). Figure 6.4 represents the signal processing software architecture.

The LLP is performed on the individual echoes in order to determine range, angular coordinates and characteristics of the obstacle portion generating them. The tracking data processing provides the tracks of intruders after pre-processing (excluding false alarms, etc.).

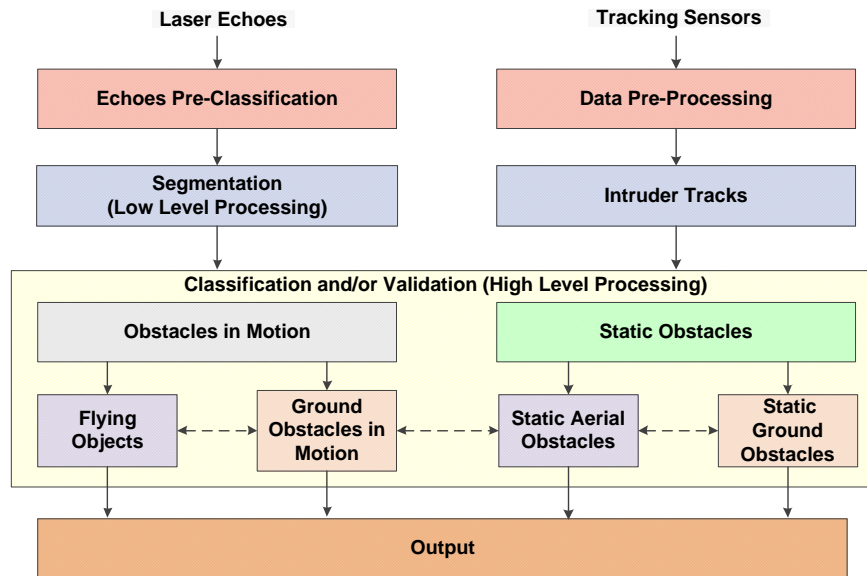


Figure 6.4. LOWAS signal processing software architecture.

The HLP analyses the LLP output to identify groups of echoes, in order to reconstruct the shape and type of the obstacle. The LOWAS is capable of automatically classifying obstacles according to the following classes:

- Wire: all thin obstacles like wires and cables (e.g., telecommunication/power lines and cableways);
- Tree: vertical obstacles of reduced frontal dimensions (e.g., trees, poles and pylons);
- Structure: extended obstacles (e.g., bridges, buildings and hills).

The single echoes are processed as soon as they are acquired. The wire LLP algorithm processes only the echoes whose magnitude is weaker than pre-defined thresholds. Subsequently, the wire HLP algorithm is employed on the subset of acquired echoes in the current frame. Clusters are merged into a single obstacle by means of iterative image segmentation, specifically implemented to identify echoes characterised by a uniform range. A statistical algorithm subsequently validates the merged echoes by verifying if the obstacle is generated by real aligned echoes or by noise data. The processing algorithms for extended obstacles (trees and structures) are also divided in two different phases: echo analysis and segmentation. The echoes already classified as extended objects are processed by a dedicated validation algorithm, since many of these are not generated by obstacles (like, for example, the ground). A well-defined number of echoes, acquired in a short time range, have some geometrical characteristics. The segmentation algorithm is responsible of detecting, merging and

validating the clusters of echoes. The integration of high-resolution databases of fixed obstacles (power lines, buildings, etc.), when flying over a well characterised operational area into the LOWAS algorithms, can support reduction of the overall processing time and provide an accurate estimation of their position. The LOWAS performs automatic prioritisation of the detected obstacles based on the risk represented according to the relevant range, and provides timely visual and aural warnings to the flight crew, including information about the detected obstacles. The dedicated signal processing algorithms grant reliable detection performance, independent from the platform motion, allowing a reconstruction of the obstacle shape without using navigation data (stand-alone integration) in slow-moving platforms characterised by a typical flight envelope (rotorcraft and fixed-wing aircraft). The LOWAS can also be integrated with the onboard navigation and guidance system to grant equally efficient reliable detection in extreme flight envelopes of high-dynamics platforms [18, 19].

## 6.7 Mathematical Algorithms

The microwave radar range equation also applies to laser systems and the power received by the detector is given by [4]:

$$P_R = \frac{P_T G_T}{4\pi R^2} \cdot \frac{\sigma}{4\pi R^2} \cdot \frac{\pi D^2}{4} \cdot \tau_{atm} \cdot \tau_{sys} \quad (6.1)$$

where  $P_T$  is the transmitter power,  $G_T$  is the transmitter antenna gain,  $R$  is the range [m],  $D$  is the aperture diameter [m],  $\tau_{atm}$  is the atmospheric transmittance and  $\tau_{sys}$  is the system transmission factor. With laser systems, the transmitter antenna gain is substituted by the aperture gain, expressed by the ratio of the steradian solid angle of the transmitter beam width  $\alpha^2$  to that of the solid angle of a sphere as given by:

$$G_T = \frac{4\pi}{\alpha^2} \quad (6.2)$$

In the far field, the transmitter beam width can also be expressed in terms of aperture illumination constant,  $K_a$  as:

$$\alpha = K_a \frac{\lambda}{D} \quad (6.3)$$

Substituting for  $G_T$  and  $\alpha$  in equation (6.1), we obtain:

$$P_R = \frac{P_T}{16R^4} \cdot \frac{\sigma}{\lambda^2} \cdot \frac{D^4}{K_a^2} \cdot \tau_{atm} \cdot \tau_{sys} \quad (6.4)$$

An aperture operating at the eye-safe wavelengths has a far-field distance of approximately 20 km [5]. As a result, it is not unusual to operate in the near-field of the

optical systems and hence the range equation is modified to account for near-field operations. This near-field effect modifies the beam width such that:

$$\alpha = \sqrt{\left(\frac{K_a D}{R}\right)^2 + \left(\frac{K_a \lambda}{D}\right)^2} \quad (6.5)$$

The range equation is dependent on the target area. The effective target cross-section is given by:

$$\sigma = \frac{4\pi}{\Omega} \rho dA \quad (6.6)$$

where  $\Omega$  is the scattering solid angle of target [sr],  $\rho$  is the target reflectivity and  $dA$  is the target area. Substituting  $\Omega$  with the value associated with the standard scattering diffuse target (Lambertian target) having a solid angle of  $\pi$  steradians, we obtain:

$$\sigma = 4 \rho_T dA \quad (6.7)$$

The cross-sectional area of a laser beam transmitted by a circular aperture from a distance is given by:

$$dA = \frac{\pi R^2}{4} \theta^2 \quad (6.8)$$

Depending on the target-laser spot relative dimensions we may distinguish three different types of targets: extended, point and linear targets. In case of a point target (Fig. 6.5-a), the target cross-section is given by:

$$\sigma_{pt} = 4 \rho_T dA \quad (6.9)$$

Hence the range equation is expressed as:

$$P_R = \frac{P_T}{4R^2} \cdot \frac{dA \rho_T}{R^2} \cdot \frac{D^4}{K_a^2 \lambda^2} \cdot \tau_{atm} \cdot \tau_{sys} \quad (6.10)$$

In case of a linear target such as a wire (Fig. 6.5-b), it can have a length larger than the illuminated area but a smaller width ( $d$ ). The target cross-section is given by:

$$\sigma_{wire} = 4 \rho_{wire} R \theta d \quad (6.11)$$

Replacing with the beam width provided in equation (6.3), the range equation is expressed as:

$$P_R = \frac{P_T}{4R^2} \cdot \frac{d \rho_{wire}}{R} \cdot \frac{D^3}{K_a \lambda} \cdot \tau_{atm} \cdot \tau_{sys} \quad (6.12)$$

In case of an extended target such as a wire (Fig. 6.5-c), all incident radiation is involved in the reflection process. Thus, for an extended Lambertian target we have a target cross-section given by:

$$\sigma_{ext} = \pi \rho R^2 \theta^2 \quad (6.13)$$

Therefore the range equation is expressed as:

$$P_R = \frac{\pi P_T}{4R} \cdot \frac{D^2 \rho}{4R} \cdot \tau_{atm} \cdot \tau_{sys} \quad (6.14)$$

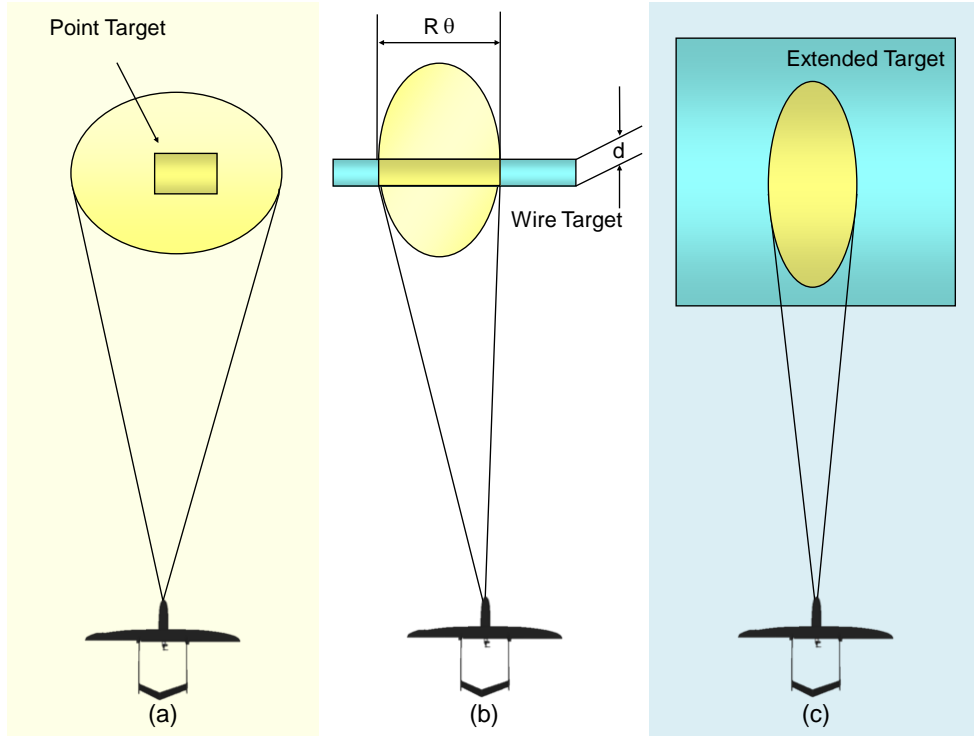


Figure 6.5. Target sections.

## 6.8 Formats and Functions

The formats and functions are made adaptive and are a combination of the following:

- Safety Line: selected when the airspeed is low;
- Wires and pylon (vertical, linear obstacles e.g. poles and bare trees): selected when the represented wire and pylon obstacles are detected within the OWS detection range;
- All obstacles: selected when the represented synthetic obstacles are those detected within the OWS detection range and
- OWS 3D (colour-coded LIDAR image): selected especially when a superimposition of Forward Looking Infrared (FLIR) images is required for low-light and night time operations.



In addition to the formats and functions above, a combination of symbols are considered for enhancing the representation of detected obstacles and to complement the decision making process:

- Distance from obstacle;
- Isolated obstacles (e.g. buildings, groups of trees, etc.);
- Integrity flags (cautions and warnings);
- Flight vector;
- Evade advice cue;
- Plan Position Indicator (PPI) and
- Terrain map.

Three general levels of alerts are defined for the LOWAS (warning, caution and advisory). These alerts are provided to the pilot through aural and visual outputs as shown in Table 6.3. Warning cues are provided as direct voice outputs, and presented in a warning panel, a Helmet-Mounted Sight/Display (HM S/D) and a Multi-Function Display (MFD). Cautions are supplied as tones and indicated in the warning panel, HM S/D and MFD while advisory alerts are presented only in the MFD.

Table 6.3. LOWAS alerts.

	<b>Tone</b>	<b>Direct Voice O/P</b>	<b>Warning Panel</b>	<b>HM S/D</b>	<b>MFD</b>
Warning cue		✓	✓	✓	✓
Caution	✓	-	✓	✓	✓
Advisory	-	-	-	-	✓

The warning cues are triggered when a detected obstacle is within the selected range or 10" from the impact point. The cautions are produced when the OWS is out of FOV or in case of a failure/degradation of the OWS functions.

## 6.9 Simulation Case Study

A conceptual representation of the overall avoidance volume obtained in relation to an identified collision threat and the avoidance trajectory generated by the SA&CA system is provided in Figure 6.6. The ground obstacles of various characteristics (natural and

man-made) including long and thin structures such as electrical cables and poles are detected. After identifying collisions, if the original trajectory of the SA&CA system host platform intersects the calculated avoidance volume, a caution flag is issued. As a result, an avoidance trajectory is generated in real-time and steering commands are provided to flight control surfaces. Realistic simulation scenarios were considered to evaluate the avoidance trajectory generation algorithm and assess its performance.

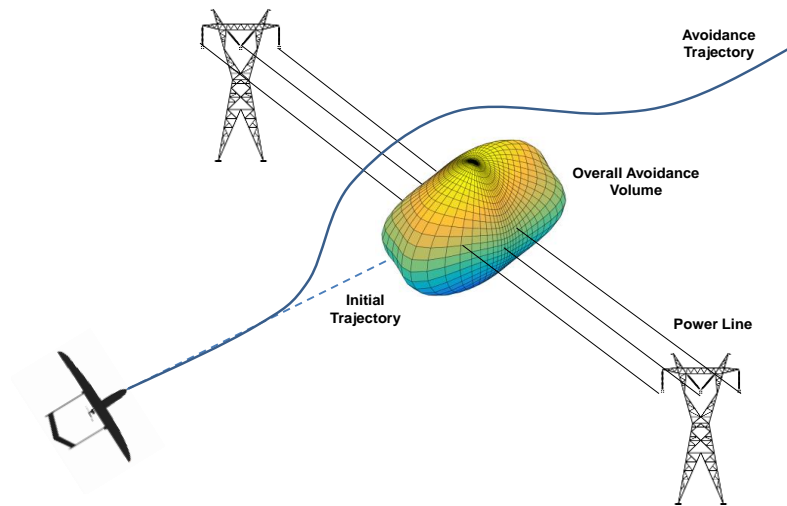


Figure 6.6. Obstacle avoidance scenario.

The scenario considered is that of an AEROSONDE™ UAV equipped with LOWAS flying towards a number of obstacles of different geometric characteristics as illustrated in Figure 6.7.

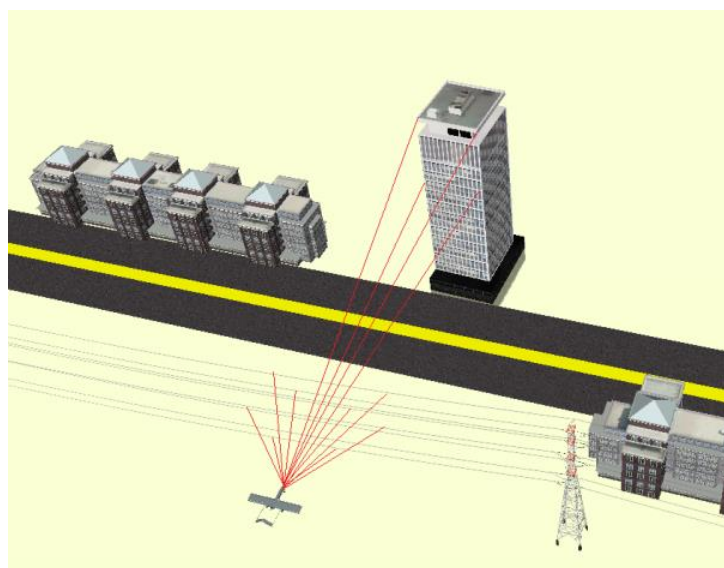


Figure 6.7. Case study scenario.

The LOWAS equipped UAV is considered to be flying at an altitude  $z = 100$  m Above-Ground Level (AGL), at a relatively low speed (20 m/s) and approaching a power transmission line consisting of a tower and a number of wires of 10 mm diameter both in front of the UAV flight path and on the left side. The altitude of the lowest wire is 80 m AGL and the altitude of the highest wire is 120 m AGL; the wires are separated by about 6.5 m vertically and 5 m laterally. The transmission lines lie approximately 100 m in front and 40 m each to the side of the UAV. The original horizontal flight trajectory would lead to a collision with the power transmission line. After a successful detection of all wires, the algorithm calculates the distances to each of them. As previously described the algorithm then recognises that the calculated distances are all comparable with the UAV size and therefore combines all wires in a single avoidance volume. The building behind the transmission line is 155 m high, 50 m in length and 50 m in width and the NG-FMS generates an additional avoidance volume for this structure. Since wire targets are assumed to extend laterally, the trajectory characterised by the greater distance (and hence optimal in this case) is the one entailing a straight climb manoeuvre. The re-join trajectory is computed using pseudospectral optimisation techniques described in [20 - 22] and in Chapter 4. The computed avoidance volumes (one for the power line and one for the building) and the optimised avoidance trajectory are depicted in Figure 6.8.

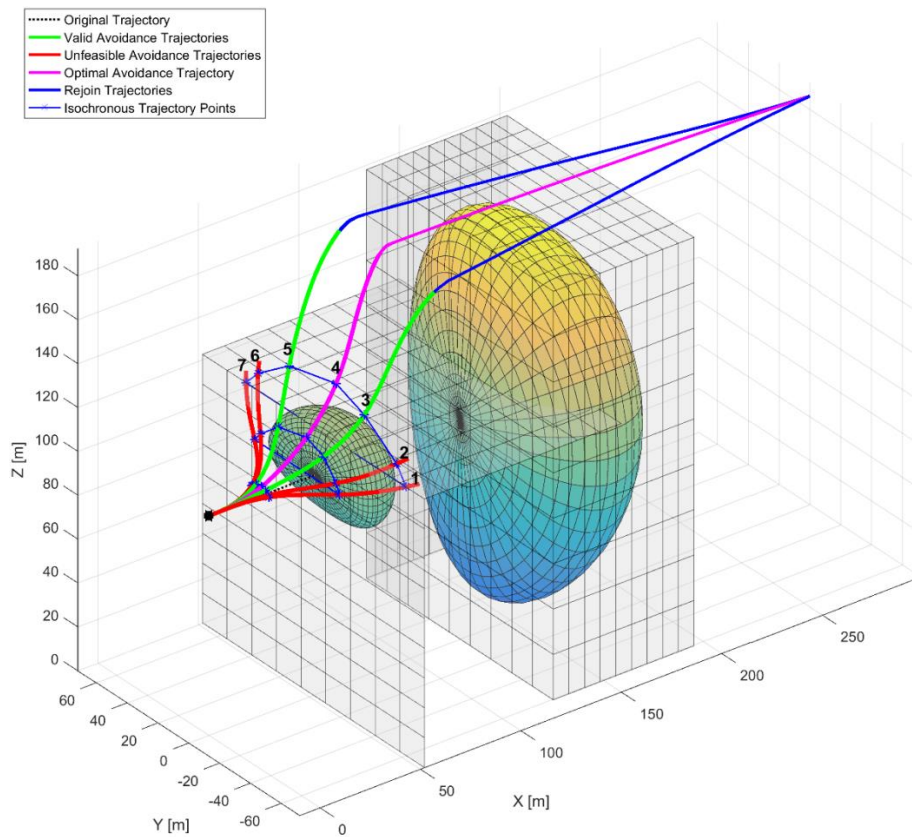


Figure 6.8. Results of the avoidance trajectory generation algorithm.

The UAV also avoids the extended target (building) by generating a smooth optimised trajectory from the safe manoeuvring point. These simulations were executed on a Windows 7 Professional workstation (64-bit OS) supported by an Intel Core i7-4510 CPU with clock speed 2.6 GHz and 8.0 GB RAM. The execution time for uncertainty volume determination and avoidance trajectory optimisation algorithms was in the order of 1.4 sec. Such an implementation makes it possible to perform the real-time separation maintenance and collision avoidance task.

## 6.10 Conclusions

The LOWAS system was proposed as one of the core non-cooperative sensors in an integrated SA&CA architecture for small-to-medium size UAS. The system architecture, mathematical models and simulation case studies performed to develop a novel Laser Obstacle Warning and Avoidance System (LOWAS) were presented. The algorithms for computing the avoidance volumes associated with obstacles and for the generation of optimal avoidance trajectories were presented along with a representative simulation case study. Tailored display formats developed for the UAV remote pilot station were presented including Safety Line (SL), Wires & Poles (W&P), all obstacles and Integrated LOWAS/FLS (ILF) formats. The demonstrated detection, warning and avoidance performance, determination of overall uncertainty volumes and avoidance trajectory generation algorithms ensure a safe avoidance of all potentially conflicting obstacles. Subsequently, a comprehensive simulation case study of the avoidance trajectory generation algorithms is accomplished using the AEROSONDE™ UAV as a test platform. It is concluded that the ground obstacle detection and trajectory optimization algorithms ensure a safe avoidance of all classes of obstacles (i.e., wire, extended and point objects) in a wide range of weather and geometric conditions, providing a pathway for possible integration of this technology into future NG-FMS architectures.

## 6.11 References

1. B.C. Breen, "Controlled Flight Into Terrain and the Enhanced Ground Proximity Warning System", IEEE Aerospace and Electronic Systems Magazine, Vol. 14, Issue 1, pp.19-24, 1999.
2. P. Novacek, "Terrain Awareness and Warning Systems – TAWS", Buyer's Guide, Pilot's Guide to Avionics Magazine, 2006.
3. B.C. Breen, "Terrain Awareness", Chapter 21, eds. C. Spitzer, U. Ferrell and T. Ferrell, Digital Avionics Handbook, Third Edition, CRC Press, 2014.

4. J. Gauci and D. Zammit-Mangion, "Obstacle Detection around Aircraft on Ramps and Taxiways through the Use of Computer Vision," Proceedings of AIAA Guidance, Navigation, and Control Conference (GNC 2009), Chicago, IL, USA, 2009
5. R. Sabatini and M. A. Richardson, "Airborne Laser Systems Testing and Analysis", RTO AGARDograph AG-300 vol. 26, Flight Test Instrumentation Series, Systems Concepts and Integration Panel (SCI-126), NATO Science and Technology Organization, 2010. Accessible at: <http://www.dtic.mil/cgi-bin/GetTRDoc?AD=ADA534869>
6. X. Yu and Y. Zhang, "Sense and Avoid Technologies with Applications to Unmanned Aircraft Systems: Review and Prospects", Progress in Aerospace Sciences, Elsevier, vol. 74, pp. 152-166, 2015. DOI: [10.1016/j.paerosci.2015.01.001](https://doi.org/10.1016/j.paerosci.2015.01.001)
7. S.I. Ali Shah and E.N. Johnson, "3D Obstacle Detection using a Single Camera", Proceedings of AIAA Guidance, Navigation, and Control conference 2009 (GNC 2009), Chicago, IL, USA, 2009.
8. A. Moses, M.J. Rutherford, and K.P. Valavanis, "Scalable RADAR-Based Sense-and-Avoid System for Unmanned Aircraft", Handbook of Unmanned Aerial Vehicles, pp. 1895-1953, Springer, 2014.
9. K.R.Noth, "Modeling and Simulation of a Ground based Sense and Avoid Architecture for Unmanned Aircraft System operations", Proceedings of 11<sup>th</sup> Integrated Communications, Navigation and Surveillance Conference: Renovating the Global Air Transportation System (ICNS 2011), Herndon, VA, USA, 2011, pp. O71-O79. DOI: [10.1109/ICNSURV.2011.5935356](https://doi.org/10.1109/ICNSURV.2011.5935356)
10. S. Ramasamy and R. Sabatini, "A Unified Approach to Cooperative and Non-Cooperative Sense-and-Avoid", Proceedings of International Conference on Unmanned Aircraft Systems (ICUAS 2015), Denver, CO, USA, 2015. DOI: [10.1109/ICUAS.2015.7152360](https://doi.org/10.1109/ICUAS.2015.7152360)
11. A. Mujumdar and R. Padhi, "Evolving Philosophies on Autonomous Obstacle/Collision Avoidance of Unmanned Aerial Vehicles", Journal of Aerospace Computing, Information, and Communication, Vol. 8, Issue 2, pp. 17-41, 2011. DOI: <http://dx.doi.org/10.2514/1.49985>
12. C. Geyer, S. Singh and L.J. Chamberlain, "Avoiding Collisions between Aircraft: State of the Art and Requirements for UAVs Operating in Civilian Airspace", Technical Report, CMU-RI-TR-08-03, Carnegie Mellon University, USA, 2008. Accessible at: <http://www.frc.ri.cmu.edu/projects/senseavoid/Images/CMU-RI-TR-08-03.pdf>
13. B. S. Goldstein and G. F. Dalrymple, "Gallium Arsenide Injection Laser Radar", Proceedings of the IEEE, Vol. 55, pp. 181-188, 1967. DOI: [10.1109/proc.1967.5437](https://doi.org/10.1109/proc.1967.5437)

14. R. Sabatini, M. A. Richardson, H. Jia and D. Zammit-Mangion, "Airborne laser systems for atmospheric sounding in the near infrared", Proceedings of SPIE 8433, Laser Sources and Applications, Photonics Europe 2012, Brussels, Belgium, 2012. DOI: [10.1117/12.915718](https://doi.org/10.1117/12.915718)
15. G. Hogg, K. Harrison and S. Minisclo, "The Anglo-French Compact Laser Radar Demonstrator Programme", AGARD-CP-563 - Low-Level and Nap-of-the-Earth (NOE) Night Operations, NATO Science and Technology Organization, 1995.
16. R. Sabatini, M.A. Richardson, A. Gardi and S. Ramasamy, "Airborne Laser Sensors and Integrated Systems", Progress in Aerospace Sciences, Elsevier, vol. 79, pp. 15–63 2015. DOI: [10.1016/j.paerosci.2015.07.002](https://doi.org/10.1016/j.paerosci.2015.07.002)
17. L. Bouwmeester, R. Clothier, R. Sabatini and G. Williams, "Autonomous Communication between Air Traffic Control and Remotely Piloted Aircraft", Proceedings of 16<sup>th</sup> Australian International Aerospace Congress (AIAC16), Engineers Australia, pp. 48-57, 2015.
18. S. Ramasamy, R. Sabatini and A. Gardi, "LIDAR Obstacle Warning and Avoidance System for Unmanned Aerial Vehicle Sense-and-Avoid", Aerospace Science and Technology, Elsevier, vol. 55, pp. 344–358, 2016. DOI: [10.1016/j.ast.2016.05.020](https://doi.org/10.1016/j.ast.2016.05.020)
19. F. Cappello, S. Ramasamy and R. Sabatini, "Multi-Sensor Data Fusion Techniques for RPAS Detect, Track and Avoid", SAE Technical Paper 2015-01-2475, SAE 2015 AeroTech Congress & Exhibition, Seattle, Washington, USA, 2015. DOI: [10.4271/2015-01-2475](https://doi.org/10.4271/2015-01-2475)
20. A. Gardi, R. Sabatini and S. Ramasamy, "Multi-Objective Optimisation of Aircraft Flight Trajectories in the ATM and Avionics Context", Progress in Aerospace Sciences, Elsevier, vol. 83, pp.1-36, 2016. DOI: [10.1016/j.paerosci.2015.11.006](https://doi.org/10.1016/j.paerosci.2015.11.006)
21. J.Z. Ben-Asher, "Optimal Control Theory with Aerospace Applications", Education Series, American Institute of Aeronautics and Astronautics (AIAA), Reston, VA, USA, 2010.
22. A.V. Rao, "Survey of Numerical Methods for Optimal Control", Advances in the Astronautical Sciences, Vol. 135, pp. 497-528, 2010.

# CHAPTER 7

## AERIAL OBSTACLES SA&CA

### CASE STUDY

*"The greater the obstacle, the more glory in overcoming it". - Molière*

#### 7.1 Introduction

The previous chapter presented a dedicated analysis and simulated case study on the application of a unified approach to SA&CA for detecting and avoiding ground targets. This chapter presents the algorithms employed in a simulated case study involving non-cooperative sensors, cooperative systems and combinations thereof. Later sections address in more details the simulated case studies performed for evaluating the SA&CA functionalities.

#### 7.2 Non-Cooperative SA&CA – FLS

Gimballed visual and thermal cameras are used for determining position and velocity estimates of the intruders. To obtain all-weather operation, thermal imaging is used in conjunction with visual imaging. Assuming the camera provides an approximate FOV of 70° with a resolution of 2.0 MP, the fusion of optical sensors with other non-cooperative sensors increases the angular accuracy. LIDAR scaled versions are used for extracting range measurements, and they provide a good FOV both in azimuth and in elevation. It allows the operator to select the azimuth orientation of the FOV among three possible directions: aligned with the platform heading (normal flight envelope) or turning left/right with respect the platform heading. This option provides an optimized coverage for turning manoeuvres at high angular speed. For stabilised obstacle detection, after image acquisition, the noise caused by the platform motion is removed. Bottom-hat morphology is performed to detect negative contrast features that correspond to the threats. Low-level tracking is achieved by utilising a number of filtering methods, one being the ad-hoc Viterbi filtering method by employing a bank of filters [1].



Let  $\alpha_n^b(i, j)$  be the filter output at time step,  $n$  of pixel  $(i, j)$  for the filter bank branch  $b$ , and  $I_n(i, j)$  be the greyscale level of pixel  $(i, j)$ , in which the ad-hoc Viterbi filter steps, for  $1 \leq i \leq H, 1 \leq j \leq W$  and all  $n$ , are carried out. The statistical test criterion for evaluation to determine the actual presence of a collision threat is given by:

$$\gamma_n = \max_{1 \leq i \leq H, 1 \leq j \leq W} [\alpha_n(i, j)] \quad (7.1)$$

where  $\gamma_n$  is the comparison parameter. An illustration of the acquired, stabilised and tracked visual image is shown in Figure 7.1 and 7.2.



Figure 7.1. Acquired and stabilised visual image.



Figure 7.2. Tracked object.

An example of an acquired thermal image [2], which is subjected to segmentation and tracking is illustrated in Figure 7.3.

A low-cost navigation and guidance system is adopted for position estimates, which includes GNSS, along with various categories of inertial and VBN sensors. When the set threshold is exceeded and the detection is continuous, high level tracking detection is performed by using an extended or unscented Kalman filter.



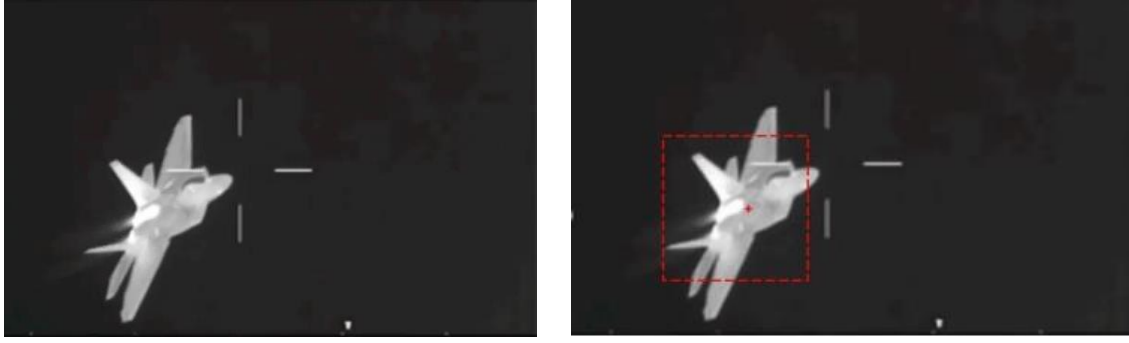


Figure 7.3. Acquired thermal image and tracked object.

The predicted state,  $\hat{x}(t)$  at time  $t$  is given by:

$$\hat{x}(t) = \begin{bmatrix} P_x(t) \\ P_y(t) \\ V_x(t) \\ V_y(t) \end{bmatrix} = \begin{bmatrix} 1 & 0 & 1 & 0 \\ 0 & 1 & 0 & 1 \\ 0 & 0 & 1 & 0 \\ 0 & 0 & 0 & 1 \end{bmatrix} \begin{bmatrix} P_x(t-1) \\ P_y(t-1) \\ V_x(t-1) \\ V_y(t-1) \end{bmatrix} + \begin{bmatrix} \frac{t^2}{2} & 0 \\ 0 & \frac{t^2}{2} \\ t & 0 \\ 0 & t \end{bmatrix} \begin{bmatrix} a_x \\ a_y \end{bmatrix} + \varepsilon(t) \quad (7.2)$$

where  $P_{x,y}(t)$  is the position in the  $x$  and  $y$  cardinal directions respectively as a function of time,  $t$ .  $V_{x,y}(t)$  is the velocity in the  $x$  and  $y$  direction respectively,  $a_{x,y}(t)$  is the acceleration and  $\varepsilon(t)$  is the prediction Gaussian noise. The Kalman Filter equations are:

$$\hat{x}_i(k|k) = \hat{x}_i(k|k-1) + W_i(k)[z_i(k) - H_i(k)x_i(k|k-1)] \quad (7.3)$$

$$P_i(k|k) = P_i(k|k-1) - W_i(k)S_i(k)W_i^T(k) \quad (7.4)$$

where:

$$W_i(k) = P_i(k|k-1)H_i^T(k)S_i^{-1}(k) \quad (7.5)$$

$$S_i(k) = [H_i(k)P_i(k|k-1)H_i^T(k) + R_i(k)] \quad (7.6)$$

where  $H_i(k)$  represents the design matrix and  $R_i(k)$  is the measurement noise covariance matrix and  $k$  is the sample time. A higher-level tracking algorithm is employed to combine the estimates instead of combining the observations from different sensors. The track fusion algorithm is defined as the weighted average variance of all the tracks and is given by:

$$\hat{x}_F(k|k) = P_F(k|k) \times \sum_{i=1}^n P_i^{-1}(k|k) \hat{x}_i(k|k) \quad (7.7)$$

$$P_F(k|k) = [\sum_{i=1}^n P_i^{-1}(k|k)]^{-1} \quad (7.8)$$

Once the tracks are fused and the states are estimated, the imminent trajectory is predicted. The errors in predicted trajectory can be derived from the quality of the measurements, reflected in the prediction error, which are expressed as:

$$\sigma^2(k + \tau|k) = \text{var}[n(k + \tau) - \hat{n}^l(k + \tau|k)] \quad (7.9)$$

where  $n(k + \tau)$  is the exhibited (modelled) trajectory and  $\hat{n}^l(k + \tau|k)$  is the predicted optimal trajectory at sample time  $k + \tau$ .

For trajectory prediction, the obstacle centre of mass, the target orientation and the geometric shape of the uncertainty volume are determined. Once the trajectory is predicted, the Risk-of-Collision (RoC) is determined by calculating the probability of a NMAC event for the predicted trajectory over the time horizon by employing Monte Carlo approximations given by:

$$P(NMAC_{(0,h_p)}) \approx \frac{1}{N_{rc}} \sum_{i=1}^{N_{rc}} \left( \min_{0 < t_p < h_p} |s_i(t_p)| < d_m \right) \quad (7.10)$$

where  $N_{rc}$  is the number of samples,  $h_p$  is defined as a future horizon up to where it is desired to predict the trajectory,  $d_m$  is the minimum distance required to avoid the obstacle and  $t_p$  is the time horizon defined for collision. The accuracy of the approximation is entirely based on the number of samples.

### 7.3 Cooperative SA&CA – ADS-B

In a cooperative traffic scenario, the ADS-B system is used to obtain the state of the intruders. The future position of the intruders is projected based on the estimate of the current state vector and the flight profile. The ADS-B measurement model adopted for intruder position and velocity estimates in  $x$  and  $y$  is given by:

$$Z(k) = \begin{bmatrix} 1 & 0 & 0 & 0 & 0 & 0 \\ 0 & 1 & 0 & 0 & 0 & 0 \\ 0 & 0 & 0 & 1 & 0 & 0 \\ 0 & 0 & 0 & 0 & 1 & 0 \end{bmatrix} \begin{bmatrix} x \\ \dot{x} \\ \ddot{x} \\ y \\ \dot{y} \\ \ddot{y} \end{bmatrix} + \begin{bmatrix} V_x(k) \\ V_{\dot{x}}(k) \\ V_{\ddot{x}}(k) \\ V_y(k) \\ V_{\dot{y}}(k) \\ V_{\ddot{y}}(k) \end{bmatrix} \quad (7.11)$$

Assuming that the velocity components,  $V_x(k)$ ,  $V_{\dot{x}}(k)$ ,  $V_{\ddot{x}}(k)$  and  $V_y(k)$  are affected only by Gaussian noise with zero mean, the standard deviation is defined by the covariance matrix given by:

$$R = \begin{bmatrix} E[V_x^2] & 0 & 0 & 0 \\ 0 & E[V_{\dot{x}}^2] & 0 & 0 \\ 0 & 0 & E[V_{\ddot{x}}^2] & 0 \\ 0 & 0 & 0 & E[V_y^2] \end{bmatrix} \quad (7.12)$$

where  $E[\cdot]$  represents the mean. Using the data fusion model described in Chapter 2 (Section 2.8), the state vector of the intruders is determined and this is propagated to

predict the future trajectories using a probabilistic model. After computing the mixing probability, the combination of the state estimate is given by:

$$\hat{x}_F(k|k) = \sum_{i=1}^r \hat{x}^i(k|k) \mu_i(k) \quad (7.13)$$

where  $\mu_i(k)$  is the mode probability update. For conflict detection, the resultant covariance matrix,  $Q$  after transformation is defined as:

$$Q = R S R^T \quad (7.14)$$

where  $S$  is the diagonal covariance matrix and  $R$  represents the transformation matrix between the heading aligned frame to that of the host aircraft coordinate frame. The probability of conflict is defined as the volume below the surface of the probability density function,  $p(x, y, z)$  representing the conflict zone. The conflict probability,  $P_c$  is expressed as:

$$P_c = \int_{-\Delta z - \Delta z_c}^{-\Delta z - \Delta z_c} \int_{-\Delta y - \Delta y_c}^{-\Delta y + \Delta y_c} \int_{-\infty}^{+\infty} p(x, y, z) dx dy dz \quad (7.15)$$

where  $\Delta y + \Delta y_c$  represents the conflict separation distance and  $\Delta x_c, \Delta y_c$  and  $\Delta z_c$  correspond to the rows of the conflict boundary matrix. The state elements transmitted are the latitude and longitude, barometric altitude, geometric altitude, and velocity. The error messages reported are Navigation Accuracy Category for Position (NACp), the Navigation Accuracy Category for Velocity (NACv), Navigation Integrity Category (NIC), Source Integrity Level (SIL), and SDA. ADS-B is also subject to several additional sources of error namely latency error, resolution error, and Message Success Rate (MSR) error. The NACp, NACv, NIC, SIL, SDA, latency error, resolution error, and MSR error provide a basis from which to derive an error characterization to model ADS-B. Given the NACp and NACv, the horizontal position and velocity can be modelled as a Rayleigh random process. From the Rayleigh process, the 95% bound on both the position and velocity error can be used to derive the variance for a Gauss-Markov process with zero-mean Gaussian noise for the North and East position and velocity. Based on values of NACp=303.8 ft and NACv=19.4 kn, the horizontal North and East position error can be modelled as a zero- mean Gaussian distribution with a standard deviation of 124 ft, and the North and East velocity can be modelled as a zero-mean Gaussian distribution with a standard deviation of 8 km. The error in the ADS-B reported vertical velocity varies with increasing vertical rate. For vertical rates between  $\pm 500$  ft/min, the vertical rate tolerance is  $\pm 46$  ft/min [3, 4].

Given the assumption that these tolerances are 95% bounds (this assumption holds good for the assessment of horizontal position and the associated uncertainty), it is estimated

that the standard deviation of the climb rate is 27.96 ft/min for vertical rates of  $\pm 500$  ft/min. Additionally the vertical rate error is effected by the resolution of the ADS-B message encoding which is 64 ft/min. Based on the received NACp, then the surveillance applications could determine whether the accuracy of transmitted geometric position is suitable for the intended purpose [3, 4]. The navigation uncertainty categories for different NACp are summarised in Table 7.1.

Table 7.1. Navigation uncertainty categories [3, 4].

<b>NACp</b>	<b>95% Horizontal Accuracy Bounds</b>	<b>Use</b>
0	EPU >18.52 km	
1	EPU <18.52 km	RNP-10 accuracy
2	EPU <7.408 km	RNP-4 accuracy
3	EPU <3.704 km	RNP-2 accuracy
4	EPU <1852 m	RNP-1 accuracy
5	EPU <926 m	RNP-0.5 accuracy
6	EPU <555.6 m	RNP-0.3 accuracy
7	EPU <185.2 m	RNP-0.1 accuracy
8	EPU <92.6 m	GPS(with SA on)
9	EPU <30 m	GPS(with SA off)
10	EPU <10 m	WAAS
11	EPU <3 m	LAAS

Table 7.2 provides the relationship between NACv and the horizontal figure of merit for velocity.

Table 7.2. Navigation uncertainty categories - velocity.

<b>NACv</b>	<b>Horizontal Velocity Error (95%)</b>
0	Unknown or >10 m/s
1	<10 m/s
2	<3 m/s
3	<1 m/s
4	<0.3 m/s

The Estimated Position Uncertainty (EPU) is a 95% accuracy bound of horizontal position. The ADS-B equipment extracts EPU from the accuracy reports provided by the navigation module. When using GNSS, EPU is also called the Horizontal Figure of Merit (HFOM). Similar to NACp, NACv is derived from 95% accuracy figure of merit for velocity. The EKF is employed to derive the accurate state vector of the intruder aircraft from the raw ADS-B measurements.

## 7.4 Simulation Case Studies

Simulation case studies were performed to test the SA&CA algorithms for aerial objects.

### 7.4.1 Tracking and Detection Performance

Tracking for the aerial objects was accomplished using Kalman filter and Track-to-Track algorithms. The covariance matrix of process noise  $Q$  and measurement noise  $R$  are given by:

$$Q = \begin{bmatrix} 0.01 & 0 & 0 & 0 & 0 & 0 \\ 0 & 0.01 & 0 & 0 & 0 & 0 \\ 0 & 0 & 0.01 & 0 & 0 & 0 \\ 0 & 0 & 0 & 0.01 & 0 & 0 \\ 0 & 0 & 0 & 0 & 0.01 & 0 \\ 0 & 0 & 0 & 0 & 0 & 0.01 \end{bmatrix} \quad (7.16)$$

$$R = \begin{bmatrix} 0.001 & 0 & 0 \\ 0 & 0.001 & 0 \\ 0 & 0 & 0.001 \end{bmatrix} \quad (7.17)$$

The initial state covariance  $P_0$  is defined as:

$$P_0 = \begin{bmatrix} 0.1 & 0 & 0 & 0 & 0 & 0 \\ 0 & 0.1 & 0 & 0 & 0 & 0 \\ 0 & 0 & 0.1 & 0 & 0 & 0 \\ 0 & 0 & 0 & 0.1 & 0 & 0 \\ 0 & 0 & 0 & 0 & 0.1 & 0 \\ 0 & 0 & 0 & 0 & 0 & 0.1 \end{bmatrix} \quad (7.18)$$

The initial conditions of the tracked object are assumed to be the following:

$$\begin{bmatrix} P_x(0) \\ P_y(0) \\ P_z(0) \\ V_x(0) \\ V_y(0) \\ V_z(0) \end{bmatrix} = \begin{bmatrix} 1 \\ 1 \\ 1 \\ 10 \\ 0 \\ 0 \end{bmatrix} \quad (7.19)$$

Given a sampling rate of 0.1 sec and the total time to be 100, the filtering results are presented below. The position in X, Y and Z are shown in Figures 7.4, 7.5 and 7.6 respectively. The 3D trajectory of the tracked object is shown in Figure 7.7.

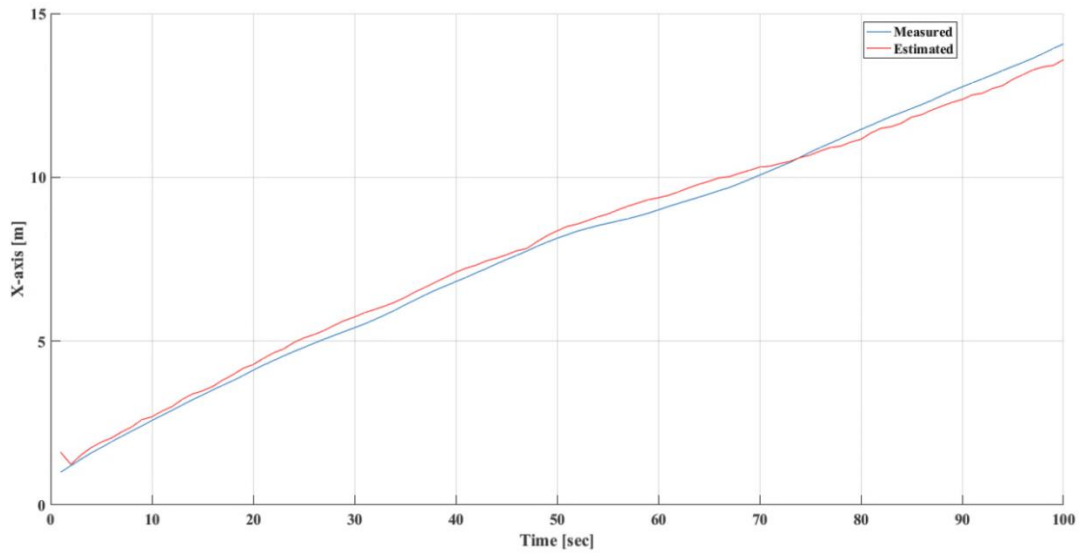


Figure 7.4. Measured and estimated X position.

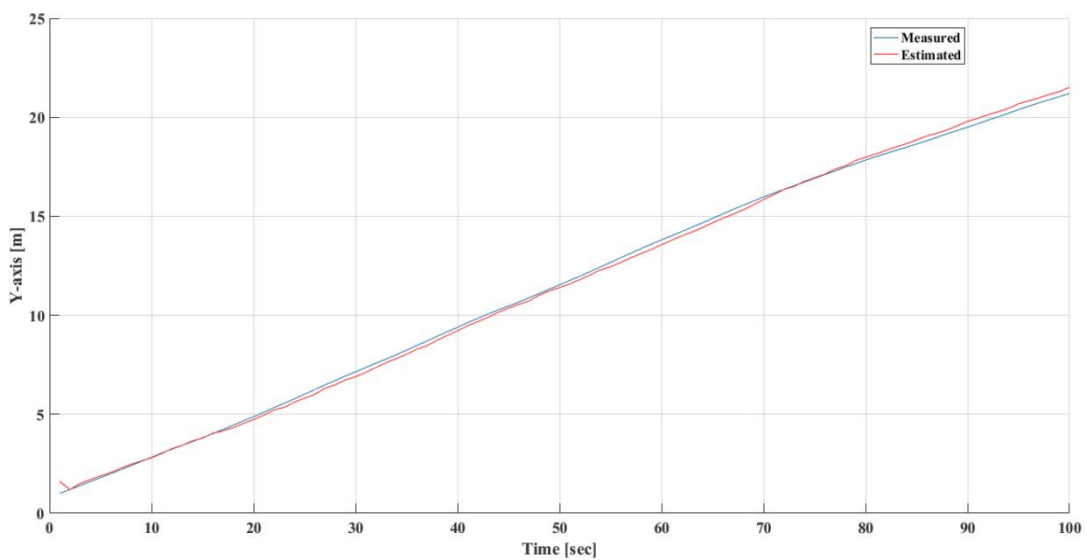


Figure 7.5. Measured and estimated Y position.

Based on the illustrated results and the given initial conditions, the Kalman filter algorithm is able to track the generated random trajectory of a point (target centroid) in the 3D plane.

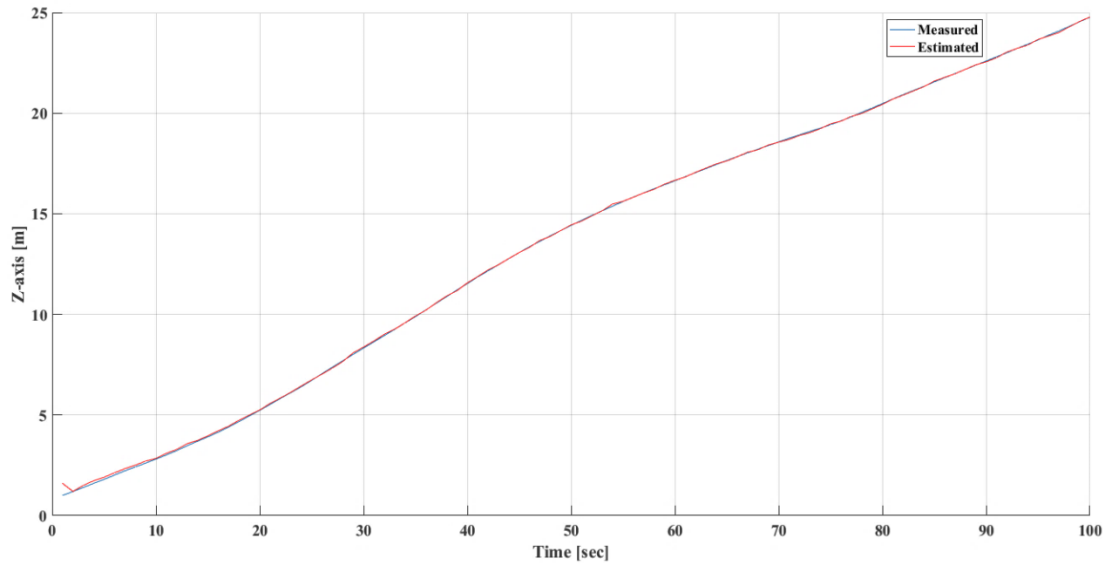


Figure 7.6. Measured and estimated Z position.

The measurement vector with a measurement noise shown in Equations 7.16 – 7.19 were used in this analysis and the resultant Mean Square Error (MSE) in X, Y and Z were obtained as shown in Figure 7.8. It is observed that the results obtained with the selected extended Kalman filter give a good performance with only one measurement. Based on the test bed architecture illustrated in Chapter 5, the accuracy of the measurement vector (tracking observable) can be increased by having more than one source (e.g. multiple tracking sensors/systems).

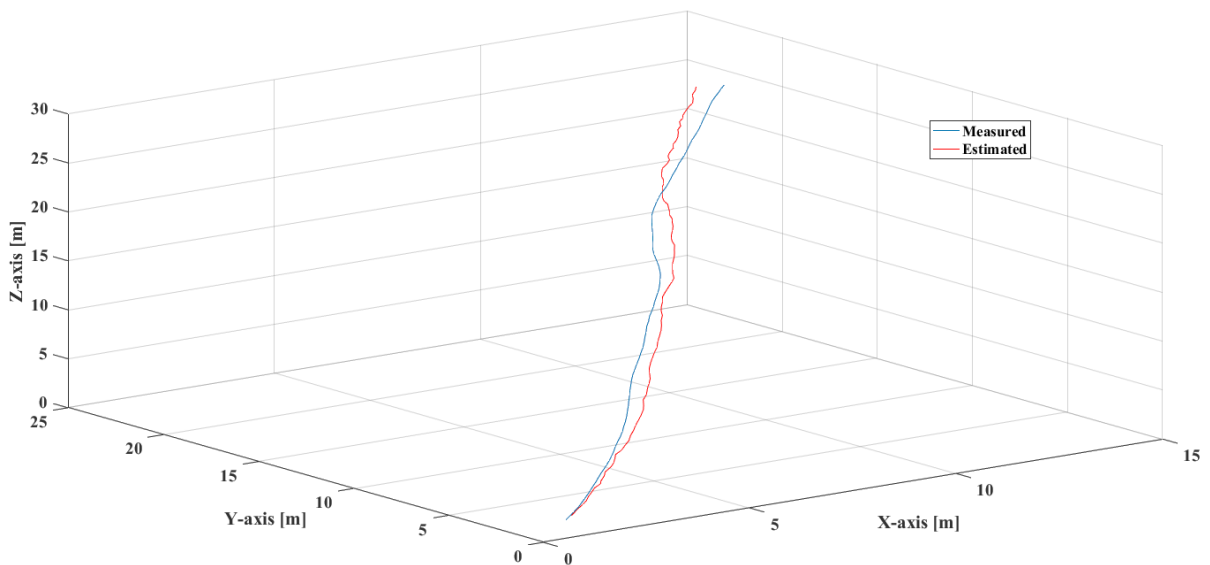


Figure 7.7. Acquired thermal image and tracked object.

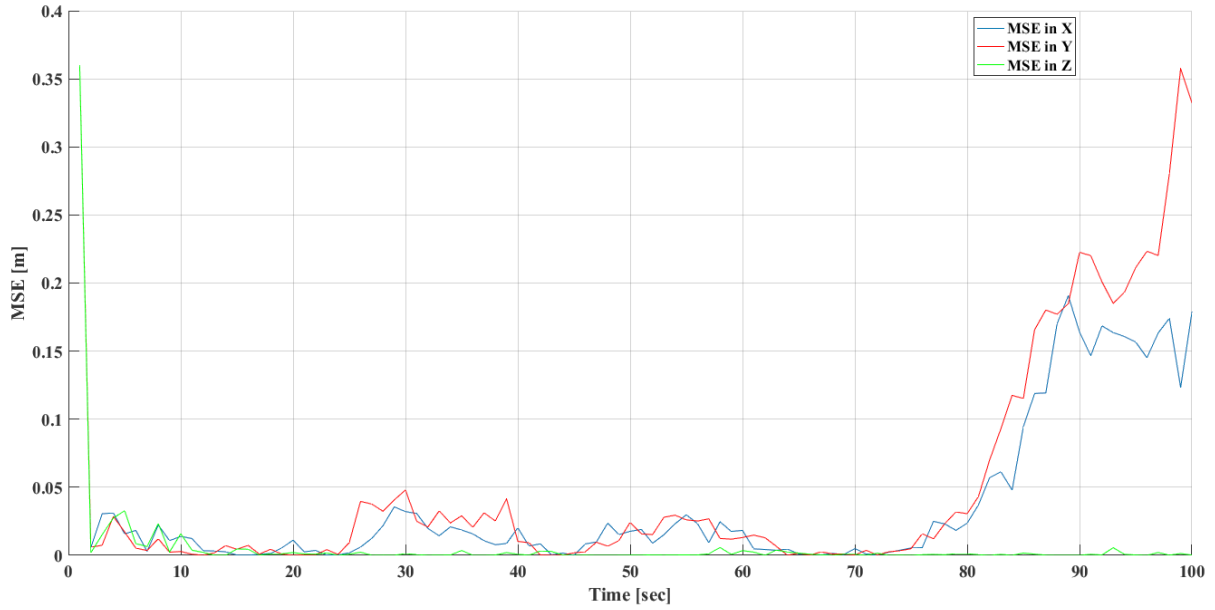


Figure 7.8. MSE in X, Y and Z.

Given the host aircraft's current position is  $[-50000, 0, 3000]$  m and the velocity is  $[200, 0, 0]$  m/s and also given an intruder in the airspace flies from an initial tracked position  $[-500, 45000, 3000]$  m with constant speed  $[0, -200, 0]$  m/s, the conflict probability is analysed for a range of covariance values. Given the position covariance for both aircraft is  $\text{diag}([1000 \times 1000, 1000 \times 1000, 15 \times 15])$  and the velocity covariance aircraft is  $\text{diag}([25, 25, 9])$ , the conflict probability results are summarised below.

The trajectory intents of the host aircraft and the intruder are shown in Figure 7.9.

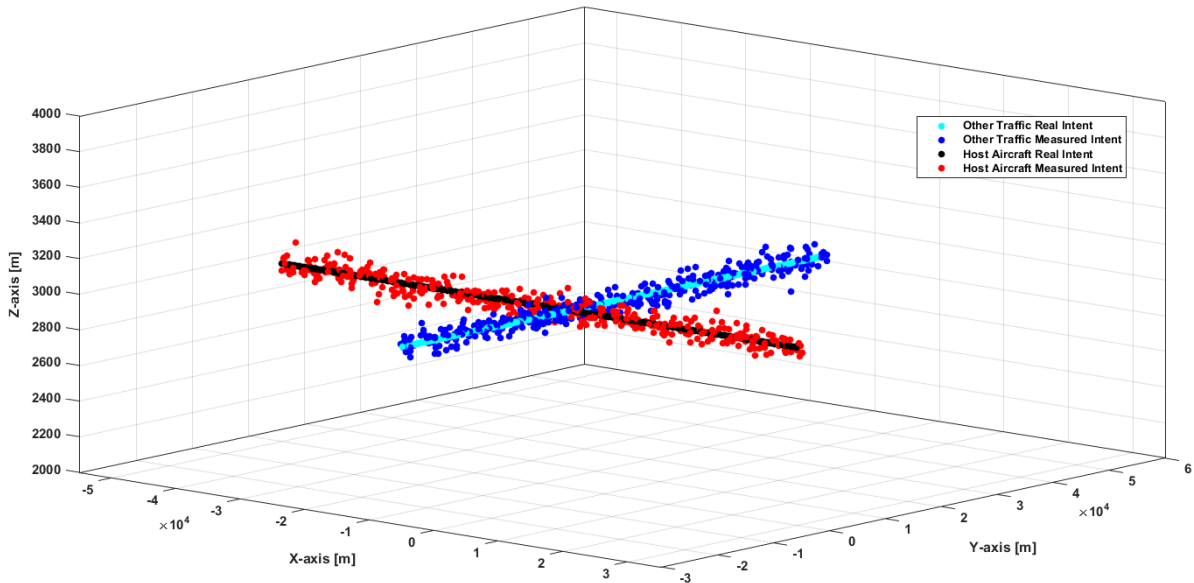


Figure 7.9. MSE in X, Y and Z.



After tracking the intruder using ADS-B reports for several seconds, the state vector estimation derived from the extended Kalman filter starts converging to the true value. Based on the last updated output from the extended Kalman filter, the conflict detection module calculates the probability of conflict within the look ahead window, which is set to 300 sec. A conflict alert is issued if the probability of conflict is greater than the detection threshold (here the threshold used is 0.7). To arrive at the threshold value, a comparison of conflict detection threshold, probability of false alert and probability of detection was performed. When the threshold is 0.7, the probability of detection is 0.9855 and probability of false alert is 0.18%. Based on this analysis, it was concluded that a good balance between false alerts and miss alerts can be derived if the detection threshold is set to be 0.7. Therefore 0.7 is used as the conflict detection threshold in this thesis. From the perspective of consequence, miss alert is worse than false alert. It is essential to keep miss alert probability as low as possible. The conflict span generated by the conflict detection module is from 171 to 241 s as seen from Figure 7.10. Given the required separation minima, the real separation between the host aircraft and other traffic does not meet the required performance from 172 to 237 s as seen from Figure 7.11.

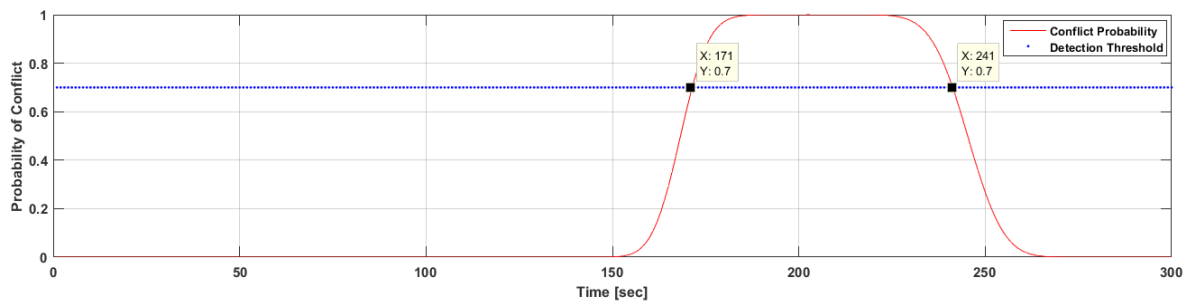


Figure 7.10. Conflict probability.

The overall avoidance volume is generated taking into account the real-time position measurements, tracking observable and relative dynamics between the two platforms and is shown in Figure 7.12.

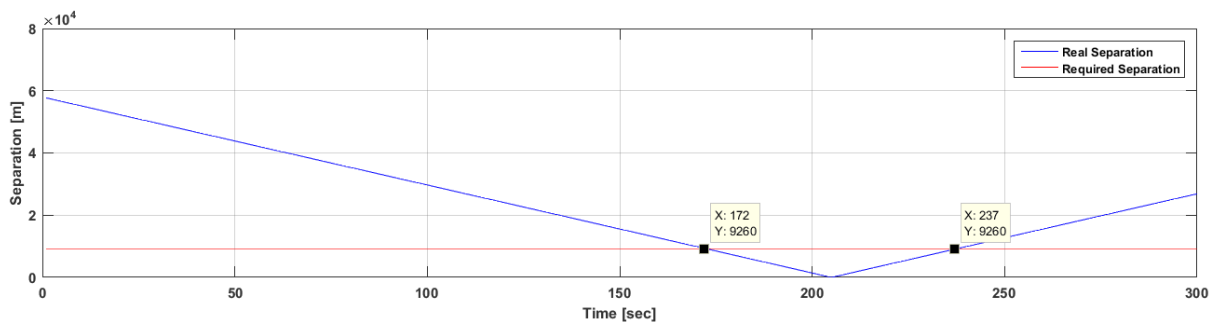


Figure 7.11. Real and required separation.

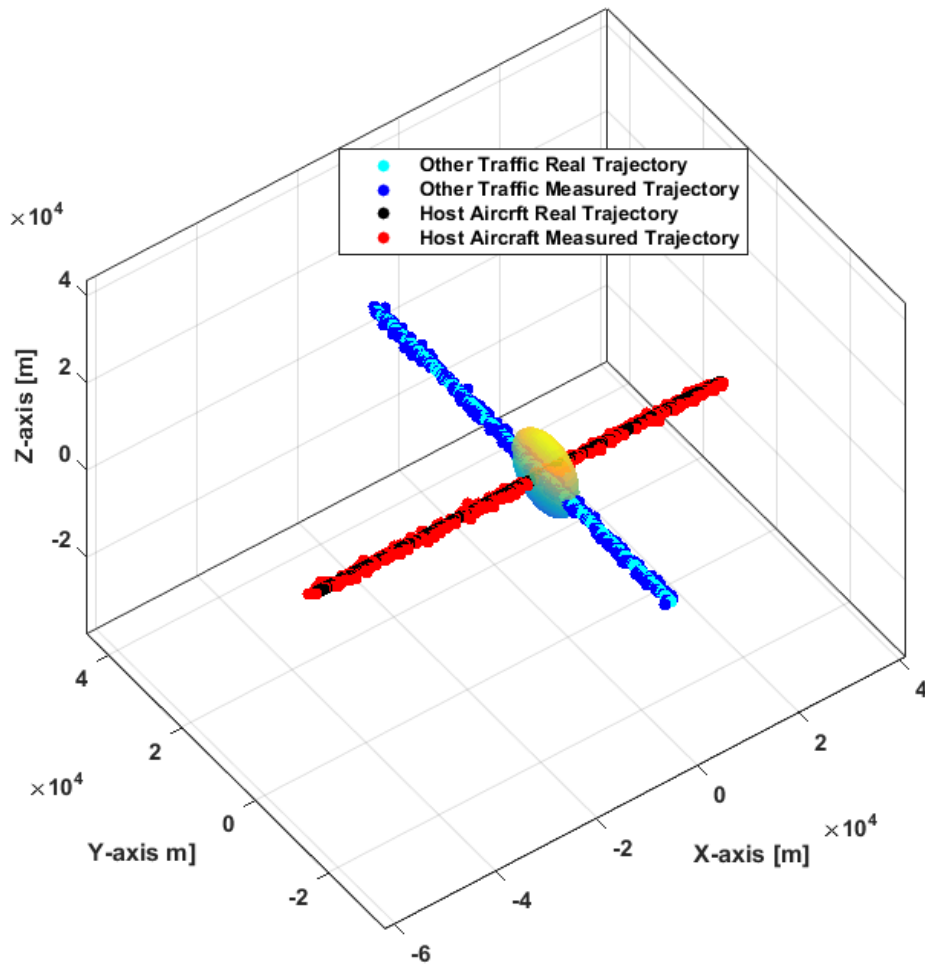


Figure 7.12. Avoidance volume at time of conflict.

The following case study considers a scenario in which objects are tracked using non-cooperative sensors (using forward-looking sensors). At the beginning of the simulation, both unmanned aircraft are placed far enough from each other that one is at the outside of the avoidance volume before being allowed to move freely according to the given initial velocities.

The given initial velocities are chosen so that both unmanned aircraft immediately move into a collision course with each other. The collision threat situation is indicated by the estimated time-to-collide and its value decreases over time and hence reduces the collision risk. The estimated and true tracks of the intruder are shown in Figure 7.13.

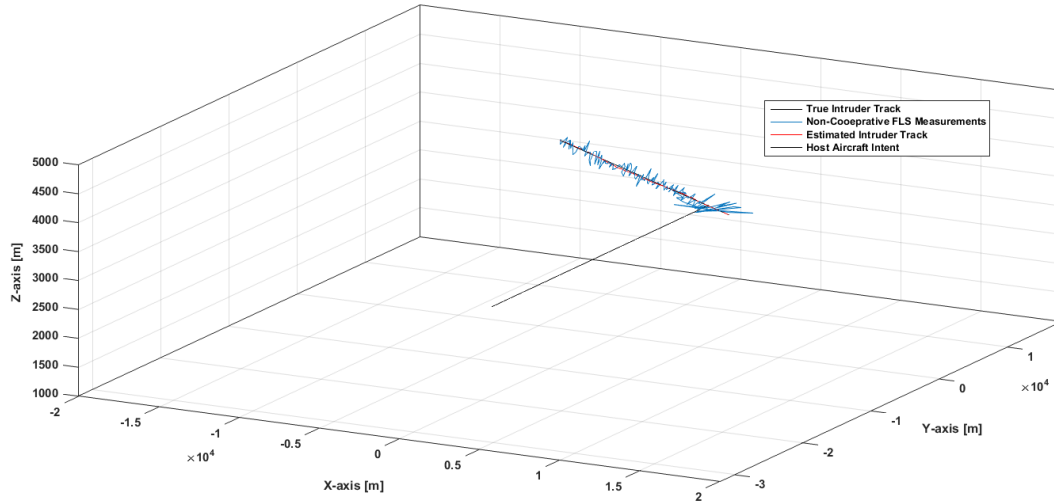


Figure 7.13. Conflict scenario.

The real as well as measured values of range, azimuth and elevation are shown in Figure 7.14.

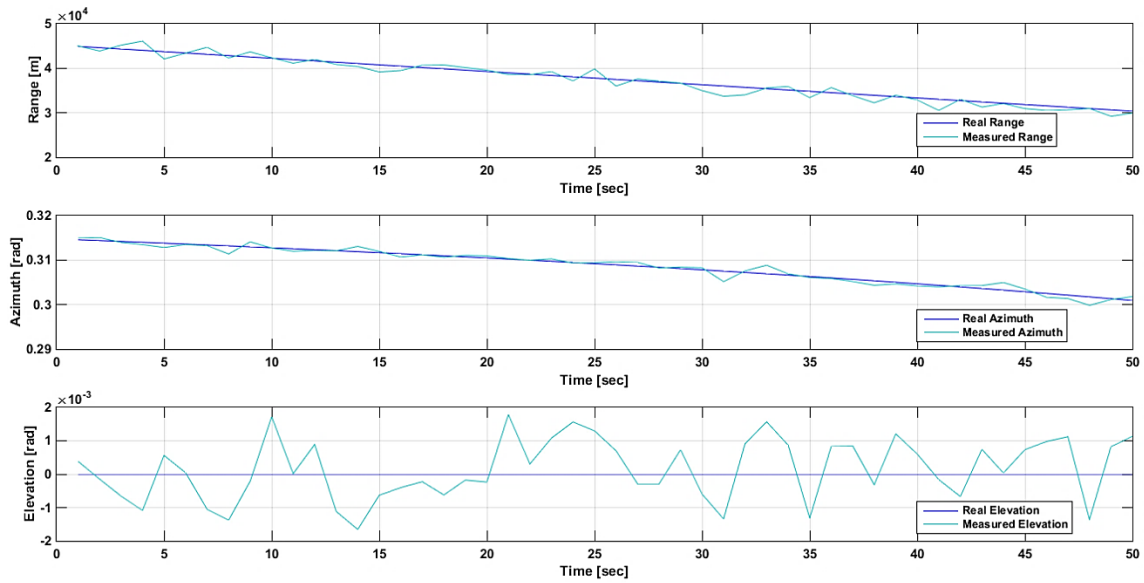


Figure 7.14. Range and bearing data.

The covariance of the measured range is 1000 m and the bearing covariance is  $0.05^\circ$ . The look-ahead window is 300 seconds. The correspondent real and required separation is shown in Figure 7.15.

It can be seen that the distance is less than the required horizontal separation, which is 5NM and occurs from 37 to 94 s. The overall avoidance volume generated, taking into account the real-time position measurements, tracking observable and relative dynamics between the two platforms, for this case is shown in Figure 7.16.

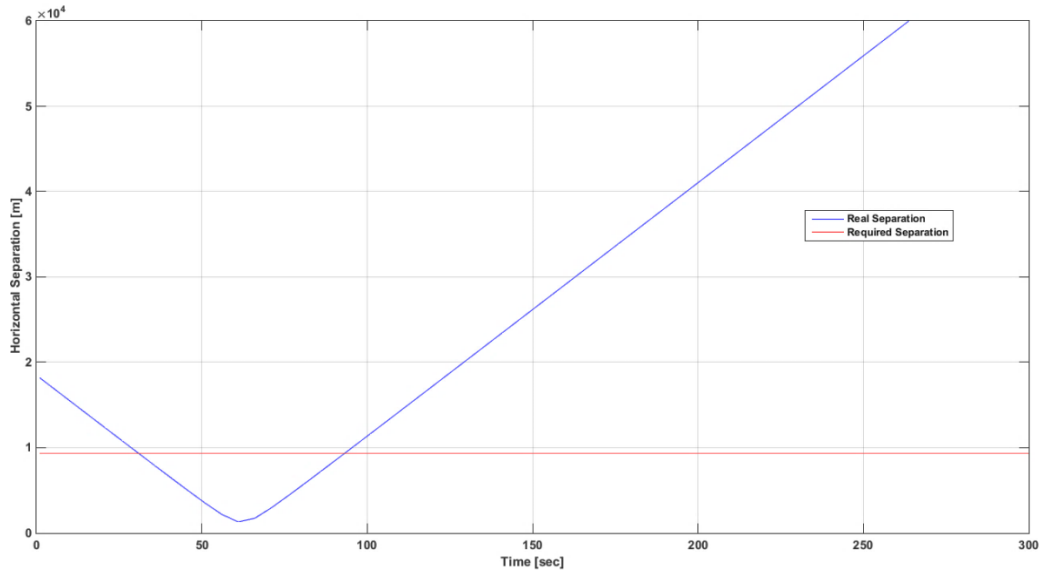


Figure 7.15. Real and required separation.

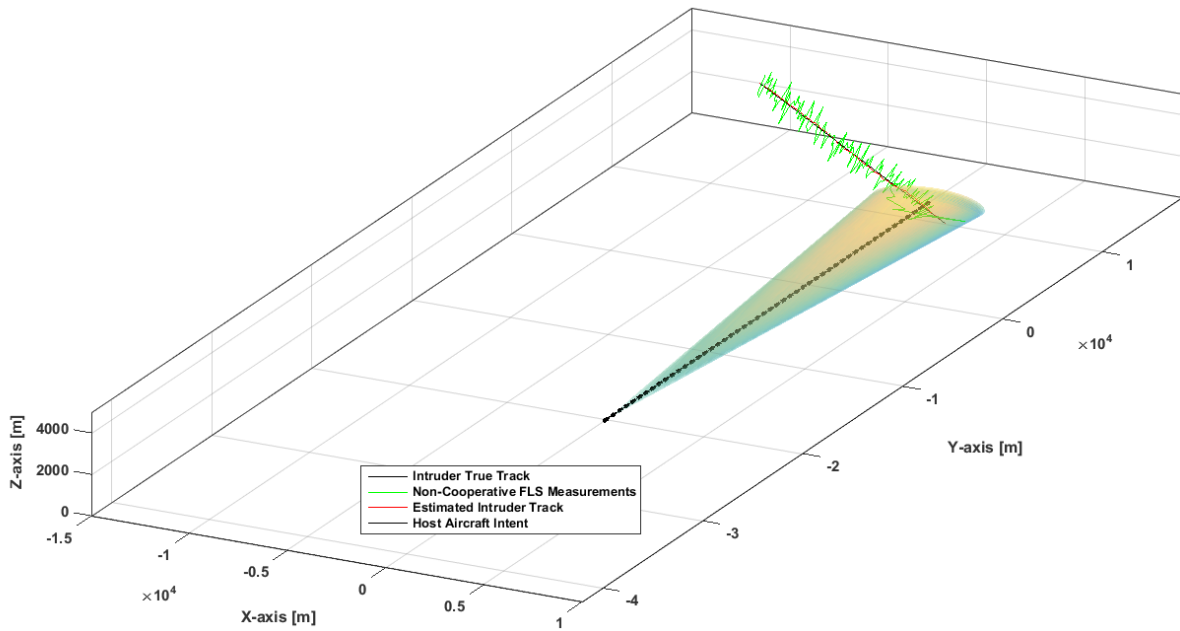


Figure 7.16. Range and bearing data.

Further simulation case studies were performed using manned and unmanned aircraft platforms (AEROSONDE™ UAS and Airbus A320 aircraft) for evaluating the computational complexity of the SA&CA functionalities. The simulations were executed on a Windows 7 Professional workstation (64-bit OS) supported by an Intel Core i7-4510 CPU with clock speed 2.6 GHz and 8.0 GB RAM. The execution time for uncertainty volume determination and avoidance trajectory optimisation algorithms was in the order of 8 sec. Such an implementation may make it possible to perform real-time separation maintenance tasks, as well as avoidance of any identified collisions

(emergency timeframes). Since the proposed algorithms are employed in a safety-critical application, it is important to explore the Worst Case Execution Time (WCET). A pure measurement-based method may not be sufficient in most SA&CA applications. But, given that the unified approach to SA&CA algorithms implemented in the NG-FMS are deterministic by design, a measurement-based method can provide an estimate of the WCET. The difficulties include the worst initial environment and overestimation of the WCET. The most demanding cases require more than 8 sec for a complete execution of the software code, but, at the same time, the WCET also depends on the number of processors, parallel computation elements and architecture design (32-bit, 64-bit, etc.)

Both cooperative and non-cooperative SA&CA cases were considered for simulation activities with the AEROSONDE™ UAS acting as the host platform. The host unmanned platform was equipped with SAA functions to carry out cooperative and non-cooperative conflict resolution and collision avoidance tasks. In the first case, it is assumed that no cooperative systems are on board the intruder. The uncertainty volume is generated in near real-time after evaluating the risk of collision at the collision point. An avoidance trajectory is generated (based on the platform dynamics) to maintain the required separation and to prevent any mid-air collisions at all of the predicted time epochs (Figure 7.17).

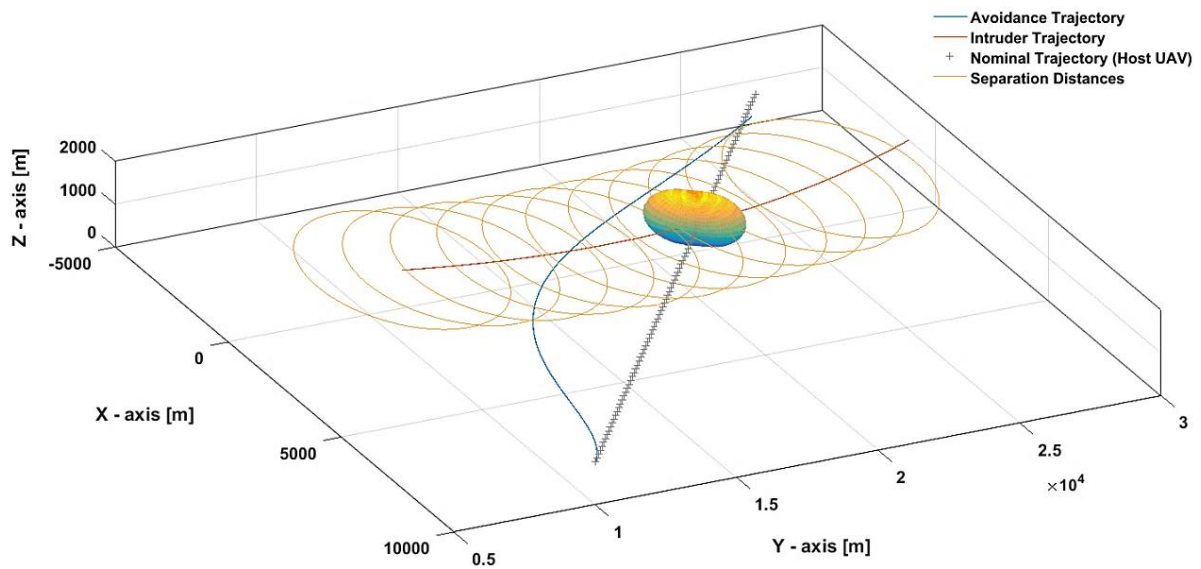


Figure 7.17. Avoidance of other traffic by host aircraft platform.

The avoidance trajectory is initiated by the SA&CA system when the probability of collision exceeded the required threshold value. Time and fuel were used in the cost functional; the aircraft dynamic model was used as a dynamic constraint, and the elevation criteria as path constraints for differential geometry or pseudospectral

trajectory optimisation algorithms. Three distinct points associated with the avoidance algorithms include:

- Break-off Point: Corresponding to the point where the host UAV initiates the avoidance trajectory (commanded by the SA&CA system). The cost function criteria adopted in this case is minimum time;
- Safe Maneuvering Point: Corresponding to the point where the host UAV can maneuver safely (any maneuver within its operational flight envelope) as it has approximately 0 ROC. From this point onwards the SA&CA cost function criteria switches to minimum time and minimum fuel to get back on the original (desired) track;
- Re-join Point: Corresponding to the point where the host UAV re-joins the original (desired) track.

After the obstacles are detected and tracked, an avoidance trajectory is generated and the corresponding action commands are executed. As a result, the intruder is evaded and the trajectory of the host aircraft is restored to its original intended path after performing the avoidance manoeuvres.

## 7.5 Conclusions

In this chapter, the algorithms used for intruder detection and avoidance were described. Simulation case studies on the application of a unified approach to Separation Assurance and Collision Avoidance (SA&CA) for detecting and avoiding aerial targets were presented. The generation of an avoidance volume, when in the presence of non-cooperative sensors (forward-looking sensors) as well as cooperative systems such as Automatic Dependent Surveillance Broadcast (ADS-B) was demonstrated. Simulation case studies were also presented for the analysis of relative dynamics between platforms.

## 7.6 References

1. R. Carnie and R. Walker, "Image Processing Algorithms for UAV Sense and Avoid", Proceedings of the 2006 IEEE International Conference on Robotics and Automation, Orlando, USA, pp. 2848-2853, 2006.
2. Flightglobal and FLIR Systems, "Farnborough Day 1 Flying Display in Infrared," 2012.
3. RTCA, "Minimum Operational Performance Standards (MOPS) for Aircraft Surveillance Applications (ASA) System", DO-317B, Radio Technical Commission for Aeronautics, Washington DC, USA, 2011.

4. RTCA, "Safety, Performance and Interoperability Requirements Document for Enhanced Air Traffic Services in Radar-Controlled Areas Using ADS-B Surveillance (ADS-B-RAD)", DO-318, Radio Technical Commission for Aeronautics, Washington DC, USA, 2009.

This page is intentionally left blank to support presswork tasks



## CHAPTER 8

# POTENTIAL UAS TRAFFIC MANAGEMENT APPLICATIONS

*"Everything, however complicated - breaking waves, migrating birds, and tropical forests - is made of atoms and obeys the equations of quantum physics. But even if those equations could be solved, they wouldn't offer the enlightenment that scientists seek. Each science has its own autonomous concepts and laws".*

- Martin Rees

### 8.1 Introduction

The integration of UAS is targeted by the UTM system to ensure safety and operation efficiency of the airspace. Some lessons learnt from low-altitude uncontrolled airspace operations of helicopters, gliders and general aviation aircraft are used in UTM system implementation. Uncertainties in navigation and tracking error measurements associated with each manned/unmanned platform (as seen by all other conflicting platforms) are required to be combined statistically to generate avoidance volumes for manual as well as autonomous operations. The unified approach to SA&CA provides the framework to generate uncertainty volumes at discrete time intervals as a function of traffic relative dynamics and thus supports the generation of dynamic geo-fences and UTM system implementation. Preliminary case studies are performed for evaluating the feasibility and potential of applying the unified approach to SA&CA in an urban environment.

### 8.2 UTM System in the CNS+A Framework

A brief introduction on UTM system implementation preliminaries was presented in Chapter 2 (Section 2.9).

Opportunities exist for UTM research and technology in several key areas including [1-7]:

- safe and efficient airspace operations including Beyond Line-of-Sight (BLoS) autonomous operations;
- tracking and locating every cooperative and non-cooperative UAS using a variety of techniques including cellular, satellite and automatic dependent surveillance technologies;
- SA&CA techniques for implementing an efficient TDA loop for avoiding any aerial and ground targets including small wires, poles, etc.;
- command, control and communications, including coordinated manned and unmanned aircraft operations;
- first/last 50 feet supported by sensors, hardware and software (algorithms) for autonomous operations;
- security considerations including providing effective countermeasures against cyber-physical attacks.

In the CNS+A framework, the general case is that of multiple manned/unmanned aircraft performing either cooperative or non-cooperative surveillance. Research is on-going on a regional as well as global scale for demonstrating the feasibility of the UTM concept [1, 2]. The UTM system provides remote pilots the information needed to maintain separation from other aircraft by reserving areas for specific routes, with consideration of restricted airspace and adverse weather conditions. The UTM concept is illustrated in Figure 8.1, highlighting CDM between UAS operation centres and UTM stakeholders.

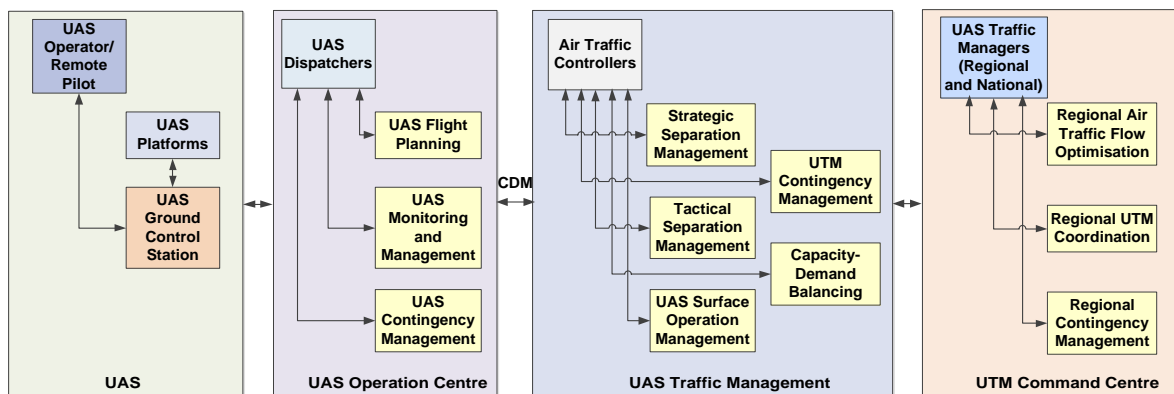


Figure 8.1. UTM system concept.

Strategic separation coordination and some tactical separation management are considered as part of UTM in addition to contingency management, surface operation management and capacity-demand balancing. In the long term, UTM research is envisaged to integrate in particular, the functionalities for trajectory prediction and

negotiation, conflict detection and resolution, separation/spacing monitoring and optimisation for mixed manned/unmanned aircraft traffic both within individual controlled airspace sectors and across multiple sectors belonging to a FIR, also considering the inbound/outbound flows from adjacent FIRs. Additionally, UTM supports functions associated with airspace design and management, geo-fencing, congestion management, authenticated operations and weather predictions. As a significant portion of the UAS fleet is specifically employed on an opportunity-basis with little to no advance planning, one of the key challenges that need to be addressed is the access of this opportunistic UAS traffic to controlled airspaces and the subsequent implications on design and development of future traffic management systems.

Typically, all flight geographies are composed of: independent conformance geography and protected geography. For an already accepted operation, if a new constraint (weather cell, security threat, ATM defined constraint, etc.) that intersects that operation's protected geography enters the UTM system, an alert will be generated by the UTM system and delivered to the concerned UAS operator/remote pilot. It is envisioned that the definition of the protected geography will be driven by a function of available data within the UTM system. Those data and the function would be available to all stakeholders, to improve understanding and collaboration within UTM. The UTM system concept can be extended to contain a number of UTM systems as shown in Figure 8.2. As an example, three UTM nodes are defined and three surveillance nodes A, B and C catering to the different UTM nodes. The surveillance nodes can provide services to more than UTM node as shown in Figure 8.2. The UTM nodes are constructed using regular polygons, which do not intersect with one another. Since UAS operations is possible across a number of UTM nodes, soft and hard handoffs can be employed based on the surveillance technology involved. All UAS platforms (different configurations and types) can be catered to using this approach.

### **8.3 Multi-UTM System**

Surveillance nodes consist of non-cooperative sensors (radar, camera, etc.) and cooperative systems (ADS-B, TCAS, etc.). These surveillance nodes are generally geographically decoupled from the UTM nodes. The UTM nodes consist of data management entities (local and global gateways). UTM nodes may or may not require coverage by surveillance nodes (i.e. depending on applications, risk, performance, etc.). However it is assumed that if a UTM node region does need surveillance, it is fully encompassed by one or more surveillance node volumes.

From Figure 8.2, it can be seen that the coverage of UTM node 1 is split by surveillance nodes A and B. The UTM node 2 is covered by the surveillance node B. The concept of a hand-off is applicable when a RPAS passes from one surveillance node to another. Surveillance nodes can also be categorised as:

- manned aircraft only (mostly cooperative),
- unmanned aircraft only (mostly non-cooperative),
- cooperative manned and unmanned aircraft only,
- cooperative manned aircraft and non-cooperative unmanned aircraft only,
- cooperative/non-cooperative (mixed equipage) manned and unmanned aircraft.

This methodology, driven by the unified approach to SA&CA, can be in turn be used to develop and manage key parameters of DAM, which include traffic density per unit volume, sector boundary optimisation, and required CNS services. The dynamic reconfiguration of airspace is performed by varying the lateral shape (different volumes obtained from the unified approach) of the control sectors, and new vertices/faces are added based on the employed SA&CA algorithms.

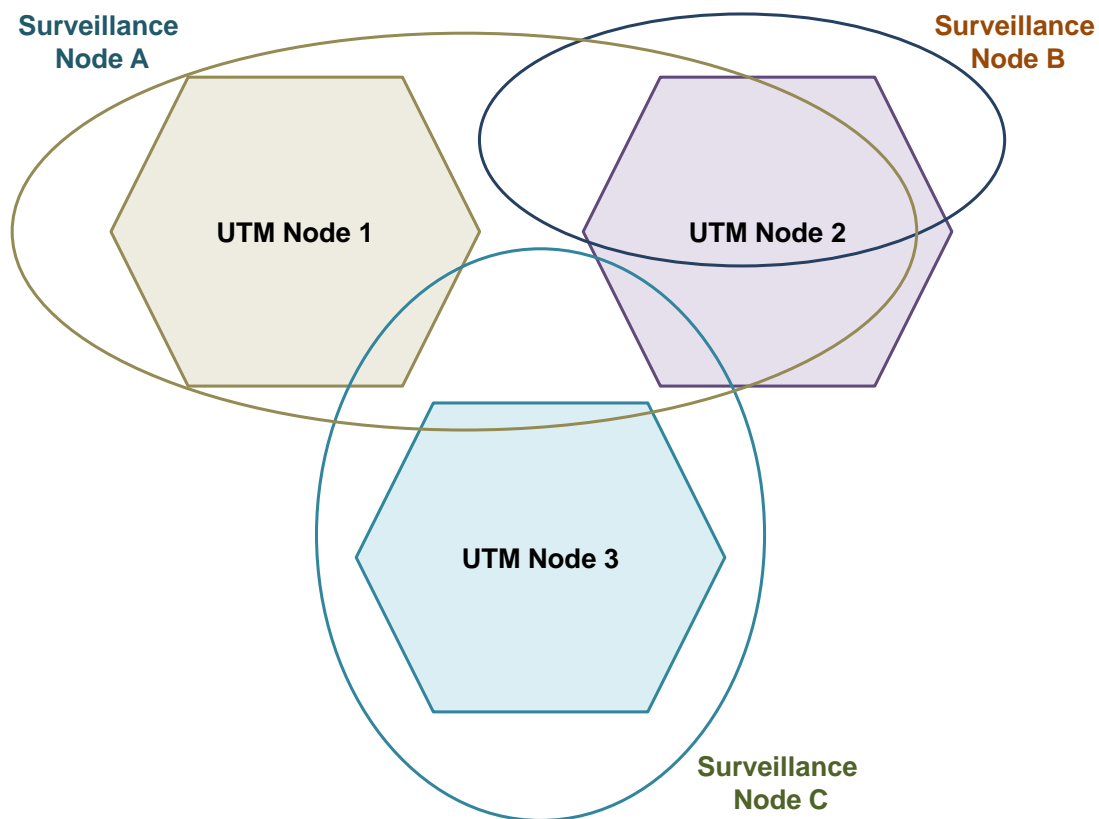


Figure 8.2. UTM and surveillance nodes.

## 8.4 Pathways to Implementation

One of our traditional conceptions of warfare and UAS operations has been severely disrupted over the last few years, in a sense that the operational space has shifted from the field to the urban environment. This shift is driving a fundamental change in the operation of UAS in a variety of civil and military applications, with concomitant implications for technology development. The systems and assets required to support open field campaigns are qualitatively different from that needed for Military Operations in Urban Terrain (MOUT). Surveillance and reconnaissance operations in cities and towns are a particular topic of interest. The urban environment is sufficiently different that the utility of conventional sensing and communication platforms is rendered problematic. In virtually all cases, the principal rationale for these vehicles is to help establish and enhance sensing and communication networks in a network-centric environment [8].

### 8.4.1 Multi-Platform Scenario

The urban space is a dynamic environment. Small buildings arise in a matter of weeks, and large buildings in months. Parked or abandoned vehicles and obstacles can be perfectly effective blockades, and require a reactive, close-in mode of sensing. In fact, geometrically, the urban space is of an entirely different scale than the traditional kind of aircraft operations. While in free-space environments the focus has been on formation flight and collective trajectory generation and tracking, urban environments impose different challenges and offer different opportunities. In some situations, UAS can assist one another, by serving as nodes or repeaters in a communications network, as lookouts, decoys, or as slaved remote sensors. In even tighter models of collaboration, multiple vehicles can be used to multi-laterate on a target signal; i.e., take signal strength and/or directional measurements that can later be combined to geolocate the target with more precision than any single vehicle-borne sensor possibly could [9].

Figure 8.3 shows one of the various possible scenarios of multi-platform operations in an urban environment. In this scenario, three airspace sectors are considered. The uncertainties in navigation and tracking associated with each manned/unmanned platform (as seen by all other conflicting platforms) are combined to generate avoidance volumes surrounding each aircraft. The avoidance volumes are computed at discrete time intervals as a function of traffic relative dynamics. The host and other traffic may be equipped with non-cooperative sensors, cooperative systems or combinations thereof. Figure 8.3 also shows a conceptual representation of the variable avoidance volume associated with aircraft 4, obtained by combining (in a statistical

sense) the navigation and tracking errors related to cooperative and non-cooperative SA&CA observations by all other aircraft at sequential time epochs as well as a function of relative dynamics.

The more recent advances in Communication, Navigation, Surveillance, ATM and Avionics (CNS+A) technologies are progressively supporting the introduction of dynamic DCB strategies. The new CNS+A technologies greatly increase the flexibility of routes and airspace configurations, which are both of great use for DCB. The novel CNS+A systems for TBO/IBO are conceived to meet the ambitious CNS performance requirements and expected to support an increase in traffic density without compromising flight safety. These include the Next Generation Flight Management System (NG-FMS), Next Generation ATM (NG-ATM) and UTM systems, supported by high-throughput, secure and reliable data links. The capacity can be therefore expressed as a function of the CNS performance as follows. The capacity factor of airspace sector  $i$  due to Communication Performance (CP) alone can be expressed as a factor of the minimum CP guaranteed by all traffic  $j$  concurrently in the sector. An example, in terms of Communication Integrity (CI) is given by [10]:

$$Cap_C \propto \min_j CI_{i,j} \quad (8.1)$$

Similar expressions hold true for Navigation Integrity (NI) and Surveillance Integrity (SI):

$$Cap_N \propto \min_j NI_{i,j} \quad (8.2)$$

$$Cap_S \propto \min_j SI_{i,j} \quad (8.3)$$

After obtaining all the avoidance volumes in airspace sector 3, the largest of the four avoidance volumes is selected as a reference to perform DCB. In addition to the CNS systems both onboard and on the ground that dictate the adherence RTSP, the SA&CA functionalities provide a methodology to perform DCB.

As shown in Chapter 5, given any two aircraft in the same or adjacent airspace sectors, the condition before collision are such that the radial distance between the host aircraft and intruder is decreasing. This is a necessary condition for a collision. Considering the scenario presented in Figure 8.3, the necessary conditions between the host aircraft (H) and the other four intruder (I) platforms are given by:

$$\frac{d||\vec{r}_{HI}||}{dt} < 0 \quad (8.4)$$

and

$$||\vec{r}_{HI}|| = ||\vec{r}_{IH}|| \quad (8.5)$$

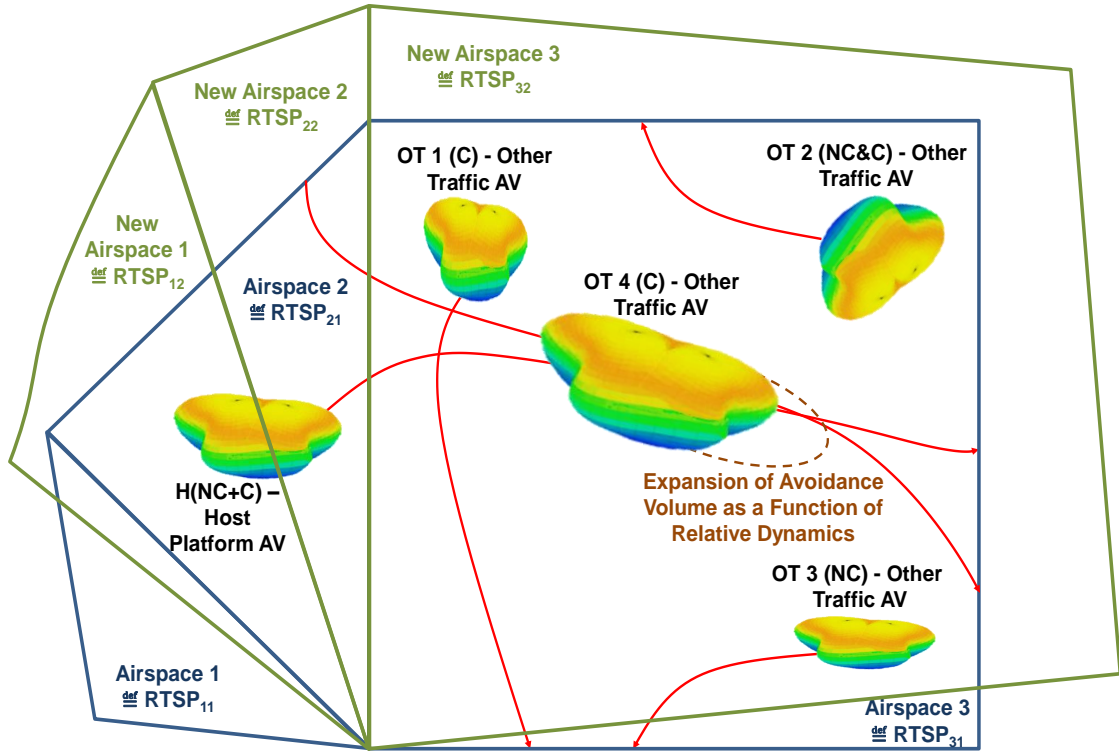


Figure 8.3. Multi-platform scenario.

where  $i = 1$  to 4 representing the number of intruders. Conditions can be described in relative perspective with respect to an observer in the host aircraft or in any of the four intruder platforms. An overall avoidance volume, given by  $\vec{r}_H + \vec{r}_{I_i}$  is defined for each intruder. The relative dynamics analysis allows expressing the rate of change of radial distance in terms of measured variables.

$$\frac{d\|\vec{r}_{HI_i}\|}{dt} = \vec{r}_{HI_i}^T \cdot \vec{v}_{HI_i} \quad (8.6)$$

$$\frac{d\|\vec{r}_{I_iH}\|}{dt} = \vec{r}_{I_iH}^T \cdot \vec{v}_{I_iH} \quad (8.7)$$

Relative position and relative velocity are obtainable from direct measurements by onboard non-cooperative sensors or cooperatives systems. The estimated time-to-collide ( $t_c$ ) is the time instance with respect to current condition when collision is estimated to occur, and is given by:

$$t_c = \frac{\|\vec{r}_{I_iH}\| - (\vec{r}_H + \vec{r}_{I_i} + \vec{r}_{clear})}{\|\vec{v}_{HI_i}\|} \quad (8.8)$$

The above condition is not sufficient for a collision to occur. For example, if trajectories of the host aircraft and an intruder are parallel to each other, collision may not occur if the separating distance between trajectories exceed certain value, namely the sum of both

object's size radii. Therefore, another condition must be identified that will make a sufficient condition for the collision condition. By identifying the angle of miss and angle of encounter, the sufficient conditions for avoiding a collision are obtained.

$$\overrightarrow{r_{HI_i}}^T \cdot \overrightarrow{v_{HI_i}} < 0 \quad (8.9)$$

or

$$\overrightarrow{r_{I_iH}}^T \cdot \overrightarrow{v_{I_iH}} < 0 \quad (8.10)$$

The vectors for relative position and velocity are given by:

$$\overrightarrow{r_{HI_i}} = \overrightarrow{r_H} - \overrightarrow{r_{I_i}} \quad (8.11)$$

$$\overrightarrow{v_{HI_i}} = \overrightarrow{v_H} - \overrightarrow{v_{I_i}} \quad (8.12)$$

$$\overrightarrow{v_{HI_i}} = \overrightarrow{v_{HI_i r}} + \overrightarrow{v_{HI_i t}} \quad (8.13)$$

where  $\overrightarrow{v_{HI_i r}}$  and  $\overrightarrow{v_{HI_i t}}$  are the radial and tangential components of the vector. The tangent angle is the angle of encounter,  $\psi$ . The radial and tangential components are given by:

$$\overrightarrow{v_{HI_i r}} = \left| \overrightarrow{v_{HI_i}} \right| \cdot \cos \psi_{HI_i} \cdot \overrightarrow{I_{HI_i r}} \quad (8.14)$$

$$\overrightarrow{v_{HI_i t}} = \left| \overrightarrow{v_{HI_i}} \right| \cdot \sin \psi_{HI_i} \cdot \overrightarrow{I_{HI_i t}} \quad (8.15)$$

where:

$$\overrightarrow{I_{HI_i r}} = \frac{\overrightarrow{r_{HI_i}}}{\left| \overrightarrow{r_{HI_i}} \right|} \quad (8.16)$$

$$\overrightarrow{I_{HI_i t}} = \overrightarrow{I_{\psi_{HI_i}}} \times \overrightarrow{I_{r_{HI_i}}} \quad (8.17)$$

#### 8.4.2 TMA Environment

In terms of granting the required levels of operational safety when considering the integration of unmanned traffic in an airspace characterised with dense air traffic, the emphasis is on CNS+A equipment that can meet strict performance requirements while also supporting enhanced ATM functionalities. These systems will enable the UTM paradigm to support flow management functions. In particular, in order to grant the required surveillance performance and SA&CA capabilities for unrestricted access to controlled airspace, UAS surveillance equipment involve a combination of non-cooperative sensors, as well as cooperative systems. In order to overcome the limitations



in current ACAS, the FAA has funded research on the Next Generation Airborne Collision Avoidance System - ACAS X.

Some of the key limitations in current ACAS include inadequate/improper coordination with ATM and/or air traffic flow management systems, lack of terrain/ground and obstacle awareness, primarily range-based presentation of traffic and unsuitability to include UAS in the framework. Therefore, taking advantage of recent advances in computational techniques and keeping pace with planned future operational concepts, Voice/data/network radio communication system and satellite communication systems data links act as the backbone for LoS and BLoS communications between air-to-air, air-to-ground and ground-to-ground systems. As an example, a deconfliction scenario in the context of an arrival point merge in the TMA is illustrated in Figure 8.4.

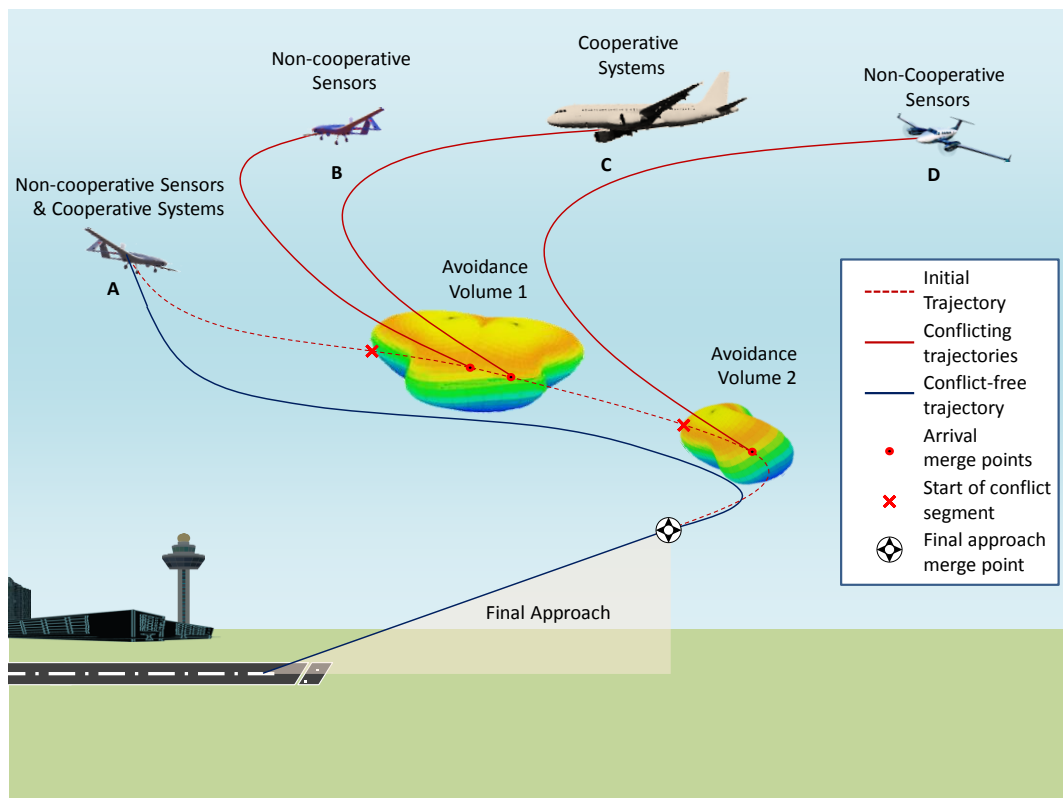


Figure 8.4. Deconfliction scenario in the TMA [11].

In this scenario, the predicted trajectory of an unmanned aircraft (traffic A) is conflicting with another unmanned aircraft (traffic B), a commercial airliner (traffic C) and a general aviation aircraft (traffic D) at three distinct points. Traffic A is equipped with both non-cooperative sensors/cooperative systems for SA&CA and traffic B has on-board non-cooperative sensors only. Traffic C is equipped with cooperative traffic collision detection and avoidance systems (e.g., based on ADS-B), whereas the general aviation

aircraft (traffic D) features a non-cooperative collision avoidance system (e.g., machine-vision/radar based). Based on the traffic data exchanged or sensed, traffic A's NG-FMS generates three distinct avoidance volumes. In this example, the volumes associated with traffics B and C are merged into a combined volume (avoidance volume 1) when the algorithm detects they are overlapping. A similar process is repeated for all four aircraft in the TMA (in this case, the TMA control service defines a sequencing approach based on first-come first-served and/or best-equipped best-served) and the resulting path constraints are fed to the 4DT planner and optimiser modules of the NG-FMS in order to generate four conflict-free trajectory solutions. These intents are then sent to the NG-ATM system. Alternatively, implementing a fully automated approach, the uncertainties in navigation and tracking associated with each manned/unmanned platform (as seen by all other conflicting platforms) are combined to generate avoidance volumes surrounding each aircraft in the TMA. The uncertainty volumes are computed at discrete time intervals as a function of traffic relative dynamics.

Figure 8.5 shows a conceptual representation of the variable avoidance volume associated with traffic A obtained by combining (in a statistical sense) the navigation and tracking errors related to cooperative and non-cooperative SA&CA observations by all other aircraft at sequential time epochs.

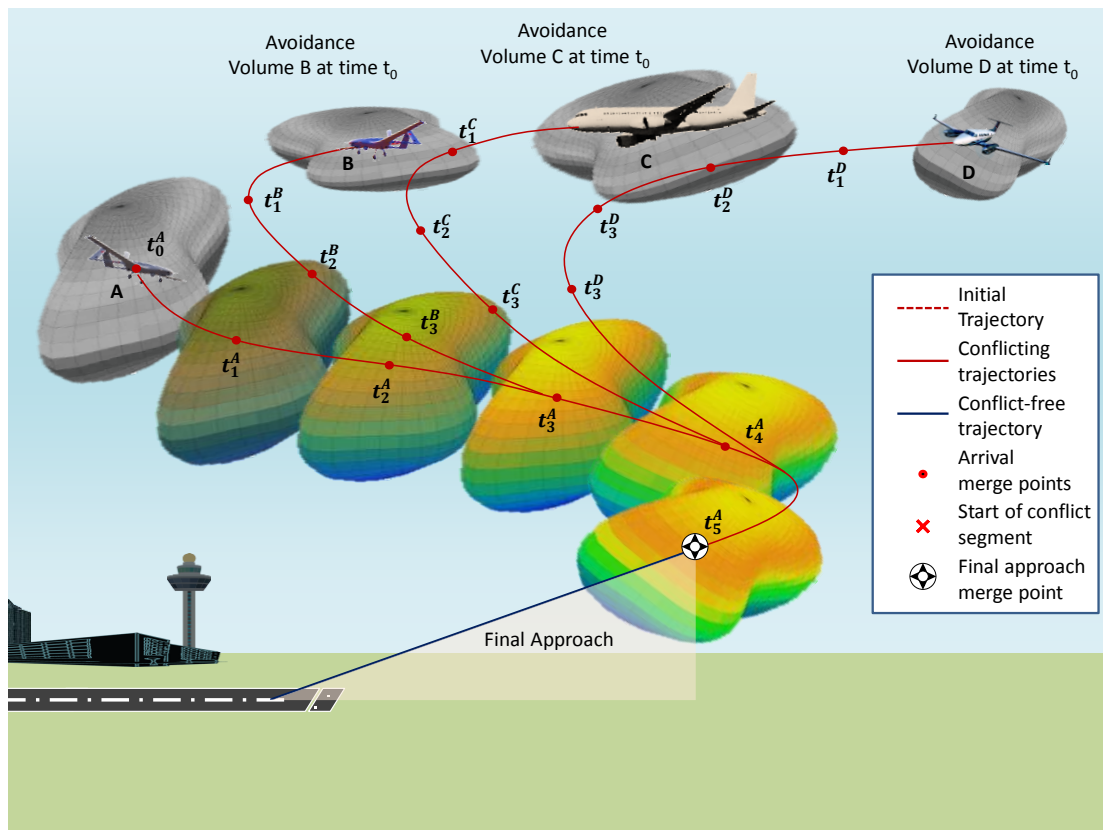


Figure 8.5. Fully autonomous deconfliction scenario in the TMA [11].

In this case, the NG-FMS exchange real-time avoidance information updates, compute the optimal 4DT to be executed by each platform and communicate these intents to the NG-ATM system. The concept of automated SA&CA operations for this scenario provide the following characteristics [12]:

- Airspace building blocks may or may not be necessary;
- Automated SA&CA;
- All aircraft are capable of automated SA&CA; or fewer unequipped aircraft and more aircraft with automated SA&CA functionalities;
- Addresses complexity management;
- Arrival intents begin at top of descent, departure corridors end at top of climb, overflight corridors may connect wind optimal user preferred routes;
- Intents are dynamic, based on DCB and weather conditions;
- Controller primarily manages air traffic flow, or else controller manages flows as well as conflicts between aircraft with mixed equipage.

## 8.5 Simulation Case Studies

The case studies performed for evaluating the feasibility and potential of applying the unified approach to SA&CA in the UTM context are presented in this section. The case studies are performed in realistic scenarios such as urban environments. Different urban environments were simulated with realistic models obtained from SketchUp™ as shown in Figure 8.6.

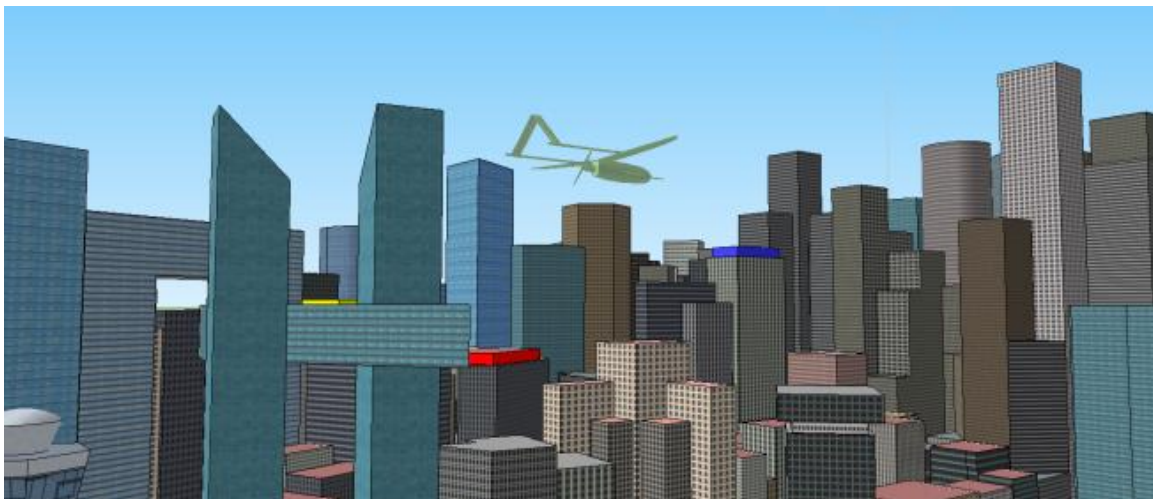


Figure 8.6. Simulated urban environment.

After conceptualising the required scenario of the urban model, the file with the Stereolithography File (STL) extension was exported to a MATLAB environment. The STL file segregates the environment to a number of objects characterised by faces and vertices of a 3D surface geometry. The surface of each object is composed of a number of oriented facets, each of them consisting of a unit normal vector to the facet and a set of three points listed in counter clockwise order representing the vertices of the facet. This representation is suitable for performing computations in a MATLAB environment. The STL standard includes two data formats including ASCII and binary. The ASCII code format was selected to support an easier implementation in MATLAB. The AEROSONDE™ was used as the UAS platform. The modelled environment and the UAV geometry imported into the MATLAB™ environment are shown in Figure 8.7.

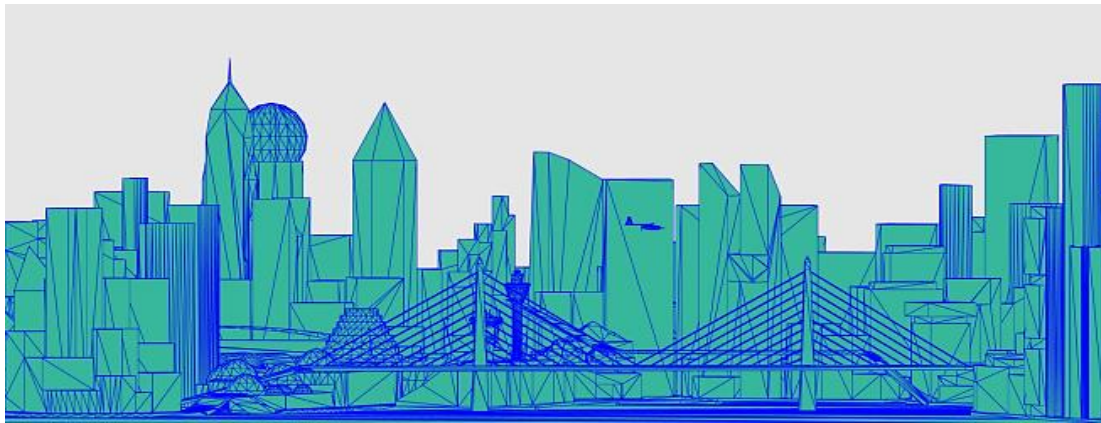


Figure 8.7. Simulated urban environment in MATLAB™.

After importing the STL file in MATLAB, all of the objects were meshed and appropriate geo-fences were constructed for trajectory planning and real-time optimisation. As an example, the vertices of ten selected objects from the scenario are shown in Figure 8.8.

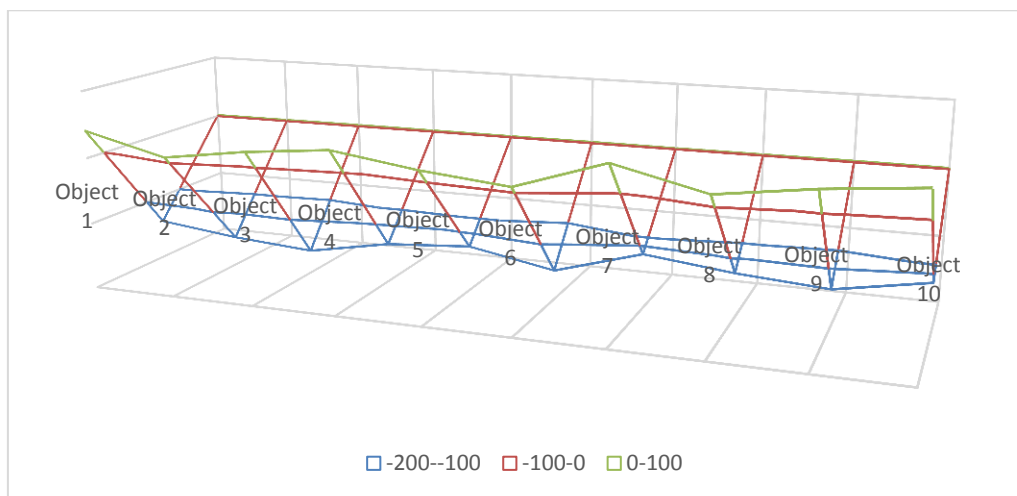


Figure 8.8. Vertices of imported objects.



The overall simulation environment is shown in Figure 8.9 and the AEROSONDE™ UAS is also highlighted. The top view (2D) of the simulation environment after importing into MATLAB is shown in Figure 8.10.

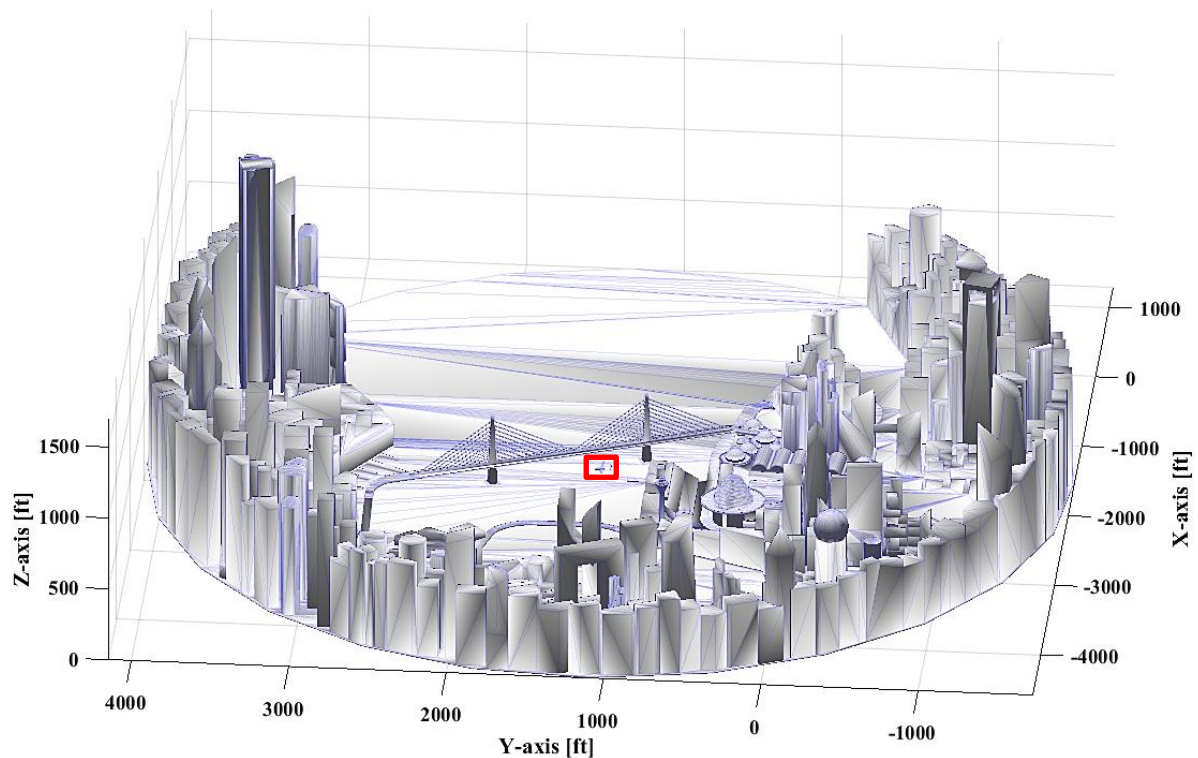


Figure 8.9. Simulated urban environment in MATLAB™ (3D).

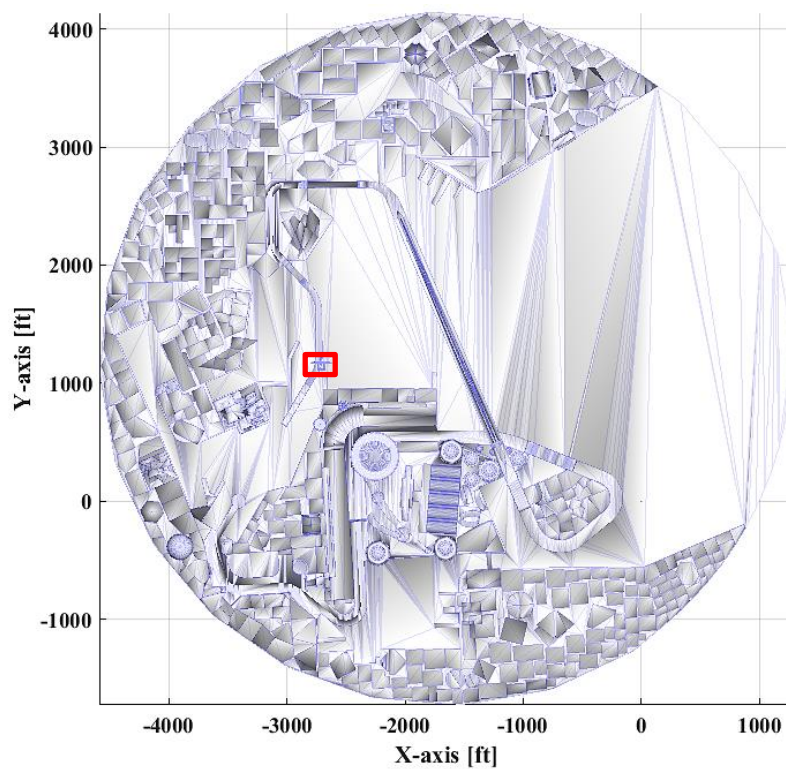


Figure 8.10. Simulated urban environment in MATLAB™ (2D).

In an UTM system, by definition, geofences can be both static and dynamic. Important landmarks such as main government headquarters are often designed to be enclosed by a static geofence while dynamic geofences are constructed around moving objects and vary depending upon the available situational awareness. However, in the unified approach to SA&CA, all geofences are considered to be dynamic, taking into consideration the errors in navigation measurements of the host platform and tracking measurements of other objects (static and dynamic), thus improving safety and efficiency of manned and unmanned aircraft operations but increasing computational overhead and cost.

Real-time trajectory optimisation takes into account the current FoV, a history database of all detected objects and the geofences to be avoided at that point of time. The UAV with the current FoV is shown in Figure 8.11.

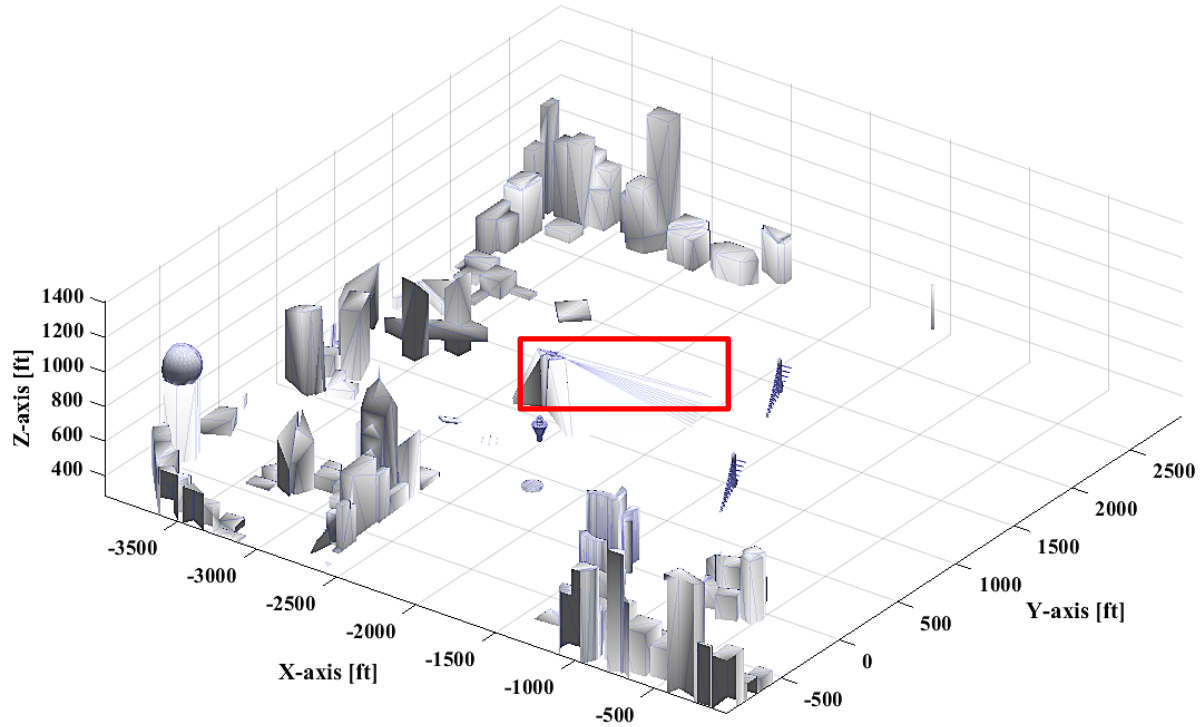


Figure 8.11. UAV and the current FoV.

The next subsequent step involves the selection of the optimal trajectory from the generated set of safe trajectories, which is then provided in the form of steering commands to the aircraft guidance subsystem of the NG-FMS. The implemented decision logics are based on minimisation of the following cost function as discussed earlier in Chapter 5:

$$J = w_t \cdot t_{SAFE} - w_d \cdot d_m(t) + \int [w_f \cdot SFC \cdot T(t)] dt \quad (8.19)$$

where, given  $T_T$  as the time-to-threat and  $T_A$  as the avoidance manoeuvre time,  $t_{SAFE}$  is the time at which the safe avoidance condition is successfully attained, defined as:

$$t_{SAFE} = T_T + 2 T_A \quad (8.20)$$

$SFC \left[ \frac{\text{kg}}{\text{N}} \cdot \text{s} \right]$  is specific fuel consumption,  $T(t)$  is thrust profile and the coefficients  $w_t, w_f, w_d$  are the weights attributed to time, fuel and distance respectively. The term  $dm(t)$  corresponds to the minimum distance from the dynamic geo-fence, which is given by:

$$d_m(t) = \min \left[ \sqrt{(x(t) - x_{GF}(t))^2 + (y(t) - y_{GF}(t))^2 + (z(t) - z_{GF}(t))^2} \right] \quad (8.21)$$

where  $x_{GF}$ ,  $y_{GF}$  and  $z_{GF}$  are the coordinates of the bounding surfaces of the dynamic geo-fence. The optimised trajectory generated in the given urban scenario at the current epoch is shown in Figure 8.12.

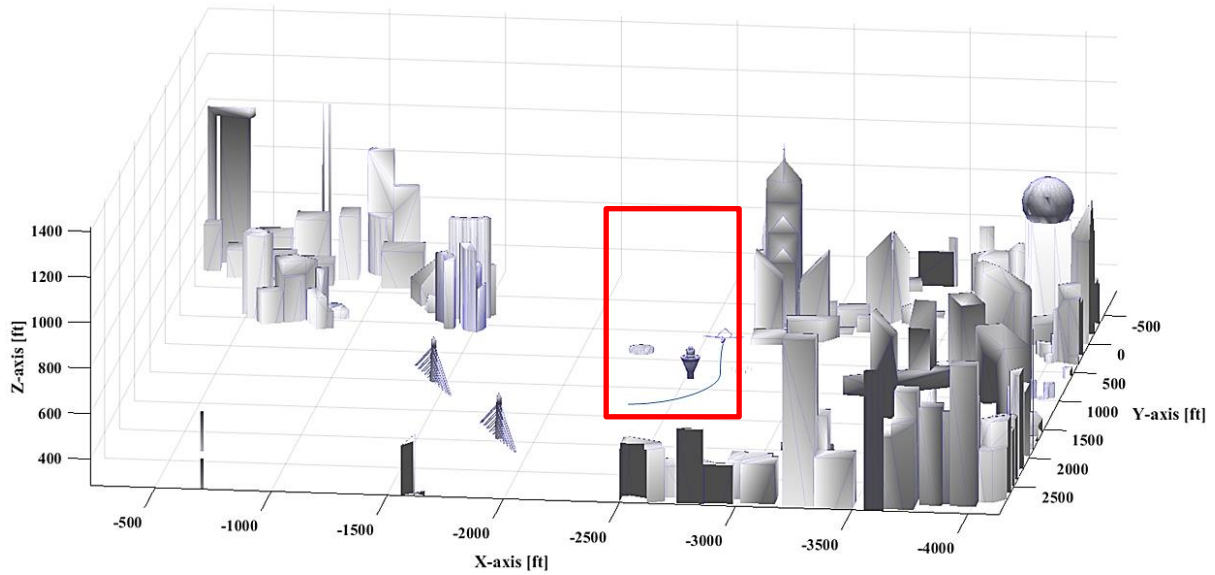


Figure 8.12. Optimised trajectory of the unmanned aircraft.

### 8.5.1 Geofences

Simulation case studies for UAS SA&CA in an UTM context demonstrated the functional capability of the NG-FMS to generate dynamic geo-fences satisfying the operational requirements of typical tactical online tasks (in the order of 84 seconds) as well as emergency scenarios (in the order of less than 10 seconds). Further Simulation case studies were performed to assess the NG-FMS algorithms ability to generate geo-fences and optimised trajectories. Figure 8.13 shows avoidance trajectory generation indicating geo-fences. In this case, a ground obstacle is detected by a non-cooperative sensor and a geo-fence is constructed around the detected obstacle. The obstacles can be categorized into point, lateral (e.g., wires) and extended structure targets. These

simulations were executed on a Windows 7 Professional workstation (64-bit OS), supported by an Intel Core i7-4510 central processing unit with clock speed 2.6 GHz and 8.0 GB RAM. The total execution time for uncertainty volume determination, as well as avoidance trajectory optimisation algorithms was in the order of 1.4 sec, supporting real-time implementation of the developed algorithms. Figure 8.13 shows the generation of an appropriate geofence for a number thin wires detected in the current FoV of the UAV.

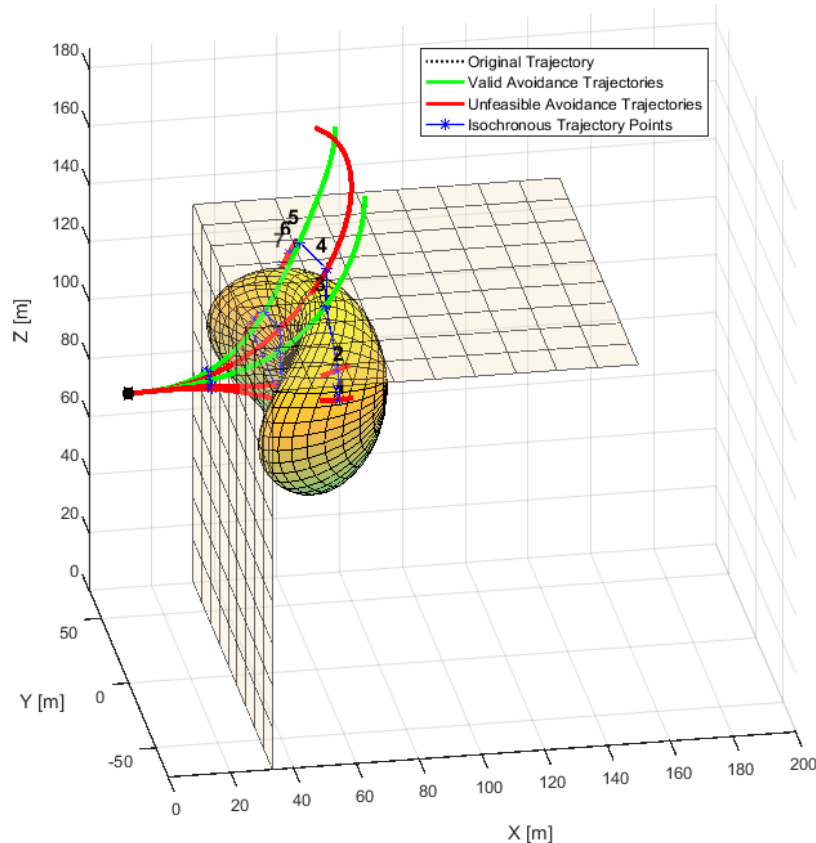


Figure 8.13. Avoidance of a ground obstacle geofence.

In the case of moving targets, a suite of non-cooperative sensors and cooperative systems can be employed to detect and re-optimize the trajectory (Figure 8.14).

If there is a possibility of a collision that is determined after evaluating the Risk-of-Collision (RoC), an uncertainty volume is computed according to the models described earlier in Chapter 4 (Section 4.2). Therefore, trajectory re-optimization routines are performed to obtain a safe avoidance of all the detected collisions. The algorithms thus support the generation of appropriate dynamic geo-fences, whose characteristics are dictated by the obstacle classification and intruder dynamics, to allow computation of the optimal avoidance flight trajectories.



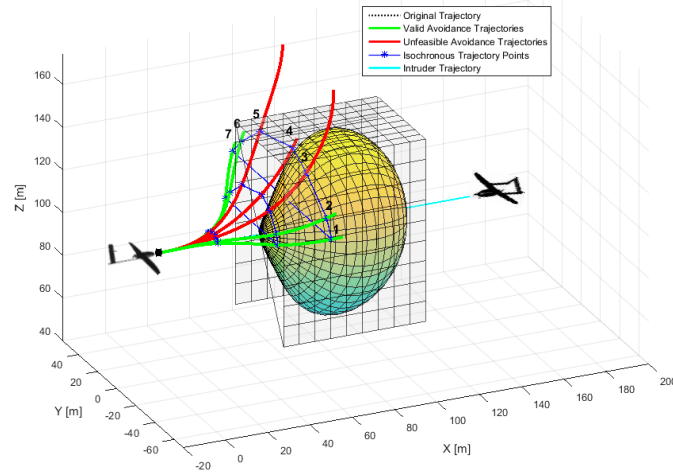


Figure 8.14. Avoidance of an aerial obstacle geofence.

### 8.5.2 Multi-Platform Coordination Scenario

A simulation case study for UAS SA&CA in a multi-platform coordination scenario was performed. In this scenario, it is assumed that the host aircraft is equipped with NG-FMS and both cooperative (ADS-B) and non-cooperative (FLS) means of intruder detection are present. Intruder 1 is not equipped with either a cooperative system or a non-cooperative sensor. Intruders 2 and 3 are equipped with ADS-B. Intruder 4 employs a NG-FMS with SA&CA algorithms. The airspace sectors are similar to the scenario described in Figure 8.3, with the host aircraft occupying an airspace sector and all other intruders occupying another airspace sector. The scenario is shown in Figure 8.15.

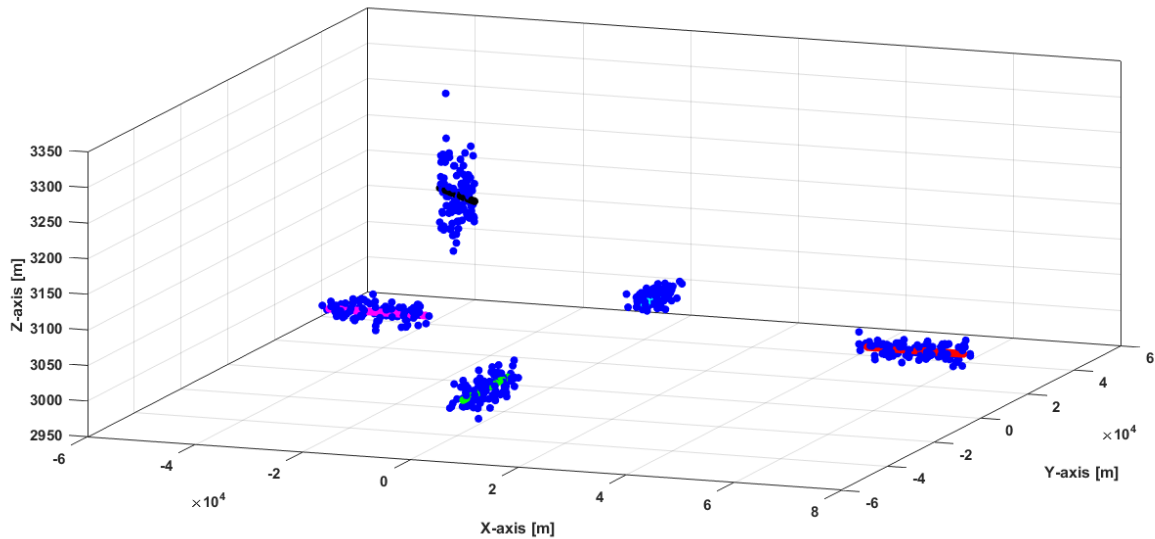


Figure 8.15. Multi-platform coordination scenario.

The uncertainties in navigation and tracking associated with each platform (as seen by all other conflicting platforms) are combined to generate avoidance volumes surrounding each aircraft. The avoidance volumes are computed at discrete time intervals as a function of traffic relative dynamics. Figures 8.16 to 8.18 show the horizontal and vertical resolution obtained between the host platform and the three intruders, which do not have a direct head-on collision probability. After obtaining all the avoidance volumes in the given airspace sectors, the largest of the four avoidance volumes are selected as a reference to perform DCB (intruder 4 in this case).

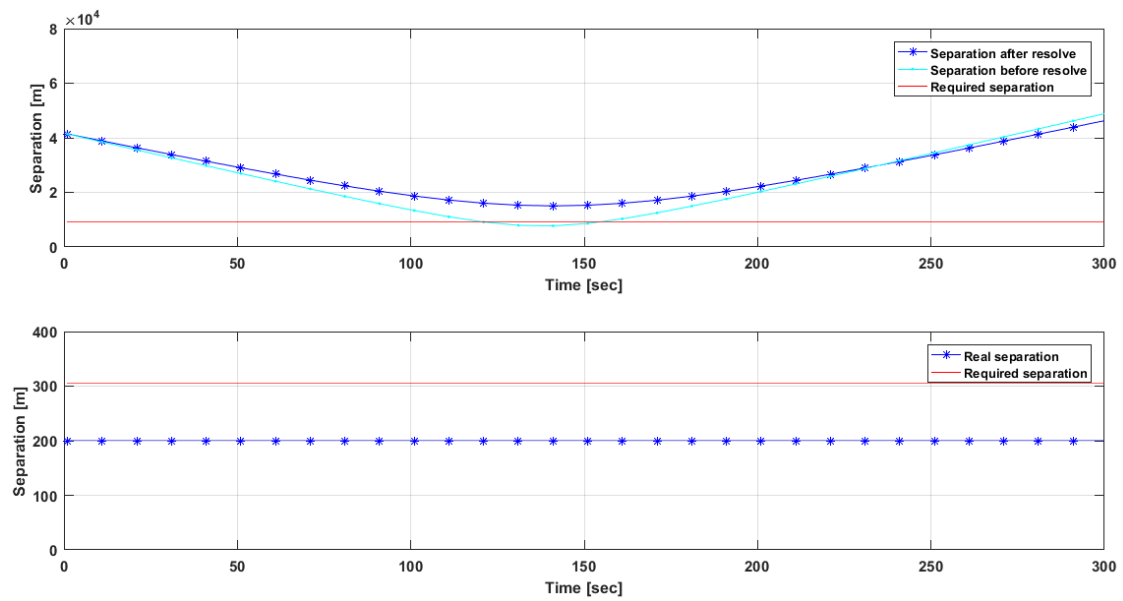


Figure 8.16. Horizontal and vertical resolution – intruder 1.

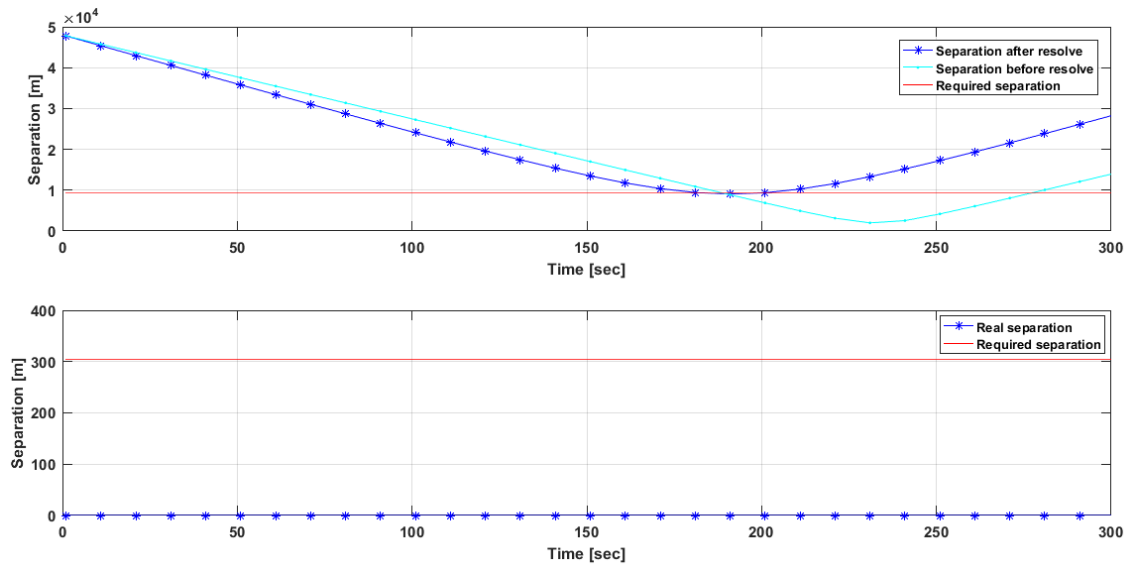


Figure 8.17. Horizontal and vertical resolution – intruder 2.

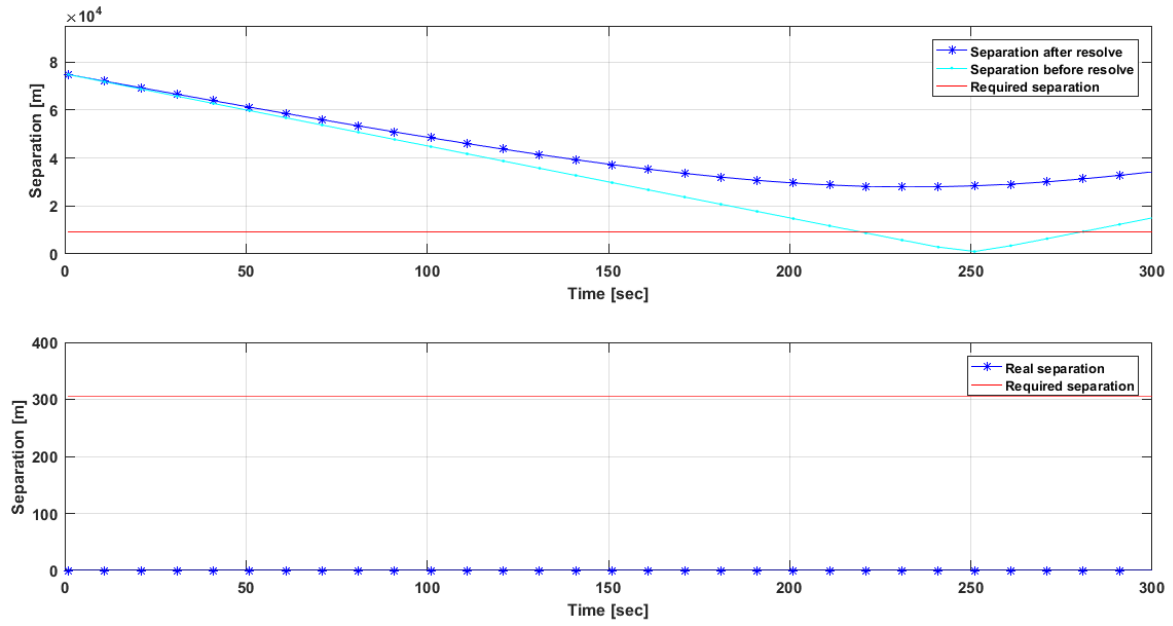


Figure 8.18. Horizontal and vertical resolution – intruder 3.

The avoidance volume generated with respect to intruder 4 dominates the DCB of airspace sector 3, along with the CNS performances available in the CNS+A network of that sector. With respect to intruder 4, since the generated avoidance trajectory deviates from the planned trajectory, a re-join trajectory command was performed to ensure that the generated intent leads back to the original trajectory. The avoidance trajectories were generated with respect to the cost function defined earlier. In the third case, both host and intruder platforms are assumed to have on board ADS-B systems.

The host unmanned platform computes an avoidance trajectory as per the rules of flight, while the other aircraft performs a step descend phase to avoid the mid-air collision. After the overall avoidance volume is computed, the avoidance trajectory and a subsequent re-join trajectory are generated by the NG-FMS as shown in Figure 8.19.

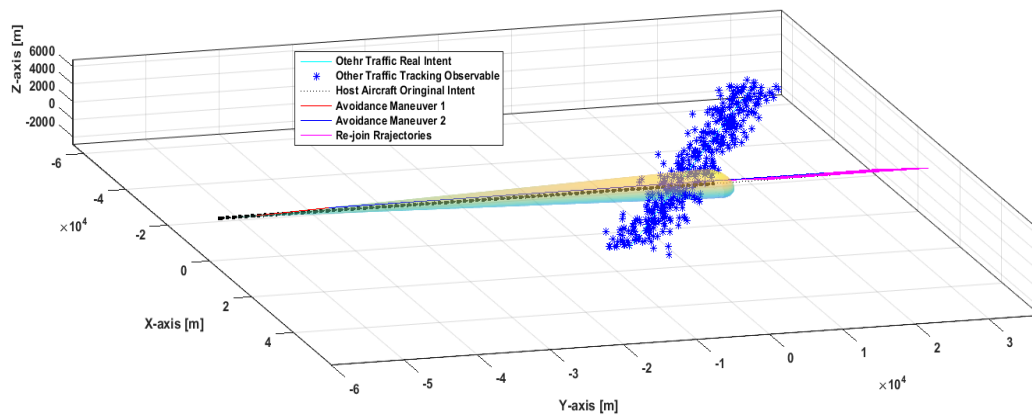


Figure 8.19. Re-optimised host platform trajectory.

## 8.6 Conclusions

The UTM system was introduced, which comprises the various elements required to support and execute UAS operations in low-altitude airspace. Specifically, the integration of small-size UAS into the airspace is targeted in the UTM system to ensure safety and operation efficiency. Some lessons learnt from low-altitude uncontrolled airspace operations of helicopters, gliders and general aviation aircraft are valuable in the UTM system implementation. Uncertainties in navigation and tracking associated to each manned/unmanned platform (as seen by all other conflicting platforms) were combined to generate avoidance volumes in all phases of flight (including low-altitude operations). The uncertainty volumes were computed at discrete time intervals as a function of traffic relative dynamics and thus support generation of dynamic geo-fences and multi UTM system implementation. Case studies were performed for evaluating the feasibility and potential of applying the unified approach to SA&CA in an urban environment.

## 8.7 References

1. P. Kopardekar, "Unmanned Aerial System (UAS) Traffic Management (UTM): Enabling Low-altitude Airspace and UAS Operations", ARC-E-DAA-TN32373, NASA Ames Research Center, NASA, Moffett Field, CA, USA, 2016.
2. J. Robinson, M. Johnson, J. Jung, P. Kopardekar, T. Prevot and J. Rios, "Unmanned Aerial System Traffic Management Concept of Operations (v0.5) (UTM CONOPS)", NASA TM draft, Moffett Field, CA, USA, 2015.
3. C.W. Johnson, "The Safety Research Challenges for the Air Traffic Management of Unmanned Aerial Systems (UAS)", Proceedings of the 6<sup>th</sup> EUROCONTROL Experimental Centre Safety Research and Development Workshop, Munich, Germany, October, Vol. 21, 2009.
4. Y. Kim, J. Jo and M. Shaw, "A Lightweight Communication Architecture for Small UAS Traffic Management (SUTM)", IEEE Integrated Communication, Navigation and Surveillance Conference (ICNS), pp. T4-1, 2015.
5. T. Prevot, J. Homola and J. Mercer, "From Rural to Urban Environments: Human/Systems Simulation Research for Low Altitude UAS Traffic Management (UTM)", 16<sup>th</sup> AIAA Aviation Technology, Integration, and Operations Conference, Washington DC, USA, p. 3291, 2016.

6. V. Milanés, J. Godoy, J. Pérez, B. Vinagre, C. González, E. Onieva and J. Alonso, "V2I-Based Architecture for Information Exchange among Vehicles", IFAC Proceedings, Vol. 43, Issue 16,, pp. 85-90, 2010.
7. P. Kopardekar, P. Lee, T. Prevot, J. Mercer, J. Homola, M. Mainini, N. Smith, A. Aweiss and K. Lee, "Feasibility of Mixed Equipage Operations in the Same Airspace", Eighth USA/Europe Air Traffic Management Research and Development Seminar (ATM2009), Napa, CA, USA, 2009.
8. T. Samad, J.S. Bay and D. Godbole, "Network-centric Systems for Military Operations in Urban Terrain: The Role of UAVs, Proceedings of the IEEE, Vol. 95, Issue 1, pp.92-107, 2007.
9. D.R.V. Rheeden, B.C. Brown, J.C. Price, B.A. Abbott, G.C. Willden, K. Chhokra, J. Scott, and T. Bapty, "Automatic Positioning of UAVs to Optimize TDOA Geolocation Performance", Proceedings of the 23<sup>rd</sup> Digital Avionics Systems Conference (DASC), pp. 24–28, 2004.
10. A. Gardi, S. Ramasamy, M. Marino, T. Kistan, R. Sabatini, M. O'Flynn and P. Bernard-Flattot, "Implementation, Verification and Evaluation of 4D Route Planning and Dynamic Airspace Functionalities in a Simulated Environment", Next Generation Air Traffic Management Systems: Multi-Objective Four-Dimensional Trajectory Optimisation, Negotiation and Validation for Intent Based Operations, THALES RMIT University Collaborative Research, Report 3, 2016.
11. A. Gardi, S. Ramasamy, R. Sabatini and T. Kistan, "Terminal Area Operations: Challenges and Opportunities", Encyclopedia of Aerospace - UAS, eds. R. Blockley and W. Shyy, John Wiley: Chichester, 2016.
12. P. Kopardekar, K. Bilimoria and B. Sridhar, "Initial Concepts for Dynamic Airspace Configuration", Proceedings of 7<sup>th</sup> AIAA Aviation Technology, Integration and Operations Conference (ATIO), Belfast, Northern Ireland, pp. 18-20, 2007.

This page is intentionally left blank to support presswork tasks

# CHAPTER 9

## CONCLUSIONS AND FUTURE DIRECTIONS

*"Great dreams of great dreamers are always transcended"*. – A.P.J. Abdul Kalam

### 9.1 Conclusions

The key design features of NG-FMS suitable for manned and unmanned aircraft operations were presented. In particular, the novel mathematical models required for the implementation of advanced SA&CA functionalities were developed. One of the key research contributions was the formulation of a unified methodology to support cooperative and non-cooperative SA&CA tasks, addressing the technical and regulatory challenges of manned and unmanned aircraft coexistence in all classes of airspace. The following section outlines the original contributions of this research project. The conclusions of this research project are further elaborated in terms of achieved research objectives in Section 9.4.

#### 9.1.1 Summary of Original Contributions

This research investigated the introduction of NG-FMS algorithms for planning and near real-time execution of 4DT functionalities in the TBO/IBO context as well as in the UTM framework. The key emphasis was on the development of a unified approach to SA&CA by considering navigation and tracking errors affecting the aircraft state vector and translating them to unified range and bearing uncertainty descriptors, which apply both to cooperative and non-cooperative scenarios. The main original contributions are summarised below:

- System architectures of the novel FMS for manned and unmanned aircraft operations;

- Adaptation of mathematical models for NG-FMS to provide 4DT optimisation and air-to-ground trajectory negotiation/validation to support TBO/IBO;
- Development of analytical models that describe a unified approach to cooperative and non-cooperative SA&CA providing the following key benefits:
  - An approach to combine the uncertainties in navigation and tracking measurements to generate overall avoidance volumes;
  - Avoidance volume determination at discrete time intervals as a function of relative dynamics (host platform and other traffic);
  - Real-time transformation of host aircraft navigation error and target tracking error affecting the state measurements to unified range and bearing uncertainty descriptors;
  - Detection and resolution of both cooperative and non-cooperative collision threats in various weather and daylight conditions; and also in case of adverse weather conditions;
  - Automatic selection of sensors/systems providing the most reliable SA&CA solution, providing robustness in all flight phases;
  - A compact and versatile parameterisation of the avoidance volume to extrapolate its actual shape and size at close encounter points with minimal data-link and computational burden;
  - Robust trajectory optimisation allowing the identification of the safest and more efficient Three-Dimensional or Four-Dimensional (3D/4D) avoidance trajectory, considering relative dynamics between the host aircraft and other traffic, airspace constraints, as well as meteorological and traffic conditions;
  - Generation of appropriate dynamic geo-fences, whose characteristics are dictated by the obstacle classification and dynamics of other platforms (including ground obstacles), to allow computation of the optimal avoidance flight trajectories;
  - Pathways to certifying SA&CA functions for both manned and unmanned aircraft (both near real-time and off-line determination of the host aircraft safe-to-fly envelope);
  - Effective utilisation of airspace resources;
  - Easier integration of automated SA&CA functionalities in airborne avionics (NG-FMS) and other ATM/UTM decision support tools.



- Recommendations for modifications and improvements in current flight management system functionalities (software modules).

### 9.1.2 Achieved Research Objectives

In this research, advanced Next Generation Flight Management System (NG-FMS) algorithms were developed for SA&CA. Specifically, a unified approach to SA&CA was developed for non-cooperative and cooperative scenarios. The conclusions of this thesis are provided below in terms of achieved research objectives:

- **Perform a detailed review of FMS and SA&CA algorithms.**

In most state-of-the-art aircraft, automated navigation and flight guidance functions are provided by a FMS, which supports the generation of safe and efficient trajectories. The hardware components of modern FMS include the MCDU and a dedicated processor. GNC and TDA loops that support automated navigation, guidance, maintenance of separation and collision avoidance tasks were identified. SA&CA functionalities and algorithms implemented in manned and unmanned aircraft were summarised.

- **Define the system level functional architecture of the NG-FMS suitable for manned and unmanned aircraft.**

The NG-FMS performs all the traditional FMS tasks including navigation, guidance, trajectory predictions, and provides auto-throttle controls for engines. Additionally, the NG-FMS communicates with a ground-based 4-PNV system, which is part of a CDM network also including AOC and ANSP. The NG-FMS software includes the multi-objective and multi-model 4DT optimisation algorithms for strategic, tactical and emergency scenarios. The avoidance of a conflict/collision involves the human pilot and/or remote pilot with data obtained from multi-sensor tracking and data fusion algorithms. The key NG-FMS software modules were also identified.

- **Develop/adapt suitable NG-FMS models and algorithms for on board planning and optimisation of 4D trajectories to support TBO/IBO in the CNS+A context.**

Suitable NG-FMS models and algorithms were developed for TBO/IBO as well as UAS operations. The trajectory planning/optimisation module of the NG-FMS performs 4DT planning and optimisation functions for pre-tactical, tactical and emergency timeframes. The 4DT optimiser includes the models pool and the constraints pool. A number of performance criteria and cost functions are used for optimisation, including minimisation of fuel consumption, flight time, operative cost, noise impact,

emissions and contrails. The databases include navigation, performance, magnetic deviation and environmental databases. The NG-FMS also incorporates the cooperative and non-cooperative SA&CA software modules. The trajectory monitoring module performs state estimation, calculating the deviations between the active 4DT intents and the estimated/predicted aircraft states.

- **Perform simulation case studies to test the validity of the NG-FMS models and algorithms for safe and efficient operations and to support environmental sustainability of aviation.**

Detailed simulation case studies were performed on manned (Airbus A380) and unmanned (AEROSONDE™) aircraft. A number of 4DT intents were generated for different flight phases. From the results of these simulation activities, the following conclusions are drawn:

- Simulation case studies demonstrated the functional capability of the NG-FMS to generate cost-effective and environmentally-friendly trajectory profiles satisfying the operational requirements of typical tactical online tasks (in the order of 72 seconds) as well as emergency scenarios (in the order of 8 seconds).
- **Recommendations for modifications and additional functionalities in current flight management system/software based on adaptation of novel algorithms and results obtained during modelling and simulation activities.**

Suitable NG-FMS models and algorithms were developed for TBO/IBO as well as UAS operations. In addition to the traditional databases including navigation, performance and magnetic deviation, new databases including demographic distribution, digital terrain elevation and environmental cost criteria databases can be integrated. The SA&CA algorithms become an integral part of the NG-FMS providing more automated functionalities. Errors affecting the CNS+A systems can be taken into account in evaluating the CNS performances (RCP, RNP, RSP and RTSP). The NG-FMS can also use a set of predefined Caution and Warning Integrity Flags (CIF/WIF) threshold parameters to trigger the generation of both caution and warning flags associated with CNS performance degradations.

- **Develop a unified approach to cooperative and non-cooperative SA&CA for manned and unmanned aircraft operations.**

Although there are a number of stand-alone SA&CA algorithms in literature, they are specific to the scenarios considered (air/ground/cooperative/non-

cooperative). A unified solution to the SA&CA is required, which also provides a solid mathematical framework to support a clear pathway to certification. Safety-critical data fusion algorithms suitable for both cooperative and non-cooperative encounters were developed for a variety of safety-critical applications. The SA&CA functions are integrated in the NG-FMS and based on mathematical algorithms that quantify in real-time the total avoidance volume in the airspace surrounding a target (static or dynamic). Data processing techniques allows the real-time transformation of navigation and tracking errors affecting the state measurements to unified range and bearing uncertainty descriptors.

- **Perform an analysis for investigating and exploring the potential of unified approach to cooperative and non-cooperative SA&CA for manned and unmanned aircraft.**

The detection equipment involve a combination of non-cooperative sensors, including active/passive FLS and acoustic sensors, as well as cooperative systems, including ADS-B and TCAS. GNSS, IMU and VBN sensor measurements (and possible augmentation from ADM) are used for navigation computation. Based on the identified state-of-the-art technologies, a typical BDL based decision tree test bed system reference architecture was presented. Implementations involving Boolean logics are generally hard wired and cannot be reconfigured, and this limits the scope of unified framework in terms of automatic decision making capability. Therefore adaptive BDL, which are based on real-time monitoring of the surveillance sensors/systems performance were implemented to provide a framework for providing autonomy in UAS operations. Sensor/system selection was defined as being based on their performance achieved at any instant of time. Covariance matrices were used for estimating sensor and system performances. After identifying the RoC, if the original trajectory of the host platform intersects the calculated avoidance volume, a caution integrity flag is issued. An avoidance trajectory is generated in real-time and the steering commands are provided to the flight control surfaces.

- **Evaluate analytical models for tracking and SA&CA, high-integrity software modules to improve safety and efficiency of air navigation and guidance services by providing automated separation maintenance and collision avoidance functions.**

Tracking and avoidance algorithms customisation was described in the context of the unified approach to SA&CA for non-cooperative and cooperative scenarios. The employment of non-cooperative sensors (e.g. forward looking sensors) and cooperative systems (e.g. ADS-B) in detecting other traffic/obstacles were

described. Simulation case studies of the detection and avoidance trajectory generation algorithms are accomplished using the AEROSONDE™ UAV as a test platform. It is concluded that obstacle detection and trajectory optimization algorithms ensure a safe avoidance of all classes of obstacles (i.e., wire, extended and point objects) and intruders in a wide range of weather and geometric conditions, providing a pathway for integration of this technology into NG-FMS architectures.

- **Perform an investigation to explore the potential of the unified approach to SA&CA to enhance the performance of UAS and coordinated (manned/unmanned) operations in the CNS/ATM and UTM context.**

The UTM System is comprised of all of the elements required to support and execute UAS operations in the low-altitude airspace. Specifically the integration of small size UAS is targeted in the UTM system to ensure safety and operation efficiency. Some lessons learnt from low-altitude uncontrolled airspace operations of helicopters, gliders and general aviation aircraft can also be helpful. Uncertainties in navigation and tracking associated with each manned/unmanned platform (as seen by all other conflicting platforms) are combined to generate avoidance volumes in all phases of flight (including low-altitude UAS operations). The uncertainty volumes are computed at discrete time intervals as a function of traffic relative dynamics, thus supporting the generation of dynamic geo-fences and multi UTM system implementation.

- **Define a pathway to certifying SA&CA for manned and unmanned aircraft operations.**

One of the fundamental limitations for certification authorities in fully certifying SA&CA functions is the inability to evaluate whether the system performance achieves comparable or superior levels of collision detection and resolution, and separation maintenance upon replacing the on board pilot with a remote pilot. The need for a certifiable SA&CA system and the implementation design drivers were presented. The pathway to certification was described, with the unified approach emerging as an innovative method in targeting successful certification by aviation regulatory bodies. By considering the nominal flight envelopes of the host UAS and other traffic as well as the on board sensors, the approach determines the attainable safety envelope. Conversely, based on a predefined (required) safety envelope and dynamics of other traffic, the software is capable of identifying the sensors that are required to be integrated in the aircraft.

## 9.2 Future Directions

The following key areas are identified for performing further research and development activities on the NG-FMS and on the unified approach to SA&CA.

- Evaluate the computational efficiency benefits of computing the avoidance volumes using tensor analysis;
- Investigate the potential of introducing CNS integrity monitoring and augmentation strategies to enhance the performance of NG-FMS for manned and unmanned aircraft. Evolutions of the NG-FMS architectures have to be explored by introducing suitable integrity monitoring and augmentation functionalities dedicated for 4DT planning, negotiation, validation and update for all flight phases.
- Further evaluate the 4DT intents generated by the NG-FMS algorithms with current flight data for paths flown by long-haul and medium-haul flights; in order to baseline the presented algorithms against current ATM operations. Evaluate further VTOL and hybrid platform operations by evaluating manoeuvring trajectories when compared to general steady flight 4D sequences.
- Further evaluate the effectiveness of advanced SA&CA functions to enhance the performance of NG-ADL by introducing the required input and output parameters for computing the data bandwidth and throughput requirements. Furthermore, the assessment of the spherical harmonics decomposition would enable an easier exchange of information for computing the overall avoidance volumes and geo-fences;
- Assess further the synergies between NG-FMS and NG-ATM algorithms by implementing advanced real-time negotiation and validation functions;
- Further investigate the potential of SA&CA algorithms to support the UTM framework for operations involving mixed equipage;
- Extend the unified approach of the SA&CA concept to real-time and close coordination of air, sea and ground operations;
- Investigate the potential of implementing NG-FMS for supervisory control of manned aircraft and swarming UAS, addressing various levels of autonomous vehicle-vehicle and ground-vehicle collaborations;
- Investigate the next generation policies and practices required to achieve the most efficient, safe, and inclusive air transportation system possible;

- Analyse the unified approach to the SA&CA framework for optimal and dynamic sharing of airspace resources between civil and military users, as well as enabling integrated civil-military ATM and UTM operations;
- Explore the potential of NG-FMS to support interoperability among air and ground systems (at signal-in-space, system and HMI<sup>2</sup> levels) and to assess the required levels of security for safer, protected and more reliable operations supported by various cyber-physical systems in a networked environment;
- Further investigate the effects of wind and wake turbulence on real-time navigation measurements, tracking observables and relative dynamics (and associated uncertainties), and the impacts on uncertainty volume generation (for automated SA&CA) in multi-platform networked operations;
- Validate the presented simulation case studies using actual flight test data (employing a host platform and a number of intruders) by assessing real-time measurements and associated uncertainties affecting navigation states (of the host aircraft platform), tracking observables (of the static or moving object) and relative platform dynamics. Provide benchmarking standards for the performance of the presented algorithms against current FMS and ATM procedures/SA&CA techniques in practice;
- Capture statistical measures of the SA&CA algorithms' performance by performing a large number of Monte Carlo simulations and by examining the boundary cases;
- Investigate the potential of the unified approach for Intelligent and Cyber-Physical Transport Systems (ICTS) applications by providing automated SA&CA functions for air, sea and ground transport as well as coordinated operations that will:
  - support an autonomous ground/sea traffic management concept of operations and real-time coordinated operations for multiple autonomous, semi-autonomous and non-autonomous platforms;
  - investigate the synergies between the unified approach to aircraft SA&CA and the methodology used in autonomous cars, specifically looking at the literature on LIDAR data processing and sensor error characterisation;
  - assist an autonomous onboard SA&CA system and centralised traffic management system to coordinate autonomous and semi-autonomously driven (by humans) vehicles and to establish proper intersection management, route diversion and communication management.

This page is intentionally left blank to support presswork tasks

This page is intentionally left blank to support presswork tasks



# APPENDICES

This page is intentionally left blank to support presswork tasks

# APPENDIX A

## UAS INTEGRATED NAVIGATION SYSTEMS

*"I am well convinced that 'Aerial Navigation' will form a most prominent feature in the progress of civilisation". - Sir George Cayley*

### A.1 Introduction

The main objective of integrated navigation systems is to develop a high performance, low-cost and low-weight/volume Navigation and Guidance System (NGS) capable of providing the required level of navigation performance in all flight phases. The NGS provides the best estimate of PVA measurements and supports the computation of the host aircraft navigation error in order to compute the overall avoidance volume given by the unified approach to SA&CA.

### A.2 Multi-sensor Data Fusion Techniques

Low-cost avionics sensors (based on satellite, inertial and vision-based techniques) are employed to provide an accurate and continuous knowledge of the aircraft navigation states. In addition to these compact and inexpensive sensors, an ADM can be adopted as a virtual sensor (i.e. knowledge-based module) to augment the state vector by computing the aircraft trajectory and attitude motion [1 - 3]. Both 3-DoF and 6-DoF ADM can be employed in the virtual sensor design. This appendix provides a summary of multi-sensor data fusion techniques implemented and also discusses the performance improvements obtained by the introduction of various integration architectures. The concentration is primarily on 6-DoF ADM implementations, pre-filtering of the ADM virtual sensor measurements to reduce the overall position and attitude error budget, as well as a considerable extension of the ADM data validity time (i.e., errors below the RNP thresholds). A key novel aspect of this approach is the employment of ADM augmentation to compensate for the shortcomings of VBN and MEMS-IMU sensors in high-dynamics attitude determination tasks. To obtain the best estimates of PVA, different sensor combinations are analysed and a BDL is implemented for sensor

selection before the centralised data fusion is accomplished. Various options are investigated for data fusion, including a traditional EKF, a more advanced UKF and a particle filter. The MSDF process is illustrated in Figure A.1.

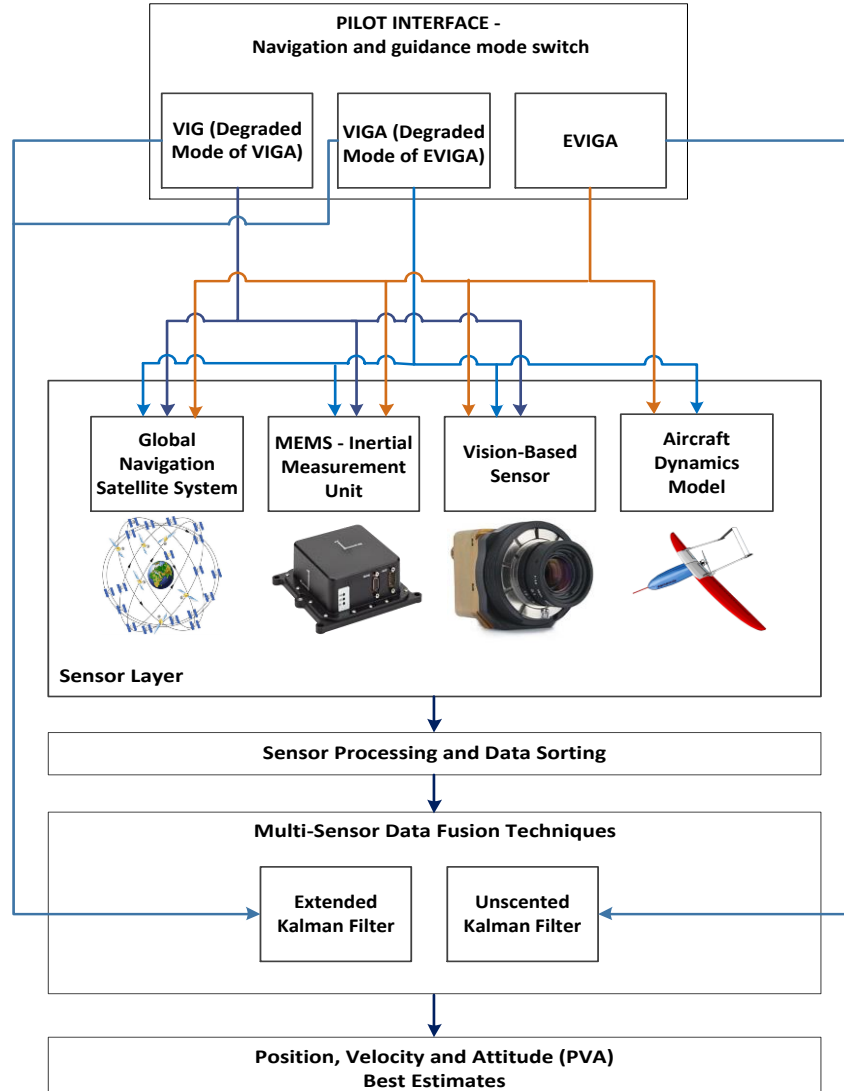


Figure A.1. Multi-sensor data fusion process.

A novel hybrid controller employing fuzzy logic and Proportional-Integral-Derivative (PID) techniques was implemented to provide effective stabilization and control of pitch and roll angles [3]. Position and velocity measurements are obtained from GNSS while PVA estimates are obtained from MEMS-based IMU and VBN sensors. Additionally, attitude data is also obtained from ADM. Data provided by these sensors is combined using an EKF/UKF. The measurements from VBN sensors, GNSS and MEMS-IMU are combined to form the VBN/IMU/GNSS (VIG) NGS integrated architecture. By taking into account the measurements also obtained from ADM, the VBN-IMU-GNSS-ADM (VIGA) NGS is

implemented. EKF is adopted in both VIG and VIGA systems. In the enhanced architecture (EVIGA), the EKF is replaced by an UKF. Additionally, an UKF is also used to process the ADM dynamics. The mathematical models developed for combining the sensor information are described below. The state vector consists of the roll angle, pitch angle and body rates of the aircraft. In order to apply the EKF techniques, the system is described in state space notation by a set of first-order non-linear differential equations:

$$\dot{x} = f(x, w) \quad (\text{A.1})$$

where  $x \in \mathbb{R}^n$  denotes the system state vector,  $f(\cdot)$  is the process function of the states and  $w \in \mathbb{R}^n$  represents a zero mean random process. The matrix of the process noise  $Q \in \mathbb{R}^{n \times n}$  is given by:

$$Q = E(ww^T) \quad (\text{A.2})$$

The measurement equation is considered to be a non-linear function of the measured states and is given by:

$$y = h(x, v) \quad (\text{A.3})$$

where  $h(\cdot)$  is the observation function,  $v \in \mathbb{R}^m$  is a zero mean random process described by the matrix of measurement noise  $R \in \mathbb{R}^{m \times m}$ :

$$R = E(vv^T) \quad (\text{A.4})$$

It is possible to rewrite the non-linear equation of measurements for systems with discrete-time measurements as:

$$y_k = h(x_k, v_k) \quad (\text{A.5})$$

As the measurement equations are non-linear, it is necessary to linearise them by a first-order approach to obtain the dynamic matrix of the system,  $F$  and the measurement matrix,  $H$ . These matrices are related to the non-linear equations and are expressed as:

$$F = \left. \frac{\partial f(x)}{\partial x} \right|_{x=\hat{x}} \quad (\text{A.6})$$

$$H = \left. \frac{\partial h(x)}{\partial x} \right|_{x=\hat{x}} \quad (\text{A.7})$$

where  $\hat{x}$  represents the mean value. The fundamental matrix is approximated by the Taylor series expansion as follows:

$$\Phi_k = I + FT_s + \frac{F^2 T_s^2}{2!} + \frac{F^3 T_s^3}{3!} + \dots \quad (\text{A.8})$$

where  $T_s$  is the sampling time and  $I$  is the identity matrix. The Taylor series are often approximated as:

$$\Phi_k \approx I + FT_s \quad (\text{A.9})$$

In the case of a linear system, the matrices:  $F$ ,  $H$  and  $\Phi$  are linear. In EKF implementation, these matrices are non-linear. The set of EKF equations for each time step are given by:

$$\hat{x}_k^- = f_k(\hat{x}_{k-1}^+) \quad (\text{A.10})$$

$$P_k^- = \Phi_k P_{k-1}^+ \Phi_k^T + Q \quad (\text{A.11})$$

$$K_k = P_k^- H^T (H P_k^- H^T + R)^{-1} \quad (\text{A.12})$$

$$\hat{x}_k^+ = \hat{x}_k^- + K_k (z_k - h_k(\hat{x}_k^-)) \quad (\text{A.13})$$

$$P_k^+ = (I - K_k H) P_k^- \quad (\text{A.14})$$

where  $k$  is the time step:  $1, 2, \dots, n$ ;  $P_k$  is the updated state covariance and  $K_k$  is the filter gain. Although the EKF provides a key advantage of linearisation of all non-linear models (i.e., process and measurement models), it can be demanding to tune the filter parameters and often provides unreliable estimates if the system non-linearities are severe. Furthermore, the accuracy of propagated mean and covariance is limited to first order due to truncations performed in the linearisation process.

Most of these EKF deficiencies are overcome by implementing an Unscented Kalman Filter (UKF). The UKF is a recursive estimator used for calculating the statistics of a random variable propagated through a non-linear system model [4 - 6]. Sigma-point Kalman Filters (SPKFs), such as the UKF, provide derivative-free higher-order approximations by fitting a Gaussian distribution rather than approximating an arbitrary nonlinear function as the EKF does [7, 8]. Furthermore, an UKF is implemented to increase the accuracy of the NGS, in addition to pre-processing the ADM measurements. It is assumed that the equations of motion for the aircraft are disturbed by uncorrelated zero-mean Gaussian noise. The UKF performance is compared with error perturbations in the system model's PVA measurements. The UKF weights and scaling parameters are given by:

$$w_m^{(0)} = \frac{\kappa}{n + \kappa} \quad (\text{A.15})$$

$$w_c^{(0)} = w_m^{(0)} + (1 - \alpha^2 + \beta) \quad (\text{A.16})$$

$$w_m^{(i)} = w_c^{(i)} = \frac{1}{2(n + \kappa)}; \quad i = 1, \dots, n \quad (\text{A.17})$$

$$w_m^{(i+n)} = w_c^{(i+n)} = \frac{1}{2(n + \kappa)}; \quad i = 1, \dots, 2n \quad (\text{A.18})$$

$$\lambda = \alpha^2 (L + \kappa) - L \quad (\text{A.19})$$

$$\gamma = \sqrt{(L + \lambda)} \quad (\text{A.20})$$

where  $\kappa$  is the secondary scaling parameter and is normally set to 0.  $\lambda$ ,  $\gamma$ , and  $m$  are the scaling parameters.  $m$  is the mean and the constant  $\beta$  is used to incorporate prior knowledge of the state distribution  $x$ . For Gaussian distributions,  $\beta = 2$  is optimal and  $\{W_i\}$  represents a set of scalar weights [9, 10].  $\alpha$  determines the spread of the sigma points around the state mean  $\hat{x}$  and is set between 0 and 1. The covariance matrix is given by  $C$ . The unscented transformation process is precisely captured in the UKF state-estimation algorithm described in the following set of equations. The noise is considered additive and the unscented transformation is non-augmented. The UKF process is initialized by using the expected mean, covariance and state vector values (i.e., PVA):

$$\hat{x}_0 = m[x_0] \quad (\text{A.21})$$

where the initial state vector estimate is  $\hat{x}_0$  and  $x_0$  is the initial state vector of the ADM:

$$P_0 = m[(x_0 - \hat{x}_0)(x_0 - \hat{x}_0)^T] \quad (\text{A.22})$$

where  $P_0$  is the initial state covariance matrix. The process model of the UKF is based upon a set of sigma points where the random vector  $x$  is approximated by  $2n + 1$  symmetric sigma points. The sigma points,  $\chi_i$  are selected based on the mean and covariance of  $x_k$ , and are obtained as follows:

$$\chi_{k-1} = [\hat{x}_{k-1} \quad \hat{x}_{k-1} + \gamma\sqrt{P_{k-1}} \quad \hat{x}_{k-1} - \gamma\sqrt{P_{k-1}}] \quad (\text{A.23})$$

where  $P$  computes the diagonal values of the state covariance matrix and results in a lower triangular matrix of the state covariance matrix.  $\gamma$  is the control parameter of the dispersion distance from the mean estimate in the computation of  $\chi_{k-1}$ , the sigma point matrix. After the sigma points are calculated, a time update for each time step  $k$  is performed and is given by:

$$\chi_{k|i}^* = f[\chi_{k-1|i}] \quad (\text{A.24})$$

$$\hat{x}_k^- = \sum_{i=0}^{2n} W_i^{(m)} \chi_{k|i}^* \quad (\text{A.25})$$

$$P_{x_k}^- = \sum_{i=0}^{2n} W_i^{(C)} [\chi_{k|i}^* - \hat{x}_k^-][\chi_{k|i}^* - \hat{x}_k^-]^T + Q_k \quad (\text{A.26})$$

$$\chi_k = [\hat{x}_k^- \quad \hat{x}_k^- + \gamma\sqrt{P_{x_k}^-} \quad \hat{x}_k^- - \gamma\sqrt{P_{x_k}^-}] \quad (\text{A.27})$$

$$\hat{y}_{k|i} = h[\chi_{k|i}] \quad (\text{A.28})$$

$$\hat{y}_k^- = \sum_{i=0}^{2n} W_i^{(m)} y_{k|i} \quad (\text{A.29})$$

In the measurement update equations listed above,  $\chi_k$  represents the unobserved state of the system. The process noise covariance matrix is represented by  $Q_k$ ,  $C$  in  $W_i^{(C)}$  is the

covariance and  $m$  in  $W_i^{(m)}$  is the mean and  $n$  is the state size. The UKF is also used to pre-process the ADM data in order to increase the ADM validity time. The UKF process model equations are expressed as:

$$P_{y_k} = \sum_{i=0}^{2n} W_i^{(C)} [\psi_{k|i} - \hat{y}_k^-] [\psi_{k|i} - \hat{y}_k^-]^T \quad (A.30)$$

$$P_{v_k} = P_{y_k} + R_k \quad (A.31)$$

$$P_{xy_k} = \sum_{i=0}^{2n} W_i^{(C)} [\chi_{k|i} - \hat{x}_k^-] [\psi_{k|i} - \hat{y}_k^-]^T \quad (A.32)$$

$$\mathcal{K}_k = P_{xy_k} P_{v_k}^{-1} \quad (A.33)$$

$$\hat{x}_k = \hat{x}_k^- + \mathcal{K}_k (y_k - \hat{y}_k^-) \quad (A.34)$$

$$P_{x_k} = P_{x_k}^- - \mathcal{K}_k P_{v_k} \mathcal{K}_k^T \quad (A.35)$$

where  $\mathcal{K}_k$  is the Kalman gain.

### A.3 Integrated Multi-sensor Data Fusion Architectures

Three different multi-sensor integrated navigation system architectures are defined, including the EKF based VIG/VIGA and the UKF based EVIGA system [2]. The VIG architecture uses VBN at 20 Hz and GPS at 1 Hz to augment the MEMS-IMU running at 100 Hz. The VIGA architecture includes the ADM (computations performed at 100 Hz) to provide attitude channel augmentation. The outputs of the navigation system were fed to a hybrid Fuzzy-logic/PID controller designed for the AEROSONDE UAS and capable of operating with stand-alone VBN, as well as data from other sensors. The implemented NGS architectures with their associated sensors are listed in Table A.1.

Table A.1. Integrated NGS systems.

NGS System	Navigation System				Filter
	GNSS	IMU	VBN	ADM	
VIG system	✓	✓	✓		EKF
VIGA system	✓	✓	✓	✓	EKF
EVIGA system	✓	✓	✓	✓	UKF

The VIG architecture is illustrated in Figure A.2. The INS provides measurements from gyroscopes and accelerometers, which are then provided to a navigation processor. Pseudorange measurements from GNSS are processed by the EKF/UKF to obtain position and velocity data. In the VIG system, the INS position and velocity provided by the navigation processor are compared with GNSS position and velocity measurements and



supplied to the EKF. A similar process is also applied to the INS and VBN attitude angles, whose differences are incorporated in the EKF measurement vector. The EKF provides estimates of the PVA errors, which are then removed from the sensor measurements to obtain the corrected PVA states. The corrected PVA and estimates of accelerometer and gyroscope biases are also used to update the INS raw measurements.

The VIGA architecture is illustrated in Figure A.2. As before, the INS position and velocity provided by the navigation processor are compared to the GNSS data to form the measurement input to the EKF. Additionally, in this case, the attitude data provided by the ADM and the INS are compared to feed the EKF at 100 Hz, and the attitude data provided by the VBN and MEMS-IMU sensors are compared at 20 Hz and input to the EKF. As in the VIG architecture, the EKF provides estimations of PVA errors, which are removed from the INS measurements to obtain the corrected PVA states. The attitude best estimate is compared with the INS attitude to obtain the corrected attitude. During the landing phase, the attitude best estimate is compared with the VBS attitude to obtain the corrected attitude. In the EVIGA architecture, EKF is replaced by an UKF (Figure A.3). Additionally, an UKF is also used to process the ADM navigation solution. The ADM operates differently to that of the VIGA system, running in parallel to the centralised UKF, and acts as a separate subsystem. The filtering of the ADM virtual sensor measurements aids in achieving reduction of the overall position and attitude error budget, and most importantly, results in considerable reduction in the ADM re-initialisation time. PVA measurements are obtained as state vectors from both the centralised UKF and ADM/UKF. These measurements are then fed into an error analysis module in which the measurement values of the two UKFs are compared. In this research, MEMS-INS errors are modeled as White Noise (WN) or Gauss-Markov (GM) processes. Simulation of the VIG, VIGA and EVIGA navigation modes shows that all integration schemes achieve horizontal/vertical position accuracies in line with CAT-I (100% of the approach flight time) and CAT-II (98.4% of the approach flight time) requirements. In all other flight phases, the VIGA system exhibits improvements in position, velocity and attitude data with respect to the VIG system. The EVIGA system shows the best performance in attitude data accuracy in addition to achieving an increased ADM validity time (validity time of 126 sec before exceeding CAT I vertical and horizontal error limits) [2].

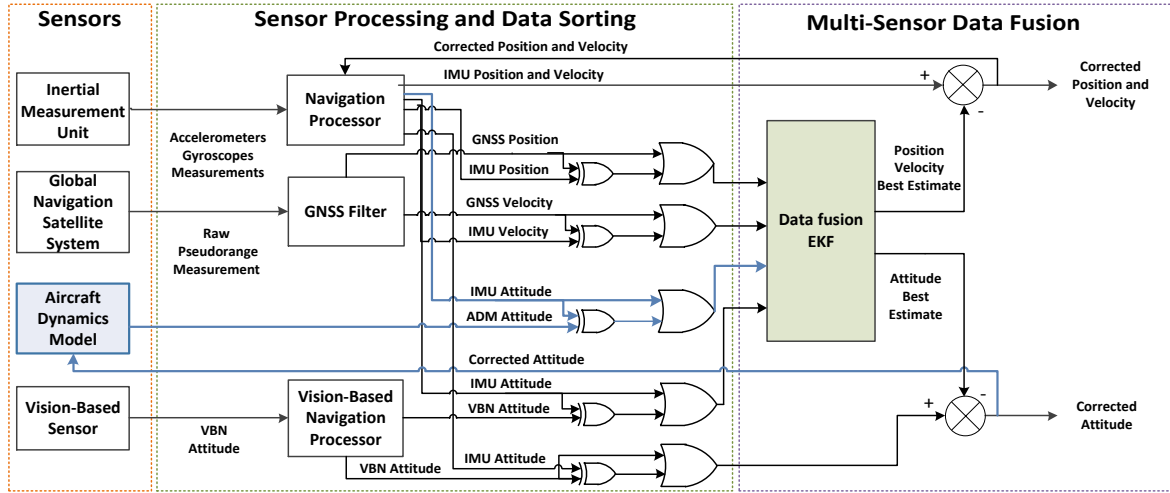


Figure A.2. VIG and VIGA architectures [1].

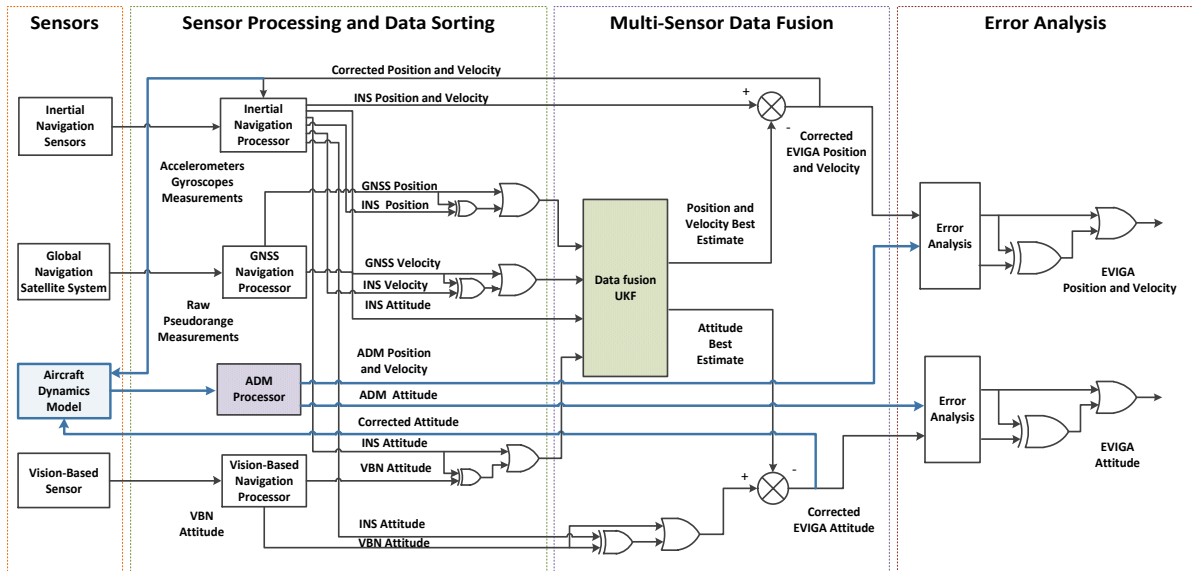


Figure A.3. EVIGA architecture [1].

## A.4 Conclusions

The design of a low-cost and low-weight/volume integrated NGS suitable for supporting the computation of navigation error required for the unified approach to SA&CA was described. Various sensors were considered for the design of the NGS. GNSS and MEMS-IMUs, with augmentation from ADM and VBN sensors, were selected for integration. Three different low-cost and low-weight/volume integrated NGS architectures were introduced. They are an EKF based VBN-IMU-GNSS-ADM (VIGA) integrated system and an UKF based (EVIGA) system. While the VIGA system used unfiltered ADM data, the EVIGA system employed an UKF for pre-filtering the ADM attitude solution to increase the ADM validity time.

## A.5 References

1. R. Sabatini, F. Cappello, S. Ramasamy, A. Gardi and R. Clothier, "An Innovative Navigation and Guidance System for Small Unmanned Aircraft using Low-Cost Sensors", *Journal of Aircraft Engineering and Aerospace Technology*, vol. 87, No. 6, pp.540-545, 2015. DOI: [10.1108/AEAT-06-2014-0081](https://doi.org/10.1108/AEAT-06-2014-0081)
2. F. Cappello, S. Ramasamy and R. Sabatini, "A Low-Cost and High Performance Navigation System for Small RPAS Applications", *Aerospace Science and Technology*, Vol. 58, pp. 529–545, 2016. DOI: [10.1016/j.ast.2016.09.002](https://doi.org/10.1016/j.ast.2016.09.002)
3. R. Sabatini, S. Ramasamy, A. Gardi, L. Rodriguez Salazar, "Low-cost Sensors Data Fusion for Small Size Unmanned Aerial Vehicles Navigation and Guidance", *International Journal of Unmanned Systems Engineering*, vol. 1, pp. 16-47, 2013. DOI: [10.14323/ijuseng.2013.11](https://doi.org/10.14323/ijuseng.2013.11)
4. E. Wan and R. Van Der Merwe, "The Unscented Kalman Filter for Nonlinear Estimation", *Adaptive Systems for Signal Processing, Communications, and Control Symposium*, Lake Louise, Alberta, Canada, pp. 153-158, 2000.
5. S.J. Julier and J.K. Uhlmann, "New Extension of The Kalman Filter to Nonlinear Systems", *AeroSense'97, Signal Processing, Sensor Fusion, and Target Recognition VI*, 1997. DOI: [10.1117/12.280797](https://doi.org/10.1117/12.280797)
6. S.J. Julier and J.K. Uhlmann, "Unscented Filtering and Nonlinear Estimation", *Proceedings of the IEEE*, Vol. 92, No. 3, pp. 401-422, March, 2004.
7. A.E. Wan, and R. Van Der Merwe, "The Unscented Kalman Filter for Nonlinear Estimation", *Adaptive Systems for Signal Processing, Communications, and Control*, The IEEE 2000 AS-SPCC Symposium, 2000.
8. R. Van Der Merwe, "Sigma-point Kalman Filters for Probabilistic Inference in Dynamic State-space Models", *Dissertation*, Oregon Health & Science University, 2004.
9. N.B. Da Silva, D.B. Wilson and K.R. Branco, "Performance Evaluation of the Extended Kalman Filter and Unscented Kalman Filter", *IEEE International Conference on Unmanned Aircraft Systems (ICUAS)*, pp. 733-741, Denver, CO, USA, 2015.
10. F. Cappello, S. Ramasamy and R. Sabatini, "Low-Cost RPAS Navigation and Guidance System using Square Root Unscented Kalman Filter", *SAE 2015 AeroTech Congress & Exhibition*, Seattle, Washington State, USA, 2015. DOI: [10.4271/2015-01-2459](https://doi.org/10.4271/2015-01-2459)

This page is intentionally left blank to support presswork tasks

## APPENDIX B

# CERTIFICATION STANDARDS AND RECOMMENDED PRACTICES

## B.1 Requirements

Tables B.1, B.2 and B.3 provide a compilation of the certification standards, AMC, GM and recommended practices encompassing the Operational (OP), Technical (TC), Safety (SAF), Human Factors (HF) as well as Test and Evaluation (TE) aspects.

Table B.1. Operational requirements.

Requirements	Two-pilot aircraft	General Aviation single-pilot aircraft	UAS (Civil   Military)
Operational	<p>FAR Parts 25 and 121</p> <p>FAR 25.1523 and Appendix D (minimum flight crew)</p> <p>FAA AC 120-100 (aviation fatigue)</p> <p>EASA AMC/GM to Annex IV – Part-CAT, Subpart D (IDE)</p> <p>ICAO Air Operator Certification and Surveillance Handbook</p> <p>ICAO Manual of Procedures for Operations Inspection, Certification and Continued Surveillance (8335 AN/879)</p>	<p>EASA Annex VIII, Part-SPO, Subparts B and C (OP, POL)</p> <p>EASA AMC &amp; GM to Annex III AMC2 ORO.FC.115 (CRM training for SPO)</p> <p>ICAO Annex 1 Section 2.1.3 (class and type ratings)</p> <p>FAA-H-8083-9A: Sect. 9-11 to 9-17 (Aviation Instructor's Handbook: SRM), FAR Part 23 and FAA AC 91-73B (procedures during taxi operations)</p> <p>EASA AMC1 FCL.720.A(b)(2)(i) (flight crew experience requirements and prerequisites)</p> <p>(AU) CASA EX43/11 (Cessna exemption)</p> <p>(NZL) CAA AC 91-11 (single-pilot IFR)</p>	<p>ICAO Manual on RPAS (10019 AN/507) Ch. 4 (certification and airworthiness), 6 (operator responsibilities), 9 (operations), 14 (integration into ATM), 15 (aerodromes)</p> <p>EASA A-NPA 2015-10 Ch. 3 (specificities of unmanned aircraft), 4 (road map)</p> <p>JARUS D.02 – FCL Recommendation</p> <p>RTCA DO-304 Ch. 1 and 2 (operational and functional requirements); Appendix D (operational functions)</p> <p>(AU) CASA AC 101-1 (design specification, maintenance and training)</p> <p>(AU) CASA DP 1529US (airworthiness framework)</p> <p>(UK) CAP 722, Sect. 5 (operations)</p>

Table B.2. Technical and safety requirements.

Requirements	Two-pilot aircraft	General Aviation single-pilot aircraft	UAS (Civil   Military)
Technical	<p>FAR 25.671 to 25.703 (control systems)</p> <p>FAR 25.1301 to 25.1337 (equipment and installation)</p> <p>FAA AR-06/2 (flight data integrity for ground-based systems)</p> <p>RTCA DO-236 (RNP for RNAV)</p> <p>RTCA DO-238 (data link systems)</p> <p>RTCA DO-289 (MASPS for surveillance)</p> <p>RTCA DO-361 (flight deck interval management)</p> <p>SAE ARP-4109/9A (FMS)</p> <p>ICAO Manual on RCP (9869 AN/462)</p> <p>ICAO Performance-based (PBN) Manual (9613 AN/937)</p> <p>ICAO Surveillance Manual (9224)</p>	<p>FAR 23.143 to 23.157 (controllability and manoeuvrability)</p> <p>FAR 23 subpart F (equipment)</p>	<p>ICAO Manual on RPAS (10019 AN/507) Ch. 10 to 13</p> <p>JARUS D.04 – Required C2 Performance</p> <p>FAA UAS Roadmap, Appendix C (goals, metrics and target dates)</p> <p>RTCA DO-304, Ch. 3 (standards assessment); Appendix G (functional allocation)</p> <p>(UK) CAP 722, Sect. 3, Ch. 1 (detect and avoid), 3 (autonomy)</p> <p><b>STANAG 4586 Appendix B1 (data link interface); Appendix B2 (C2 interface)</b></p> <p><b>DOD 11-S-3613 Ch. 4 to 7 (UAS roadmap)</b></p>
Safety	<p>FAR 25.1309 (equipment, systems and installations)</p> <p>FAA AC 25.1309-1A (System design and analysis)</p> <p>SAE ARP-4754A (systems development and design)</p> <p>SAE ARP-4761 (safety assessment for systems)</p>	<p>FAR 23.1309 (equipment, systems and installation)</p>	<p>JARUS AMC RPAS.1309 (safety assessment of RPAS)</p> <p>EUROCAE ER-010 (system safety objectives and assessment criteria)</p> <p>(UK) CAP 722, Sect. 4, Ch. 4 (safety assessment)</p> <p>ICAO Manual on RPAS (10019 AN/507) Ch. 7</p>

Table B.3. Human factors and T&E requirements.

Requirements	Two-pilot aircraft	General Aviation single-pilot aircraft	UAS (Civil   Military)
Human Factors	<p>FAA-STD-004 (human factors program)</p> <p>FAA TC-13/44 (flight deck controls and displays)</p> <p>FAA AC 25.1302-1 (design and methods of compliance for systems and equipment)</p> <p>ARINC 837 (cabin HMI)</p> <p>ICAO Human Factors Training Manual (9683 AN/950) Part 2</p> <p>(UK) CAP 737 (flight crew human factors)</p>	<p>FAA TC-14/42 (portable weather applications)</p> <p>(AU) CAAP 5.59-1(0) (single-pilot human factors)</p>	<p>(UK) CAP 722, Sect. 3, Ch. 2 (human factors in UAS operations)</p> <p>RTCA DO-344, Vol. 2, Appendix D (control station human factors considerations)</p>
			<p><b>STANAG 4586 Appendix B3 (HMI)</b></p> <p><b>DOD 11-S-3613 Ch. 10 (manned-unmanned teaming)</b></p>
T&E	<p>RTCA DO-178C (software)</p> <p>RTCA DO-278, Ch. 6 (CNS/ATM software integrity)</p> <p>RTCA DO-297, Ch. 5 (integrated modular avionics)</p> <p>RTCA DO-335, Ch. 9 (automatic flight guidance/control)</p> <p>RTCA DO-356 (security)</p> <p>ASTM F3153-15 (verification of avionics systems)</p> <p>FAA TC-16/4 (verification of adaptive systems) and FAA AC 20-157 (reliability assessment plan)</p> <p>FAA AC-25-7C (flight test) (AU) CASA AC 21-47(0) (flight test safety) (AU) CASA AC 60-3(0) (flight simulators for validation)</p>	<p>Flight Standardization Board Report: Embraer EMB-500, EMB-505</p> <p>Flight Standardization Board Report: Cessna Citation 525C</p>	<p><b>IDA Paper 3821 (operational test and evaluation: lessons learnt)</b></p>

This page is intentionally left blank to support presswork tasks



# APPENDIX C

## ELEMENTS OF HUMAN MACHINE INTERFACE & INTERACTIONS

*"Although humans today remain more capable than machines for many tasks, by 2030 machine capabilities will have increased to the point that humans will have become the weakest component in a wide array of systems and processes. Humans and machines will need to become far more closely coupled, through improved human-machine interfaces and by direct augmentation of human performance". -*

Werner J.A. Dahm

### C.1 Introduction

This appendix provides a summary of some key elements of HMI<sup>2</sup> for NG-FMS. In particular, the formats and functions required for supporting automated SA&CA functionalities are presented. Some elements of the adaptive HMI<sup>2</sup> system that dynamically assists pilots and operators based on real-time detection of their physiological and cognitive states are described. With an appropriate system implementation, pilot error can be avoided and enhanced synergies can be attained between humans and machines, improving the total system performance. Moreover, the implementation of suitable decision logics (based on the estimated cognitive states of the pilot or remote pilot) allows a continuous and optimal reconfiguration of the automation levels.

### C.2 Human Machine Interface and Interactions

HMI<sup>2</sup> systems are essential for providing inputs as well as receiving information from avionics systems. The key focus is on the interfaces required for the exchange of information between the NG-FMS and the displays for pilot (manned aircraft) and remote pilot (unmanned aircraft). Generally, Electronic Flight Instrument System (EFIS)

displays are employed, which are the Primary Flight Display (PFD) and Navigation and Tactical Display (NTD). EFIS displays enable continuous monitoring of flight information as well as the required parameters. Additionally, they also allow the pilots to implement corrective measures if required (e.g. avoidance of ground obstacles). The PFD provides information on thrust and control commands generated by the NG-FMS. Track of flight plan, instantaneous position, Distance-To-Destination (DTD) based waypoints for all flight phases, sectorisation of flight plan into segments, sections and integral steps are displayed on the NTD. Other relevant information including navigation aids, airports, altitude/speed/time constraints and wind information are also displayed on the NTD. In order to support time based operations, the key parameters for 4-Dimensional Trajectory-Based Operations (TBO) have to be identified and included in the trajectory prediction component of the current FMS. Furthermore, functions and formats that support full 4D information, and human factors consideration for evaluation of the 4D trajectory information have to be analysed considering mixed equipage. Novel forms of HMI<sup>2</sup> are required for the NG-FMS in order to enable time based operations. Furthermore, recent research activities have been performed to identify the specific requirements for single-pilot and UAS operations. Specifically, the HMI<sup>2</sup> drivers for effective sharing of information between NG-FMS and NG-ATM/GCS will vary significantly from the manned version, wherein the control shifts from a pilot to a remote pilot perspective. As pointed out in STAGNAG 4586, there is a need of greater levels of interoperability and therefore a significant evolution of the HMI<sup>2</sup> design is required [1, 2]. The new formats and functions development activities focus on:

- 4D trajectory navigation and guidance;
- Next generation communications including LoS and BLOS data links;
- Vehicle configuration data including telemetry data (specifically for UAS);
- Automated SA&CA for non-cooperative and cooperative scenarios;
- Monitoring of integrity by the generation of predictive (caution) and reactive (warning) flags;
- Monitoring of CNS+A performance metrics including RCP, RNP, RSP and RTSP.

The current state-of-the-art small-to-medium range commercial aircraft employ a two person flight comprised of a Pilot Flying (PF) and a Pilot Non-Flying (PNF). In such flight deck configurations, the flight tasks are distributed between the PF and PNF. The PF takes the direct responsibility of directing the aircraft in line with the approved flight plan and continuously monitors the flight path for any deviations. On the other hand, the roles of the PNF as 'pilot monitoring' are primarily focussed on monitoring the position of aircraft,

controlling and monitoring radio transmissions, assisting the PF in high workload situations, cross monitoring the actions of PF and taking over flight tasks in case of incapacitation of PF. Based on the role allocations, the presence of a PNF is beneficial. In particular, the PNF reduces the PF's workload, however, an additional workload, associated with team management, is introduced. According to statistics obtained between the years 2002 - 2011, 37% of all fatal accidents were caused by a failure in Crew Resource Management (CRM) [3]. Another widely recognised advantage is that the PNF reduces the probability of inadvertent errors made by PF. Nevertheless, several limitations such as memory and attention problems affect the monitoring and corrective role of the PNF. In order to avoid these errors, modern commercial aircraft are equipped with electronic checklist functionalities that enable efficient cross-checking of PNF tasks.

Under current regulations, all large commercial aircraft are required to be flown by a flight crew, consisting of not less than two pilots (FAR 14 CFR 121.385) [4]. However, authorities also specify that all aircraft must be capable of being operated by a single pilot from either seat, which means the current flight deck design is natively ready for single pilot and UAS operations. Another constraint specifically for regional aircraft is that they must be able to operate not only in big aerodromes but also from smaller airports that might have fewer navigation and landing aids to support automated landings. In all cases, CRM is an essential operational policy for two pilots to fly a commercial aircraft.

In the existing design, the aircraft is directed by a NG-FMS that coordinates with the autopilot during most flight phases. Throughout the past few years, aircraft designers have created a variety of modes for achieving an extensive range of functionalities. For example, Airbus A320 has nine auto throttle modes, ten VNAV modes and seven LNAV modes. However, such a large number of modes have emerged as a factor of confusion for the pilot, leading to additional risks during the flight. In order to minimise hazards, researchers and industries have committed to simplify the most complicated and confusing systems. Commercial airliners, especially regional airliners, are the core users of small and medium range commercial aircraft.

In the TBo/UTM context, SA&CA is handled in a distributed system, where the pilot/remote pilot is designated with some of the conventional ATCo's responsibilities in order to achieve increased capacity-demand balancing. Eurocontrol has identified three levels of delegation for achieving SA&CA. They are: limited, where the ATCo performs conflict detection and resolution tasks while the pilot executes the ATCo's decision; extended, where the ATCo performs conflict detection, and delegates the conflict resolution to be executed by the pilot; full, where the ATCo delegates full

responsibility to the pilot for detection and resolution of any conflicts as well as execution of avoidance trajectory manoeuvre [5]. The concept of distributed control acts to provide higher levels of delegation for SA/CA tasks, since highly centralised ATM systems limit the air traffic density within a specified sector.

In addition to delegation of tasks between ATCo and pilots, the responsibility for SA&CA can also be delegated between the human operator and the automation system [6]. A highly distributed system relies on the pilot/controller as well as human-automation integration, and hence requires high levels of integrity for each component of the system. To address human-machine teaming in the CNS+A context, three human factor concepts are discussed. These are: situational awareness, trusted autonomy and ergonomics.

Situational awareness has featured prominently in aviation-related human factors research over the past few decades [7, 8]. A loss of situational awareness has been a major cause of aircraft accidents and incidents. Increased levels of automation in the flight deck have provided opportunities for increased situational awareness, by reducing the need for constant vigilance over low level flight tasks. The pilot can therefore expend the cognitive resources on higher level tasks. A typical example is the automated navigation and guidance services provided by state-of-the-art FMS. However, higher levels of automation can also lead to a loss of situational awareness due to automation complacency, which is detrimental to the overall system performance. Additionally, the lack of low-level vigilance might impede the pilot's response to emergencies such as loss of self-separation.

Trusted autonomy plays an increasingly important role in systems with high levels of delegation including ATCo-pilot/pilot-co-pilot/system-pilot interactions. As an example, radio phraseology and crew resource management provides a framework for building trust through proper communication and decision making protocols. With higher levels of automation, human-machine teaming becomes a key issue, and automation trust is required for optimal performance. Over- or lack-of trust results in non-optimal human-machine teaming scenarios [9]. In lack-of trust situations, the pilot allocates excessive vigilance for automation-monitoring or outright rejects the automation commands. When conflicting instructions are provided, the pilot executes the commands from the agent (person or system) in whom or which a greater level of trust is allocated to. Over- or lack of trust might result in making an incorrect decision.

In line with ergonomics theory, the functional design of systems can be described as to complement the human operator's work or cognitive processes. SA&CA technologies

shall factor in these considerations when designing the feedback mechanisms such as advisories, warnings and resolutions. Appropriate feedback shall be prioritized in terms of overall urgency, and shall be sufficient to draw the pilot's attention without leading to any distraction of the current task. The identification and resolution of the conflict shall be timely, i.e. sufficient time for the pilot to react, and easily comprehensible, i.e. not requiring a high cognitive effort to process. Feedback may consist of visual, aural or haptic cues. Visual feedback is the primary information channel for the pilot, and is constantly being refined based on the functions of the flight crew. Synthetic vision can enhance the pilot's situational awareness via integration into a PFD [10]. Terrain data stored in the system is fused with navigational data, surveillance data and flight data [11]. The location of the next waypoint in the ND shows up in the PFD as series of indicator rings. The optimal route, represented as a magenta line in the ND, shows up as a 'tunnel-in-the-sky' in the PFD, along with the optimal pitch, bank angle and airspeed. Nearby aircraft communicate their position and attitude to the NG-FMS via the ADS-B system and are displayed in the ND as well as the pilot's FoV in the PFD. Auditory feedback takes the form of a standard message, or a warning siren. Ergonomic design of this feedback channel requires tailoring the frequency and volume of the sound to achieve its desired effect. Haptic interfaces provide feedback through the pilot's sense of touch. It can be integrated into control devices, like the yoke and rudder, with force displacement gradients during separation loss to provide warnings against incorrect manoeuvres.

### **C.3 Formats and Functions for Automatic SA&CA**

The employment of distinct alerting and display for warnings (and cautions) about time-critical external conditions, such as collision with other traffic, terrain, turbulent weather areas, wind shear and wake vortices has two main issues both in unmanned and manned aviation. These issues include lack of information in tactical and emergency scenarios and lack of information flow among the various alerting systems. The formats and functions for automatic SA&CA can be supported by the existing list derived from TCAS implementations [12 - 14]. By the extensive use of a combination of non-cooperative sensors and cooperative systems, the effective range of conflict detection can be extended to 100 NM or more (typically by the employment of ADS technology). ADS-B messages contain a more extensive and accurate set of information including 3D position, ground and vertical speed, track information and Identification of other traffic (by call signs). The CDTI, which was introduced in manned aviation for the display of 3D position relative to the own ship can be modified to include the information obtained

after the TDA processes. The symbology for an integrated CDTI display for automated SA&CA is summarised in Table C.1.

The CDTI functions with a primary purpose of attention cueing and with a secondary purpose as a tactical guidance display. Additional information about other traffic, including call signs, can be added by the pilot/remote pilot and also can be configured to be decluttered using adaptive forms of HMI<sup>2</sup>.

Table C.1. Symbology of CDTI display.

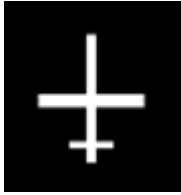
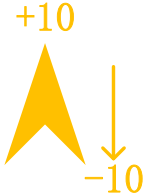


Symbology	Information
	Own aircraft
	Other traffic that might lead to a conflict. 1000 feet above and descending with 10 feet per second. The predicted conflict will not happen in 3 minutes.
	Other traffic leading to a conflict. 2000 feet below and climbing with 10 feet per second. The predicted conflict will happen within 3 minutes.
	Non-conflict other traffic within look ahead time. 3000 feet above and level. Call sign of the aircraft is Qantas aircraft flight QF12.

Figure C.1 shows the CDTI display tailored for SA&CA. The target data is obtained after the TDA process involving information from all available non-cooperative sensors and cooperative systems. In this example, two other aircraft are detected in the surrounding airspace and shown in the display. Additionally the state information of each detected aircraft is also provided in the display. The white circles indicate the distance in hundreds of metres (NM can be used specifically for manned aircraft and helicopters). From Figure

B.1, the relative geometry and movement is shown clearly. This is crucial to help the pilot/remote pilot to build a 3D situational awareness picture and react accurately (as well in a timely fashion) against any threat.

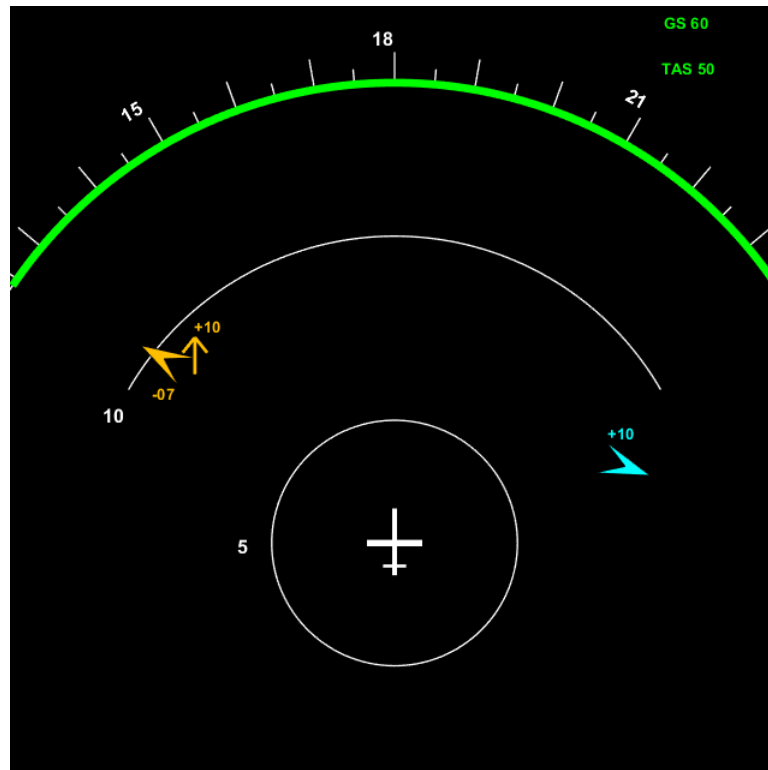


Figure C.1. CDTI display showing other traffic.

Furthermore, conflict resolution information and the re-optimised trajectory can be added to the PFD (Figure C.2). The resolution display shows red and green bands on the heading, velocity and vertical velocity scale as displayed in Figure C.3. The red band indicates the region to be avoided, for which the detected conflicts were not resolved (failure to do so leads to a collision). The green band presents the possible resolution provided by the conflict resolution mechanism after a re-optimised trajectory is generated for eliminating any collisions in the re-planned path. The green band indicates that the probability of conflict is decreased under a certain threshold dictated by the risk of collision. In practice, aural annunciations are inhibited below 1500 feet Above-Ground Level (AGL). The SA&CA conflict aural warning and resolution annunciation are integrated with other aural alerts. The preference for aural alerts depends on the phase of flight. During take-off and landing flight phases, the wind shear detection system as well as Ground Proximity Warning System (GPWS) and ground Obstacle Warning (and avoidance) System (OWS) are given higher priority over other alerts. Therefore the SA&CA aural conflict (aural warning and resolution annunciation) is activated when a wind shear or GPWS or OWS alert is active. In addition, the separation

assurance responsibility relies on ATM system information, other than the onboard system.  
Table C.2 summarises the list of aural annunciations.

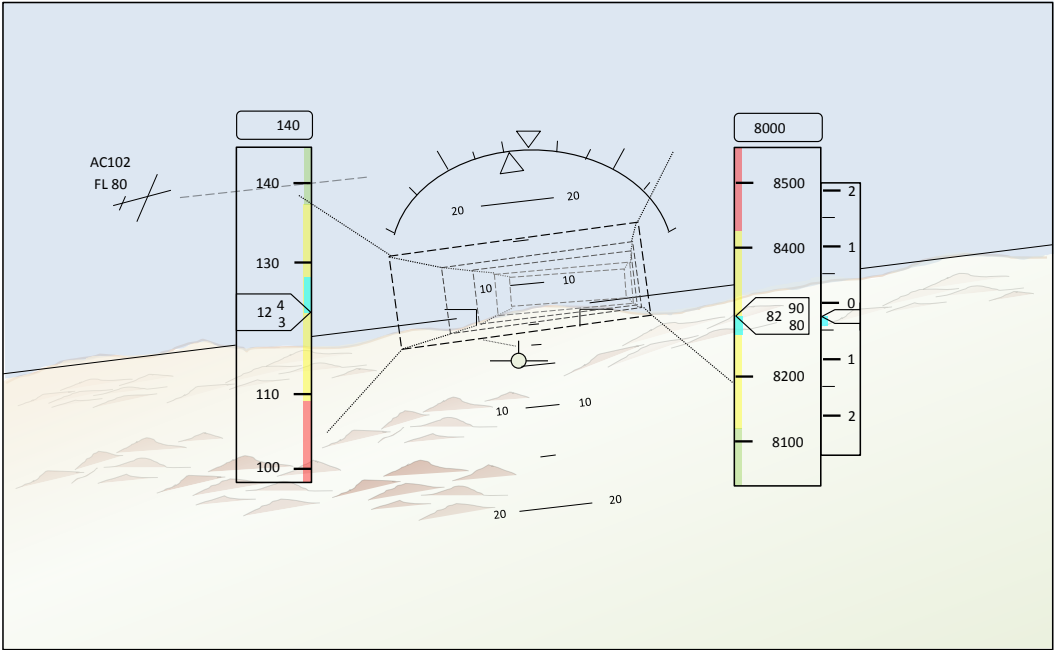


Figure C.2. PFD display showing resolution information.

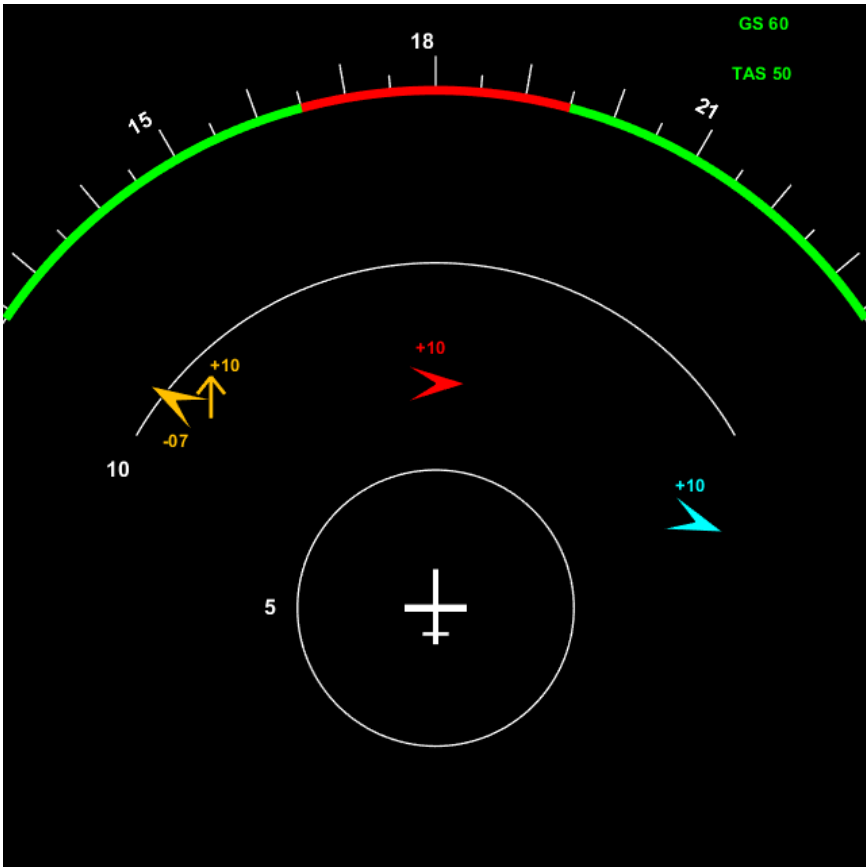


Figure C.3. CDTI display showing resolution information.



Table C.2. Aural annunciations.

<b>SA&amp;CA Function</b>	<b>Aural Annunciation</b>
Conflict Alert	Conflict, Conflict
Climb Resolution	Climb, Climb
Descend Resolution	Descend, Descend
Speed change resolution	Speed up/down
Ground track change resolution	Turn left/right
Conflict resolved	Clear
Resolution to climb/turn right	Climb/turn right

## C.4 Information Display

Different formats are presented on the ground pilot display units according to the characteristics of detected obstacles. The obstacle information can be combined in the CDTI as shown earlier in Figure C.1. In this display, obstacles/other traffic depicted in red indicate an assessed conflict in the immediate time frame. Specifically, obstacles that are identified as conflicts are indicated with a triangle encircled in the cross-sections of the avoidance volumes. Avoidance volumes are represented as white circles, corresponding to the maximum cross-sections of the avoidance volume bounding spheres. The maximum altitude of the obstacles relative to the aircraft's current position is indicated in red beside the avoidance volumes. Other traffic Obstacles/other traffic in yellow indicate a possible conflict in the tactical time frame (within 5 to 20 minutes). Obstacles/other traffic in amber indicate that there exists a lower probability of collision. In the first case (Figure C.4), two obstacles are detected corresponding to a) wire obstacles and b) extended structure.

In this case, a "CLIMB" command is issued and communicated to the ground pilot (remotely controlled) or automatically performed by the aircraft. Geo-fences are generated for the detected obstacles and are integrated in the TID as shown in Figure C.5.

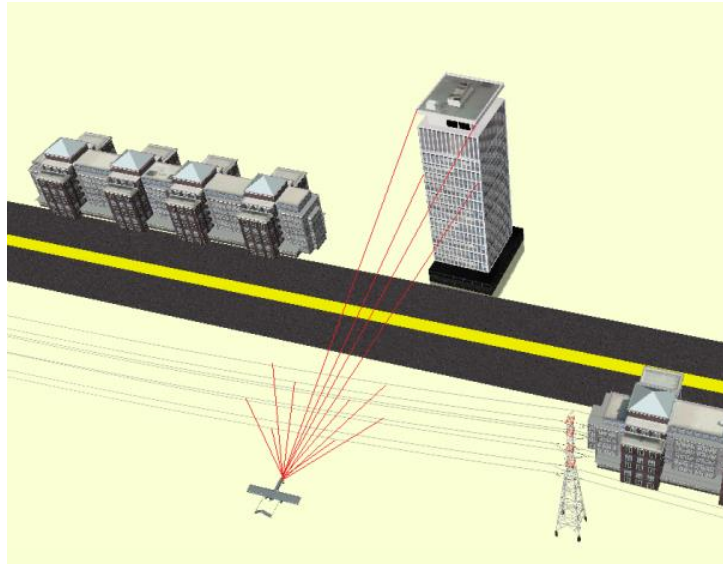


Figure C.4. Case 1 - Detection of wires and an extended structure.



Figure C.5. CDTI – Case 1.

Guidance and resolution information is provided to the ground pilot and to the autopilot to implement full automated functionalities. The resolution information is categorised as:

- horizontal guidance: the directive wedges and chords supporting avoidance of any conflict;
- vertical guidance: the desired altitude required to avoid any conflict;
- vertical rate guidance: the desired vertical speed required to avoid any conflict;

- auditory alerts: similar to the Resolution Advisories (RAs) provided by TCAS II;
- text based commands: guidance commands including "CLIMB", "DESCEND", "TURN RIGHT" and "TURN LEFT".

In the second case, one extended structure (e.g. tall building) is detected and trajectory re-optimisation is performed to avoid a collision (Figure C.6). In this case, a “CLIMB UP”/“TURN LEFT”/“TURN RIGHT” command is issued and communicated to the ground pilot (remotely controlled) or automatically executed by the aircraft. The TID for this scenario is shown in Figure C.7.

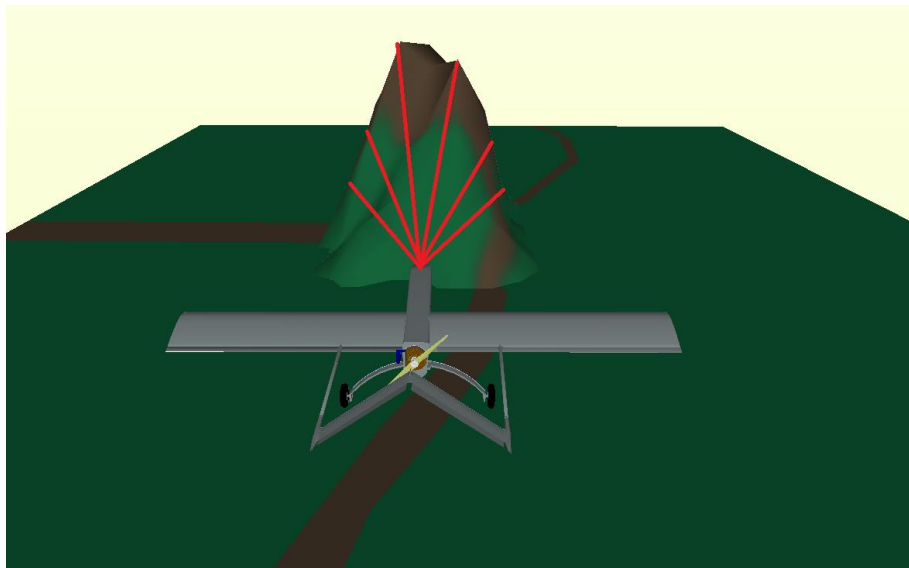


Figure C.6. Case 1 - Detection of wires and an extended structure.

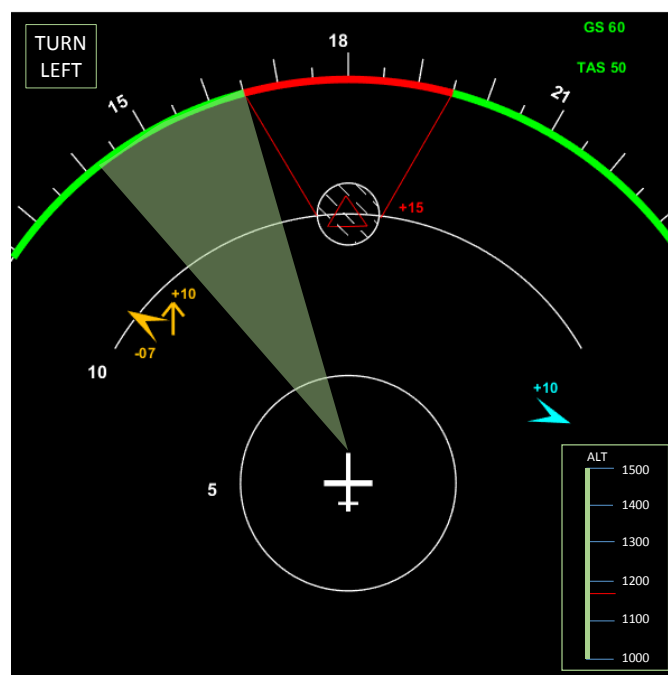


Figure C.7. TID - Case 2.

In the third case, a single small extended structure (e.g. a tree) is detected by the SA&CA algorithms (Figure C.8). In this case, a “CLIMB UP”/” TURN LEFT”/”TURN RIGHT” command is issued and communicated to the ground pilot (remotely controlled) or automatically performed in autonomous mode. The TID for this scenario is shown in Figure C.9.

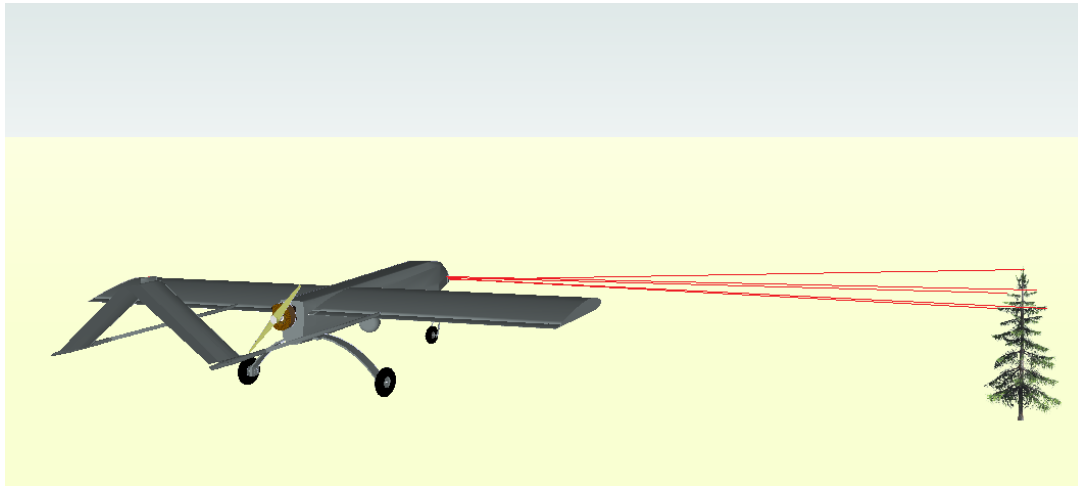


Figure C.8. Case 3 - Detection of wires and an extended structure.



Figure C.9. TID - Case 3.

After estimating the tracking observables of other traffic, steering commands are automatically issued to the autopilot and also communicated to the ground pilot.

## C.5 Adaptive HMI<sup>2</sup>

Adaptive HMI<sup>2</sup> are intended to assist human operators by using several intelligent functions including managing displayed information, adaptive alerting, assessing the situation, determining the human conditions and recommending timely responses. This set of functions employs models of the human operators, the human operators' cognition and intentions, and the situation. Additionally, adaptive HMI<sup>2</sup> integrates several state-of-the-art technologies for achieving an optimum interaction between the pilot and a virtual (automation) system [15, 16]. The adaptive HMI<sup>2</sup> architecture is illustrated in Figure C.10.

The novel functions required are:

- Continuous cognition assessment;
- Environment and operations assessment;
- Dynamic task allocation;
- Adaptive alerting.

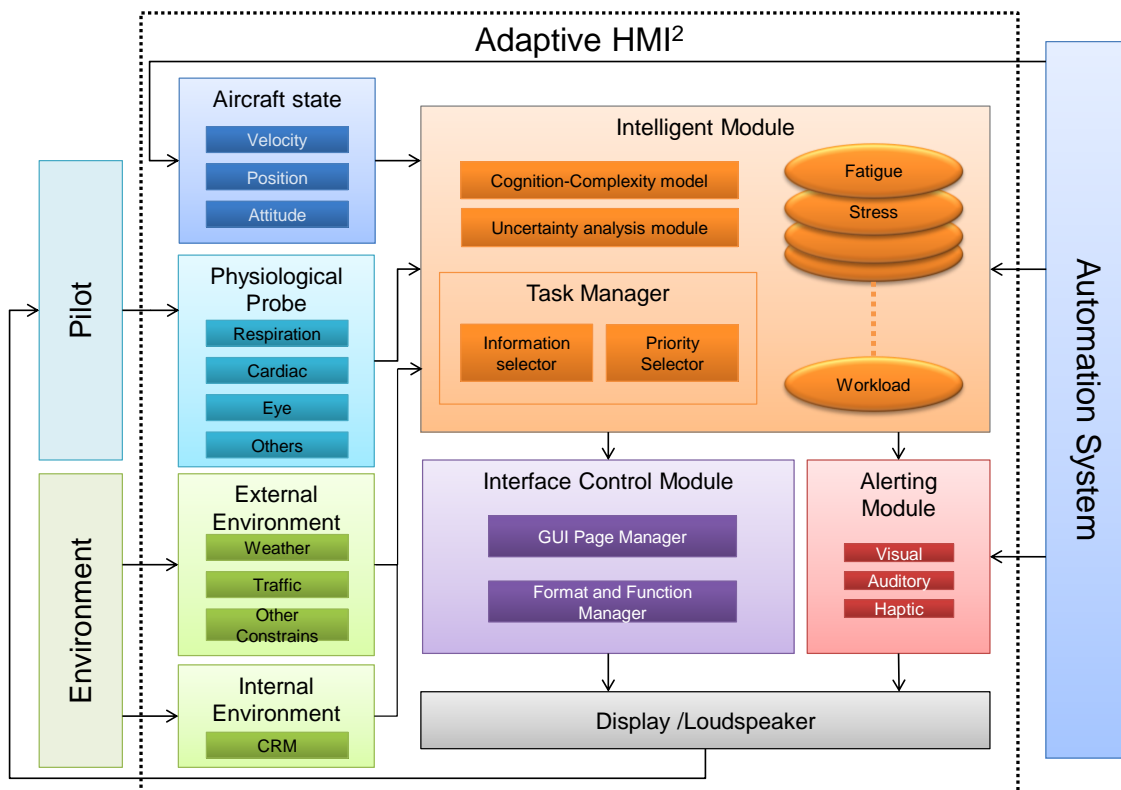


Figure C.10. Adaptive HMI<sup>2</sup> architecture.

The adaptive HMI integrates several state-of-the-art technologies for achieving an optimum interaction between the pilot and the automation system. The first introduced technology is the Head-Up Display (HUD), which has been equipped on the Boeing B787 aircraft. The HUD provides enhanced vision and enables the single pilot to operate the aircraft with greater ease. Another technology that is envisaged to be adopted is the use of touch screens. The integration of adaptive HMI<sup>2</sup> into NG-FMS is shown in Figure C.11.

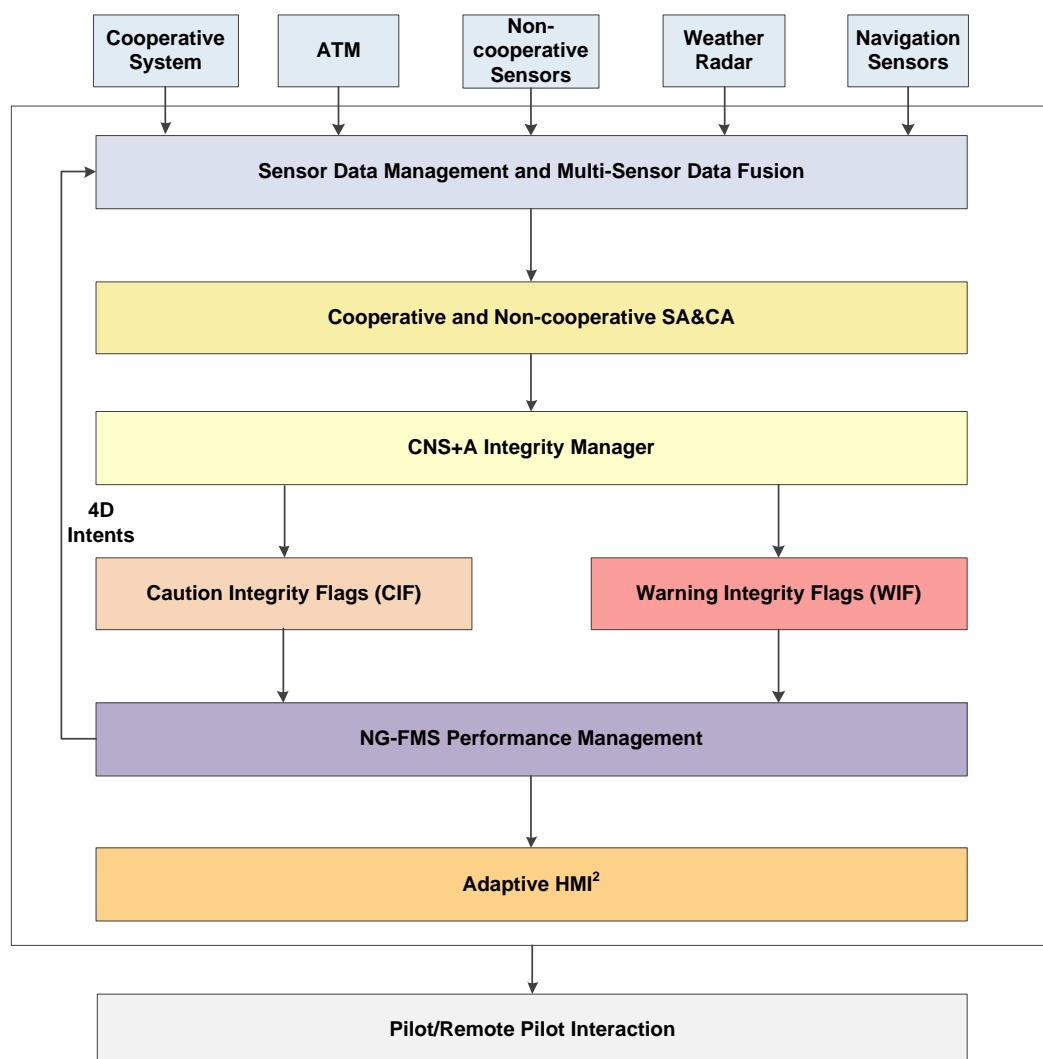


Figure C.11. Adaptive HMI<sup>2</sup> integration in the NG-FMS.

Using this technology, the hand-eye coordination problems can be reduced, leading to a faster operation and a reduction in the opportunity for errors. Currently, automatic speech recognition technology is used for conducting checklist tasks. The automation system attends to the call while the pilot interacts with the voice instructions and

completes the cross checking by the communication system. This technology reduces the heads-down time so that the pilot can concentrate on his primary tasks. It also enables interactivity between the pilot and his virtual assistant, which leads to a significant reduction in workload. These technologies make a more intuitive and user-friendly interface, which naturally eases the workload for pilots. Additionally, the adaptive HMI<sup>2</sup> enhances the situational awareness of the pilot by displaying a real-time status of some key parameters, such as automation level and control authority, in a status mode display. The multimodal alerts, including visual, aural and haptic, are provided to keep the pilot in the loop in case of abnormal conditions or emergencies.

The design features of NG-FMS provide increased inner-loop automation, creating a greater shift in the pilot's responsibilities from low-level, tactical tasks like aviating and navigating, towards higher-level, strategic tasks like managing and decision-making. However, the pilot is still responsible for directing the aircraft during all phases of flight, either in terms of having the final authority to approve a specific decision made by the system, or in response either to external events, or during different flight phases. In particular, perhaps the most important technological advancement required to support fully autonomous flight (FMS for single pilot operations during pilot incapacitation and for unmanned aircraft) is proving safety in the presence of anomalies such as unexpected traffic, on board failures, and conflicting data. Current aircraft automation is mostly considered rigid in the sense that designers have favoured simplicity over adaptability in their strategies.

The adaptive HMI<sup>2</sup> is introduced within the NG-FMS, providing it with the capability of adaptive automation and thus enhancing the system's adaptability to unanticipated events. The integration allows the NG-FMS to estimate the pilot's cognitive state through a combination of physiological sensors as well as external complexity inputs from the NG-FMS subsystems. Through beyond-line-of-sight communication datalinks, adaptive HMI<sup>2</sup> provides periodic updates to the ground-based flight crew. During transitions between strategic and tactical tasks, adaptive HMI<sup>2</sup> is able to monitor and aid the pilot, and if necessary, support making the transition. For example, in the event of pilot overload or incapacitation, the adaptive HMI<sup>2</sup> reduces the pilot's workload by either assuming responsibility of some of these functionalities, or by allocating them to the ground-based flight crew.

## C.6 Conclusions

After an introductory note on HMI<sup>2</sup> systems for NG-FMS, the formats and functions required for SA&CA were presented. In particular, the formats and functions developed for ground obstacle SA&CA were described. The appendix also presented the emergence of adaptive HMI<sup>2</sup> systems. With an appropriate system implementation, pilots' errors can be reduced and enhanced synergies can be attained between human and machine, improving the total system performance. Moreover, the implementation of suitable decision logics (based on the estimated cognitive states of the pilot or remote pilot) allows a continuous and optimal reconfiguration of the automation levels. The design of adaptive HMI<sup>2</sup> is still very much in the research phase, as experimental measurements and results, especially in real-world flight situations, are yet to be fully captured and evaluated.

## C.7 References

1. J.T. Platts, M.L. Cummings and R.J. Kerr, "Applicability of STANAG 4586 to Future Unmanned Aerial Vehicles", Proceedings of AIAA Infotech Aerospace Conference, Rohnert Park, California, USA, 2007.
2. R. Franklin, "STANAG 4586, NATO Network Enabled Capability Service Oriented Architecture Working Group–Status Overview Presentation", STANAG 4586, 2010.
3. CAA, "Global Fatal Accident Review 2002 to 2011", CAA CAP 1036, 2013.
4. FAA, "FAA Federal Aviation Regulations (FARS), 14 CFR", Section 385, Composition of Flight Crew, 2015.
5. E. Hoffman, J.P. Nicolaon, C. Pusch and K. Zeghal, "Limited Delegation of Separation Assurance to Aircraft", The Freer-Flight Evolutionary Air-ground Cooperative ATM Concepts, EUROCONTROL, 1999.
6. J.P. Dwyer and S. Landry, "Separation Assurance and Collision Avoidance Concepts for the Next Generation Air Transportation System", Human Interface, Part II, HCII 2009, pp. 748–757, Springer-Verlag, Berlin-Heidelberg, 2009.
7. C.D. Wickens, J. Lee, Y. Liu and G.S. Becker, "An Introduction to Human Factors Engineering", Pearson Education Inc., USA, 2004.
8. V.J. Gawron, "Human Performance. In Human Performance, Workload, and Situational Awareness Measures Handbook", Second Edition, CRC Press, pp. 13-86, 2008.
9. J.D. Lee and K.A. See, "Trust in Automation: Designing for Appropriate Reliance", Human Factors: The Journal of the Human Factors and Ergonomics Society, vol. 46, pp. 50-80, 2004.



10. G.L. Calhoun, M.H. Draper, M.F. Abernathy, M. Patzek and F. Delgado, "Synthetic Vision System for Improving Unmanned Aerial Vehicle Operator Situation Awareness", Defense and Security, International Society for Optics and Photonics, pp. 219-230, 2005.
11. S. Temel and N. Unaldi, "Opportunities and Challenges of Terrain Aided Navigation Systems for Aerial Surveillance by Unmanned Aerial Vehicles", Wide Area Surveillance, Springer, Berlin-Heidelberg, pp. 163-177.
12. Radio Technical Commission for Aeronautics, TCAS I Functional Guidelines, RTCA DO-184, Washington DC, 1983.
13. Radio Technical Commission for Aeronautics, Report – Assessment and Recommendations on Visual Alerts and Aural Annunciations for TCAS II, RTCA DO-299, 2009.
14. J. Meyer, M. Göttken, C. Vernaleken and S. Schärer, "Automatic Traffic Alert and Collision Avoidance System (TCAS) Onboard UAS", Handbook of Unmanned Aerial Vehicles, Springer Netherlands, pp. 1857-1871, 2015.
15. J. Liu, A. Gardi, S. Ramasamy, Y. Lim and R. Sabatini, "Cognitive Pilot-Aircraft Interface for Single-Pilot Operations", Knowledge-Based Systems, Elsevier, 2016. DOI: [10.1016/j.knosys.2016.08.031](https://doi.org/10.1016/j.knosys.2016.08.031)
16. Y. Lim, J. Liu, S. Ramasamy and R. Sabatini, "Cognitive Remote Pilot-Aircraft Interface for UAS Operations", Proceedings of the 2016 International Conference on Intelligent Unmanned Systems (ICIUS 2016), Xi'an, Shaanxi Province (China), August 2016.

This page is intentionally left blank to support presswork tasks

# APPENDIX D

## LIST OF RELEVANT PUBLICATIONS

Some of the key findings of this research work are documented in this section.

### D.1 Scientific Dissemination

#### Book Chapters:

1. A. Gardi, S. Ramasamy, R. Sabatini and T. Kistan, "Terminal Area Operations: Challenges and Opportunities", Encyclopedia of Aerospace - UAS, eds. R. Blockley and W. Shyy, John Wiley: Chichester, 2016. DOI: [10.1002/9780470686652.eae1141](https://doi.org/10.1002/9780470686652.eae1141)
2. R. Sabatini, A. Gardi, S. Ramasamy, T. Kistan and M. Marino, "Modern Avionics and ATM Systems for Green Operations", Green Aviation, Chapter 27, eds. R. Blockley et al., John Wiley: Chichester, 2016. ISBN: 978-1-118-86635-1

#### Journal Papers:

1. S. Ramasamy, R. Sabatini and A. Gardi, "LIDAR Obstacle Warning and Avoidance System for Unmanned Aerial Vehicle Sense-and-Avoid", Aerospace Science and Technology, vol. 55, pp. 344–358, 2016. DOI: [10.1016/j.ast.2016.05.020](https://doi.org/10.1016/j.ast.2016.05.020)
2. S. Ramasamy, R. Sabatini and A. Gardi, "A Novel Unified Analytical Framework for Aircraft Separation Assurance and UAS Sense-and-Avoid", Journal of Intelligent & Robotic Systems, pp. 1-20, 2017.
3. F. Cappello, S. Ramasamy and R. Sabatini, "A Low-Cost and High Performance Navigation System for Small RPAS Applications", Aerospace Science and Technology, 2016. DOI: [10.1016/j.ast.2016.09.002](https://doi.org/10.1016/j.ast.2016.09.002)
4. R. Sabatini, F. Cappello, S. Ramasamy, A. Gardi and R. Clothier, "An Innovative Navigation and Guidance System for Small Unmanned Aircraft using Low-Cost Sensors", Journal of Aircraft Engineering and Aerospace Technology, 2015. DOI: [10.1108/AEAT-06-2014-0081](https://doi.org/10.1108/AEAT-06-2014-0081)
5. S. Ramasamy, R. Sabatini, A. Gardi and T. Kistan, "Next Generation Flight Management System for Real-Time Trajectory Based Operations", Applied

- Mechanics and Materials, vol. 629, pp. 344-349, 2014. DOI: [10.4028/www.scientific.net/AMM.629.344](https://doi.org/10.4028/www.scientific.net/AMM.629.344)
6. S. Ramasamy, M. Sangam, R. Sabatini and A. Gardi, "Flight Management System for Unmanned Reusable Space Vehicle Atmospheric and Re-entry Trajectory Optimisation", Applied Mechanics and Materials, vol. 629, pp. 304-309, 2014. DOI: [10.4028/www.scientific.net/AMM.629.304](https://doi.org/10.4028/www.scientific.net/AMM.629.304)
  7. J. Liu, A. Gardi, S. Ramasamy, Y. Lim and R. Sabatini, "Cognitive Pilot-Aircraft Interface for Single-Pilot Operations", Knowledge-Based Systems, 2016. DOI: [10.1016/j.knosys.2016.08.031](https://doi.org/10.1016/j.knosys.2016.08.031)
  8. Y. Lim, B. Vincent, S. Ramasamy, J. Liu and R. Sabatini, "Commercial Airliner Single Pilot Operations: System Design Drivers and Pathways to Certification", IEEE Aerospace and Electronic Systems Magazine, 2017. DOI: [10.1109/MAES.2017.160175](https://doi.org/10.1109/MAES.2017.160175)
  9. Y. Lim, S. Ramasamy, A. Gardi, T. Kistan and R. Sabatini, "Cognitive Human-Machine Interfaces and Interactions for Unmanned Aircraft", Journal of Intelligent & Robotic Systems, pp. 1-19, 2017.
  10. A. Gardi, R. Sabatini and S. Ramasamy, "Multi-Objective Optimisation of Aircraft Flight Trajectories in the ATM and Avionics Context", Progress in Aerospace Sciences, vol. 83, pp.1-36, 2016. DOI: [10.1016/j.paerosci.2015.11.006](https://doi.org/10.1016/j.paerosci.2015.11.006)

### Conference Proceedings:

1. S. Ramasamy, R. Sabatini and A. Gardi, "A Unified Approach to Separation Assurance and Collision Avoidance for UAS Operations and Traffic Management", Proceedings of the IEEE International Conference on Unmanned Aircraft Systems (ICUAS 2017), Miami, FL, USA, pp. 920-928, June 2017.
2. S. Ramasamy, R. Sabatini and A. Gardi, "A Unified Approach to Separation Assurance and Collision Avoidance for Flight Management Systems", Proceedings of the 35<sup>th</sup> AIAA/IEEE Digital Avionics Systems Conference (DASC2016), Sacramento, CA, USA, September 2016. DOI: [10.1109/DASC.2016.7777964](https://doi.org/10.1109/DASC.2016.7777964)
3. S. Bijjahalli, S. Ramasamy and R. Sabatini, "Masking and Multipath Analysis for Unmanned Aerial Vehicles in an Urban Environment", Proceedings of the 35<sup>th</sup> AIAA/IEEE Digital Avionics Systems Conference (DASC2016), Sacramento, CA (USA), September 2016. DOI: [10.1109/DASC.2016.7778029](https://doi.org/10.1109/DASC.2016.7778029)
4. S. Ramasamy, R. Sabatini and A. Gardi, "Cooperative and Non-Cooperative Sense-and-Avoid in the CNS+A Context: A Unified Methodology", Proceedings of the IEEE International Conference on Unmanned Aircraft Systems (ICUAS 2016), Arlington, VA, USA, pp. 531-539, June 2016. DOI: [10.1109/ICUAS.2016.7502676](https://doi.org/10.1109/ICUAS.2016.7502676)

5. S. Ramasamy and R. Sabatini, "Communication, Navigation and Surveillance Performance Criteria for Safety-Critical Avionic Systems", SAE Technical Paper 2015-01-2544, SAE 2015 AeroTech Congress & Exhibition, Seattle, Washington, USA, September 2015. DOI: [10.4271/2015-01-2544](https://doi.org/10.4271/2015-01-2544)
6. F. Cappello, R. Sabatini and S. Ramasamy, "Multi-Sensor Data Fusion Techniques for RPAS Detect, Track and Avoid", SAE Technical Paper 2015-01-2475, SAE 2015 AeroTech Congress & Exhibition, Seattle, Washington (USA), 2015. DOI: [10.4271/2015-01-2475](https://doi.org/10.4271/2015-01-2475)
7. S. Ramasamy, A. Gardi, J. Liu and R. Sabatini, "A Laser Obstacle Detection and Avoidance System for Manned and Unmanned Aircraft Applications", Proceedings of the IEEE International Conference on Unmanned Aircraft Systems (ICUAS 2015), Denver, CO, USA, June 2015. DOI: [10.1109/ICUAS.2015.7152332](https://doi.org/10.1109/ICUAS.2015.7152332)
8. S. Ramasamy, R. Sabatini and A. Gardi, "Novel Flight Management Systems for Improved Safety and Sustainability in the CNS+A Context", Proceedings of the AIAA/IEEE Integrated Communication, Navigation and Surveillance Conference (ICNS 2015), Herndon, VA, USA, April 2015. DOI: [10.1109/ICNSURV.2015.7121225](https://doi.org/10.1109/ICNSURV.2015.7121225)

#### **Technical Reports (THALES Australia):**

1. A. Gardi, S. Ramasamy, M. Marino, T. Kistan, R. Sabatini, M. O'Flynn and P. Bernard-Flattot, "Implementation, Verification and Evaluation of 4D Route Planning and Dynamic Airspace Functionalities in a Simulated Environment", Next Generation Air Traffic Management Systems: Multi-Objective Four-Dimensional Trajectory Optimisation, Negotiation and Validation for Intent Based Operations, THALES RMIT University Collaborative Research, Report 3, 2016.
2. M. Marino, A. Gardi, S. Ramasamy, T. Kistan, R. Sabatini, M. O'Flynn and P. Bernard-Flattot, "System Level Implementation, Verification Requirements and Simulation Case Studies for 4D Route Planning and Dynamic Airspace Functionalities", Next Generation Air Traffic Management Systems: Multi-Objective Four-Dimensional Trajectory Optimisation, Negotiation and Validation for Intent Based Operations, THALES RMIT University Collaborative Research, Report 2, 2015.

This page is intentionally left blank to support presswork tasks